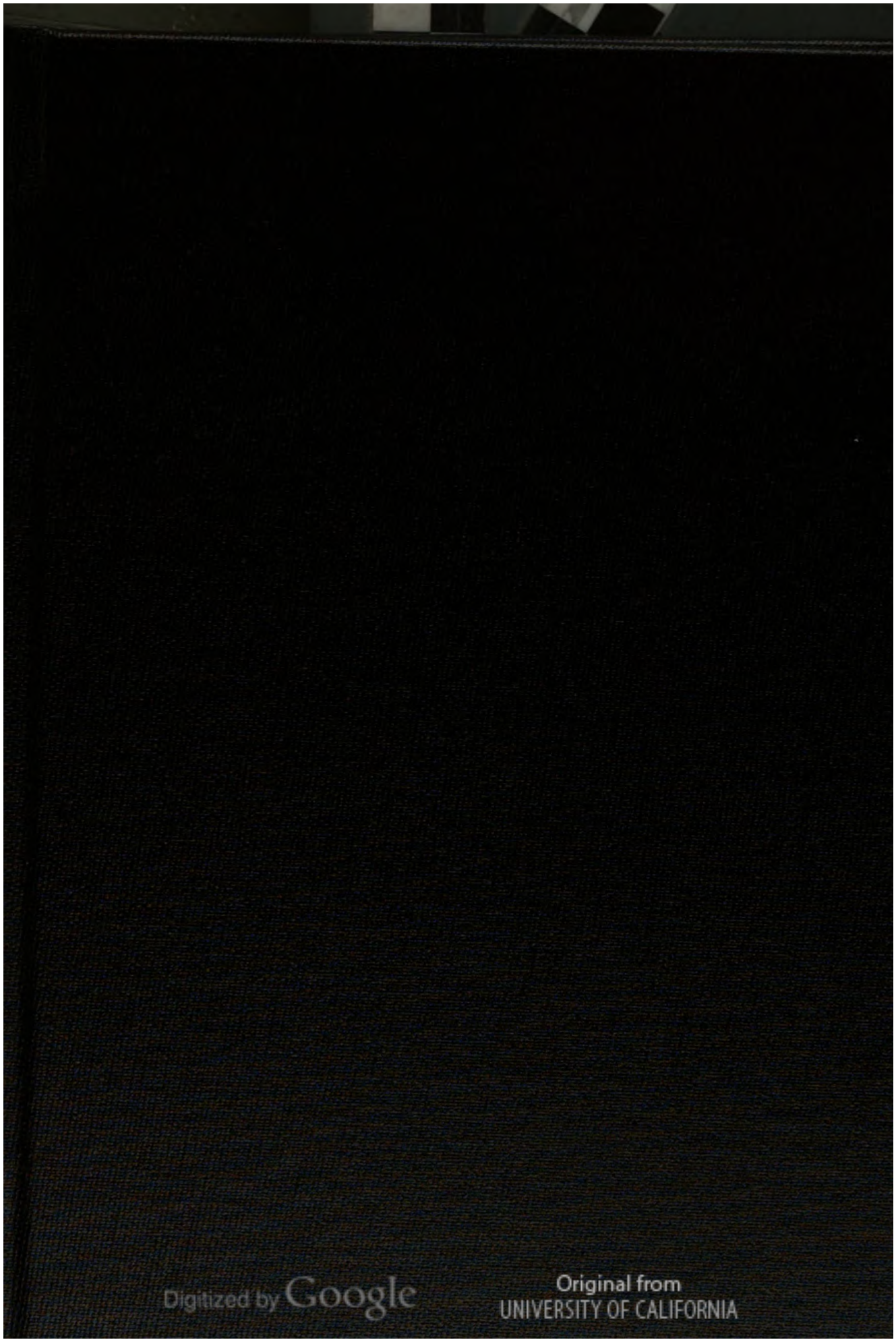

Mechanical Springs

MACHINE DESIGN

SERIES

THE PENTON PUBLISHING CO., CLEVELAND 13, OHIO, U. S. A.
PUBLISHERS OF STEEL • MACHINE DESIGN • THE FOUNDRY • NEW EQUIPMENT DIGEST • REVISTA INDUSTRIAL

Mechanical Springs

by

A. M. Wahl
Westinghouse Electric & Manufacturing Company

First Edition

PUBLISHED BY
PENTON PUBLISHING COMPANY
CLEVELAND, OHIO
1944

THE PENTON PUBLISHING COMPANY
CLEVELAND, OHIO
London: 2 Caxton St., Westminster, S.W. 1

Printed in U.S.A.

FOREWORD

This book presents the fundamental principles underlying the design of mechanical springs and brings together in convenient form for the designer of machines the more important developments in spring theory and testing which have taken place within recent years. Although mechanical springs often represent important components of modern machines and devices, in the past such springs too often have been designed on the basis of empirical or "rule of thumb" methods which do not take full account of the limitations of the materials used or of the mechanical stresses set up during operation. This is particularly true for applications where fatigue or repeated loading is involved. As a consequence, unsatisfactory operation or even mechanical failure has resulted in many cases.

It is the author's hope that the present book may contribute something toward the avoidance of such conditions by helping to put the specification of springs on a more rational basis. To this end, the results of researches carried out under the direction of the Special Research Committee on Mechanical Springs of the American Society of Mechanical Engineers and, more recently, those of the War Engineering Board Spring Committee of the Society of Automotive Engineers, have been freely drawn upon. Much of the material in the book has also been based on research reported in the *Transactions* of the A.S.M.E., the *Journal of Applied Mechanics*, the *S.A.E. Journal* and the author's series of articles published in *Machine Design* during the past several years.

Because of the importance of the helical compression or tension spring a relatively large amount of space has been devoted to this type. Not only have the theoretical aspects of stress calculation of this type of spring been treated in considerable detail, but much emphasis also has been laid upon the fatigue properties of such springs, as well as on the fatigue problem of spring materials in general. This has been done since it is the author's experience that the limitations due to the endurance properties of materials are apt to be overlooked by

designers. Other important aspects of the helical spring design problem treated in various chapters include creep effects under static loading, buckling, lateral loading, vibration and surging.

Besides the helical spring, the fundamentals of design of other important spring types including disk, Belleville, flat, leaf, torsion, spiral, volute and ring springs have been treated. Because of its military importance, the volute type of spring has been discussed in considerable detail.

Although rubber is not ordinarily thought of as a spring material, the extensive application of rubber springs and mountings in recent years has made the inclusion of a chapter on this subject appear advisable. Since the subject of vibration is intimately tied up with the application of rubber mountings, some of the fundamentals of vibration absorption and isolation also have been discussed.

It should be emphasized that in a book of this nature it is not possible to cover all the factors which enter into the choice of a spring for a given application. Consequently the author feels that for best results in any particular design, close cooperation should be maintained between the designer and the spring manufacturer in order to benefit from the latter's experience and judgment. However, a knowledge of the fundamentals should assist in judging the feasibility of a design.

The preparation of this book would not have been possible without the support of the Westinghouse Electric and Manufacturing Co. In this connection the author's thanks are due, in particular, to L. W. Chubb, Director, Research Laboratories, and to R. E. Peterson, Manager, Mechanics Department. Thanks are also due to R. L. Wells of the Laboratories, and to Tore Franzen, Maurice Olley, B. Sterne and H. O. Fuchs of the S.A.E. War Engineering Board Spring Committee. The encouragement given to much of the author's research by S. Timoshenko and J. M. Lessells is greatly appreciated. To L. E. Jermy, Editor, *Machine Design*, and to J. W. Greve, Associate Editor, the writer is further indebted for valuable suggestions concerning the presentation.

A. M. WAHL

East Pittsburgh, Pa.
May 4, 1944

CONTENTS

CONTENTS

CONTENTS

LIST OF SYMBOLS

Symbol	Definition	Units
a	= constant	—
a	= radius, distance	inch
b	= constant	—
b	= width	inch
c, C	= constants	—
c	= distance	inch
c	= spring index	—
c	= damping factor	lb-sec/in.^{2}
d, D	= diameter	inch
D	= plate rigidity	lb-in.
e	= distance from neutral axis to center of gravity	inch
e	= eccentricity of loading	inch
E	= modulus of elasticity	lb/sq in.
f	= frequency of vibration	cycles/sec
F	= force	lb
g	= acceleration of gravity	in./(sec)^2
G	= modulus of rigidity	lb/sq in.
h	= thickness	inch
h	= initial cone height	inch
I	= moment of inertia of area	in.^{4}
I_p	= polar moment of inertia	in.^{4}
k, K	= constants	—
K	= spring constant	lb/in.
K	= stress multiplication factor	—
K_c	= stress concentration factor due to curvature	—
K_f	= fatigue strength reduction factor	—
K_t	= theoretical stress concentration factor	—
l	= length	inch
m	= temperature coefficient of modulus	degrees^{-1}
m	= reciprocal of Poisson's ratio	—
m	= integer, constant	—
m_h, m_t	= bending and twisting moments per inch	in.-lb/in.
m_1, m_2	= bending moments per inch	in.-lb/in.
M	= bending moment, moment	in.-lb
n	= constant, integer	—
n	= number of turns, number of leaves, etc.	—
n	= per cent deflection of rubber slab	—
n	= factor of safety	—
N	= number of solid coils (helical spring)	—
N	= normal force	lb
p	= load per inch	lb/in.
P	= load	lb
P_y	= load for complete yielding	lb

LIST OF SYMBOLS

Symbol	Definition	Units
q	= sensitivity index	—
q	= ratio	—
q	= pressure per unit area	lb/sq in.
Q	= shear load, lateral load	lb
r, R	= radius	inch
R	= radial load	lb
S	= tension per unit length	lb/in.
t	= thickness	inch
t	= time	sec
t	= temperature	degrees
T	= torque, twisting moment	in.-lb
U	= energy stored in spring per unit volume	in.-lb/in.^{3}
V	= volume	in.^{3}
V	= energy stored per unit volume	in.-lb/in.^{3}
W	= weight	lb
x, y, z	= rectangular co-ordinates	—
x	= distance along beam	inch
y	= deflection of beam at any point	inch
z	= constant	—
α	= angle, helix angle	degrees or radians
α	= ratio, outer to inner radius	—
β	= angle, angular deflection	degrees or radians
β	= constant, ratio	—
γ	= constant, ratio	—
γ	= angle, angle of shear	degrees or radians
γ	= weight per unit volume	lb/in.^{3}
δ	= deflection	inch
ϵ	= distance	inch
ϵ	= small quantity	—
θ	= angular deflection, angle	radians
$\dot{\theta}$	= angular velocity ($d\theta/dt$)	radians/sec
κ	= curvature	in.$^{-1}$
λ	= small quantity	—
μ	= Poisson's ratio	—
μ	= coefficient of friction	—
ρ	= radius	inch
σ	= normal stress	lb/sq in.
σ_o, σ_v	= static, variable components of normal stress	lb/sq in.
σ_m	= maximum stress	lb/sq in.
σ_y	= yield stress in tension	lb/sq in.
σ_e	= endurance limit in bending	lb/sq in.
σ_e	= equivalent stress based on strength theory	lb/sq in.
$\sigma_1, \sigma_2, \sigma_3$	= principal stresses	lb/sq in.
τ	= shear stress	lb/sq in.
τ_o, τ_v	= static and variable components of shear stress	lb/sq in.
τ_e	= endurance limit in shear	lb/sq in.
ϕ	= angle of rotation, angular deflection	radians or degrees
ψ	= constant	—
ζ, ξ	= co-ordinates	—
ω	= angular velocity, circular frequency	radians/sec

MECHANICAL SPRINGS

CHAPTER I

GENERAL CONSIDERATIONS IN SPRING DESIGN

A mechanical spring may be defined as an elastic body whose primary function is to deflect or distort under load and which recovers its original shape when released after being distorted. Although most material bodies are elastic and will distort under load, they are not all considered as springs. Thus a beam of structural steel will deflect slightly when a weight is placed on it; however, it is not considered as a spring because its primary purpose is not to deflect under load but rather to remain rigid.

On the other hand, the helical spring used in the ordinary spring scales, *Fig.* 1, is designed so as to deflect by a relatively large amount when loaded. Consequently, the deflection and load may easily be determined. This, therefore, functions as a spring.

Provided the material is not stressed beyond the elastic limit, the usual type of spring will have a straight-line load-deflection diagram as shown in *Fig.* 2. This means that the deflection is proportional to the load, i.e., if the load is doubled; the deflection will be doubled. The relation will hold true even if the acting load is a torque or moment, provided linear deflection is replaced by angular deflection.

Not all springs have linear load-deflection diagrams, however. In some cases load-deflection diagrams as shown in *Fig.* 3 may be found. Curve *A* may be obtained with a thin flat circular plate loaded to a large deflection. Curve *B* may result from

an initially-coned disk (or Belleville) spring. These two spring types are discussed in Chapters XV and XIV, respectively. Because of friction and contact between turns, the ordinary clock spring also does not have a linear torque-angle characteristic, as discussed in Chapter XVIII.

FUNCTIONS OF SPRINGS

Among the primary functions of springs the following are perhaps the most important:

1. To Absorb Energy and Mitigate Shock: In order to absorb energy without excessive peak loads the spring must deflect by

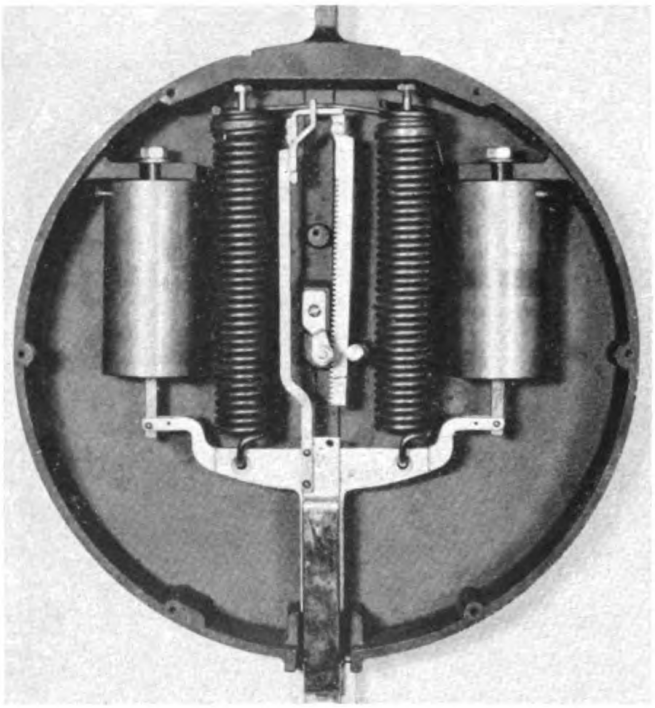

—Courtesy, John Chatillon & Sons

Fig. 1—Heavy-duty scale springs

a considerable amount. An example of the use of a spring to absorb energy is the draft-gear spring shown in *Fig.* 4. Another example is the automotive springs for independent suspension of front wheels, *Fig.* 5, which must be able to absorb the energy of impact when the car goes over a bump. These also function as mechanical supports for the vehicle.

2. To Apply a Definite Force or Torque: An automotive valve spring supplies the force which holds the valve follower against the cam; a watch spring supplies the torque necessary to overcome the friction in the driving mechanism. Sometimes springs are

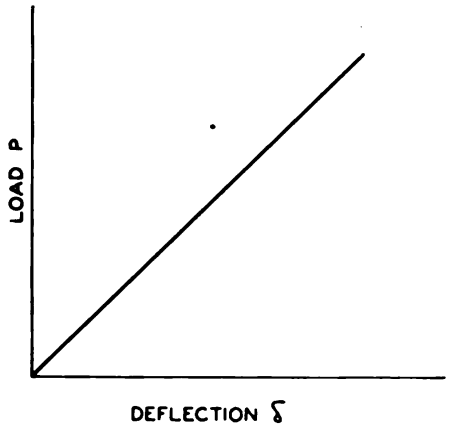

Fig. 2 — Linear load-deflection curve of typical spring

used to apply a definite gasket pressure as in the high-voltage condenser-bushing gasket springs shown in *Fig.* 6. The function of these springs is to maintain an oil-tight gasket seal regardless of expansions due to temperature change. Lockwashers commonly used under nuts and bolt heads also function essentially as springs

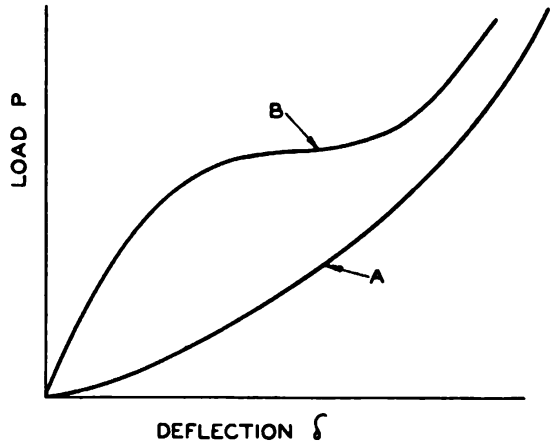

Fig. 3 — Nonlinear load-deflection curves

to apply a definite force regardless of slight changes in the bolt length due to vibration, temperature changes, etc. This force tends to prevent the bolt from unwinding even though vibration is present.

3. To Support Moving Masses or To Isolate Vibration: The usual purpose of springs used to support moving or vibrating masses

is to eliminate or to reduce vibration or impact. Thus electric motors are frequently spring supported to prevent the transmission of objectionable vibration to the foundation. Likewise, the springs used in automobile suspensions not only tend to mitigate shock due to irregularities in the road surface (Point 1) but also pre-

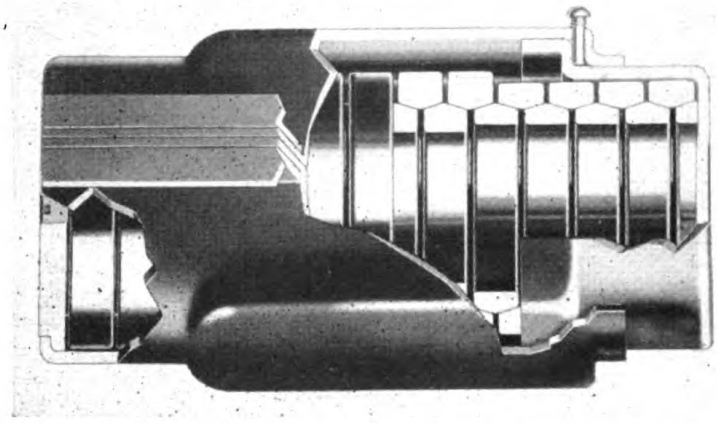

—Courtesy, Edgewater Steel Co.

Fig. 4—Sectional view of ring spring in draft gear

vent the transmission to the car body of objectionable vibration to the presence of regular waves (wash-board) in the road contours. Similarly the springs on a railway car, *Fig.* 7, tend to prevent the transmission of impact shocks from truck irregularities. An interesting application of the use of springs to support a vibrating mass is the tub support in an automatic washing machine, *Fig.* 8. By supporting the tub flexibly on springs, transmission of vibration due to unbalanced masses in the eccentrically-loaded tub is greatly reduced.

4. To Indicate or Control Load or Torque: One of the most im-

Fig. 5—Helical springs for independent suspension of front wheels

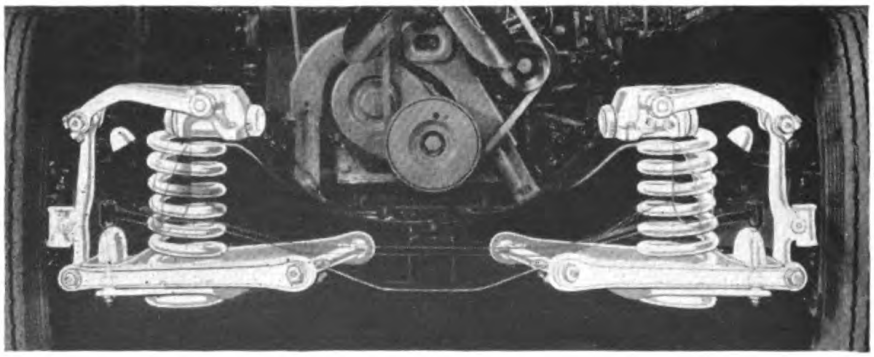

portant functions of springs is that of furnishing a flexible member which will deflect by a considerable amount when subject to a load or torque. By the use of suitable mechanisms this deflection is transferred to a pointer which indicates the amount of load or torque. An example is the scale spring in *Fig.* 1.

5. To Provide an Elastic Pivot or Guide: Sometimes one or more flat springs may be used in combination to function as an elastic pivot. Because of low internal friction such pivots often have real advantages over bushings or antifriction bearings. Thus the flexible elements of the gimbal mountings for the Mt. Palomar telescope,

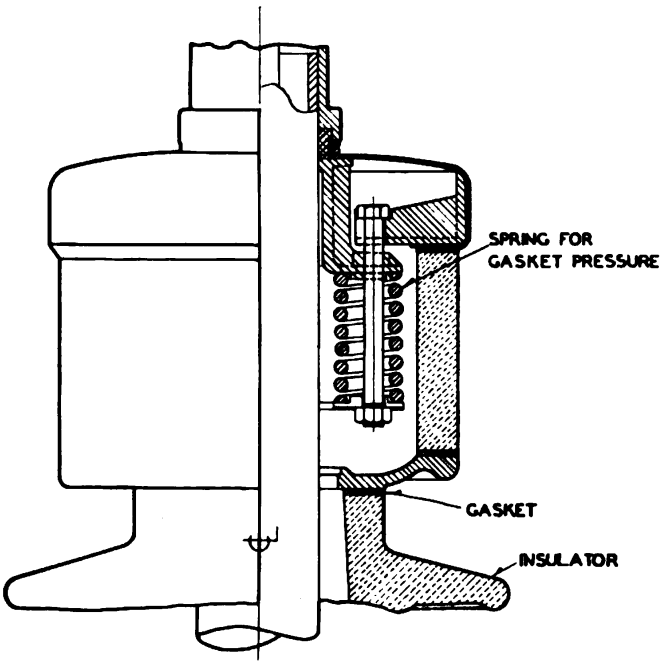

Fig. 6—Spring used for maintaining gasket pressure

Fig. 9, which consists of a group of straight bars radially disposed around the telescope axis can be considered essentially as a spring application where an elastic pivot is required. An application where flat springs serve as guides is in the balancing machine, *Fig.* 10.

SPRING MATERIALS

Because springs must usually deflect by a considerable degree for a given load, it follows that a relatively large amount of energy must be stored when the spring is in the deflected position. Since both the deflection and load for most springs are propor-

tional to stress and since energy is proportional to deflection times load, it follows that in general the amount of energy which may be stored is proportional to the *square* of the stress. Hence for best results relatively high working stresses must be used. This explains why most spring materials have high tensile strengths and are worked at much higher stresses than in other fields.

The most widely used material for springs at present is carbon steel. In the smaller sizes of wire, for an .8 to .9 per cent carbon steel by cold drawing and patenting, ultimate tensile strengths varying from 230,000 to 400,000 pounds per square inch (depending on the size of the wire) may be obtained. This type of material is known as music wire. In the larger sections, by using one per cent carbon steel and heat treating after forming, the ultimate strength may reach 200,000 to 240,000 pounds per square inch. Similar values may be obtained from chrome-vanadium and alloy steel. Properties of various spring mate-

Fig. 7—Leaf and coil springs on New York Central "Mercury"

rials are tabulated in Chapter XXIII. In the larger sizes, helical springs are usually heat treated after forming, the latter being done hot. Smaller sizes of helical springs, on the other hand, are usually wound cold from pretempered material or music wire. After winding, a stress relieving low-temperature heat treatment is usually given[1].

[1]Typical specifications for different spring materials, including data on heat treatment, are given in Chapter XXIII.

Where corrosion effects are present, stainless steel springs of 18 per cent chromium, 8 per cent nickel composition are frequently used. This material (which is also used for high-temperature applications) may have a tensile strength varying from

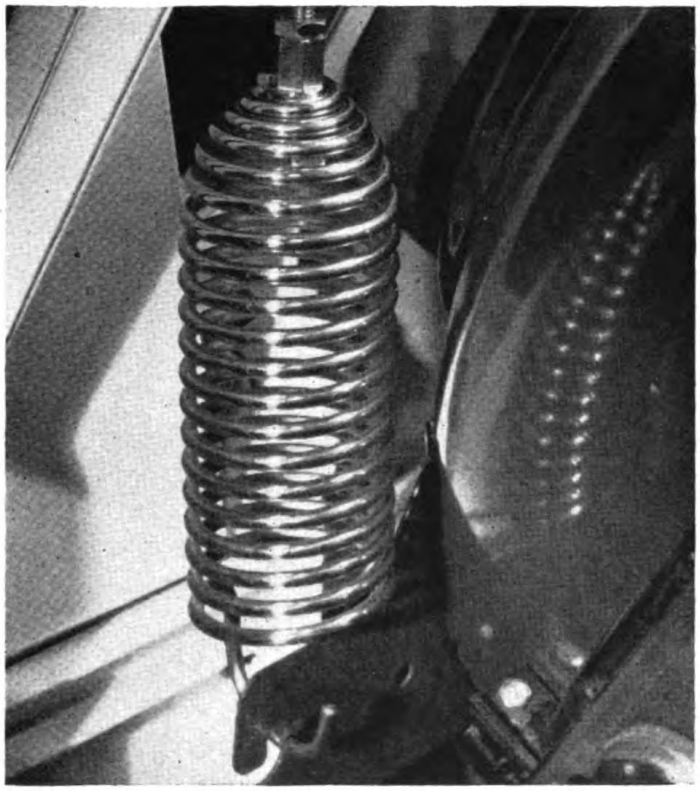

Fig. 8—Spring support for automatic washer

180,000 pounds per square inch for 3/16-inch wire to 280,000 pounds per square inch for 1/32-inch wire. Phosphor bronze also is used where corrosion is present. This material, however, has considerably less strength than stainless steel, values of ultimate tensile strength around 100,000 pounds per square inch are being obtained.

TYPES OF LOADING

Static Loading—In many cases, springs are subject to a load (or deflection) which is constant or which is repeated but a few

times during the life of the spring. Such springs are known as *statically-loaded* springs. Examples are safety valve springs where the valve is expected to pop off but a few times during its life; springs for producing gasket pressure, typified by the condenser bushing springs in *Fig.* 6; springs in circuit-breaker mechanisms where the breaker operates but a few times in its life.

In the design of statically-loaded springs it is frequently important that the spring maintain its calibration to a sufficient degree. Thus in the case of a spring compressed by a given amount this means that as time goes on, the load should not drop off by more than a small amount (usually a few per cent). This phenomenon of load loss is known as *relaxation.* For example, in a safety-valve spring, if there is some loss in load due to relaxation of the material after a period of time, the valve will pop off at lower pressure than that for which it was designed. Similarly for springs used to produce gasket pressure, relaxation of the

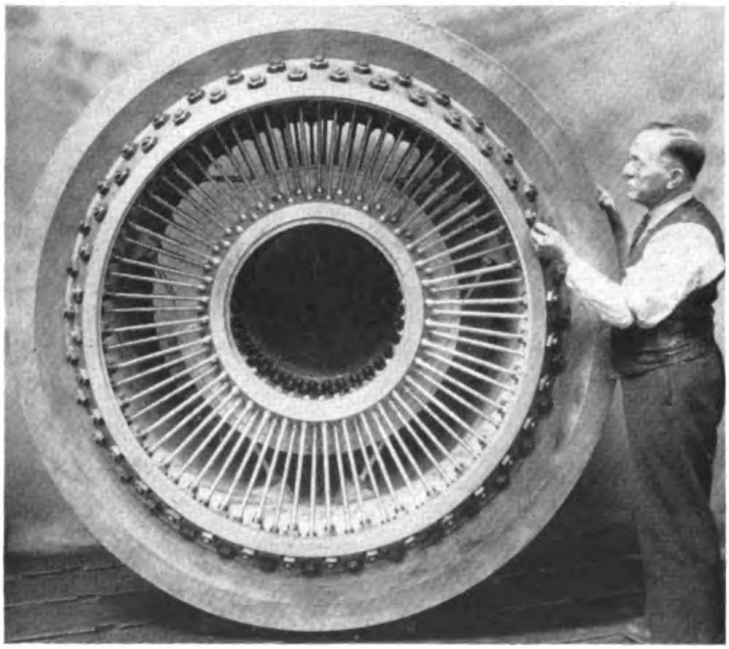

Fig. 9—Flexible elements for gimbal of Mt. Palomar telescope

material will result in loss of pressure. While some loss in pressure usually may be tolerated, too much renders the spring ineffective for application as a sealing device.

If the spring is subject to a constant *load* rather than a constant *deflection* and if the stress is too high, there will be a slow deflection with time. This is usually known as *settage* and is due

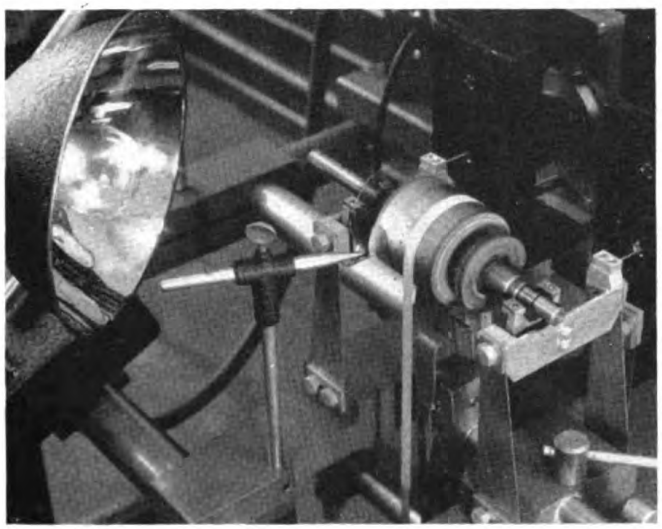

Fig. 10—Flat springs used in balancing machine

to creep or plastic flow of the material. In many cases this is undesirable also. Thus, if the spring is used to support a given load as in the case of a knee-action car, settage of the spring will allow a deflection of the wheels relative to the car. Such a deflection may have a bad effect on the steering mechanism. Another example is the trolley base springs shown in *Fig.* 11. If settage of these springs should occur, objectionable loss in pressure between trolley wheel and overhead wire would result. Therefore the springs must be designed so that this set is kept small.

At normal temperatures, if the peak stress in the spring is kept well below the elastic limit or yield point of the material, trouble from set or relaxation will seldom occur. Hence in design, where high temperatures are not involved, the maximum stress is taken equal to the yield point divided by the factor of safety. Frequently this factor of safety is taken equal to 1.5 although lower values may be used in many cases. Some of the factors which influence the choice of a factor of safety are discussed later on, Page 24.

At elevated temperatures the effects of creep or relaxation are

increased. In such cases the design stress should be based on actual creep or relaxation tests. Unfortunately, not much data of this kind are available to designers, although some tests were reported recently by F. P. Zimmerli[2]. These tests indicated that for ordinary carbon-steel springs, the effects of temperatures below about 350 degrees Fahr. were not very pronounced. Above 400 degrees Fahr. the use of stainless-steel springs is indicated. This question is further discussed in Chapter V.

In the design of springs subject to *static* loading it is suggested that for the usual spring material which has some ductility (although of course not as much as structural materials), stress concentration effects such as those due to curvature may be neglected. For example, in a simple plate with a small hole and subject to a tension load, theoretical analysis based on the theory of elasticity shows that, for *elastic* conditions, the peak stress at the edge of the hole is around three times the stress some distance away[3]. For fatigue or repeated loading this peak stress is important. However, for static loads the usual practice in machine design is to neglect such stress concentration effects[4], since these peak stresses are localized and may be relieved by plastic flow as a consequence of the material ductility. Available evidence also points to the fact that similar stress concentration effects such as those due to curvature in helical springs may be neglected where static loads are involved.

Variable Loading—In many spring applications the load does not remain constant, but varies with time. For example, an automotive valve spring is initially compressed by a given amount during assembly but, during operation, it is compressed periodically by an additional amount. It may, therefore, be considered to operate between a minimum and a maximum load or stress. In such a case the spring is said to be subject to *variable* or *fatigue* loading. *Fig.* 12 shows such stress cycles for such a spring subject to a continuous cyclic stress between the minimum stress σ_{min} and the maximum value σ_{max}. This is equivalent to a static or

[2]"Effect of Temperature on Coiled Steel Springs at Various Loadings", *Transactions* A.S.M.E., May, 1941, Page 363. Also "Relaxation Resistance of Nickel Alloy Springs", by Betty, et al, *Transactions* A.S.M.E., July, 1942, Page 465.

[3]Timoshenko—*Strength of Materials*, Part II, Second Edition, 1941, Van Nostrand, page 312, gives a further discussion of stress concentration; also *Theory of Elasticity*, McGraw Hill, 1934, page 75.

[4]For a further discussion article by C. R. Soderberg on "Working Stresses", *Transactions* A.S.M.E., 1933, APM 55-16 is recommended. Also Timoshenko—*Strength of Materials*, page 482.

constant stress σ_0 equal to half the sum of maximum and minimum stresses on which is superimposed a variable stress σ_v. The variable stress is equal to half the difference between σ_{max} and σ_{min}, the proper algebraic sign being considered. The discussion concerning bending stress σ in this chapter also applies, in general, to torsion stresses.

More often, however, the loading condition is much more complicated than that indicated in *Fig.* 12. For example, an

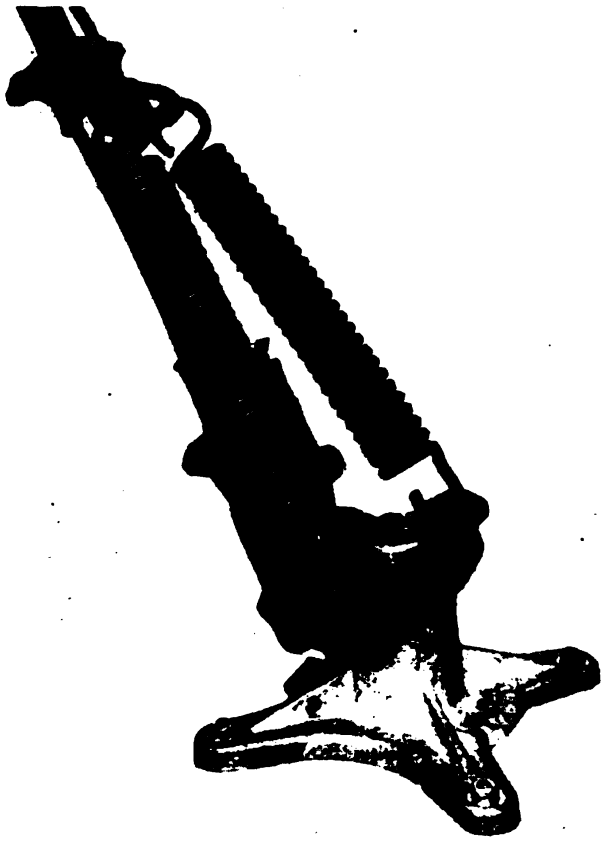

Fig. 11—Trolley-base springs

automobile knee-action spring, *Fig.* 5, is subject to practically a constant load when the car is traveling over smooth pavement. In passing over rough dirt roads, however, the spring may be subject to an irregular loading condition with stress cycles of

varying amplitude as indicated in *Fig.* 13. The same thing is also true of freight car and locomotive springs. In such cases the determination of allowable stresses is more difficult, particularly since fatigue test data giving results for cases where the variable component of stress changes with time are almost wholly lacking[5].

In many applications, springs are subject to loads or stresses which vary more or less continuously between a minimum and a maximum value. The difference between the maximum and the minimum stress is known as the *stress range;* this is also twice the variable component of stress σ_v. This stress range is of particular importance when fatigue or repeated loading is involved since for many materials the endurance range is practically constant provided the yield point is not exceeded.

If the limiting variable stress σ_v which the spring will just stand is plotted against the mean stress σ_o on which σ_v is superimposed, an *endurance diagram* such as that shown in *Fig.* 14 will be obtained. Thus any point *P* on this curve means that, if

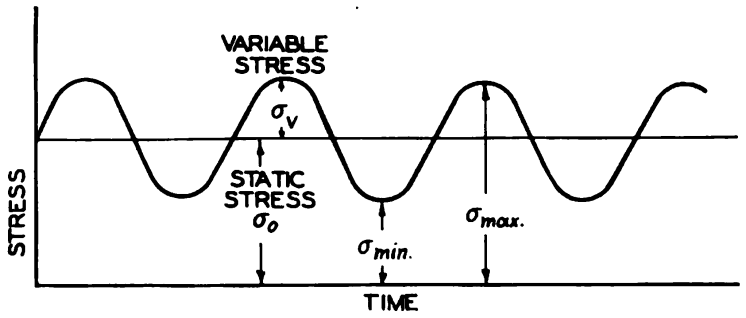

Fig. 12—Variable stress superimposed on a static stress

the mean stress is σ_o, a variable stress larger than σ_v if superimposed on the stress σ_o will eventually cause fatigue failure; conversely, one smaller than σ_v will not cause fatigue failure of the spring.

It is interesting to note that when the static component of the stress σ_o is zero, a condition of completely reversed stress is obtained. The variable stress σ_v for zero σ_o should therefore

[5]B. F. Langer—"Fatigue Failure from Stress Cycles of Varying Amplitude", *Journal of Applied Mechanics*, December, 1937, gives a further discussion of this problem. Also "Damage and Overstress in the Fatigue of Ferrous Metals", by Russell and Welcker, *Proceedings* A.S.T.M., 1936, Part 2, page 118.

correspond to the usual endurance limit σ_e for completely reversed stress in either torsion or bending (depending on whether torsion or bending stresses are considered). On the other hand, when the variable stress is low, tests show that the curve tends to approach the ultimate strength σ_u. Of course, for high values of mean stress considerable creep may be expected to occur so

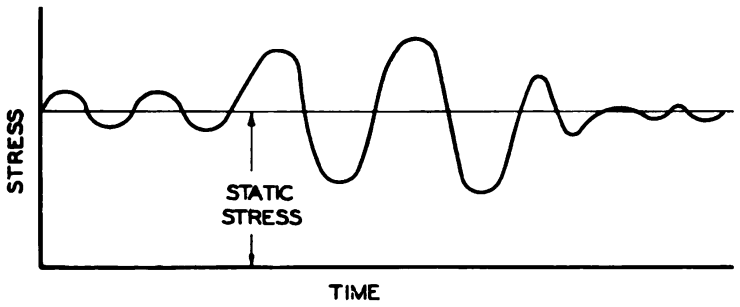

Fig. 13—Stress cycles of variable amplitude

that the problem becomes one of avoiding excessive settage or loss in load.

Another way of plotting endurance or fatigue test results for variable stress conditions is shown in *Fig.* 15. Here two curves *a* and *b* representing σ_{max} and σ_{min} respectively are plotted equidistant from the dot and dash line *c* which represents the mean stress σ_o. The *a* and *b* curves represent upper and lower limits of actual stress just required to cause fatigue failure for stress ranges between points on the same vertical line. It is clear that at any point *P* the ordinate of the mean stress line *c* represents the static or mean component of stress σ_o while the vertical

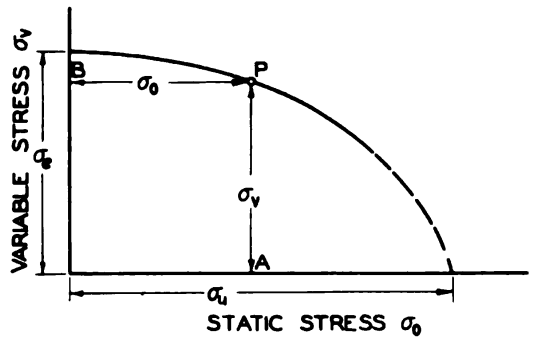

Fig. 14 — Typical experimental line of fatigue failure for combined static and variable stress

distance between the mean stress line and either the upper or lower curve gives the variable stress component σ_v. The upper curve *a* represents $\sigma_o + \sigma_v$ while the lower curve *b* represents $\sigma_o - \sigma_v$. The maximum and minimum values of stress σ_{max}

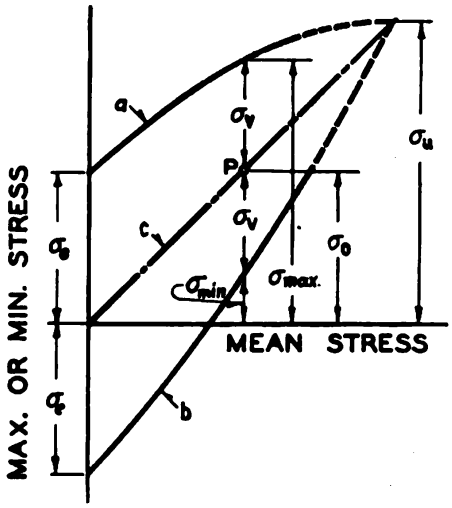

Fig. 15—Alternate method of representation of fatigue test results for static and variable stress

and σ_{min} corresponding to any combination of static and variable stresses σ_o and σ_v may be read directly from the curves *a* and *b* as indicated.

A simple method[6] of determining working stress is to replace the actual endurance curve by a straight line connecting the yield point σ_y and the endurance limit σ_e as shown in *Fig.* 16. This line may, however, be considerably below the actual endurance curve so that working stresses determined in this manner may be somewhat too conservative. However, the method is of advantage in many cases on account of its simplicity.

Using this method, a combination of static and variable stresses represented by any point *P* on the line *AB* connecting the points at distances σ_e/n and σ_y/n is defined as having a factor of safety of *n*. If σ_{wo} is the static component of the *working* stress and σ_{wv} the variable component, from the geometry of *Fig.* 16 it may be shown that the factor of safety may

[6]This method was suggested by Soderberg—"Factor of Safety and Working Stresses", *Transactions* A. S. M. E., 1930, APM 52-2.

be expressed by the following relation:

$$n = \frac{1}{\frac{\sigma_{wo}}{\sigma_y} + \frac{\sigma_{wr}}{\sigma_e}} \quad \ldots\ldots\ldots\ldots\ldots\ldots\ldots\ldots\ldots\ldots\ldots\ldots\ldots\ldots\ldots\ldots\ldots\ldots\ldots\ldots\ldots\ldots (1)$$

This relation holds for torsion as well as for bending, provided the values σ_y and σ_e are taken as the yield point and endurance limits in torsion respectively. Torsion stresses, however, will be represented by the Greek letter τ.

More accurate results for most spring steels will usually be obtained by using an elliptical relationship between the values of static and variable stresses necessary to cause fatigue failure. For torsion stresses the endurance curve will be represented by

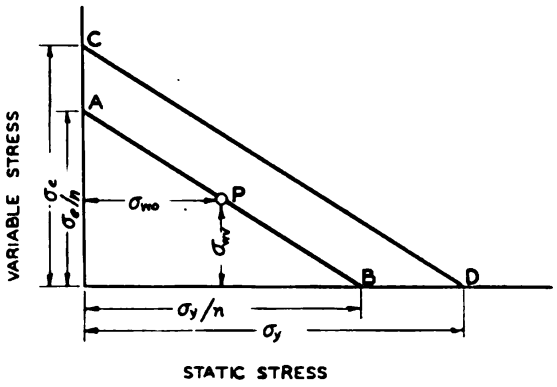

Fig. 16—Simplification of experimental curve of fatigue failure with method of defining safety factor

the quadrant of the ellipse, *ACB* in *Fig.* 17 and intersecting the coordinate axes at τ_y and τ_e. If it be assumed that no stress should exceed the yield strength, the dotted portion of this ellipse should be replaced by the line *CB* extending at an angle of 45 degrees to the abscissae. This is done since, when the variable and static components of stress represented by points on *CB* are added, the maximum stress will just equal the yield stress. On the basis of this elliptical law, the factor of safety n becomes

$$n = \frac{1}{\sqrt{\left(\frac{\sigma_{wo}}{\sigma_y}\right)^2 + \left(\frac{\sigma_{wr}}{\sigma_e}\right)^2}} \quad \ldots\ldots\ldots\ldots\ldots\ldots\ldots\ldots\ldots\ldots\ldots\ldots\ldots\ldots\ldots\ldots\ldots\ldots\ldots\ldots\ldots\ldots (2)$$

where the symbols have the same meaning as those used in Equation 1.

The results of some fatigue tests are plotted in *Fig.* 17 to enable a comparison to be made between the elliptical and the straight line relationships in the case of torsional fatigue stressing. The triangles represent the results obtained by Weibel[7] in tempered Swedish steel wire tested both in pulsating (0 to maximum) and in reversed torsion, the surface of the wires being in the "as received" condition. While these results show rather high values, they are among the few available for such a comparison. The circles in *Fig.* 17 represent test results by Hankins[8] on specimens of silico-manganese spring steel with machined surfaces. It may be seen that in these cases the elliptical law agrees closely with the test results. It should be noted,

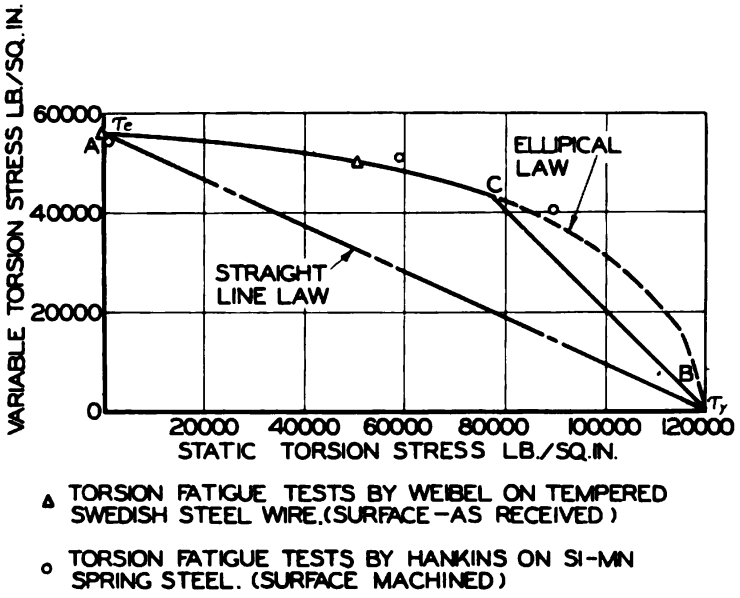

Fig. 17—Elliptical curve representing fatigue failure and comparison with torsion endurance test results

however, that the straight line law, *Fig.* 16, is safer to use in practice, particularly where complete test data are lacking.

In calculating the static or mean stress σ_v, the consensus of

[7] "The correlation of Spring Wire Bending and Torsion Tests"—E. E. Weibel, *Transactions* A.S.M.E., November, 1935, page 501.

[8] "Torsional Fatigue Tests on Spring Steels"—G. A. Hankins, Dept. of Scientific & Industrial Research, (British) Special Report No. 9.

opinion at present is that stress-concentration effects may be neglected for ductile materials[9]. This is consistent with neglecting stress-concentration effects where static loads only are involved. Since stress peaks due to curvature in helical-com-

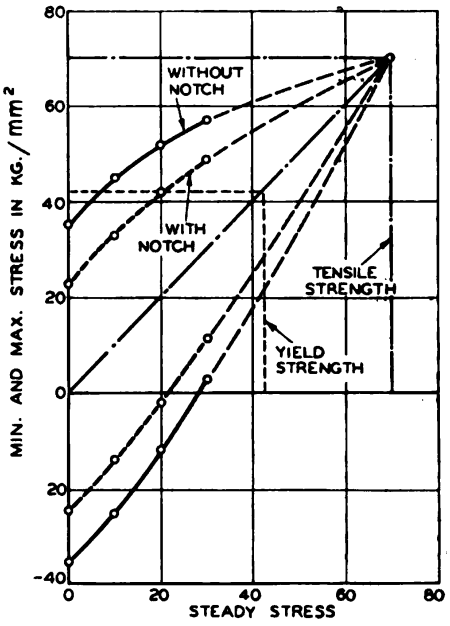

Fig. 18—Notch effect in fatigue stressing with initial tension, .7 per cent carbon steel (Stahl und Eisen, Volume 52, Page 660)

pression and torsion springs are localized, it is believed that for design purposes they may be considered as due to stress concentration effects and hence may be neglected in computing σ_m. It should be noted that the effect of direct shear in helical-compression springs should be considered, because this is not a localized stress. In figuring the variable component σ_v, however, stress concentration may not be neglected.

Some evidence in support of this method lies in certain fatigue tests on notched bars under combined static and variable stress. The results of one such test[10] on .7 per cent carbon steel bars are given in *Fig.* 18, the full lines being results for specimens without stress concentration and the dashed lines for notched specimens. It may be seen that the mean or static

[9]Ductile materials are defined by Soderberg as those having elongations over 5 per cent, which includes most spring materials.

[10]*Federstaehle*—Houdremont and Bennek, Stahl und Eisen, Vol. 52, page 660. Also, discussion by R. E. Peterson of Report of Research Committee on Fatigue of Metals, *Proceedings* A.S.T.M., 1937, Vol. 37, Part 1, Page 162.

stress represented by the dot and dash line is not diminished by the stress-concentration effect, while the variable stress represented by the vertical distance between either the full lines or the dashed lines is diminished in a more or less constant ratio by the stress concentration effect of the notch. While it must be admitted that available fatigue test data made for the purpose of evaluating stress-concentration effects under combined static and variable stress are rather meagre, it is believed that, until further test data are at hand, stress increases due to curvature in practical springs may be treated in this manner. An application of this method to the determination of working stresses in helical springs is given in Chapter VI.

Another method of treating the problem of combined static and variable stress is to calculate the stress range by taking stress-concentration effects (due to curvature, for example) into account. In the usual cases where stress concentration is present, the peak stress at the location of stress concentration will not exceed the yield point since the material will merely yield at this point. Hence, the maximum point of the stress range σ_{max} will be the yield point stress of the material. To determine the factor of safety, the endurance range of the material is compared with the range calculated in this manner[11]. A further condition to be satisfied is that the stress at maximum load, calculated by neglecting stress concentration, must not exceed the yield point of the material, since otherwise excessive yielding may occur. Application of this method in the design of helical springs is also illustrated in Chapter VI.

INFREQUENT OPERATION

Where springs are subject to relatively few cycles of loading, the permissible working stress may be considerably increased over that allowable for an infinite number. Examples of such springs are those used in certain control mechanisms. A typical stress-cycle graph for helical compression springs of carbon steel stressed from zero to a maximum is shown in

[11]To take into account the fact that the material may not be fully sensitive to stress concentration (i.e., that the actual stress range as found by test may be greater than the calculated figure using theoretical stress concentration factors), a reduction in the stress range may be made, provided test data are available. Further discussion of sensitivity is given in "Two- and Three-Dimensional Cases of Stress Concentration and Comparison with Fatigue Tests"—Peterson and Wahl, *Journal of Applied Mechanics*, March, 1936.

Fig. 19. It appears that for this type of stress application, the stress required to cause failure in ten thousand cycles of stress application may be about twice as great as that required to cause failure in ten million cycles. Provided some permanent set would not be objectionable, this suggests that a considerably higher working stress could be used if the spring is to be subject

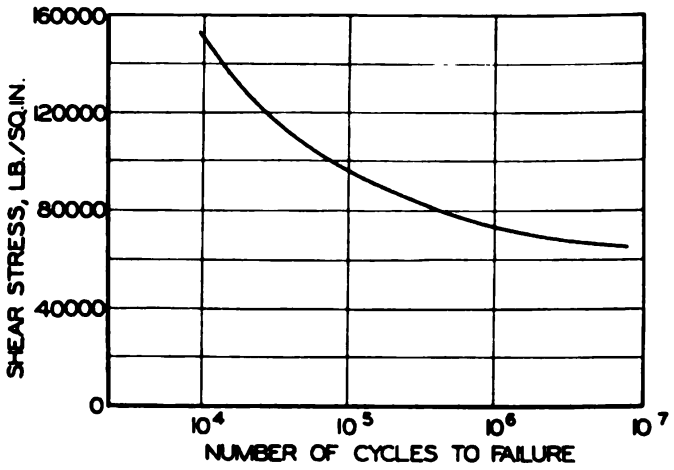

Fig. 19—Typical stress-cycle curve for helical springs

to relatively few stress cycles. It must not be inferred however, that a large increase in the working stress is usually possible when the loadings are relatively few. In most cases the increased permanent set would probably interfere with the operation of mechanisms of which the springs form an integral part.

SURFACE CONDITIONS AND DECARBURIZATION

It has been found that the surface condition in spring steels has a marked effect on the fatigue strength of the material. The reason for this is that in the manufacture of springs, because of heating during the heat-treating and forming operations, the surface layer is decarburized to some extent. Thus there is, in effect, a thin layer of low-carbon steel (which is relatively weak) over the body of the spring which is composed of the relatively strong high-carbon or alloy steel. Under fatigue or repeated loading conditions the weaker low-carbon steel on the surface may develop a crack which then spreads across the

section as a consequence of the high stress concentration at the base of the crack. Actual tests have shown that a very thin layer of this decarburized material is sufficient to greatly weaken the spring during fatigue.

A great deal of work on the effect of surface conditions on the fatigue strength of springs has been carried out by the National Physical Laboratory in England. The results of this work on actual plates as used in leaf springs show conclusively that this decarburized layer on the surface combined with the stress concentration effect of surface irregularities produced by manufacturing operations may reduce the actual endurance range to one-half or even less of that to be expected on the basis of tests on machined or ground specimens. For example, fatigue tests on 2 by ⅜-inch bars of heat treated .61 per cent carbon commercial spring steel (as used in leaf springs) made by Batson and Bradley[12] showed an endurance range with the surface machined and ground of 0 to 128,000 pounds per square inch. When the surface was left untouched, the endurance range dropped to 0-42000 pounds per square inch, a reduction of about two-thirds. The stress-cycle curves of *Fig.* 20 are plotted from data published by these experimenters and show the tremendous effect due to surface conditions in this particular case. Although this probably represents an unusually great reduction in strength, the stress data do show how important are the surface conditions.

Similar results were obtained by Hankins and Ford[13] who found for one silico-manganese steel a ±60,000 pounds per square inch endurance limit in reversed bending on specimens which had been heat treated after grinding to size. In this case there was a decarburized surface layer left there by the heat-treating process. When the tests were made on specimens of the same steel and given the same heat treatment but having a thin layer of surface material ground off *after* heat treatment, the endurance limit increased to ±103,000 pounds per square inch. Further tests were made on specimens which had been heat treated in a neutral atmosphere in such a way as to prevent the formation of a decarburized layer; in this case the endurance limit was

[12] "Fatigue Strength of Carbon and Alloy Steel Plates as Used for Laminated Springs", *Proceedings* Institute of Mechanical Engineers, 1931, Page 301.

[13] "Mechanical and Metallurgical Properties of Spring Steels as Revealed by Laboratory Tests"—Hankins and Ford. *Journal Iron and Steel Institute*, 1929, No. 1, Page 317.

±107,000 pounds per square inch or practically the same as for the specimens ground after heat-treatment. This indicates that the decarburized layer left by the usual heat treatment was to a large extent responsible for the lower endurance limits found on specimens which had not been machined after heat treatment. These tests are extremely interesting in that they afford an indication of what may be done by means of special heat treatments for increasing the fatigue strength of actual springs.

This reduction in endurance strength because of surface effects has also been observed in reversed torsion fatigue tests by Lea and Heywood[14] on chrome-vanadium spring steel wires. These investigators found that, where the wires had been ma-

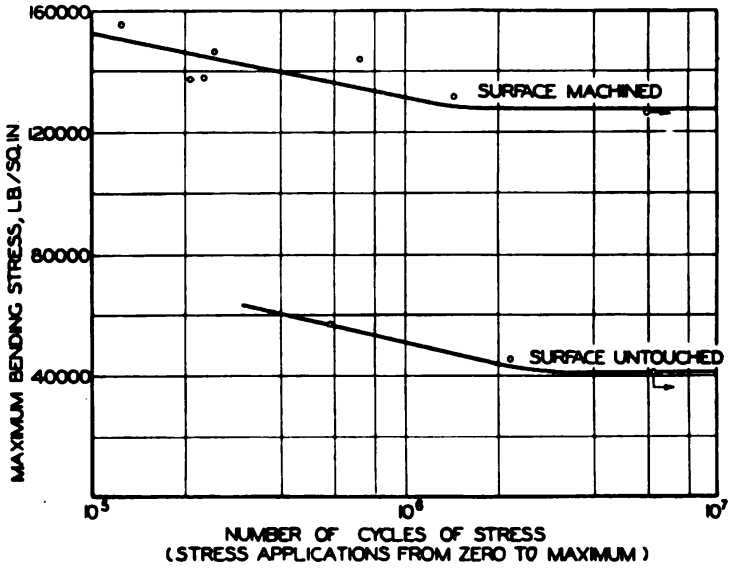

Fig. 20—Stress-cycle curves for .61 per cent carbon commercial spring steel plate. (From tests by Batson and Bradley, *Proceedings I.M.E.*, 1931, Page 301)

chined and polished, the torsional endurance limits were increased to almost twice the value obtained from specimens in the unmachined condition. Swan, Sutton, and Douglas[15] also report for chrome-vanadium steel under pulsating torsional

[14] "The Failure of Some Steel Wires Under Repeated Torsional Stresses"—Lea and Heywood, *Proceedings* Institute of Mechanical Engineers, 1927, Page 403.

[15] "Investigation of Steels for Aircraft Engine Valve Springs", *Proceedings* Institute of Mechanical Engineers, 1931, Vol. 120, Page 261.

stress (from ¼ maximum to the maximum), an increase of around 50 per cent in endurance range where the specimens were machined and polished. The results of these various tests show the importance of the surface conditions of spring steels when under torsion fatigue stressing. On the other hand, it should be mentioned that torsion fatigue tests on Swedish valve spring wires by Weibel[7] showed practically no difference in the torsional endurance limit between specimens with the surface untouched and those having the surface layer ground off. Probably this may be explained by the fact that this material has a very good surface condition so that the effect of decarburization was small.

Recently a process of shot-blasting helical springs has been developed which increases the endurance range by 50 per cent or more for the smaller springs[16]. This process consists of propelling small steel shot at high velocity against the spring surface, using an air blast or a centrifugal type of machine. Apparently the peening action of steel shot propelled against the surface of the spring tends to cold work and thus increase the strength of the weak or decarburized surface layer. This method seems to offer an economical way of obtaining satisfactory fatigue life in springs without the expense of grinding the surface after heat treatment. However, shot blasting or shot peening, as it is also called, can not be expected to give satisfactory results where excessive decarburization or surface defects are present. A further discussion of this is given in Chapter IV.

CORROSION EFFECTS

In cases where springs are subject to even mildly corrosive action while under fatigue stressing, the endurance limit for most ordinary materials is reduced greatly. In such cases, fatigue tests must be carried out for many more than the usual ten million cycles[17]. A large number of corrosion fatigue tests on spring materials, carried out by McAdam[18], show the tre-

---

[16]F. P. Zimmerli—"How Shot Blasting Increases Fatigue Life", *Machine Design*, Nov. 1940, Page 62. Also Lessells and Murray—"The Effect of Shot Blasting and Its Bearing on Fatigue", *Proceedings* A.S.T.M. Vol. 41, 1941, Page 659.

[17]"Corrosion-Fatigue of Metals"—H. J. Gough, *Engineer*, Vol. 154, 1932, Page 284.

[18]"Fatigue and Corrosion Fatigue of Spring Materials"—D. J. McAdam, Jr., *Transactions* A.S.M.E., 1929, APM 51-5.

mendous reduction in the endurance limit for spring materials subject to either fresh or salt-water corrosion fatigue. For spring steels subject to fresh-water corrosion fatigue, the value of endurance limit obtained was but one-fourth to one-ninth that obtained by tests on specimens in air. Higher values of endurance limit under corrosion conditions were obtained on corrosion-resistant steels, while cadmium-plated springs showed much higher endurance limits under such conditions, i.e., about twice the value was obtained for a spring steel with a plating than without. These examples show that the spring designer must either protect the springs from corrosive action, or else use extremely low working stresses. Even then, if corrosion is present, there is no assurance that eventual fatigue failure will not occur, if a sufficiently large number of stress repetitions of stress take place.

VARIATIONS IN DIMENSIONS

Another factor which the spring designer should keep in mind is that there is always an unavoidable variation in the size of wire or plate used in making springs. The effect of these variations may often be large, especially when it comes to obtaining proper load-deflection characteristics. For example, in the case of helical springs, a cumulative variation in both coil and wire diameter of only 1 per cent will result in a 7 per cent change in the load-deflection characteristic of the spring. Thus for a .1-inch wire, a 1 per cent variation would correspond to a change in diameter of only .001-inch. Such variations are easily possible in commercial practice. Hence, it may be necessary to allow the spring manufacturer some leeway in choosing the other spring dimensions to compensate for unavoidable variations in sizes of commercial wire stock. For example, if the wire for making helical springs happens to be slightly undersize, the spring manufacturer may be able to compensate for this by slightly reducing the coil diameter. In most cases, this slight reduction in coil diameter would not be detrimental to the operation of the spring. In commercial springs, actual stresses and load-deflection characteristics may easily deviate by 5 to 10 per cent from the calculated values and this must be considered in design. If special precautions are to be taken by the spring

maker, such variations may be reduced, but at increased expense. A further discussion of this is given in Chapter VIII.

FACTOR OF SAFETY

In choosing the factor of safety, n (as defined in Equation 1) the designer must be guided by many considerations. If the consequences of failure are serious, then a higher factor must be used; while if a broken spring causes but little inconvenience, it may be possible for the designer to lower the factor of safety. Where springs are made of uniform and high-grade material and where close control of the manufacturing process is maintained, lower factors of safety may be used. If, in addition, accurate test data on the particular spring materials employed are available for cases where the test conditions approximate the service conditions, the design factor of safety may again be reduced. On the other hand, ignorance of the peak loads acting or of the effect of unknown factors such as corrosion or temperature effects may dictate an increase in this factor.

It is the primary purpose of this book to acquaint the designer with the fundamentals underlying spring design in order to enable him to make an intelligent selection of springs for a given purpose. Nevertheless, it is advisable, in cases where important spring applications are concerned to have the design confirmed by consultation with the spring manufacturer, in order to benefit from the latter's experience.

CHAPTER II

HELICAL ROUND-WIRE COMPRESSION AND TENSION SPRINGS

Springs of most importance in machine design are helical round-wire compression or tension types. They are made in a wide variety of sizes and used in tremendous quantities. Among the reasons for wide acceptance and general use are the following:

1. LOW COST: Helical springs are relatively cheap to manufacture, particularly if large enough quantities are required to justify the use of automatic spring-winding machinery.
2. COMPACT: Springs are relatively compact, a considerable amount of material being squeezed into a small space.
3. EFFICIENT: The material is stressed fairly efficiently unless the spring index (ratio of coil diameter to wire diameter) is too low. This is further discussed in Chapter XXII.

The field of application of the helical spring is as broad as that of machine design itself. Several of the more important practical applications of helical springs have already been mentioned, Chapter I. In the automotive field these include independent suspension of front wheels, *Fig.* 5, suspension of rear wheels, and valve springs. Railroads are large users of helical springs particularly for freight and passenger car suspensions. In the manufacture of electrical equipment, springs are used in tremendous quantities in switchgear and control equipment, circuit breaker mechanisms, etc. Innumerable other applications might also be mentioned. A typical application of a helical spring in a circuit breaker mechanism is shown in *Fig.* 21.

Because of the practical importance of this type of spring, a relatively large amount of space is devoted to it in this book. The present chapter discusses the theory for stress and deflection calculation in helical springs, the application of this theory in practical work being covered in subsequent chapters. The

theory as given in this chapter will be limited to springs where the deflections per coil are not too large (not more than half the coil radius). The effects of large pitch angles, however, are considered.[1] This includes most practical springs.

The general theory for calculating helical tension springs is essentially the same as that used for compression springs However, because of the effects of the end loops which are usually used in tension springs, additional concentrations of stress may be expected. For this reason a lower working stress is usually advisable unless a special type of end fastening is used. In the present chapter, effects due to end turns both in compression and tension springs are excluded from the theoretical discussion; these effects are considered later in Chapters VIII and XI.

ELEMENTARY THEORY--LARGE INDEX AND SMALL HELIX ANGLE

For calculating helical springs, the elementary theory as commonly given in textbooks on strength of materials or machine design is based on the assumption that the spring may be considered essentially as a straight bar under torsion. This assumption is approximately true where the *spring index* is large and where the helix angle is small. Since the elementary theory does not take into account the difference in fiber length between the inside and outside of the coil which arises because of the curvature of the spring bar or wire, considerable error will be involved if this theory is used for springs with small or moderate indexes.

Stress Calculations—Briefly the elementary theory is as follows: If a spring of large index under an axial load P as shown in *Fig.* 22 is compressed between two parallel plates as indicated in *Fig.* 23, the resultant load in general will be slightly eccentric to the axis as shown. This eccentricity is neglected, however, in the present discussion. Referring to *Fig.* 22, each individual element of the spring coil may be considered to be subject to a torque moment Pr where r = mean coil radius. In *Fig.* 24 one of these elements of length dx is cut from the

[1]Effects of large initial pitch angles combined with large deflections are considered in Chapter III.

coil by two planes perpendicular to the bar axis. Assuming that these planes do not warp or distort during deformation, it follows that the shearing deformations and hence the shearing stress will have a linear distribution along a radius as shown. This is identical with the stress distribution in a straight bar under torsion. Therefore at a distance ρ from the center O

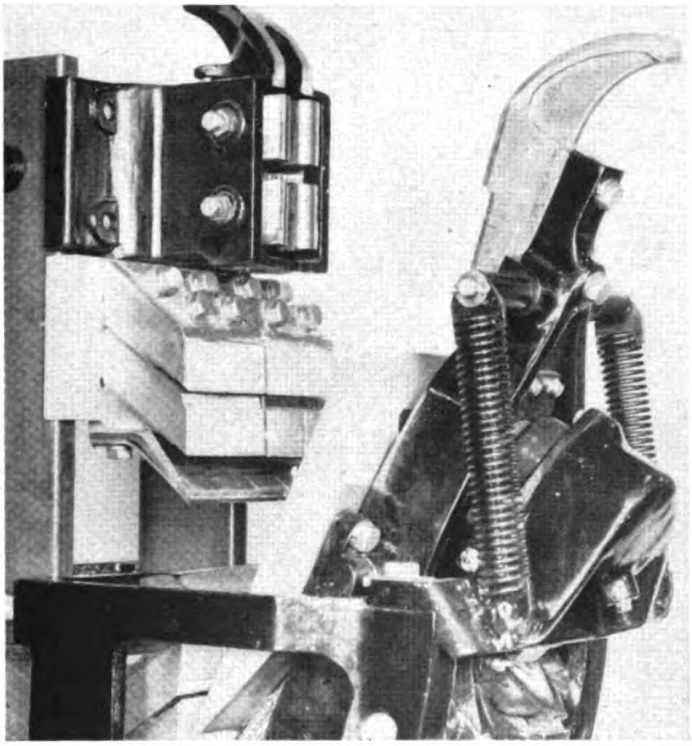

Fig. 21—Application of helical spring in a circuit breaker

the shearing stress will be $\tau = 2\rho\tau_m/d$ (from similar triangles) where τ_m = maximum shearing stress at the surface of the bar and d = bar diameter. The moment taken up by the shaded ring of width $d\rho$ at a radius ρ will be $dM = 2\pi\rho^2 d\rho(2\rho\tau_m/d)$ and the total torque moment Pr will be

$$Pr = \int_0^{d/2} dM = \int_0^{d/2} \frac{4\pi\tau_m\rho^3}{d} d\rho = \frac{\pi d^3\tau_m}{16} \quad \ldots\ldots\ldots\ldots\ldots\ldots\ldots\ldots (3)$$

or solving for the maximum stress τ_m

$$\tau_m = \frac{16Pr}{\pi d^3} \quad \ldots\ldots (4)$$

This is the ordinary formula for calculating stress in helical springs commonly given in textbooks or handbooks. As stated before, it will be in considerable error for springs with small indexes for two reasons: (1) The effect of direct shear stress due to the axial load P is neglected; and (2) The increase in stress due to the difference in fiber length between the inside

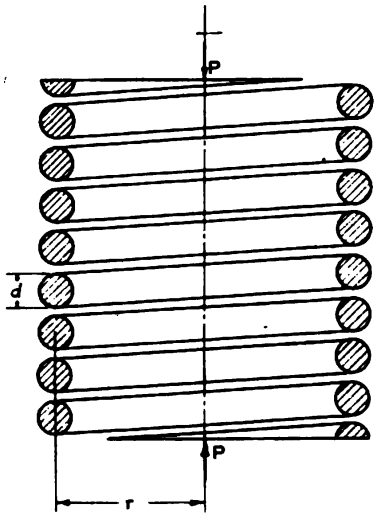

Fig. 22—Helical spring of large index, axially loaded

of the coil and the outside produced by wire curvature is not considered. These effects will be more fully discussed later.

Deflection Calculations — To calculate *deflection* of the spring, the following procedure may be employed. Considering an element *ab* on the surface of the bar and parallel to the axis (*Fig.* 24), this element, after deformation, will rotate through a small angle γ to the position *ac*. From elastic theory this angle γ will be equal to τ_m divided by the shearing modulus of elasticity G. Thus from Equation 4,

$$\gamma = \frac{\tau_m}{G} = \frac{16Pr}{\pi d^3 G} \quad \ldots\ldots (5)$$

Since the distance $bc = \gamma\, dx$, for small angles such as are being considered, the elementary angle $d\alpha$ through which one cross section rotates with respect to the other will be equal to

$2\gamma dx/d$. Again assuming that the spring may be considered as a straight bar of length $l=2\pi nr$ where $n=$number of *active* coils, the total angle β representing the angular deflection of one end of the bar with respect to the other will be, using Equation 5,

$$\beta=\int_0^{2\pi nr}\frac{2\gamma}{d}dx=\int_0^{2\pi nr}\frac{32Pr}{\pi d^4G}dx=\frac{64Pr^2n}{Gd^4} \quad \ldots\ldots\ldots\ldots\ldots\ldots (6)$$

Since the effective moment arm of the load P is equal to r, the deflection at the load will be

$$\delta=\beta r=\frac{64Pr^3n}{Gd^4} \quad \ldots\ldots\ldots\ldots\ldots\ldots\ldots\ldots\ldots\ldots\ldots\ldots\ldots\ldots\ldots\ldots (7)$$

This is the commonly used formula for spring deflections. In contrast with the ordinary *stress* formula, which may be in con-

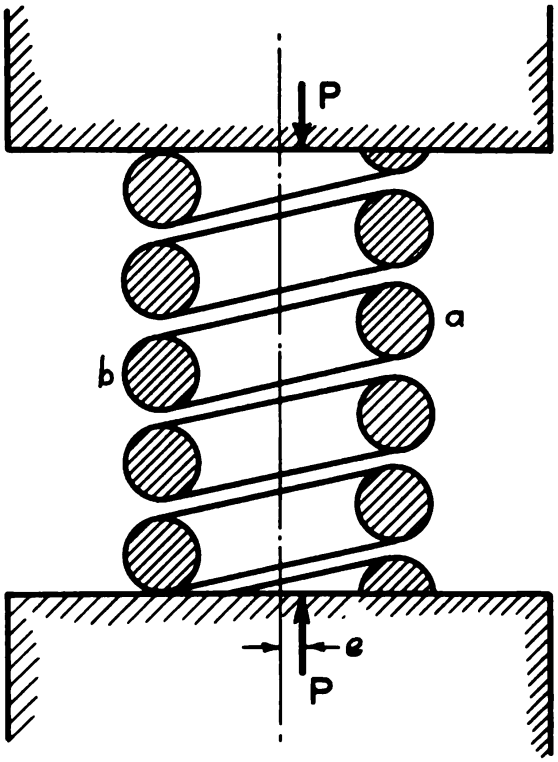

Fig. 23—Resultant eccentricity of loading between parallel plates. (Stress is greater at b than at a)

siderable error, this deflection formula is quite accurate even for fairly small spring indexes and for large helix angles. Tests

carried out to check the accuracy of this equation are discussed in Chapter IV.

APPROXIMATE THEORY—SMALL OR MODERATE INDEX CONSIDERING CURVATURE EFFECTS

A typical fatigue fracture of a heavy helical spring which failed under fatigue loading is shown in *Fig.* 25. It will be noted that the failure starts from a fatigue crack near the inside of the coil and progresses at an angle of about 45 degrees to the axis of the bar[2]. Since such failures are typical of heavy helical

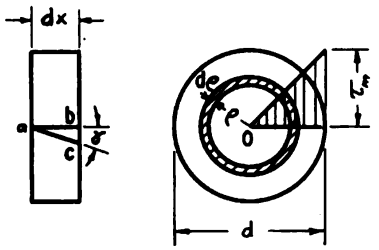

Fig. 24—Cross-sectional element of spring under torsion (elementary theory)

springs which usually have rather small indexes, it may be expected that the maximum stress occurs at the inside of the coil near point *a'*, *Fig.* 26*a*. The reasons for the existence of the maximum stress at this point are: First, the fiber length along the inside of the coil is much less which means that a higher shearing stress is present for a given angular rotation of adjacent cross sections. Thus in *Fig.* 26*b*, if the radial sections *bb'* and *aa'* rotate through a small angle with respect to each other and about the bar axis, the inside (and shorter) fiber *a'b'* will be subject to a much higher shearing stress because of its short length than the outside fiber *ab* which is longer. Second, the stress on the inside fiber *a'b'* is increased because the shear stress due to the direct axial load *P* is *added* to that due to the torque moment *Pr* at this point. In the outside fiber *ab* this stress is *subtracted* from that due to the torque moment. The result is that the stresses on the inside of the coil reach values around 2½ times those on the outside for springs of index 3, as may be shown both by test (Chapter IV) and theory; for larger indexes

[2]This type of fracture with the fractured surface making an angle of 45 degrees with the axis is typical of fatigue fracture of a straight cylindrical bar under alternating torsion.

this difference is, of course, not so pronounced.

Stress Calculation—The exact solution of the problem of determining stress in springs of small index is complicated (see Page 38), but an approximate solution which is sufficiently accurate for practical use (within about 2 per cent for practical springs) may be derived as follows[3]:

A small helix angle is assumed since this assumption is valid for nearly all practical springs. Considering an element of an axially-loaded spring with mean radius of curvature r cut by two neighboring radial cross sections aa' and bb' as shown in *Fig.*

Fig. 25—Typical fatigue failure

27*a*, the forces acting on this element are resolved into a twisting moment $M=Pr$ acting in a radial plane and a direct axial shearing force P. The stresses set up by this twisting moment are

[3]This method of derivation differs in several respects from an approximate solution given by A. Roever, "Beanspruchung Zylindrische Schraubenfedern mit Kreisquerschnitt." *V.D.I.* 1913. Page 1907, but the final numerical results are only slightly different. See also author's paper "Stresses in Heavy Closely Coiled Helical Springs", *Transactions* A.S.M.E., 1929 paper A.P.M., 51-17.

first considered and later are superimposed on the stresses due to the direct shear load P.

Under the action of the moment $M=Pr$ the two cross-sections aa' and bb' will rotate with respect to each other through a small angle $d\beta$. As mentioned before, this will result in much higher stresses on the inside fiber $a'b'$ particularly for springs of small index. The shear stress τ acting over the cross section *Fig.* 27*b* may be considered as divided into an axial component τ_a, parallel to the axis of the spring and a transverse component τ_t perpendicular to the spring axis.

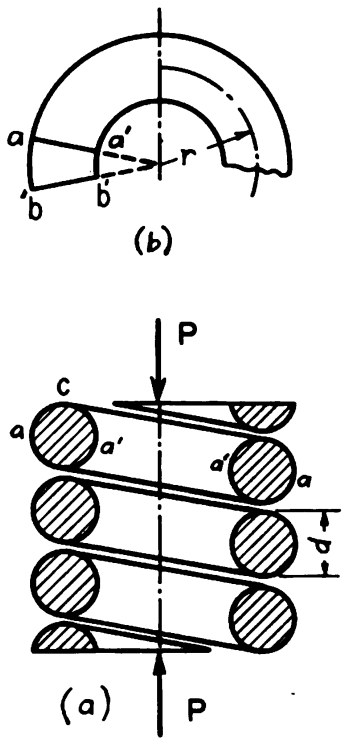

Fig. 26—Heavy helical spring axially loaded

If it is assumed that the two neighboring cross sections aa' and bb' rotate relative to each other and about an axis ee' perpendicular to their surfaces and passing through their centers O, the distribution of the axial components of the stress along a transverse diameter perpendicular to the spring axis will be somewhat as shown by the shaded area of *Fig.* 28. Such a distribution of stress due only to a moment would not be possible since the area to the right of the center O is greater than that to the left and hence an external force could be needed to secure equilibrium. If, however, rotation occurs about some point O', *Fig.* 29, which is displaced toward the axis of the spring, instead of about point O, a distribution of stress is obtained which is possible under the action of a pure moment M. From conditions of symmetry the transverse stress components τ_t will be in statical equilibrium when rotation occurs about any point on the axis aa' *Fig.* 27*b*. Point O' may be found as follows:

Under the assumption of rotation about O', the stress τ acting on any element dA with coordinates x and y may be found. When the sections aa' and bb' have rotated through a small angle

$d\beta$ with respect to each other, the relative movement of the ends of the filament dd' corresponding to dA will be $d\beta(x^2+y^2)^{\frac{1}{2}}$

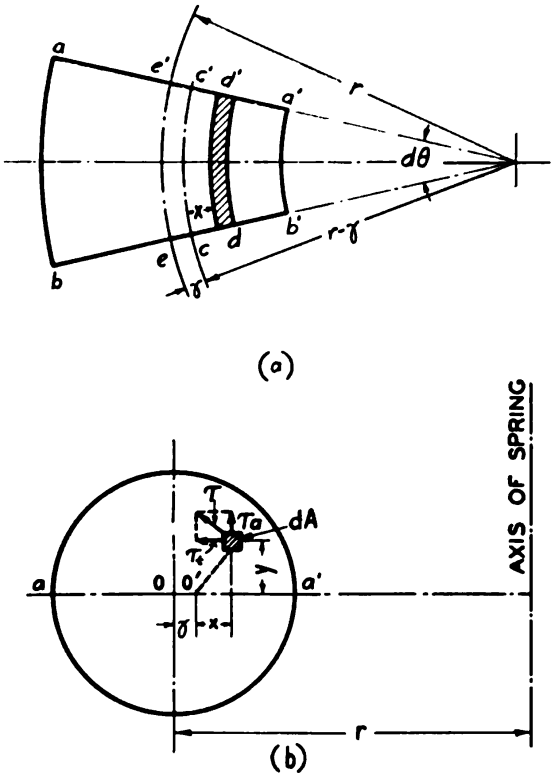

Fig. 27—Element of coil of helical spring

and, since the length of dd' is $(r-\gamma-x)d\theta$, the shearing stress τ acting on this element will be

$$\tau=\frac{Gd\beta\sqrt{x^2+y^2}}{(r-\gamma-x)d\theta} \qquad (8)$$

The axial component τ_a of this stress will be, *Fig.* 27,

$$\tau_a=\frac{\tau x}{\sqrt{x^2+y^2}}=\frac{xGd\beta}{(r-\gamma-x)d\theta} \qquad (9)$$

Under the assumptions made, this distribution of stress is identical with that in a curved bar[4] and the distribution of the

[4]For example, Timoshenko, *Strength of Materials*, Van Nostrand, Part 2, Second Edition, Page 65, gives a discussion of curved bar theory.

stresses τ_a is hyperbolic in form, *Fig.* 29. This distance γ is determined from the condition that the integral of $\tau_a dA$ (where dA is the element of area) must be zero when taken over the cross-section. From curved bar theory the distance γ may be expressed approximately as[5]:

$$\gamma = \frac{d^2}{16r}\left(\frac{1}{1+\frac{d^2}{16r^2}}\right) \approx \frac{d^2}{16r} \qquad (10)$$

The term $d^2/16r^2$ is neglected in the denominator since in practical springs $d/2r$ seldom greater than 1/3 and hence $d^2/16r^2$ is small compared to unity. Putting Equation 10 in 9,

$$\tau_a = \frac{xGd\beta}{\left(r - \frac{d^2}{16r} - x\right)d\theta} \qquad (11)$$

Further, it is assumed that the ordinary formula for angle of twist of circular bars (Equation 6) will apply with sufficient

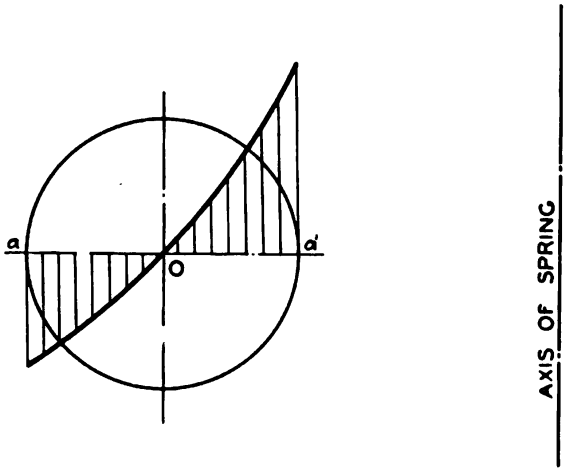

Fig. 28—Shearing stress distribution along a transverse diameter, rotation about the center

accuracy for the calculation of $d\beta/d\theta$ (borne out by actual tests, as discussed in Chapter IV). Thus

$$\frac{d\beta}{d\theta} = \frac{32Mr}{\pi d^4 G} \qquad (12)$$

where $M = Pr$. Putting this in Equation 11,

[5]Timoshenko, loc. cit., Page 74.

$$\tau_a = \frac{32xMr}{\pi d^4\left(r - \frac{d^2}{16r} - x\right)} \quad \ldots\ldots (13)$$

From this equation it is clear that the maximum value of τ_a will occur when $x = d/2 - d^2/16r$, i.e., at point a' in *Fig.* 27*b*.

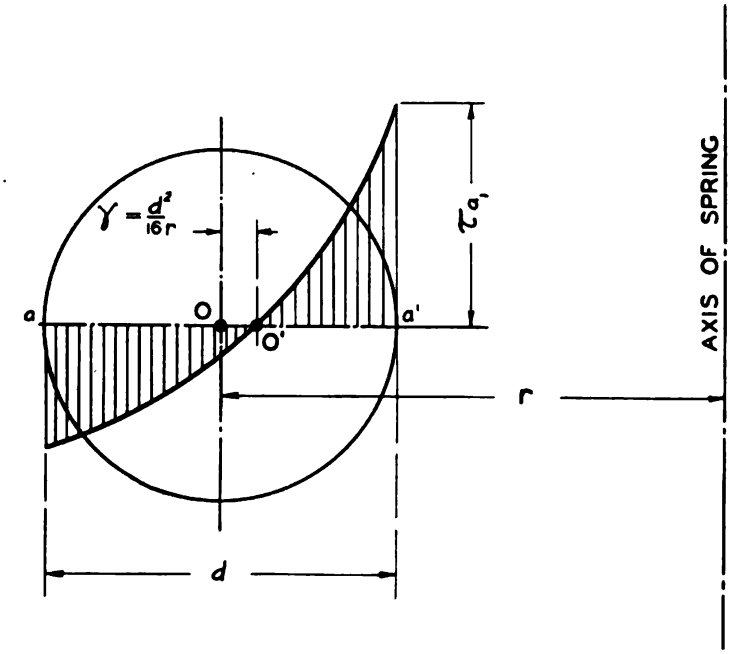

Fig. 29—Stress distribution along a transverse diameter, assuming rotation about the point O'

Putting this value in Equation 13 and also putting the spring index $c = 2r/d$, the stress at a' in *Fig.* 29 becomes

$$\tau_{a1} = \frac{16M}{\pi d^3}\left(\frac{4c-1}{4c-4}\right) \quad \ldots\ldots (14)$$

Likewise, the stress at point a (*Fig.* 29) on the outside of the coil, putting $x = -d/2 - d^2/16r$ in Equation 13 and dropping the negative sign, will be

$$\tau_{a2} = \frac{16M}{\pi d^3}\left(\frac{4c+1}{4c+4}\right) \quad \ldots\ldots (15)$$

In an actual spring where a load P acts along the axis, as

mentioned previously, the external forces acting over the cross section may be resolved into a twisting moment $M=Pr$ and a direct axial shear force P, assuming that the pitch angle is small. Stresses due to the twisting moment may be found by substituting Pr for M in Equations 14 and 15. On these stresses the shearing stress at a and a' (*Fig. 27b*) due to the direct axial load P must be superimposed. It appears reasonable to take for this stress that given by the theory of elasticity at the outer edges of the neutral surface of a cantilever of circular cross section loaded by a force P. This theory[6] gives a value of stress equal to $4.92P/\pi d^2$. Adding this stress to that due to the moment Pr from Equation 14 the maximum stress τ_{max} at a' may be expressed

$$\tau_{max}=\frac{16Pr}{\pi d^3}\left(\frac{4c-1}{4c-4}+\frac{.615}{c}\right) \quad \ldots\ldots (16)$$

This is an approximate expression for the maximum stress in a helical round-wire spring, axially loaded. Comparing the results obtained by using this formula with those of a more elaborate investigation by Goehner (see Page 42), it may be shown that for practical springs where the index c is equal to 3 or more, this formula is within 2 per cent of the more exact formula. Such differences are negligible from a practical standpoint. This equation also agrees well with experimental results including strain measurements on actual springs (Chapter IV).

The stress at the outside of the coil at a, (*Fig. 28b*), may be found by using Equation 15 and *subtracting* the stress due to direct shear because it acts in the opposite direction, giving

$$\tau_{min}=\frac{16Pr}{\pi d^3}\left(\frac{4c+1}{4c+4}-\frac{.615}{c}\right) \quad \ldots\ldots (17)$$

Comparison with experimental results indicates that this equation is also approximately correct.

From Equation 16, the maximum shearing stress in a helical spring may be written

$$\tau_{max}=\frac{16Pr}{\pi d^3}K \quad \ldots\ldots (18)$$

[6] Timoshenko—*Theory of Elasticity*, McGraw-Hill, Page 290.

where the stress correction factor K is

$$K = \frac{4c-1}{4c-4} + \frac{.615}{c} \qquad (19)$$

It is thus seen that the maximum stress is simply the stress given by the ordinary formula of Equation 4 multiplied by a factor K which is greater than unity and which depends on the spring index c. For convenience in calculation values of K are plotted as functions of the spring index c in *Fig.* 30. It is seen that for a spring of index 3 the factor $K = 1.58$, which means that

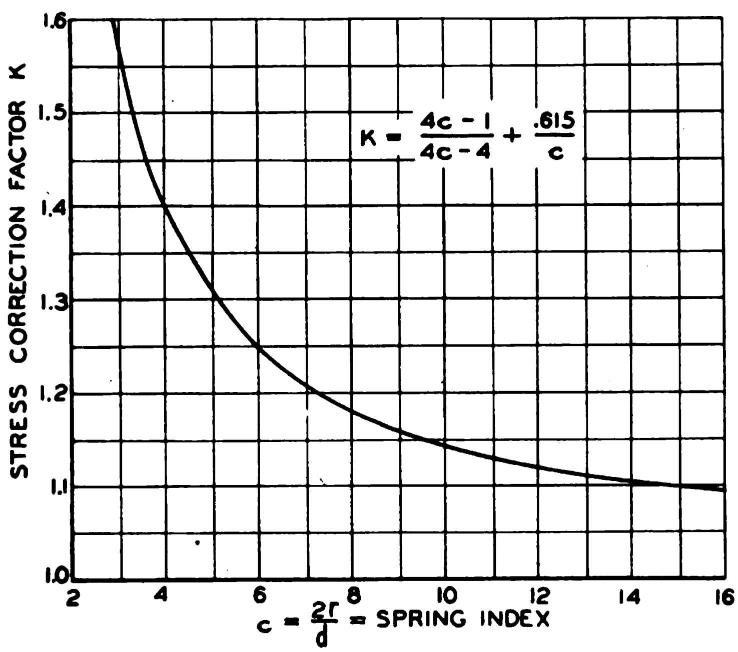

Fig. 30—Stress correction factor for helical round wire compression or tension springs

the stress given by the ordinary formula must be multiplied by this amount for the maximum stress.

It should be mentioned here that the stresses derived hold only as long as elastic conditions prevail, i.e., as long as the yield point or elastic limit of the material is not exceeded. If this is not the case, the maximum stress may be less than that calculated. However, even for such cases where yielding occurs, the formula

will still give the range in stress which is of most importance from a fatigue standpoint. Further discussion of the use of Equation 18 for fatigue loading is given in Chapter VI.

EXACT THEORY

The approximate theory developed in the preceding section for calculating stress in helical springs of small or moderate index is, as mentioned previously, sufficiently accurate for most practical purposes (results being accurate to within 2 per cent for spring indexes greater than three). Where greater accuracy is desired, the exact method of calculation developed by Goehner[7] may be used. This method will be briefly outlined[8].

Stress Calculation—Referring to *Fig.* 31, if $\tau_{\theta z}$ and $\tau_{r\theta}$ are the components of shearing stress acting on the element *A* of a radial cross section of the spring as shown, the coordinates of *A* being ρ and z and if the pitch angle is small so that the elements of the springs may be considered under pure torsion, all shear stress components except $\tau_{\theta z}$ and $\tau_{r\theta}$ may be assumed zero. With this assumption from the theory of elasticity, the conditions of equilibrium in cylindrical coordinates give the following partial differential equation

$$\frac{\partial \tau_{r\theta}}{\partial \rho} + \frac{\partial \tau_{\theta z}}{\partial z} + \frac{2\tau_{r\theta}}{\rho} = 0 \qquad (20)$$

The theory of elasticity also requires that the following equations (derived from what are known as the "compatibility equations") must be satisfied:

$$\frac{\partial^2 \tau_{\theta z}}{\partial \rho^2} + \frac{1}{\rho}\frac{\partial \tau_{\theta z}}{\partial \rho} + \frac{\partial^2 \tau_{\theta z}}{\partial z^2} - \frac{\tau_{\theta z}}{\rho^2} = 0 \qquad (21)$$

$$\frac{\partial^2 \tau_{r\theta}}{\partial \rho^2} + \frac{1}{\rho}\frac{\partial \tau_{r\theta}}{\partial \rho} + \frac{\partial^2 \tau_{r\theta}}{\partial z^2} - \frac{4\tau_{r\theta}}{\rho^2} = 0 \qquad (22)$$

---

[7] O. Goehner, "Schubspannungsverteilung im Querschnitt einer Schraubenfeder", *Ing.-Arch.* Vol. 1, 1930, Page 619; "Schubspannungsverteilung im Querschnitt eines gedrillten Ringstabs mit Anwendung auf Schraubenfedern", *Ing.-Arch.* Vol. 2, 1931, Page 1; "Spannungsverteilung in einem an den Endquerschnitten belasteten Ringstabsektor", *Ing.-Arch.* Vol. 2, 1931, Page 381; and "Die Berechnung Zylindrische Schraubenfedern," *V.D.I.*, March 12, 1932, Page 269.

[8] *Theory of Elasticity*—S. Timoshenko, McGraw-Hill, Page 355, gives a more complete discussion of the method.

To solve Equations 20, 21 and 22 a stress function ϕ is introduced. Taking

$$\tau_{r\theta} = \frac{Gr^2}{\rho^2}\left(\frac{\partial\phi}{\partial z}\right) ; \tau_{\theta z} = -\frac{Gr^2}{\rho^2}\left(\frac{\partial\phi}{\partial\rho}\right) \quad \ldots\ldots\ldots\ldots\ldots\ldots (23)$$

Equation 20 is satisfied. By substitution of Equation 23 in 21 and 22, the following equations are obtained

$$\frac{\partial}{\partial\rho}\left(\frac{\partial^2\phi}{\partial\rho^2} + \frac{\partial^2\phi}{\partial z^2} - \frac{3}{\rho}\frac{\partial\phi}{\partial\rho}\right) = 0 \quad \ldots\ldots\ldots\ldots\ldots\ldots\ldots (24)$$

$$\frac{\partial}{\partial z}\left(\frac{\partial^2\phi}{\partial\rho^2} + \frac{\partial^2\phi}{\partial z^2} - \frac{3}{\rho}\frac{\partial\phi}{\partial\rho}\right) = 0 \quad \ldots\ldots\ldots\ldots\ldots\ldots\ldots (25)$$

This means that the expression in parenthesis must be a constant which may be denoted by $-2c'$. Thus,

$$\frac{\partial^2\phi}{\partial\rho^2} + \frac{\partial^2\phi}{\partial z^2} - \frac{3}{\rho}\frac{\partial\phi}{\partial\rho} + 2c' = 0 \quad \ldots\ldots\ldots\ldots\ldots\ldots\ldots (26)$$

It will be found advantageous to introduce new coordinates as follows:

$$\xi = r - \rho \; ; \; \zeta = z$$

Then Equation 26 becomes

$$\frac{\partial^2\phi}{\partial\xi^2} + \frac{\partial^2\phi}{\partial\zeta^2} + \frac{3}{r\left(1 - \frac{\xi}{r}\right)}\frac{\partial\phi}{\partial\xi} + 2c' = 0 \quad \ldots\ldots\ldots\ldots\ldots\ldots (27)$$

Since in general ξ/r may be considered small,

$$\frac{1}{1 - \frac{\xi}{r}} = 1 + \frac{\xi}{r} + \frac{\xi^2}{r^2} + \text{---} \quad \ldots\ldots\ldots\ldots\ldots\ldots\ldots\ldots (28)$$

This makes it possible to solve Equation 27 by means of a series of successive approximations. From the condition that the resultant shearing stress at the boundary of the cross section

must be tangent to the boundary, the function ϕ may be shown to be constant along the boundary. With this condition the expression for ϕ becomes:

$$\phi=\phi_0+\phi_1+\phi_2+ --- \qquad (29)$$

where

ϕ_0 satisfies $$\frac{\partial^2\phi_0}{\partial\xi^2}+\frac{\partial^2\phi_0}{\partial\zeta^2}+2c'=0$$

ϕ_1 satisfies $$\frac{\partial^2\phi_1}{\partial\xi^2}+\frac{\partial^2\phi_1}{\partial\zeta^2}+\frac{3}{r}\frac{\partial\phi_0}{\partial\xi}=0$$

ϕ_2 satisfies $$\frac{\partial^2\phi_2}{\partial\xi^2}+\frac{\partial^2\phi_2}{\partial\zeta^2}+\frac{3}{r}\frac{\partial\phi_1}{\partial\xi}+\frac{3\xi}{r^2}\frac{\partial\phi_0}{\partial\xi}=0;\ etc.$$

From Equations 23, using $\rho=r+\xi$,

$$\tau_{r\theta}=\frac{G}{\left(1-\frac{\xi}{r}\right)^2}\frac{\partial\phi}{\partial\zeta}\ ;\qquad \tau_{\theta z}=\frac{G}{\left(1-\frac{\xi}{r}\right)^2}\frac{\partial\phi}{\partial\xi} \qquad (30)$$

The total twisting moment acting over the spring cross section will be

$$M_t=-\int\int(\tau_{r\theta}\zeta+\tau_{\theta z}\xi)d\xi d\zeta \qquad (31)$$

Again the function $1/(1-\xi/r)^2$ in Equations 30 may be expanded in series form as follows:

$$\frac{1}{\left(1-\frac{\xi}{r}\right)^2}=1+\frac{2\xi}{r}+\frac{3\xi^2}{r^2}+ --- \qquad (32)$$

The determination of $\tau_{r\theta}$ and $\tau_{\theta z}$ by means of successive approximations has been carried out in this general manner by Goehner[7] with the following results for round-wire, helical springs.

Maximum shearing stress for a circular ring sector with zero pitch angle is

$$\tau_{max}=\frac{16Pr}{\pi d^3}\,\frac{\left(\frac{c}{c-1}+\frac{1}{4c}+\frac{1}{16c^2}\right)}{\left(1+\frac{3}{16}\,\frac{1}{c^2-1}\right)} \qquad (33)$$

where $c=2r/d$.

This formula is accurate to within one per cent even for

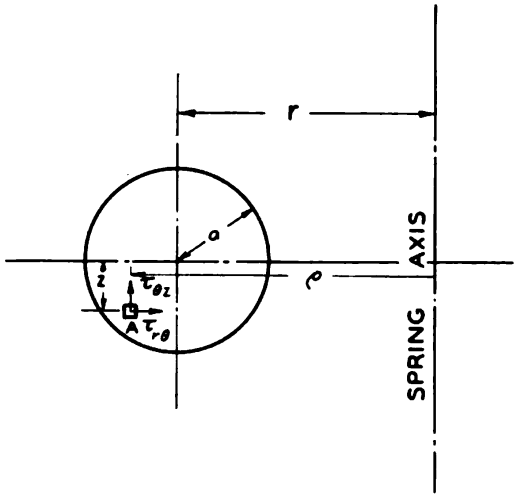

Fig. 31—Torsion stress components in cross-section of helical spring (exact theory)

indexes c as low as 2½. It does not apply accurately, however, where the pitch angle is appreciable.

For practical springs where the pitch angle α is not zero, the more exact formula for maximum shear stress becomes

$$\tau_{max}=\frac{16Pr\cos\alpha}{\pi d^3}\times \left\{\frac{\frac{1}{1-\frac{d}{2\rho'}}+\frac{1}{4}\left(\frac{d}{2\rho'}\right)+\frac{1}{16}\left(\frac{d}{2\rho'}\right)^2}{1+\frac{\frac{3}{16}\left(\frac{d}{2\rho'}\right)^2}{1-\left(\frac{d}{2\rho'}\right)^2}}+\left[.62\left(\frac{d}{2\rho'}\right)+\frac{.53\left(\frac{d}{2\rho'}\right)^2}{1-\frac{d}{2\rho'}}\right]\tan^2\alpha\right\} \qquad (34)$$

where $\rho'=r/\cos^2\alpha=$ actual radius of curvature of the helix taking the pitch angle into account. The first term of this equation

corresponds to Equation 33 where the actual radius of curvature is used instead of r. The second term of this equation arises because of the angularity of the shear load $P \cos \alpha$. The term in the denominator of the second part of the right side of Equation 34 is used to replace the series which arises in the calculation. Although Equation 34 is considered very accurate, it is cumbersome for practical calculations; for such cases the following formulas may be used with an accuracy within one per cent:

1. For indexes $2r/d$ greater than 3 and for pitch angles α less than 16 degrees, the maximum shearing stress is

$$\tau_{max} = \frac{16Pr \cos \alpha}{\pi d^3}\left(\frac{1}{1 - \frac{d}{2\rho'}} + \frac{1}{4}\left(\frac{d}{2\rho'}\right) - \frac{1}{8}\left(\frac{d}{2\rho'}\right)^2\right) \quad (35)$$

where $\rho' = r/\cos^2\alpha$

2. For indexes greater than 4 and $\alpha < 20$ degrees.

$$\tau_{max} = \frac{16Pr \cos \alpha}{\pi d^3}\left[\frac{1}{1 - \frac{d}{2\rho'}} + \frac{1}{4}\left(\frac{d}{2\rho'}\right)\right] \quad (36)$$

3. Where $\alpha < 12$ degrees (which includes most practical cases) the following formula for τ_{max} expressed in terms of spring index is most convenient and is to be preferred:

$$\tau_{max} = \frac{16Pr \cos \alpha}{\pi d^3}\left(1 + \frac{5}{4c} + \frac{7}{8c^2} + \frac{1}{c^3}\right) \quad (37)$$

It should be noted that if $\cos \alpha = 1$, Equation 37 differs by less than 2 per cent from Equation 16 derived by approximate methods, for spring indexes of three or more.

Equations 33 to 37 give the shearing stress due to the twisting moment $Pr \cos \alpha$ and the direct shear $P \cos \alpha$. However, there is also a bending stress σ_{max} present due to the bending moment $Pr \sin \alpha$ and a direct tension or compression stress due to the direct load $P \sin \alpha$. To get the maximum equivalent stress in the spring this bending stress σ_{max} must be combined with the torsion stress τ_{max} on the basis of a *strength theory* (Page 44).

To calculate this maximum bending stress σ_{max} the results

of curved-bar theory[4] may be used. A somewhat more accurate method is to apply the general equations of the theory of elasticity as was done by Goehner[5]. This involves essentially the setting up of the equilibrium equations and the compatibility

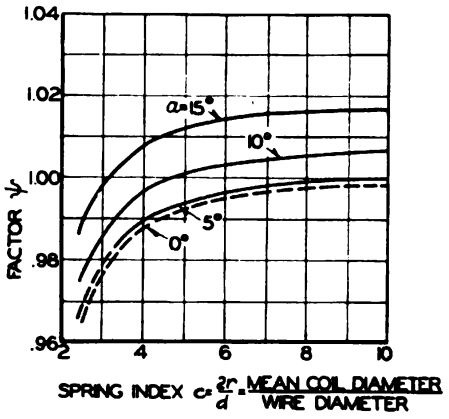

Fig. 32—Curves for finding ψ in the spring deflection formula for various spring indexes c and pitch angles α

equations in cylindrical coordinates and their solution by a method of successive approximations, similar to that previously used for the calculation of torsion stress τ_{max}. Final results are:

The maximum bending stress:

$$\sigma_{max}=\frac{32Pr\sin\alpha}{\pi d^3}\left\{1+\frac{6m^2+9m+4}{8m(m+1)}\left(\frac{d}{2\rho'}\right)+\left(\frac{25m^3+41m^2+28m+8}{48m^2(m+1)}\right)\frac{\left(\frac{d}{2\rho'}\right)^2}{\left(1-\frac{d}{2\rho'}\right)}+\frac{1}{8}\frac{d}{r}\right\}\quad\ldots\ldots(38)$$

where m=Poisson's constant=reciprocal of Poisson's ratio.

For Poisson's ratio=.3 this formula simplifies to

$$\sigma_{max}=\frac{32Pr\sin\alpha}{\pi d^3}\left\{1+.87\frac{d}{2\rho'}+\frac{.64\left(\frac{d}{2\rho'}\right)^2}{\left(1-\frac{d}{2\rho'}\right)}+\frac{1}{8}\frac{d}{r}\right\}\quad\ldots\ldots(39)$$

where $\rho'=r/\cos^2\alpha$. The last term in the brackets $d/8r$ yields the

[5] *Ing. Archiv.*, 1931, Page 381. Also *Theory of Elasticity*—Timoshenko, Page 361.

stress due to the direct tension or compression which is $4\,P \sin \alpha/\pi d^2$; the remainder yields the stress due to the bending moment $Pr \sin \alpha$. Again the denominator $1—d/2\rho'$ represents approximately the series which arises from the method of successive approximations.

Equations 38 and 39 need only be used for relatively large pitch angles and small indexes. For the usual case the following formulas may be used with sufficient accuracy:

$$\sigma_{max}=\frac{32Pr \sin \alpha}{\pi d^3}\left[1+\frac{8m^2+11m+4}{8m(m+1)c}+\frac{25m^3+41m^2+28m+8}{48m^2(m+1)c^2}\right] \quad \ldots\ldots\ldots\ldots\ldots\ldots (40)$$

or taking $m=10/3$ corresponding to Poisson's ratio $=.3$

$$\sigma_{max}=\frac{32Pr \sin \alpha}{\pi d^3}\left(1+\frac{1.12}{c}+\frac{.64}{c^2}\right) \quad \ldots\ldots\ldots\ldots\ldots\ldots\ldots\ldots (41)$$

To find the equivalent stress in the spring, the shearing stress τ_{max} and the bending stress σ_{max} which act at a given point should, as mentioned before, be combined according to a *theory of strength*. One strength theory which is widely used at present is the *maximum-shear theory*, which states that failure is determined by the maximum shearing stress at any point in a stressed body[10]. It may be shown from elastic theory that if a bending stress σ_{max} and a shearing stress τ_{max} act at a given point, the equivalent shear stress τ_e based on the maximum shear theory is[11]

$$\tau_e=\sqrt{(\tau_{max})^2+\frac{(\sigma_{max})^2}{4}}=\tau_{max}\sqrt{1+\frac{(\sigma_{max})^2}{4(\tau_{max})^2}} \quad \ldots\ldots\ldots\ldots\ldots\ldots (42)$$

Another strength theory which is coming more and more into favor is the *shear-energy theory*[12] (also known as the *von Mises-Hencky* theory). This theory states that failure will occur when the shear energy (or energy of distortion) of the highest stressed

[10]For example Timoshenko—*Strength of Materials*, Part 2, Second Edition, Page 473 gives a further discussion of strength theories.

[11]Timoshenko, loc. cit., Part 1, Page 122.

[12]Timoshenko, loc. cit. Part 2, Page 479 gives a further discussion of this theory. Also "Plasticity"—A. Nadai, *Eng. Soc. Monographs*, McGraw-Hill, 1931.

element is equal to the shear energy of an element in an axially stressed specimen at the yield point (or at the endurance limit if the theory is applied to fatigue failure). If σ_1, σ_2, and σ_3 are the principal stresses at failure, a mathematical statement of the foregoing is:

$$(\sigma_1-\sigma_2)^2+(\sigma_2-\sigma_3)^2+(\sigma_1-\sigma_3)^2=2\sigma_c^2=\text{Constant} \quad \ldots\ldots\ldots\ldots\ldots\ldots (43)$$

In this case σ_c may refer either to the yield point or the endurance limit.

The expression on the left side of this equation can be shown to be proportional to the shear-energy or energy of distortion stored in the material. This energy is equal to the total energy stored minus the energy of three-dimensional tension or compression.

It may be shown that when a bending stress σ_{max} and a torsion stress τ_{max} act simultaneously as in this case, the equivalent torsion stress according to the *shear-energy theory* is

$$\tau_e=\tau_{max}\sqrt{1+\frac{(\sigma_{max})^2}{3(\tau_{max})^2}} \quad \ldots\ldots\ldots\ldots\ldots\ldots\ldots\ldots\ldots\ldots\ldots\ldots\ldots\ldots\ldots\ldots (44)$$

This equation is derived by determining the principal stresses from Mohr's circle for a case of combined tension and shear[13]. In this case these principal stresses are

$$\sigma_1=\frac{\sigma_{max}}{2}+\sqrt{\frac{(\sigma_{max})^2}{4}+(\tau_{max})^2} \quad \ldots\ldots\ldots\ldots\ldots\ldots\ldots\ldots\ldots\ldots\ldots\ldots\ldots\ldots\ldots\ldots (45)$$

$$\sigma_2=\frac{\sigma_{max}}{2}-\sqrt{\frac{(\sigma_{max})^2}{4}+(\tau_{max})^2} \quad \ldots\ldots\ldots\ldots\ldots\ldots\ldots\ldots\ldots\ldots\ldots\ldots\ldots\ldots\ldots\ldots (46)$$

$$\sigma_3=0 \quad \ldots\ldots\ldots\ldots\ldots\ldots\ldots\ldots\ldots\ldots\ldots\ldots\ldots\ldots\ldots\ldots\ldots\ldots\ldots\ldots\ldots\ldots\ldots\ldots (47)$$

Equation 47 follows since no normal stress acts on the surface of the spring. Substituting Equations 45 and 46 in Equation 42 and taking the equivalent shear stress $\tau_e=\sigma_c/1.73$ (which is the shear stress equivalent to a simple tension stress σ_c), Equation 44 is obtained.

Unless the pitch angle is unusually large σ_{max} will be small

[13]The derivation of these formulas for principal stress for combined tension and shear is given in *Strength of Materials*, loc. cit., Part 1, Page 48.

compared to τ_{max} so that in general for most practical springs τ_c will differ but slightly from τ_{max}.

It should be noted that the formulas given in this chapter apply rigidly only as long as the deflections per turn are small (relative to the coil diameter) so that the coil radius and pitch angle may be considered constant. These conditions usually apply with sufficient accuracy in practical springs where the index is not large, since for small or moderate indexes excessive stresses are set up when the deflections per turn approach the mean coil radius.

EXAMPLE: As an example of the application of the more exact formulas given in this chapter, assuming a spring with an index of 3 and a pitch angle $\alpha = 12$ degrees, so that Equation 37 may be used. Then $\cos \alpha = .978$ and $\tan \alpha = .2126$. Using Equation 37

$$\tau_{max} = \frac{16Pr}{\pi d^3} 1.551 \cos \alpha$$

Similarly from Equation 41

$$\sigma_{max} = \frac{32Pr}{\pi d^3} 1.444 \sin \alpha$$

Hence

$$\frac{\sigma_{max}}{\tau_{max}} = 2 \tan \alpha \frac{1.444}{1.551}$$

Assuming that the *maximum-shear theory* applies, by substitution in Equation 42,

$$\tau_c = \frac{16Pr}{\pi d^3} 1.547$$

If the *shear-energy theory* be taken as a basis, by substitution in Equation 44,

$$\tau_c = \frac{16Pr}{\pi d^3} 1.557$$

This differs but slightly from the value obtained by using the

maximum-shear theory. It also differs by only about 1½ per cent from the value derived previously by approximate methods and neglecting the pitch angle (Equation 16). This indicates that the approximate method is accurate enough for most purposes.

Deflection Calculation—Assuming that the spring deflection per turn is not large[14] relative to the coil radius and that the pitch angle may be considered very small, the spring deflection is[15]

$$\delta = \frac{64Pr^3n}{Gd^4}\left(\frac{1}{1+\frac{3}{16}\left(\frac{1}{c^2-1}\right)}\right) \qquad (48)$$

where c is the spring index. It is seen that this is simply the ordinary deflection formula, Equation 7 multiplied by a term in brackets which depends on the spring index. The larger the spring index, the nearer will this term approach unity. However, even for the exceptionally small index of 3, the term in the brackets of Equation 48 is equal to .977 which indicates that the deflection will be about 2.3 per cent smaller than that calculated from the usual formula. However, for best accuracy the pitch angle should be considered.

If the pitch angle of the spring is considered, the procedure is as follows: From elastic theory[16] it may be shown that the twist per unit length of a helical spring is

$$\theta = \frac{\sin\alpha\cos\alpha}{r} - \frac{\sin\alpha_o\cos\alpha_o}{r}$$

where α and α_o are the final and initial pitch angles, respectively. This assumes that the deflection is small so that the coil radius r may be considered constant. Multiplying this by the torsional rigidity C yields the twisting moment $M_t = Pr\cos\alpha$. Likewise the bending moment $Pr\sin\alpha$ will be equal to the flexural rigidity EI multiplied by the exact expression for the change in curvature, which is

$$\Delta\kappa = \frac{\cos^2\alpha}{r} - \frac{\cos^2\alpha_o}{r} \qquad (49)$$

[14]The case of large deflections (which may occur without excessive stress only for large indexes) is treated in Chapter III.

[15]Goehner, *V.D.I.* 1932, Page 272.

[16]For example Love—*Theory of Elasticity*, third edition, Cambridge Univ. Press, Page 421.

The total length of the spring wire or bar will be

$$l=\frac{2\pi nr}{\cos\alpha} \quad \ldots\ldots (50)$$

Using these expressions and the results of elastic theory, a more exact expression for the deflection of helical springs has been derived[17]. This more accurate formula, which assumes small deflections, may be written

$$\delta=\frac{64Pr^3n}{Gd^4}\psi=\delta_o\psi \quad \ldots\ldots (51)$$

where

$$\psi=\frac{\cos\alpha}{1+\frac{3}{16}\frac{\cos^4\alpha}{c^2-1}}+\frac{2G}{E}\sin\alpha\tan\alpha \quad \ldots\ldots (52)$$

δ_o = nominal deflection figured by usual formula, Equation 7, ψ = a constant depending on the spring index $c=2r/d$ and on the pitch angle α. In *Fig.* 32 values of the constant ψ have been plotted as functions of the spring index c for various pitch angles α. In making the calculations, a ratio $G/E=.38$ was taken (corresponding approximately to Poisson's ratio=.3), which holds with sufficient accuracy for most spring materials. However, a relatively large change in this ratio G/E will have but a negligible effect on the value of ψ. The dashed curve for zero pitch angle cannot be realized in practical springs because of interference between the coils; also a part of the curve for 5 degrees pitch angle is shown dashed since it cannot be realized. It may be seen that for practical springs where the pitch angle is usually less than 10 degrees and for the smaller indexes the value of ψ is less than unity, which means that the actual deflection is slightly *smaller* than the nominal deflection, Equation 7. This seems surprising at first since one would expect that the direct shear would act to increase the deflection over that given by Equation 7. Tests to be described later (Chapter IV), however, tend to bear out this conclusion. It should be noted that in actual springs the effect is usually very small; thus for indexes $c>2.5$ and pitch angles $\alpha<15$ degrees, the deviations between

[17]Goehner, loc. cit.

the more exact formula and the ordinary formula Equation 7 will be under 2½ per cent. For most springs where $\alpha < 10$ degrees and $c > 4$ the difference is under one per cent, a figure which is usually negligible in practice since other factors such as the effects of variations in coil and wire size, shape of end turns, and modulus of rigidity will ordinarily be greater than this. In certain cases, however, as for example in certain instrument springs, to obtain maximum accuracy, it may be desirable to use the factor ψ of Equation 52 in making deflection calculations.

EXAMPLE: Assuming a steel spring of the following dimensions: Outside diameter ¾ in., mean coil radius $r = .286$ in., wire diameter $d = .177$ in., 4 active turns, spring index $(2r/d) = 3.28$, initial pitch angle 7½ degrees, working load 140 lb, the deflection figured from the nominal formula for these dimensions is $\delta_n = .0745$. For a pitch angle of 7½ degrees and index $c = 3.2$ from *Fig.* 32 $\psi = .985$. The deflection calculated by the more accurate formula is then $\delta = \psi\delta_n = .985(.0745) = .0733$ in.

CHAPTER III

OPEN-COILED HELICAL SPRINGS AND SPRINGS WITH LARGE DEFLECTIONS—THEORY

Unless extreme accuracy is required the theory developed in Chapter II for close-coiled helical springs is satisfactory for the practical calculation of spring deflections and stresses where the initial pitch angle is under 10 degrees and the deflection per turn less than, say, half the coil radius. However, for cases where the initial pitch angle is large or where the deflection per turn is large, some error in the use of the usual formula, Equation 7, for calculating spring deflections will result. This error approaches 15 per cent for initial pitch angles around 20 degrees and deflections per turn equal to the initial coil radius. The reason for this error in the usual formula is partly that the pitch angle was assumed zero in the previous derivation and partly because the coil radius changes with deflection. Thus when a compression spring is compressed from the initial position shown in *Fig.* 33*a* to that shown in *Fig.* 33*b*, the mean coil radius increases from r_o to r. Since the spring deflection, other things being equal, is proportional to the cube of the coil radius, it follows that the spring becomes more flexible as it is compressed. The opposite effect, of course, occurs in tension springs.

Errors due to neglecting the effect of pitch angle may be eliminated by using the more accurate formula, Equation 51, which takes the pitch angle into account. If the spring deflections per turn are large, however, this formula will also be somewhat in error at the larger deflections since the change in coil radius with deflection was neglected in the derivation.

The discussion in this chapter will be limited to springs of large index since the effects due to changes in the pitch angle and coil radius are most pronounced in such springs. For springs of small or moderate index high stresses are set up before the deflection becomes large enough so that changes in pitch angle or coil radius are of importance. Hence Equation 51 may be used in such cases.

When an open-coiled helical spring is subject to an axial tension giving a large deflection, there is a tendency for the coils to unwind; in other words, one end of the spring tends to rotate with respect to the other about the spring axis. If this rotation can take place freely and without restraint, we have the condition of an axially-loaded spring as indicated in *Fig.* 34. This is approximately the condition in tension springs with hooked ends where the hooks are not rigidly held but have some freedom to rotate about the spring axis. If, however, the ends are prevented from rotation by friction (as is usually the case in compression springs) or by clamping, end moments acting about the axis of the coil are set up which tend to prevent this rotation. For this reason, it is necessary to distinguish two cases:

1. Open-coiled helical spring axially loaded and with ends free to rotate about the spring axis and
2. The same except that ends are fixed so that rotation about the spring axis is prevented.

SPRINGS WITH ENDS FREE TO ROTATE

Calculation of Stress—An open-coiled helical spring of large pitch angle as shown in *Fig.* 34 is subject to a tension load P, the ends being assumed free to rotate about the coil axis. If α is the helix or pitch angle and r the actual coil radius, the forces and moments acting on the element A of length ds will be, *Fig.* 34*b*, a bending moment $Pr \sin \alpha$, a twisting moment $Pr \cos \alpha$, a shear force $P \cos \alpha$ and a tension force $P \sin \alpha$. The shear stress τ due to the twisting moment $Pr \cos \alpha$ will be equal to this moment divided by the torsional section modulus for a spring of large index c. Thus

$$\tau = \frac{16Pr \cos \alpha}{\pi d^3} \qquad (53)$$

Likewise the bending stress σ due to the bending moment $Pr \sin \alpha$ will be, for large index c

$$\sigma = \frac{32Pr \sin \alpha}{\pi d^3} \qquad (54)$$

Since the spring index is assumed large, stresses due to the

direct shear load $P \cos \alpha$ and the tension $P \sin \alpha$ will be neglected for the present. Thus on an element of the surface of the coil the two stresses σ and τ are acting as indicated in *Fig.* 34*c*. As mentioned previously in Chapter II these stresses may be combined according to the *maximum-shear theory* and, therefore Equation 42 may be used. Hence the equivalent shear stress τ_e is

$$\tau_e = \frac{1}{2}\sqrt{\sigma^2 + 4\tau^2} \quad \ldots\ldots (55)$$

Using the values of σ and τ given by Equations 53 and 54 in this, and simplifying, the expression for equivalent shear stress becomes

$$\tau_e = \frac{16Pr}{\pi d^3}\sqrt{\sin^2\alpha + \cos^2\alpha} = \frac{16Pr}{\pi d^3} \quad \ldots\ldots (56)$$

This follows since the term under the radical is unity.

If the maximum-shear theory applies, this equation shows that the maximum equivalent shear stress is equal to that given by the ordinary formula $16\,Pr/\pi d^3$ regardless of the pitch angle

TABLE I

Comparison of Maximum-Shear and Shear-Energy Theories

Pitch Angle	Ratio τ_e'/τ_e
0	1.000
5	1.001
10	1.006
15	1.012
20	1.020
30	1.040

(effects due to curvature and direct shear being neglected), providing the coil radius r is taken as that actually existing when the spring is loaded. As shown in *Fig.* 33, this will be different from the initial coil radius r_o at zero load.

Applying the *shear-energy theory* of strength (as discussed in Chapter II), values of σ and τ given by Equations 53 and 54 should be used in Equation 43. If this is done an equivalent shear stress is obtained equal to

$$\tau_e' = \frac{16Pr}{\pi d^3}\sqrt{\cos^2\alpha + \frac{4}{3}\sin^2\alpha} \quad \ldots\ldots (57)$$

A comparison between Equations 56 and 57 shows that, when applied to a helical spring, the difference between the results given by the two theories (maximum-shear and shear-energy) is under 2 per cent for pitch angles under 20 degrees and under 4 per cent for angles below 30 degrees, (TABLE I).

In view of the small difference between the two theories,

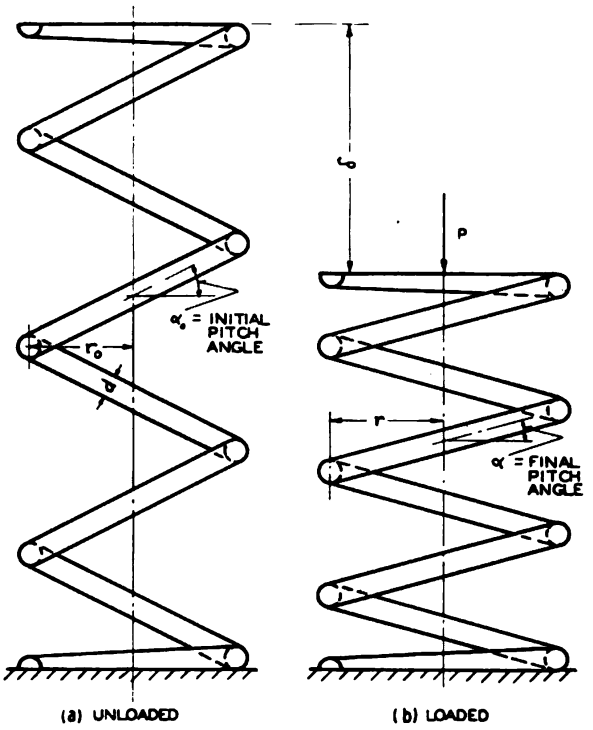

Fig. 33—Open-coiled spring with large deflection

the simpler formula, Equation 56 will be used in the following:

In calculating springs, it is simpler for the designer to use the coil radius r_o at zero load as a basis for calculation since it is a quantity easily measured. It is shown, Page 57, that for an axially-loaded spring the actual coil radius is given by $r = K_2 r_o$ where K_2 is a function of the ratio δ_o/nr_o between nominal deflection per turn and initial coil radius, and of the initial pitch angle α_o (pitch angle at zero load). The nominal deflection δ_o as figured from the ordinary deflection formula using the initial coil radius, Equation 7, is

$$\delta_o = \frac{64Pr_o^3 n}{Gd^4} \quad \text{.....(58)}$$

Thus K_2 may be expressed as a function δ_o/nr_o and of α_o and the equivalent stress becomes, from Equation 56,

$$\tau_c = \frac{16Pr}{\pi d^3} = \frac{16Pr_o K_2}{\pi d^3} \quad \text{.....(59)}$$

This stress is thus expressed simply as the ordinary formula for stress $16\ Pr_o/\pi d^3$ multiplied by a factor K_2 which may be

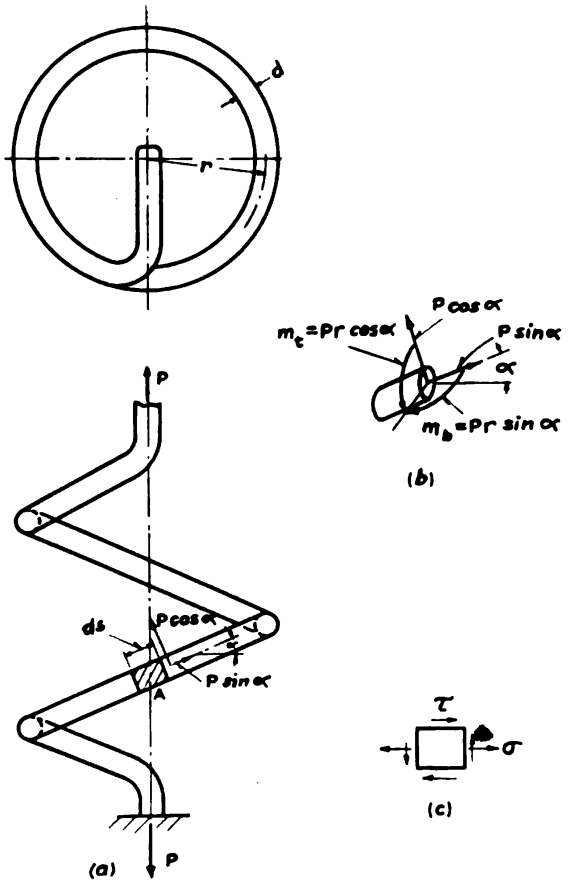

Fig. 34—Open-coiled helical spring with axial load

obtained from the curves of *Fig.* 35 if α_o and δ_o/nr_o are known. Values of δ_o/nr_o may be calculated from Equation 58 for a given load P. It should be noted that negative values of δ_o/nr_o cor-

respond to compressions, positive values to extensions. The factor K_2 is greater than unity for open-coiled compression springs since the coil radius increases as the spring is compressed; the opposite effect occurs in tension springs.

From the curves of *Fig.* 35 it may be seen that, if the initial

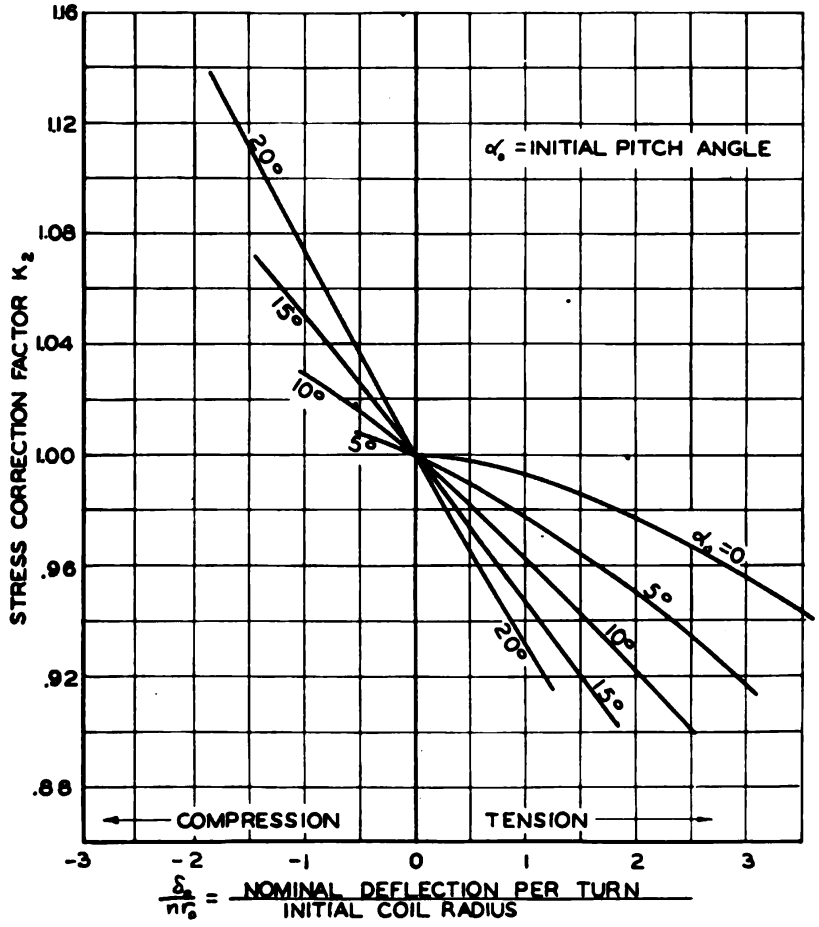

Fig. 35—Stress correction factor K_2 (Spring ends free to rotate)

pitch angle is below 15 degrees and the calculated deflection per turn δ_o/n is not more than the initial coil radius r_o, the errors in the stress formula due to pitch angle changes are under 6 per cent. This error may reach 15 per cent if the angle α_o reaches 20 degrees and the deflection per turn exceeds the initial coil diameter. In most actual applications where $\alpha_o <$

15 degrees and $\delta_o/nr_o < .5$, the error is under 3 per cent and, therefore, may be neglected for most practical purposes.

During this discussion, in order to determine the effect of pitch angle change, the increase in stress due to bar curvature and direct shear have been neglected. As an approximation to obtain the maximum stress, the stresses figured in this way should also be multiplied by the curvature correction factor K as given in Equation 19. Even for spring indexes between 10 and 20, this factor will vary from 1.07 to 1.14 and is thus of importance. A more accurate, but more complicated, method is to use expression for τ_{max} and σ_{max} given by Equations 34 and 38, Chapter II.

Calculation of Deflections—Assuming a helical spring axially loaded with the ends free to rotate as the spring deflects, *Fig.* 34, it is shown by the theory of elasticity[1] that the change in bar or wire curvature as the spring deflects from an initial pitch angle α_o to a different pitch angle α is

$$\Delta\kappa = \frac{\cos^2\alpha}{r} - \frac{\cos^2\alpha_o}{r_o} \qquad (60)$$

where r_o and r are the coil radii corresponding to the initial and final values of pitch angle. This equation is similar to Equation 49 except that the change in coil radius is considered. From *Fig.* 34 the bending moment causing this change in curvature is $m_b = Pr \sin \alpha$. This must be equal to the flexural rigidity EI multiplied by the change in curvature $\Delta\kappa$. Thus

$$Pr \sin \alpha = EI(\Delta\kappa)$$

where E = modulus of elasticity, I = moment of inertia of cross-section or using Equation 60:

$$P = \frac{EI}{r \sin \alpha}\left(\frac{\cos^2\alpha}{r} - \frac{\cos^2\alpha_o}{r_o}\right) \qquad (61)$$

From elastic theory[1] it may also be shown that the twist $\Delta\theta$ in the wire per unit length, as the spring deflects from a pitch angle α_o to a pitch angle α is

[1]Love—*Theory of Elasticity*, Cambridge University Press, Third Edition, Page 421.

$$\Delta\theta = \frac{\sin\alpha\cos\alpha}{r} - \frac{\sin\alpha_o\cos\alpha_o}{r_o} \quad \ldots\ldots (62)$$

This when multiplied by the *torsional rigidity* GI_p (for round wire) will yield the twisting moment m_t. This latter is, from *Fig.* 34, $m_t = Pr\cos\alpha$. Thus

$$Pr\cos\alpha = GI_p(\Delta\theta)$$

or using Equation 62

$$P = \frac{GI_p}{r\cos\alpha}\left(\frac{\sin\alpha\cos\alpha}{r} - \frac{\sin\alpha_o\cos\alpha_o}{r_o}\right) \quad \ldots\ldots (63)$$

where G=modulus of rigidity and I_p=polar moment of inertia of wire cross section.

Using Equations 61 and 63,

$$P = \frac{EI}{r_o^2}\,\frac{r_o}{r}\left(\frac{\cos^2\alpha_o - \frac{r_o}{r}\cos^2\alpha}{\sin\alpha}\right) \quad \ldots\ldots (64)$$

$$\frac{r_o}{r} = \frac{1}{K_2} = \frac{\sin\alpha_o\cos\alpha_o\tan\alpha + \frac{EI}{GI_p}\cos^2\alpha_o}{\cos^2\alpha\left(\frac{EI}{GI_p} + \tan^2\alpha\right)} \quad \ldots\ldots (65)$$

Assuming that the active length l of the spring remains con-

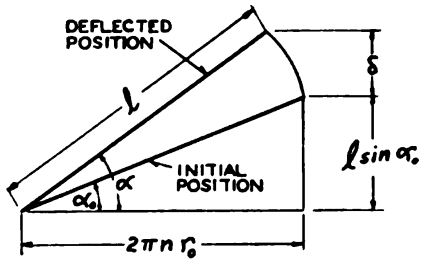

Fig. 36—Developed spring length with large pitch angle

stant (which is reasonable for springs of large index) the spring length may be developed on the helix cylinder as indicated in *Fig.* 36. From the geometry of this figure as the angle changes

from α_o to α the total spring deflection δ becomes

$$\delta = l(\sin \alpha - \sin \alpha_o)$$

Since $l \cos \alpha_o = 2\pi n r_o$, where n is the total number of active coils, this equation may be written:

$$\delta = \frac{2\pi n r_o}{\cos \alpha_o}(\sin \alpha - \sin \alpha_o) \quad \ldots\ldots\ldots\ldots\ldots\ldots\ldots\ldots\ldots\ldots\ldots\ldots (66)$$

Using Equations 64 and 66 the total deflection δ of the spring may be expressed as the nominal deflection δ_o (calculated from Equation 58) multiplied by a factor ψ_1. Thus

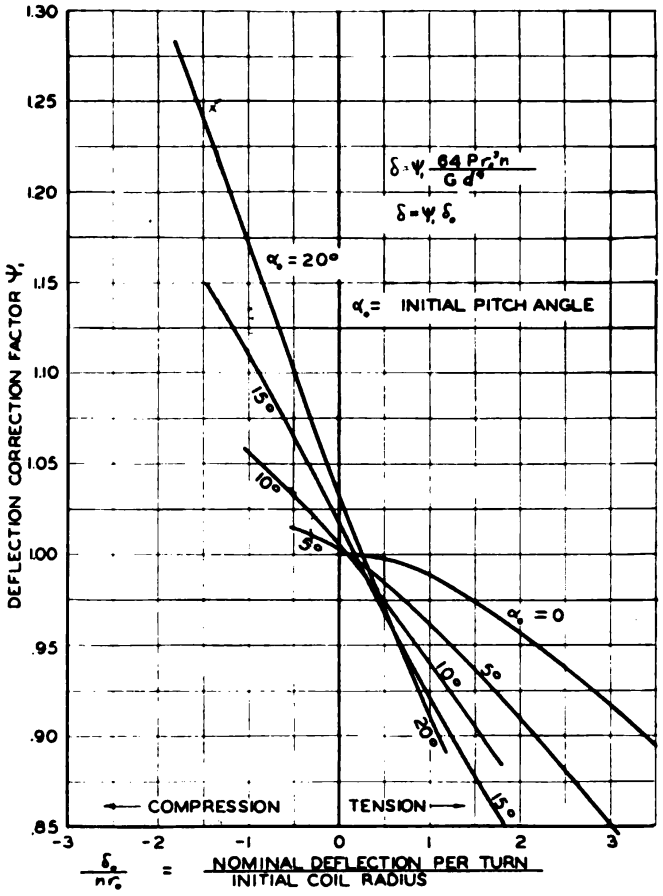

Fig. 37—Curves for finding deflection correction factor ψ_1, spring ends free to rotate

$$\delta = \psi_1 \delta_o = \psi_1 \frac{64 P r_o^3 n}{G d^4} \quad \ldots\ldots (67)$$

The factor ψ_1 depends on the initial pitch angle α_o, the ratio E/G between bending and shear moduli, and on the ratio δ_o/nr_o between nominal deflection per turn and initial coil radius. Values

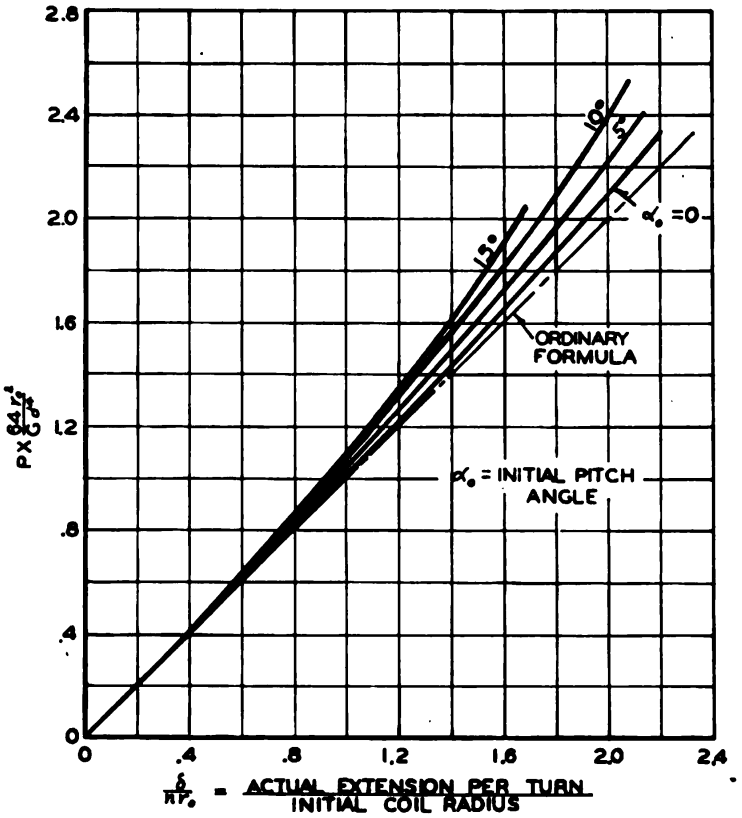

Fig. 38—Load extension diagrams for open-coiled helical tension spring, spring ends free to rotate

of ψ_1 have been calculated for a ratio $E/G=2.6$ (which applies approximately for most spring steels) and the results plotted in *Fig.* 37 for various values of α and δ_c/nr_o. Although a value of $E/G=2.6$ corresponding to Poisson's ratio $=.3$ has been assumed, it is believed that a considerable change may be had in this ratio with only an insignificant change in the final results.

A study of the curves of *Fig.* 37 shows that for pitch angles below 10 degrees and deflections per turn less than half the coil

radius, $\delta_o/nr_o < .5$, the error in the usual spring deflection formula is not over about 3½ per cent, i.e., ψ_1 does not differ from unity by more than about 3½ per cent. For pitch angles around 20 degrees and deflections per turn equal to the coil radius, however, the error may reach 15 per cent.

To use *Fig.* 37 for practical calculations of open-coiled helical springs it is merely necessary to determine the deflection δ_o for the given load P using the ordinary spring formula, Equation 58, or by means of spring tables or charts. From this value of δ_o the

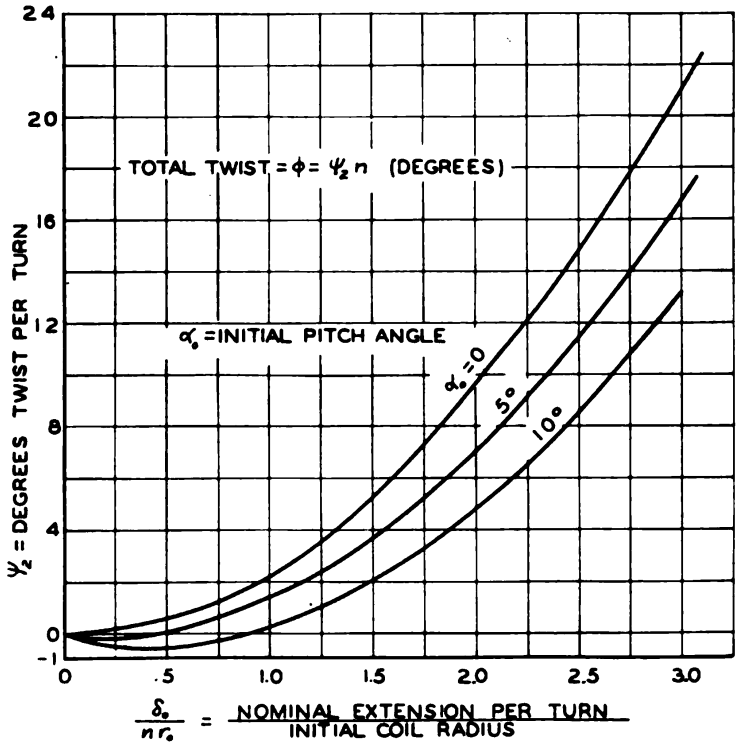

Fig. 39—Curves for calculating twist of spring ends. Tension springs with ends free to rotate

ratio δ_o/nr_o may be found. Then knowing this and the initial pitch angle α_o, the factor ψ_1 may be read from *Fig.* 37. The maximum deflection under the load P will then be equal to $\psi_1\delta_o$.

To show how the load-deflection diagrams deviate from a straight line for various initial pitch angles α_o and for various amounts of deflection, the curves of *Fig.* 38 have been plotted, using Equation 67, for tension springs where the ends are fastened

so that restraint against rotation about the spring axis is small. The ordinates of this curve represent values of $P \times 64r_o^2/Gd^4$ and are directly proportional to the load, while the abscissas represent actual extensions per turn divided by initial coil radius. These curves are concave upward, which means an increase in spring rate (in pounds per inch deflection) with load. This would be expected for tension springs since the coil radius r decreases with load. The straight dot-dash line represents the deflection as figured by the ordinary formula. In this case it may be seen that for larger deflections and pitch angles there is a considerable deviation from the straight line representing the ordinary formula.

Unwinding of Spring Ends—When a tension spring is extended, as is well known, the coils tend to unwind, at least at larger deflections. The amount of this unwinding may be calculated as follows: From *Fig.* 36, the angle in radians subtended by the projection of the total spring length in the unloaded position on a plane perpendicular to the axis will be

$$\phi_1 = \frac{l \cos \alpha_o}{r_o} \quad \ldots\ldots (68)$$

In the loaded position this angle will change to

$$\phi_2 = \frac{l \cos \alpha}{r} \quad \ldots\ldots (69)$$

Change in angle ϕ or the relative rotation of one end with respect to the other will be the difference in these values.

$$\phi = \phi_2 - \phi_1 = l\left(\frac{\cos \alpha}{r} - \frac{\cos \alpha_o}{r_o}\right)$$

or since from *Fig.* 36, $l = 2\pi n r_o / \cos \alpha_o$,

$$\phi = \frac{2\pi n r_o}{\cos \alpha_o}\left(\frac{\cos \alpha}{r} - \frac{\cos \alpha_o}{r_o}\right) \quad \ldots\ldots (70)$$

where ϕ is expressed in radians.

Using Equations 66 and 67 this angle may be expressed in terms of α_o and δ_o/nr_o as before. Expressing ϕ in degrees:

$$\phi = \psi_2 n \quad \ldots\ldots (71)$$

where ψ_2 is the twist per turn in degrees and may be read from *Fig.* 39 if α_o and δ_o/nr_o are known. It will be noted from this figure that ψ_2 becomes slightly negative for small values of δ_o/nr_o and for initial pitch angles greater than zero. This means that for small deflections the spring has a slight tendency to wind up. This is due to the fact that the distortions of the elements of the coil under axial load are in such a direction as to cause this winding-up effect. As the spring deflection increases, this tendency is overbalanced by the change in pitch angle which causes an unwinding of the coil.

SPRINGS WITH ENDS FIXED AGAINST ROTATION

Calculation of Deflection—Where the spring ends are fixed, i.e., prevented from rotating about the axis of the spring during deflection (this condition is realized in many compression springs

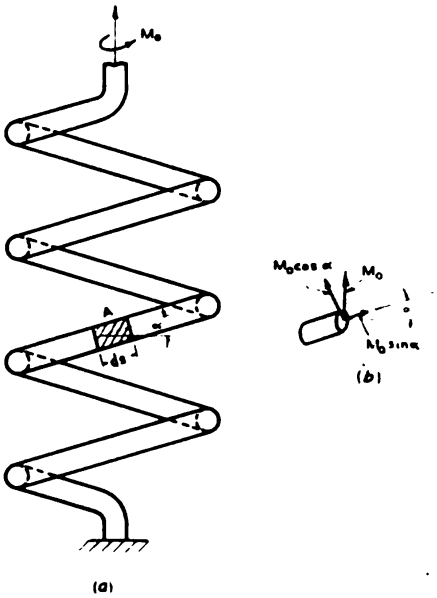

Fig. 40—Open-coiled helical spring with end moments. Moments are represented by vectors

where the friction between the ends and the supporting plate prevents relative rotation), a similar analysis may be made to that for the case where rotation occurs without restraint. In this case, $\phi=0$, it is necessary to take into account the moment acting at the spring ends which prevents the coils from unwinding.

From Figs 34 and 40 if a moment M_o and a load P are acting on the spring simultaneously as indicated, the bending and twisting moments m_b and m_t acting on the wire will be

$$m_b = M_o \cos \alpha - Pr \sin \alpha \quad (72)$$

$$m_t = M_o \sin \alpha + Pr \cos \alpha \quad (73)$$

The components $M_o \cos \alpha$ and $M_o \sin \alpha$ of the axial moment M_o are indicated by vectors in *Fig. 40b*.

The change in curvature of the wire $\Delta\kappa$ due to the moment m_b is equal to the moment divided by the flexural rigidity EI. Using Equation 60,

$$\Delta\kappa = \frac{m_b}{EI} = \frac{\cos^2 \alpha}{r} - \frac{\cos^2 \alpha_o}{r_o} \quad (74)$$

Likewise the twist $\Delta\theta$ becomes, from Equation 62,

$$\Delta\theta = \frac{m_t}{GI_p} = \frac{\sin \alpha \cos \alpha}{r} - \frac{\sin \alpha_o \cos \alpha_o}{r_o} \quad (75)$$

Substituting Equations 72, and 73 in Equations 74 and 75 two equations may be obtained, from which the following formulas for P and M_o may be found:

$$P = \frac{GI_p \cos \alpha}{r}\left(\frac{\sin \alpha \cos \alpha}{r} - \frac{\sin \alpha_o \cos \alpha_o}{r_o}\right) - \frac{EI \sin \alpha}{r}\left(\frac{\cos^2 \alpha}{r} - \frac{\cos^2 \alpha_o}{r_o}\right) \quad (76)$$

$$M_o = \frac{GI_p \sin \alpha}{r}\left(\frac{\sin \alpha \cos \alpha}{r} - \frac{\sin \alpha_o \cos \alpha_o}{r_o}\right) + EI \cos \alpha\left(\frac{\cos^2 \alpha}{r} - \frac{\cos^2 \alpha_o}{r_o}\right) \quad (77)$$

In addition, since the ends of the spring are prevented from rotation, ϕ_1 and ϕ_2 as given by Equations 68 and 69 are equal which means that

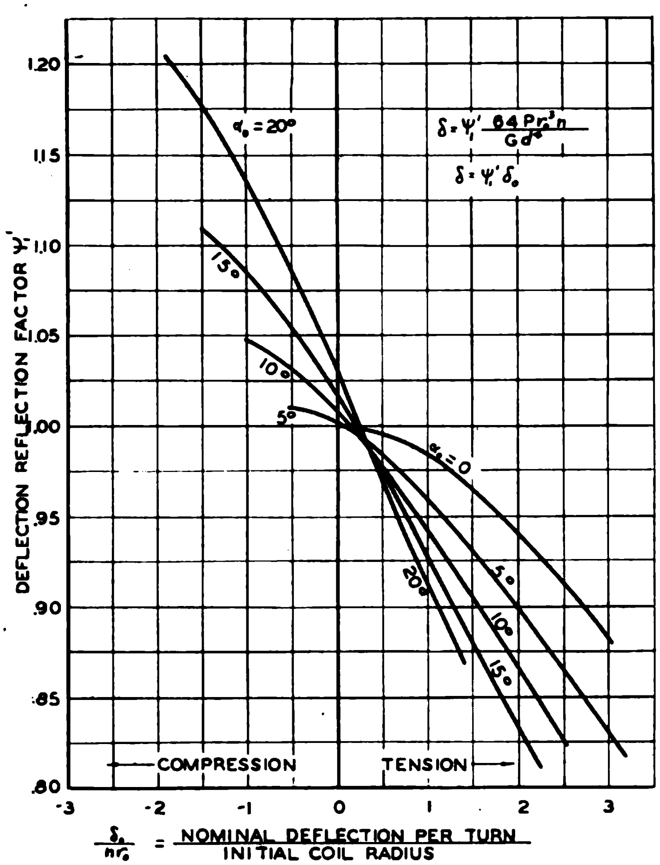

Fig. 41—Curve for finding deflection correction factor ψ_1'
Spring ends are fixed against rotation

$$\frac{\cos\,\alpha_o}{r_o}=\frac{\cos\,\alpha}{r}$$

or

$$r=r_o\frac{\cos\,\alpha}{\cos\,\alpha_o} \quad \text{(78)}$$

Using Equation 78 in Equations 76 and 77 and simplifying,

$$\psi_1'=\frac{\sin\,\alpha-\sin\,\alpha_o}{\cos^2\alpha_o\left[\sin\,\alpha-\sin\,\alpha_o+\frac{EI}{GI_p}\tan\,\alpha(\cos\,\alpha_o-\cos\,\alpha)\right]} \quad \text{(79)}$$

where ψ_1' is a factor corresponding to ψ_1 for the case where no

moment acts at the ends, Equation 67. By using Equations 66 and 67, the factor ψ_1' may be expressed in terms of initial pitch angle α_0 and δ_0/nr_0 as before, and the results are given on the curves of *Fig.* 41. Comparison of *Figs.* 37 and 41 indicates that the difference between the two cases, i.e., ends fixed or free, is not great at the smaller values of δ_0/nr_0. At larger values there are some deviations.

Load deflection diagrams as determined for compression springs with fixed ends by using Equation 79 are given in *Fig.* 42. It is seen that at the larger pitch angles and deflections there is

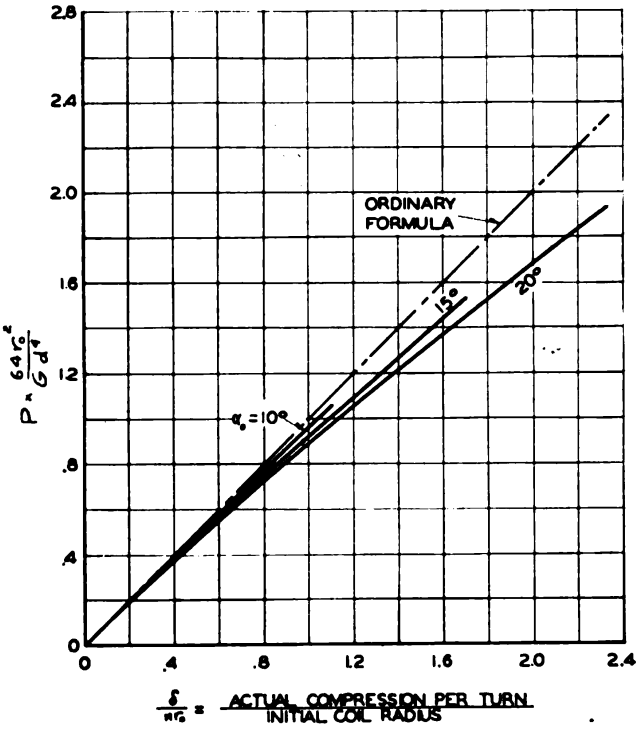

Fig. 42—Load-compression diagrams for open-coiled compression spring. Ends fixed against rotation

considerable deviation from the straight line calculated from the usual formula. It should be noted that the question of buckling of compression springs is not considered here[2]. Where the buckling load is exceeded, the curves of *Figs.* 41 and 42 may still be used if guides are provided to prevent lateral movement.

[2]Chapter IX discusses methods of determining buckling loads in compression springs.

Similar load-deflection curves for tension springs with ends restrained from rotation about the spring axis are given in *Fig.* 43. This condition will apply approximately for tension springs having hooks which fit into a hole in a plate, so that, when the spring is extended, the hook cannot rotate appreciably. It also holds where

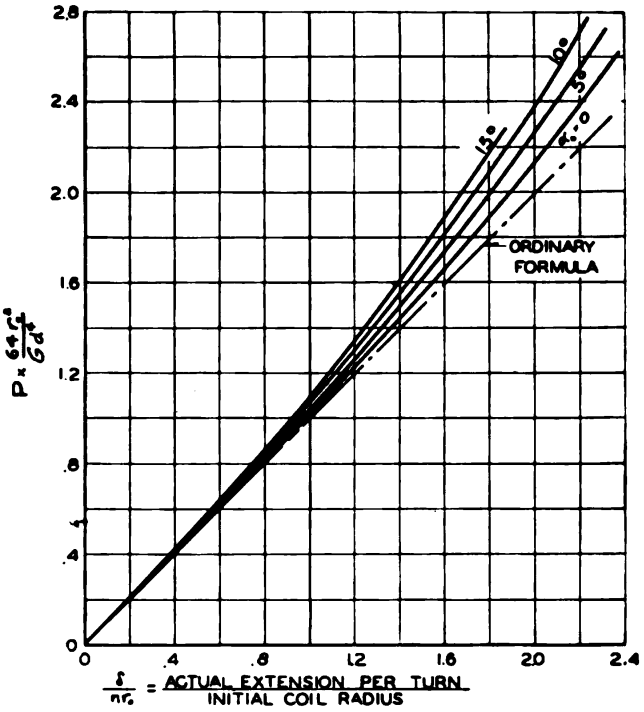

Fig. 43—Load-extension diagrams for open-coiled helical tension springs. Ends fixed against rotation

the spring is fitted with spring ends which are in turn fastened in a mechanism to prevent any rotation.

Calculation of Equivalent Stress—For axially-loaded helical springs with fixed ends, the stress is modified by the presence of the fixing moment M_o at the ends of the spring. From Equations 72 and 73 the bending and twisting moments acting on the wire cross section may be calculated. Assuming, as before, that the *maximum-shear theory* of strength is valid, the equivalent shear stress from Equation 55, for a circular wire cross section becomes

$$\tau_e = \frac{1}{2}\sqrt{\sigma^2 + 4\tau^2} = \frac{16}{\pi d^3}\sqrt{m_b^2 + m_t^2}$$

Substituting values of m_b and m_t given by Equations 72 and 73 in this and simplifying,

$$\tau_o = \frac{16}{\pi d^3}\sqrt{M_o^2 + (Pr)^2}$$

Using the values of M_o and Pr given by Equations 76 and 77, this equation may be reduced to

$$\tau_o = \frac{16 Pr_o}{\pi d^3} K_2' \qquad (80)$$

where K_2' is a factor by which the usual formula $\tau = 16\ Pr_o/\pi d^3$ must be multiplied to obtain the actual stress. Values of K_2' are

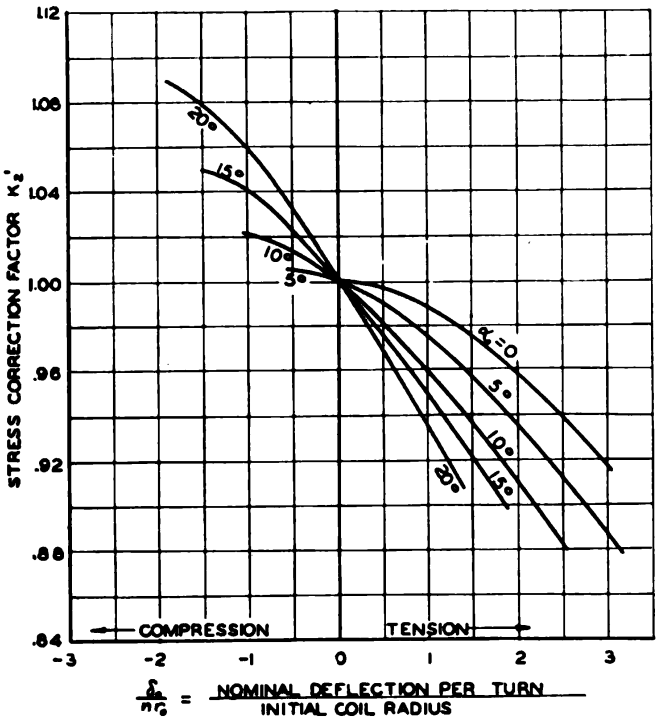

Fig. 44—Stress correction factor K_2', ends fixed

plotted as functions of α_o and of δ_o/nr_o in *Fig.* 44. It should be noted that as mentioned previously additional stresses due to curvature will be present, and these may be taken into account by using the formulas of Chapter II.

In general the analysis of this chapter indicates that where

large deflections are present, the error in the usual deflection formula, Equation 7, should be considered. This error may approach 15 per cent for initial pitch angles near 20 degrees and deflections per turn equal to the coil radius. For usual applications where the initial pitch angle is under 10 degrees and the deflection per turn less than half the coil radius, the results indicate an error in the usual formula of less than 3½ per cent. Hence, unless maximum accuracy is desired, these effects due to pitch angle change and change in coil diameter may usually be neglected.

CHAPTER IV

STATIC AND FATIGUE TESTS ON HELICAL SPRINGS AND SPRING MATERIALS

In order to check on the validity of the formulas derived in Chapter II for stress in round wire helical springs, a series of strain measurements using Huggenberger extensometers was carried out on actual helical springs of the type used in railway applications and on semicoils cut from these springs[1]. The springs tested had indexes around 3 with an outside diameter of 6 inches and a bar diameter of 1½ inches. This low index was chosen because in some cases values as low as this are used in actual practice. Furthermore, the use of a low index spring in the tests meant that the difference between the results calculated by the ordinary formulas and those calculated by more exact theory would be considerable. Hence, a better experimental check could be obtained.

STRAIN MEASUREMENTS

Since the dimensions of the full-sized springs were such as to make it impossible to place an extensometer on the inside of the coil (where the maximum stress occurs), semicoils were cut from actual springs and loaded in such a way as to simulate the loading of a complete spring under an axial load. To do this, two steel arms were welded to the semicoil as shown in *Fig.* 45. These arms were then loaded by special eyebolts having spherical points so as to obtain axial loads. A photograph of the semicoil in position in the testing machine with the extensometer placed at the inside of the coil at the point of maximum stress is shown in *Fig.* 46. To measure the torsion stress in the coil, the extensometer points were placed a to b and a' to b' at 45 degrees to the axis, *Fig.* 45, of the bar[2]. From these strain measure-

[1]Author's paper "Stresses in Heavy Closely Coiled Helical Springs," *Transactions* A.S.M.E. 1929, A.P.M. 51-17 gives further details.

[2]A pure shear stress consists essentially of a tension stress combined with an equal compression stress at right angles thereto; both of these stresses being at 45 degrees to the shear stress. Thus strain measurements taken at 45 degrees to the shear stress axis allow determination of the latter.

ments and from formulas based on elastic theory, it is possible to calculate the shear stress, provided the modulus of elasticity and Poisson's ratio are known[3]. By using a relatively short gage length (one centimeter), the peak stress can be found with sufficient accuracy. The arrangement of *Fig.* 46 thus makes possible the measurement of peak stress on the inside of the coil

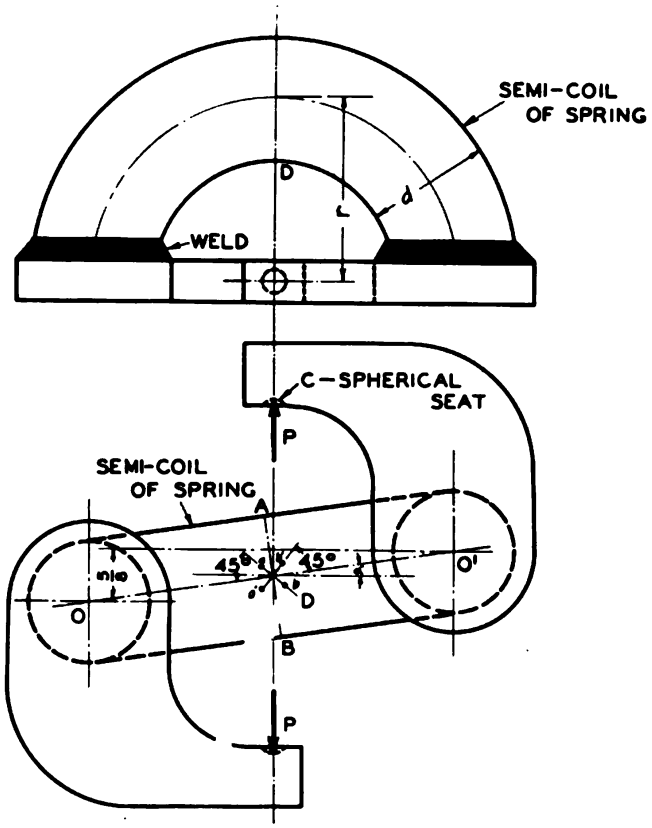

Fig. 45—Spring semicoil test arrangement

while at the same time the axial-loading condition in a complete spring is simulated.

Comparisons with Stress Formulas—Load-stress curves obtained from the strain measurements on the outside and the inside of a semicoil are shown by the full lines in *Fig.* 47. Similar results were also obtained by tests on a different semicoil. For comparison with the test results the dashed lines representing the calculated theoretical values taken from Equation 18 for the

[3]See, for example, Timoshenko—*Strength of Materials*, Second Edition, part 1, Page 52.

stress at the inside of the coil and from Equation 17 for the stress at the outside are also shown. It will be noted that the theoretical results obtained from Equations 17 and 18 agree within a few per cent with the experimental results. The dashed

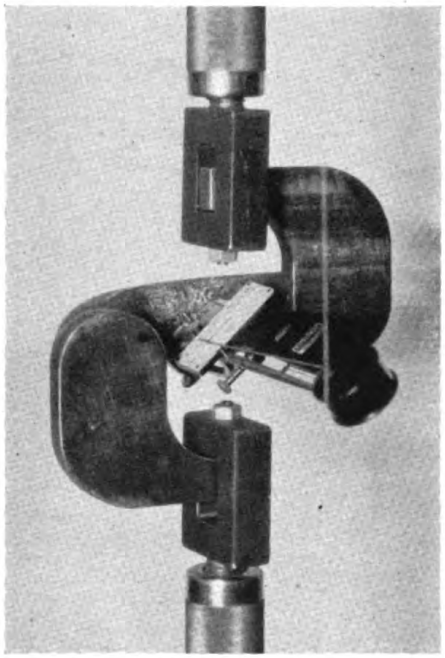

Fig. 46—Semicoil of helical spring in testing machine. Extensometer is at point of maximum stress on inside of coil

line representing the stress calculated from the ordinary formula which neglects the effects of curvature and direct shear is about midway between the two experimental curves and is considerably in error as far as the maximum stress is concerned. It is also of interest to note that the measured stress on the inside of the coil is around 2½ times that on the outside. For springs of larger index this difference, of course, would be considerably less pronounced.

To show that these tests on semicoils were representative of tests on complete springs axially loaded, a complete spring was tested in compression as shown in *Fig.* 48. As before, extensometers having a one centimeter gage length were applied at the outside of the coils to measure strains at 45 degrees to the axis of the wire. Load-stress curves obtained in this manner on diametrically opposite sides of the spring are shown in *Fig.* 49. The open circles represent stress on one side, the full circles stress on a diametrically opposite side of the spring. It may be

seen that the stress on one side is about 10 per cent higher than that on the opposite side at the higher loads. The reason for this is to be found in the fact that, because of the presence of the end coils, the load will be slightly eccentric to the spring axis (further

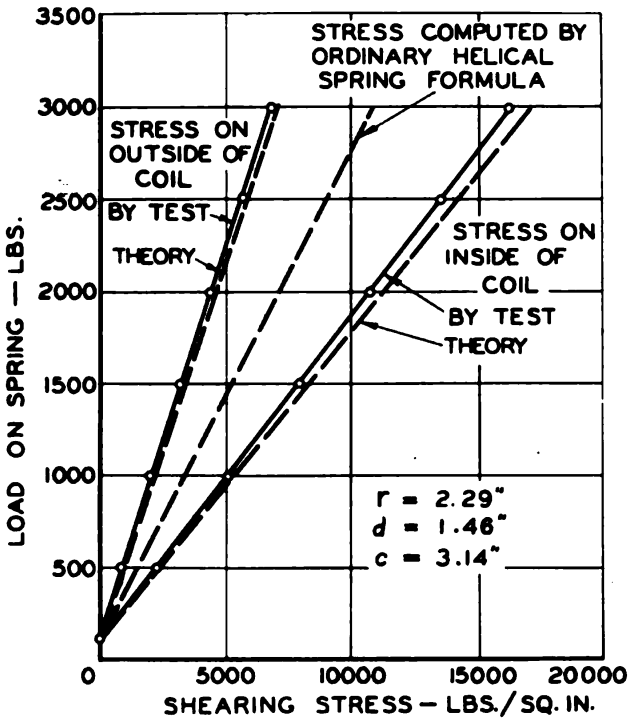

Fig. 47—Load-stress curves for semicoil

discussed in Chapter VIII). The dashed line on this figure represents the stress on the outside of the spring as calculated from Equation 17.

In *Fig.* 50 the average test curve (which gives the stress due to the axial load only) is shown together with the calculated curve from the same formula. It is of interest to note that this test curve practically coincides with that obtained on the outside of the semi-coil, *Fig.* 47, up to a load of 3000 pounds, thus indicating that the semicoil tests do simulate the loading of a complete spring. For comparison the stress curve computed from the ordinary stress formula, Equation 4, which neglects curvature and direct-shear effects is also shown.

These tests thus indicate that for small indexes the simple

stress formula for helical springs may be in considerable error. They also indicate that the approximate formula of Equation 18 is sufficiently accurate for calculating stresses in helical springs, elastic conditions being assumed.

DEFLECTION TESTS

To check on the usual deflection formula, Equation 7, for helical springs, tests on actual springs were carried out some years ago under the author's direction[4]. These tests also serve as a check on the more exact deflection formula of Equation 51 which takes into account effects due to spring index and pitch angle.

Essentially the test method was to wind three tension springs with indexes of 9.5, 4.7 and 2.7 from a single bar of carbon spring steel of ⅝-inch diameter. A total of nine springs cut from three bars of steel were tested. The method of testing is indicated in *Fig.* 51, the load being applied through an eye-

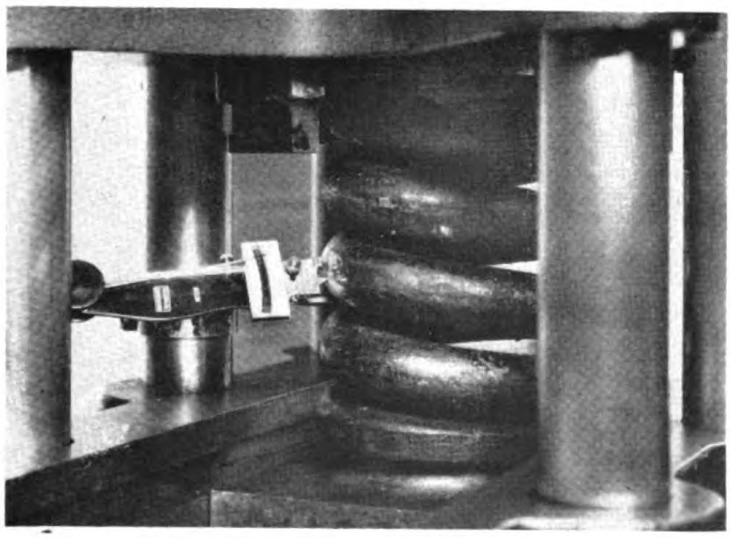

Fig. 48—Extensometer used to measure stress

bolt as indicated. Deflections were measured between the punch marks *a-a'* and *b-b'* in the body of the spring to eliminate the disturbing effects of the end turns. By taking an average

[4]"Further Research on Helical Springs of Round and Square Wire", *Transactions* A.S.M.E., 1930, Page 217.

on opposite sides, the unavoidable effect of slight eccentricities of loading were eliminated. It was found that the test load-deflection curves were almost exactly straight lines. A typical test curve for a spring of large index is shown in *Fig.* 52, the mean or average being shown. On this curve the circles represent test points on one side of the spring, the crosses represent those on the diametrically opposite side. Because of the unavoidable slight eccentricity of loading, these do not coincide.

By tests on the spring of large index made from a given bar of material, the torsional modulus of rigidity could be determined from Equation 7 for that particular bar. Average wire diameters were obtained by measuring d_1, d_2, d_3 and d_4, *Fig.* 51 with a micrometer for each coil after the test. To do this it

TABLE II

Values of Modulus of Rigidity

Bar No.	Modulus of Rigidity, G (lb./sq. in.)
1	11.45×10^6
2	11.46×10^6
3	11.50×10^6

was necessary to cut up the spring. Coil diameters were found by measuring diameters D_1 and D_2, correction being made for pitch angle. The results on the determination of modulus of rigidity for the three bars tested are shown in TABLE II.

These results indicate that the modulus varied by less than ½ per cent between the different bars and, hence, that the mate-

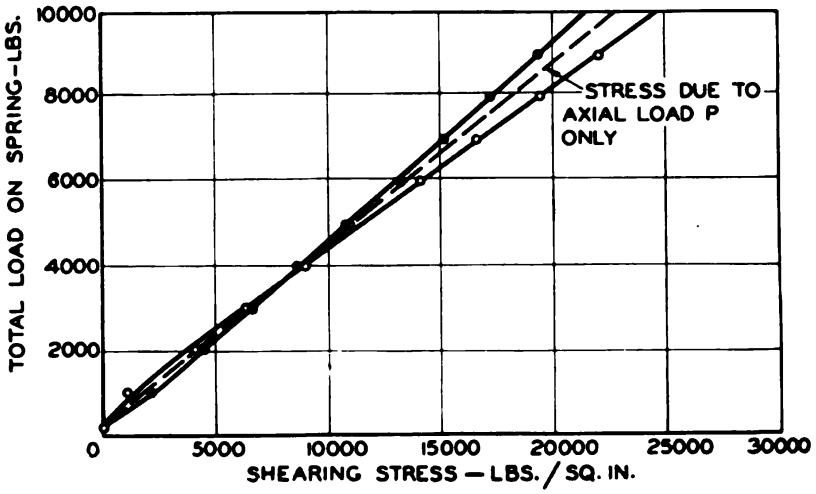

Fig. 49—Load-stress curves on complete spring

rial used for the tests was uniform.

Calculated Values Compared—For the springs of smaller index it was found that as indicated by the theoretical curves of *Fig.* 32, the actual deflection was in most cases slightly *less* than that figured by the ordinary deflection formula, i.e., ψ was less than unity. A typical test curve for a spring of small index

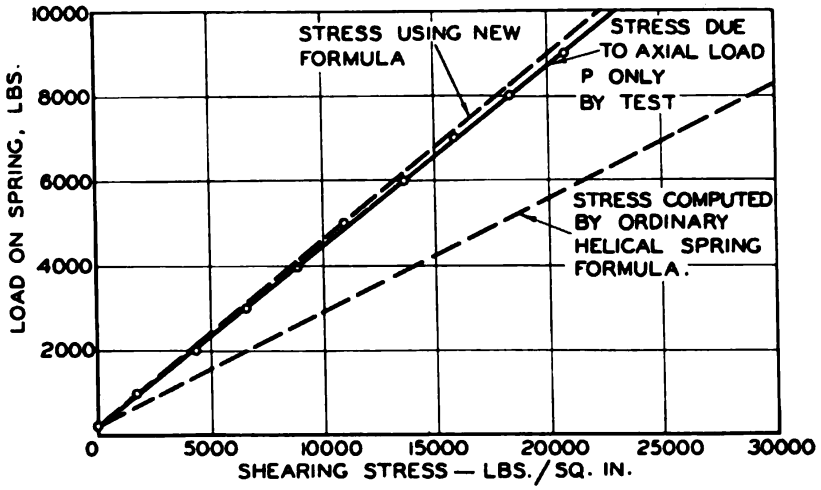

Fig. 50—Load-stress curves for complete spring under axial loading

is shown by the full line of *Fig.* 53, this curve representing the average value as measured on diametrically opposite sides. The curve calculated from ordinary deflection formula, Equation 7, is shown dashed.

A summary of test results obtained on six springs having indexes of 2.7 or 4.7 is given in TABLE III, which shows the percentage deviation between the test curves and the curves calculated from the ordinary formula, Equation 7, for the various springs tested. A negative deviation means that the deflection was slightly less than that calculated by means of the ordinary formula. It may be seen that the average test deviation (for springs made from three bars 1, 2, and 3) was —1.7 per cent for springs of index 2.7 and —1.0 per cent for springs of index 4.7 The deviations calculated by using the factor ψ of *Fig.* 32 for the known pitch angle and spring index were —2.4 per cent and —0.7 per cent. It is thus seen that the average test values are within .7 per cent of the corresponding calculated values using the more accurate method. This indicates that slightly

more accurate values of spring deflections may be obtained by multiplying the deflections figured by the ordinary formula by the factor ψ of Equation 52 or *Fig.* 32. It should be mentioned,

TABLE III

Measured and Calculated Deviations* from Ordinary Helical Spring Formula

Spring Index	Bar No. 1	Bar No. 2	Bar No. 3	Av. Test Deviation	Calculated Deviation
(D/d)	(%)	(%)	(%)	(%)	using factor ψ
2.7	—3	0	—2.2	—1.7	—2.4
4.7	—1.3	—1.6	0	—1.0	— .7

*All deviations negative, i.e., deections were slightly less than calculated from ordinary formula Equation 7. Effect of pitch angle considered.

however, that the usual deflection formula for helical springs is sufficiently accurate for most practical purposes.

VARIATIONS IN MODULUS OF RIGIDITY

For accurate calculation of deflections in helical springs, knowledge of the value of *modulus of rigidity* or *torsional modulus G* for use in the deflection formula Equation 7 is necessary. For several reasons, the effective torsional modulus of a helical spring (which should be used in the spring formula) may differ somewhat from that to be expected on the basis of torsion tests on straight bars of the same material with ground and polished surfaces. Among the reasons for this difference are effects of overstraining of the material, presence of a decarburized layer on the surface, and residual stresses resulting from the manufacture of the spring.

Effects of some of these factors will be discussed in connection with test data available in the literature relative to the modulus of rigidity of actual springs and spring materials. Unfortunately, this data shows that the effective torsion modulus for any given material may vary from an average figure by several per cent in individual cases.

Effects of Overstraining—The value of modulus of rigidity is reduced to some extent by overstraining the material. However, there is a tendency for a part of this reduction to be lost after the material has stood for some time. Adams[5] found that by overstraining straight bars of high-carbon spring steel in

[5]*Carnegie Scholarship Memoirs*, Iron & Steel Institute, 1937, Page 1.

torsion, a reduction of several per cent in the modulus of rigidity was obtained although this decrease could be eliminated by a proper low temperature heat treatment after the overstraining. Similar results were obtained by Pletta, Smith, and Harrison[6], on actual helical springs made from ¾-inch diameter bar. These investigators found decreases in the torsional modulus varying from about 1 to 5 per cent depending on the amount of overstraining, and a tendency of the modulus to partially recover its initial value after the spring has stood for a considerable length of time.

Effects of Surface Decarburization—A factor which is of considerable importance in fixing the effective torsional modulus is the degree of decarburization of the wire surface in the com-

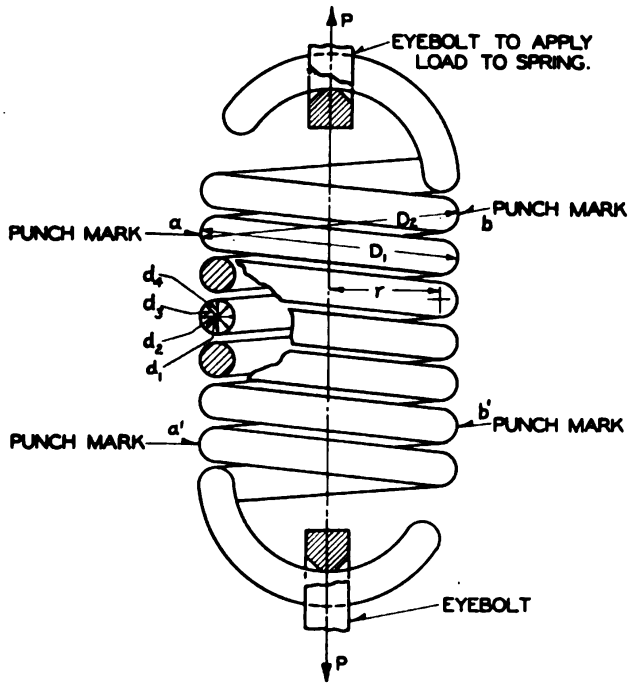

Fig. 51—Testing helical spring for deflection

pleted spring. It is clear that, if there is a decarburized layer of material on the surface, when the spring is stressed this material will act like low-carbon steel and will yield at a relatively

[6]"The Effect of Overstrain on Closely Coiled Helical Springs and the Variation of the Number of Active Coils with Load" by Pletta, Smith and Harrison, Eng. Exp. Station *Bulletin* No. 24, Virginia Polytechnic Inst.

low load. At higher loads the spring will, therefore, act to some extent as if the layer of decarburized material were not present; in other words, the load-deflection rate will be roughly that corresponding to a bar or wire having a diameter equal to the actual diameter minus twice the thickness of the decarburized layer. Since the actual diameter is used in the spring formula, this effect is the same as if the effective modulus of rigidity were decreased. For example, a spring of ½-inch hot-wound stock may be assumed to have a decarburized layer extending .01-inch into the material. At the higher loads, since the decarburized layer contributes but little to strength, the load-deflection rate corresponds to a bar diameter of $.5-2(.01)=.48$-inch or 4 per cent under size. Since the load-deflection rate varies as the fourth power of the wire size, Equation 7, this means a reduction of approximately 16 per cent in the former, or a decrease in effective modulus of rigidity of 16 per cent. In many cases, spring

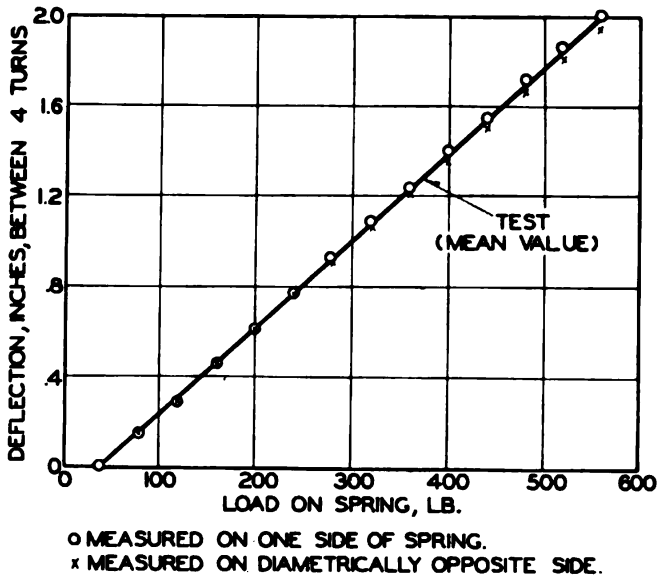

Fig. 52—Typical load-deflection diagram for helical spring of large index ($c = 9.5$)

manufacturers assume a modulus figure of about 10 per cent less for hot-rolled carbon spring steel than for hard-drawn materials. The above example shows that a decarburized layer around 6 mils thick in ½-inch diameter stock would be sufficient

to account for this lower modulus value. Such a layer may easily occur in hot-wound spring materials.

Effect of Temperature—In general the modulus of rigidity of spring materials drops with increase in temperature. This means that the deflection of a spring under a given load will be

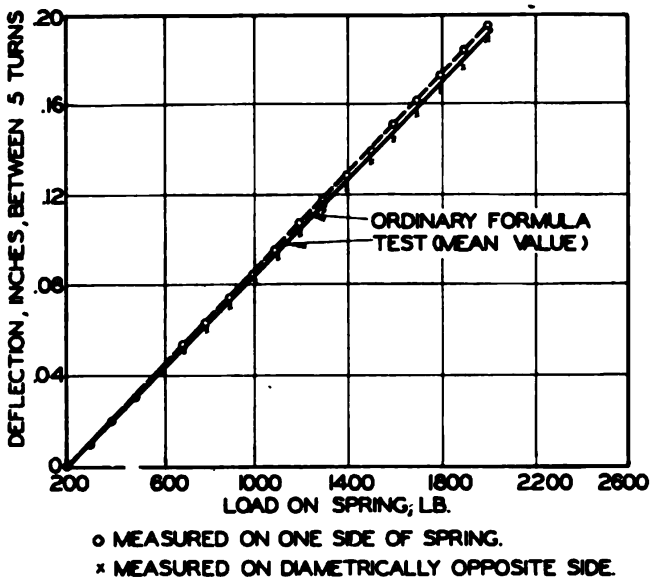

Fig. 53—Typical load-deflection diagram for spring of small index (c = 2.7). Note that mean deflection of two sides is slightly below the theoretical value

larger at higher temperatures. However, available test data on the effects of temperature are limited. One of the few investigations made along this line is that carried out by Keulegan and Hauseman[7] who investigated the change in modulus of rigidity for a limited range of temperature (from —50°C. to +50°C) for various spring materials. These investigators found that within this range for most materials the modulus of rigidity could be represented approximately by

$$G = G_o(1 - mt) \quad \ldots\ldots (81)$$

where G=modulus of rigidity at 0°C, m=temperature coefficient of modulus, and t=temperature, C.

[7]Bureau of Stds. Jl. of Res., Vol. 10, 1933, Page 305. See also Brombacher & Melton, N.A.C.A. Tech. Report No. 358, 1930.

Average values of m obtained by these investigators for various spring materials are given in TABLE IV. For example, for music wire an increase in temperature from 0 to 50 degrees Cent. would mean a drop in the torsional modulus equal to

TABLE IV

Temperature Coefficients of Modulus of Rigidity G*
(—20C to 50C)

Material	Grade	Coefficient m (per °C)
Oil-tempered steel	.66% C	.00025
Music wire		.00026
Chrome-vanadium steel†	.98% Cr. .24% Va	.00026
Stainless steel‡	18% Cr 8% Ni	.00040
Monel metal‡		.00032
Phosphor bronze‡		.00040

*Data given by Keulegan and Hauseman, Bureau of Standards Journal of Research. Vol. 10, 1933, Page 345.
†Quenched and tempered.
‡Hard drawn.

$m \times 50G = .00026 \times 50G = .013G$ or 1.3 per cent in this range. Where extreme accuracy is desired (as in instrument springs) such effects may be important.

A rough idea of how the modulus of rigidity drops with temperature varying from -100 degrees Fahr. to 600 or 800 degrees Fahr. may be obtained from the curves of *Fig.* 54. These were obtained by drawing smooth curves through test data published by Zimmerli and his collaborators[8]. Since the actual test data reported showed considerable irregularities and scatter, these curves should be considered as giving only a rough indication of the trend of modulus change with temperature.

DETERMINATION OF MODULUS OF RIGIDITY

In general there are three methods which have been used to determine the modulus of rigidity for spring materials:

1. DEFLECTION METHOD: Measurements of deflection in helical springs in tension or compression
2. DIRECT METHOD: Measurements of twist of a straight bar in a torsion testing machine
3. TORSIONAL PENDULUM METHOD: Measurements of the period of a torsional pendulum from which by known formulas the modulus of rigidity may be determined.

Deflection Method—In using the first method, deflections

[8] *Proceedings* A.S.T.M., 1930, Part II, Page 356.

are measured on actual helical springs loaded in testing machines. As mentioned previously it is advisable to measure these deflections between coils in the body of the spring to eliminate uncertainties due to the effects of end coils. Also to eliminate effects due to unavoidable eccentricities of loading it is advisable to measure deflections on diametrically opposite sides of the coil. An average of these values then is taken. If the deflection δ_n between n turns of the spring is found, the modulus of rigidity G may be found from

$$G=\frac{64Pr^3n}{\delta_n d^4} \qquad (82)$$

This equation is obtained by solving Equation 7 for G, the other symbols having the same meanings as before. Slightly higher

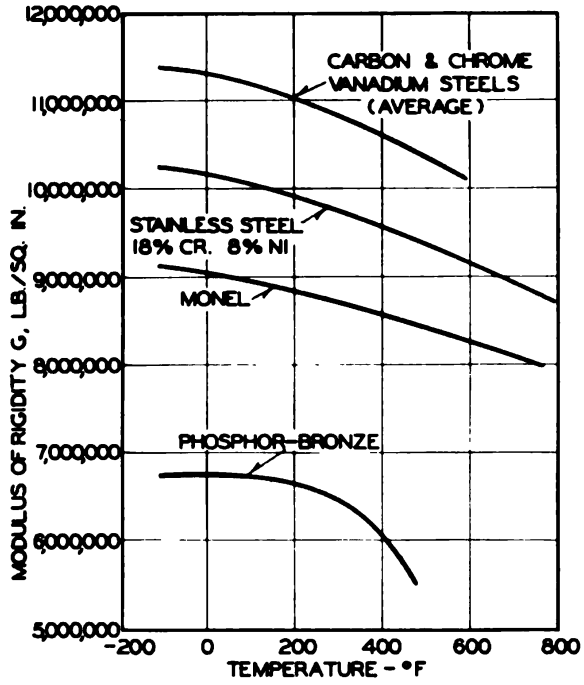

Fig. 54—Temperature effect on modulus of rigidity for various materials

accuracy may be had, particularly for small indexes, by dividing δ_0 by the factor ψ taken from *Fig.* 32. However, for indexes larger than 5 this factor may be neglected in most cases. It

should be emphasized that, for accurate results, careful measurements of the spring dimensions at many points are necessary. Usually this means that the spring must be cut up after the test to measure the average wire diameter.

In the past, there has been some reluctance on the part of investigators to use the deflection method on the ground that errors in the spring formulas may introduce unknown errors in the results. It is the author's opinion that the questions regarding inaccuracy of the formula have been settled, both experimentally and theoretically, and that the results are reliable if the precautions mentioned are carried out. In addition, the deflection method has the advantage that the modulus of rigidity is measured on the complete spring and, hence, may be more representative of material wound up to form actual springs. It is possible that there may be some difference between the material as coiled into a spring and heat treated and straight bars of spring material as required by the other methods discussed.

Direct Method—In using the direct method for finding the torsional modulus, a straight, round bar of the spring material is twisted in a torsion testing machine. To eliminate disturbances near the clamped ends it is advisable to measure twist along a definite gage length of the material under torsion by means of some kind of a torsion measuring device. One method which may be used is to attach mirrors on the bar a certain distance apart. Angular deflections of these mirrors are measured by a telescope and scale. If θ is the angle of twist *in radians* as thus measured in the gage length l the modulus of rigidity is found from[9]

$$G=\frac{32Tl}{\pi d^4\theta} \qquad (83)$$

where T=torque producing the twist, l=gage length, d=bar diameter.

Measurements in which the overall angular movement of the head of the testing machine are measured are subject to error since there is a certain indefinite amount of twist in the clamping jaws near the ends of the specimen and this may introduce appreciable error in the results.

[9]This equation is easily derived from the known formula for angular twist of a straight bar in torsion. See *Strength of Materials*—Timoshenko, Part I, Page 261.

Torsional Pendulum Method—In the third or torsional pendulum method a weight is supported by the spring wire and vibrated in torsion. The frequency of oscillation f in cycles per second is measured; from this the torsional modulus G may be calculated from the equation

$$G=\frac{128\pi lIf^2}{d^4} \quad \ldots\ldots (84)$$

where I=mass moment of inertia of pendulum bob, l=effective length of wire, and d=wire diameter as before. This equation may easily be derived from the known equation.

$$f=\frac{1}{2\pi}\sqrt{\frac{K}{I}} \quad \ldots\ldots (85)$$

where K=torsional spring constant of the wire[10].

The bar should be relatively long to reduce, as much as possible, the indeterminate effects due to clamping at the ends of the bar or rod. In this test, of course, the material is subject to a combination of torsion and tension stress, the latter being due to the weight of the pendulum bob.

Carbon Spring Steels—A summary of available test data on modulus of rigidity of carbon spring steel is given in TABLE V. Individual test data were obtained by various investigators, using one of the three test methods described previously, i.e., deflection, direct, or torsional pendulum method. In each case the source of the data together with the method used is indicated in the footnotes to the table.

Item 1 of TABLE V represents an average figure calculated from the deflection measurements between coils of helical springs reported by Edgerton, the modulus figure being an average for tests on three springs. In using the test data, deflections beyond the approximate elastic limit of the spring material were not used, since practical springs are seldom loaded to such high values. Item 2 refers to a torsion test of a ½-inch diameter bar of carbon spring steel, as tested by Adams, while Item 3 refers to the same material after overstraining at a torque about 50

[10]For example Den Hartog—*Mechanical Vibrations*, McGraw-Hill, 1940, Page 43.

per cent above the torque corresponding to the proportional limit, followed by a mild heat treatment at 228 degrees Cent. The reduction in modulus of rigidity from 11.82 to 11.14 $\times$ 10^6 pounds per square inch by this treatment gives an idea of the reduction which may result from stressing helical springs far beyond the proportional limit of the material. This investigator showed

TABLE V

Values of Modulus of Rigidity *G* for Carbon Spring Steels

No.	Material	Heat Treatment	Wire or Bar Diameter (in.)	Modulus of Rigidity (lb./sq.in.$\times 10^7$)	Investigator
1	1% C steel, basic, open hearth	Q & T*	¾	11.6	Edgerton[1]
2	1% C steel	Q & T*	½	11.82	Adams[2]
3	1% C steel	Q & T*, O-MHT†	½	11.14	Adams[3]
4	1% C steel	Q & T*	9/16	11.2	Wahl[4]
5	1% C steel	Q & T*	⅝	11.47	Wahl[5]
6	.67% C steel	Oil tempered	.028-.08	11.12	Sayre[6]
7	Music wire		.035	11.4	Brombacher & Melton[7]
8	Hard-drawn wire			11.4	Sayre[6]

*Q & T = Quenched and tempered.

†O-MHT = Overstrained, mild heat treatment.

[1]These values of *G* are average values calculated from spring deflection tests reported by Edgerton, *Transactions* A.S.M.E., October, 1937, Page 609. Deflection method used for tests.

[2]*Carnegie Scholarship Memoirs, Journal* Iron & Steel Inst., 1937, Page 1-55. Average value with no overstrain. Direct method used for tests.

[3]Value of *G* obtained by overstraining at a torque about 50 per cent above that corresponding to the proportional limit. (By using higher temperatures in the heat treatment *G* could be restored to its original value.) Direct method used.

[4]Unpublished test data. Deflection method used.

[5]*Transactions* A.S.M.E., 1930, Page 217. Deflection method used.

[6]*Transactions* A.S.M.E., 1934, Page 556. Torsional pendulum method.

[7]N.A.C.A. Report No. 358, 1930, Page 568. Torsional pendulum method.

that by increasing the temperature of the mild heat treatment from 228 degrees Cent. to 275 degrees Cent. this reduction in the modulus figure due to overstraining was practically eliminated.

A comparison of the various modulus figures TABLE V indicates that a variation in the torsional modulus of carbon spring steels from, say, 11.1 $\times$ 10^6 to 11.8 $\times$ 10^6 for various conditions may be expected, the value of 11.5$\times$$10^6$ pounds per square inch being perhaps a good average figure. It should also be noted that variations of ± 5 per cent may be obtained in some cases while, as mentioned before, even larger variations are possible if the spring wire has a decarburized layer of appreciable thickness. The higher value of 11.82 $\times$ 10^6 obtained by Adams

was probably due to the fact that no decarburized layer was present while the material was not overstrained. The lower values of G found for the other cases are probably due largely to either or both of these two effects. These latter figures are, however, more representative of those to be expected.

Alloys, Stainless, Monel and Phosphor Bronze—A summary of available test data on the modulus of rigidity of spring materials other than carbon steels is given in TABLE VI.

On the basis of this data rough average values of the modulus of rigidity may be taken as: 11.5×10^6 pounds per

TABLE VI

Modulus of Rigidity of Alloy Steels, Stainless, Monel Metal and Phosphor Bronze

Material	Heat Treatment	Wire or Bar Diameter (Inches)	Modulus of Rigidity G (lb./sq.in. $\times 10^6$)	Investigator
Cr-Va steel*	Q. & T.†	½	11.75	Adams[1]
Cr-Va steel§	Q. & T.†	.148	11.2	Zimmerli, Wood Wilson[2]
Cr-Va steel	Q. & T.†	.375	11.45	Berry[3]
Stainless steel§§	A. & C. D.‡	.148	10.5	Zimmerli, et al[2]
Stainless steel§§	C. D.‡	.04-.162	10.8	Wahl[4]
Monel metal	A. & C. D.‡	.125	9.1	Zimmerli, et al[2]
Phosphor bronze	A. & C. D.‡	.09	6.7	Zimmerli, et al[2]
Phosphor bronze			6.3	Sayre[5]
Phosphor bronze		.081	6.2	Brombacher & Melton[6]

†Q. & T. = quenched and tempered.

‡A. & C. D. = annealed and cold drawn.

*1.38% Cr, .17% Va, .21% Ni.

§1.06% Cr, .17% Va.

§§18% Cr, 8% Ni.

[1]*Carnegie Scholarship Memoirs*, Iron & Steel Institute, 1937, Pages 1-55. Direct method used. Material not overstrained.

[2]*Proceedings* A.S.T.M., 1930, Part II, Page 357. Direct method used.

[3]*Proceedings* Inst. Mech. Engrs., 1938, Page 460. Direct method used.

[4]Unpublished test data. Deflection method. Average of 14 springs.

[5]*Transactions* A.S.M.E., 1934, Page 556. Torsional pendulum tests.

[6]N.A.C.A. *Technical Report* No. 358, 1930, Page 568. Direct method used.

square inch for chrome vanadium steels, 10.6×10^6 for stainless steel (18% Cr, 8% Ni), 9×10^6 for Monel metal, 6.4×10^6 for phosphor bronze. Again it should be noted that individual test values may deviate from these averages by several per cent.

FATIGUE TESTS

In recent years a great many investigations have been made to determine the endurance properties of helical springs under fatigue or repeated loading. The usual method of fatigue

testing is illustrated by the tests of automotive knee-action springs shown in *Fig.* 55. The results of such tests are of direct interest to designers and engineers who are responsible for the selection of springs operating under fatigue loading. Another important example is the valve spring used in internal combustion engines.

A survey of the literature shows that there are considerable differences in the endurance limits or limiting stress ranges for helical springs as reported by the various investigators. The reason for this lies mainly in the fact that the endurance limit of a helical or other type of spring is very much dependent on the surface condition of the spring wire or bar. Slight surface flaws or defects and surface decarburization resulting from the manufacturing process may result in a considerable reduction in the limiting endurance range. The low values reported in the literature in certain cases may be due to this. A further reason for variation in the results obtained lies in the fact that different spring indexes may be used. Since the sensitivity of different materials to stress concentration effects due to bar curvature varies, some difference in results would be expected. This is further discussed in Chapter VI.

Small-Size Springs—Among the more important investigations of the fatigue of helical springs, the tests conducted by Zimmerli[11] should be mentioned. These tests consisted of endurance tests with various stress ranges on small-sized helical springs as used for automotive valve springs. A typical endurance diagram as obtained on chrome-vanadium steel springs in this investigation is shown in *Fig.* 56, the stress ranges actually used being represented by the vertical lines between the circles and the line of minimum stress[12]. The circles with the arrows attached represent upper limits of the range which did not cause failure within ten million cycles, while the plain circles represent ranges which did. On the basis of these tests the estimated limiting endurance range is represented by the upper dashed curve. From this diagram it may be seen that the limiting endurance ranges are about as follows for this material: 0 to 77,000, 20,000 to 88,000, 40,000 to 98,000, 60,000 to 108,000

[11] "Permissible Stress Range for Small Helical Springs" F. P. Zimmerli, *Engineering Res. Bulletin* No. 26, University of Michigan, July 1934.

[12] This type of endurance diagram has been previously discussed in Chapter I.

pounds per square inch. This means that the spring could be expected to operate indefinitely within any of these ranges. Similar diagrams were obtained on other spring materials.

A summary of the results obtained by Zimmerli together with those obtained by other investigators is included in TABLE VII. Pertinent data including kind of material, heat treatment,

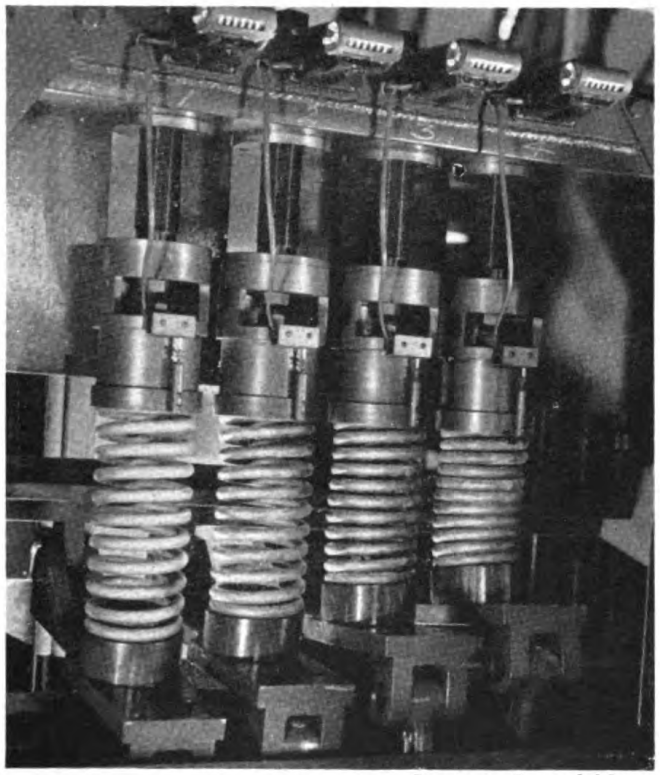

—Courtesy, General Motors

Fig. 55—Fatigue tests of knee action helical springs

ultimate strength, modulus of rupture, yield strength of the material in torsion, hardness, wire size, coil diameter, number of coils, and spring index are given together with values of the limiting endurance range. Where several values of limiting endurance range are given, diagrams similar to those of *Fig.* 56 may easily be constructed for a given material. In all cases the correction factor K of Equation 18 was used to calculate the stress range. A typical fatigue failure of a large helical spring is shown in *Fig.* 25 Page 31.

Other important investigations, the results of which are

TABLE VII

Limiting Endurance Ranges of Helical Compression Springs°

Coil Dia. D inches	Wire Dia. d inches	Index D/d	No. of Active Coils	Material	Heat Treatment§	Hardness	Modulus of Rupture (Torsion) lb./sq. in.	Elastic Limit or Yield Point (Torsion) lb./sq. in.	Ultimate Strength (Tension) lb./sq. in.	Limiting Endurance Range§§ lb./sq. in.	Investigator
1.7	.16	10.6		Cold Drawn Wire			155000		202000	25000 to 56000**	Lea and Dick[1]
1.5	.128	11.7		C.D. Wire .63% C		360 Brinell	143000		184000	25000 to 66000**	"
1.087	.163	6.67	6	C.D. Wire .93% C		51 Rock. C	216000	118000 E.L.	282000	20000 to 80000 40000 to 95000	Zimmerli[2]†††
1.10	.148	7.44	6	Pretempered Wire .65% C .64% Mn		43 Rock. C	184000	110000 E.L.	203000	20000 to 72000 40000 to 85000 60000 to 98000	"
1.10	.148	7.44	6	Cr Va Steel 1.12% Cr .12% Va	O.Q. 1650°F D 900°F	41 Rock. C	152000	107000 E.L.	202000	12000 to 84000 23000 to 92000 50000 to 105000	"
1.10	148	7.44	6	Pretempered Wire 75% C .32% Mn	Blued at 475°F for 20 minutes	44 Rock. C	180000	111000 E.L.	216000	20000 to 80000 40000 to 92000 60000 to 105000	"
1.10	147	7.5	6	Stainless Steel 17.4% Cr 8.9% Ni	Blued at 700°F 25 min. after winding	42 Rock. C	172000		216000	20000 to 45000 40000 to 62000 60000 to 79000	"
1.06	.162	6.5	3¾	Valve Spring Wire 65% C .58% Mn	Heated to 750°F after coiling				204000	20000 to 95000 20000 to 135000†	Zimmerli[3]†††
	.148	6-7		Music Wire SAE 1095 and Cr Va SAE 6150						20000 to 90000 20000 to 135000†	"
	.148	6-7		Stainless Steel 18-8						20000 to 65000 20000 to 110000†	"
	.148	6-7		Phosphor Bronze SAE 81						20000 to 35000 20000 to 50000†	"
2.69	.56	4.8	6½	Cr Va Steel .52%C .88% Cr .21% Va	Wound hot O.Q. 1600°F D. 810°F	477-488 Brinell	183000	141000 Y.P.	237000	0 to 77000‡	Johnson[4]***
2.69	.56	4.8	6½	High Carbon Electric Steel 1.04% C .36% Mn	Wound cold	430-470 Brinell	194000	126000 Y.P.	237000	0 to 93000‡	"
2.69	.56	4.8	6½	High Carbon Open Hearth Steel .91% C .38% Mn	Wound hot O.Q. 1575°F D. 940°F	438-450 Brinell	173000	118000 Y.P.	225000	0 to 68000‡	"
2.69	.56	4.8	6½	Beryllium Bronze Be 97.60% Cu 2.38%	Wound cold Heated 2 hrs. at 520°F after coiling	303 Brinell	110000	95000 Y.P.	166000	0 to 33000‡	"

3.75	¾	5	7½	Carbon O.H. Steel 1.05% C .36% Mn	Wound hot O.Q. 1620°F D. 700°F		153100	119000 Y.P.	206200	0 to 72700	Edgerton[5]
2.25	¾	3	7½	"	"		153100	119000 Y.P.	206200	0 to 92200	"
3.75	¾	5	7½	Carbon Electric Steel 1.05% C .21% Mn	Hot wound O.Q. 1640°F D. 700°F		164200	94500 Y.P.	205200	0 to 58200††	"
3.75	¾	5	7½	Silicon Vanadium Steel .63% Si .17% Va	Hot wound O.Q. 1570°F D. 850°F		175000	129000 Y.P.	205000	0 to 62800	"
3.75	¾	5	7½	Carbon Electric Steel	Hot wound O.Q. 1550°F D. 850°F		171000	129000 Y.P.	200600	0 to 75600	"
1⅞	.135	14		Valve Spring Carbon Steel .63% C .72% Mn	Q 1650°F D. 900°F Wound cold Heated at 600°F	43 Rock. C	171000	98000 E.L.	214000	0 to 68000 20000 to 86000 40000 to 105000	Tatnall[6]
1⅞	.135	14		Commercial Carbon Steel .50% C .89% Mn	Q 1650°F D. 800°F	44.5 Rock. C	178000	107000 E.L.	228000	0 to 53000 20000 to 70000 40000 to 85000	"
1⅞	.135	14		Cold Drawn Commercial Carbon Steel		30 Rock. C	145000		191000	0 to 46000 40000 to 85000	"
.437	.063	7		Music Wire	Cold Wound Heated at 500-535°F after winding					0 to 76000	Hengsten-berg[7]
1.9	.225	8.4		"	"					0 to 65000	"
1.75	.250	7		"	"					0 to 56000	"
1.77	.225	7.9		Electric Carbon Steel .8-.95% C .5% Mn	Heat treated after forming	390-425 Brinell				0 to 69000	"
2.0	.250	8		Carbon Steel .55-.7% C .9-1.2% Mn	Cold wound Heated at 500-535°F after winding					0 to 56000	"

* All stress values corrected for bar curvature and direct shear by multiplying by stress correction factor K. All values refer to compression springs except where otherwise noted.

** Low values attributed to surface injury due to drawing. Tension springs used in these tests.

*** No cracks shown by magnaflux test of springs.

§ Q. and D. = quenched and drawn; O.Q. = oil quenched; C.D. = cold drawn.

† After shot-blasting.

‡ These values estimated for 10^7 cycles. Actua ltests run to 10^6 cycles ony.

†† Low value probably due to incorrect heat-treatment.

††† In all of Zimmerli's tests wire showing surface defects was rejected.

§§ Where more than one stress range is listed for a given material these correspond approximately in most cases to actual stress ranges used in the tests. Thus, for example, in the fifth row of the table, for CrVa spring steel, tests showed that springs of this material will withstand indefinitely a stress range from 12,000 to 84,000, from 23,000 to 92,000 or from 50,000 to 105,000 lb./sq. in. From these figures endurance diagrams similar to *Fig.* 56 may be drawn.

1 *Proc. Inst. Mech. Engrs.*, Vol. 120, 1931, p. 661.
2 *Univ. of Michigan Engineering Research Bul.* No. 26.
3 *Machine Design, Nov.* 1940, p. 62.
4 *Iron Age*, March 15, 1934, p. 12.
5 *Trans. A.S.M.E.*, Oct. 1937, p. 609.
6 *Wire and Wire Products*, Oct. 1937, p. 577.
7 Tests carried out at Westinghouse Research Laboratories.

summarized in TABLE VII are those by Johnson[13] at Wright Field and those made under the direction of the special research committee on Mechanical Springs of the A.S.M.E. and reported by Edgerton[14]. Both of these investigations covered tests on the larger sized helical springs (around ¾-inch bar diameter) and were made using a stress range from zero to maximum.

TABLE VIII gives a summary of expected limiting stress range as estimated from the data of TABLE VII and assuming a low minimum stress, say below 10,000-20,000 pounds per square

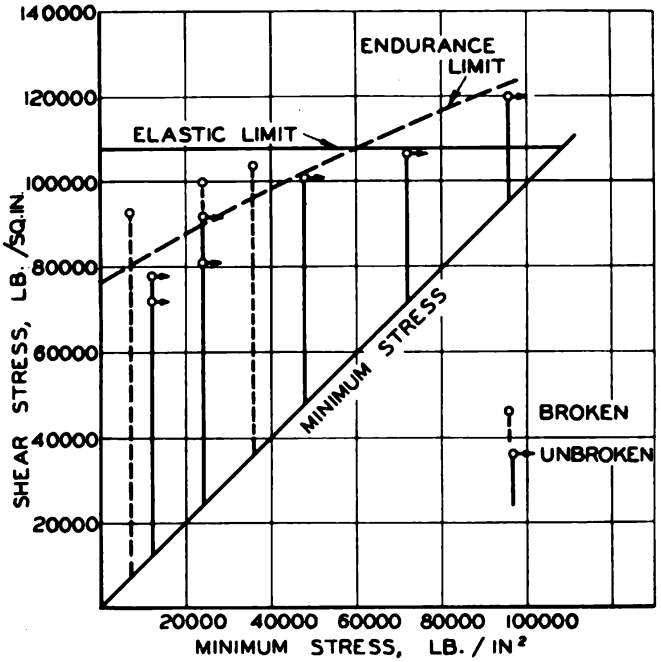

Fig. 56—Typical diagram of endurance tests on helical springs of chrome-vanadium steel. From tests by Zimmerli

inch. This table covers the smaller wire sizes. Thus the limiting stress range of 60,000 for cold-wound carbon steel wire means that the spring will withstand a range of 60,000 pounds per square inch from a low minimum stress, i.e., ranges such as 0 to 60,000, 5,000 to 65,000, or 10,000 to 70,000 pounds per square inch. The figures refer to results as estimated from tests reported by various in-

[13] "Fatigue Characteristics of Helical Springs", *Iron Age*, March 15, 1934, Page 12.

[14] "Abstract of Progress Report No. 3 on Heavy Helical Springs", *Transactions* A.S.M.E. October, 1937, Page 609.

vestigators. As will be seen there are considerable differences between the results reported by different investigators for the same or similar materials. The reason for this is that the quality

TABLE VIII

Limiting Stress Ranges Small-Size Helical Springs*

(Assuming Range from Minimum Stress Near Zero)

Material	Approx. Wire Dia. (inches)	Index (D/d)	Limiting Stress Range§ (lb./sq. in.)	Investigator
Cold-drawn wire	.13-.16	10-11	41000** 31000**	Lea & Dick
	.16	6	60000	Zimmerli
	.135	14	46000	Tatnall
Music wire	.25	8	56000	Hengstenberg
	.063	7	76000	"
	.148	6-7	70000	Zimmerli
	.148	6-7	115000†	"
Valve spring wire .65% C	.162	6.5	75000	"
			115000†	"
	.135	14	68000	Tatnall
Carbon steel wire (Cold wound)	.148	7.4	60000	Zimmerli
	.148	7.4	52000	"
	.135	14	53000	Tatnall
	.25	8	56000	Hengstenberg
Cr-Va steel SAE 6150	.148	7.4	70000	Zimmerli
			115000†	"
Stainless steel 18-8	.148	6-7	45000	"
			90000†	"
Phos bronze SAE 81	.148	6-7	15000	"
			30000†	"

* Values computed by using factor K to take into account bar curvature and direct shear. Compression springs used except where noted.
† Shot blasted.
** Values obtained on tension springs.
§ Maximum stress of range found by adding minimum stress to stress range given in this column. Thus for CrVa steel range might be 0 to 70,000, 5000 to 75,000, or 10,000 to 80,000 lb./sq. in. Variations in range listed for the same type of material may be due to differences in quality of material or to differences in spring index or wire size.

of the material may be different and the wire size or spring index may vary. These factors may change the limiting endurance range. Thus from TABLE VIII for cold-wound carbon steel the limiting ranges as reported by various investigators are 60,000, 52,000, 53,000, and 56,000 pounds per square inch. Such variations may easily be expected even in materials supposedly the same. The low values of 41,000 to 31,000 reported by Lea and Dick on springs of cold-drawn wire may probably be explained by inferior quality of material and by the fact that tension springs were used in the tests.

Shot-Blasting—The large increase in endurance range of helical springs due to shot-blasting[17], or shot-peening as it is also

called, is especially noteworthy. By this process it appears possible to raise the endurance range to values which may be expected on ground and polished bars tested in torsion. Thus, from Zimmerli's tests, shot-blasted helical springs of chrome-vanadium steel will have an endurance range in zero to maximum torsion of 115,000 pounds per square inch. This compares with a value of 128,000 found by Johnson on ground and polished bars of chrome-vanadium steel for a range from zero to maximum in torsion[16] and with a value of only 70,000 pounds per square inch for springs without the shot blasting treatment. (TABLE VIII).

For satisfactory results a proper size of shot and peening intensity must be used. Manufacturers frequently check the latter by means of a standard A-type specimen, 3 inches long by ¾-inch wide by .051-inch thick treated to Rockwell *C* 44-50. This strip is supported on a heavy plate and subjected to the same intensity of shot blast as the spring. After peening the deflection of the strip is measured on a 1.25-inch chord. From

TABLE IX

Limiting Stress Ranges for Larger-Sized Helical Compression Springs*

(minimum stress near zero)

Material	Bar Diameter (in.)	Index (D/d)	Limiting Stress Range (lb./sq.in.)	Investigator
O.H. Carbon steel	.56	4.8	68000	Johnson
	.75	5.0	72700	Edgerton
Cr.-vanadium steel	.56	4.8	77000	Johnson
Beryllium bronze	.56	4.8	33000	Johnson

See footnote of Table VIII.

data obtained from J. O. Almen the following values are satisfactory: For ½-inch wire diameter springs, shot size .040 and deflection .016-inch on a 1.25-inch chord with the standard *A* specimen. For coil springs and torsion bars of 1.25-inch diameter bar or larger, shot size .060, deflection .012 to .015-inch on a *C* specimen which has a thickness of .0938-inch but is otherwise similar to the *A* specimen. For flat springs .020-inch thick, shot size .013, deflection .003-inch on an *A* specimen[15].

[15]Additional data on this is given in the articles: Zimmerli—*Machine Design*, Nov. 1940, Page 62. "New Trails in Surface Finishing", *Steel*, July 5, 1943, Page 102. J. O. Almen—"Peened Surfaces Improve Endurance of Machine Parts", *Metal Progress*, Feb., May, Sept. 1943. "Improving Fatigue Strength of Machine Parts", *Mechanical Engineering*, Aug. 1943, Page 553.

[16]Chapter XXIII gives more data on endurance limits of spring materials (as distinct from those of helical springs).

It should be noted that the high endurance ranges which are obtained from shot blasting cannot ordinarily be utilized in de-

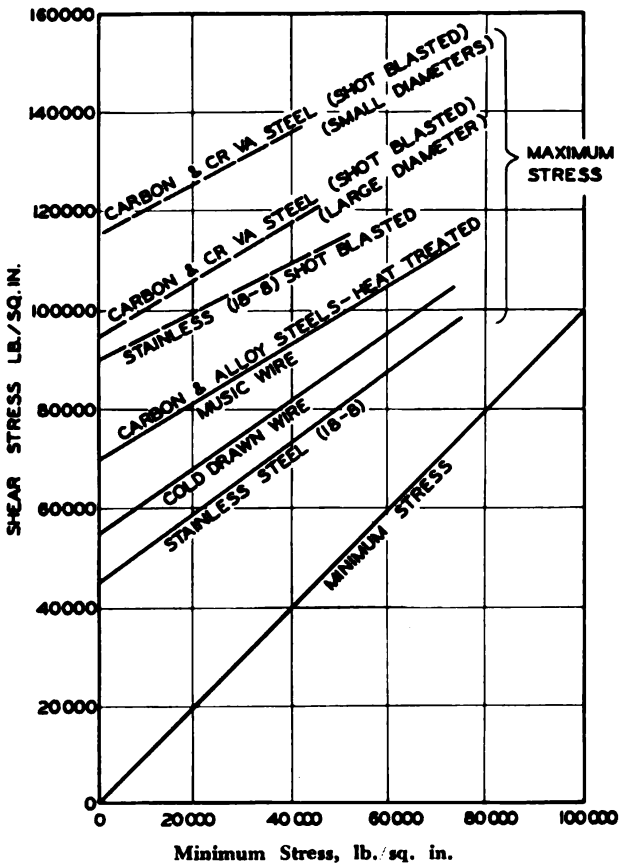

Fig. 57—Approximate endurance diagrams for good quality helical springs. Limiting stress range read vertically between line of minimum stress and lines for each material representing maximum stress. Curvature correction factor K used

sign, since, if too high a stress is used, excessive creep or load relaxation may occur. (This is discussed in Chapter V). However, the use of the shot-blast treatment greatly reduces the danger of fatigue failure so that the problem becomes mainly one of avoiding excessive set or load loss.

Large-Size Springs—Estimated limiting stress ranges for low minimum stresses for the larger-sized springs are summarized in TABLE IX.

On the basis of the data given in TABLES VII and IX, the curves of *Fig.* 57 showing the value of endurance ranges which may be expected from good-quality helical compression springs have been plotted. These curves hold roughly for springs having indexes between 5 and 10. For larger indexes, somewhat lower values may be expected and vice versa for the smaller indexes. Since these curves represent rough average values, considerable deviation in individual instances may be obtained. Because of stress concentration near the hook ends of tension springs, somewhat lower values of endurance ranges than those given in *Fig.* 57 may also be found.

FATIGUE TESTS ON SPRINGS WITH FEW STRESS CYCLES

Not much data appears to be available in the literature for helical springs subject to but a small number of stress cycles. The following data may be mentioned. Zimmerli[11] found on .148-inch diameter valve spring wire (SAE 6150, index 7.4) a life of 166,000 to 192,000 cycles for a stress range of 86,000, the minimum stress being 7100 pounds per square inch (curvature correction included in this and following data). Edgerton[14] found a life varying from 120,000 to 250,000 cycles for hot-wound carbon steel springs of index 5 at a stress range of 100,000 pounds per square inch (minimum stress zero). H. O. Fuchs[17] made tests on 7 springs of centerless ground wire (446 Brinell) shot-peened and preset, .648-inch diameter wire, index 7.3. These had a life varying from 170,000 to 409,000 cycles at a stress range between 43,000 minimum to 138,000 pounds per square inch maximum. On 9 similar springs of .628-inch diameter wire, the life varied from 73,000 to 178,000 cycles at a stress range between 49,000 to 151,000 pounds per square inch.

The fatigue test data given in this chapter apply only for springs at normal temperature with no corrosion present. In particular, shot blasting begins to lose its effectiveness at temperatures about 500 degrees Fahr. [15]. It should be emphasized that the full values of stress ranges found in fatigue tests should not be used in design. As discussed in Chapter I, a margin of safety to take into account unavoidable uncertainties, is required.

[17] Private communication.

CHAPTER V

HELICAL SPRINGS UNDER STATIC LOADING

Calculation of stress in helical springs based on elastic theory has been treated extensively in Chapter II. It should be noted, however, that such calculations based on proportionality between stress and strain do not apply rigidly after the elastic limit or yield point of the material has been exceeded. Although the formulas given in Chapter II are of basic importance in practical design, a consideration of what happens when the elastic limit of the material has been exceeded is of value in

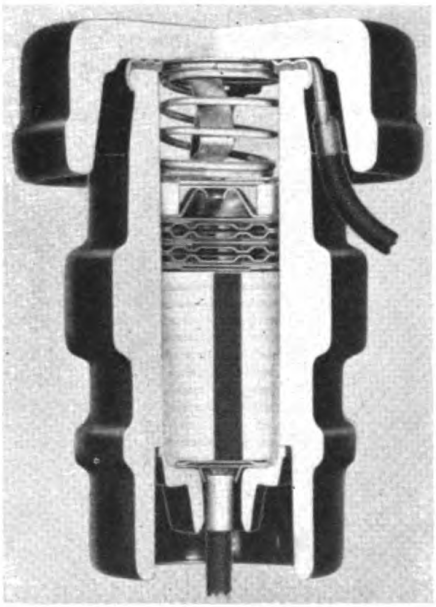

Fig. 58—Statically loaded helical spring in lightning arrester

the determination of allowable stress for helical springs. In the present chapter, a rational basis for the choice of working stress in springs under *static* loading based on such considerations will be outlined, while in Chapter VI the question of *fatigue* or *variable* loading will be discussed.

A statically-loaded helical spring may be defined as one subject to a constant load or to a load repeated but a relatively few times during the life of the spring. A spring loaded less than about 1000 times during its life would usually be considered as statically loaded in contrast to fatigue loading involving possibly millions of cycles.

Some of the more important applications of statically-loaded helical springs have already been mentioned in Chapter I. These include safety-valve springs, springs to provide gasket pressure (*Fig.* 6) and springs in mechanisms which operate only occasionally. Innumerable other applications might also be cited, such as the springs in lightning arresters *Fig.* 58. Here the function of the spring is to maintain a definite space relationship between the disks of the arrester, regardless of temperature change.

When a spring is subject to fatigue or repeated loading, failure may occur by the development of a fatigue crack which causes eventual fracture of the spring (*Fig.* 25). Fracture of the material practically never occurs, however, where springs are subject to static loads; in such cases the designer must guard against excessive creep or loss in load (which takes place if too-high working stresses are used). These effects are particularly pronounced at elevated temperatures. If a small amount of creep or load loss can be tolerated, a higher working stress may be used than would be the case otherwise.

A factor which is of particular importance in the design of helical springs subject to static loading is the *spring index*, i.e., the ratio between coil diameter and wire diameter. Where the spring index is small, the highest stress is concentrated near the inside of the coil. When the load is calculated by taking this stress into account, as will be seen later, a higher value is permissible for small index springs than would be the case for springs of larger indexes.

STRESS CALCULATIONS

Assuming that the peak stress is below the elastic limit, in a spring of small index subject to a static load and normal operating temperature, the stress distribution along a transverse diameter is shown approximately by the line *bc* in *Fig.* 59*a*. The

peak shearing stress *ab* in this case is calculated by Equation 18 which is based on elastic conditions.

From *Fig.* 59*a* it is seen that, for a spring of small index, the stress *ab* on the inside of the coil is much larger than the stress *a'c* on the outside of the coil, i.e., most of the high stress is con-

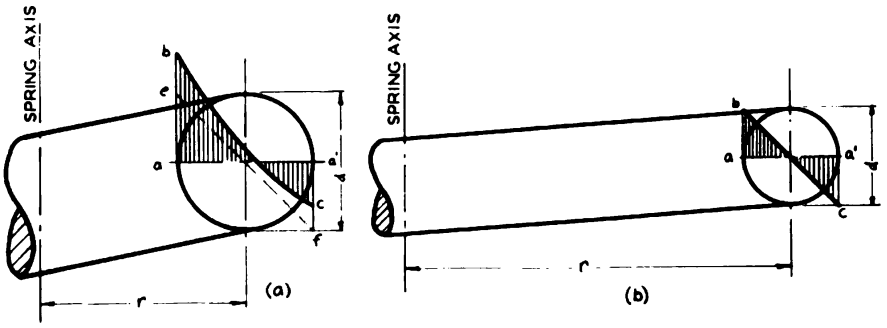

Fig. 59—Distribution of stress along transverse diameter of bar of helical spring (elastic conditions). Small index at *a*, large index at *b*

centrated near point *a*. This means that a condition of *stress concentration* exists, as is shown graphically by *Fig.* 60*a* where the peak stress is concentrated in the relatively small shaded area near *a*.

When the spring index is large, conditions are considerably different, as shown in *Fig.* 59*b*. Here the stress *ab* on the in-

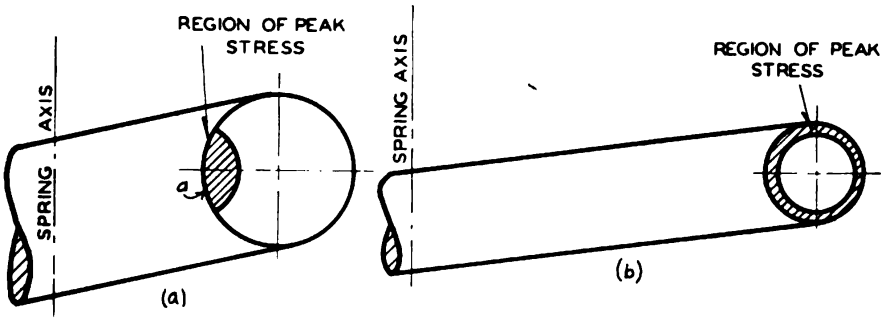

Fig. 60—Relative distribution of regions of peak stress in cross-section of bar of helical spring, small index at *a* and large index at *b* (for the spring of small index most of the stress is concentrated near the inside of the coil at *a*)

side of the coil is only a little larger than the stress *a'c* on the outside. In this case the peak stress is given approximately by taking $K=1$ in Equation 18. This follows from Equation 19

which reduces to $K=1$ for very large value of the index c. For large indexes the highest stresses are located in the ring-shaped shaded area shown in *Fig. 60b* instead of being concentrated in a relatively small region near the inside of the coil as is the case where the index is small (*Fig. 60b*). In other words, in the case of the spring of small index only a relatively small portion of its cross-sectional area is subject to stresses near the peak, while

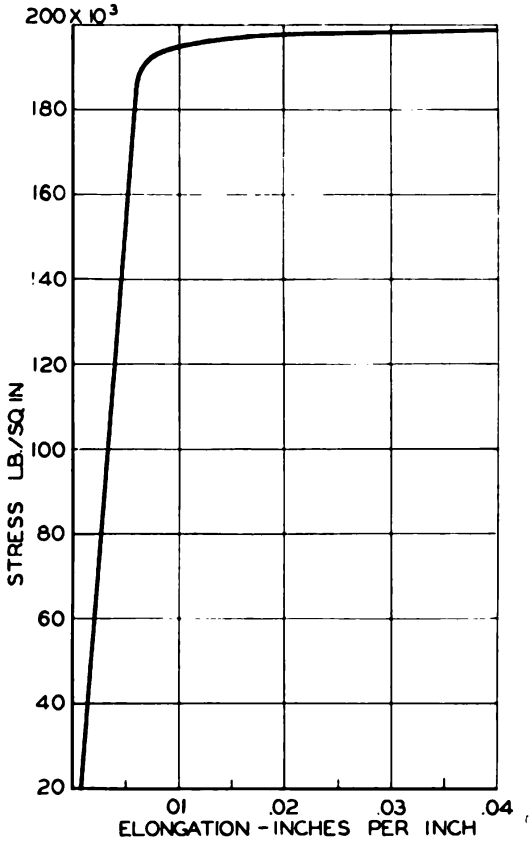

Fig. 61—Stress-strain diagram for chrome-vanadium spring steel

in the case of the spring of large index, a relatively large part of the cross section is subject to such stresses. Hence if the load is increased so that yielding occurs over the entire cross-section of the bar or wire it is clear that the spring of small index will be able to carry a much larger load than would be expected on the basis of the maximum stress calculated from Equation 18 which assumes purely elastic conditions. The reason for this is that, after the elastic limit is passed and yielding be-

gins, most of the cross-section will be effective in carrying load even for small indexes; since a good share of the cross-section of the spring of large index is already subject to stresses near the peak, the increase in load necessary to produce complete yielding over the entire section will not be so great as in the case of the small index spring, where only a small part of the section is initially subject to stresses near the peak.

Most helical spring materials have considerable ductility (although, of course, much less than have structural materials). For example, a tension stress-strain diagram of a typical chrome-vanadium steel as used for small helical springs[1] is shown in *Fig.* 61. It is seen that this has a shape of tensile stress-strain diagram characteristic of a ductile material with a fairly sharply defined yield point. Since most of the useful spring materials have elongations greater than 5 per cent in 2 inches, and stress-strain diagrams similar to that of *Fig.* 61, (although they may have a greater slope after the yield point has been passed) it appears reasonable to treat these as ductile materials. In such cases, where static loads are involved, as brought out in Chapter I, it is usual practice to neglect stress concentration effects in design[2]. This means that the stress augment to bar curvature (which may be considered a stress concentration effect) may be neglected in calculating the stress under static-load conditions.

Calculations Neglecting Curvature—To calculate the stress in the spring by neglecting stress concentration due to bar or wire curvature, the procedure is as follows: Assuming a helical compression or tension spring under a load P and neglecting effects due to the end turns and pitch angle, the torsion moment at any point along the bar will be equal to Pr while the direct shear will be equal to P. The distribution of torsion stress along a transverse diameter due to the moment Pr will be as shown in *Fig.* 62*a* while the peak torsion stress τ_1 due to this moment alone will be that given by the usual formula (Equation 4). Thus

$$\tau_1 = \frac{16Pr}{\pi d^3} \qquad (86)$$

On this stress must be superimposed the shear stress τ_2 due to

[1] *Engineering Research Bulletin* No. 26, University of Michigan, gives other similar diagrams.

[2] "Working Stresses"—C. S. Soderberg, *Transactions* A.S.M.E., 1933, APM 55-16.

the direct shear load P, which for our purposes may be considered uniformly distributed over the cross-section[3]. This stress will be assumed distributed as shown in *Fig.* 62*b* and is

$$\tau_2 = \frac{4P}{\pi d^2} \quad (87)$$

Maximum stress will be obtained by superposition of the distributions of *Fig.* 62*a* and *b* giving a resultant distribution shown in *Fig.* 62*c*. The maximum stress, τ_m, thus obtained by neglecting stress concentration effects, is

$$\tau_m = \tau_1 + \tau_2 = \frac{16Pr}{\pi d^3} + \frac{4P}{\pi d^2} \quad (88)$$

This equation may be written

$$\tau_m = \frac{16Pr}{\pi d^3} K_s \quad (89)$$

where

$$K_s = 1 + \frac{.5}{c} \quad (90)$$

The factor K_s, which will be called a *shear-stress multiplication factor* is plotted as a function of spring index c in *Fig.* 63.

Thus for static loads it appears logical to use Equation 89 (derived on the assumption that stress concentration effects may be neglected). In order to form an idea of the margin of safety of the spring against yielding, the stress computed by Equation 89 should be compared with the yield point of the material in torsion, which for most spring materials may be taken as about 57 per cent of the tension yield point.

LOAD FOR COMPLETE YIELDING

There is a somewhat different (and perhaps more logical) approach to the problem of designing a spring for static load

[3]Actually there will be some non-uniformity in the distribution of the shear stress but since this will have a similar effect to that of stress concentration due to bar curvature it will be neglected.

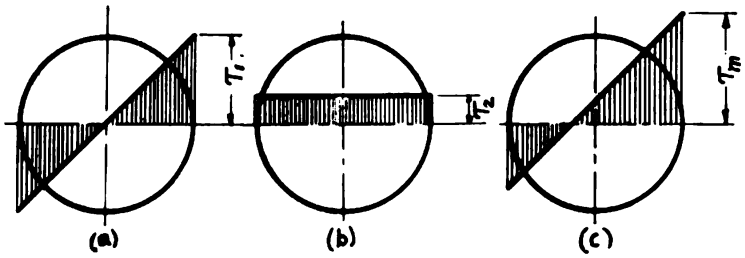

Fig. 62—Superposition of stresses in helical spring—stress concentration due to bar curvature neglected. At *a* is shown stress due to torsion moment, *b* is stress due to direct shear, and *c* superposition of stresses shown at *a* and *b*

conditions. This method is based on the consideration of the load required to produce complete yielding of the material in the spring, the working load being then taken as a certain percentage of the load required to produce complete yielding. If a spring material gives a stress-strain curve similar to that of *Fig.* 61, it may be expected that after exceeding the yield point the distribution of stress across a transverse diameter will be something like that shown in Fig. 64*a* for a spring of small index and in *Fig.* 64*b* for one of large index. Actually it may be expected that for many materials some rise in the stress-strain

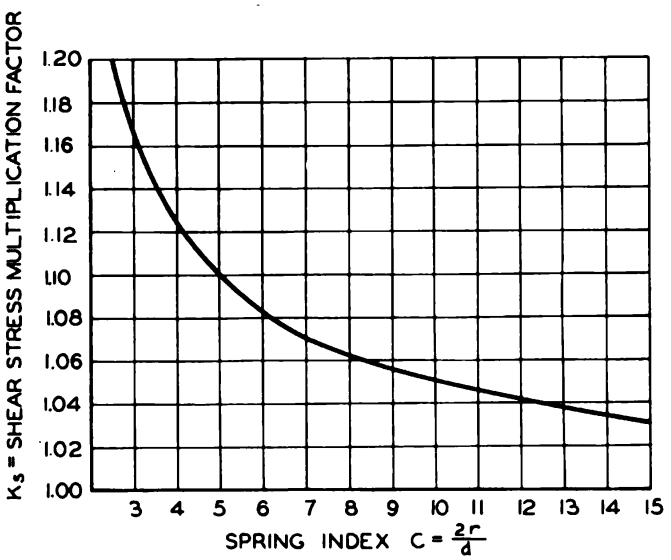

Fig. 63—Curve for finding shear stress multiplication factor K_s. This factor takes into account effects due to direct shear load but not to bar curvature

curve after passing the yield point will take place due to the cold working effect so that actually the curves of *Fig.* 64 will be approximately trapezoidal in form. However, the assumption of a rectangular distribution, which lends itself to simplicity in analysis, will be sufficiently accurate. Because of the necessity for carrying a considerable direct-shear load, particularly where

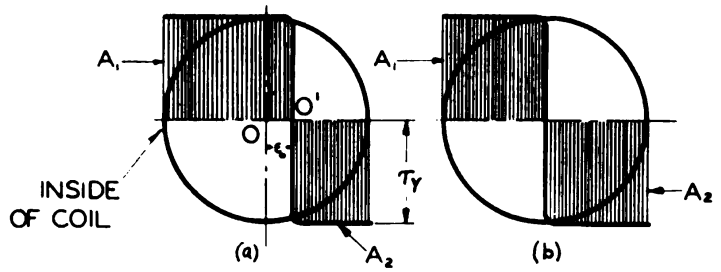

Fig. 64—Assumed distribution of torsion stress under plastic conditions for springs of different indexes. At *a* is shown small index, large index at *b*. For the smaller indexes the area A_1 is much greater than A_2 to take care of the direct shear load

the spring index is small, it may be expected that in such cases the area A_1 will be greater than A_2 in *Fig.* 64*a*. On the other hand, if the index is large, these two areas will be about the same, *Fig.* 64*b*. Due to this effect, the point O' where the stress is zero is shifted by an amount ϵ_0 from the geometrical center O.

The calculation of the load P_y at which complete yielding over the entire cross section occurs represents a problem in plastic flow which is extremely complicated for low index springs. This is true since a determination of the directions of the resultant shear stress at all points of the cross section under yielding is necessary to evaluate the shear force and moment. However, an approximate solution based on reasonable assumptions may be obtained as follows:

It is assumed that the directions of the resultant shear stress during yielding at all points of the cross section may be represented by a series of circles as shown in *Fig.* 65*a*. The centers of successive circles are displaced so that each circle intersects the transverse axis BB' at equal intervals between BO' and $O'B'$ where O' represents the point of zero stress (the line BB' represents an axis transverse to the spring axis). If no strain hard-

ening is assumed, i.e., if the resultant shear stress is taken equal to the shearing yield point τ_y at all points and the direction taken along each circle, it is possible to calculate the resultant moment and shear load for a given displacement ϵ_o of the point O' from the center O. From this the spring index may be found.

Referring to *Fig.* 65*b*, the circle with center at A represents one of the circles of *Fig.* 65*a*. On the basis of the assumption of equal spacing of the points of intersection of the circles between $O'B$ and $O'B'$, the radius ρ' of this circle will be

$$\rho' = \frac{O'D}{1 - \frac{2\epsilon_o}{d}} \quad \ldots\ldots (91)$$

Using this formula for any point D along $O'B$, a series of circles may be constructed as in *Fig.* 65*a*.

Considering a small element dA at radius ρ and angle θ, *Fig.* 65*c*, this element will be acted on by a shear force $\tau_y dA$ making an angle ψ with the radius OC. The area is

$$dA = \rho d\rho d\theta \quad \ldots\ldots (92)$$

The moment of this shear force about the center O will be

$$dM_y = \tau_y (\sin \psi) \rho dA$$

Using Equation 92 in this,

$$dM_y = \tau_y (\sin \psi) \rho^2 d\rho d\theta) \quad \ldots\ldots (93)$$

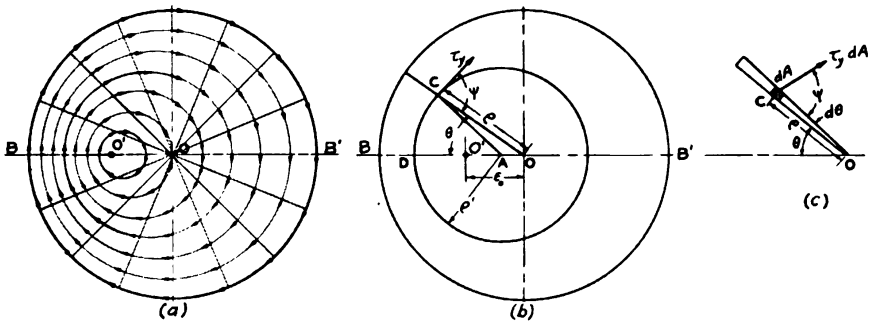

Fig. 65—Schematic diagram of resultant shear stress direction over cross section for low index helical spring under yielding. Point of zero stress O' is displaced from geometrical center O away from spring axis

The total moment acting will be the integral of these elementary moments over the whole cross section. Thus the moment M_y for complete yielding over the section becomes

$$M_y = \int_0^{d/2} \int_0^{2\pi} \tau_y (\sin \psi) \rho^2 d\rho d\theta \quad \ldots\ldots (94)$$

In this $\sin \psi$ is a complicated function of both ϵ_o, ρ and θ and for this reason integration of Equation 94 in general terms is difficult. However, by assuming a given ϵ_o and d and by drawing the circles as shown in *Fig.* 65*a*, the value of $\sin \psi$ can be found for any given angle θ and radius ρ. Drawing equally spaced radii from the center of the cross section O as indicated in *Fig.* 65*a* and plotting the value of $\tau_y \rho^2 \sin \psi$ along each radius as a function of distance ρ, the integral of Equation 94 may be evaluated. This involves the determination of the area under the curve for each radius, multiplying by a constant depending on the angular spacing of the radii and adding the total. In this way the total moment M_y for a given ϵ_o and d may be obtained.

The resultant shear load P_y over the cross section may be obtained in a similar manner. Referring to *Fig.* 65*c* the vertical component of the shear force acting on the element dA is

$$dP_y = -\tau_y \sin(\psi - \theta) dA$$

The negative sign is used since the shear force is considered positive downward. Using the expression for dA given by Equation 92 in this

$$dP_y = -\tau_y \sin(\psi - \theta) \rho d\rho d\theta \quad \ldots\ldots (95)$$

The total vertical shear force P_y acting over the section for complete yielding will be the integral of these elementary forces taken over the section. Hence

$$P_y = -\int_0^{d/2} \int_0^{2\pi} \tau_y \sin(\psi - \theta) \rho d\rho d\theta \quad \ldots\ldots (96)$$

Again this may be evaluated by drawing circles as in *Fig.* 65*a*, drawing equally spaced radial lines, measuring $\psi - \theta$, and plotting the function $\tau_y \rho \sin(\psi - \theta)$ along each radius, and finding the area under each curve. By adding these with proper

algebraic sign and multiplying by a constant, the resultant shear force P_y for a given ϵ_o and bar diameter d is found.

Since $M_y = P_y r$ where r = coil radius,

$$r = \frac{M_y}{P_y}$$

Hence, if the values of M_y and P_y obtained by graphical or numerical integration of Equations 94 and 96 are known, the coil radius r may be found for a given ϵ_o and d. From this the spring index $2r/d$ is obtained.

If it is assumed that the spring is essentially a straight bar acted on by a torsion moment $M_y' = P_y' r$, direct shear being neglected, the value of M_y' for constant yield stress τ_y is

$$M_y' = 2\pi \int_0^{d/2} \tau_y \rho^2 d\rho = \frac{\pi d^3 \tau_y}{12} \quad \ldots\ldots\ldots\ldots\ldots\ldots\ldots\ldots\ldots\ldots\ldots\ldots\ldots\ldots\ldots\ldots (97)$$

Comparing this equation with Equation 3, it is seen that the moment M_y' (or load P_y') for complete yielding of a large index spring is about 33 per cent higher than that at which yielding starts (obtained from Equation 3 by taking $\tau_m = \tau_y$). In actual springs because of strain hardening and other effects, higher percentage values may be expected, however.

By comparing values of M_y' (Equation 97) for a large index spring and M_y (Equation 94) for a small index spring, an estimate of the effect of the direct shear load is possible. The ratio M_y'/M_y may be considered comparable to the factor K_s (Equation 90) derived previously by neglecting stress concentration effects. Although a complete solution of this problem obtained by using Equations 94 and 97 for various spring indexes is not available at this writing, the indications at present are that the ratios M_y'/M_y are considerably less than K_s as given by Equation 90. However, because of possible inaccuracies in the assumptions made regarding the shear stress directions, *Fig.* 65*a*, and because of strain hardening effects not considered, the more conservative value of K_s given by Equation 90 will be retained for design purposes.

If the yield stress in torsion τ_y is known, the load at which complete yielding of the spring occurs (where the load deflec-

TABLE X

Load and Deflection per Turn for Statically-Loaded Helical Springs*

Outside Diameter of Springs (inches)

Wire Diam. inches		1/8	5/32	3/16	1/4	5/16	3/8	7/16	1/2	5/8	3/4	7/8	1	1-1/8	1-1/4
.014	P	.912	.720	.596	.441	.352	.293								
	y	.0228	.0378	.0570	.106	.172	.253								
.016	P	1.372	1.09	.900	.664	.529	.438	376							
	y	.0189	.0319	.0478	.0910	.1465	.218	.302							
.018	P	1.98	1.55	1.275	.952	.753	.625	.538	.470						
	y	.0162	.0273	.0413	.0794	.1285	.191	.266	.352						
.020	P	2.73	2.15	1.76	1.31	1.04	.860	.735	.644						
	y	.0139	.0238	.0365	.0702	.114	.169	.234	.312						
.022	P	3.66	2.87	2.37	1.75	1.395	1.145	.981	.855	.686					
	y	.0119	.0207	.0319	.0620	.102	.151	.208	.279	.449					
.024	P	4.77	3.76	3.07	2.28	1.81	1.50	1.27	1.115	.888					
	y	.0104	.0183	.0284	.0557	.0918	.137	.191	.254	.410					
.026	P	6.15	4.80	3.97	2.92	2.31	1.91	1.62	1.42	1.13					
	y	.00915	.0163	.0257	.0499	.0830	.125	.173	.231	.373					
.028	P	7.76	6.08	4.93	3.66	2.90	2.39	2.03	1.77	1.41	1.18				
	y	.00811	.0146	.0228	.0457	.0756	.114	.160	.214	.344	.506				
.030	P	9.60	7.5	6.12	4.52	3.59	2.93	2.52	2.19	1.74	1.445				
	y	.00715	.0130	.0206	.0416	.0685	.1045	.1475	.198	.317	.468				
.032	P	11.8	9.12	7.52	5.47	4.31	3.56	3.07	2.66	2.12	1.77	1.51			
	y	.00638	.0116	.0188	.0383	.0638	.0960	.1365	.182	.294	.437	.603			
.034	P	14.4	11.1	9.07	6.64	5.22	4.32	3.68	3.23	2.54	2.12	1.80	1.56		
	y	.00574	.0106	.0172	.0351	.0591	.0899	.1265	.170	.275	.407	.563	.762		
.036	P		13.3	10.8	7.94	6.21	5.14	4.35	3.82	3.01	2.51	2.15	1.86		
	y		.00962	.0156	.0327	.0549	.0835	.118	.159	.257	.382	.529	.701		
.038	P		15.6	12.8	9.32	7.30	6.05	5.15	4.52	3.54	2.97	2.54	2.20	1.96	
	y		.00869	.01435	.0299	.0508	.0782	.1105	.150	.241	.361	.500	.662	.842	
.040	P		18.3	15.1	10.9	8.55	7.05	6.05	5.23	4.16	3.42	2.96	2.57	2.28	
	y		.00792	.0132	.0277	.0475	.0728	.104	.140	.228	.338	.472	.625	.800	
.042	P		21.6	17.5	12.8	9.80	8.24	7.00	6.06	4.84	3.99	3.40	2.98	2.65	2.37
	y		.0073	.0121	.0259	.0439	.0685	.0978	.132	.217	.320	.445	.591	.760	.941
.044	P			20.1	14.6	11.45	9.46	8.06	6.98	5.57	4.62	3.92	3.41	3.03	2.72
	y			.0111	.0239	.0415	.0641	.0910	.1235	.204	.304	.419	.558	.717	.897
.046	P			23.2	16.8	13.2	10.85	9.21	8.01	6.35	5.27	4.48	3.92	3.48	3.14
	y			.0104	.0224	.0389	.0605	.0858	.118	.193	.289	.401	.533	.685	.856
.048	P			26.6	19.2	15.0	12.3	10.5	9.17	7.24	6.00	5.10	4.46	3.94	3.55
	y			.00952	.0209	.0368	.0571	.0821	.112	.185	.275	.380	.509	.651	.820
.051	P			32.5	23.1	18.1	14.9	12.6	10.9	8.68	7.20	6.13	5.35	4.74	4.27
	y			.00856	.0189	.0338	.0525	.0752	.103	.170	.256	.356	.476	.611	.763
.055	P				29.3	22.9	18.8	15.9	13.8	10.9	9.05	7.72	6.70	5.95	5.35
	y				.0166	.0302	.0472	.0685	.0933	.155	.234	.326	.434	.558	.704
.059	P				36.5	28.4	23.3	19.8	17.1	13.5	11.1	9.56	8.35	7.37	6.63
	y				.0147	.0268	.0426	.0620	.0853	.143	.212	.300	.403	.518	.649
.063	P				45.3	34.9	28.6	24.1	20.9	16.6	13.6	11.6	10.1	9.02	8.10
	y				.0131	.0241	.0385	.0565	.0778	.131	.198	.278	.372	.482	.603
.067	P				54.8	42.1	34.7	29.3	25.2	19.9	16.4	14.1	12.2	10.8	9.70
	y				.0117	.0218	.0354	.0519	.0715	.121	.183	.258	.347	.447	.557
.071	P					50.6	41.1	34.5	30.2	23.7	19.7	16.7	14.6	12.9	11.6
	y					.0197	.0319	.047	.0659	.111	.170	.241	.325	.417	.524
.074	P					57.4	46.8	39.7	34.2	27.1	22.3	18.9	16.5	14.7	13.2
	y					.0183	.0302	.0446	.0621	.106	.161	.229	.307	.398	.503
.078	P					68.0	55.5	46.8	40.3	31.8	26.0	22.3	19.4	17.2	15.4
	y					.0166	.0275	.0414	.0576	.0987	.150	.214	.289	.375	.471
.082	P					80.2	64.7	54.8	47.0	37.1	30.4	26.0	22.5	20.0	18.0
	y					.0152	.0252	.0382	.0535	.0925	.141	.202	.272	.353	.444
.086	P						75.5	63.3	54.9	42.9	35.1	29.9	26.0	23.1	20.8
	y						.0234	.0354	.050	.086	.132	.190	.256	.332	.420
.090	P						83.5	70.3	60.8	47.5	39.2	33.2	28.8	25.7	23.2
	y						.0212	.0326	.0462	.0808	.124	.178	.241	.314	.397
.106	P							122.	104.	81.2	66.8	57.0	49.2	43.4	38.9
	y							.0246	.0356	.0630	.0987	.143	.196	.255	.324
.121	P								159.	121.	101.	85.5	73.5	65.3	58.0
	y								.0283	.0516	.082	.120	.164	.217	.273
.135	P								224.	174.	141.	120.	103.	91.0	81.7
	y								.0230	.0431	.0695	.102	.141	.187	.239
.148	P									231.	188.	159.	137.	121.	108.
	y									.0367	.060	.0891	.124	.165	.212
.162	P									309.	249.	211.	183.	160.	142.
	y									.0311	.0517	.0778	.110	.145	.186
.177	P										330.	266.	240.	210.	187.
	y										.0442	.0668	.0955	.127	.165
.207	P													343.	303.
	y													.101	.132
.225	P														394.
	y														.116

*Effect of curvature neglected.

TABLE X (continued)

Wire Diam. inches		Outside Diameter of Springs (inches)													
		1-3/8	1-1/2	1-5/8	1-3/4	1-7/8	2	2-1/4	2-1/2	2-3/4	3	3-1/2	4	4-1/2	5
.048	P	3.25													
	y	.998													
.051	P	3.89	3.55												
	y	.937	1.12												
.055	P	4.85	4.45	4.11											
	y	.860	1.03	1.22											
.059	P	6.01	5.50	5.08											
	y	.782	.955	1.13											
.063	P	7.33	6.71	6.20	5.75										
	y	.737	.887	1.05	1.23										
.067	P	8.82	8.06	7.45	6.90	6.45									
	y	.686	.828	.985	1.15	1.32									
.071	P	10.5	9.58	8.87	8.22	7.68	7.20								
	y	.645	.775	.922	1.07	1.24	1.43								
.074	P	11.9	10.9	10.0	9.33	8.68	8.12								
	y	.610	.739	.876	1.03	1.19	1.36								
.078	P	14.0	12.7	11.7	10.9	10.2	9.54								
	y	.579	.696	.825	.970	1.12	1.28								
.082	P	16.3	14.8	13.6	12.7	11.8	11.1								
	y	.548	.656	.780	.915	1.06	1.22								
.086	P	18.7	17.2	15.7	14.7	13.6	12.8	11.3							
	y	.515	.624	.740	.870	.989	1.15	1.48							
.090	P	21.9	19.1	17.6	16.2	15.0	14.7	12.6							
	y	.490	.592	.702	.825	.946	1.09	1.40							
.106	P	35.4	32.5	29.9	27.6	25.7	24.1	21.2	19.1	17.3					
	y	.402	.487	.582	.681	.790	.905	1.15	1.46	1.78					
.121	P	52.9	48.4	44.4	41.1	38.4	36.1	31.7	28.5	25.9	23.8				
	y	.342	.415	.494	.582	.677	.780	1.00	1.25	1.53	1.85				
.135	P	73.6	66.7	62.0	57.5	53.6	50.0	44.4	39.5	35.9	32.9				
	y	.297	.367	.434	.510	.595	.685	.890	1.11	1.36	1.63				
.148	P	98.	88.7	81.5	75.5	70.8	66.0	59.1	52.5	47.5	43.5				
	y	.264	.320	.385	.455	.534	.612	.797	1.00	1.22	1.47				
.162	P	128.	117.	107.	100.	92.5	87.3	77.2	69.0	62.5	57.1				
	y	.235	.285	.342	.405	.473	.550	.715	.903	1.11	1.33				
.177	P	168.	154.	141.	131.	121.	114.	101.	90.5	81.8	74.8				
	y	.208	.255	.307	.364	.425	.493	.642	.811	.995	1.20				
.207	P	275.	250.	228.	211.	196.	183.	161.	145.	130.	121.	103.			
	y	.167	.206	.247	.296	.347	.403	.525	.670	.829	1.01	1.41			
.225	P	355.	321.	297.	271.	252.	236.	208.	187.	170.	154.	132.	114.		
	y	.147	.183	.223	.264	.311	.361	.475	.600	.746	.905	1.27	1.69		
.263	P	572.	520.	477.	437.	410.	381.	335.	300.	270.	249.	211.	184.	164.	
	y	.115	.145	.177	.212	.252	.295	.386	.492	.610	.748	1.05	1.41	1.83	
.283	P		653.	600.	550.	513.	478.	422.	375.	339.	311.	266.	232.	204.	183.
	y		.129	.159	.190	.226	.264	.351	.447	.556	.680	.962	1.30	1.67	2.10
.307	P			780.	709.	660.	615.	543.	483.	434.	396.	339.	296.	262.	236.
	y			.140	.169	.201	.235	.313	.401	.501	.611	.870	1.17	1.52	1.93
.331	P				897.	833.	775.	682.	608.	547.	498.	426.	370.	329.	294.
	y				.150	.180	.210	.282	.364	.454	.557	.793	1.07	1.39	1.75
.363	P					1110.	1030.	908.	811.	730.	668.	563.	487.	436.	390.
	y					.154	.182	.246	.320	.402	.494	.702	.950	1.24	1.57
.394	P						1330.	1170.	1040.	938.	858.	724.	630.	558.	499.
	y						.161	.218	.282	.358	.442	.631	.859	1.12	1.42
.430	P							1530.	1370.	1230.	1115.	950.	824.	725.	652.
	y							.189	.249	.315	.391	.565	.768	1.00	1.28
.460	P								1690.	1510.	1380.	1170.	1010.	892.	797.
	y								.224	.286	.354	.515	.700	.922	1.17
.500	P								2170.	1960.	1780.	1510.	1310.	1150.	1030.
	y								.196	.251	.311	.456	.630	.827	1.05

Stress of 100,000 lb./sq. in. is used for convenience. For any other stress τ, values of P (load in lb.) and y (deflection per turn) should be multiplied by $\tau/100{,}000$. Deflections are based on a torsion modulus $G=11.4\times10^6$. lb./sq. in. For any other value of G, deflections given should be multiplied by the ratio $11{,}400{,}000/G$.

tion diagram flattens out provided the spring does not become solid) may be calculated approximately for no strain hardening by solving Equation 89 for P and multiplying by 1.33. However, as indicated previously, for low index springs this calculated

load will usually be somewhat below the actual load obtained by tests since K_s as given by Equation 90 is probably somewhat high and since strain hardening effects come into the picture.

APPLICATION OF FORMULAS TO SPRING TABLES

To facilitate the application of Equations 89 and 7 in the design of statically loaded helical springs TABLE X, has been computed. This table gives loads and deflections per turn at a stress of 100,000 pounds per square inch and a torsion modulus of 11.5×10^6 pounds per square inch as computed from Equations 89 and 7 for various standard outside coil diameters and wire sizes. The music wire gage is used for sizes up to .090 and the National Wire Gage for sizes from .106 to ½-inch.

Although stresses of 100,000 pounds per square inch may actually be used in some practical cases, it should be noted that this stress is used in the table for convenience only and is not necessarily the recommended working stress. The actual working stress for a statically-loaded spring should be equal to the yield stress of the spring material divided by a factor of safety (Chapters IV and XXIII give data on the yield points of spring materials). If the yield stress in tension is known, the yield stress in torsion may be taken as about 57 per cent of that in tension. This factor .57 is based on the shear-energy theory discussed in Chapter 2. Values of factor of safety as used in practice may vary from 1.5 to as low as 1.25 in some cases.

To use TABLE X for any value of stress other than 100,000 pounds per square inch, the loads and deflections given in the table should be modified in the same ratio. As an example, assuming a spring of one inch outside diameter and .135-inch wire, from TABLE X the load and deflection per turn are 103 pounds and .141-inch, respectively, at 100,000 pounds per square inch stress figured from Equations 89 and 7. If the material used is music wire with an ultimate strength of 260,000 pounds per square inch in this size and a yield point in tension of about .8 this or 208,000 pounds per square inch, the yield point in torsion is then 57 per cent of this or about 120,000. Assuming a factor of safety of 1.5 based on the yield point is desired, this gives a working stress of $120000/1.5 = 80{,}000$ pounds per square inch. This means that the permissible loads

and deflections per turn, under these conditions would be 80 per cent of those given in the table. In the case cited, the allowable deflection per turn would be .80(.141) = .113-inch and the permissible load would be .80(103) = 82.5 pounds.

To facilitate computation for intermediate coil and wire diameters not given in TABLE X, the charts of *Figs.* 66 and 67 have been plotted. In *Fig.* 66 the ordinate represents load at

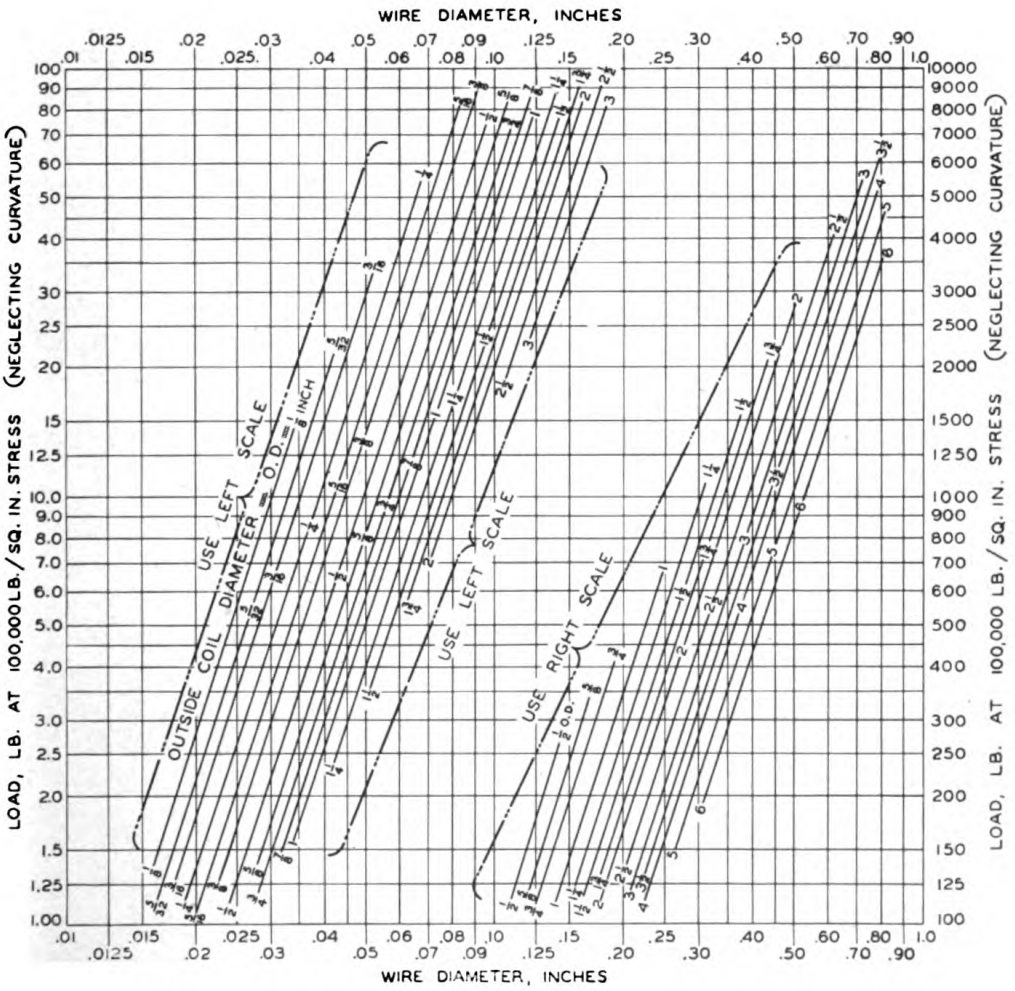

Based on a stress of 100,000 lb./sq. in. To find load at any other stress τ, loads given must be multiplied by $\tau/100{,}000$. Not to be used for fatigue loading

Fig. 66—Chart for calculating loads in statically-loaded helical springs

100,000 pounds per square inch torsion stress (calculated by neglecting the stress increase due to curvature) while the abscissa represents wire diameter. Each curve represents a given outside diameter of the spring. Thus for a wire size of .090-inch and an outside diameter of ½-inch the load at 100,000 pounds per square inch stress is about 61 pounds.

In *Fig.* 67 the deflections per turn represented by the ordinates are plotted against wire diameter for various outside coil diameters. Thus for a wire size of .106-inch and a coil outside diameter of ½-inch, the deflection per turn is .035-inch. It should be noted that a small error will result in reading the results from the charts of *Figs.* 66 and 67 and for best accuracy Equations 89 and 7 should be used. These charts, however, are sufficiently accurate for most practical purposes.

Curvature Effects—Frequently, spring tables or charts based on Equation 18 which yield the peak stress including curvature effects are available, (Chapter VII). These tables may also be used provided that the stress on which the table or chart is based be divided by a factor K_c where $K_c = K/K_s$, values of K and K_s being obtained from Equations 19 and 90. The value of K_c represents the stress concentration effect due primarily to wire or bar curvature, while K_s represents the increased stress due to the direct shear of the axial load. This follows since $K = K_c K_s$. For convenience in calculation, values of K_c are given in *Fig.* 68 as functions of spring index c. Thus, if a table or chart is based on a stress of 100,000 pounds per square inch and if the spring index is 6 and $K_c = 1.15$, the stress calculated by neglecting curvature would be 100000/1.15 or 87000 pounds per square inch. This latter would then be compared with the yield point.

Examples—As an example of this design procedure for statically-loaded springs, a spring may be considered of index 3, chrome-vanadium steel having a tension yield stress of around 190,000 pounds per square inch and a yield stress in torsion about 57 per cent of this or 110,000 pounds per square inch. Assuming that a factor of safety of 1.5 based on the yield stress in torsion is to be used, the working stress for the static-load condition as figured by using Equation 89 would then be 110,000/1.5 = 73,000 pounds per square inch. For an index 3, the factor $K_c = 1.35$ (*Fig.* 68); hence the allowable stress as figured by using Equation 18 (which includes curvature effects)

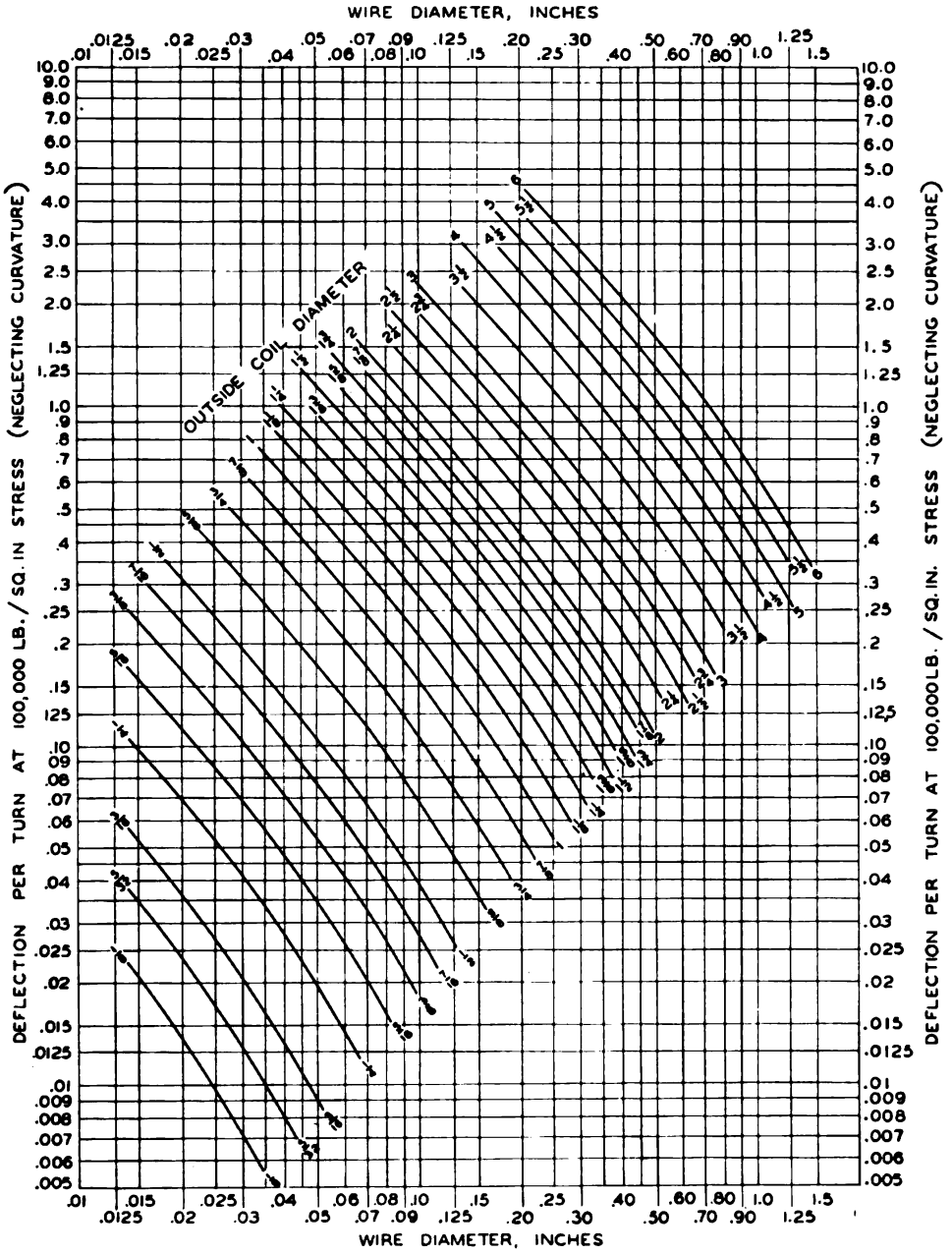

For any other stress τ, values should be multiplied by $\tau/100{,}000$. Also, if the modulus G is other than 11.4×10^6, values should be multiplied by 11,400,000/G

Fig. 67—Chart for calculating deflections in statically-loaded helical springs of round wire. Based on torsion modulus, $G = 11.4 \times 10^6$ lb./sq. in.

would be 73000 (1.35) = 98000 pounds per square inch. If charts based on this equation are used (such as those given in Chapter VII) the other spring proportions such as active turns, coil and wire diameters, free and solid heights, are determined.

As a second example: A spring has an index of 15 with other conditions the same as in the previous example. For an index 15, the factor $K_c = 1.06$ from *Fig.* 68. Again assuming an allowable stress figured by neglecting stress concentration, equal to 2/3 the yield stress in torsion or 73000 pounds per square inch, the allowable stress figured from Equation 18 would be 73000 (1.06) = 77,400 pounds per square inch. This stress is lower than the allowable value in the previous example. This illustration shows how the peak calculated stress (with curvature considered) would vary with the spring index, assuming that the same margin is being maintained between the working load and the load required to cause complete yielding.

CREEP AND RELAXATION UNDER ELEVATED TEMPERATURES

In the previous discussion the determination of working stress for statically-loaded helical springs was based on the yield point of the material, normal temperatures being assumed. As long as the working stress is kept well below this point, no trouble from creep or set should be experienced, provided the operating temperature is not more than about 200 degrees Fahr. for ordinary spring steels.

For higher operating temperatures it is not usually sufficient to base the design on the yield point or elastic limit of the material. The best method of determining working stresses in such cases is to make actual creep or relaxation tests at various temperatures. Unfortunately, there is not a great deal of data available as to the amount of loss of load which may be expected. The most comprehensive series of tests so far carried out to determine relaxation or loss of load in helical springs have been those reported by Zimmerli[4]. These tests were made by compressing helical springs by a given amount in a special test fixture. This compressed spring was then put into a furnace and left for a period of time varying from three days for the

[4] "Effects of Temperature on Coiled Steel Springs at Various Loadings"—F. P. Zimmerli, *Transactions* A.S.M.E., May, 1941, Page 363.

carbon and low-alloy steel springs to ten days for the stainless steel springs. After this heating, the springs were removed from

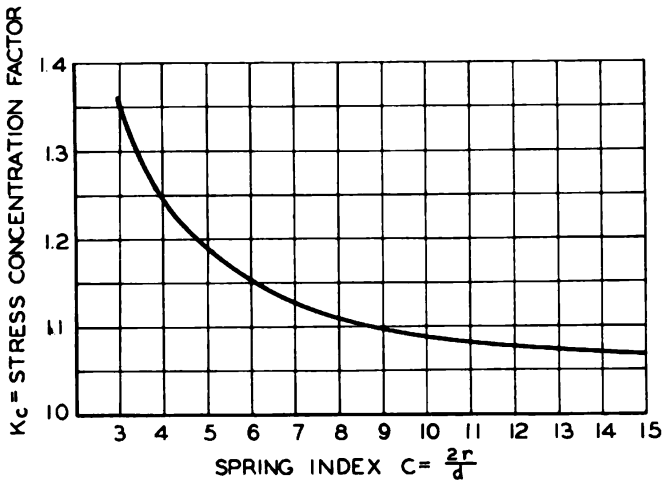

Fig. 68—Curve for finding stress-concentration factor K_c

the test fixture and the loss in free height determined. From this loss in free height (due to permanent set) the percentage loss in load could be calculated.

Load Loss Tests—The results obtained by Zimmerli are summarized in TABLE XI for various spring materials. The values given in this table represent percentage loss in load in a period of three days at the temperature listed, except for the stainless steel springs where the tests were run ten days. The stresses were figured with curvature correction, Equation 18. If figured without curvature correction these values would be about 10 per cent lower. The actual tests were made with springs which had been subjected to various bluing or stress relieving temperatures for periods of thirty minutes. In the table the values of load loss obtained at the optimum bluing temperatures are listed. If stress relieved at lower temperatures, the values of load loss were usually considerably greater. It appears that at the lower bluing temperatures not all the coiling stresses are removed; when these latter are combined with the load stresses a greater set takes place than would be the case otherwise.

From this table it appears that, at stresses of 100,000 pounds per square inch or about 90,000 figured without curvature correction, about ten per cent load loss may be expected within three days for music wire or the .6 per cent carbon steel wire, when

subject to temperatures of 350 degrees Fahr. Somewhat lower values may be expected for the chrome-vanadium steel. Stainless steels of the 18-8 type showed a load loss of only about four per cent at 350 degrees Fahr. which increased to 11.5 per cent at 550 degrees Fahr. at the same stress (100,000 pounds per square inch). These latter tests were run for ten days. For very long periods of time higher load losses may be expected.

On the basis of his work Zimmerli concluded that the usual spring steels are reliable when stressed to not more than 80,000 pounds per square inch (or to about 72,000 pounds per square inch figured without curvature correction) at temperatures up to 350 degrees Fahr. Above this temperature and up to 400 degrees Fahr. erratic results may be expected, while ordinary spring steels cannot be used for temperatures above 400 degrees Fahr. He also concluded that "stainless steels of the 18-8 type resist temperature and stress better than others, except high-speed."

A further conclusion drawn from this series of tests was that, for small wires, springs heat-treated after coiling showed no advantage over those wound from pretempered wire properly blued. Also the best bluing temperature was found to be in the

TABLE XI

Percentage Loss in Load for Helical Springs at Elevated Temperatures

Material	Diameter (in.)	Temperature (F)	Bluing Temp.‡ (F)	Loss in Load at 80,000 lb./sq.in. Stress* (%)	Loss in Load at 100,000 lb./sq.in. Stress* (%)	Rockwell Hardness
Music wire	.148	250	700	2.5	4.7	48
.91% C .31% Mn		350	700	7	10	48
Music wire	.062	250	700	2.5	3.5	51
.91% C .31% Mn		350	700	7	7.5	51
Carbon steel	.148	250	800	3	4.5	45
.66% C .76% Mn		350	700	6	10	45
Carbon steel	.062	250	800	3	3.5	43
.59% C .75% Mn		350	700	6	8.5	47
Cr-Va steel	.148	250	800	2	4	45.5
.87% Cr .18% Va		350	800	4	7	45.5
Cr-Va steel	.062	250	700	1.5	2.5	49
.97% Cr .18% Va		350	800	3.5	5	46.5
Stainless steel	.148	350	800	3	3	43.5
		450	700	3.5	5.5	45
18.2% Cr 9.2% Ni		550	800	9.5	11.5	43.5
		250	800	1.3	2	43
Stainless steel	.062	350	800	2	4	45.5
19.2% Cr 9.1% Ni		450	800	3.5	5.5	45.5
		550	800	9	11.5	45.5

*Stresses calculated with curvature correction. If calculated without curvature correction about 10 per cent lower values would be obtained.

‡Values have been reported for optimum bluing (or stress relieving) temperatures. Greater losses in load may usually be expected for bluing temperatures other than those listed.

highest which can be had without objectionable lowering of hardness or physical properties. For further details on this the reader is referred to the original article[4].

Analytical Method of Calculations—Some analytical methods have been developed by Nadai[5] for calculating creep and relaxation. A brief resume of these methods will be given:

It is first assumed as an approximation that the spring is essentially a bar under pure torsion. This will be approximately true for large index springs. Letting P = load on spring, r = mean coil radius, d = wire diameter, and θ the angle of twist per unit length along the wire, the twisting moment will be $M = Pr$. If γ = unit shear at a distance ρ from the center of the wire cross section. Then

$$\gamma = \rho\theta \qquad (98)$$

As is common in creep problems the unit shear strain γ will be assumed to consist of an elastic part γ' and a plastic part γ''. Thus, using Equation 98,

$$\gamma = \gamma' + \gamma'' = \rho\theta \qquad (99)$$

From elastic theory, the following relation holds:

$$\gamma' = \frac{\tau}{G} \qquad (100)$$

where τ=shear stress at radius ρ (*Fig.* 24, Chapter II) and G = modulus of rigidity of the material.

Differentiating Equation 99 with respect to time t,

$$\frac{\partial\gamma}{\partial t} = \frac{\partial\gamma'}{\partial t} + \frac{\partial\gamma''}{\partial t} = \rho\dot{\theta} \qquad (101)$$

where the dot denotes differentiation with respect to time.

Assuming that $\partial\gamma''/\partial t = g(\tau)$ where $g(\tau)$ is a function of shear stress τ only, using Equation 100 and by substitution in Equation 101,

$$\frac{1}{G}\frac{\partial\tau}{\partial t} + g(\tau) = \rho\dot{\theta} \qquad (102)$$

[5] "The Creep of Metals Under Various Stress Conditions"—A. Nadai, *Th. von Karman Anniversary Volume*, 1941. Also bibliography given in this reference.

The axial load P is given by

$$P=\frac{M}{r}=\frac{2\pi}{r}\int_0^a \tau\rho^2 d\rho \quad (103)$$

where $a=d/2=$radius of wire.

Steady Creep—To calculate the *steady creep* of the spring under a constant load P, it will be assumed that the shear stress τ at elevated temperatures is governed by a power function law. This has been found to agree with tests over limited ranges of strain rates. This gives, using Equation 101,

$$\tau=\tau_o\left(\frac{d\gamma}{dt}\right)^k=\tau_o(\rho\dot{\theta})^k \quad (104)$$

where $(0\leq k\leq 1)$. In this k is an exponent which depends on the temperature and can be determined by actual creep tests.

Substituting this value of τ into Equation 103, and integrating

$$P=\frac{2\pi}{r}\int_0^a \tau\rho^2 d\rho=\frac{2\pi(\dot{\theta})^k\tau_o a^{3+k}}{(3+k)r} \quad (105)$$

For *steady creep*, after sufficient time has elapsed so that the stresses due to creep become constant, the expression $\partial\tau/\partial t=0$ in Equation 102. Solving for the value of $\dot{\theta}$ by using Equation 105 and substituting in Equation 104,

$$\tau=\frac{(3+k)Pr}{2\pi a^3}\left(\frac{\rho}{a}\right)^k \quad (106)$$

In *Fig.* 69 the distribution of stress over the cross-section for *steady creep* under a load P is indicated by the curved line which may be obtained by calculating τ as a function of ρ from Equation 106. The straight line which represents the initial stress distribution (for a spring of large index) is also shown.

It should be noted that the distribution of stress given by Equation 106 only occurs after a considerable time has elapsed. To calculate the stress distribution for the intermediate period, procedure may be as follows: From Equation 105 since P is assumed constant:

$$\frac{\partial P}{\partial t}=0 \quad or \quad \int_0^a \rho^2 \frac{\partial \tau}{\partial t} d\rho = 0$$

Using in this the value of $\partial\tau/\partial t$ given by Equation 102,

$$\frac{\dot{\theta} a^4}{4} = \int_0^a \rho^2 g(\tau) d\rho \quad \ldots\ldots (107)$$

Using Equation 107 in Equation 102 and rearranging terms the following integro-differential equation results:

$$\frac{1}{G} \frac{\partial \tau}{\partial t} = \frac{4\rho}{a^4} \int_0^a g(\tau) \rho^2 d\rho - g(\tau) \quad \ldots\ldots (108)$$

The solution of this equation for $t = 0$ is the usual formula:

$$\tau = \frac{2Pr\rho}{\pi a^4}$$

For $t = \infty$ the solution is given by Equation 106.

Relaxation—To calculate the *relaxation* or loss in load of a spring initially compressed (or extended) to a given length,

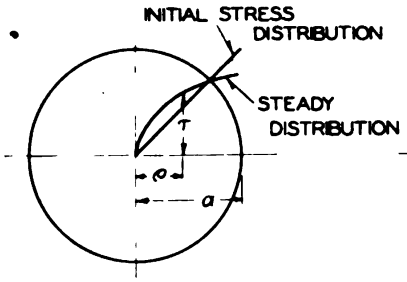

Fig. 69—Initial and steady distribution of stress for spring subject to creep

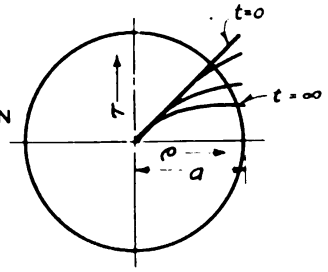

Fig. 70—Stress distribution during relaxation of spring showing time effect

the procedure is as follows: Since the length of the spring does not change with time, the angle of twist per unit length θ remains constant. Hence $\dot{\theta} = 0$. Using Equation 102 the following differential equation is obtained:

$$\frac{1}{G} \frac{\partial \tau}{\partial t} + g(\tau) = 0 \quad \ldots\ldots (109)$$

To integrate this, a power function is again assumed:

$$g(\tau)=\frac{\partial\gamma^{p}}{\partial t}=C\tau^{n} \quad \ldots\ldots (110)$$

where C is a given constant.

Substituting this into Equation 109,

$$\frac{\partial\tau}{\partial t}+GC\tau^{n}=0 \quad \ldots\ldots (111)$$

Integrating this with respect to time and determining the integration constant from the condition that for $t = 0$, a linear stress distribution over the cross section occurs,

$$\frac{1}{\tau^{n-1}}-\frac{1}{\tau_i^{n-1}}=(n-1)CGt$$

In this $\tau_i=\tau_0\,\rho/a$ is the initial stress distribution. Solving for τ,

$$\tau=\tau_i\left(\frac{1}{1+(n-1)CGt\tau_i^{n-1}}\right)^{1/(n-1)} \quad \ldots\ldots (112)$$

Shear Stresses—The distribution of shearing stresses over the cross-section for various times t is illustrated by *Fig.* 70. It should be noted that the peak stress drops considerably as time goes on while the stress distribution tends to flatten out and approach a more uniform distribution. After a considerable period of time the shear stresses approach the value:

$$\tau=\frac{1}{[(n-1)CGt]^{1/(n-1)}} \quad \ldots\ldots (113)$$

Using this value and assuming a rectangular distribution of stress, the expression for load P at large values of t becomes

$$P=\frac{2\pi\tau a^{3}}{3r}=\frac{2\pi a^{3}}{3r}\left[\frac{1}{(n-1)CGt}\right]^{1/(n-1)} \quad \ldots\ldots (114)$$

The exponent n must be obtained from relaxation tests.

More exact expressions for load may be obtained by using the value of τ given by Equation 112 in Equation 103 and evaluating the integral numerically or graphically.

CHAPTER VI

FATIGUE OR VARIABLE LOADING OF HELICAL SPRINGS

In the previous chapter a rational basis for determining working stresses in helical springs subject to static or infrequently repeated loading was discussed. In cases where springs are subject to fatigue or repeated loading, as for example in automotive valve springs, a somewhat different approach to the problem of determining working stress is necessary. In the case of helical springs, the problem is complicated by the fact that the spring is usually subject to a load (or stress) which varies from a minimum value to a maximum. As shown in Chapter I this is equivalent to a constant or a steady load on which is superimposed a variable or alternating load. Thus in the case of the automotive valve spring, the constant component of the load is determined by the initial compression of the spring while the variable component is determined by the valve lift.

If all spring stresses are calculated by means of the curvature correction factor K, Equation 18, conservative design will result. This procedure appears justified if the spring is subject to a considerable range of stress in fatigue. Where there is a considerable static load component on which is superimposed a variable load component, however, it appears logical to neglect stress concentration effects due to curvature in figuring stresses from the static component of the load. In this connection there has been a general opinion among spring engineers that the use of the factor K will result in too low values of working load; in other words that the stresses computed this way are too high. This view was confirmed to a certain extent by the results of a series of carefully made fatigue tests on small helical springs of different indexes carried out by Zimmerli[1]. These showed that the limiting stress range in fatigue, when figured by using the K factor, was higher for the springs of smaller indexes. Similar results were reported by Edgerton[2] in connec-

[1] *Transactions* A.S.M.E., January, 1938, Page 43.
[2] *Transactions* A.S.M.E., October, 1937, Page 609.

tion with fatigue testing work on heavy helical springs by the A.S.M.E. Special Research Committee on Mechanical Springs. These tests will be discussed later.

A further reason why the full stress-concentration effect corresponding to the curvature correction factor K does not always occur (even for fatigue loading) lies in the fact that some materials are not fully sensitive to stress concentration. In other words, when such materials are tested by means of specimens having notches, holes, or fillets, the fatigue strength reduction produced by the presence of such "stress raisers" is not as great as that to be expected based on theoretical stress-concentration factors. These so-called theoretical stress-concentration factors may be determined either by analytical means using the theory of elasticity[3], by strain measurements, or by photoelastic tests[4].

This lack of sensitivity to stress concentration effects is in general more pronounced in the smaller sized specimens and for the low-carbon steels, while on the other hand the fine-grained, high-strength alloy steels are very sensitive to such effects[5]. In the case of helical springs, the decarburization of the surface layer which occurs during heat treatment and the effects of shot-blast treatments, if used, represent further factors which tend to reduce sensitivity to stress-concentration.

METHODS OF CALCULATION

In accordance with the previous discussion and that of Chapter I a method of evaluating working stress in helical springs under variable loading based on the following assumptions will be described:

1. Stress concentration effects due principally to bar or wire curvature in helical springs may be neglected in figuring the static component of stress
2. Relation between the limiting value of the static and variable stress components at failure follows a linear law

[3]For example *Theory of Elasticity*—Timoshenko, McGraw-Hill. Also Neuber *Kerbspannungslehre*, Springer, Berlin for methods of determining stress concentration factors by analytical methods.

[4]Frocht, M. M.—*Photoelasticity*, Vol. I, Wiley.

[5]Papers by R. E. Peterson on "Correlating Data from Fatigue Tests of Stress Concentration Specimens", *Timoshenko Anniversary Volume*, Macmillan, 1938, and "Application of Stress Concentration Factors in Design", *Proceedings Society for Experimental Stress Analysis*, Vol. 1, No. 1, Page 118, discuss this. Also article by Peterson and Wahl, *Journal of Applied Mechanics*, March, 1938, Page A-15 and discussion December, 1936, Page A-146.

3. Tensile and fatigue properties of the material are the same in springs of different indexes, assuming the same size wire
4. Effects of eccentricity of loading due to end turns are neglected
5. Residual stresses produced by heat-treatment or overstressing the springs may be neglected.

These factors will be discussed more fully later. For the present, full sensitivity of the material to stress concentration will also be assumed. Later the effects of variations in the sensitivity index of the material (due to surface decarburization, shot blasting, etc.) will be considered.

Full Sensitivity to Stress Concentration—Referring to *Fig.* 71, the dashed line shows a typical experimental curve of failure for materials under a combination of static and variable stress. The ordinates represent values of variable stress which will just cause failure when superimposed in the static stresses shown by the abscissas. Assuming that fatigue tests are made on a spring of large index ($c = \infty$) so that $K_c = 1$, and letting τ_e' denote the endurance limit in a zero to maximum stress range obtained

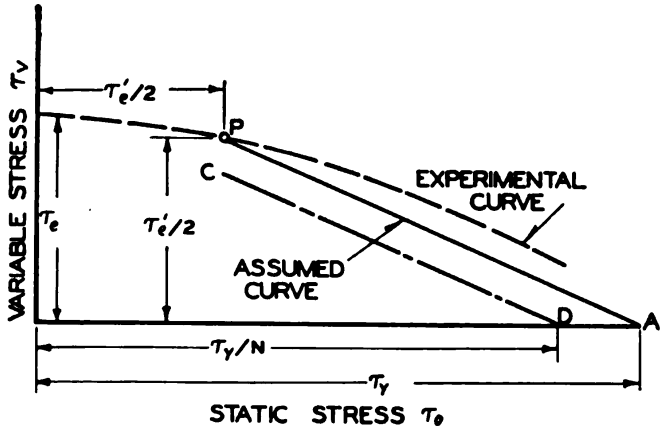

Fig. 71—Application of straight line law, to helical springs when endurance limit τ'_e for pulsating load application (zero to maximum) and yield stress τ_y are known

on this spring, then the point P on the diagram is determined. For this case (0 to maximum stress) both the static and variable components are equal to $\tau_e'/2$. As an approximation, the experimental curve may be replaced by the straight line PA drawn to intersect the axis of abscissas at τ_y, the torsional yield point

of the material[6]. This is done since in general no stress should exceed the yield point[7]. To apply this diagram in actual design, it may be assumed that the spring is operating under a fatigue stress range from τ_{min} to τ_{max} where these stresses are figured by using the full curvature correction factor $K = K_c K_s$ (see Page 110). Then the variable component of stress τ_v is

$$\tau_v = \frac{\tau_{max} - \tau_{min}}{2} \quad \ldots\ldots (115)$$

This, of course, presupposes full sensitivity to stress concentration. The static component of stress τ_o, when figured by neglecting stress concentration effects due to bar curvature, then becomes

$$\tau_o = \frac{\tau_{max} + \tau_{min}}{2K_c} \quad \ldots\ldots (116)$$

The right side of the last equation is divided by $K_c = K/K_s$ since this factor has already been used in figuring τ_{max} and τ_{min};

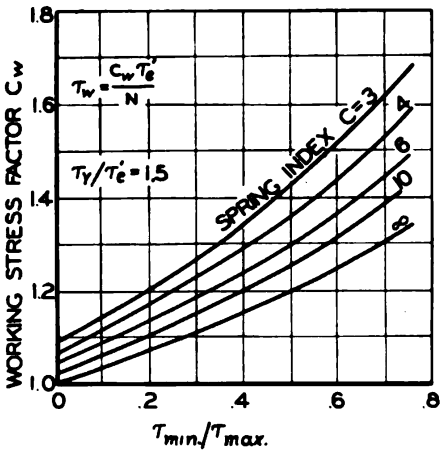

Fig. 72—Chart for determining working stress factor C_w for $\tau_y/\tau'_e = 1.5$ and $q = 1$

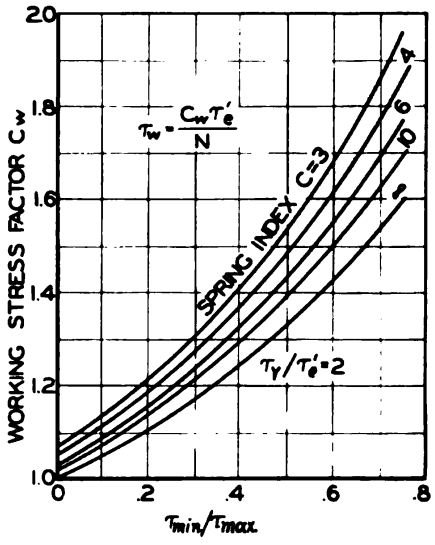

Fig. 73—Chart for determining working stress factor for C_w for $\tau_y/\tau'_e = 2$ and $q = 1$

[6]If the yield point is not sharply defined, as an approximation it may be taken as that point where the plastic strain is .2 per cent. See "Concerning the Yield Point in Tension—J. M. Lessells, *Proceedings* A.S.T.M., 1928, Page 387.

[7]The ultimate strength in torsion could be substituted for τ_y if desirable. In some cases this would give results in closer agreement with tests, but the results obtained by using the yield point will, in general, be on the safe side.

therefore, to neglect stress concentration effects due to curvature division by K_c is necessary. An analytical expression for the line *PA, Fig.* 71, in terms of τ_o and τ_v is

$$\frac{\tau_o}{\tau_y}+\frac{\tau_v}{\frac{\tau_e'}{2}\left(\frac{\tau_y}{\tau_y-\tau_e'/2}\right)}=1 \quad \ldots\ldots (117)$$

This is merely the equation of a straight line passing through points P and A. Substituting the values of τ_v and τ_o given by

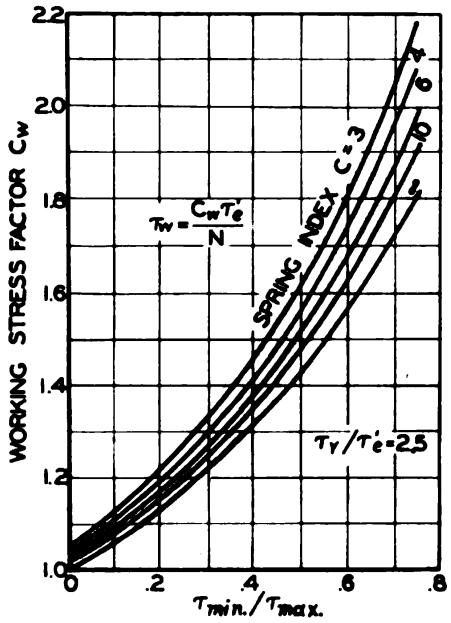

Fig. 74—Chart for determining working stress factor C_w for $\tau_y/\tau'_e = 2.5$ and $q = 1$

Equations 115 and 116 in this equation,

$$\tau_{max}=\frac{2\tau_y}{\frac{1}{K_c}\left(1+\frac{\tau_{min}}{\tau_{max}}\right)+\left(\frac{2\tau_y}{\tau_e'}-1\right)\left(1-\frac{\tau_{min}}{\tau_{max}}\right)} \quad \ldots\ldots (118)$$

This equation gives the maximum stress[8] τ_{max} in terms of K_c, τ_y, τ_{min}/τ_{max} and τ_y/τ_e' and may be written

$$\tau_{max}=C_w\tau_e' \quad \ldots\ldots (119)$$

where the factor C_w is a function of K_c, τ_y, τ_{min}/τ_{max} and τ_y/τ_e',

[8]It is assumed that the variable component of stress is not greater than the static component, i.e., that only stress conditions corresponding to the line *PA* in *Fig.* 71 are considered. This is almost always the case.

$$C_w = \frac{\frac{2\tau_y}{\tau_e'}}{\frac{1}{K_c}\left(1+\frac{\tau_{min}}{\tau_{max}}\right)+\left(\frac{2\tau_y}{\tau_e'}-1\right)\left(1-\frac{\tau_{min}}{\tau_{max}}\right)} \quad \ldots\ldots\ldots\ldots\ldots (120)$$

Since K_c is a function of spring index c, values of C_w may be plotted in the form of charts for various spring indexes, and various values of τ_y/τ_e'.

For design purposes the value of τ_{max} given by Equation 119 is divided by a factor of safety N so that the working stress becomes

$$\tau_w = C_w \frac{\tau_e'}{N} \quad \ldots\ldots\ldots\ldots\ldots\ldots\ldots\ldots\ldots\ldots\ldots\ldots\ldots\ldots\ldots\ldots\ldots\ldots (121)$$

It may be shown that this amounts to assuming a line *CD*, *Fig* 71, parallel to the line *PA* and intersecting the axis of abscissas at a distance τ_y/N from *O*. Any combination of variable and static stresses which falls on the line *CD* is thus assumed to have a factor of safety *N*.

For convenience in calculation, charts showing the relation between C_w and τ_{min}/τ_{max} for various spring indexes at given values of τ_y/τ_e' are given in *Figs.* 72, 73 and 74. These charts have been computed using the expression for C_w given in Equation 120 and assuming a definite value of τ_y/τ_e'. Thus in *Fig* 73 the latter ratio is taken equal to 2. These charts show clearly how the maximum permissible stress increases with increase in τ_{min}/τ_{max} and that this increase is greater for the springs of smaller index. However, this increase in allowable stress will be limited by creep and relaxation effects as discussed in Chapter V.

Material not Completely Sensitive to Stress Concentration —A similar procedure may be used for cases where the spring material is not fully sensitive to stress concentration. It will be assumed that the "sensitivity index" of the material (which is a measure of the actual sensitivity to stress concentration) has been determined for the given material and wire size by actual fatigue tests[9]. This sensitivity index q is defined as

$$q = \frac{K_f - 1}{K_c - 1} \quad \ldots\ldots\ldots\ldots\ldots\ldots\ldots\ldots\ldots\ldots\ldots\ldots\ldots\ldots\ldots\ldots\ldots\ldots (122)$$

[9]References of footnote 5 give a further discussion of "sensitivity index."

where K_f=fatigue strength reduction factor, i.e., the ratio of endurance limit without stress concentration to endurance limit with stress concentration present. Here K_c is again the theoretical stress concentration factor due to bar or wire curvature. For materials completely insensitive to stress concentration $K_f=1$ and from Equation 122, $q=0$. For materials fully sensitive, $K_f=K_c$ and hence $q=1$. Thus the more sensitive materials, such as the fine-grained alloy steels in the larger sizes, would show larger values of q than would materials not sensitive to stress concentration. As mentioned previously, the surface condition of wire or bar would also have an effect on the sensitivity and hence on the index.

To take into account the effect of lack of sensitivity to stress concentration, the stress range $\tau_{max}-\tau_{min}$ should be calculated by using the fatigue strength reduction factor K_f rather than the theoretical factor K_c. If q is known, by solving for K_f in Equation 122,

$$K_f=1+q(K_c-1) \quad \ldots\ldots (123)$$

It is, however, assumed that τ_{max} and τ_{min} have already been calculated in the usual way by using the curvature correction factor $K=K_s K_c$. Therefore, if the value of $\tau_{max}-\tau_{min}$ is multiplied by K_f/K_c, a reduced value of variable stress τ_v will be obtained which will take into account the sensitivity effect. Hence,

$$\tau_v=\left(\frac{\tau_{max}-\tau_{min}}{2}\right)\frac{K_f}{K_c} \quad \ldots\ldots (124)$$

Using Equation 123 in this,

$$\tau_v=\frac{(\tau_{max}-\tau_{min})}{2}\ \frac{[1+q(K_c-1)]}{K_c} \quad \ldots\ldots (125)$$

Substituting Equations 116 and 125 in Equation 117,

$$\tau_{max}=\frac{2\tau_y}{\frac{1}{K_c}\left(1+\frac{\tau_{min}}{\tau_{max}}\right)+\left(\frac{2\tau_y}{\tau_e'}-1\right)\left(1-\frac{\tau_{min}}{\tau_{max}}\right)\left(\frac{1+q(K_c-1)}{K_c}\right)} \quad (126)$$

It is seen that where $q=1$ (full sensitivity) this equation reduces to Equation 118. For $q=0$ (no stress concentration ef-

fect) the denominator of this equation is in effect divided by K_c which means that stress concentration effects due to curvature as represented by K_c are neglected entirely both for the static and variable stress components. This is equivalent to using the factor K_s of Equation 90.

From Equation 126 is obtained:

$$C_w = \frac{2\tau_y/\tau_c'}{\frac{1}{K_c}\left(1+\frac{\tau_{min}}{\tau_{max}}\right)+\left(\frac{2\tau_y}{\tau_c'}-1\right)\left(1-\frac{\tau_{min}}{\tau_{max}}\right)\left(\frac{1+q(K_c-1)}{K_c}\right)} \quad (127)$$

This also reduces to Equation 120 when $q=1$.

Charts showing C_w as a function of spring index c for a sensitivity index $q=½$ and for τ_y/τ_c' equal to 1.5, 2.0, and 2.5 are given in *Figs.* 75, 76 and 77, respectively. These charts are

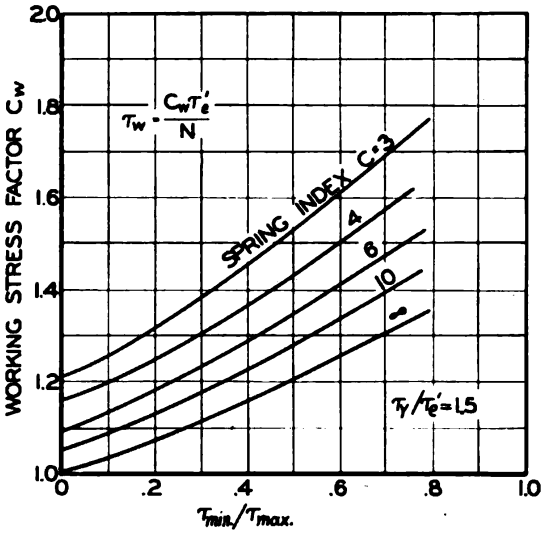

Fig. 75—Chart for determining working stress factor C_w for τ_y/τ'_c = 1.5 and q = ½

given merely as examples to show the effect of a reduction in the sensitivity of the material as measured by the index c on the allowable stress τ_w. From these figures, it may be seen that for materials not sensitive to stress concentration the allowable working stress is considerably higher for the springs of smaller index as compared to the larger index springs.

Application of Charts—To illustrate the application of the charts of *Figs.* 72 to 77 in practical work, the following conditions may be assumed: A spring of ¼-inch wire diameter and

¾-inch mean coil diameter, i.e., $c=3$. Fatigue tests on springs of large index and on the same size wire subjected to a pulsating load (0 to maximum) yield a value of endurance limit $\tau_e'=$ 60,000 pounds per square inch, while torsion tests show a yield

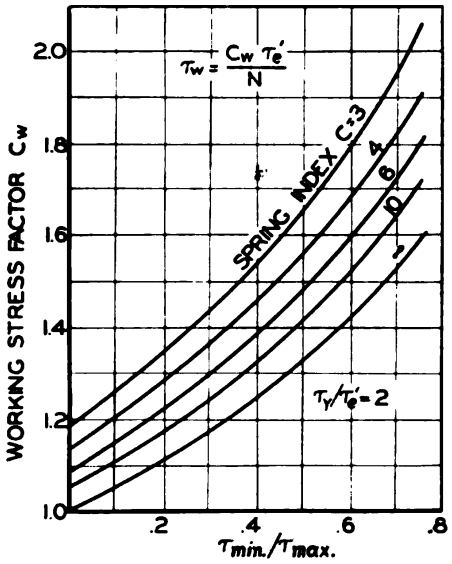

Fig. 76—Chart for determining working stress factor C_w for $\tau_y/\tau'_e = 2$ and $q = ½$

point in torsion of 120,000 pounds per square inch. Further the spring is under a fatigue stress range from τ_{min} to τ_{max} where $\tau_{min}=.5\tau_{max}$ (both stresses being computed by using the factor K).

To be on the safe side, full sensitivity of the material is assumed ($q=1$). Since $\tau_y/\tau_e'=2$, the chart of *Fig.* 73 applies. From this chart for an index $c=3$, $C_w=1.53$ when $\tau_{min}/\tau_{max}=.5$. Thus, on this basis fatigue failure may be expected at $\tau_{max}= C_w \tau_e'=1.53\times60{,}000=92{,}000$ pounds per square inch (Equation 119). Assuming a factor of safety $N=1.5$, the working stress would be, from Equation 121, $\tau_w=C_w\tau_e'/N=92{,}000/1.5=$ 61,000 pounds per square inch (the stress being figured by using the factor K). If the spring index were 10 instead of 3, the factor C_w would be 1.39, *Fig.* 73, and the working stress $\tau_w=$ $1.39\times60{,}000/1.5=56{,}000$ pounds per square inch, assuming factor of safety $N=1.5$.

To show the effect of a reduction in the sensitivity index q, endurance tests on springs of considerably smaller index in this particular wire size may be assumed to show a value of $q=½$.

Then using the chart of *Fig.* 76 ($\tau_y/\tau_e'=2$, $q=\frac{1}{2}$) $C_w=1.65$ for $c=3$ and $\tau_{min}/\tau_{max}=\frac{1}{2}$. In this case, the allowable working stress, using a factor of safety $N=1.5$, would be $\tau_w=C_w\,\tau_e'/N=1.65\times60{,}000/1.5=66{,}000$ pounds per square inch.

Limitations of Method—A fundamental limitation in the design method previously discussed for springs under variable loading lies in the assumption that the stress concentration factor K_c may be neglected in figuring the static component of the stress, even for springs under fatigue loading. As brought out in Chapter V, where the load is purely static, this appears reasonable; however, further tests will be required to establish the validity of this assumption when applied to combinations of static and variable stress. The alternative method discussed in the following section (Page 131) does not, however, involve this limitation.

A further limitation of the method is the assumption of a linear relation between the static and variable stress components necessary to cause fatigue failure, i.e., a straight line *PA* in *Fig.* 71 is assumed to be the actual limiting curve. Usually the experimental results will be somewhat above this line as indicated. Hence, if the value of the zero to maximum endurance limit τ_e' is determined by actual tests on a spring of large index and having the wire size under consideration, it appears that if the line *PA* is used as a basis, the calculated results will be on the safe side. In this connection it is necessary to determine the value of τ_e' by tests on the actual wire size used, since the endurance values may change considerably between small and larger sizes.

It has also been assumed that the line of failure *PA* tends to approach the yield point in torsion. In many cases it will be found that this line approaches the ultimate strength in torsion[10]. In such cases the latter could be used instead of τ_y in applying the charts and formulas. If this is done, however, a higher factor of safety should be used than otherwise.

In deriving the formulas for C_w, it has been assumed that the endurance properties of the material do not change between springs of small and large index assuming a given wire size. Although this appears to be a reasonable assumption, there are

[10]University of Michigan *Engineering Research Bulletin* No. 26 mentioned previously, Page 86, discusses this further.

cases where it may not be strictly true. For example, in cold-wound springs of a given wire size, springs coiled to smaller diameters will be subjected to the greatest amount of cold working, and hence such springs may possess somewhat different endurance properties than would otherwise be expected. If a stress-relieving treatment is given, this difference may be slight. A similar result may be expected where springs are quenched after coiling, since the effect of the heat treatment may be different for springs of different indexes. The shot-blast treatment frequently given springs (Chapter IV) will probably also introduce variations in the sensitivity index.

It is common practice, in the manufacture of compression springs, to compress the spring solid, thus giving it a permanent set. The effect of this is to introduce residual stresses of op-

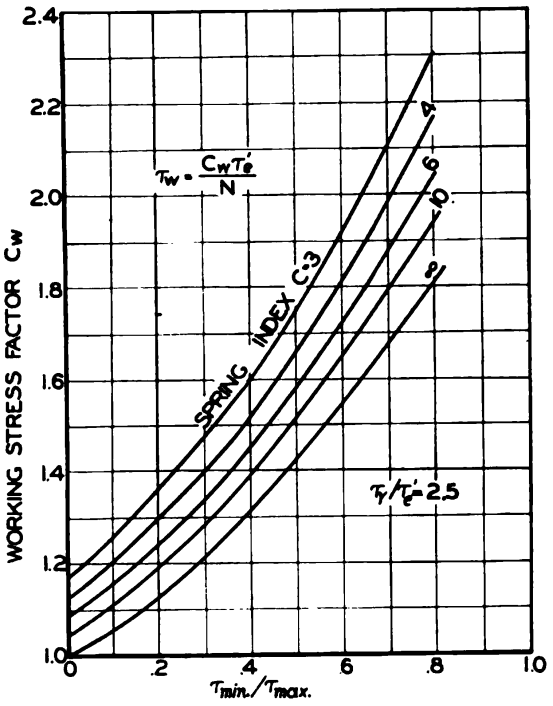

Fig. 77—Chart for determining working stress factor C_w for $\tau_y/\tau'_e = 2.5$ and $q = \frac{1}{2}$

posite sign so that when the spring is under the working load, the peak stress will be reduced by the amount of such residual stresses. For this reason the tendency will be for the fatigue strength to be increased because of the presence of these stresses. Because of the sharper curvature of the springs having smaller

indexes, it will be easier to introduce such residual stresses in these springs. Thus it may happen that the fatigue strength of the springs of smaller index may be increased by such treatment to a relatively greater extent than is the case for springs of large index.

In the present analysis the effects of eccentricity of loading due to the end coils have been neglected. These effects may increase the maximum stress from 4 to 30 per cent, depending on the shape and form of the end turns, and on the total number of turns. Further discussion of this will be given in Chapter VIII.

COMPARISON OF THEORETICAL AND TEST RESULTS

To the author's knowledge the most comprehensive series of tests yet made to check the effect of spring index on endurance strength of helical springs were those carried out by Zimmerli[11]. He made a series of tests on springs of .148-inch diameter pretempered Swedish valve-spring wire, having indexes c varying from 3.5 to 12. It will be of interest to compare these test results with those obtained by the application of the charts of *Figs.* 72, 73 and 74 which assume full sensitivity to stress concentration ($q=1$). Values of the minimum and maximum points (τ_{min} and τ_{max}) of the limiting stress ranges as found by Zimmerli for the various indexes are given in the second and third columns of TABLE XII.

To determine the zero to maximum endurance limit τ_e', for a spring of large index, the test results for $c=11.9$ are used as a basis taking $\tau_{min}=19{,}000$ pounds per square inch, $\tau_{max}=91{,}000$ pounds per square inch, and $\tau_{min}/\tau_{max}=.21$. Assuming tentatively $\tau_y/\tau_e'=1.5$, from Equation 119, $\tau_{max}=1.11\ \tau_e'$ for $\tau_{min}/\tau_{max}=.21$. Solving, $\tau_e'=91{,}000/1.1=82{,}700$ pounds per square inch. Since the yield point in torsion for the material will be around 120,000 pounds per square inch (or somewhat above the elastic limit in torsion), it may be assumed that $\tau_y/\tau_e'=1.5$ with sufficient accuracy allowing the use of *Fig.* 72. Using the value of C_w thus found and assuming the minimum values of the stress range τ_{min} as given, the limiting values of maximum stress τ_{max} were computed using the chart of *Fig.* 72 and Equation 119. The computed values of τ_{max} thus obtained are given

[11] *Transactions* A.S.M.E., January, 1938, Page 43.

in the fifth column of TABLE XII. For comparison, values of the limiting stress range $\tau_{max} - \tau_{min}$ as found by test and as determined by calculation are given in the last two columns.

Comparison of the figures in these last two columns indicates that the test and calculated values of limiting stress range differ by only a few per cent. This offers some indication that

TABLE XII

Theoretical and Test Values of Limiting Stresses

Spring Index	Limiting Stresses from Fatigue Tests*		Calculated		Limiting Range in Stress $\tau_{max} - \tau_{min}$	
	τ_{min}	τ_{max}	τ_{min}	τ_{max}	By test	Calculated
c	(lb./sq.in.)	(lb./sq.in.)	(lb./sq.in.)	(lb./sq.in.)	(lb./sq.in.)	(lb./sq.in.)
3.5	14,000	100,000	14,000	95,500	86,000	81,500
4.55	19,000	94,000	19,000	96,000	75,000	77,000
7.0	19,000	93,000	19,000	93,500	74,000	74,500
9.1	19,000	90,000	19,000	92,000	71,000	73,000
11.9	19,000	91,000	19,000	91,000	72,000	72,000

*These stresses figured using the curvature correction factor K.

the method of determining working stress, using Equation 118 which assumes full sensitivity to stress concentration ($q=1$), will give results in fair agreement with actual fatigue tests, at least for some materials and wire sizes.

Tests by Edgerton mentioned previously were made on two groups of springs coiled from ¾-inch diameter bar stock, one group of index 3 and the other of index 5. The endurance limits calculated by the use of the conventional formula, Equation 4, were practically the same for the two groups of springs, while the endurance limits calculated by using the K factor differed considerably. This would indicate that for these springs neither the bar curvature nor the direct shear stress have any effect on the endurance. This is in contrast to the previously discussed tests by Zimmerli which do show that the wire curvature does tend to reduce the endurance range even in small size springs. It is clear that further test data will be required before definite conclusions may be drawn.

ALTERNATIVE METHOD OF CALCULATION

The previously discussed method of evaluating working stress in helical springs under variable loading is based on the assumption that stress-concentration effects due to curvature

may be neglected in calculating the static component of the stress. This is in line with the method proposed by Soderberg (Page 17) for evaluating working stresses. An alternative, however, and possibly somewhat simpler method is the following:

Assuming the spring is operating between maximum and minimum loads P_{max} and P_{min}, then the range in load will be $P_{max}-P_{min}$. The range in torsion stress τ_r is then computed from the range in load using the full curvature correction factor K. (When further test data are available regarding sensitivity indexes for various materials, the value of K may be reduced to $K_s K_f$ where K_f depends on the sensitivity index q and is given by Equation 123. In the absence of actual test data or experience, however, it is suggested that a sensitivity index q equal to unity be used in design.)

Peak stress τ_{max} is then calculated from the load P_{max} using the curvature correction factor K. If this peak stress is above the torsional yield point, the latter value is taken as the maximum stress of the range, since in nearly all cases localized yielding will limit the peak stress to this value. Then the actual limiting stress range is taken as the test value with the peak stress equal to the yield point in torsion. However, if the peak stress τ_{max} is below the torsional yield point, then the actual endurance range with this value of τ_{max} is taken as a basis. This may be found from endurance diagrams of the type shown in *Fig.* 56 or from data similar to that given in TABLE VII, Page 88.

Usually it will be found that, if the peak stress does not exceed the yield point in torsion, there will not be much variation in the value of the endurance range for various peak stresses. Hence for practical purposes, an approximate figure of limiting range equal to the range with the peak stress equal to the yield point may be taken as a conservative figure. The allowable stress range, figured by using the factor K, would then be this limiting endurance range divided by the factor of safety[12].

In addition, to avoid excessive permanent set the stress at the maximum load P_{max}, calculated by neglecting curvature correction as discussed in Chapter V, should not exceed the allowable value for static loading. This alternative method of design for variable loading appears to be promising and is some-

[12] A further discussion of this method was given in a paper on "Helical Spring Design Stresses for a Standard Code" *Transactions* A.S.M.E., July 1942, Page 476.

what simpler than that discussed previously. Further test data, however, would be desirable to differentiate between the two methods. It is possible that either would be sufficiently good for practical use.

Example—As an example of the use of this method: A carbon steel spring is 2 inches outside coil diameter, ½-inch bar diameter, and index of three, subject to continuous alternating load between a maximum of 1700 pounds and a minimum of 1200 pounds. Using Equation 18 the stress at the peak load calculated with curvature correction will be 82,000 pounds per square inch. This is somewhat below the torsional yield point. For a range in load of 1700—1200=500 pounds the stress range will be 24,100 pounds per square inch. From TABLE IX, Page 92, for a heat-treated, carbon-steel spring the endurance range for zero to maximum load application with a peak stress of 82,000 pounds per square inch, may be estimated as about 70,000 pounds per square inch. This gives a factor of safety of 70,000/24,100=2.9 on the stress range. At the peak load the stress figured without curvature correction, Equation 89, is 61,000 pounds per square inch. Since the expected torsional yield point of this material should be about 110,000 pounds per square inch, TABLE VII Page 88, the factor of safety with respect to yielding would be 110,000/61,000=1.8.

CHAPTER VII

PRACTICAL SELECTION AND DESIGN OF HELICAL COMPRESSION SPRINGS

It is the primary purpose of this chapter to present data on working stresses, as well as charts and tables, which may be used by the designer to facilitate the practical selection of helical springs for given applications. Although the methods of evaluating working stresses described in the preceding two chapters provide a rational approach to the design problem, in many cases the additional work involved by the use of these more rational methods is not warranted. This is particularly true if only a few springs of certain characteristics are required, for example, to fit into a given mechanism, plenty of space being available. In such cases the use of the spring tables given here may be all that is necessary.

On the other hand, there may be cases when the proper functioning of a certain spring is vital to the successful operation of a given machine while at the same time, the available space is limited. In such case, a considerable amount of time spent in studying the spring requirements on the basis of the methods of Chapters V and VI would probably be justified. Even where these methods are used, however, the choice of the proper spring is facilitated by the use of the charts and tables given in this chapter.

WORKING STRESSES USED IN PRACTICE

To aid the designer in cases where a quick selection of springs is necessary, a review of suggested working stress values, obtained from various sources, is desirable[1]. In utilizing these it should be remembered that for best results, a considerable amount of judgment is required and for this reason in important applications consultation with a spring manufacturer usually will be advisable.

[1]Working stresses are discussed further in author's article, *Transactions* A.S.M.E., 1942, Page 476.

In TABLE XIII a tabulation of working stresses used as a basis for helical spring design by Westinghouse Elec. & Mfg. Co. is given. These working stress values, which should be used primarily as a guide in spring selection, apply to springs made of good quality steel, such as music or oil-tempered wire, hot-wound springs, heat treated after forming. In most cases the

TABLE XIII

Working Stresses in Shear-Helical Compression Springs of Steel*

Wire Diameter (in.)	Severe Service (lb./sq.in.)	Average Service (lb./sq.in.)	Light Service (lb./sq.in.)
Up to .085	60,000	75,000	93,000
.085 to .185	55,000	69,000	85,000
.186 to .320	48,000	60,000	74,000
.321 to .530	42,000	52,000	65,000
.531 to .970	36,000	45,000	56,000
.971 to 1.5	32,000	40,000	50,000

*For springs of good-quality spring steel. All stresses based on the use of a curvature correction factor. The table does not hold where corrosion effects or high temperature are present. For phosphor bronze springs 50 per cent and for rust-resisting steel 75 per cent of these values are used.

values of stresses listed in TABLE XIII will be found to be conservative and may often be increased after a careful study of spring requirements.

To facilitate spring selection based on the stresses listed in TABLE XIII the tables on Pages 138 to 149 are given.

From TABLE XIII it may be seen that lower stresses are used for the larger wire sizes and for severe service in accordance with practical experience. The classification of particular applications as severe, average, or light service depends to a considerable extent on the judgment of the designer. In general, however, springs subject to continuous fatigue stressing in pulsating load application, where the ratio of minimum to maximum stress is one-half or less, as in valve springs, for example, would be considered severe service. On the other hand, a spring subject to but a few applications of load during its life or to practically a constant load at normal temperature would be light service.

For ordnance applications where space is at a premium, much higher working stresses are suggested by the S.A.E. War Engineering Board Spring Committee (*Manual* on "Design and Application of Helical and Spiral Springs for Ordnance"). Suggested values of working stress in compression springs of music

wire range from 190,000 for .015-diameter to 140,000 for .15-diameter wire with considerable lower values for tension springs. For carbon-steel compression springs, hot wound and heat treated after coiling, suggested values of stress vary from 116,000 for ⅜-inch diameter to 80,000 for 1-inch diameter bar. These

TABLE XIV

Allowable Stresses for Helical Springs

Material	Maximum Working Stress, (lb./sq.in.)	Maximum Solid Stress, (lb./sq.in.)
Music wire	70,000	120,000
Oil-tempered wire	60,000	100,000
Hard-drawn spring wire	50,000	80,000
Stainless steel (18-8)	50,000	80,000
Monel metal	35,000	70,000
Phosphor bronze	35,000	70,000
Brass	25,000	50,000

stresses are calculated without curvature correction and apply tc indexes from 4 to 9. Use of these stresses assumes that cold setting and shot blasting operations are used to obtain maximum strength. Such high stress values should not be used where long life or fatigue endurance is required.

As another example of working stresses used in practice, the values listed in TABLE XIV are suggested in a pamphlet published by Barnes-Gibson-Raymond Division of Associated Spring Corp. These values refer to maximum working stress and to maximum solid stress. Where possible it is further suggested the stress range in the spring be limited to ½ to 2/3 the maximum working stress.

The American Steel & Wire Company in their *Manual of Spring Engineering* suggest for springs of plain carbon steels

TABLE XV

Recommended Maximum Torsional Design Stresses for Helical Compression Springs Under Average Service Conditions*

(Plain Carbon Steels)

Wire diameter (in.)	Music Wire (lb./sq in.)	Tempered Steel (lb./sq.in.)	Hard-Drawn Steel (lb./sq.in.)
.020 to .030	100,000	100,000	90,000
.031 to .092	90,000	100,000	80,000
.093 to .176	90,000	90,000	80,000
.177 to .282	.....	90,000	70,000
.283 to .436	.....	85,000	
.437 to .624	.....	80,000	Cold wound for OD > 3 inches
.437 to .624	.....	90,000	Hot wound for OD < 3 inches
.625 to .874	.....	90,000	Hot wound
.875 to 1.249	.....	80,000	Hot wound
1.25 to 1.5	.....	80,000	Hot wound

*Curvature correction included.

under average service conditions values of maximum design stress as given in TABLE XV.

For helical springs of other spring materials, safe working stresses in torsion are suggested by this company as follows:

Material	(Pounds Per Square Inch)
Stainless steel	80,000
Phosphor bronze	50,000
Monel metal	50,000
Brass	40,000

It should be noted that these suggested stresses and those in TABLE XV are for *average* service conditions defined as non-corrosive atmosphere, normal temperatures, and with slowly varying or static loads. In individual cases, where fatigue or other conditions are present, lower values of stress will be required, while in still other cases higher values may be possible.

SPRING TABLES

To facilitate the selection of springs for a given purpose, spring tables have been computed, based on the stresses of TABLE XIII for severe service. TABLE XVI applies to carbon-steel springs of good quality such as music or oil-tempered wire, or hot-wound helical springs. The allowable loads P are based on the stresses indicated while the deflections per turn y were determined from these loads using a modulus of rigidity of 11.4×10^6 pounds per square inch. This latter value applies to most carbon steels with sufficient accuracy. The total deflection of the spring will of course be equal to the deflection y per turn multiplied by the number of active turns. For a different value of the shear modulus G the deflections given in the table should be multiplied by $11.4 \times 10^6/G$. For working stresses other than those listed, values of loads and deflections may be taken proportional to the stress.

In TABLES XVII and XVIII similar tabulations are given for stainless steel and phosphor bronze helical compression springs. TABLE XVII for stainless steel springs is based on stresses equal to 75 per cent of those of TABLE XVI while TABLE XVIII for phosphor bronze springs is based on stresses equal to 50 per cent of those for carbon steel. The shear modulus used in com-

(*Continued on Page* 152)

Table

Load *P* and Deflection per turn *y* for Carbon

Severe

Outside Diameter

At 60,000 lb. per square inch

Wire Diam.		1/8	5/32	3/16	1/4	5/16	3/8	7/16	1/2	5/8	3/4
.014	P	.493	.398	.334	.252	.203	.169				
	y	.0123	.0209	.0319	.0606	.0990	.146				
.016	P	.726	.588	.494	.375	.302	.253	.217			
	y	.0100	.0174	.0266	.0514	.0838	.126	.174			
.018	P	1.03	.836	.700	.534	.428	.360	.310	.271		
	y	.00840	.0147	.0227	.0445	.0730	.110	.153	.203		
.020	P	1.39	1.14	.957	.729	.588	.491	.424	.371		
	y	.00706	.0126	.0198	.0390	.0645	.0965	.135	.180		
.022	P	1.82	1.50	1.27	.967	.781	.652	.561	.493	396	
	y	.0059	.0108	.0171	.0343	.0572	.0857	.119	.161	.259	
.024	P	2.33	1.93	1.63	1.25	1.01	.845	.727	.638	.512	
	y	.00510	.00940	.0151	.0305	.0512	.0774	.109	.146	.236	
.026	P	2.93	2.42	2.07	1.59	1.28	1.07	.915	.810	.652	
	y	.00437	.00822	.0134	.0272	.0461	.0700	.0980	.132	.215	
.028	P	3.60	3.01	2.55	1.98	1.60	1.34	1.15	1.01	.813	.679
	y	.00376	.00724	.0118	.0247	.0418	.0638	.0903	.122	.198	.292
.030	P	4.34	3.66	3.11	2.41	1.96	1.63	1.41	1.24	1.00	.834
	y	.00323	.00634	.0105	.0222	.0381	.0581	.0828	.112	.182	.270
.032	P	5.18	4.38	3.76	2.90	2.35	1.98	1.72	1.50	1.21	1.02
	y	.00280	.00560	.00942	.0203	.0348	.0533	.0765	.103	.168	.252
.034	P	6.07	5.20	4.47	3.48	2.83	2.39	2.05	1.82	1.45	1.22
	y	.00241	.00497	.00850	.0184	.0321	.0496	.0707	.0957	.157	.234
.036	P	6.97	6.11	5.26	4.10	3.34	2.82	2.42	2.14	1.71	1.44
	y	.00206	.00441	.00763	.0169	.0295	.0458	.0654	.0891	.146	.219
.038	P	8.08	7.00	6.14	4.80	3.89	3.30	2.84	2.52	2.00	1.70
	y	.00179	.00390	.00690	.0154	.0271	.0426	.0610	.0838	.136	.206
.040	P	8.97	8.05	7.12	5.56	4.53	3.83	3.33	2.91	2.35	1.96
	y	.00151	.00348	.00624	.0141	.0252	.0395	.0574	.0778	.129	.193
.042	P		9.14	8.12	6.41	5.16	4.45	3.83	3.37	2.72	2.28
	y		.00308	.00563	.0130	.0231	.0370	.0536	.0732	.122	.183
.044	P		10.4	9.15	7.27	5.99	5.06	4.40	3.86	3.12	2.61
	y		.00273	.00506	.0119	.0217	.0343	.0496	.0684	.114	.172
.046	P		11.6	10.4	8.26	6.83	5.76	5.02	4.40	3.56	2.98
	y		.00244	.00465	.0110	.0202	.0321	.0468	.0646	.108	.163
.048	P		12.9	11.7	9.38	7.69	6.54	5.67	5.02	4.04	3.39
	y		.00216	.00418	.0102	.0189	.0303	.0444	.0613	.103	.155
.051	P		14.8	13.6	11.1	9.18	7.81	6.77	5.96	4.82	4.05
	y		.00179	.00359	.00907	.0171	.0276	.0405	.0560	.0947	.144
.055	P			16.5	13.7	11.4	9.73	8.45	7.45	6.04	5.06
	y			.00296	.00780	.0150	.0244	.0363	.0504	.0857	.131
.059	P			19.6	16.6	13.9	11.9	10.4	9.16	7.44	6.24
	y			.00242	.00670	.0131	.0218	.0326	.0456	.0788	.119
.063	P				20.0	16.8	14.4	12.5	11.1	9.02	7.57
	y				.00578	.0116	.0194	.0293	.0413	.0714	.110
.067	P				23.3	19.9	17.2	15.0	13.3	10.8	9.09
	y				.00498	.0103	.0175	.0266	.0376	.0656	.101
.071	P				27.1	23.4	20.1	17.7	15.7	12.8	10.8
	y				.00430	.00910	.0156	.0241	.0342	.0602	.0932
.074	P					26.1	22.7	19.9	17.7	14.5	12.2
	y					.00831	.0146	.0224	.0321	.0565	.0881
.078	P					30.2	26.4	23.2	20.7	16.9	14.2
	y					.00738	.0131	.0205	.0296	.0524	.0820
.080	P					32.4	28.3	25.0	22.2	18.2	15.4
	y					.00698	.0125	.0196	.0282	.0504	.0793
.082	P					34.6	30.3	26.8	23.8	19.5	16.5
	y					.00658	.0118	.0187	.0271	.0486	.0766

*Based on stresses indicated. For other working stresses, load and deflection may be taken in proportion.

†Curvature effects included.

XVI

Steel, Round Wire, Helical Springs†

Service*

of Spring (in.)

⅛	1	1⅛	1¼	1⅜	1½	1⅝	1¾	1⅞	2		Wire Diam.
										P y	.014
										P y	.016
										P y	.018
										P y	.020
										P y	.022
										P y	.024
										P y	.026
										P y	.028
										P y	.030
.869 .348										P y	.032
1.04 .325	.906 .442									P y	.034
1.24 .305	1.08 .406									P y	.036
1.46 .287	1.27 .382	1.14 .490								P y	.038
1.70 .271	1.48 .360	1.32 .463								P y	.040
1.95 .255	1.72 .341	1.53 .438	1.38 .548							P y	.042
2.25 .241	1.97 .322	1.75 .414	1.58 .520							P y	.044
2.56 .229	2.25 .306	2.01 .395	1.81 .494	1.64 .605						P y	.046
2.92 .217	2.56 .292	2.27 .375	2.05 .472	1.88 .578						P y	.048
3.48 .202	3.06 .272	2.72 .351	2.46 .440	2.24 .540	2.06 .650					P y	.051
4.36 .184	3.83 .248	3.42 .321	3.08 .405	2.80 .495	2.57 .596	2.38 .708				P y	.055
5.38 .169	4.72 .228	4.21 .296	3.80 .372	3.46 .465	3.17 .550	2.93 .652				P y	.059
6.51 .156	5.73 .210	5.12 .274	4.62 .345	4.21 .423	3.86 .510	3.57 .606	3.32 .709			P y	.063
7.85 .144	6.88 .195	6.13 .253	5.54 .319	5.06 .394	4.64 .476	4.29 .566	3.98 .663	3.73 .768		P y	.067
9.29 .134	8.18 .182	7.29 .236	6.59 .298	6.01 .369	5.50 .444	5.10 .530	4.74 .620	4.43 .719	4.17 .827	P y	.071
10.5 .127	9.25 .172	8.25 .224	7.45 .284	6.78 .349	6.24 .424	5.77 .504	5.36 .592	5.00 .686	4.69 .786	P y	.074
12.3 .118	10.8 .161	9.67 .210	8.72 .266	7.94 .329	7.29 .398	6.74 .474	6.28 .557	5.86 .645	5.50 .740	P y	.078
13.2 .114	11.7 .156	10.4 .204	9.40 .258	8.56 .318	7.85 .386	7.28 .461	6.76 .541	6.33 .628	5.93 .722	P y	.080
14.3 .111	12.5 .151	11.2 .198	10.1 .250	9.22 .310	8.45 .375	7.82 .447	7.29 .526	6.80 .611	6.39 .701	P y	.082

(Continued on next page)

Table XVI

Load *P* and Deflection per turn *y* for Carbon

Severe

Outside Diameter

At 55,000 lb. per square inch

Wire Diam.		5/16	3/8	7/16	1/2	5/8	3/4	7/8	1	1 1/8	1 1/4	1 3/8	1 1/2	1 5/8
.086	*P*	35.7	31.6	28.1	25.1	20.6	17.4	15.0	13.2	11.8	10.7	9.72	8.95	8.26
	y	.00532	.00981	.0157	.0229	.0413	.0652	.0945	.130	.170	.216	.267	.325	.387
.090	*P*	38.9	34.6	30.8	27.6	22.6	19.2	16.6	14.6	13.1	11.8	10.8	9.92	9.16
	y	.00474	.00879	.0143	.0210	.0384	.0610	.0889	.122	.160	.204	.253	.307	.366
.091	*P*	42.1	37.5	33.4	29.9	24.6	20.8	18.1	15.9	14.2	12.9	11.7	10.8	9.96
	y	.00456	.00856	.0138	.0205	.0373	.0594	.0870	.119	.157	.200	.248	.301	.360
.102	*P*		49.4	45.1	40.6	33.6	28.6	24.8	21.9	19.6	17.7	16.2	14.9	13.7
	y		.00652	.0110	.0166	.0312	.0505	.0743	.103	.136	.174	.216	.264	.315
.106	*P*		55.2	50.0	45.3	37.5	31.9	27.8	24.5	21.9	19.8	18.1	16.7	15.4
	y		.00597	.0101	.0154	.0291	.0472	.0700	.0974	.129	.165	.206	.251	.300
.121	*P*		76.1	70.7	65.1	54.8	47.0	40.9	36.1	32.5	29.3	26.8	24.6	22.8
	y		.00409	.00737	.0116	.0230	.0382	.0574	.0804	.108	.138	.173	.211	.254
.135	*P*			93.4	86.9	74.6	64.2	56.1	49.6	44.6	40.6	37.0	33.8	31.5
	y			.00546	.00893	.0185	.0316	.0480	.0680	.0915	.119	.149	.186	.221
.148	*P*				111	95.9	83.3	73.2	64.7	58.3	53.0	48.6	44.6	41.3
	y				.00705	.0152	.0266	.0410	.0586	.0796	.104	.131	.161	.195
.162	*P*				137	123	107	95.2	84.3	76.0	69.0	63.0	58.4	54.0
	y				.00538	.0124	.0222	.0351	.0505	.0690	.0904	.115	.142	.172
.177	*P*					154	137	122	109	98.3	89.4	81.9	75.6	70.1
	y					.00991	.0184	.0295	.0433	.0597	.0788	.101	.125	.153

At 48,000 lb. per square inch

.207	*P*									135	122	113	104	96.8
	y									.0398	.0531	.0687	.0861	.105
.225	*P*										156	144	132	124
	y										.0458	.0597	.0752	.0929
.263	*P*											223	207	194
	y											.0450	.0576	.0721
.283	*P*												256	239
	y												.0504	.0632
.307	*P*													306
	y													.0548

At 42,000 lb. per square inch

.331	*P*													
	y													
.363	*P*													
	y													
.394	*P*													
	y													
.430	*P*													
	y													
.460	*P*													
	y													
.500	*P*													
	y													

†Curvature effects included.

• Table based on stresses indicated. For other working stresses, load and deflection may be taken in proportion.

(Continued)

Steel, Round Wire, Helical Springs†

Service *

of Spring (in.) ———————————————————

1¾	1⅞	2	2¼	2½	2¾	3	3½	4	4½	5	5½	6		Wire Diam.
7.70 .456	7.19 .528	6.76 .608	6.00 .782										P y	.086
8.52 .432	7.96 .501	7.47 .575	6.66 .742	6.00 .930									P y	.090
9.26 .423	8.66 .491	8.13 .565	7.25 .728	6.53 .911									P y	.0915
12.8 .372	11.9 .432	11.2 .498	10.0 .642	9.02 .808	8.20 .987								P y	.102
14.3 .353	13.4 .412	12.6 .474	11.2 .612	10.1 .771	9.20 .945	8.47 1.14							P y	.106
21.2 .300	19.9 .351	18.7 .404	16.6 .524	15.0 .662	13.7 .813	12.6 .982							P y	.121
29.4 .261	27.6 .306	25.8 .354	23.0 .461	20.7 .580	18.9 .718	17.4 .864							P y	.135
38.5 .232	36.1 .272	34.0 .315	30.6 .412	27.3 .520	24.9 .640	22.9 .777							P y	.148
50.4 .205	47.1 .241	44.4 .280	39.7 .368	35.7 .466	32.6 .576	29.9 .696							P y	.162
65.4 .182	61.3 .215	57.6 .250	51.4 .328	46.5 .417	42.4 .516	39.0 .628							P y	.177
90.4 **127**	**84.8** **.150**	**79.8** **.176**	**71.3** **.232**	**64.4** **.298**	**58.9** **.370**	**54.2** **.451**	**46.6** **.636**						P y	.207
115 **112**	**108** **.133**	**102** **.156**	**91.3** **.208**	**82.6** **.266**	**75.4** **.332**	**69.3** **.406**	**59.7** **.576**	**52.4** **.773**					P y	.225
181 **0874**	**171** **.105**	**161** **.124**	**144** **.166**	**131** **.215**	**119** **.269**	**110** **.331**	**94.8** **.471**	**82.8** **.634**	**74.4** **.830**				P y	.263
224 **.0774**	**211** **.0930**	**199** **.110**	**179** **.149**	**162** **.193**	**148** **.243**	**137** **.299**	**118** **.428**	**104** **.582**	**92.4** **.758**	**83.5** **.958**			P y	.283
282 **.0672**	**267** **.0814**	**252** **.0965**	**227** **.131**	**206** **.171**	**188** **.217**	**173** **.267**	**150** **.385**	**132** **.525**	**118** **.685**	**107** **.873**	**97.0** **1.08**	**89.3** **1.30**	P y	.307
307 **.0512**	**289** **.0623**	**274** **.0744**	**247** **.102**	**224** **.134**	**205** **.170**	**189** **.211**	**164** **.305**	**144** **.416**	**129** **.546**	**116** **.691**	**106** **.856**	**97.4** **1.04**	P y	.331
	377 **.0526**	**356** **.0631**	**323** **.0876**	**294** **.116**	**269** **.148**	**249** **.184**	**215** **.268**	**189** **.368**	**170** **.484**	**153** **.616**	**140** **.764**	**128** **.927**	P y	.363
		451 **.0544**	**408** **.0759**	**372** **.101**	**341** **.130**	**316** **.163**	**274** **.239**	**241** **.329**	**216** **.434**	**195** **.555**	**178** **.693**	**164** **.838**	P y	.394
			522 **.0646**	**478** **.0872**	**440** **.113**	**406** **.142**	**353** **.210**	**313** **.292**	**279** **.386**	**252** **.494**	**231** **.617**	**212** **.752**	P y	.430
				582 **.0772**	**534** **.101**	**495** **.127**	**431** **.190**	**381** **.265**	**341** **.352**	**308** **.452**	**282** **.564**	**259** **.690**	P y	.460
				734 **.0660**	**677** **.0868**	**629** **.110**	**548** **.166**	**486** **.234**	**436** **.313**	**395** **.404**	**360** **.505**	**332** **.619**	P y	.500

Table

Load *P* and Deflection per turn *y* for Stainless

Severe

Outside Diameter

At 45,000 lb. per square inch

Wire Diam.		⅛	5/32	3/16	¼	5/16	⅜	7/16	½	⅝	¾
.014	*P*	.369	.299	.251	.189	.152	.127				
	y	.0100	.0170	.0260	.0494	.0805	.119				
.015	*P*	.452	.370	.311	.233	.187	.156	.134			
	y	.00901	.0155	.0238	.0456	.0742	.110	.152			
.0162	*P*	.565	.459	.388	.292	.237	.196	.169			
	y	.00804	.0139	.0213	.0412	.0674	.100	.140			
.0173	*P*	.685	.557	.471	.354	.286	.239	.204	.180		
	y	.00728	.0128	.0198	.0380	.0628	.0930	.129	.172		
.0181	*P*	.784	.638	.538	.407	.326	.275	.236	.208		
	y	.00680	.0119	.0186	.0361	.0592	.0885	.123	.164		
.0204	*P*	1.10	.898	.761	.580	.467	.391	.336	.295		
	y	.00555	.00989	.0156	.0309	.0512	.0768	.107	.143		
.0230	*P*	1.55	1.28	1.08	.831	.669	.555	.480	.421	.340	
	y	.00445	.00824	.0131	.0263	.0442	.0659	.0930	.124	.202	
.0258	*P*	2.14	1.78	1.51	1.16	.936	.782	.676	.592	.478	
	y	.00359	-.00678	.0109	.0224	.0380	.0572	.0810	.108	.177	
.0286	*P*	2.88	2.40	2.05	1.57	1.28	1.06	.918	.808	.648	.546
	y	.00293	.00568	.00935	.0194	.0333	.0504	.0716	.0964	.156	.233
.032	*P*	3.89	3.28	2.82	2.18	1.76	1.48	1.29	1.12	.908	.765
	y	.00228	.00456	.00767	.0165	.0283	.0434	.0623	.0838	.137	.205
.035	*P*	4.89	4.22	3.66	2.84	2.31	1.94	1.68	1.47	1.19	.990
	y	.00181	.00382	.00658	.0144	.0251	.0387	.0556	.0748	.124	.184
.038	*P*	6.06	5.25	4.60	3.60	2.92	2.48	2.13	1.89	1.50	1.28
	y	.00146	.00318	.00562	.0125	.0221	.0347	.0497	.0682	.111	.168
.040	*P*	6.73	6.04	5.34	4.17	3.40	2.87	2.50	2.18	1.76	1.47
	y	.00123	.00283	.00508	.0115	.0205	.0372	.0467	.0634	.105	.157
.041	*P*	7.18	6.45	5.62	4.46	3.64	3.09	2.70	2.36	1.90	1.59
	y	.00115	.00266	.00476	.0110	.0197	.0311	.0452	.0614	.102	.153
.048	*P*		9.68	8.78	7.04	5.77	4.90	4.25	3.76	3.03	2.54
	y		.00176	.00340	.00830	.0154	.0247	.0361	.0499	.0839	.126
.050	*P*		10.5	9.67	7.88	6.49	5.50	4.78	4.23	3.43	2.86
	y		.00154	.00307	.00769	.0143	.0230	.0340	.0470	.0795	.120
.054	*P*			11.8	9.72	8.16	6.93	5.98	5.28	4.31	3.60
	y			.00253	.00656	.0126	.0206	.0304	.0420	.0721	.109
.059	*P*			14.7	12.5	10.4	8.92	7.75	6.87	5.58	4.68
	y			.00197	.00545	.0107	.0175	.0265	.0371	.0642	.0969
.063	*P*				15.0	12.6	10.8	9.38	8.32	6.76	5.68
	y				.00471	.00944	.0158	.0238	.0336	.0581	.0896
.072	*P*				21.0	18.3	15.8	13.8	12.3	10.0	8.46
	y				.00336	.00720	.0125	.0192	.0275	.0481	.0747
.080	*P*					24.3	21.2	18.8	16.6	13.6	11.6
	y					.00568	.0102	.0160	.0230	.0410	.0646

*Based on stresses indicated. For other working stresses, load and deflection may be taken in proportion.

†Curvature effects included.

XVII

Steel, Round Wire, Helical Springs†

Service*

of Spring (in.)

⅛	1	1⅛	1¼	1⅜	1½	1⅝	1¾	1⅞	2		Wire Diam.
										P y	.014
										P y	.015
										P y	.0162
										P y	.0173
										P y	.0181
										P y	.0204
										P y	.0230
										P y	.0258
										P y	.0286
.652 .283										P y	.032
.851 .256	.748 .341									P y	.035
1.10 .234	.952 .311	.853 .399								P y	.038
1.28 .221	1.11 .293	.990 .377								P y	.040
1.36 .213	1.20 .285	1.07 .367	.966 .459							P y	.041
2.19 .176	1.92 .238	1.70 .305	1.54 .384	1.41 .470						P y	.048
2.46 .169	2.18 .227	1.92 .292	1.74 .365	1.58 .448	1.45 .540					P y	.050
3.08 .153	2.74 .207	2.43 .268	2.18 .335	1.99 .411	1.83 .497	1.69 .588				P y	.054
4.04 .138	3.54 .186	3.16 .241	2.85 .303	2.60 .379	2.38 .448	2.20 .531				P y	.059
4.88 .127	4.30 .171	3.84 .223	3.46 .281	3.16 .344	2.93 .415	2.68 .493	2.49 .577			P y	.063
7.27 .107	6.40 .145	5.69 .188	5.16 .239	4.68 .294	4.31 .356	3.97 .421	3.71 .497	3.46 .576	3.25 .660	P y	.072
10.0 0928	8.78 .127	7.80 .166	7.03 .210	6.42 .259	5.90 .314	5.47 .375	5.06 .441	4.76 .511	4.45 .589	P y	.080

(*Continued on next page*)

Table XVII

Load *P* and Deflection per turn *y* for Stainless

Severe

Outside Diameter

At 41,250 lb. per square inch

Wire Diam.		5/16	3/8	7/16	1/2	5/8	3/4	7/8	1	1 1/8	1 1/4	1 3/8	1 1/2	1 5/8
.0915	*P*	31.6	28.1	25.0	22.4	18.4	15.6	13.6	11.9	10.6	9.68	8.78	8.10	7.47
	y	.00371	.00697	.0112	.0167	.0304	.0484	.0708	.0969	.128	.163	.202	.245	.293
.106	*P*		41.4	37.5	34.0	28.1	23.9	20.8	18.4	16.4	14.8	13.6	12.5	11.6
	y		.00486	.00822	.0125	.0237	.0384	.0570	.0793	.105	.134	.168	.204	.244
.121	*P*		57.1	53.0	48.8	41.1	35.2	30.7	27.1	24.4	22.0	20.1	18.4	17.1
	y		.00333	.00600	.00949	.0187	.0311	.0467	.0655	.0879	.112	.141	.172	.207
.135	*P*			70.0	65.2	57.0	48.2	42.1	37.2	33.4	30.4	27.8	25.4	23.6
	y			.00444	.00727	.0151	.0251	.0391	.0554	.0745	.0969	.121	.151	.180
.148	*P*				83.2	71.9	62.5	54.9	48.5	43.7	39.8	36.4	33.4	31.0
	y				.00574	.0124	.0216	.0334	.0477	.0648	.0847	.107	.131	.159
.162	*P*				103	92.2	80.2	71.4	63.2	57.0	51.8	47.2	43.8	40.5
	y				.00438	.0101	.0181	.0286	.0411	.0562	.0736	.0936	.116	.140
.177	*P*					116	103	91.5	81.8	73.7	67.0	61.4	56.7	52.6
	y					.00807	.0150	.0240	.0353	.0486	.0642	.0822	.102	.125

At 36,000 lb. per square inch

.192	*P*								89.8	81.3	74.2	68.2	62.7	58.4
	y								.0266	.0370	.0492	.0634	.0785	.0963
.207	*P*									101	91.5	84.8	78.0	72.6
	y									.0324	.0432	.0559	.0701	.0855
.225	*P*										117	108	99.0	93.0
	y										.0373	.0486	.0612	.0756
.244	*P*										147	136	126	117
	y										.0321	.0421	.0536	.0664
.263	*P*											167	155	146
	y											.0366	.0469	.0587
.283	*P*												192	179
	y												.0410	.0515
.307	*P*													230
	y													.0446

At 31,500 lb. per square inch

.331	*P*													
	y													
.363	*P*													
	y													
.394	*P*													
	y													
.430	*P*													
	y													
.460	*P*													
	y													
.490	*P*													
	y													

° Table based on stresses indicated. For other working stresses, load and deflection may be taken in proportion.

† Curvature effects included.

(Continued)

Steel, Round Wire, Helical Springs†

Service*

of Spring (in.)

1¾	1⅞	2	2¼	2½	2¾	3	3½	4	4½	5	5½	6		Wire Diam.
6.94 .344	6.50 .400	6.10 .460	5.44 .593	4.90 .742									*P* *y*	.0915
10.7 .287	10.0 .335	9.45 .386	8.40 .498	7.58 .628	6.90 .769	6.35 .928							*P* *y*	.106
15.9 .244	14.9 .286	14.0 .329	12.4 .427	11.2 .539	10.3 .662	9.45 .800							*P* *y*	.121
22.0 .212	20.7 .249	19.4 .288	17.2 .375	15.5 .472	14.2 .585	13.0 .703							*P* *y*	.135
28.9 .189	27.1 .221	25.5 .256	23.0 .335	20.5 .423	18.7 .521	17.2 .632							*P* *y*	.148
37.8 .167	35.3 .196	33.3 .228	30.0 .300	26.8 .379	24.5 .469	22.4 .567							*P* *y*	.162
49.0 .148	46.0 .175	43.2 .204	38.6 .267	35.9 .339	31.8 .420	29.2 .511							*P* *y*	.177
54.4 .116	51.0 .136	48.1 .160	42.8 .209	38.7 .267	35.2 .332	32.4 .402	28.0 .568						*P* *y*	.192
67.8 103	63.6 .122	59.8 .143	53.5 .189	48.3 .243	44.2 .301	40.6 .367	35.0 .518						*P* *y*	.207
86.2 .0912	81.0 .108	76.5 .127	68.5 .169	62.0 .210	56.6 .270	52.0 .331	44.8 .469	39.3 .629					*P* *y*	.225
110 .0808	103 .0958	96.7 .113	87.0 .151	79.0 .194	71.9 .243	66.4 .298	56.9 .422	50.0 .570	44.8 .740				*P* *y*	.244
136 .0711	128 .0855	121 .101	108 .135	98.2 .175	89.2 .219	82.5 .269	71.1 .383	62.1 .516	55.8 .676				*P* *y*	.263
168 .0630	158 .0757	149 .0896	134 .121	122 .157	111 .198	103 .243	88.5 .348	78.0 .474	69.3 .617	62.6 .780			*P* *y*	.283
212 .0547	200 .0663	189 .0786	170 .107	154 .139	141 .177	130 .217	112 .313	99.0 .427	88.5 .558	80.2 .711	72.8 .879	67.0 1.06	*P* *y*	.307
230 .0417	217 .0507	206 .0606	185 .0831	168 .109	154 .138	142 .172	123 .248	108 .339	96.8 .444	87.0 .563	79.5 .697	73.0 .847	*P* *y*	.331
	283 .0428	267 .0514	242 .0713	220 .0944	202 .121	187 .150	161 .218	142 .300	128 .394	115 .501	105 .622	96.0 .755	*P* *y*	.363
		338 .0443	306 .0618	279 .0822	256 .106	237 .133	206 .195	181 .268	162 .353	146 .452	134 .564	123 .682	*P* *y*	.394
			396 .0526	362 .0710	333 .0920	308 .116	267 .171	237 .238	212 .314	190 .402	174 .502	160 .612	*P* *y*	.430
				436 .0629	400 .0822	371 .103	323 .155	286 .216	256 .287	231 .368	212 .459	194 .561	*P* *y*	.460
				521 .0559	481 .0733	444 .0928	390 .140	343 .196	308 .263	278 .339	255 .423	234 .518	*P* *y*	.490

Table

Load *P* and Deflection per turn *y* for Phosphor

Severe

Outside Diameter

At 30,000 lb. per square inch

Wire Diam.		1/8	9/64	5/32	1/4	5/16	3/8	7/16	1/2	5/8	3/4
.0142	*P*	.255	.208	.174	.132	.106	.0887				
	y	.0114	.0196	.0297	.0568	.0921	.137				
.0159	*P*	.357	.290	.243	.184	.148	.124	.107			
	y	.00968	.0167	.0257	.0492	.0810	.120	.167			
.0179	*P*	.504	.410	.346	.262	.211	.177	.152	.133		
	y	.00805	.0141	.0220	.0426	.0702	.105	.146	.194		
.0201	*P*	.702	.576	.486	.372	.298	.249	.215	.188		
	y	.00662	.0119	.0187	.0372	.0608	.0912	.127	.170		
.0226	*P*	.986	.811	.686	.525	.422	.352	.304	.266	.214	
	y	.00542	.00990	.0157	.0316	.0526	.0798	.111	.148	.239	
.0254	*P*	1.37	1.13	.960	.738	.598	.498	.430	.378	.304	
	y	.00432	.00811	.0131	.0268	.0452	.0682	.0965	.130	.209	
.0285	*P*	1.89	1.58	1.35	1.03	.841	.704	.606	.533	.427	.358
	y	.00344	.00664	.0110	.0227	.0389	.0592	.0839	.113	.183	.272
.032	*P*	2.59	2.19	1.88	1.45	1.18	.993	.858	.750	.606	.508
	y	.00266	.00532	.00895	.0193	.0331	.0506	.0726	.0980	.160	.239
.036	*P*	3.48	3.06	2.63	2.05	1.67	1.41	1.21	1.07	.858	.718
	y	.00196	.00419	.00724	.0161	.0280	.0435	.0622	.0846	.139	.208
.040	*P*	4.48	4.02	3.56	2.78	2.26	1.92	1.66	1.46	1.18	.982
	y	.00143	.00331	.00592	.0134	.0239	.0375	.0545	.0739	.123	.183
.045	*P*		5.48	4.89	3.90	3.21	2.71	2.35	2.07	1.67	1.40
	y		.00245	.00460	.0109	.0200	.0316	.0461	.0634	.106	.159
.051	*P*		7.42	6.79	5.53	4.59	3.90	3.38	2.98	2.41	2.02
	y		.00170	.00341	.00862	.0162	.0262	.0385	.0532	.0900	.137
.057	*P*			9.05	7.57	6.34	5.39	4.68	4.14	3.37	2.81
	y			.00254	.00688	.0132	.0219	.0325	.0454	.0780	.118
.064	*P*				10.4	8.74	7.52	6.58	5.82	4.74	3.96
	y				.00532	.0107	.0180	.0276	.0384	.0666	.102
.072	*P*				14.0	12.2	10.5	9.22	8.20	6.68	5.62
	y				.00393	.00841	.0146	.0223	.0320	.0561	.0868
.081	*P*					16.7	14.5	12.9	11.5	9.38	7.96
	y					.00642	.0114	.0181	.0262	.0468	.0740

* Table based on stresses indicated. For other working stresses, load and deflection may be taken in proportion.

†Curvature effects included.

XVIII

Bronze, Round Wire, Helical Springs†

Service*

of Spring (in.)

⅛	1	1⅛	1¼	1⅜	1½	1⅝	1¾	1⅞	2		Wire Diam.
										$\frac{P}{y}$	.0142
										$\frac{P}{y}$	.0159
										$\frac{P}{y}$	.0179
										$\frac{P}{y}$	.0201
										$\frac{P}{y}$	.0226
										$\frac{P}{y}$	.0254
										$\frac{P}{y}$	.0285
434 331										$\frac{P}{y}$	.032
618 293	.541 .386									$\frac{P}{y}$	.036
818 257	.741 .342	.660 .440								$\frac{P}{y}$	.040
1.21 224	1.05 .298	.938 .384	.845 .482	.773 .592						$\frac{P}{y}$	.045
1.74 192	1.53 .258	1.36 .334	1.23 .418	1.12 .513	1.03 .618					$\frac{P}{y}$	.051
2.42 168	2.13 .226	1.90 .296	1.71 .366	1.56 .452	1.43 .544	1.32 .647				$\frac{P}{y}$	.057
3.43 146	3.00 .196	2.68 .255	2.42 .322	2.20 .394	2.03 .478	1.87 .566	1.74 .663			$\frac{P}{y}$	.064
4.86 125	4.26 .170	3.79 .220	3.43 .278	3.12 .342	2.87 .416	2.66 .494	2.47 .580	2.31 .672	2.16 .770	$\frac{P}{y}$	.072
6.90 107	6.04 .145	5.40 .190	4.85 .241	4.44 .298	4.08 .362	3.78 .432	3.52 .506	3.27 .586	3.08 .674	$\frac{P}{y}$	.081

(*Continued on next page*)

Table XVII

Load *P* and Deflection per turn *y* for Phosphor

Seven

Outside Diameter

At 27,500 lb. per square inch

Wire Diam.		5/16	3/8	7/16	1/2	5/8	3/4	7/8	1	1 1/8	1 1/4	1 3/8	1 1/2	1 5/8
.091	*P*	20.7	18.4	16.4	14.8	12.2	10.2	8.90	7.86	7.02	6.32	5.76	5.28	4.9
	y	.00439	.00819	.0133	.0196	.0361	.0568	.0833	.115	.151	.192	.237	.287	.344
.102	*P*		24.7	22.6	20.3	16.8	14.3	12.4	11.0	9.80	8.85	8.10	7.45	6.8
	y		.00620	.0104	.0158	.0296	.0480	.0706	.0978	.129	.165	.205	.251	.299
.114	*P*		33.2	30.5	27.8	23.2	19.8	17.2	15.2	13.7	12.4	11.2	10.3	9.5
	y		.00466	.00814	.0126	.0244	.0402	.0596	.0832	.111	.143	.178	.217	.260
.129	*P*			42.0	39.3	32.8	28.3	24.7	21.8	19.6	17.7	16.2	14.8	13.8
	y			.00593	.00967	.0193	.0326	.0492	.0692	.0931	.120	.151	.184	.223
.144	*P*				51.5	44.6	38.6	33.8	30.0	27.0	24.5	22.4	20.7	19.1
	y				.00720	.0154	.0266	.0409	.0586	.0790	.103	.130	.160	.193
.162	*P*				68.5	61.5	53.5	47.6	42.2	38.0	34.5	31.5	29.2	27.0
	y				.00512	.0118	.0211	.0333	.0480	.0656	.0859	.109	.135	.163
.182	*P*						74.0	65.6	58.9	53.2	48.6	44.4	41.0	38.2
	y						.0165	.0267	.0391	.0541	.0720	.0915	.114	.140

At 24,000 lb. per square inch

.204	*P*									64.4	58.8	54.1	49.8	46.4
	y									.0388	.0517	.0669	.0834	.103
.229	*P*										81.8	75.4	69.9	65.2
	y										.0422	.0550	.0696	.0860
.258	*P*											106	98.8	91.8
	y											.0444	.0568	.0705
.284	*P*												129	120
	y												.0476	.0596

At 21,000 lb. per square inch

.325	*P*													156
	y													.0408
.365	*P*													
	y													
.410	*P*													
	y													
.460	*P*													
	y													

° Table based on stresses indicated. For other working stresses, load and deflection may be taken in proportion.

†Curvature effects included.

(Continued)

Bronze, Round Wire, Helical Springs†

Service*

of Spring (in.)

1¾	1⅞	2	2¼	2½	2¾	3	3½	4	4½	5	5½	6		Wire Diam.
4.56 .404	4.26 .468	3.99 .539	3.56 .697	3.20 .870									*P* *y*	.091
6.40 .353	5.95 .405	5.60 .474	5.00 .610	4.51 .768	4.10 .938	3.78 1.13							*P* *y*	.102
8.90 .307	8.31 .358	7.82 .413	7.00 .538	6.28 .672	5.74 .828	5.26 .998							*P* *y*	.114
12.9 .264	12.0 .307	11.3 .355	10.1 .462	9.07 .584	8.28 .717	7.56 .870							*P* *y*	.129
17.8 .229	16.6 .267	15.7 .310	13.9 .403	12.6 .512	11.5 .630	10.6 .762							*P* *y*	.144
25.2 .195	23.6 .229	22.2 .266	19.8 .350	17.8 .442	16.3 .547	15.0 .661							*P* *y*	.162
35.6 .167	33.3 .197	31.4 .229	28.1 .302	25.3 .384	23.0 .474	21.1 .574	18.2 .807						*P* *y*	.182
43.4 .124	40.6 .146	38.3 .171	34.3 .226	31.0 .289	28.3 .360	25.9 .436	22.3 .616						*P* *y*	.204
60.6 .104	56.8 .123	53.8 .145	48.2 .193	43.6 .248	39.7 .309	36.0 .377	31.4 .534	27.6 .720					*P* *y*	.229
85.9 .0859	80.7 .102	76.0 .121	68.2 .162	61.8 .210	56.6 .263	51.8 .321	45.0 .461	39.3 .620	35.1 .807				*P* *y*	.258
113 .0732	107 .0883	101 .105	90.4 .141	81.8 .182	74.8 .230	69.1 .284	59.6 .406	52.3 .550	46.6 .716	42.2 .908			*P* *y*	.284
146 .0504	138 .0612	130 .0728	117 .100	106 .131	97.5 .166	90.0 .206	77.8 .298	68.4 .407	61.0 .532	55.0 .674	50.1 .832	46.2 1.01	*P* *y*	.325
	192 .0496	181 .0596	163 .0822	150 .109	136 .139	126 .173	110 .254	96.7 .349	86.5 .458	77.9 .582	71.0 .722	65.0 .874	*P* *y*	.365
		250 .0476	229 .0672	209 .0897	192 .116	177 .145	154 .215	136 .297	122 .394	110 .501	100 .624	92.2 .760	*P* *y*	.410
			316 .0540	291 .0734	267 .0960	248 .121	216 .181	190 .252	170 .335	154 .430	141 .536	130 .656	*P* *y*	.460

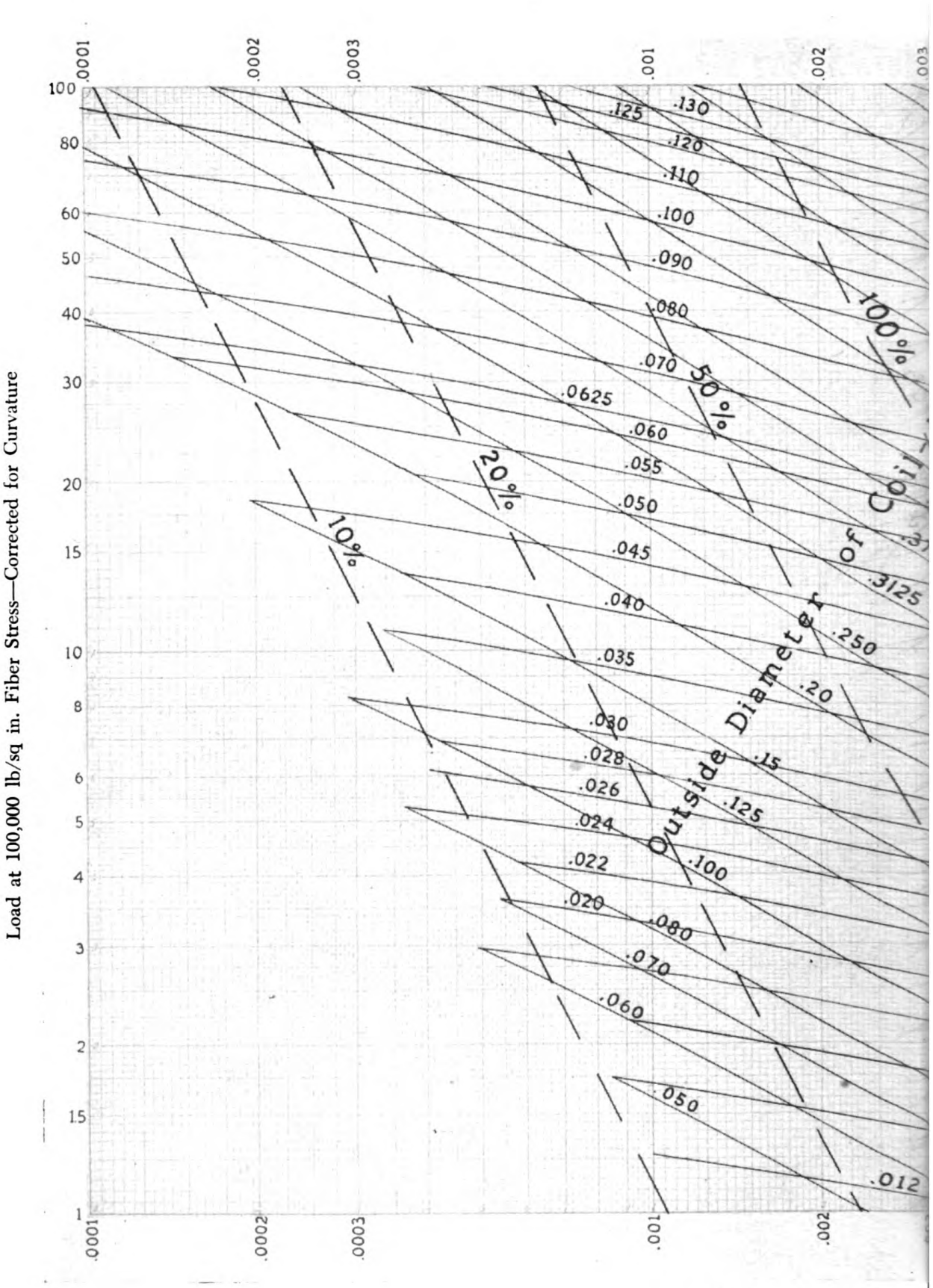

Fig. 78—Design Chart for helical compression

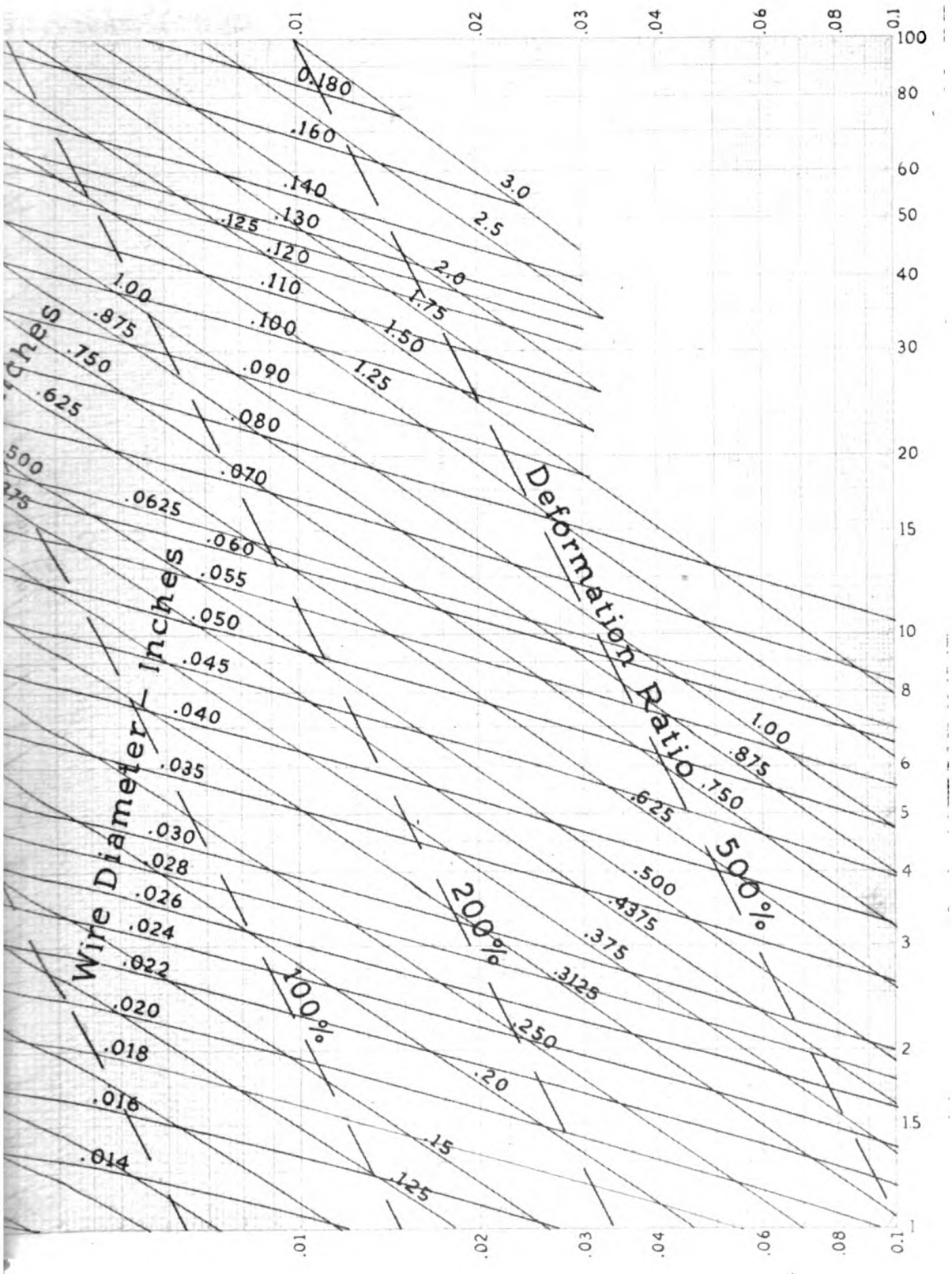

—Courtesy, Wallace Barnes Co.

f Load per Active Coil
Elasticity = 11,500,000 lb per sq in.)
r tension springs (Load range 1 to 100 pounds)

puting TABLE XVII for stainless steel was 10.5×10^6 while that used in calculating TABLE XVIII for phosphor bronze springs was 6×10^6 pounds per square inch. For other values of modulus G, the deflections per turn given in TABLE XVII should be multiplied by $10.5 \times 10^6/G$, those in TABLE XVIII by $6 \times 10^6/G$. For average or light service these loads and deflections may be increased in proportion to working stress (see TABLES XIII and XV).

As an example of the use of the spring tables: A steel compression spring is required for a mechanism to give 160 pounds at a deflection of .8-inch. The space available is such that an outside diameter of 2 inches may be used. If the spring is subject to severe service, from TABLE XVI for .263-inch wire diameter and 2 inch outside diameter the allowable load is 161 pounds and the allowable deflection per turn .124-inch. To obtain .8-inch deflection would require $.8/.124 = 6.45$, say 6½, active turns or about 8 to 8½ total turns (Chapter VIII discusses evaluation of end turns). This would take a spring of about $1.1(8.5)\ (.263) + .8 = 3.26$ inches free length, allowing 10 per cent extra length for space between the turns when the spring is compressed at a load of 160 pounds. The length at a load of 160 pounds would be 2.46 inches, and the solid length about 10 per cent less or about 2.2 inches. The stress at the solid length would be about 10 per cent above the stress on which the table is based or 52,800 pounds per square inch, a relatively low stress. A further discussion of allowable values for maximum stress when the spring is compressed solid will be given in Chapter VIII.

DESIGN CHARTS

Two useful design charts[1], prepared with the curvature correction factor included, are shown on *Figs.* 78 and 79. For convenience, these charts are based on a value of 100,000 pounds per square inch working stress and a torsional modulus $G = 11.5 \times 10^6$ pounds per square inch. It should be emphasized that this value of stress is used mainly for convenience and is not necessarily the recommended working stress. The

[1]These charts were published by Wallace Barnes Co. in *The Mainspring* for June and August, 1940, and are reproduced through the courtesy of this company.

chart of *Fig.* 78 covers the range in load between one and 100 pounds, that of *Fig.* 79, between 100 and 10,000 pounds.

In these charts the ordinates represent load at 100,000 pounds per square inch torsion stress, the abscissas, inches deflection per pound of load per active coil. Thus the abscissa, when multiplied by number of active turns will yield the reciprocal of the spring constant in pounds per inch. The set of lines inclined at about 15 degrees to the horizontal in these charts represents wire diameters, while the set inclined at about 30 degrees represents outside coil diameters. The intersection of any line of one set with that of the other set fixes the load at 100,000 pounds per square inch stress and the deflection per pound of load per active turn. Thus, for example, if the wire size is .04-inch and the outside coil diameter ¼-inch, the load at 100,000 pounds per square inch stress will be 9.3 pounds and the deflection per pound of load per turn will be .0025-inch. If there are 10 active turns the spring constant will be $1/.025 = 40$ pounds per inch. The load at any other stress τ different from 100,000 pounds per square inch will be in direct ratio to the stress; thus for an allowable stress of 60,000 pounds per square inch the load in the above example becomes 9.3 (60,000/100,000) = 5.58 pounds.

If the load and working stress are known the required spring size may easily be read from the charts of *Figs.* 78 and 79. Thus, assuming a working stress of 60,000 pounds per square inch is to be used with a working load of 30 pounds, the working load at 100,000 pounds per square inch will be direct ratio to the stress or 30 (100,000/60,000) = 50 pounds. From the chart it is seen that a wide variety of sizes will yield this value of load. For example, a wire size of .100-inch and an outside coil diameter of ¾-inch will come close to it. In this size the spring will have a deflection of about .002-inch per pound of load per active turn or .06-inch per turn at 30 pound load, assuming a steel spring with $G = 11.5 \times 10^6$ pounds per square inch. If, say, ¼-inch deflection is required at 30 pounds load the number of active coils required would be .25/.06 or slightly more than four. If the actual modulus G is different from 11.5×10^6 pounds per square inch a correction in deflection may be made to take this into account by multiplying the deflection by $11.5 \times 10^6/G$.

(*Continued on Page* 156)

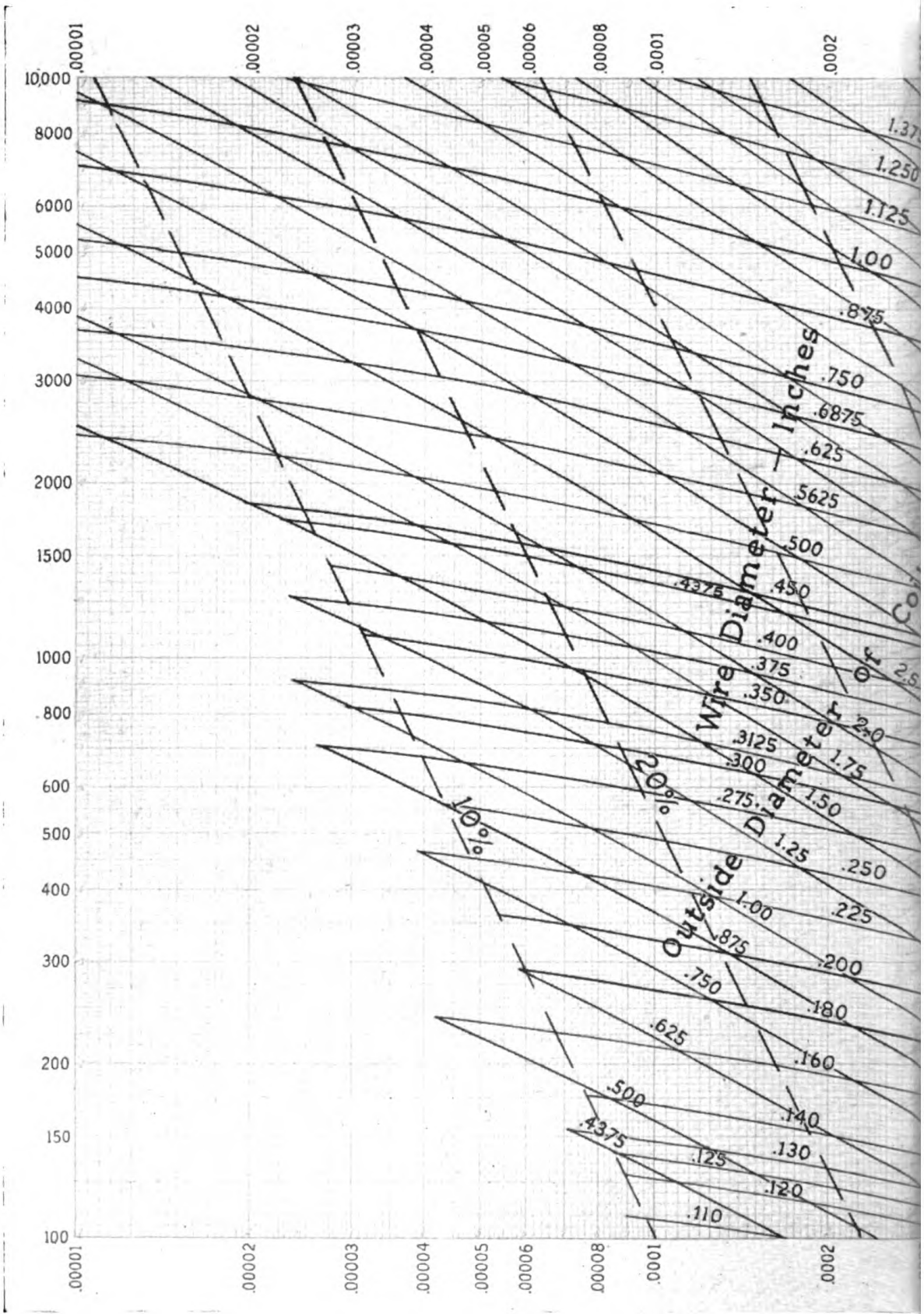

Fig. 79—Design chart for helical compression or t

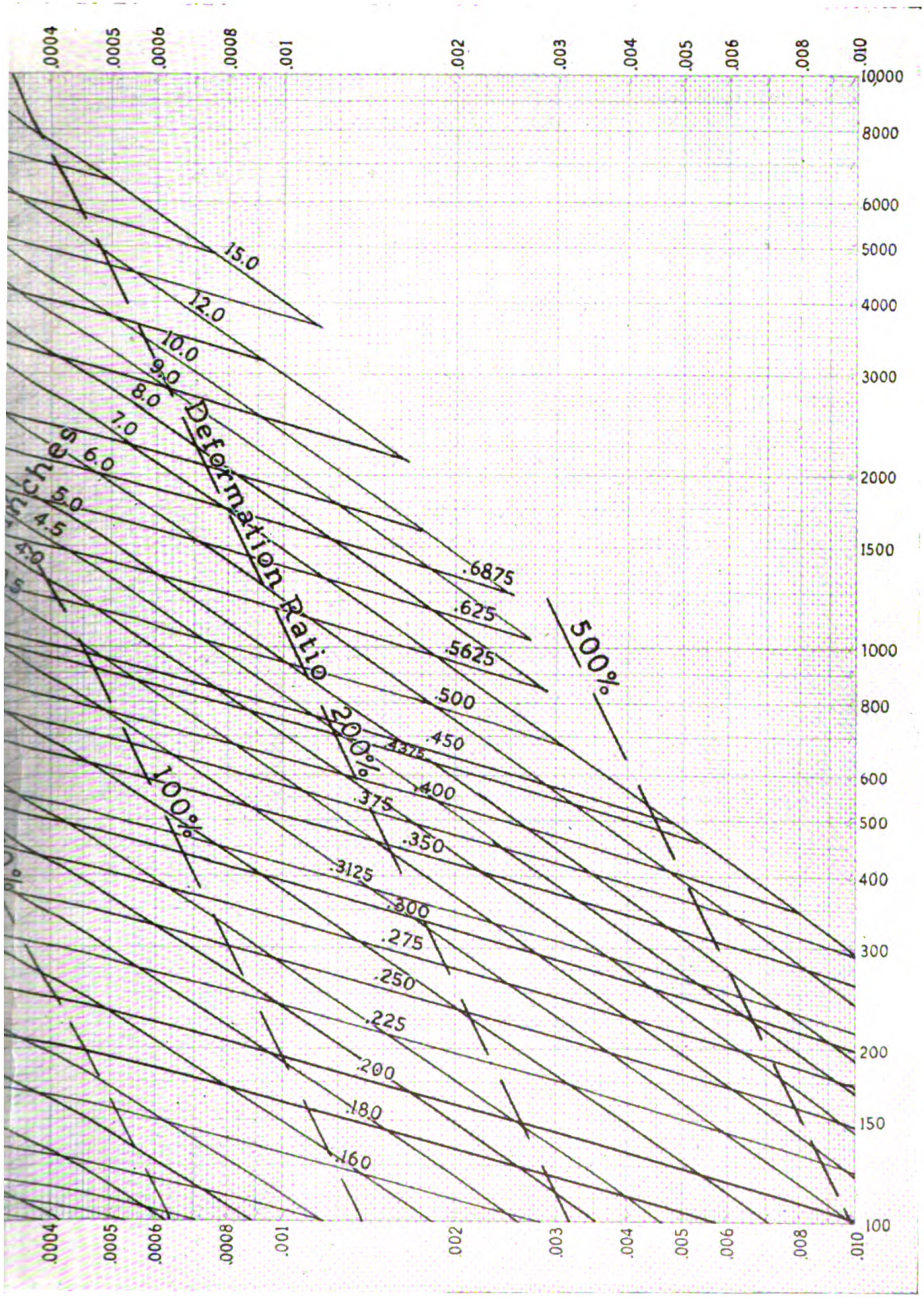

d of Load per Active Coil

—Courtesy, Wallace Barnes Co.

lasticity = 11,500,000 lb per sq in.)

sion springs (Load Range 100 to 10,000 pounds)

On the charts of *Figs.* 78 and 79 a series of dashed lines at about 70 degrees to the horizontal are shown. These represent *deformation ratio,* defined as the ratio of the deflection at 100,000 pounds per square inch stress to the net solid height of the active coils in the spring. It is clear that springs with a large deformation ratio will have a large deflection compared to the solid height and vice versa. Thus a spring of .100-inch wire and an outside coil diameter of ¾-inch (as used in the previous example) will have a deformation ratio of almost 100 per cent at 100,000 pounds per square inch, *Fig.* 79. This means that the deflection at 100,000 pounds per square inch stress will be about equal to the solid height. At 60,000 pounds per square inch the deformation ratio will be about 60 per cent.

It should be noted that there will always be a small inaccuracy in reading these design charts. This error should not, however, exceed 3 per cent and will usually be within 2 per cent. In this connection, it should be noted that because of manufacturing tolerances, variations in wire size, and in coil diameter, the actual deviation between test and calculated results will usually be more than 2 per cent, unless special precautions in manufacturing have been taken. For a further discussion of this, Chapter VIII considers these variables. This means that the charts of *Figs.* 78 and 79 should be sufficiently accurate for most practical purposes. However, in cases where maximum accuracy is desired, calculation may be made using Equations 7 and 18, or TABLES XVI, XVII or XVIII may be used.

CHAPTER VIII

OTHER DESIGN CONSIDERATIONS—HELICAL COMPRESSION SPRINGS

Some of the various considerations, other than working stress, which are important in designing helical compression springs will be briefly discussed in this chapter. These include types of end turns, allowances for end coils, effects of eccentricity of loading, effects of variation in spring dimensions, variation in modulus of rigidity, stress at solid compression. The effect of combined axial and lateral loading together with buckling problems will be discussed in the following chapter.

EFFECTS DUE TO END TURNS

Usual types of end turns employed in helical compression springs are shown in *Fig.* 80. The most common type—ends set up and ground or forged, indicated in *Fig.* 80*a*—has the advantage that there is less eccentricity of loading (and hence a lower stress for a given load) than would be the case where the ends are made as indicated in *Fig.* 80*b, c* or *d.* In *Fig.* 80*b* the ends are simply squared and closed, while in *Fig.* 80*c,* the ends are left plain without any grinding. This type of spring would give the highest amount of eccentricity of loading. The spring of *Fig.* 80*d* is the same as that at *c* except that the ends have been ground so that at least ½ turn at each end is flat. In *Fig.* 80*e,* a spring with 2½ turns set up is shown.

An accurate determination of deflection in helical compression springs requires that the effect of the end turns be estimated with reasonable accuracy. Some experimental and analytical work by Vogt[1] indicates that for the usual design of end coil with ends squared and ground, *Fig.* 80*a*, the number of active coils is equal to the number of completely free coils plus ½. (The number of free coils in this case is determined by the number of turns between tip contact points.) Thus if a com-

[1] "Number of Active Coils in Helical Springs", *Transactions* A.S.M.E., June, 1934, Page 468.

pression spring has 10 free coils and 12 total coils (tip to tip of bar) then on this basis the number of active coils would be 10½, and ¾ of a turn would be inactive at each end. However, when the load is increased, there is some progressive seating of the end turns so that the number of completely free coils decreases with the load, and this increases the number of inactive turns.

Pletta, Smith, and Harrison[2] made a series of careful tests on commercial springs using a special setup to determine the end-turn effect. The results of these tests indicate that at *zero load* the number of active turns was equal to $n' + ½$ where n' is the number of completely free coils at zero load. As the load increases, however, the number of inactive coils was found to increase, due to seating of the end coils, the amount of increase varying from .5 to one turn at usual working loads, with an average of about .7-turn. Since for calculation purposes the average number of active turns in the range from no load to working load is of primary interest (this would be used in the deflection formula), it appears reasonable to subtract about half of this decrease from the number of active turns. This gives a figure for average active turns varying from n' to $n' + ¼$. Because the total number of turns is $n' + 2$ for the usual type of end turn, *Fig.* 80*a*, this means that the inactive turns found in these tests varied from about 1¾ to 2 with an average of 1.85.

An analysis made by H. C. Keysor[3] indicates that the total number of inactive coils in the spring is approximately equal to 1.2 as a deduction from "solid turns" based on the commonly used practice of taking the number of "solid turns" equal to the solid height divided by bar or wire diameter. Since for the usual shape of end coil, *Fig.* 80*a*, the "solid turns" are equal to the "total turns" measured from tip to tip of bar, minus ½ turn, this figure of 1.2 would be equivalent to a deduction of 1.7 turn from "total turns".

Some additional data on inactive turns was given by Edgerton[4] based on the research of the Special Research Committee for Mechanical Springs of A.S.M.E. The average value obtained by Edgerton was 1.15 as a deduction from "solid turns"

[2]"The Effect of Overstrain on Closely Coiled Helical Springs and the Variation of the Number of Active Coils with Load", Virginia Polytechnic Institute, Engineering Experimental Station *Bulletin* No. 24.

[3]"Calculation of the Elastic Curve of a Helical Compression Spring"—H. C. Keysor, *Transactions* A.S.M.E., May, 1940, Page 319.

[4]Discussed in MACHINE DESIGN, December, 1939, Page 53.

or 1.65 as a deduction from total turns.

Taking the results of these investigations as a basis, it appears that for the usual design of end coil the number of inactive coils may vary from about 1.65 to 2 considered as a deduction from total turns. Probably a mean value of 1¾ inactive coils would be as good a figure as any to use in practice. For the higher loads possibly a figure somewhat higher may be justified, while a lower figure may be used for lower loads. The seating of the coils as the load increases also tends to produce a slight curvature of the load-deflection diagram. For further details, the reader is referred to the investigation by Pletta and his associates[2].

The preceding discussion has been concerned only with the usual type of end turn. Test results concerning the other types

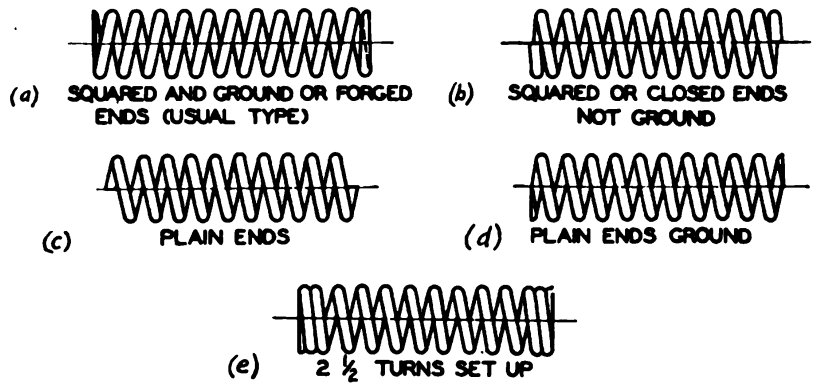

Fig. 80—Types of end turns as used in helical compression springs

of end coils shown in *Fig.* 80 are lacking, but approximate values of inactive coils are as follows: For plain ends, *Fig.* 80*c*, active turns are $n-½$ where n=total turns; for plain ends ground, *Fig.* 80*d*, active turns are $n-1$. *If* 2½ turns at each end are set up and ground as in *Fig.* 80*e* the active turns may be taken roughly as $n-5$.

ECCENTRICITY OF LOADING

If a compression spring of usual design is compressed between two parallel plates as in a testing machine (*Fig.* 23), it will be found that in general the resultant load is displaced from the spring axis by a small amount e as indicated in this figure.

The effect of this eccentric loading is to increase the stress on one side of the spring diameter and decrease it on the other as indicated, for example, by the load-stress diagram of *Fig.* 49 which shows a higher stress on one side of the spring than on the other.

An analysis of the effect of this eccentricity of loading based on certain assumptions has also been carried out by Keysor[3]. Because of the complexity of the analysis, it will not be given here. However, the final results of the analysis are given in the curve of *Fig.* 81, the ordinates representing ratio e/r between eccentricity e and coil radius r and the abscissas being the number of turns n' between tip contact points. The total number of turns n for the usual design will be equal to $n' + 2$. It is seen that the eccentricity ratio fluctuates between zero and maximum values, the zero values occuring approximately at $n' =$ ½, 1½, 2½ . . . . etc. Theoretically it should be possible to get axial loading (i.e., zero eccentricity) by choosing n' to conform with these values. However, because of variations in actual springs and possibly also because of errors in the assumptions made, axial loading cannot in general be realized in practice[5]. For practical design, therefore, the envelope of the curve as indicated in *Fig.* 81 should be employed.

For calculating the ratio e/r the following expressions given by Keysor may be used:

$$\frac{e}{r} = 1.123(Z-1) \qquad (128)$$

$$Z = 1 + \frac{.5043}{N} + \frac{.1213}{N^2} + \frac{2.058}{N^3} \qquad (129)$$

where N = number of solid coils. This will be approximately 1½ turns greater than the number of coils n' between tip contact points, i.e., $N = n' + 1.5$. By using these equations the ratio e/r may be calculated. As an approximation it may be assumed that where the spring index is fairly large the stress will be increased in the ratio $1 + e/r$ as compared with the stress for purely axial loading.

Some tests have been made by the writer which give a rough check on this formula. These were carried out in con-

[5]This is borne out also by experiments made by Pletta and Maher—"Helix Warping in Helical Compression Springs", *Transactions* A.S.M.E., May 1940, Page 327.

nection with an application where it was desired to obtain as nearly as possible a central load on a helical compression spring. The tests were made on small helical springs using a special three-point loading fixture so arranged that the eccentricity of loading could be determined. Essentially this consisted of a flat plate with provision for attaching dead weights 120 degrees apart on equal radii. When equal loads were applied at equal

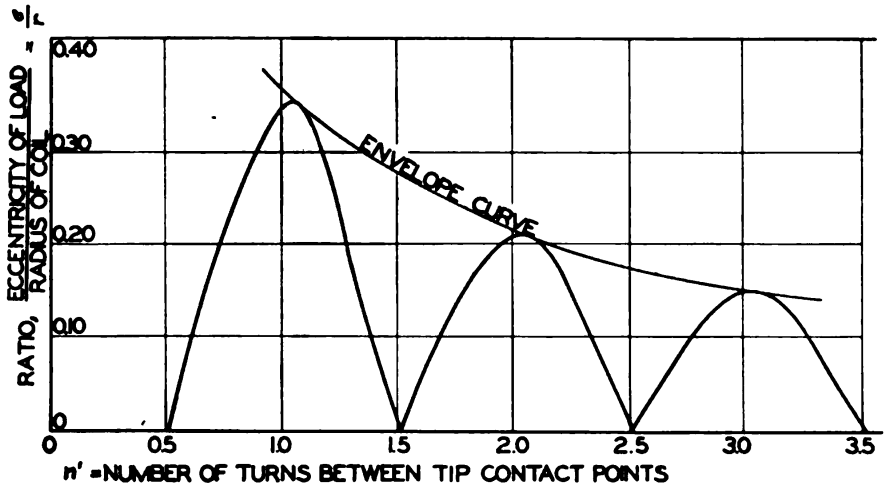

Fig. 81—Ratio e/r between eccentricity and coil radius as a funtion of n' based on analysis by Keysor

radii, in general it was found that the loading planes at each end of the spring were not parallel. The loads were then adjusted to give parallelism of these loading planes; from the magnitude of the required loads the eccentricity of loading could be calculated.

The results of these tests are summarized in TABLE XIX, the spring outside diameter, wire diameter, number of turns n', and load being given. Springs tested had ground end coils of the usual form. In the last column the values of the ratio e/r between eccentricity and coil radius as calculated from Equations 128 and 129 are given. For comparison the test values of e/r as measured on these various springs are also given in the next to the last column.

It will be seen that in most cases the agreement between calculated and test values is sufficiently good for practical use, especially if it is considered that the test springs were hand made and no particular care was taken in forming the end turns.

TABLE XIX

Tests To Determine Eccentricity of Loading in Helical Springs

Spring No.	Outside Diameter (in.)	Wire Diameter (in.)	Turns Between Tip Contact Points n'	Total Load (lb.)	Load Eccentricity / Coil Radius = e/r Test		Calculated*
0	2⅞	.177	4	34	.12		.12
1	2⅞	.177	4	34	.04		.12
2	2⅞	.177	4¼	31	.09		.11
3	2⅞	.177	4½	29	.14		.11
4	2¾	.177	2	38	.19		.23
5	2¾	.177	2	38	.13	.19 av.	.23
6	2¾	.177	2	38	.24		.23
7	2¾	.177	2¼	32	.22		.21
8	2¾	.177	2¼	32	.27	.21 av.	.21
9	2¾	.177	2¼	29	.13		.21
10	2¾	.177	2½	30	.30		.19
11	2¾	.177	2½	30	.22	.24 av.	.19
12	2¾	.177	2½	30	.20		.19

*Using Equations (128) and (129), taking N = n' + 1.5.

For best results the increase of the stress due to eccentricity should be taken into account in design, particularly if the number of coils is small.

EFFECT OF VARIATIONS IN DIMENSIONS

Another factor which the designer should consider is the effect of slight variations in spring wire or coil diameters on the load-deflection characteristic of springs. For example, as will be shown later, a one per cent change in the mean-coil diameter means a 3 per cent change in the load-deflection characteristic while a one per cent change in the wire diameter results in a 4 per cent change in the deflection characteristic.

Allowable Variations—Allowable variations in commercial spring-wire diameters as listed in A.S.T.M. standards for various materials are given in TABLE XX. From these an idea of the probable variations in wire diameter of actual springs may be determined.

As may be seen from this table, music wire of .064-inch diameter may vary by ±.001-inch from the nominal value or by about 1½ per cent. This means a 6 per cent possible change in the load-deflection characteristic due to this variation. However, if the wire is 1½ per cent undersize, the spring maker might compensate for it by reducing the coil diameter by 2 per cent. In

this manner the load-deflection characteristic may be brought back to the design value. If springs are to be held to relatively close tolerance, it is well to allow some leeway on the coil diameter or on the total number of turns, since otherwise the cost may be excessive.

Manufacturing Tolerances—In winding springs cold, there is always some "spring back". In other words, the inside diam-

TABLE XX

Allowable Variations in Commercial Spring Wire Sizes

Material	A.S.T.M. Specification (No.)	Wire Diameter (in.)	Permissible Variation (in.)
Hard-drawn spring wire	A-227-39T	.028 to .072	±.001
Chrome-vanadium spring wire	A-229-39T	.073 to .375	±.002
Oil-tempered wire	A-231-39T	.376 and over	±.003
Music wire	A-228-39T	.026 and under	±.0003
		.027 to .063	±.0005
		.064 and over	±.001
Carbon-steel valve-spring wire	A-230-39T	.093 to .148	±.001
		.149 to .177	±.0015
Chrome-vanadium valve-spring wire	A-232-39T	.178 to .250	±.002

eter of the spring after winding will be slightly greater than the diameter of the mandrel as a consequence of the elastic and plastic properties of the material. Although this effect may be compensated for by using a slightly smaller mandrel, for different materials it may be expected that some variations in coil diameter will still remain.

As an example of actual variations in coil diameters to be expected in practice, the tolerances given by one spring manufacturer[6] are listed in TABLE XXI. It may be seen that these tolerances depend both on the spring index D/d and on the mean diameter D.

Deflection—The effect of small variations in coil diameter and wire diameter may be estimated quantitatively as follows: The ordinary deflection formula for helical springs (Equation 7) is

$$\delta = \frac{64Pr^3n}{Gd^4}$$

In this formula r and d are the *nominal* mean coil radius and wire diameter, respectively. Supposing that the *true* mean

[6] *Manual of Spring Engineering* published American Steel and Wire Co., Page 97.

coil radius and wire diameter are $r_o = r(1+\epsilon)$ and $d_o = d(1+\lambda)$ where ϵ and λ are small quantities, relative to unity, the true deflection then becomes

$$\delta_1 = \frac{64Pr^3(1+\epsilon)^3 n}{Gd^4(1+\lambda)^4}$$

Since it has been assumed that ϵ and λ are small relative to unity, the squares and higher powers may be neglected. Hence this equation may be written with sufficient accuracy (since $(1+\epsilon)^3 \approx 1+3\epsilon$ and $1/(1+\lambda)^4 \approx 1-4\lambda$):

$$\delta_1 = \frac{64Pr^3n}{Gd^4}(1+3\epsilon-4\lambda) \quad \ldots\ldots\ldots\ldots\ldots\ldots\ldots\ldots\ldots\ldots\ldots\ldots\ldots\ldots\ldots\ldots (130)$$

It is seen that the true deflection δ_1 is merely the nominal deflection δ multiplied by a term $1+3\epsilon-4\lambda$ which depends on ϵ and λ. Supposing now that the actual mean coil diameter or radius is one per cent greater than the nominal, i.e., $\epsilon = .01$, while at the same time the true wire diameter is one per cent *less* than the nominal or $\lambda = -.01$. Putting these values of ϵ and λ in Equation 130,

$$\delta_1 = 1.07\frac{64Pr^3n}{Gd^4}$$

In other words, under such conditions with a one per cent *cumulative* variation in coil and wire diameter from the nominal values the actual deflection will be 1.07 times the nominal deflection or 7 per cent greater.

Example—As a practical example, an actual case examined by the author will be discussed. This spring was made of nominal 9/16-inch wire or $d = .5625$ inch. After cutting up the spring and measuring the dimensions, it was found that the average wire diameter was .551-inch which would correspond to an error in the wire size of $(.5625-.551)/.5625 = 2.04$ per cent, i.e., $\lambda = -.02$. Assuming the true mean coil diameter of this spring were equal to the nominal, i.e., that $\epsilon = 0$, then from Equation 130, the true deflection δ_1 would be $1-4\lambda = 1.08$ times the calculated value. The actual coil diameter, however, had been made about 2 per cent less than the nominal, which meant that ϵ was $-.02$ Using this value in Equation 130 the true deflection becomes 1.02 times the nominal deflection. Thus, the

actual coil diameter had been made slightly smaller than the nominal value by the spring maker to compensate for the decreased diameter of the wire used.

In a similar manner it may be shown that one per cent variation in the wire diameter means approximately a 3 per cent variation in the stress; a one per cent change in the coil diameter, a one per cent change in stress. Usually, the stress does not have

TABLE XXI

Tolerances on Spring Coil Diameters *

(Close Cold-Wound Helical Springs)

Mean Coil Diameter (in.)	Variations in Diameter D/d = 4 (in.)	D/d = 8 (in.)	D/d = 12 (in.)
1/8	±.003	±.0035	±.005
1/8 to 3/16	.0035	.005	.0065
3/16 to 1/4	.005	.0065	.0085
1/4 to 3/8	.0065	.0085	.0105
3/8 to 1/2	.0085	.0105	.0130
1/2 to 3/4	.0105	.0130	.0155
3/4 to 1	.0130	.0155	.0230
1 to 1 1/2	.0155	.0205	.0318
1 1/2 to 2	.0185	.0313	.0408
2 to 3	.030	.0430	.0528
3 to 4	....	.0550	.0730
4 to 5	....	.0725	.095
5 to 6	....	....	.125
6 to 7	....	....	.165
7 to 8	....	....	.210

*Data from American Steel & Wire Co.

to be held to such close limits as the deflection; however, a consideration of the effect of commercial variations in wire size on stress may be advisable for certain highly stressed springs.

EFFECT OF MODULUS OF RIGIDITY

An accurate calculation of the deflection of actual springs requires not only that the effective turns be known, but also that the modulus of rigidity of the spring material be known with good accuracy. As indicated in the discussion of Chapter IV the modulus values reported in the literature vary considerably. In particular, the effect of a decarburized layer only a few mils thick reduces the modulus by several per cent.

On the basis of the results given in TABLES V and VI a good average figure for modulus of rigidity for carbon and alloy steels is 11.5×10^6 pounds per square inch. However, for hot-wound,

carbon-steel springs of hot-rolled material in the larger sizes, some manufacturers recommend a modulus figure of 10.5×10^6 pounds per square inch. On the basis of the test data given in

TABLE XXII

Average Values for Modulus of Rigidity

Material	Modulus of Rigidity (lb./sq. in.)
Music wire	11.5×10^6
Carbon steel	11.5×10^6
Chrome-vanadium steels	11.5×10^6
Hard-drawn stainless	10.5×10^6
Monel metal	9×10^6
Phosphor bronze	6×10^6

Chapter IV the following average figures given in TABLE XXII may be used for various spring materials. It should be noted, however, that deviations of several per cent may occur.

STRESS AT SOLID COMPRESSION

In the design of compression springs it is desirable to choose the coil pitch such that when the spring is compressed solid, no appreciable permanent set will occur. The reason for this is that usually in operation the spring may at times be compressed solid and, if under these conditions it takes a set, the load at working deflections will be changed. Thus the spring will no longer have its initial characteristics.

Overstressing—If a compression spring is initially wound with a coil pitch sufficiently great so that the elastic limit of the material is exceeded when the spring is compressed solid, the distribution of stress along a diameter of the cross section is shown in *Fig.* 82*b* for a spring of large index[7]. At low loads before the elastic limit is reached the distribution is approximately linear as shown in *Fig.* 82*a*. After the load is released, the residual stress distribution will be like that in *Fig.* 82*c*.

For a spring of large index these residual stresses may be calculated approximately from the condition that the moment of the stress represented by the triangle *obc* about point *o* must be equal to the moment of the stresses represented by the area *oadc*. When normal load is again applied the resultant stress

[7]For a discussion of methods of calculation of loads for complete yielding, see Chapter V, Page 102.

will be as indicated in *Fig.* 82*d*. It is clear that the maximum stress at this load has been reduced by the overstressing, since residual stresses of opposite sign are induced and these subtract from the stresses due to the working load. However, in this process of cold-setting or overstressing, the free length has also been decreased. If the initial free length of the spring is made greater than the specified free length by the proper amount, the final free length may be held to the specified value. At the same time, by means of this overstressing process, a higher calculated stress at solid compression may be permissible.

It will be found that beyond a certain limit, there will be no additional gain by using this process. In other words, beyond a certain initial free length, the final length after the setting operation will be the same. The reason for this is that the stress-strain curve tends to flatten out (*Fig.* 61) so that a higher

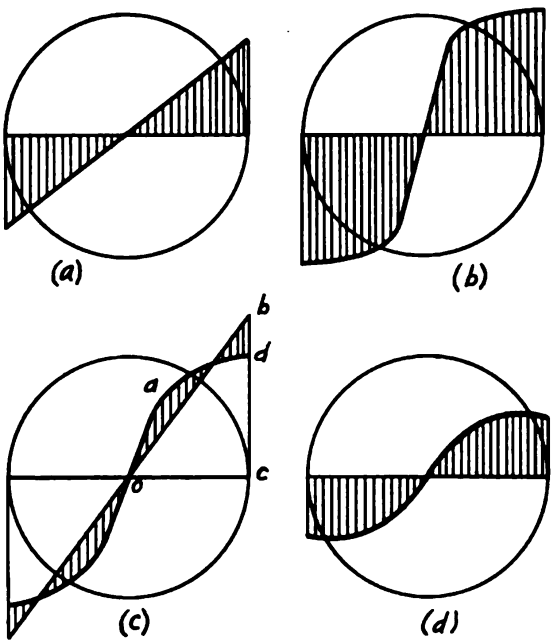

Fig. 82—Distribution of stresses over cross section of helical spring of large index; (*a*), stress distribution of normal load before cold-setting; (*b*) distribution above elastic limit; (*c*) residual stress after cold-setting with load removed; (*d*) stress at normal load after setting

TABLE XXIII

Suggested Torsion Stresses at Solid Compression for Helical Springs*

Material	Diameter (in.)	Stress at Solid Compression up to which it is not necessary to remove set (lb./sq. in.)	Maximum Stress at Solid Compression with all set removed (lb./sq. in.)
Music Wire			
	up to .032	130,000	180,000
	.032 to .062	110,000	170,000
	.062 to .125	100,000	160,000
	.125 and over	90,000	150,000
Hard-drawn spring wire			
	up to .032	120,000	170,000
	.032 to .062	100,000	160,000
	.062 to .125	90,000	150,000
	.125 and over	80,000	140,000
Oil-tempered wire			
	.125 and over	80,000	140,000
18-8 stainless hard drawn			
	up to .125	85,000	140,000
	over .125	75,000	120,000
Phosphor bronze			
	General sizes	40,000	70,000

*Curvature correction included.

strain does not give an appreciably greater torsion moment. If exceeded, excessive cold work and loss of ductility may occur.

Recovery—Another effect which occurs when this type of operation is performed is what is known as "recovery." Thus immediately after the settage operation on a compression spring, the free length of the spring will be a certain value; on standing for some time, however, if the settage stress is too high, the free length will increase slightly. This again will change the load-deflection characteristics of the spring and is objectionable in many cases (such as, for example, instrument springs).

Allowable Stresses—Suggested stresses at solid compression for various spring materials as given by Wallace Barnes Co.[1] are listed in TABLE XXIII. In the third column is given the stress at solid compression up to which it is not necessary to remove set while in the last column is tabulated the stress at solid compression which may be used after all set is removed through repeated compressions of the spring. It should be remembered that the high calculated stresses given in the fourth column will not actually be reached due to yielding of the material.

[1] *The Mainspring*, February, 1941.

CHAPTER IX

COMBINED LATERAL AND AXIAL LOADING; BUCKLING OF HELICAL COMPRESSION SPRINGS

If a compression spring is made too long relative to its diameter, it will be found that at a certain load, a sudden sidewise buckling will occur. This phenomenon is essentially similar to the buckling of a long slender column when the load exceeds the critical load. In the design of helical compression springs, it is necessary to guard against this lateral buckling by choosing the spring proportions in such a way that the critical or buckling load will always be greater than any load encountered in service. If this is not done, some sort of lateral support (such as a hollow tube for a guide) must be provided.

BUCKLING

Calculation of the buckling load for helical springs may be carried out in essentially the same manner as that used in column theory[1]. However, the analysis in the case of the spring differs from that used in ordinary column theory in that it is necessary to consider the decrease in length under load. In the case of the usual steel column, on the other hand, this decrease is small and may be neglected. The reason for this lies in the high modulus of elasticity of most structural materials, which is such that the change in length from no load to full load is usually less than .1 per cent. This is not true, however, for a material like rubber with a very low modulus of elasticity. Besides the change in length under load, it is also necessary to consider the deformations of the spring due to lateral shearing forces. In addition it will be assumed that the spring is close coiled so that the pitch angle may be considered as small.

[1]For a good discussion of column theory see *Theory of Elastic Stability* by Timoshenko, McGraw-Hill, 1936. A discussion of buckling of helical springs is also given here. For additional references on the buckling of springs see articles by E. Hurlbrink, *Zeit, Ver. d. Ing.* V. 54, Page 138, 1910; by R. Grammel, *Zeit Angew. Math. Mech.*, V. 4, Page 384, 1924; and by Biezeno and Koch, *Zeit Angew Math. Mech.* V. 5, Page 279, 1925.

Letting l_o=free length of spring; l=length of spring after compression; n=number of active coils; r=mean coil radius; α_o, β_o, γ_o equal the compressive, flexural, and shearing rigidities of the spring in its unstressed condition[2] and α, β, γ are the same quantities after compression of the spring.

Critical Load—It may be shown from column theory that if the shearing deformations in a column with hinged ends are considered, the critical load is[3]

$$P_{cr}=\frac{P_e}{1+\frac{\kappa_1 P_e}{AG}} \quad \ldots\ldots (131)$$

In this AG/κ_1 is the shearing rigidity of the column and P_e is the Euler critical load $\pi^2 EI/l^2$, EI being the flexural rigidity of the column. The Euler critical load is that figured by considering only the flexural rigidity and neglecting shearing deformations.

Applying these formulas to a spring with shear rigidity γ and flexural rigidity β, the critical load becomes

$$P_{cr}=\frac{\pi^2\beta}{l^2}\left(\frac{1}{1+\frac{\pi^2\beta}{l^2\gamma}}\right) \quad \ldots\ldots (132)$$

For a close-coiled spring the compressive, flexural and shearing rigidities will all be inversely proportional to the number of coils per unit length (Equations 135, 141, and 144). Hence

$$\alpha=\alpha_o\frac{l}{l_o}\ ; \qquad \beta=\beta_o\frac{l}{l_o}\ ; \quad \gamma=\gamma_o\frac{l}{l_o} \quad \ldots\ldots (133)$$

Substituting Equation 133 in Equation 132,

$$P_{cr}=\frac{\pi^2\beta_o}{l\,l_o}\,\frac{1}{1+\frac{\pi^2\beta_o}{l^2\gamma_o}} \quad \ldots\ldots (134)$$

Using Equation 7, Chapter II, compressive rigidity becomes

[2]By compressive rigidity is meant the ratio of load to deflection per unit of length for the case of a bar under direct compression. For a bar of cross-sectional area A and modulus of elasticity E the compressive rigidity is equal to AE. Likewise the flexural rigidity is the ratio of bending moment to curvature for a beam in pure bending and is equal to modulus of elasticity times moment of inertia of the cross-section. The shearing rigidity is equal to the ratio of shearing force to shearing deflection per unit of length and for a beam is equal to modulus of rigidity times cross-sectional area GA, multiplied by a constant depending on the shape of the section.

[3]Timoshenko, loc. cit., Page 140.

$$\alpha_o = \frac{Gd^4 l_o}{64r^3 n} \quad \ldots\ldots (135)$$

Since the length is l when the spring is compressed to the critical load P_{cr}, the following equation holds:

$$\frac{l_o - l}{l_o} = \frac{64 P_{cr} r^3 n}{G d^4 l_o} \quad \ldots\ldots (136)$$

Using Equation 136 in Equation 135,

$$\frac{l_o - l}{l_o} = \frac{P_{cr}}{\alpha_o}$$

or, solving for P_{cr}

$$P_{cr} = \left(1 - \frac{l}{l_o}\right)\alpha_o \quad \ldots\ldots (137)$$

Equating values of P_{cr} given by Equations 134 and 137, the following relation is obtained

$$\frac{\alpha_o (l_o - l)}{l_o} = \frac{\pi^2 \beta_o}{l\, l_o} \frac{1}{1 + \frac{\pi^2 \beta_o}{l^2 \gamma_o}}$$

Letting $z = l/l_o$, then this equation may be reduced to

$$z^3 - z^2 + \frac{\pi^2 z \beta_o}{l_o^2}\left(\frac{1}{\gamma_o} + \frac{1}{\alpha_o}\right) - \frac{\pi^2 \beta_o}{l_o^2 \gamma_o} = 0 \quad \ldots\ldots (138)$$

Flexural Rigidity—Calculation of the flexural rigidity β of the spring may be accomplished by determining the angular twist of a single coil of the spring under the action of a moment transverse to the plane of the coil as indicated in *Fig.* 83. This may be done by considering a quarter coil subject to a moment M at its end as indicated in *Fig.* 84. The moment is here represented by a vector. At a cross section at an angle ϕ the bending moment M_b will be $M \cos \phi$ while the twisting moment M_t will be $M \sin \phi$. Considering a length $ds = rd\phi$, the total component of angular twist about the axis of the moment will be

$$d\theta = \frac{M_b ds \cos \phi}{EI} + \frac{M_t ds \sin \phi}{GI_p} \quad \ldots\ldots (139)$$

In this case EI and GI_p are the flexural and torsional rigidities of the wire cross section, respectively. The twist due to the bending moment M_b must be multiplied by $\cos \phi$ to obtain the component along the axis y—y of the moment; that due to M_t must be multi-

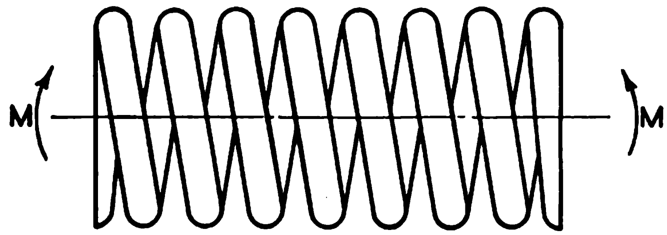

Fig. 83—Spring subjected to transverse moment

plied by $\sin \phi$. The moment of inertia in bending of the section is taken as I, that in torsion as I_p. Substituting $M_b = M \cos \phi$, $M_t = M \sin \phi$ and $ds = r d\phi$ in Equation 139 gives

$$d\theta = \frac{rM}{EI} \cos^2 \phi d\phi + \frac{rM}{GI_p} \sin^2 \phi d\phi$$

The total angular twist θ for a complete turn will be four times the integral of this between $\phi = 0$ and $\phi = \pi/2$. Thus:

$$\theta = 4 \int_0^{\pi/2} \left(\frac{rM}{EI} \cos^2 \phi + \frac{rM}{GI_p} \sin^2 \phi \right) d\phi$$

Integrating this,

$$\theta = \frac{\pi M r}{EI} \left(1 + \frac{EI}{GI_p} \right) \qquad \text{(140)}$$

If the free length is l_o, the number of turns per inch axial length will be n/l_o. This means that the angular deflection in one inch axial length will be $n\theta/l_o$. This will be also equal to the curvature $1/\rho$. Hence, taking $I_p = 2I$ for a circular cross section of the spring bar,

$$\frac{1}{\rho} = \frac{n}{l_o} \theta = \frac{n\pi}{l_o} \frac{Mr}{EI} \left(1 + \frac{E}{2G} \right)$$

From this the flexural rigidity β_o, which is the ratio of bending moment to curvature, is seen to be

$$\beta_o = \frac{2l_oEIG}{n\pi r(2G+E)} \quad \ldots\ldots (141)$$

Shearing Rigidity—To calculate the shearing rigidity, the deformation of a single ring (or coil) under a shear force Q is considered, *Fig.* 85*a*. Considering the deformation of the quarter turn shown in *Fig.* 85*b*, the bending moment at an angle ϕ

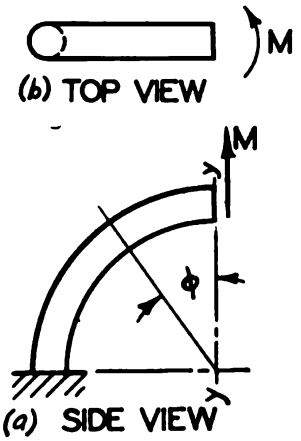

Fig. 84—Quarter coil under moment transverse to plane of coil

will be $Qr \sin \phi$; this divided by EI and multiplied by ds will give the angular deflection $d\theta$ in a length ds. Hence

$$d\theta = \frac{Qr}{EI} \sin \phi ds \quad \ldots\ldots (142)$$

The deflection along the axis y—y will be this angle multi-

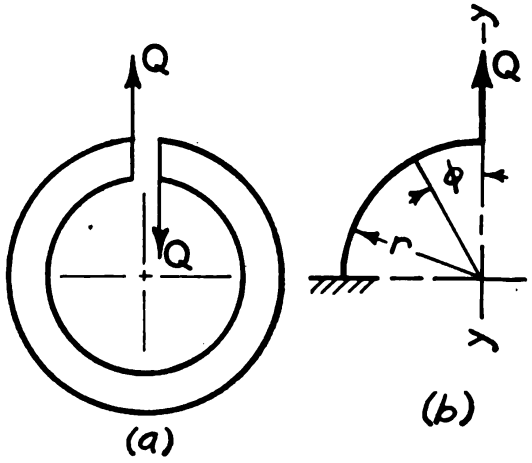

Fig. 85—Single spring turn under shear force

plied by $r \sin \phi$. This gives, using Equation 142,

$$dy = d\theta r \sin \phi = \frac{Qr^2 \sin^2 \phi ds}{EI}$$

Taking $ds = r \sin \phi$, integrating between 0 and $\pi/2$, and multiplying by 4 to get the shearing deflection y for a complete turn of spring,

$$y = 4\int_0^{\pi/2} \frac{Qr^3 \sin^2 \phi d\phi}{EI} = \frac{\pi Qr^3}{EI} \quad \ldots\ldots (143)$$

Since there will be n/l_o turns per inch axial length, the total shearing deflection per inch axial length will be

$$\frac{ny}{l_o} = \frac{\pi n}{l_o} \frac{Qr^3}{EI}$$

From this the shearing rigidity, or ratio of shearing force to deflection per unit length, becomes

$$\gamma_o = \frac{l_o EI}{\pi n r^3} \quad \ldots\ldots (144)$$

Substituting expressions in Equations 135, 141, and 144 for α_o, β_o, γ_o in Equation 138 and taking $G = E/2(1+\nu)$ where ν = Poisson's ratio,

$$z^3 - z^2 + (3+2\nu)mz - m = 0 \quad \ldots\ldots (145)$$

where

$$m = \frac{\pi^2 r^2}{l_o^2 (2+\nu)} \quad \ldots\ldots (146)$$

It will be found that this equation has one real positive root which determines the critical value of z at which buckling occurs. If this value of z is known, the corresponding critical load is, using Equation 137,

$$P_{cr} = \frac{\alpha_o (l_o - l)}{l_o} = \alpha_o (1 - z) \quad \ldots\ldots (147)$$

The results, by solving Equation 145, may be expressed:

$$P_{cr} = C_B l_o C_K \quad (148)$$

where C_K = spring constant of spring or load per inch deflection, and C_B = a factor depending on the ratio l_o/r between free length and coil radius. P_{cr} = critical or buckling load.

For a spring with hinged ends as was assumed in the derivation, the factor C_B is given by the lower curve *a* in *Fig.* 86. A spring loaded between two pivots as indicated in *Fig.* 87*b* might

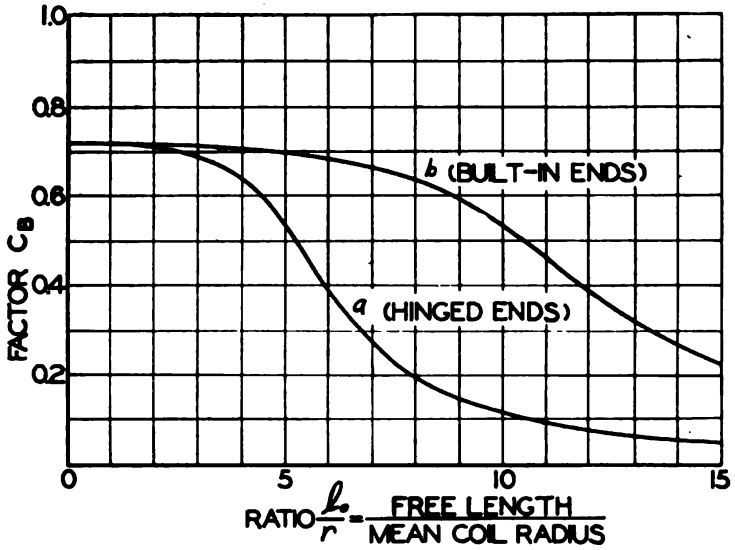

Fig. 86—Curve for finding buckling load factor C_B. Curve *a* for spring with fixed ends; curve *b* for hinged ends

be considered approximately as a spring with hinged ends provided that the distance *h* is small compared to the free length.

Fixed Spring Ends—Where the ends of the spring may be considered as fixed, a similar analysis may be carried out. The results may be written in the same form as Equation 148 except that the buckling load factor C_B is now to be taken from the upper curve *b* of *Fig.* 86. The case of built-in ends is simulated when a helical spring is compressed between parallel plates as indicated in *Fig.* 87*a*, but because of incomplete fixity of the ends and of load eccentricity, buckling load may be lower than calculated[4].

Since for a spring of circular wire the spring constant C_K is

[4]See article by Biezeno and Koch, loc. cit. for a further discussion of this problem. Tests carried out by these investigators show good agreement with the analysis provided that the number of coils is not too small and that the coils do not touch before buckling occurs. Also comments in *Machine Design*, July 1943, Page 144.

$Gd^4/64r^3n$, from Equation 7, Equation 148 may be written as

$$P_{cr} = C_B l_o \frac{Gd^4}{64r^3n} \quad \text{.....(149)}$$

The factor C_B may also be considered as the ratio of the critical deflection (at which buckling occurs) to the free length. Thus, if $C_B = .4$, buckling may be expected at a deflection equal to $.4l$.

Although the results of tests show agreement with Equation 148 for usual conditions, some inaccuracy may be expected due to variations in spring dimensions and the effect of end turns.

Example—As an example of the use of the buckling load factor C_B in calculating the buckling load, a steel helical compression spring has the following dimensions: Free length $l_o = 6$ inches, mean coil radius $r = .75$-inch, outside diameter = 1.75 inches, wire diameter $d = .25$-inch, active turns $n = 12$. From the chart of *Fig.* 79 (Chapter VII) for these dimensions the spring constant $C_K = 142$ pounds per inch. From *Fig.* 86 the buckling factor C_B is found equal to .64 for $l_o/r = 6/.75 = 8$. It will be assumed that the spring is compressed between parallel surfaces so that the ends are completely restrained from rotation; hence curve *b* of *Fig.* 86 for fixed ends may be used. Then

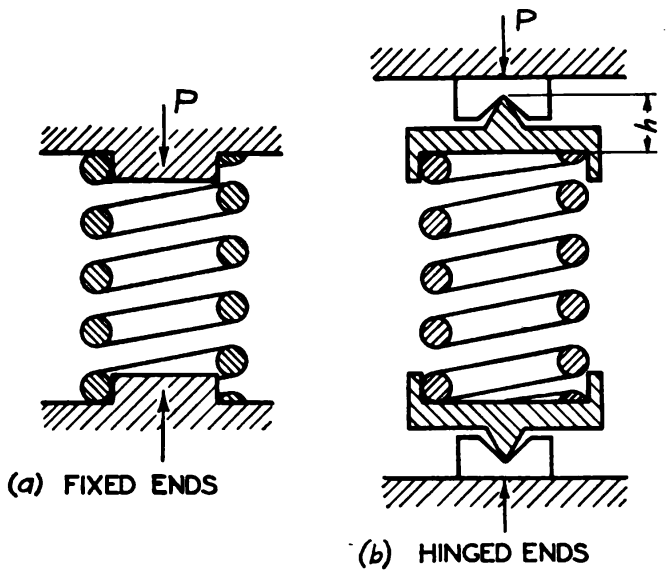

Fig. 87—Springs with fixed and hinged ends

from Equation 148 the calculated buckling load P_{cr} is $C_B l_o C_K = (.64)(6)142 = 545$ pounds. Assuming a maximum working stress of 60,000 pounds per square inch the actual load on the

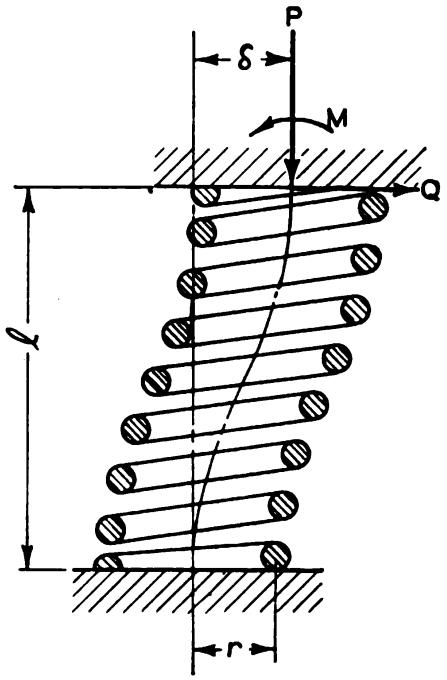

Fig. 88—Helical spring under combined lateral and axial load

spring would be (from the chart of *Fig.* 79, Chapter VII) $P = 190$ pounds, taking 60 per cent of the value for 100,000 pounds per square inch. Under these conditions there is a considerable margin between the working load and the buckling load. If, however, the ends of the spring were hinged as indicated in *Fig.* 87*b*, so that no restraint due to rotation occurs, then using curve *a* of *Fig.* 86, the constant $C_B = .2$. In this case $P_{cr} = C_B l_o C_K = .2(6.0)142 = 170$ pounds. Hence, with this type of end fastening there would be danger of such a spring buckling before the working load of 190 pounds was reached.

COMBINED AXIAL AND LATERAL LOADING

Deflection—Helical springs are sometimes called on to withstand not only axial loads, but also transverse loads as indicated in *Fig.* 88 where the force Q represents the transverse load. Examples of such applications are certain types of railway

trucks in which the helical springs must transmit lateral loads combined with axial loads. In certain refrigerator mechanisms where the compressor is supported on helical springs, these latter are called upon to absorb lateral forces due to the unbalanced reciprocating mechanism as well as axial loads due to the weight of the unit.

For calculation of the lateral deflections of a spring under such conditions the combined effect of the axial load P and the lateral load Q must be considered. In general the larger the axial load relative to the buckling load the larger the effect of the former on the deflection.

The case of a spring loaded both axially and transversely as indicated in *Fig.* 88 may be considered as a column under combined axial and transverse loads[5]. It is also essentially the same as a cantilever spring under combined axial and transverse loading, *Fig.* 154 Chapter XVI. The procedure in calculating such a spring is as follows: First the lateral deflection of the spring is calculated as though there were no axial load. Assuming the deflection calculated in this way is δ_o, the critical load P_{cr} is found from Equation 148 for the case of built-in ends using curve *b* of *Fig.* 86. If P is the axial load acting on the spring, the ratio P/P_{cr} is thus found. As will be shown later in Chapter XVI the magnification in the deflection due to the axial load will be given approximately by[6]

$$C_1 = \frac{1}{1 - P/P_{cr}} \qquad (150)$$

Values of C_1 as a function of P/P_{cr} are given in *Fig.* 156 of Chapter XVI. Then the actual lateral deflection will be

$$\delta = C_1 \delta_o \qquad (151)$$

To calculate the deflection δ_o which would occur if no axial load were acting the results of beam theory may be used. The simple cantilever spring loaded by a lateral load Q (*Fig.* 147 Chapter XVI) may be considered as two cantilevers of length $l/2$. This gives a deflection due to bending of

[5] Timoshenko, *Theory of Elastic Stability*, Page 4.

[6] A more exact method of determining this factor is given in the reference of Footnote 5. This shows that the approximate expression is sufficiently accurate for practical use.

$$\delta_1 = \frac{Ql^3}{12EI}$$

In this case EI is the flexural rigidity of the cantilever.

To apply this to the laterally loaded helical spring of *Fig.* 88 the flexural rigidity β given by Equation 141 is used, taking instead of l_o the compressed length l under the load P. Thus

$$\delta_1 = \frac{Ql^3}{12\beta} \quad \ldots\ldots (152)$$

To this must be added the deflection due to direct shear which is simply the load divided by the shearing rigidity γ and multiplied by the length l. To find γ Equation 144 is used taking l instead of l_o. Then the shearing deflection becomes

$$\delta_s = \frac{Ql}{\gamma} \quad \ldots\ldots (153)$$

The total deflection δ_o is the sum of δ_1 and δ_s. Thus, using Equations 152 and 153,

$$\delta_o = \frac{Ql^3}{12\beta} + \frac{Ql}{\gamma} \quad \ldots\ldots (154)$$

For the usual steel springs, $E = 30 \times 10^6$ pounds per square inch and $G = 11.5 \times 10^6$ pounds per square inch. Using these values in Equation 154 and simplifying, the expression for the deflection δ_o without axial load becomes:

$$\delta_o = \frac{2Qnr}{10^6 d^4}(.204l^2 + 1.06r^2) \quad \ldots\ldots (155)$$

This value of δ_o is then used in Equation 151 to calculate the lateral deflection δ.

Increase in Stress—Because of this lateral deflection there will also be an increase in stress. An accurate calculation of this would involve the end turns and would be very complicted. As a rough estimate the stress may be computed as follows: The torsion moment due to the axial load P will be Pr. The effective radius r will be increased by an amount $\delta/2$ due to the eccentric loading effect. Thus the torsion moment due to P becomes equal to $P(r+\delta/2)$. In addition the lateral force Q produces a

torsion moment $Ql/2$. This results in a total torsion moment of

$$M_t = P\left(r + \frac{\delta}{2}\right) + \frac{Ql}{2} \quad \text{.....(156)}$$

The shearing stress due to the moment M_t will be obtained by using the approximation $(4c-1)/(4c-4)$ for the effect of curvature where c is the spring index, as indicated in Equation 14 Chapter II. Hence

$$\tau_1 = \frac{16M_t}{\pi d^3}\,\frac{4c-1}{4c-4}$$

or using Equation 156

$$\tau_1 = \frac{16Pr}{\pi d^3}\left(\frac{4c-1}{4c-4}\right)\left(1 + \frac{\delta}{2r} + \frac{Ql}{2Pr}\right) \quad \text{.....(157)}$$

To this is added a stress due to the direct shear load equal to

$$\tau_s = \frac{16Pr}{\pi d^3}\left(\frac{.615}{c}\right)$$

(This value is obtained from the second term in the brackets of Equation 16). The direct shear stress at the inside of the coil due to the lateral force Q will be zero. Hence the maximum shear stress is

$$\tau = \tau_1 + \tau_s \quad \text{.....(158)}$$

This calculation should be considered as very rough. Since for the usual case τ_1 is much greater than τ_s, it may be expected that the effect of lateral loading is to increase the stress in the ratio:

$$C_l = 1 + \frac{\delta}{2r} + \frac{Ql}{2Pr} \text{ approximately} \quad \text{.....(159)}$$

In general the axial force P is much larger than Q, and for this case the shear stresses are of primary importance. In a similar way, the bending stresses may be calculated.

Example—As an example: A steel spring has the following dimensions: Outside diameter=5 inches, mean coil radius r=2⅛ inches, bar diameter d=¾-inch, free length l_o=9½ inches, active coils n=8.

From *Fig.* 79, for a spring of ¾-inch wire and 5 inches

outside diameter at a load of 1100 pounds the deflection per turn is found to be .188-inch or 1.5 inches for 8 active coils. Thus the spring constant $C_K = 1100/1.5 = 732$ pounds per inch. The ratio $l_o/r = 9.5/2.13 = 4.48$ and from *Fig.* 86 the buckling load factor $C_B = .7$. Using these values in Equation 148 the critical load P_{cr} becomes

$$P_{cr} = C_B l_o C_K = .7(9.5)732 = 4860 \text{ lb}$$

Assuming that the actual axial load P on this spring is 2400 pounds, then $P/P_{cr} = 2400/4860 = .494$. From Equation 150, the deflection magnification factor C_1 is 2. To calculate the deflection δ_o Equation 155 is used. The value of l used in this equation is the free length l_o minus the deflection due to a load of 2400 pounds. This latter will be $2400/C_K = 2400/732 = 3.28$ inches. Thus $l = 9.5 - 3.28 = 6.22$ inches. Assuming a lateral load $Q = 200$ pounds, by substitution in Equation 155,

$$\delta_o = \frac{2(200)(8) \times 2\frac{1}{8}}{10^6(\frac{3}{4})^4}\left[.204(6.22)^2 + 1.06(2\tfrac{1}{8})^2\right] = .274 \text{ inches}$$

From Equation 151 the deflection at a lateral load of 200 pounds (for $C_1 = 2$) is

$$\delta = C_1\delta_o = 2(.274) = .548 \text{ inches}$$

Thus it is seen that in this case the actual deflection with axial load present is twice that calculated by neglecting the effect of the axial load.

From *Fig.* 79 the stress at an axial load of 3050 pounds is 100,000 pounds per square inch with curvature correction considered. At 2400 pounds axial load the stress would be $2400(100{,}000)/3050 = 78{,}500$ pounds per square inch. From Equation 159 the factor C_l for determining the increase in stress due to the lateral load is

$$C_l = 1 + \frac{\delta}{2r} + \frac{Ql}{2Pr} = 1.25 \text{ for } \delta = .548,\ Q = 200 \text{ lb}$$

This means that an increase in stress to $1.25(78{,}500) = 98{,}000$ pounds per square inch may be expected due to the lateral load.

TEST DATA

A series of tests on a great many different springs was carried out by Burdick, Chaplin, and Sheppard[7]. The tests were made by supporting a steel plate or table on four springs. This steel plate carried the axial load while the transverse load was supplied by a turnbuckle. In this manner essentially the loading conditions of *Fig.* 88 were obtained. Results of these tests showed a considerable scatter between test values of lateral deflection and those calculated by using Equations 151 and 155. The range in deviation in the test points was from about 60 per cent to 125 per cent of the theoretical values, most of the test results, however, being within 20 per cent of the calculated values.

Similar tests carried out by Lehr and Gross in Germany[8] showed deviations around 20 per cent or more between calculated and test deflections. By taking special precautions in clamping the ends of the spring and by accurately determining the effective length and number of turns, these investigators found it possible to obtain good agreement between theory and test in the case of laterally loaded compression springs. For this reason it appears that the chief causes of the discrepancy between test and theory lies in (1) imperfect clamping of the end windings, which allows a slight rotation under loading while no rotation is assumed in the theory, and (2) inaccuracy in determining the effective number of turns and length of the spring.

In practice, for the usual compression springs with the conventional design of end turns the designer may, therefore, expect actual deviations as much as 20 per cent and even more from the calculated values of lateral deflection as obtained from Equation 151.

---

[7] "Deflection of Helical Springs under Transverse Loading" by Burdick, Chaplin and Sheppard, *Transactions* A.S.M.E., October, 1939, Page 623.

[8] *Die Federn*, published by V.D.I., Berlin, 1938, Page 100.

CHAPTER X

HELICAL SPRINGS FOR MAXIMUM SPACE EFFICIENCY

A problem which frequently arises in helical spring design is that of selecting a spring with given load and deflection characteristics, the space available being limited. Since load times deflection is proportional to energy, this means that a certain amount of energy must be stored within the given space. A consideration of how the possible energy storage varies with spring index is therefore of interest.

SINGLE SPRINGS

A logical approach to this problem is to calculate the energy stored in a compression spring when the coils just touch and the spring is solid, the stress at solid compression being assumed to be the maximum allowable value. The amount of energy stored in the spring is then calculated for various spring indexes. For a given volume of space occupied by the spring the amount of energy which can be stored will be a maximum at a definite value of spring index. However, this optimum value will depend on whether the spring has variable or static loading[1].

Solid and Free-Height Volume—For statically loaded compression springs where the springs are compressed nearly solid in practice, the actual space occupied by the spring will approximate the solid-height volume, i.e., the volume occupied by a cylinder of diameter equal to the outside spring diameter and length equal to the active height of the spring (this neglects the space occupied by the end turns). Hence, for applications involving statically loaded springs, the use of solid-height volume appears to be logical as a criterion of efficiency of space utilization. On the other hand, where the spring is under variable loading with a zero to maximum stress range, the space

[1]This method of approach is similar to that used by J. Jennings (*Engineering*, August 15, 1941, Page 134). However, the method used by the author differs from that used by Jennings in that a distinction is made between static and variable loading. Also the usual deflection formula is used instead of the Wood formula used by Jennings, since the former is quite accurate (see Chapter IV).

occupied by the spring when unloaded may be much larger than the solid-height volume. In this case the *free-height* volume, or the volume occupied by the active part of the spring when unloaded probably is a more representative criterion than solid height volume[2]. However, it should be mentioned that the application of the criterion of free-height volume is complicated by the fact that a value of allowable stress at solid compression must be assumed. If a low stress is used, the difference between the results obtained by using the free-height and those obtained using the solid-height volume would be much less than those obtained by using a high stress.

In most practical applications where springs are subject to a considerable amount of initial compression, a criterion of space occupied intermediate between the free and solid-height values would appear to be most representative. This volume will depend both on the amount of initial compression and on the allowable stress at solid height. In addition, for best accuracy, the end turns should be considered. To avoid all these complications, the simple criterion of solid-height volume will be used in what follows, primarily as a convenient guide for judging the efficiency of space utilization.

Infrequent Loading—To apply this criterion, the potential energy stored in the spring due to a load P and a deflection δ will first be calculated. This stored energy is

$$U=\frac{1}{2}P\delta \qquad (160)$$

The deflection δ of the spring is given by Equation 7. Substituting this value of δ in Equation 160 the stored energy becomes

$$U=\frac{32P^2r^3n}{Gd^4} \qquad (161)$$

where the symbols have the usual meanings.

Variable Loading—If the load acting on the spring is variable as, for instance, that in an automotive valve spring, the peak torsional stress in the spring as figured using the curvature correction factor of Equation 19, may, as a first approximation,

[2]See discussion on this subject by E. Latshaw, *Machine Design*, March, 1942, Page 84. In this discussion a number of curves based on free-height volume and a stress of 120,000 pounds per square inch are given.

be used as a measure of the load carrying ability[3]. This stress is, from Equation 18,

$$\tau_m = K\frac{16Pr}{\pi d^3} \quad \ldots\ldots (162)$$

where the factor K is given by Equation 19.

Solving this formula for P and substituting in Equation 161 the expression for stored energy becomes

$$U = \frac{\pi^2}{8}\frac{rnd^2\tau_m^2}{GK^2} \quad \ldots\ldots (163)$$

In accordance with the criterion of solid-height volume discussed previously, this energy must be stored in a volume equal to that of a cylinder with a diameter equal to the outside coil diameter $(2r+d)$ and a length equal to the active length nd of the spring when the latter is fully compressed. This neglects the effect of pitch angle, which is small for practical springs. The solid-height volume is thus

$$V = nd\frac{\pi}{4}(2r+d)^2 = \frac{nd^3\pi}{4}(c+1)^2$$

or

$$nd^3 = \frac{4}{\pi}\frac{V}{(c+1)^2} \quad \ldots\ldots (164)$$

where c is the spring index.

Substituting Equation 164 in 163 an expression for total stored energy is obtained:

$$U = C_v\frac{\tau_m^2 V}{4G} \quad \ldots\ldots (165)$$

where C_v is a constant depending on the spring index c and is

$$C_v = \frac{\pi c}{K^2}\frac{1}{(c+1)^2} \quad \ldots\ldots (166)$$

This equation shows that, for a given volume of space occupied and a given peak stress, the energy stored depends only on the energy coefficient C_v which in turn depends only on the

[3]See Chapter VI for a more complete discussion of this.

spring index. Values of C_v are plotted against spring index c in the lower curve of *Fig.* 89. This curve shows that for variable loads and for a single spring the maximum energy is stored in a given space and at a given peak stress if the spring index is

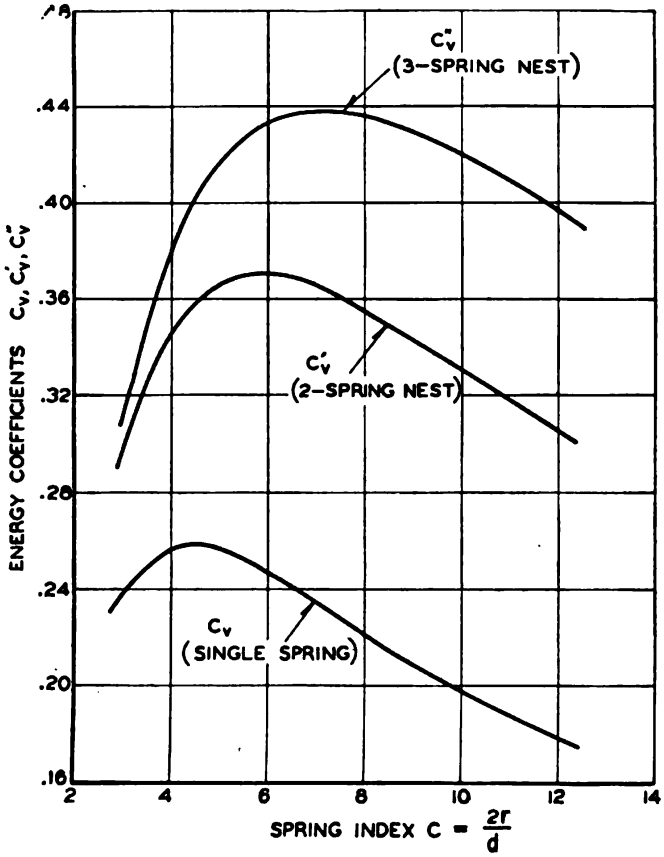

Fig. 89—Energy coefficients for variable loads

between 4 to 5. However, it should be noted that if the free-height volume had been taken as a basis this optimum value of the index would have been somewhat less[4]. Thus, if a stress of 120,000 pounds per square inch is assumed, the optimum index is around 3 to 4 provided the free-height volume is used as the criterion of efficiency of space utilization.

Maximum Energy Storage—Where the load is *static* or repeated only a few times during the service life of the spring as

[4]See discussion by E. Latshaw, loc. cit.

discussed in Chapter V indications are that curvature effects (but not those due to direct shear) may be neglected in calculating the stress. In this case the stress τ_s should be calculated by Equation 89 which is

$$\tau_s = \frac{16Pr}{\pi d^3} K_s$$

where K_s is given by Equation 90 and takes into account the stress produced by the direct shear load.

Using this equation instead of Equation 162 and proceeding in a similar way as before, the energy stored becomes

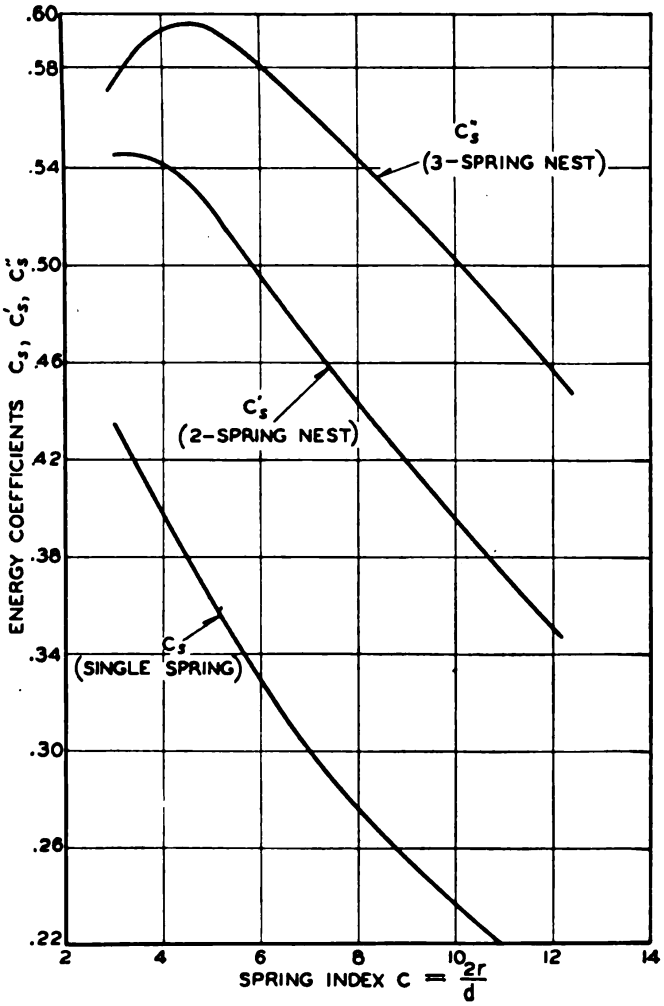

Fig. 90—Energy coefficients for static loads

$$U = C_s \frac{\tau_s^2 V}{4G} \quad \text{.....(167)}$$

where

$$C_s = \frac{\pi c}{K_s^2} \frac{1}{(c+1)^2} \quad \text{.....(168)}$$

Plotting C_s as a function of the spring index c, the lower curve of *Fig.* 90 is obtained. This curve indicates a maximum value of C_s at the smallest practical spring index. This means that where *static loads* are involved, maximum energy storage using one spring only will be obtained in a given space by using the smallest practical value of the index (which will usually be around three).

SPRING NESTS

A common method of increasing the amount of energy which may be stored in a given space is to use a *spring nest*, i.e., a combination of two or more springs telescoped one within

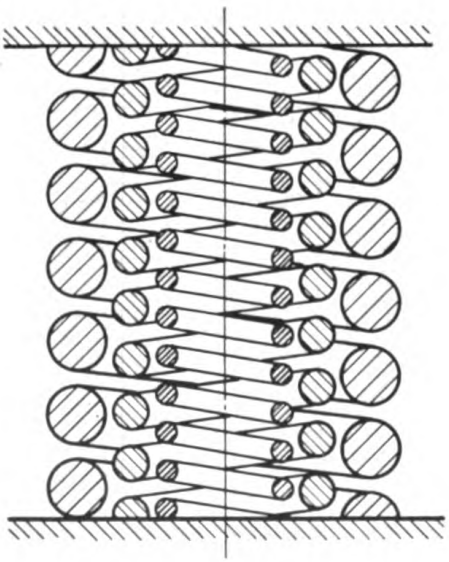

Fig. 91—Three-spring nest of helical springs

the other as indicated in *Fig.* 91. A practical example of the use of such a nest is shown in *Fig.* 92 which represents an end view of a three-spring nest for a locomotive tender truck.

For maximum energy storage the solid lengths of all the springs composing the nest should be the same. Assuming a nest composed of two springs, this means that

$$n_1 d_1 = n_2 d_2 \quad \ldots\ldots (169)$$

In this equation and those following the subscripts 1 and 2 refer to the outer and inner springs of the nest, respectively. In addition, it will be assumed that the free lengths of the springs com-

(Photo, courtesy Baldwin-Locomotive Works)

Fig. 92—Three-spring nest for locomotive tender

prising the nest are also the same. This means that the total deflection of each spring is the same at any given load, i.e., that

$$\delta_1 = \delta_2 \quad \ldots\ldots (170)$$

Variable Loading—For variable loading the deflection is given by using Equations 7 and 18.

$$\delta_1=\frac{4\pi r_1^2\tau_1 n_1}{Gd_1K_1}\ ;\quad \delta_2=\frac{4\pi r_2^2\tau_2 n_2}{Gd_2K_2} \qquad \text{.....(171)}$$

In terms of the spring indexes c_1 and c_2 these equations may be written

$$\delta_1=\frac{\pi c_1^2 n_1 d_1\tau_1}{GK_1}\ ;\qquad \delta_2=\frac{\pi c_2^2 n_2 d_2\tau_2}{GK_2} \qquad \text{.....(172)}$$

If the same maximum stress in each spring is assumed, $\tau_1=\tau_2$. Also, since $n_1d_1=n_2d_2$ from Equation 169 this means that the spring indexes c_1 and c_2 (and hence also the curvature correction factors K_1 and K_2) should be the same if $\delta_1=\delta_2$. If the spring indexes are made the same, the energy coefficients C_v (which depend only on the indexes) will be the same for both springs. Using Equation 165 this means that the total energy stored will be given by

$$U=C_v\frac{V_1\tau_1^2}{4G}+C_v\frac{V_2\tau_2^2}{4G}$$

where V_1 and V_2 are the volumes enclosed by the outer and inner springs respectively when compressed solid. Since $\tau_1=\tau_2=\tau_m$ this equation may be written

$$U=C_v\frac{V_1\tau_m^2}{4G}\left(1+\frac{V_2}{V_1}\right) \qquad \text{.....(173)}$$

If the two springs just touch, the outer diameter of the inner spring will be equal to the inner diameter of the outer spring, i.e., $2r_1-d_1=2r_2+d_2$. Using Equation 164 this gives

$$V_1=\frac{\pi}{4}n_1d_1^3(c_1+1)^2$$

$$V_2=\frac{\pi}{4}n_2d_2(2r_1-d_1)^2=\frac{\pi}{4}n_2d_2d_1^2(c_2-1)^2$$

Since $c_1=c_2=c$ and $n_1d_1=n_2d_2$, from these equations is obtained:

$$\frac{V_2}{V_1}=\left(\frac{c-1}{c+1}\right)^2 \qquad \text{.....(174)}$$

Substituting this in Equation 173, for a two-spring nest,

$$U = C_v' \frac{\tau_m^2 V}{4G} \quad \text{.....(175)}$$

where

$$C_v' = C_v \left[1 + \left(\frac{c-1}{c+1} \right)^2 \right] \quad \text{.....(176)}$$

and V = volume enclosed by outer spring.

Values of the energy coefficient C_v' are plotted against spring index in *Fig.* 89. From this it is seen that for a two-spring nest *under variable loading,* the maximum energy storage is obtained for spring indexes around 5 to 7. These values are somewhat higher than those obtained for a single spring; however, they are also higher than would be the case if the free-height volume had been taken as a basis. Thus for example the analysis by Latshaw mentioned previously[2] indicates an optimum value of index for a two-spring nest equal to about 4, based on an allowable stress of 120,000 pounds per square inch. For a lower assumed stress this value of spring index would be higher.

A similar analysis based on solid-height volume may be made for a three-spring nest. This gives, for energy stored,

$$U = C_v'' \frac{\tau_m^2 V}{4G} \quad \text{.....(177)}$$

where

$$C_v'' = C_v \left[1 + \left(\frac{c-1}{c+1} \right)^2 + \left(\frac{c-1}{c+1} \right)^4 \right] \quad \text{.....(178)}$$

the constant C_v being given by Equation 166.

Values of C_v'' plotted against c in *Fig.* 89 show that for a three-spring nest under the assumptions of equal deflection and equal solid height, the maximum energy is stored in a given volume of space if springs having indexes around 6 to 8 are used. Again these values will be lower if the free-height volume is used as a basis.

Static Loading—For a spring nest subject to static loading the analysis may be made in exactly the same way as before, except that the stress τ_s is figured from Equation 89 which neglects the stress augment due to curvature, and instead of C_v the factor C_s (Equation 168) is used. Results of this analysis are:

For a two-spring nest, statically loaded, the stored energy becomes

$$U = C_s' \frac{\tau_s^2 V}{4G} \quad \text{.....(179)}$$

where

$$C_s' = C_s \left[1 + \left(\frac{c-1}{c+1} \right)^2 \right] \quad \text{.....(180)}$$

For a three-spring nest, statically loaded, stored energy is

$$U = C_s'' \frac{\tau_s^2 V}{4G} \quad \text{.....(181)}$$

where

$$C_s'' = C_s \left[1 + \left(\frac{c-1}{c+1} \right)^2 + \left(\frac{c-1}{c+1} \right)^4 \right] \quad \text{.....(182)}$$

Values of C_s' and C_s'' are plotted against spring index c in *Fig.* 90. From these it appears that for *static loads* the maximum energy storage in a given space will be had by using springs with indexes around 3 to 4 for a two-spring nest and with indexes of 4 to 5 for a three-spring nest. These optimum values are somewhat lower than those obtained for springs under variable loading, based on the criterion of solid-height volume. However, if the criterion of free-height volume is used for springs under variable loading, the difference between the optimum values of index for the two kinds of loading will be small. In any case, the results do indicate that where maximum energy storage within a given space is a primary consideration, a rather low value of index should be used, say around 3 for a single spring and about 3½ or 4 for two or three-spring nests.

Application of formulas—Assuming the designer requires a spring with a definite load and deflection for a given application, the amount of energy stored is fixed. By using the formulas of this chapter, the *minimum* amount of space required for the spring can be found for a given peak stress. Actually, other practical considerations may dictate larger space requirements than those indicated, but the formulas should give a rough indication of the space needed.

CHAPTER XI

TENSION SPRINGS

Design of helical tension and combination tension-compression springs differs from that of compression springs in that the effect of the end turns in reducing allowable stress should be considered.

HELICAL TENSION SPRINGS

Unless special care is taken in manufacture a fairly sharp curvature of the wire or bar at the point where the hook joins the body of the spring, at *A*, *Fig.* 93*b*, may occur. This curvature will result in additional stress concentration which is not considered in the usual method of stress calculation for helical springs. Thus at point *A* a half end turn is bent up sharply so that the radius r_1 is relatively small, which tends to result in a high concentration of stress. For this reason, most failures of tension springs occur at such points and this is one reason why a somewhat lower working stress is usually recommended for tension springs as compared with compression springs. This stress-concentration effect may be reduced, and the strength increased, by shaping the end turn so that the minimum radius of curvature is as large as possible.

Another factor which must be considered in tension springs is the effect of *initial tension.* By certain methods of coiling the spring it is possible to bring the coils together in such a way that an initial load must be applied before the coils will begin to separate. The amount of this initial load is limited to a value corresponding to a stress around 6000 to 25,000 pounds per square inch (figured by neglecting curvature effects), the exact value depending on the spring index. After separation of the coils begins, the slope of the load-deflection diagram is the same as that which would be obtained for a spring with no initial tension. In many mechanisms the initial tension is important.

Stress in End Loops—Although an exact calculation of stress in the end loops of helical springs is complicated, a rough

estimate for the case shown in *Fig.* 93 (which has a sharp bend at points A and A') may be made as follows: The bending moment at A' (where the sharp bend begins) due to the load P is Pr approximately. The *nominal* bending stress at this point will be $32Pr/\pi d^3$ since $\pi d^3/32$ is the section modulus of a circular sec-

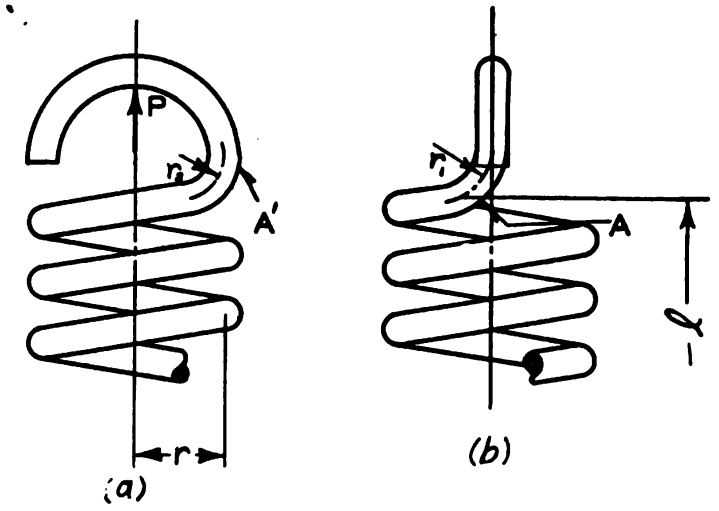

Fig. 93—Tension spring with half-loop coil end

tion. (Note: This is twice as great as the nominal torsion stress $16Pr/\pi d^3$ due to the torsion moment Pr). The maximum bending stress will be this value multiplied by a factor K_1 where K_1 is a stress concentration factor depending on the ratio $2r_2/d$, the radius r_2 being the radius at the start of the bend in the plane of the hook, as indicated in *Fig.* 93. An estimate of K_1 may be obtained from the curve of *Fig.* 180, Chapter XVII, for torsion springs which applies to round wire in bending. To this bending stress must also be added the direct tension stress $4P/\pi d^2$. This gives a maximum bending stress at point A' equal to

$$\sigma = \frac{32Pr}{\pi d^3} K_1 + \frac{4P}{\pi d^2} \qquad (183)$$

At the point A, *Fig.* 93*b* near the point where the bend joins the helical portion of the spring the stress condition is principally torsion. Calculation may be made as follows: From Equation 14, Chapter II, for the case of pure torsion acting on a curved bar, the approximate expression for stress concentration

factor is $(4c_1-1)/(4c_1-4)$ where in this case c_1 is to be taken as $2r_1/d$, the radius r_1 being the radius of curvature of the bend, *Fig. 93b*. The maximum stress due to the torsion moment Pr will then be

$$\tau_1=\frac{16Pr}{\pi d^3}\left(\frac{4c_1-1}{4c_1-4}\right) \quad \text{.....(184)}$$

There is also a direct shear stress present at point A due to the axial load. This direct shear, however, does not act at the inside of the bend where the torsion stress given by Equation 184 would exist. Consequently, Equation 184 may be taken as an approximate expression for the maximum stress at point A. If r_1 is small, c_1 will also be small, and the quantity in the paren-

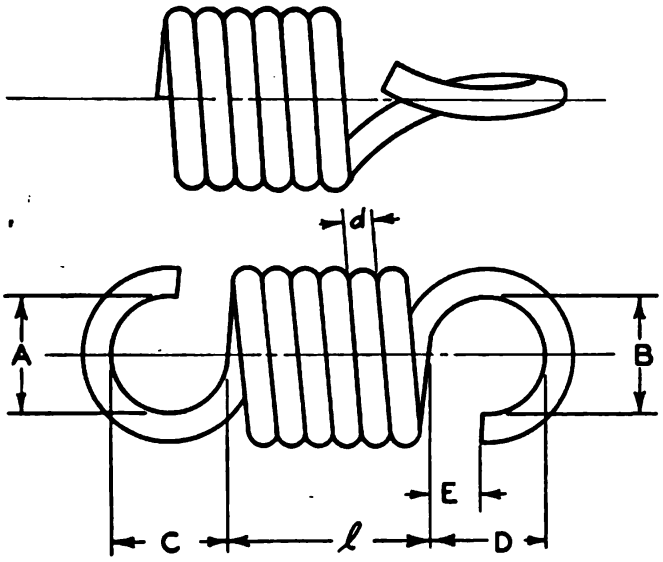

Fig. 94—Tension spring with full loop turned up. Dimensions A, B, C, D are approximately equal to the inside diameter of the spring, $E=B/3$ approximately, $l=d\ (n'+1)$ where n′=number of turns in dimension l between points where loops begin. Working turns $n=n'+1$, approximately

thesis of this equation may be large. This means a high stress concentration effect, and shows the advisability of keeping r_1 as large as possible.

Between points A' and A there will be a combination of

bending and torsion stresses which depend on the shape of the bend as well as on the radii r_1 and r_2. Since the peaks of these bending and shearing stresses do not occur at the same point, the combination of the two presents considerable complication and will not be discussed here. For practical purposes Equations 183 and 184 are probably sufficient.

For the commonly used type of tension spring with a full loop turned up as indicated in *Fig.* 94, the minimum radius of curvature will be considerably larger, and the stress concentration effect smaller, than is the case with the spring shown in *Fig.* 93 where a half loop is turned up. Dimensions as commonly used for these springs are also indicated in *Fig.* 94.

Effect of End Coils on Deflection of Tension Springs—To find the total number of active turns in a tension spring, the number of turns between points where the loop begins is determined first. To this is added the deflection due to the end coils. Tests made by Sayre[1] indicate that a half coil turned up to form a loop as indicated in *Fig.* 93 is equivalent to .1 full-coil as far as deflection is concerned. Thus, if a spring had n' turns between points where the loops start, the total active turns would be $n'+.2$ the extra .2 turn being the equivalent of two loops. This conclusion may be shown analytically as follows. The half coil turned up to form a loop is equivalent to the quarter-turn of *Fig.* 85*b*, Chapter IX, loaded as shown. Using Equation 143 the deflection of this quarter-turn becomes

$$\delta_1 = \frac{\pi}{4}\,\frac{Pr^3}{EI}$$

where in this case r is the mean radius of the loop (taken equal to the mean spring radius). Since for most spring materials the modulus of elasticity $E=2.6G$, approximately, where $G=$ modulus of rigidity, this equation may be written

$$\delta_1 = \frac{\pi}{4}\,\frac{Pr^3}{2.6G}\times\frac{64}{\pi d^4} = .096\left(\frac{64Pr^3}{Gd^4}\right)$$

or $\delta_1 = .1\delta_o$, approximately, where δ_o is the deflection per turn given by Equation 7.

For the full coil turned up, *Fig.* 94, the experimental work of Sayre[1] indicates a deflection equal to .5-turn. In this case the

[1] *Transactions* A.S.M.E., 1934, Page 558.

total number of active coils would be $n'+1$ where n' is again the number between points where the loops begin.

Initial Tension—The amount of initial tension which can be put into a spring depends primarily on the spring index $2r/d$, the higher the index the lower the initial tension values. The values of stress corresponding to practical values of initial tension listed in TABLE XXIV were published by Wallace Barnes Co.[2]. These values are calculated from Equation 4, curvature effects being neglected. Hence the initial tension load may be figured from these values of stress using the formula

$$P_1 = \frac{\pi \tau_1 d^3}{16r} \quad \text{(185)}$$

where τ_1 = initial tension stress.

As an example calculation for finding initial tension load: A tension spring has a 2-inch outside diameter and ¼-inch wire diameter so that the index $2r/d=7$. When wound with maxi-

TABLE XXIV

Torsional Stress Corresponding to Initial Tension

Spring Index (2r/d)	Initial Tension Stress Pounds Per Square Inch
3	25,000
4	22,500
5	20,000
6	18,000
7	16,200
8	14,500
9	13,000
10	11,600
11	10,600
12	9,700
13	8,800
14	7,900
15	7,000

mum initial tension the stress, from TABLE XXIV, due to initial tension will be τ_1 = 16,200 pounds per square inch. From Equation 185 the initial tension load becomes

$$P_1 = \frac{\pi(16200)\ (\tfrac{1}{4})^3}{16(\tfrac{7}{8})} = 57 \text{ lb.}$$

By changes in the method of winding, values of initial tension

[2] *The Mainspring*, April, 1941.

less than this may also be obtained.

. **Shapes of End Coils**—Usually the end turns of tension springs are made in the simple forms indicated in *Figs.* 93 and 94 where either a half or a full turn is bent up to form a loop. In many practical applications, however, a wide variety of end loop designs, some of which are shown in *Fig.* 95, may be used.

Some of these designs, particularly where the loop or hook is at the side, will result in a considerably greater stress in the spring than that calculated on the basis of an axial load, Equa-

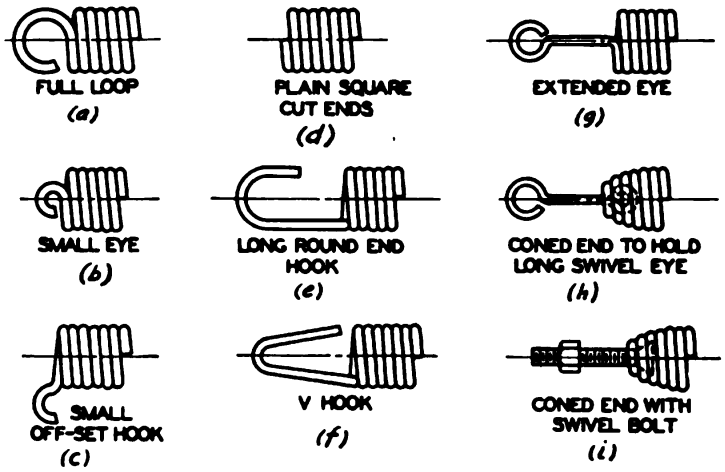

Fig. 95—Various types of end loops for tension springs

tion 18. Thus, if the loop is at the side, the moment arm of the load on which the maximum torsion stress in the spring depends is practically twice that which would exist if a purely axial load were applied to the same spring. This means a doubling of the stress for a given load.

Sometimes in the actual loading of tension springs, even if the usual type of end loop is used, the line of action of the load may still be displaced by a considerable amount from the axis of the spring. In this case a considerable increase in stress may also occur and should be considered by the designer.

Often tension springs are made with plain ends, *Fig.* 95*d*. Special fixtures called "spring ends" are attached to these as indicated in *Fig.* 96*a*. When using these, the spring is close wound and the ends of the spring are spread apart by screwing the spring into the holes. In this case an initial stress corresponding to

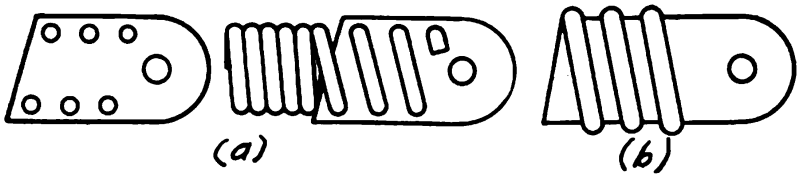

Fig. 96—Two types of spring ends for tension springs

the spreading apart of the turns near the ends is set up. This initial stress will correspond to a load equal to the initial tension in the spring plus the load corresponding to the distance the end coils are spread. A second type of spring end is shown in *Fig. 96b*. This is screwed into the ends of the spring coil.

Some expedients to reduce stress in the end coils are indicated in *Figs.* 97 and 98. In *Fig.* 97 the diameter of end coils is gradually reduced before the end loop is formed. Then, when the end loop is bent up, the moment arm of the load at the point where the curvature of the wire is the sharpest will be small. Thus the peak stress in the spring is reduced accordingly. Such

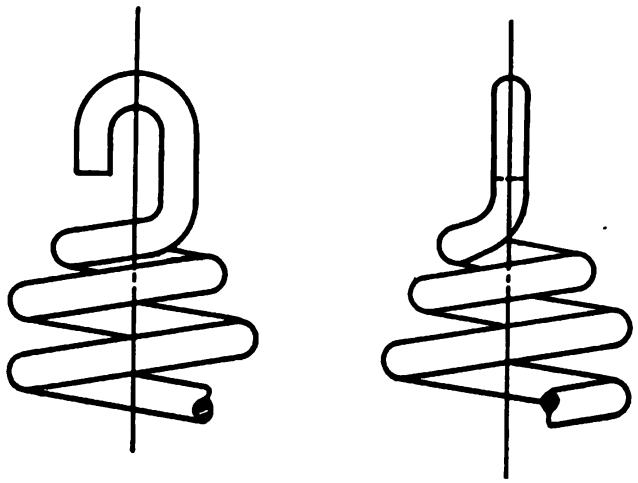

Fig. 97—End coil for reduced stress in tension spring

a design, while more expensive than the usual form of end loop, is worth while where high stresses are unavoidable.

Another method of reducing the stress in the spring is to use a U-shape piece having hooks at each end to fit over the spring wire. By means of this arrangement a sharp curvature

of the spring wire or bar at points of high stress is avoided and the maximum stress in the spring reduced. In addition this type of construction is frequently of advantage in mechanism where springs are subject to a whipping action as, for example, when one end of the spring is attached to a bell-crank which travels through a given arc and stops suddenly. In this case the end of the spring is stopped when the spring itself has a velocity transverse to its axis. For such applications the swivel action provided by the design of *Fig.* 98 is of advantage in reducing the stress[3]. On the other hand, a spring fastened rigidly at its ends by a plug would be subject to rather high stress at these points due to this whipping action.

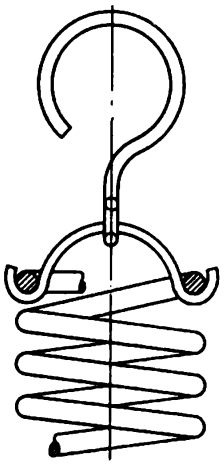

Fig. 98—Method of supporting end loops to avoid bending stress due to whipping action

Working Stresses — For tension springs with the usual design of end loop, *Figs.* 93 and 94, where the curvature may be rather sharp, it is to be expected that the strength will be appreciably lower than for compression springs of the same material and heat treatment. This is particularly true where the spring is subject to fatigue or repeated loading since in this case the stress concentration effect due to the sharp curvature would be emphasized. Also it is difficult to preset tension springs properly since either the initial tension will be lost or excessive space will result between turns. Because of lack of favorable residual stresses more creep or load loss may, therefore, be expected than for properly preset compression springs. For these reasons, a reduction of working stress to 75 or 80 per cent of that for compression springs is frequently made.

TENSION-COMPRESSION SPRINGS

Often it is desirable for a spring to exert both tension and compression loads. A case in point is a crank-type fatigue testing machine used for testing full-sized impulse turbine blades[4].

[3]For further discussion of this see *The Mainspring*, August, 1939.

[4]See article by R. P. Kroon—"Turbine Blade Fatigue Testing", *Mechanical Engineering*, Vol. 62, Page 531.

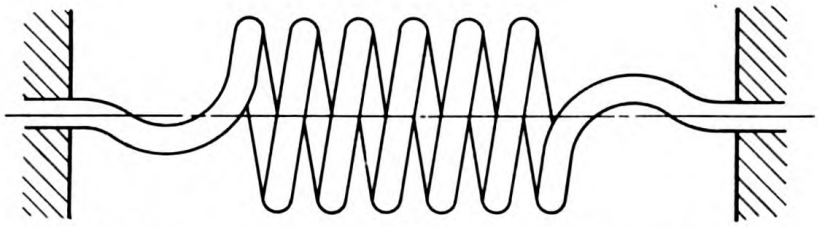

Fig. 99—Tension-compression spring. The spring is clamped at both ends so that both tension and compression loads may be exerted

In this case nine springs having the shape shown in *Fig.* 99 are clamped around the periphery of two circular plates as shown in *Fig.* 100. One of these plates is moved back and forth by a crank arrangement connected to a crosshead. By this means an alternating load varying between tension and compression is applied to the turbine blade specimen which is heated at the same time, thus simulating the temperature and vibration conditions occurring in service. In making such springs, care should be taken so that the end coils have a gradual transition between the body of the spring and the straight portion of the end. In this manner the curvature of the end turns may be reduced and the effects of stress concentration minimized as much as possible. The advantage of the arrangement of *Fig.* 100 is that a definite load is maintained on the test specimen even if deflections of the latter occur, due to various causes.

In designing tension-compression springs, it should be borne in mind that if the stress is completely reversed, the stress range will be *twice* that of a spring subject to pulsating (zero to maximum) stress of the same peak value. Thus if the endur-

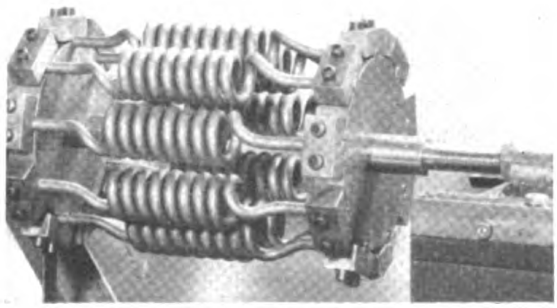

Fig. 100—Assembly of tension - compression springs for crank-type fatigue testing machine

ance limit is 70,000 pounds per square inch for springs tested in a zero to maximum range (this is an average value for springs of this type, Chapter IV) the expected endurance limit would be about ±35,000 pounds per square inch in the case of a tension-compression spring for the same material. Additional stress concentration effects near the end turns would tend to reduce the endurance range below this value. On the other hand, the endurance range in reversed stress may be somwhat greater than that to be expected in a zero to maximum stress range. In general it, therefore, appears that usually a working stress about half the allowable value for a zero to maximum range may be employed for such springs.

In the springs used in Fig. 100, which have a wire diameter of .5-inch and an index of 3.5, working stresses of ±25,000 pounds per square inch, figured with curvature correction, have been used without failure in service.

CHAPTER XII

SQUARE AND RECTANGULAR-WIRE COMPRESSION SPRINGS

Square or rectangular-wire compression or tension springs have advantages in many applications. For example, in the design of precision spring scales, a rectangular cross-section enables the designer to obtain a more nearly linear load-deflection characteristic[1]. An application of this type utilizing rectangular bar springs is the heavy duty scales of *Fig.* 1 Chapter I. Another illustration of the use of such springs is the set of interchangeable iso-elastic springs in *Fig.* 101 made for a testing machine.

A further advantage of the square or rectangular-bar section is that more material may be packed into a given space for such sections than would be possible for round wire. However, this advantage is partially nullified by the fact that the efficiency of utilization of the material for the rectangular section is not as great. Where static loads are involved and springs are cold-set, a more uniform stress distribution occurs and this difference in efficiency between round and rectangular wire may be small.

SPRINGS OF LARGE INDEX, SMALL PITCH ANGLE

If the pitch angle is not too large, a helical tension or compression spring of square or rectangular wire and of large index[2] may be considered essentially as a bar of square or rectangular cross section subject to a torsion moment Pr, *Fig.* 102 where P is the axial load and r the mean coil radius. To calculate the torsional rigidity and stress in a rectangular bar under torsion, Prandtl's "membrane analogy" may be used[3].

Membrane Analogy—This analogy may be briefly described as follows: A stretched membrane having a rectangular shape is subject to a uniform tension at its edges, combined with

[1]For a further discussion of this point together with theoretical results see paper by Sayre and de Forest—"New Spring Formulas and New Materials in Precision Spring Scale Design" presented at the Annual A.S.M.E. Meeting, December, 1934.

[2]In this case, the index may be considered as the ratio $2r/a$ between mean diameter and thickness of wire cross-section *Fig.* 102.

[3]Timoshenko's *Theory of Elasticity*, McGraw-Hill, 1934, Page 239, gives a more complete discussion of this analogy.

a uniform lateral pressure causing it to bulge out. The Prandtl analogy states that the maximum slope of the membrane at any point represents the shearing stress at the corresponding point in the twisted bars, and that the volume enclosed

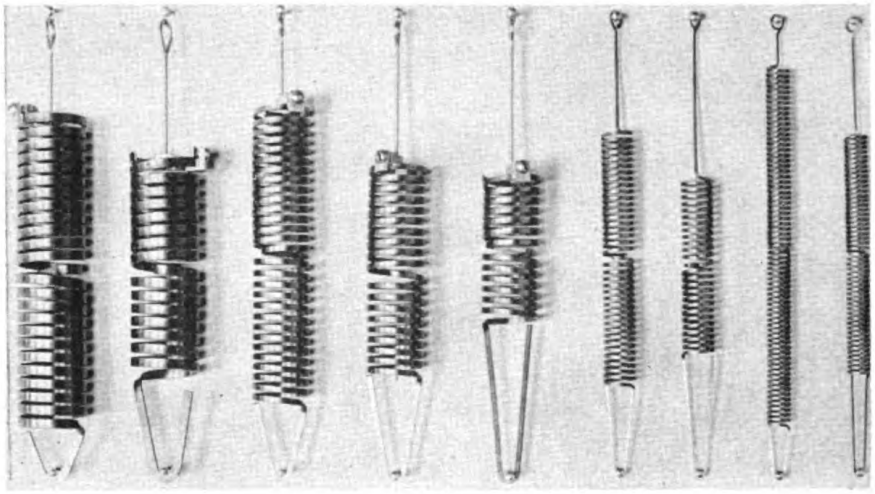

—Courtesy John Chatillon and Sons

Fig. 101—Set of interchangeable rectangular bar springs made for a testing machine. Rates vary from 1/10 to 2½ pounds per inch deflection

within membrane and plane of its edges represents torque.

It may also be shown[1] that the deflections of a loaded membrane must satisfy the partial differential equation:

$$\frac{\partial^2 z}{\partial x^2} + \frac{\partial^2 z}{\partial y^2} = -\frac{q}{S} \qquad \text{(186)}$$

where z is the deflection of the membrane at any point having the coordinates x and y, q is the pressure per unit of area of the membrane, and S the tension force in the membrane itself per unit length of the boundary. In addition the deflection z must be zero at the edges.

Referring to *Fig.* 103 which represents a rectangular cross section with sides a and b where $(b>a)$, the deflection z of the membrane may be expressed in series form as follows:

$$z = \sum_{n=1,\ 3,\ 5,\ \ldots}^{\infty} b_n \cos \frac{n\pi x}{a} \cdot Y_n \qquad \text{(187)}$$

[1]Timoshenko, loc. cit., Page 240.

where Y_n is a function of y only. By proper choice of Y_n, the membrane Equation (186) may be satisfied.

By substitution of Equation 187 in Equation 186 and expanding the right side of Equation 186 in the form of a Fourier's series, the expression for Y_n may be determined. The final results become

$$z=\frac{4qa^2}{S\pi^3}\sum_{n=1,3,5}^{\infty}\frac{1}{n^3}(-1)^{(n-1)/2}\left(1-\frac{\cosh\frac{n\pi y}{a}}{\cosh\frac{n\pi b}{2a}}\right)\cos\frac{n\pi x}{a} \quad \ldots\ldots\ldots (188)$$

From the membrane analogy, the shearing stress at any point is proportional to the slope of the membrane at the corresponding point, the term q/S being replaced by $2G\theta$ where

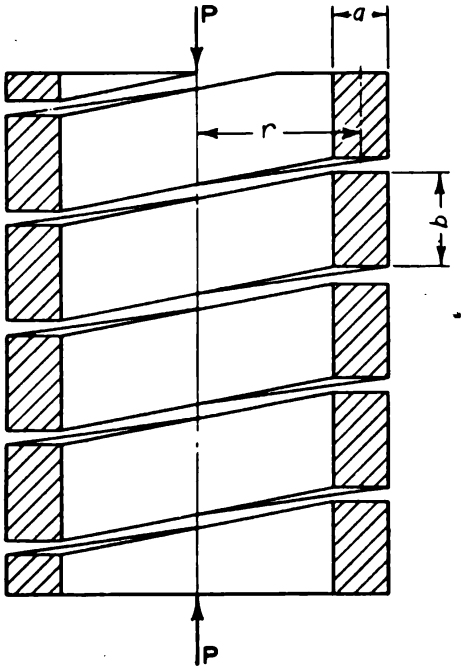

Fig. 102 — Helical spring of rectangular wire axially loaded

G=modulus of rigidity and θ the angular twist per unit length. By differentiating Equation 188 and taking $y=0$, $x=a/2$, the maximum stress τ_m (at the mid-points of the long sides) becomes

$$\tau_m = \frac{8G\theta a}{\pi^2} \sum_{n=1,3,5}^{\infty} \frac{1}{n^2} \left(1 - \frac{1}{\cosh \frac{n\pi b}{2a}} \right) \quad \ldots\ldots (189)$$

or

$$\tau_m = k(2G\theta a) \quad \ldots\ldots (190)$$

where k depends on b/a, from TABLE XXV.

The torque M_t may be determined in terms of the angular twist θ by taking twice the volume under the deflected membrane, the ratio q/S being again replaced by $2G\theta$. Since twice this volume is given by

TABLE XXV

Factors for Computing Rectangular Bars in Torsion

b/a	k	k_1	k_2
1.	.675	.1406	.208
1.2	.759	.166	.219
1.5	.848	.196	.231
2.	.930	.229	.246
2.5	.968	.249	.258
3.	.985	.263	.267
4.	.997	.281	.282
5.	.999	.291	.291
10.	1.000	.312	.312
∞	1.000	.333	.333

$$V = 2 \int_{-a/2}^{+a/2} \int_{-b/2}^{+b/2} z\,dx\,dy$$

by using Equation 188 for z and taking $q/S = 2G\theta$ the expression for torque becomes

$$M_t = \frac{1}{3} G\theta a^3 b \left(1 - \frac{192a}{\pi^5 b} \sum_{n=1,3,5\ldots}^{\infty} \frac{1}{n^5} \tanh \frac{n\pi b}{2a} \right)$$

This equation may be written

$$M_t = k_1 G\theta a^3 b$$

Solving for θ,

$$\theta = \frac{M_t}{k_1 a^3 b G} \quad \ldots\ldots (191)$$

where k_1 depends on the ratio b/a and may be obtained from TABLE XXV.

By substituting the value of θ given by Equation 191 in Equation 190 the maximum stress τ_m may be determined in terms of M_t. Thus,

$$\tau_m = \frac{M_t}{k_2 a^2 b} \quad \text{.....(192)}$$

The factor k_2 may be taken from TABLE XXV.

For a rectangular-wire helical spring of large index and small pitch angle, the twisting moment $M_t = Pr$ where r = mean coil radius, *Fig.* 102. The maximum shearing stress then becomes

$$\tau_m = \frac{Pr}{k_2 a^2 b} \quad \text{.....(193)}$$

It should be noted that this equation assumes a large index, i.e., the stress increase due to curvature and direct shear is neglected. These latter effects will be considered later.

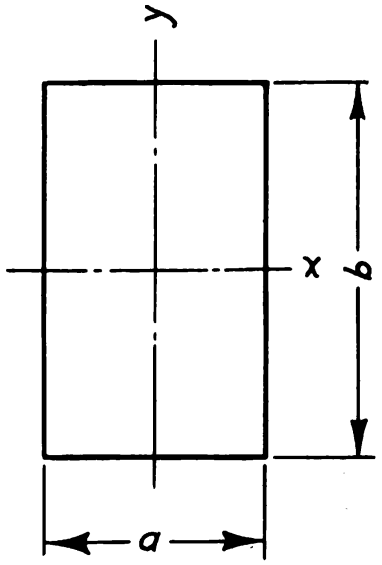

Fig. 103—Rectangular bar section

For *square-wire springs* where $a = b$, this equation reduces to

$$\tau_m = \frac{4.8Pr}{a^3} \quad \text{.....(194)}$$

From Equation 191 the angular twist θ per unit length may be found, taking $M_t = Pr$. The total angular twist will be $2\pi nr\theta$ and the deflection δ, this value multiplied by the coil radius r. Thus $\delta = 2\pi nr^2\theta$, or using Equation 191

$$\delta = \frac{2\pi Pr^3 n}{k_1 a^3 b G} \quad \text{.....(195)}$$

where k_1 is taken from TABLE XXV.

For *square-wire springs* where $a = b$ this equation reduces to

$$\delta = \frac{44.6\ Pr^3 n}{Ga^4} \quad \text{.....(196)}$$

Although in deriving this deflection equation a large index is tacitly assumed, a more exact calculation based on elastic theory[5] shows that for an index greater than four the error will be under 2 per cent. This is in contrast to the stress formula which may be considerably in error even for indexes greater than 4.

For *large pitch angles* or *large deflections* a theory may be developed for square-wire springs similar to that described in Chapter III for round wire springs.

SQUARE-WIRE SPRINGS OF SMALL INDEX

If the spring be assumed simply as a square bar under a torsion moment Pr, the use of the *membrane analogy* yields an expression for maximum shear stress which is given by Equation 194. For large spring indexes this value of stress will be approximately correct, but for small or moderate indexes the error will be considerable. In such cases, as for round wire, a more exact analysis shows that to obtain the maximum stress, the ordinary stress formula must be multiplied by a factor K' depending on the spring index to account for curvature and direct shear.

Small Pitch Angles—The factor K' may be computed from

[5]Goehner, O.—*Die Berechnung Zylindrischer Schraubenfedern* V.D.I. Vol. 76, Page 269.

elastic theory in a similar way as for the case of round wire, Chapter II. In this case the analysis[6] shows that for small pitch angles and indexes greater than three an expression for the factor K', correct to within 1 per cent, is

$$K' = 1 + \frac{1.2}{c} + \frac{0.56}{c^2} + \frac{0.5}{c^3} \quad \ldots\ldots (197)$$

Where $c = 2r/a$ = spring index.

Thus the maximum torsion stress for *square wire* becomes

$$\tau_m = K' \frac{4.8Pr}{a^3} \quad \ldots\ldots (198)$$

Values of K' are plotted as functions of spring index $2r/a$ in *Fig.* 104. Comparison of this figure with the corresponding curve for round wire (*Fig.* 30 Chapter II) shows that the values

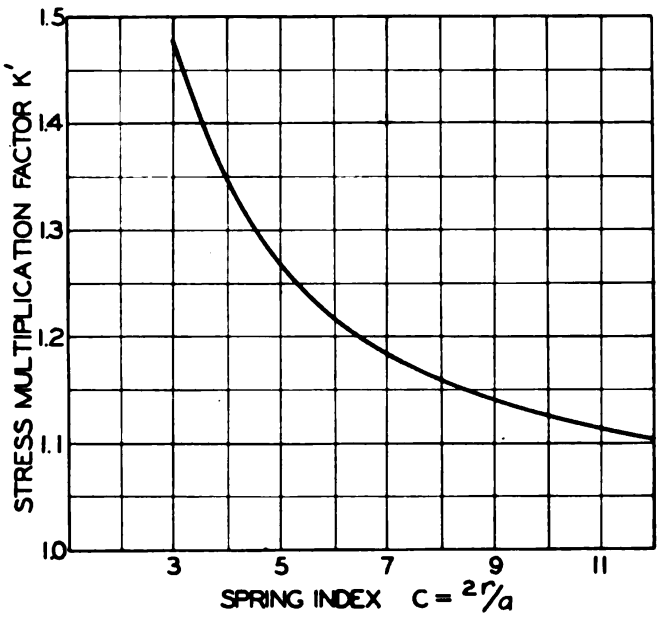

Fig. 104—Stress multiplication factor K' for square-wire helical springs (Index $2r/a > 3$)

of K' are somewhat under the K values for round wire, the difference being about 7 per cent for an index of 3, and 4 per cent for an index of 4.

In general when a square-wire spring is wound, as a con-

[6]Goehner, loc. cit., Page 272.

sequence of plastic deformation during coiling the section becomes trapezoidal as indicated in *Fig.* 105. In such cases an approximation may be had by taking an average value of a equal to

$$a=\frac{b_1+b_2+2a_1}{4} \quad \text{(199)}$$

and taking the spring index equal to $2r/a_1$ for finding K'. The stress measurements on rectangular-wire springs to be discussed later indicate that this method is sufficiently accurate.

To calculate deflections in square-wire springs of small index, Equation 196, derived on the basis of a straight bar in torsion will give results correct to within 4 per cent for spring indexes over three. The application of the more exact calculation based on elastic theory[6] yields the following expression valid for small indexes and small pitch angles:

$$\delta=\frac{44.6Pr^3n}{Ga^4}\left(\frac{c^2-1}{c^2-.69}\right)=\delta_o\left(\frac{c^2-1}{c^2-.69}\right) \quad \text{(200)}$$

The term outside the parentheses represents deflection δ_o based on the torsion of a straight bar, Equation 196, while the fraction involving c represents the effect of the spring index. For an index of 3 this fraction is .963 which means a deflection about 3.7 per cent less than that figured from the usual formula in Equation 196. For an index of 4 the deflection will be about 2 per cent less.

The charts of *Figs.* 78 and 79 which apply to round wire helical springs may also be used for an approximate calculation of loads and deflections in square wire springs at given stresses. It is merely necessary to calculate the load and deflection at the given working stress in the corresponding round-wire spring, i.e., one having the same outside coil diameter, number of turns and a wire diameter equal to the average side of the square cross section. The loads thus found are multiplied by the factor 1.06 and the deflections by .738 to find those for the square wire spring at the given stress. For best accuracy, however, Equations 198 and 200 should be used instead of the charts mentioned.

Large Pitch Angles; Exact Theory—Applying the more exact theory in a similar manner as outlined in Chapter II to

a square-wire section, the following more exact formulas have been developed[7]. These take into account the effect of pitch angle α.

Maximum shear stress is

$$\tau_m = \frac{4.8Pr\cos\alpha}{a^3} \times \left[1 + 1.20\left(\frac{a}{2\rho}\right) + .56\left(\frac{a}{2\rho}\right)^2 + \frac{1}{2}\left(\frac{a}{2\rho}\right)^3 + \frac{.62\left(\frac{a}{2\rho}\right)\tan^2\alpha}{1 - \frac{a}{2\rho}} \right] \quad (201)$$

where $\rho = r/\cos^2\alpha$. Where the index $c = 2r/a > 3$ and $\alpha < 10$ degrees, this equation may be expressed as

$$\tau_m = \left(\frac{4.8Pr\cos\alpha}{a^3}\right) K' \quad (202)$$

where K' is given by Equation 197 or *Fig.* 104.

If α is between 10 and 20 degrees and $c < 3$, the following expression for maximum torsion stress holds:

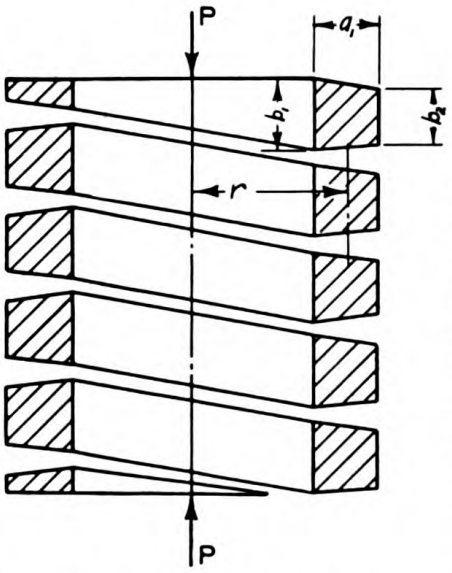

Fig. 105 — Section of helical spring coiled from square wire tends to become trapezoidal in form after coiling

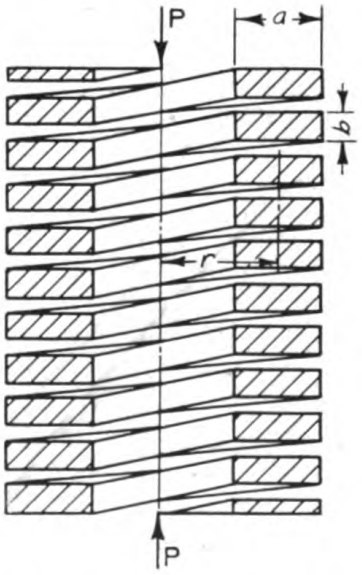

Fig. 106—Helical spring coiled flatwise from rectangular wire. Effect of bar curvature complicates exact calculation

[7]These equations were derived by Goehner, loc. cit., Page 271, using methods similar to those discussed in Chapter II.

$$\tau_m = \frac{4.8Pr\cos\alpha}{a^3}\left[1 + \frac{1.2}{c} + \frac{.56}{c^2}\right] \quad \text{.....(203)}$$

The bending stress σ_m which occurs as a result of the pitch angle may be calculated using curved-bar theory, taking the bending moment equal to $Pr \sin \alpha$ and using a similar procedure to that used in Chapter II. The bending and torsion stresses σ_m and τ_m may then be combined in a similar way to get the maximum equivalent shear stress. In general, for practical springs this equivalent stress will not be greatly different from the maximum torsion stress τ_m.

A more accurate expression for calculating the effect of pitch angle on deflection may be derived in a similar way as was done for round wire springs, Equation 51. The analysis shows that the deflection δ is given by

$$\delta = \psi' \delta_o \quad \text{.....(204)}$$

where δ_o = deflection of square-wire spring figured from the usual formula, Equation 196, and

$$\psi' = \frac{\cos\alpha}{1 + \dfrac{.31\cos^4\alpha}{c^2 - 1}} + 1.69\frac{G}{E}\sin\alpha\tan\alpha \quad \text{.....(205)}$$

It will be seen that this equation is similar to Equation 51 for round-wire springs. For example, if $c=3$ and $\alpha=10$ degrees, the calculated value of ψ' from Equation 205 is .97, which means that the deflection will be about 3 per cent lower than that calculated by neglecting the pitch angle and curvature effect.

RECTANGULAR-WIRE SPRINGS

An exact calculation of rectangular-wire springs is complicated if the effect of bar curvature in increasing the stress is considered. This is particularly true if the spring is coiled flatwise as in *Fig.* 106.

Small Pitch Angles—Where the long side of the cross section is parallel to the spring axis and where the ratio b/a is between 1 and 2.5 as in *Fig.* 102, an approximate expression for shearing stress (for small pitch angles) is:

$$\tau_m = K' \frac{Pr(3b+1.8a)}{b^2a^2} \quad \ldots\ldots (206)$$

where K' is obtained from Equation 197 or the curve of *Fig.* 104 using $c=2r/a$. Where b/a is between 2.5 and 3 this equation will give results accurate to within a few per cent for indexes c>4; when c is between 3 and 4 the error may be as much as 7 per cent.

Where the long side of the rectangle is parallel to the spring axis (*Fig.* 102) and $b>3a$, an approximation for stress[8] is

$$\tau_m = \frac{3}{2} \frac{P(2r+a)}{a^2(b-.63a)} \quad \ldots\ldots (207)$$

Formulas based on elastic theory have also been developed for calculating stress in rectangular-bar springs[8]. It should be noted that the maximum torsion stress in a rectangular bar under torsion is normally at that midpoint of the long sides of the rectangle. This will also be true where the bar is coiled in the form of a spring of large index. For smaller indexes, however, the maximum stress tends to occur at the inside of the coil because of curvature and direct shear effects. Thus two opposing effects here tend to come into play. Where the spring is coiled flatwise, *Fig.* 106, the peak stress may occur either on the short or on the long sides depending on the spring index and the ratio b/a.

Charts for Calculating Stress—For practical calculations of stress in rectangular bar springs the curves of *Fig.* 107, based on those calculated by Liesecke[9] from Goehner's equations for stress in rectangular bar springs may be used.

Referring to the dimensions shown on the sketches in *Fig.* 107 the maximum shearing stress τ_m in the spring is given by

$$\tau_m = \beta \frac{Pr}{ab\sqrt{ab}} \quad \ldots\ldots (208)$$

where a and b are sides perpendicular and parallel to spring axis, respectively, and r = mean coil radius. β = a factor to be taken from *Fig.* 107 depending on the ratio a/b or b/a and

[8]Liesecke, *Zeit.* V.D.I., 1933, Vol. 77, Page 892.
[9]Liesecke, loc. cit., Page 425.

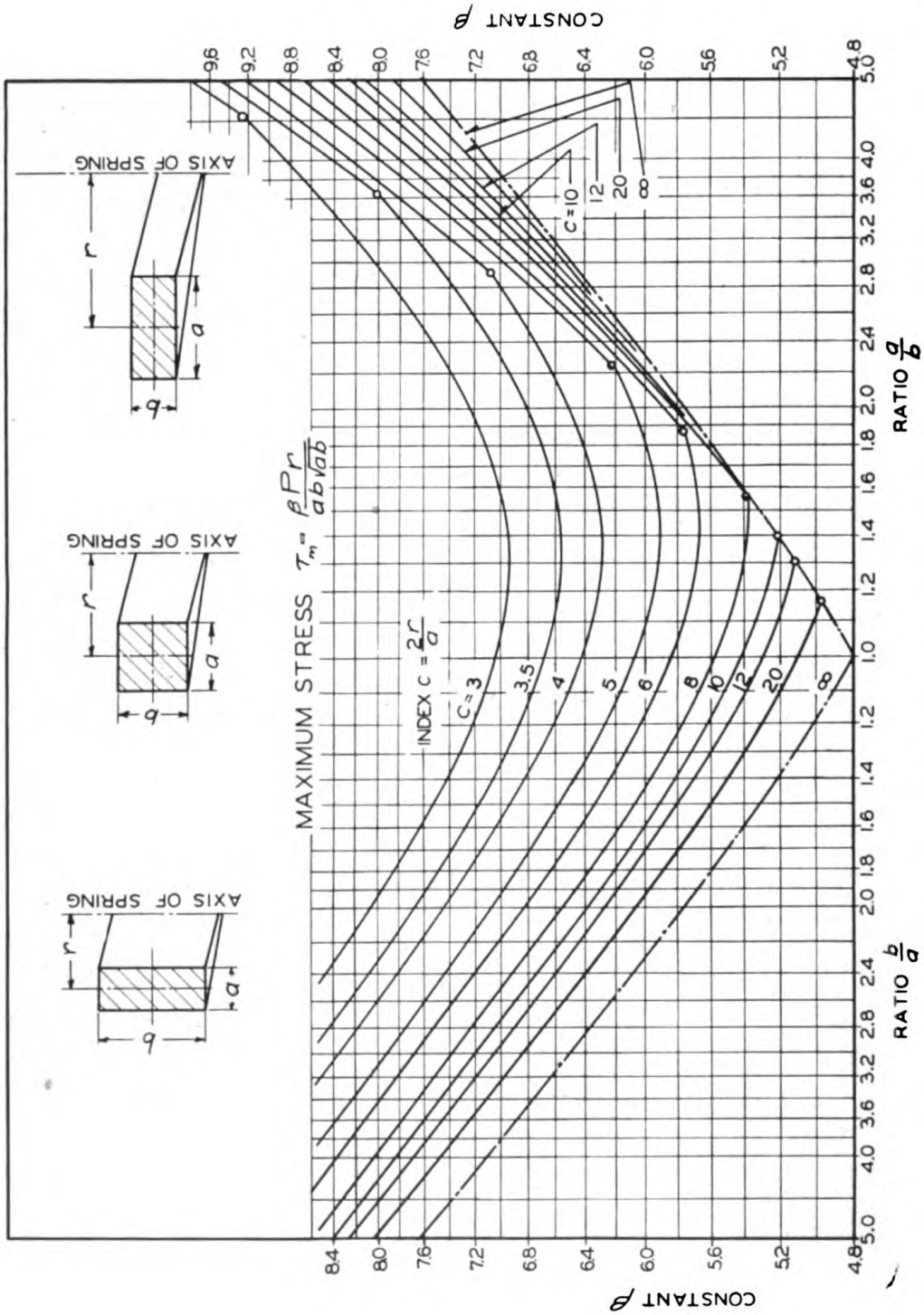

Fig. 107—Curves for calculating stress in rectangular wire helical springs (based on charts by Liesecke VDI, 1933, page 425)

on the spring index $c=2r/a$. Each curve represents a given spring index. Interpolation is used for intermediate values of c.

It should be noted that in this case b always represents the side of the section parallel to the axis of the spring; hence, it may also be the short side.

EXAMPLE: As an example of the use of the chart of *Fig.* 107 for calculation of maximum stress in a rectangular-wire spring, a spring is coiled flatwise as indicated on the figure.

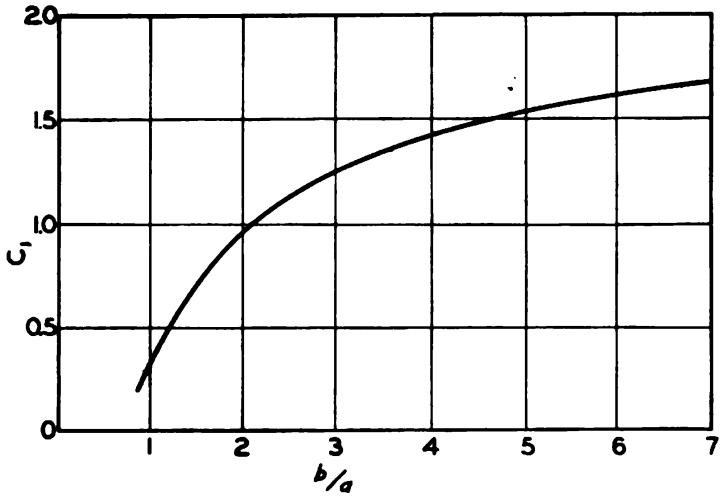

Fig. 108—Curve for factor C_1 for rectangular bar springs

Letting $a=$½-inch, $b=$¼-inch, $a/b=2$, $r=1.5$ inch, $c=2r/a=6$, load $P=300$ pounds, from *Fig.* 107 for $a/b=2$ and $c=6$, $\beta=5.88$. Hence the maximum stress τ_m becomes

$$\tau_m=\beta\frac{Pr}{ab\sqrt{ab}}=\frac{5.88(300)1.5}{\frac{1}{4}(\frac{1}{2})\sqrt{\frac{1}{8}}}=60{,}000 \text{ lb/sq in.}$$

Calculation of Deflections—To calculate deflections in rectangular-bar springs having large indexes (say greater than 8), the following formula, based on torsion of a straight bar of rectangular section, will yield results accurate to within a few per cent where the pitch angle is not large:

$$\delta=\frac{19.6Pr^3n}{Ga^3(b-.56a)} \qquad (209)$$

In this formula, b represents the long side and a the short side of the cross section.

A more accurate formula for rectangular wire springs of large index is the following[10]

$$\delta=\frac{2\pi Pr^3n}{GC''} \quad \text{.....(210)}$$

where

$$C''=a^3\left[\frac{b}{3}-.209a\left(\tanh\frac{\pi a}{2b}+.004\right)\right] \quad \text{.....(211)}$$

If $b/a>2.7$ this factor reduces to

$$C''=a^3(b/3-.21a) \quad \text{.....(212)}$$

Where the long side of the rectangle is parallel to the spring axis as in *Fig.* 102, Equation 210 will yield results accurate to within a few per cent even for indexes as low as 3, the accuracy increasing with the spring index. If higher accuracy is desired, the chart of *Fig.* 109 should be used.

Where the spring is coiled flatwise as in *Fig.* 106, Equation 210 will also give results accurate to within a few per cent, for spring indexes greater than five. In the case of such springs for the smaller indexes, and for larger indexes where higher accuracy is wanted the following equation may be used[10]:

$$\delta=\frac{2\pi Pr^3n}{GC''\left(1+\frac{C_1}{c^2-1}\right)} \quad \text{.....(213)}$$

where C_1 is a factor depending on b/a and is given by the curve of *Fig.* 108. The term C'' is given by Equation 211 or Equation 212. It is seen that the right side of Equation 213 is equal to the corresponding term in Equation 210 divided by a factor C_2 where

$$C_2=1+\frac{C_1}{c^2-1}$$

Where the spring index $c=3$ and $b/a=4$, $C_2=1.18$, i.e.,

[10]Goehner, loc. cit., Page 271. It is assumed that the pitch angle is under 12 degrees.

the results given by Equation 210 for such cases may be around 18 per cent in error. For large values of c the factor C_2 becomes practically unity and Equations 210 and 213 become identical to each other.

The calculation of deflection in rectangular-wire springs for small pitch angles may be simply carried out by the use of the chart[11] of *Fig.* 109. In this case the maximum deflection is given by

$$\delta = \gamma \frac{8Pr^3n}{a^2b^2G} \qquad \text{.....(214)}$$

[11]Liesecke, V.D.I., 1933, Page 892.

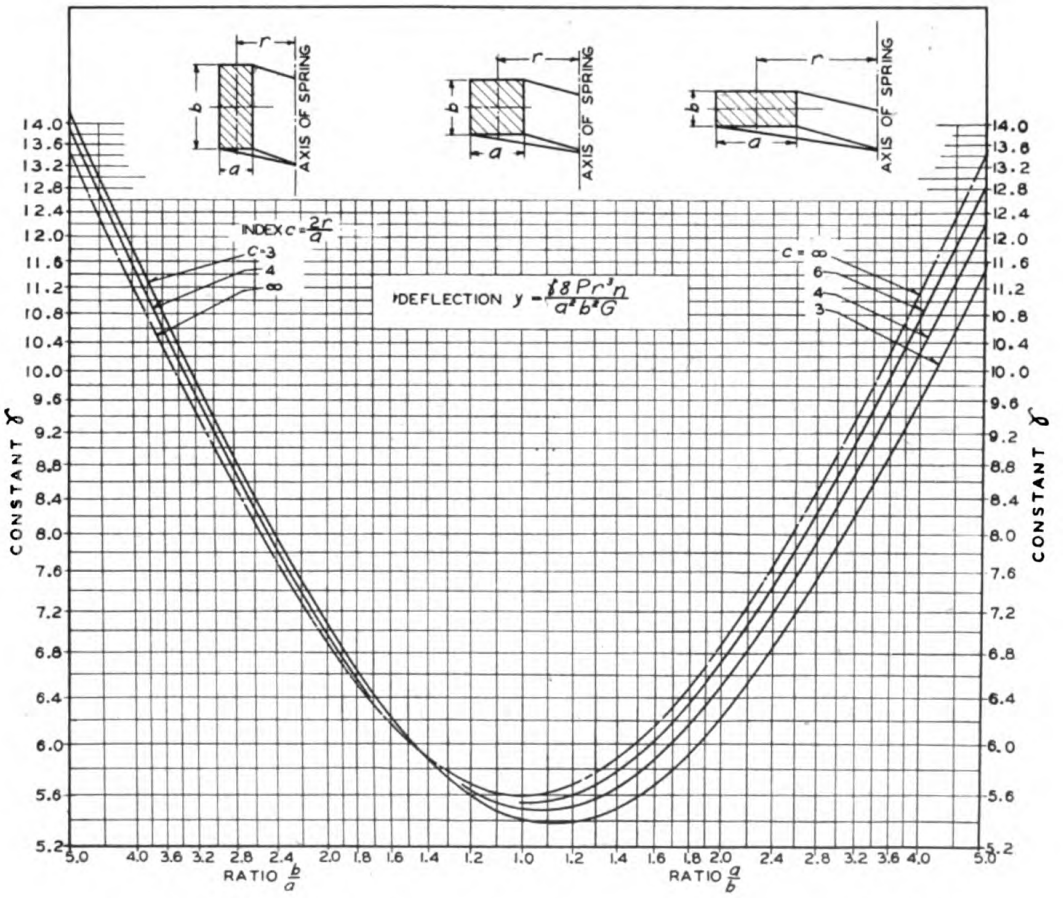

Fig. 109—Curves for calculating deflections in rectangular-wire helical springs (Based on charts by Liesecke, VDI, 1933 P. 892)

where the constant γ depends on the ratio a/b or b/a, *Fig.* 109. In using this equation b is taken as the side parallel to the spring axis and a the side perpendicular thereto. If the spring is

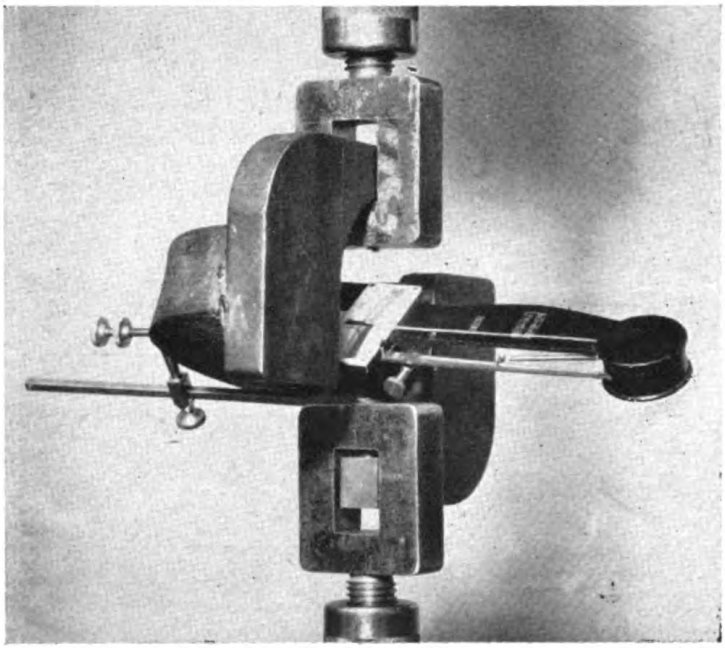

Fig. 110—Semicoil of square-wire helical spring in position in testing machine

coiled flatwise, the ratio a/b is taken, while if it is coiled edgewise a ratio b/a is taken.

EXAMPLE: A spring is coiled flatwise with $a=\frac{1}{2}$-inch, $b=\frac{1}{4}$-inch, $r=1.5$ inch, index $c=2r/a=6$, $P=300$ pounds, number of active turns $n=5$, $G=11.5\times10^6$ pounds per square inch (steel). From *Fig.* 109 the constant $\gamma=6.7$ for $a/b=2$, $c=6$. From Equation 214,

$$\delta=\gamma\frac{8Pr^3n}{a^2b^2G}=\frac{6.7\times8\times300\times3.37\times5}{\frac{1}{4}\times\frac{1}{16}\times11.5\times10^6}=1.51\text{ inch.}$$

In certain instances, it has been the practice in spring design to use a value of modulus of rigidity G for rectangular-bar springs different from that used in circular-bar springs of the same material. Since there is no good reason why the modulus of rigidity should be different for springs of the same

material, this probably has been done to compensate for inaccuracy in certain commonly used empirical deflection and stress formulas for rectangular bar springs. Comparisons[12] of some of these formulas used in practice with the more exact theory for springs of large index show considerable errors up to 100 per cent, depending on the ratio b/a. It is the author's opinion that the formulas given here will yield more satisfactory results for the calculation of such springs than will the empirical formulas which have, at times, been used in the past.

Large Pitch Angles—An exact calculation of stress in rectangular-wire springs with large pitch angles is complicated and will not be discussed here. However, an approximation sufficiently accurate for most practical purposes may be obtained by using the chart of *Fig.* 107 and neglecting the pitch angle.

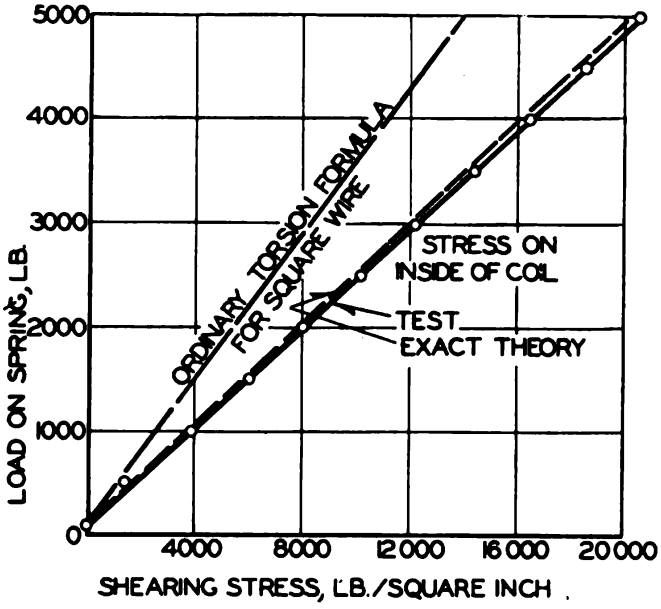

Fig. 111—Load-stress curves for semicoil, $c = 3.07$

For calculating deflections for rectangular-wire springs the following approximate expression takes pitch angle into account[13]:

$$\delta = \frac{2\pi P r^3 n}{C'' G} \psi_1 \qquad (215)$$

[13]See author's article in *Machine Design*, July, 1930 for further details of this comparison.

[12]*V.D.I.*, Vol. 76, Page 271.

The factor ψ_1 is expressed by

$$\psi_1 = \frac{\cos \alpha}{1 + \frac{C_1 \cos^4 \alpha}{c^2 - 1}} + \frac{GC''}{EI} \sin \alpha \tan \alpha \quad \ldots\ldots\ldots\ldots\ldots\ldots\ldots\ldots\ldots\ldots (216)$$

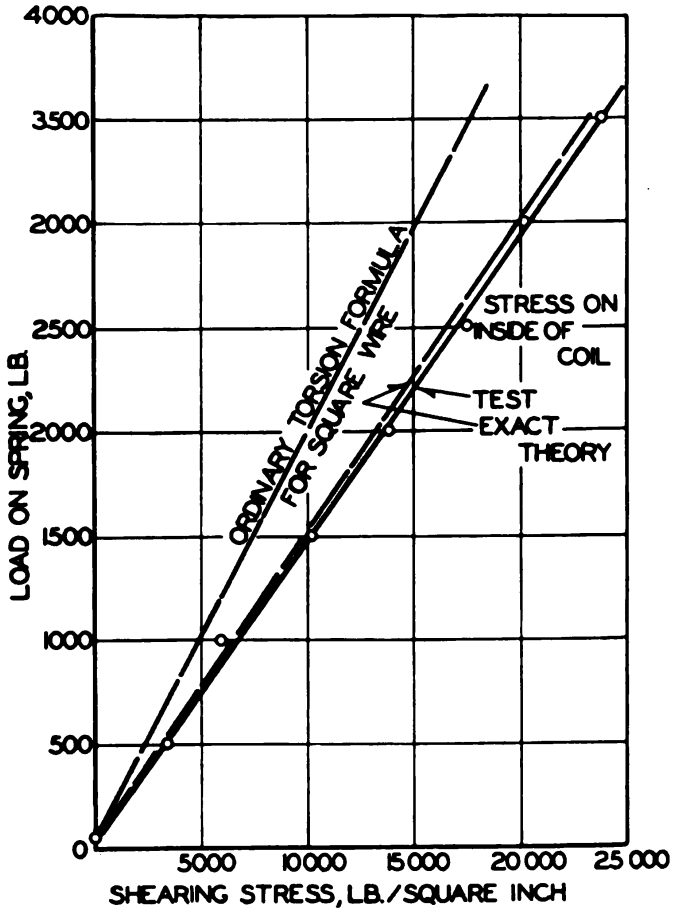

Fig. 112—Load-stress curves for semicoil, $c = 4.14$

C'' is given by Equation 211 or 212 and EI = flexural rigidity of the wire cross section about an axis parallel to the spring axis.

TESTS ON SQUARE-WIRE SPRINGS

To check the stress formula, Equation 198, for square-wire springs some strain measurements were made on semicoils cut

from actual square-wire springs. The strain measurements were made in the same manner as those carried out on round-wire springs, Chapter IV. A semicoil was cut from an actual square-wire helical spring and two arms were welded on as indicated in *Fig.* 110 which represents the semicoil in position in a testing machine. The eyebolts shown have spherical points so that the coil is under a purely axial load as is the case in a complete spring axially loaded. The Huggenberger extensometer used to measure stress is also shown in position on the inside of the coil where the maximum stress occurs. Shearing stresses plotted against load are represented by the full lines in *Figs.* 111 and 112 which show the results of two tests on two coils, one of index 3.07 and the other of index 4.14. For comparison, dashed curves representing the stress calculated by the more exact formula, Equation 198, are also shown. It may be seen that the results calculated from this more exact expression agree well with the test results. For comparison a curve representing the stress calculated by the ordinary torsion formula for square wire, Equation 194, (which neglects curvature effects) is also given. In both cases this latter curve shows considerable deviation from the test curve.

APPLICATION OF FORMULAS TO STATIC AND FATIGUE LOADING

It should be noted that the formulas for stress given in this chapter for square and rectangular bar springs are based on elastic conditions. Where fatigue loading is involved the formulas should give the maximum stress range which is of primary interest. However, for static loading these formulas neglect the effects of plastic flow with resultant increased ability of the spring to carry load. In such cases an analysis similar to that of Chapter V for round wire would be required; this is, however, beyond the scope of this book. In the absence of more detailed information, use of rectangular-bar formulas which neglect curvature and direct shear (Equation 206 taking $K' = 1$) would probably be justified where static loading only is concerned.

CHAPTER XIII

VIBRATION AND SURGING OF HELICAL SPRINGS

In the usual calculation of stress and deflection in helical springs, it is tacitly assumed that the load is applied (or the spring compressed) at a slow rate[1] so that additional dynamic stresses due to impact or vibration do not occur. In most practical spring applications this assumption is probably realized with sufficient accuracy. There are a large number of applications, however, where dynamic effects due to surge or vibration

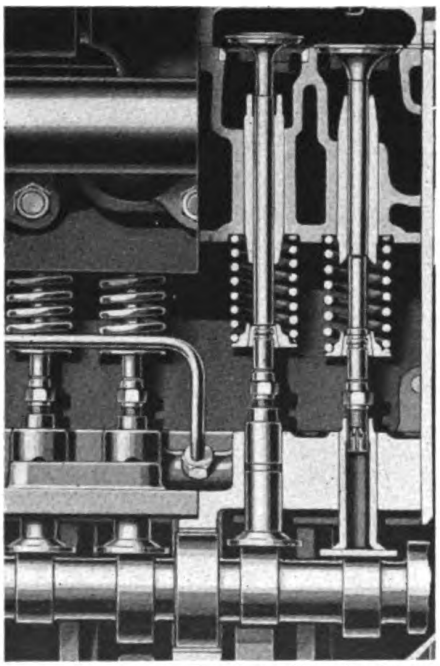

—Courtesy, Chrysler Corp.

Fig. 113 — Automotive valve spring and gear assembly

are of great importance. The additional vibratory stresses thus set up must be taken into account by the designer if fatigue failure is to be avoided. The most important example of such

[1]By a slow rate is meant one in which the time of application of the load is large compared to the natural period of vibration of the spring.

applications is the aircraft or automotive engine valve spring. A sectional view of a typical automotive valve spring and gear is shown in *Fig.* 113, while a sketch of a typical valve-gear drive showing the arrangement is shown in *Fig.* 114*a*.

Surging—A typical valve-lift curve showing valve lift plotted against time is shown in *Fig.* 114*b*. This latter curve also represents the compression of the end of the spring (beyond a

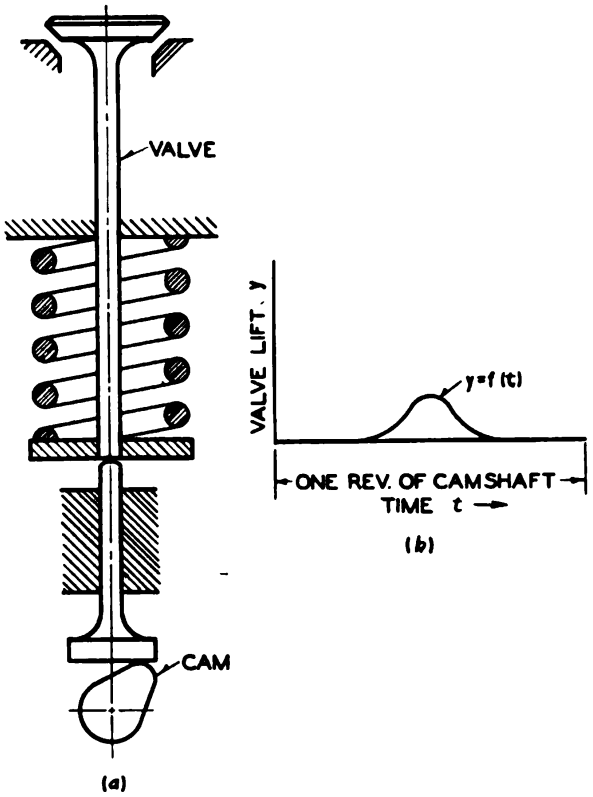

Fig. 114—Schematic valve spring and gear for internal combustion engine

given initial value) plotted against time. It is clear that, if the engine speed is high, a sudden compression of the end of the spring will cause a compression wave to travel along the spring which will be reflected from the end, the time for the wave to travel from one end of the spring to the other being dependent on the natural frequency of the spring. This phenomenon of wave travel along a spring may easily be demon-

strated by taking a long flexible spring, such as a curtain rod spring, and holding it stretched between the two hands. If one end is suddenly moved by moving one hand, a compression or extension wave will be seen to travel back and forth along the spring. This is essentially the same as surging of valve springs.

Another interesting application of dynamically loaded springs is the crank-type fatigue testing machine shown in *Fig.* 100, Chapter XI. Where machines of this type are to operate at high speeds, spring vibration should be considered.

DESIGN CONSIDERATIONS

Resonance—In the design of springs subject to a rapid reciprocating motion (such as valve springs), it is important to avoid, in so far as possible, resonance between the frequency of the alternating motion of the end of the spring and one of the natural frequencies of vibration of the spring. Usually the lowest natural frequency is of the most importance. For a spring compressed between parallel plates the first mode of vibration (corresponding to the lowest natural frequency) will consist of a vibratory motion of the middle portion of the spring with the ends remaining stationary. The second mode of vibration (corresponding to a higher frequency) will have a node (or point of zero motion of the coils) in the middle of the spring, while maximum motion of the coils occurs at points ¼ and ¾ of the length distant from a given end of the spring. The natural frequencies corresponding to these modes of vibration may be calculated by methods discussed later.

Principal Frequencies—For example, if a spring is subject to a reciprocating motion by means of a simple crank arrangement as indicated in *Fig.* 115, provided the ratio r/l between crank radius and connecting rod length is not too large, the expression for the spring displacement from its position at top dead center is given with sufficient accuracy by the equation[2]:

$$y=\left(r+\frac{r^2}{4l}\right)-r\left(\cos\omega t+\frac{r}{4l}\cos 2\omega t\right) \quad \ldots\ldots\ldots\ldots\ldots\ldots\ldots (217)$$

In this ω is the speed of the crank in radians per second

[2]Den Hartog, *Mechanical Vibrations*, Second Edition, McGraw-Hill, 1940, Page 209, derives this equation.

($\omega = \pi N/30$ where N = speed in revolutions per minute).

This equation shows that for springs subject to oscillation by means of a simple crank there are two principal frequencies with which to be concerned:

1. Fundamental frequency of rotation as represented by the *cos* ωt term of Equation 217.

2. Frequency twice this value represented by the *cos* $2\omega t$ term of Equation 217.

Thus to avoid trouble from resonance, the spring should be stiff enough so that its lowest natural frequency, calculated from Equation 236, is considerably higher than twice the frequency of rotation of the crankshaft.

Where a spring is deflected by a cam as in valve springs, the valve lift curve $y = f(t)$ (*Fig.* 114*b*) is not a simple sine function consisting primarily of one or two terms as in the case a crank but instead a complicated function, which may be assumed to consist of a large number of sinusoidal terms (a Fourier's series). Thus the expression for valve lift y may be written as follows:

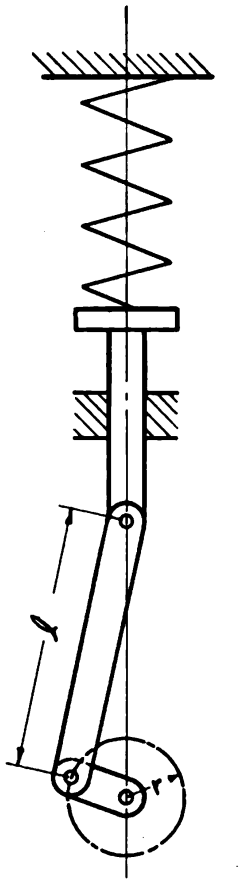

Fig. 115—Helical spring subject to reciprocating motion

$$y = f(t) = c_o + c_1 \sin(\omega t + \phi_1) + c_2 \sin(2\omega t + \phi_2) + \ldots + c_\mu \sin(\mu\omega t + \phi_\mu) + \ldots \quad (218)$$

Thus the motion of the end of the spring may be considered as a fundamental wave having a circular frequency ω equal to 2π times the camshaft speed in revolutions per second, on which is superimposed harmonics of 2, 3, 4 . . . . times this frequency; the amplitudes of these harmonics are c_2, c_3, c_4 . . . . For purposes of analysis each of these harmonics may be assumed to act independently. In practice harmonics as high as the twentieth may have to be considered.

Surge Stresses—In general, it should be noted that the amplitudes of motion of these higher harmonics, represented by the terms c_1, c_2, etc., decrease as the order of the harmonic increases[3]. Usually it will be found difficult to avoid resonance within certain engine speed ranges between one of the higher harmonics and a natural frequency (usually the lowest) of the spring. When this takes place, severe vibration or surging occurs due to resonance effects and this may increase the stress range in the spring by 50 per cent or more. This is true even though the amplitude of the particular harmonic in resonance may be relatively small, since there is a large magnification of the motion under such conditions.

To reduce stresses due to such resonant vibrations in valve springs several methods are open. In the first place the natural frequency of the spring may be as high as possible so that resonance will occur only for the higher order harmonics (which are usually of lower amplitude). Hence an improvement is obtained since the stresses set up by resonance with these higher harmonics are not as great as those set up by resonance with lower harmonics of greater amplitude.

Another method of reducing surge stresses in valve springs is to shape the cam contour so as to reduce the amplitudes of the harmonics which are of importance in the speed range within which the engine is to be used. For example, it might be found that for an engine with an operating range from 2000 to 3000 revolutions per minute the tenth, eleventh, and twelfth harmonics are in resonance with the lowest natural frequency of the valve springs in this speed range. Hence a cam contour such as to give a low value for these harmonics would be of advantage in this case. In many cases it is possible by a change in the cam contour to reduce the magnitudes of the harmonics to low values within certain speed ranges[4].

By reducing or varying the pitch of the coils near the ends of the spring, an improvement often may be obtained. The reason for this is that if resonance occurs with one harmonic, these end coils will close up thus changing the natural frequency

[3]The numerical values of the amplitudes of the various harmonics may be determined by harmonic analysis for any given valve lift curve.

[4]This is further discussed in "Schwingungen in Schraubenfoermigen Ventilfedern" by A. Hussmann, Dissertation, T. H. Berlin, published by Deutschen Versuchsanstalt fuer Luftfahrt, Berlin-Adlershof, 1938.

of the spring. This tends to throw it out of resonance[5]. Friction dampers, consisting of a three-pronged device with the prongs pressing against the center coils of the spring have also been used to damp out resonant oscillations[6].

EQUATION FOR VIBRATING SPRING

To calculate natural frequency and vibratory characteristics of a spring it is first necessary to derive the differential equation of motion. To do this, an element A (shown cross-hatched)

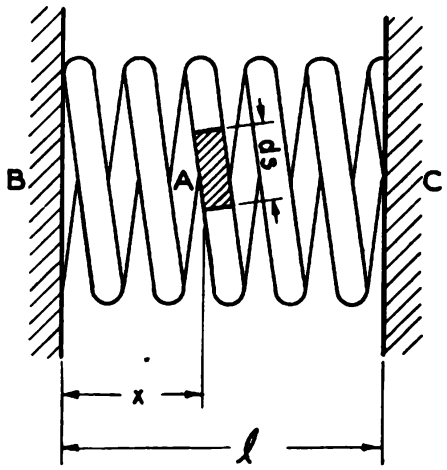

Fig. 116—Helical spring compressed between parallel plates

of the helical spring in *Fig.* 116 compressed between the two flat plates B and C is considered. It is assumed that when the spring is not vibrating, the element A of length ds, is at a distance x from the left end of the spring. The active length of the compressed portion of the spring is taken as l, while the effect of pitch angle will be neglected. The deflection of the small element A from its mean position (or position when the spring is at rest) at any time t will be designated y. If $\pi d^2/4$ is the cross-sectional area of the wire, γ the weight of the spring material per unit of volume and g the acceleration of gravity, the mass of the element A is $\pi d^2 \gamma ds/4g$ and the force required to accelerate the element will be

[5]*Die Federn*, by Gross and Lehr, Page 115, published by V.D.I., Berlin, 1938.

[6]*The Surging of Engine Valve Springs*, by Swan and Savage, Sp. Rep. No. 10, Dept. of Sci. & Ind. Research, London.

$$F_a = \frac{\pi d^2 \gamma ds}{4g} \frac{\partial^2 y}{\partial t^2} \quad \text{.....(219)}$$

This follows from the equation force equals mass times acceleration since the acceleration of this element is $\partial^2 y/\partial t^2$. The partial derivative is used since y is a function of both s and t.

The change in y in a distance ds will be $(\partial y/\partial s)ds$. For a complete turn this change will be $\triangle y = 2\pi r\ \partial y/\partial s$ where r = mean coil radius and the total force P acting at a distance x will be, from the ordinary spring deflection formula, Equation 7,

$$P = \frac{Gd^4 \Delta y}{64r^3} = \frac{Gd^4}{64r^3} 2\pi r \frac{\partial y}{\partial s} \quad \text{.....(220)}$$

In this G is the modulus of rigidity.

The change in the force P in a length ds will be $(\partial P/\partial s)ds$, and this will be the net force F_b acting to accelerate the element A. Thus by differentiation of Equation 220, this force becomes

$$F_b = \frac{\partial P}{\partial s} ds = \frac{\pi}{32} \frac{Gd^4}{r^2} \frac{\partial^2 y}{\partial s^2} ds \quad \text{.....(221)}$$

Damping Forces—In addition there are damping forces present due to various causes including:

1. Internal hysteresis in the spring material
2. Air damping
3. Damping due to friction in the end turns
4. Damping due to loss of energy in the supports.

An exact method of taking all these sources of damping into account would be hopelessly complicated. For mathematical convenience the damping force is assumed proportional to the velocity of motion. This means that, if c is the damping force per unit length of the wire per unit of velocity, the damping force F_d is

$$F_d = c \frac{\partial y}{\partial t} ds \quad \text{.....(222)}$$

This force opposes the elastic force F_b. Hence, from equilibrium,

$$F_a = F_b - F_d$$

or substituting Equations 219, 221 and 222 in this and dividing by ds

$$\frac{\pi d^2\gamma}{4g}\frac{\partial^2 y}{dt^2}=\frac{\pi}{32}\frac{Gd^4}{r^2}\frac{\partial^2 y}{\partial s^2}-c\frac{\partial y}{\partial s} \quad \ldots\ldots (223)$$

Since $s=2\pi rnx/l$ where l = active length of spring, and n the number of active turns

$$\frac{\partial y}{\partial s}=\frac{l}{2\pi rn}\frac{\partial y}{\partial x} \text{ and } \frac{\partial^2 y}{\partial s^2}=\frac{l^2}{4\pi^2 r^2 n^2}\frac{\partial^2 y}{\partial x^2}$$

Thus by substitution of these values in Equation 223 and rearranging terms, the following differential equation is obtained:

$$\frac{\partial^2 y}{\partial t^2}+2b\frac{\partial y}{\partial t}=a^2\frac{\partial^2 y}{\partial x^2} \quad \ldots\ldots (224)$$

where

$$W=\frac{\pi^2}{2}d^2nr\gamma=\text{weight of active part of spring} \quad \ldots\ldots (225)$$

$$k=\frac{Gd^4}{64r^3n}=\text{spring constant} \quad \ldots\ldots (226)$$

$$a=l\sqrt{\frac{kg}{W}} \quad \ldots\ldots (227)$$

$$b=\frac{c'g}{2W} \quad \ldots\ldots (228)$$

In this the term b is a measure of the equivalent damping in the spring. In general b will vary with such factors as kind of material, amplitude of motion, design of end turns, rigidity of support, and can only be determined by actual tests on vibrating springs[7]. If the damping is zero, $b=0$ and Equation 224 reduces simply to

$$\frac{\partial^2 y}{\partial t^2}=a^2\frac{\partial^2 y}{\partial x^2} \quad \ldots\ldots (229)$$

This is the same form as the well-known equation for longi-

[7]See for example article by C. H. Kent, *Machine Design*, October, 1935, for a report of such tests. Also references of footnotes 4 and 6.

tudinal wave transmission in prismatical bars, a being the velocity of motion of the wave along the bar[8].

NATURAL FREQUENCY

To calculate the natural frequency of a spring, it is permissible to neglect damping since the small amount of damping present in actual springs does not affect the natural frequency appreciably. Hence for this purpose the simpler differential equation (229) may be used. To solve this equation, the instantaneous deflection y at any point of the spring is assumed to be the product of two functions, one a function of x only, and the other a function of t only. Thus,

$$y=\phi(x)\cdot\psi(t) \qquad (230)$$

where $\phi(x)$ and $\psi(t)$ are functions of x and t respectively. Then

$$\frac{\partial^2 y}{\partial t^2}=\frac{d^2\psi}{dt^2}\cdot\phi(x);\ \frac{\partial^2 y}{\partial x^2}=\frac{d^2\phi}{dx^2}\cdot\psi(t)$$

Substituting these in Equation 229,

$$\frac{d^2\psi}{dt^2}\cdot\phi(x)=a^2\frac{d^2\phi}{dx^2}\cdot\psi(t)$$

or

$$\frac{1}{\psi(t)}\frac{d^2\psi}{dt^2}=\frac{a^2}{\phi(x)}\frac{d^2\phi}{dx^2}$$

This equation can only be satisfied if both members of this equation are equal to a constant, say $-\omega^2$. Then

$$\frac{d^2\psi}{dt^2}+\omega^2\psi(t)=0 \qquad (231)$$

$$\frac{d^2\phi}{dx^2}+\frac{\omega^2\phi(x)}{a^2}=0 \qquad (232)$$

Solutions of these equations are

$$\psi(t)=A_1 sin\ \omega t+B_1 cos\ \omega t \qquad (233)$$

$$\phi(x)=A_2 sin\ \frac{\omega x}{a}+B_2 cos\ \frac{\omega x}{a} \qquad (234)$$

[8]Timoshenko—*Vibration Problems in Engineering*, Second Edition, Page 309, Van Nostrand.

where A_1, A_2, B_1, B_2 are arbitrary constants depending on the boundary conditions of a given problem.

By substituting Equations 233 and 234 in Equation 230 a solution is obtained which satisfies the differential Equation 229. This solution is

$$y=(A_1 sin\ \omega t+B_1 cos\ \omega t)\left(A_2 sin\ \frac{\omega x}{a}+B_2 cos\ \frac{\omega x}{a}\right)$$

Spring Ends Fixed—If both ends of the spring are assumed as fixed or clamped, this means that regardless of the value of t,

$$y=0 \text{ for } x=0;\ y=0 \text{ for } x=l.$$

The first of these conditions requires that $B_2=0$, while the second requires that $sin\ \omega l/a=0$. This means that the following relations hold:

$$\frac{\omega l}{a}=\pi,\ 2\pi,\ 3\pi \cdots etc.$$

or

$$\omega=\frac{\pi a}{l},\ \frac{2\pi a}{l},\ \frac{3\pi a}{l} \cdots etc.$$

Since $\omega=2\pi f$ where f is a natural frequency of the spring, these equations show that the natural frequencies are in the ratios 1:2:3, etc.

Using the value of a given by Equation 227, the expression for the natural frequency of the spring (in cycles per second) becomes

$$f=\frac{\omega}{2\pi}=\frac{m}{2}\sqrt{\frac{kg}{W}} \qquad (235)$$

where $m=1, 2, 3 \ldots$ is the order of the vibration, i.e., $m=1$ for the first mode, 2 for the second mode, etc.

Using the expressions for the spring constant k and spring weight W given by Equations 226 and 225, the *lowest* natural frequency, $m=1$, becomes

$$f=\frac{d}{2\pi r^2 n}\sqrt{\frac{Gg}{32\gamma}} \quad \text{.....(236)}$$

This lowest frequency is usually of most importance in practice.

The equation shows that for a given material the natural frequency of a helical spring is proportional to the wire diameter and inversely proportional to the product of the coil diameter and the number of active coils. For the usual steel springs where $G=11.5\times10^6$ pounds per square inch and $\gamma=.285$ pounds per cubic inch, the formula for *lowest* natural frequency reduces to the simple expression

$$f_1=\frac{3510d}{r^2n} \text{ cycles per second} \quad \text{.....(237)}$$

One Spring End Free—For a spring with one end free and the other clamped, the lowest natural frequency would be equal to that of a similar spring twice as long but with both ends clamped. For such a spring Equation 237 may be used if the number of turns is taken as twice the actual number in the spring.

Example—As an example of the use of these equations in calculating natural frequency, assuming a steel spring clamped at both ends, with $d=.3$-inch, $r=1$-inch, $n=6$ and using Equation 237, the lowest natural frequency becomes

$$f_1=\frac{3510\times.3}{(1)^2\times6}=175 \text{ cycles per second.}$$

In the second mode of vibration the spring frequency will be double this or 350 cycles per second.

One Spring End Weighted—For a spring with a weight hanging on its end as shown in *Fig.* 117, the lowest natural frequency of the system may be calculated as follows: It is known that where a mass is deflected by a certain amount δ under its own weight (the mass of the spring being small compared to that of the weight), the natural frequency in cycles per second may be taken as[9]

$$f=\pi\sqrt{\frac{1}{\delta}} \quad \text{.....(238)}$$

[9]Den Hartog—*Mechanical Vibrations*, Page 45.

In the case where the mass is supported by a helical spring of appreciable weight as indicated in *Fig.* 117 it has been found that, if the weight of one third of the spring is added to that of the mass W_m, the calculated deflection may be used for figuring the natural frequency. If W is the spring weight, Equation 225, and k the spring constant in pounds per inch deflection, the frequency in cycles per second becomes

$$f=\pi\sqrt{\frac{k}{W_m+W/3}} \qquad (239)$$

SURGING OF ENGINE VALVE SPRINGS

Since most aircraft and automobile engines run at variable speeds, as mentioned previously, it is practically impossible to avoid resonance between one of the higher harmonics of the valve lift curve and a natural frequency of the spring at some speed of operation. When this occurs the amplitudes of vibration and the resulting stress in the spring depend primarily on the amplitude of the harmonic which is in resonance and on the amount of damping in the spring (represented by the damping term b in Equation 224).

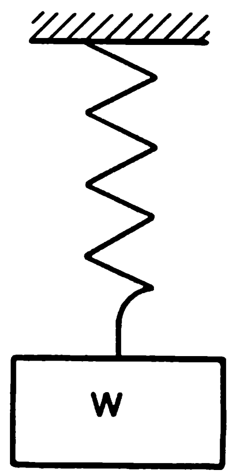

Fig. 117—Weight on helical spring

To obtain the additional stress in the spring, due to this vibration it is assumed that one end of the spring in *Fig.* 116, say end C, is oscillated through an amplitude represented by the function

$$y_o=c_n \sin \omega_n t \qquad (240)$$

In this c_n represents the amplitude of the particular harmonic of the valve lift curve which is in resonance with a natural frequency f_n of the spring, usually the lowest. The circular frequency of this particular harmonic is taken as $\omega_n=2\pi f_n$. The amplitude of motion and stress due to this harmonic may be determined by solving the differential Equation 224 in conjunction with the proper boundary conditions. This stress is then superimposed on the static stress due to the valve lift as indicated

in *Fig.* 118. Here the dot-dash line represents the stress due to the valve lift only, the maximum value being τ_o. On this is superimposed a higher frequency vibration represented by the stress τ_v which is due to resonance with a given harmonic of the valve lift curve.

To solve Equation 224 for the *steady state* condition, the deflection y at any point x from the end of the spring is assumed given by

$$y = F(x) \sin \omega_n t \qquad (241)$$

and $\omega_n = 2\pi f_n$. The function $F(x)$ is a function of x only. This method neglects the transient oscillations due to sudden speed changes which are of no concern here. The assumption represented by Equation 241 is justified since, for a forced vibration of a given frequency, all parts of the spring must vibrate at this frequency.

The boundary conditions are: For $x=0$ *Fig.* 116, $y=0$ regardless of time t since one end of the spring is assumed fixed in space. For $x=l$, $y=c_n \sin \omega_n t$ since the other end of the spring is assumed to have a harmonic motion of amplitude c_n produced by the harmonic of Equation 218 which is in resonance with the natural frequency.

A solution of the differential Equation 224 satisfying these boundary conditions has been obtained by Hussmann[10].

For small values of damping such as occur in practical springs the solution reduces to the relatively simple form:

$$y_{max} = \frac{2c_n f_n}{b\lambda} \sin (2\pi f_n t + \phi) \qquad (242)$$

where y_{max} = maximum amplitude of motion in the spring and ϕ is a given phase angle. From this solution, for small damping, the maximum variable stress obtained is

$$\tau_v = \tau_{st} \frac{2\pi f_n}{b} \qquad (243)$$

In this the stress τ_{st} is the static stress induced by compressing the spring by an amount c_n. This equation indicates that

[10] See reference of Footnote 4.

the variable stress τ_v, *Fig.* 118 is inversely proportional to the damping factor b and directly proportional to the frequency f_n and the stress τ_{st}. The latter, in turn, is proportional to the amplitude c_n of the particular harmonic in resonance.

Tests have shown that the damping factor b in actual springs may be low enough that a magnification of 100 to 300 times occurs, i.e., τ_v may be around 100 to 300 times τ_{st}. It has also been found[10] that the damping factor b varies with the amount of

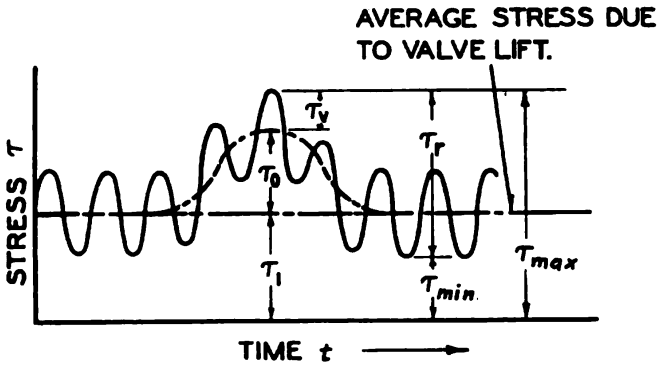

Fig. 118—Superposition of vibration stresses on stresses due to direct compression for valve spring

initial compression of the spring and that it increases with the amplitude c_n of the harmonic in resonance. This is reasonable since at low amplitudes the internal damping of the spring material due to hysteresis will be lower. Also for extremely high initial compressions, higher values of b are found, resulting from damping caused by impact between turns. At medium initial compressions, values of the damping factor are lower while, at very low compressions, these values again rise because of damping due to clashing and lifting of the end turns from the supports.

Values of b varying from about 1 sec^{-1} at lower amplitudes of vibration to 10 sec^{-1} at the higher amplitudes have been obtained in tests[10], most values being between 2 and 4.

As an example of the use of Equation 243 assuming that the lowest natural frequency f_n of the spring is equal to 200 cycles per second and that the camshaft speed is 1200 revolutions per minute, this means that resonance between this natural

frequency of the spring and the tenth harmonic of the valve lift curve may occur. Assuming also that tests on springs under similar conditions have shown a damping factor $b=5$ sec^{-1}, Equation 243 shows

$$\tau_v = \frac{2\pi \times 200 \tau_{st}}{5} = 251 \tau_{st}$$

If τ_o is the stress due to compression of the spring by an amount equal to the valve lift, and if the alternating stress due to the tenth harmonic of the lift curve is, for example, $.002\tau_o$ (as found

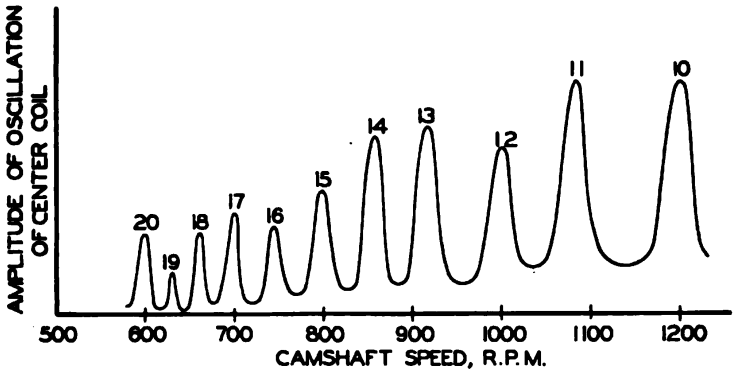

Fig. 119—Typical shape of resonance curve for valve spring. Order of harmonic noted at each resonance peak

from harmonic analysis), the alternating stress due to resonance with this harmonic will be $251 \times .002\ \tau_{st}$ or about $.5\tau_o$. This means that, in this case, the stress range will be increased to 2 times its value with no vibration.

From *Fig.* 118 the total stress range in the spring is

$$\tau_r = \tau_o + 2\tau_v \quad \ldots\ldots (214)$$

If τ_1 is the stress due to initial compression of the spring with the valve in the closed position, the range in stress will be from a minimum value $\tau_{min} = \tau_1 - \tau_v$ to a maximum value $\tau_{max} = \tau_1 + \tau_o + \tau_v$. By comparison with endurance diagrams such as those shown in Chapter IV the relative margin of safety of the spring against fatigue failure may be estimated.

A typical resonance curve similar to those obtained by actual

tests on valve springs is shown in *Fig.* 119. In this curve the amplitude of oscillation of the middle coil of a valve spring is plotted against camshaft speed. It is seen that this curve consists of various peaks spaced at intervals, each peak being due to a definite harmonic in the valve lift curve (indicated by the number shown). Thus the peak marked 10 is due to the tenth harmonic of the valve lift curve, i.e., to a vibration frequency of $10 \times 20 = 200$ cycles per second for a camshaft speed of 1200 revolutions per minute. The amplitudes of these peaks vary since the amplitudes (values of the c's of Equation 218) of the various harmonics are different.

DESIGN EXPEDIENTS

In the design of springs subject to rapid reciprocating motion, such as valve springs, the following expedients are often helpful:

1. Use of spring with a high natural frequency
2. Change in pitch of coils near end of spring
3. Avoidance, where possible of resonance between natural frequency of the spring and an exciting frequency
4. Change in shape of cam so as to reduce the magnitude of the harmonics of the valve lift curve within certain speed ranges of practical importance.

By using the methods given, in conjunction with test results, estimates of stress ranges in actual springs under vibration conditions can be made and in this way the margin of safety against fatigue failure determined.

CHAPTER XIV

INITIALLY CONED DISK (BELLEVILLE) SPRINGS

Where space is limited in the direction of load application, the use of initially coned disk springs is frequently of advantage. Such springs, which are also known as Belleville springs, consist essentially of circular disks of constant thickness and have an initial dish, *Fig.* 120. By a suitable variation of the ratio h/t between initial cone height and disk thickness, it is possible to obtain load-deflection curves having a wide variety of shapes as indicated by the curves of *Fig.* 121. For example, referring to this figure, a load-deflection characteristic for a ratio $h/t=2.75$ has the shape represented by Curve *A*. Such a shape may be desirable when a snap-acting device is being designed. By reducing the ratio h/t to 1.5 a load-deflection curve similar to Curve *B* is obtained. This type of spring, known as the "constant load" type shows a considerable range of deflection within which the load is practically constant. Such a characteristic is highly desirable in many applications, such as for example,

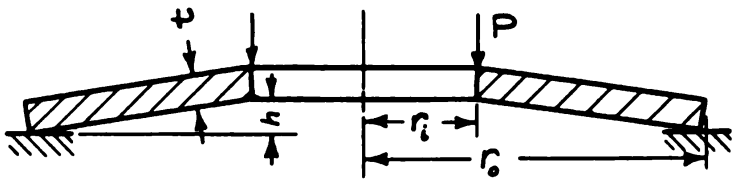

Fig.120—Initially-coned disk (Belleville) spring

where a constant load applied to a gasket is necessary. By varying h/t a variety of intermediate shapes, *Fig.* 122, is possible.

A typical example of the application of such springs is the spring washer used in copper oxide rectifiers to provide a constant pressure for holding a stack of rectifier disks together. Other applications include springs for producing gasket pressure in special types of capacitors and in condenser bushings for electrical equipment. In such cases, springs with the characteristic shown by Curve *B Fig.* 121 have been found advantage-

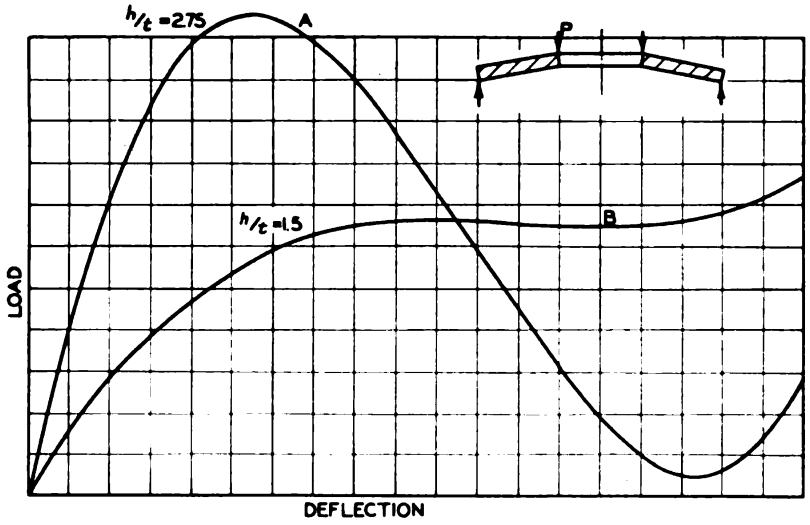

Fig. 121—Two types of load-deflection curves that are obtainable by using initially-coned disk springs

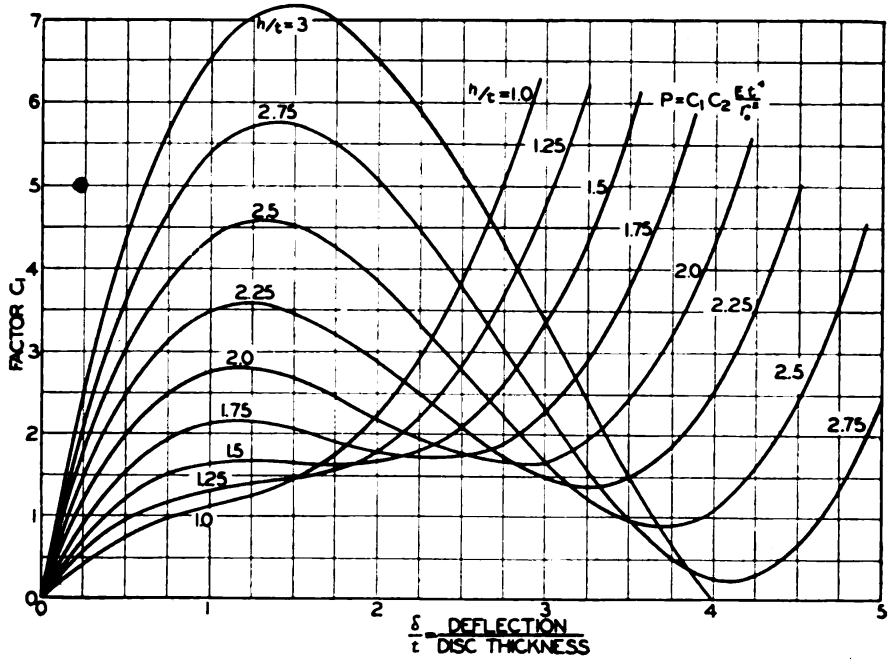

Fig. 122—Curves for finding deflection factor C_1 for initially-coned disk springs. Load-deflection characteristic curves will be similar

ous since such springs will supply approximately constant gasket pressure for a considerable variation of deflection due to temperature change or to other causes. Such deflection changes may be produced for example by temperature changes as a con-

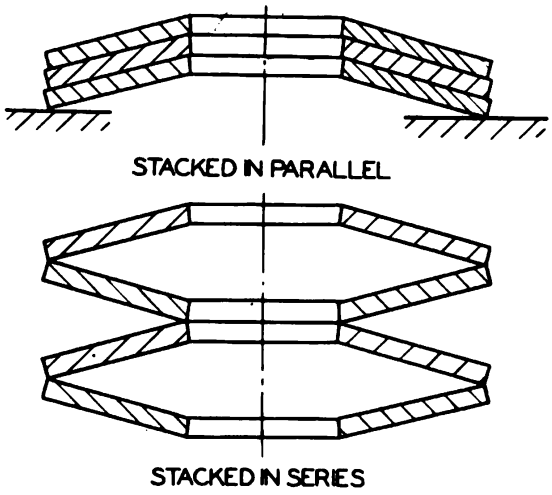

Fig. 123—Methods of stacking initially-coned disk springs

sequence of the difference in expansion coefficients between the porcelain insulation and the copper parts of electrical equipment of this type.

Initially-coned disk springs may be stacked in series or in parallel as shown in *Fig.* 123. By stacking the springs in parallel a higher load is obtained for a given deflection; stacking the springs in series means a larger deflection at the given load. However, if springs are stacked in series, ratios of h/t between cone height and thickness greater than about 1.3 should not ordinarily be used since instability or snap action is apt to occur, and an irregular load-deflection characteristic will then result.

THEORY

The application of the mathematical theory of elasticity to the calculation of initially coned disk springs is extremely complicated[1]. However, a practical solution of the problem may be obtained by making the assumption that during deflection,

[1]See for example, *Theory of Plates and Shells*—S. Timoshenko, McGraw Hill, 1940, Page 475.

radial cross sections of the disks rotate without distortion as shown by the dotted outline in *Fig.* 124*c*. If the ratio r_o/r_i between outer radius and inner radius is not too large, tests show that such an assumption will yield sufficiently accurate results for practical computation, at least as far as deflections are concerned. In addition, calculations on flat circular plates with

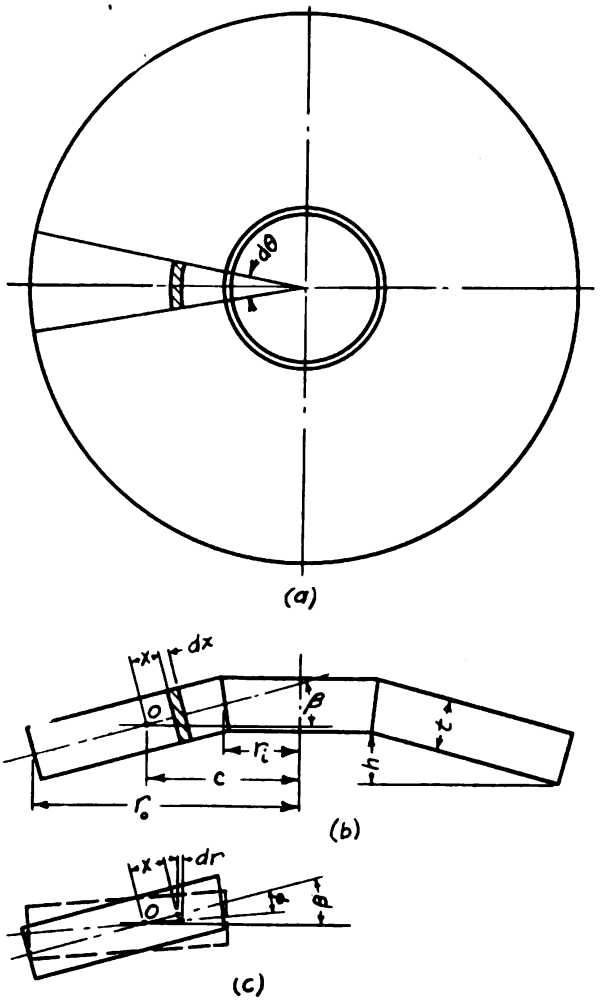

Fig. 124—Initially-coned disk spring dimensions

central holes have also been made on the basis of this assumption, i.e., that radial cross-sections rotate without distortion, and these have yielded good results when compared with those

of the elastic flat-plate theory[2]. For example, comparison between the exact and approximate solutions[3] shows that where the ratio r_o/r_i between outer and inner radii is not over 3 (which includes most practical cases) the error in deflection made by using this method is not over about 5 per cent, while the error in stress is under 9 per cent.

The solution for the initially coned disk spring which follows is based on the assumption of rotation of radial cross sections without distortion and is due to Almen and Laszlo[4]. These investigators also show some deflection tests which indicate that the assumption is satisfactory for practical use.

Considering a section of an initially coned disk spring cut out by two radial planes subtending a small angle $d\theta$, *Fig.* 124*a*, under the action of the external load, a radial cross section rotates about point O as indicated by the dashed outline of *Fig.* 124*c*. Considering an elementary strip of length dx at a distance x from O, the deformation under these assumptions consists essentially of a radial displacement dr and a rotation ϕ, the latter being the total rotation of the cross section about point O during deflection. The displacement dr causes a uniform tangential strain in the element dx (the small differences in radial distance from the axis of the spring between the upper and lower portions of the element dx are here neglected). The rotation ϕ produces a tangential bending strain which is zero at the neutral surface and a maximum at the upper and lower surfaces of the spring. The stresses due to the movements dr and the angle ϕ produce moments about point O which resist the external moment.

The stress due to the radial displacement dr may be calculated as follows: The mean circumferential length of the element dx before deflection is

$$l_1 = (c - x \cos \beta)d\theta$$

where β is the initial dish angle. After deflection this length becomes

---

[2]The exact solution is described in Chapter XV.

[3]A. M. Wahl and G. Lobo, Jr.—"Stresses and Deflections in Flat Circular Plates with Central Holes", *Transactions* A.S.M.E., 1930, A.P.M. 52-3. Also S. Timoshenko—*Strength of Materials*, Van Nostrand, Part 2, 1941, Page 179.

[4]"The Uniform Section Disk Spring", *Transactions* A.S.M.E., 1936, Page 305. A similar solution for radially tapered springs is given by W. A. Brecht and the writer "The Radially Tapered Disc Spring", *Transactions* A.S.M.E., 1930, A.P.M. 52-4.

$$l_2=[c-x\ cos(\beta-\phi)]d\theta$$

The change in length is

$$l_1-l_2=d\theta[x\ cos(\beta-\phi)-cos\ \beta]$$

or

$$l_1-l_2=d\theta[x\ sin\ \beta\ sin\ \phi-x\ cos\ \beta(1-cos\ \phi)] \quad (245)$$

It will be further assumed that the angles β and ϕ are small (as is the case in practical springs) so that

$$cos\ \beta\approx 1;\ sin\ \beta\approx\beta;\ sin\ \phi\approx\phi;\ 1-cos\ \phi\approx\frac{\phi^2}{2}$$

The last expression for 1—*cos* ϕ is obtained by using the cosine series and neglecting terms above the second degree.

Using these in Equation 245,

$$l_1-l_2=d\theta x\phi\left(\beta-\frac{\phi}{2}\right) \quad (246)$$

The unit elongation in the tangential direction will be, using Equation 246,

$$\epsilon_1=\frac{l_1-l_2}{l_1}=\frac{x\phi\left(\beta-\frac{\phi}{2}\right)}{c-x} \quad (247)$$

Neglecting the effect of the radial stresses which are assumed to be small, the stress is obtained by multiplying this by $E/(1-\mu^2)$ where E=modulus of elasticity and μ=Poisson's ratio. Thus the stress due only to the radial motion dr becomes

$$\sigma_1'=\frac{\epsilon_1 E}{1-\nu^2}=\frac{-Ex\phi\left(\beta-\frac{\phi}{2}\right)}{(1-\mu^2)(c-x)} \quad (248)$$

where the negative sign signifies compression. The factor 1—μ^2 is used because lateral contraction or expansion of elements of the strip are prevented; this expression may also be obtained from the known formula for calculating stresses from strains in two-dimensional states of stress[5].

[5]See, for example, Timoshenko—*Strength of Materials*, 1941, Part 1, Page 52.

The moment about point O due to the tangential stresses acting on the element dx will be

$$dM' = \sigma_1' t dx d\theta x \sin(\beta - \phi)$$

or taking $\sin(\beta - \phi) \approx \beta - \phi$ for small angles and using Equation 248:

$$dM' = \frac{Et d\theta \phi (\beta - \phi)\left(\beta - \frac{\phi}{2}\right) x^2 dx}{(1-\mu^2)(c-x)}$$

Integrating this from $x = c - r_o$ to $x = c - r_i$,

$$M_1' = \frac{Et d\theta \phi (\beta - \phi)\left(\beta - \frac{\phi}{2}\right)}{1-\mu^2}\left[\frac{r_o^2 - r_i^2}{2} - 2c(r_o - r_i) + c^2 \log_e \frac{r_o}{r_i}\right] \quad (249)$$

To calculate the tangential stress due to the bending strain set up by the rotation ϕ of the element dx, *Fig.* 124*b*, it is necessary to multiply the change in curvature in the tangential direction by the plate rigidity[6] which is

$$D = \frac{Et^3}{12(1-\mu^2)} \quad \ldots\ldots (250)$$

This corresponds to flexural rigidity in the case of beams. Letting κ_2 be the change in curvature of the element during deflection, then the bending moment acting on element dx due to this change in curvature will be

$$dM_2 = D\kappa_2 dx = \frac{Et^3}{12(1-\mu^2)} \kappa_2 dx \quad \ldots\ldots (251)$$

The initial tangential curvature of the element in the unloaded disk is approximately $\sin \beta/(c-x)$ while the curvature in the deflected position is $\sin(\beta - \phi)/c - x$. The change in curvature is then

$$\kappa_2 = \frac{\sin \beta - \sin(\beta - \phi)}{c-x} \approx \frac{\phi}{c-x}$$

Using this in Equation 251,

[6] Timoshenko, loc. cit., Part II, Page 120, gives a further discussion of plate rigidity.

$$dM_2 = \frac{Et^3\phi dx}{12(1-\mu^2)(c-x)} \quad \ldots\ldots (252)$$

The tangential stress σ_1'' at the surface will be this value dM_2 divided by the section modulus of the element dx which is $t^2dx/6$. Hence using Equation 252,

$$\sigma_1''_{max} = \frac{6dM_2}{t^3dx} = \frac{E\phi t}{2(1-\mu^2)(c-x)} \quad \ldots\ldots (253)$$

At a distance y from the neutral axis (taken positive in an upward direction) this stress will be

$$\sigma_1'' = \frac{-E\phi y}{(1-\mu^2)(c-x)} \quad \ldots\ldots (254)$$

where the negative sign is used to signify compression.

The component of the moment dM_2 which acts in a radial direction will be, using Equation 252,

$$dM_1'' = 2dM_2\frac{d\theta}{2} = \frac{Et^3\phi d\theta dx}{12(1-\mu^2)(c-x)}$$

Integrating this from $x=c-r_o$ to $x=c-r_i$, the moment M_1'' due only to the angular motion of the elements of the section becomes

$$M_1'' = \frac{Et^3\phi d\theta}{12(1-\mu^2)}\int_{c-r_o}^{c-r_i}\frac{dx}{c-x} = \frac{Et^3\phi d\theta \log(r_o/r_i)}{12(1-\mu^2)} \quad \ldots\ldots (255)$$

The total moment about point O thus becomes, using Equations 249 and 255,

$$M_1 = M_1' + M_1''$$

or

$$M_1 = \frac{E\phi d\theta}{1-\mu^2}\left\{\left[\frac{1}{2}(r_o^2-r_i^2) - 2c(r_o-r_i) + c^2\log_e\frac{r_o}{r_i}\right]\times\right.$$

$$\left.(\beta-\phi)\left(\beta-\frac{\phi}{2}\right)t + \frac{t^3}{12}\log_e\frac{r_o}{r_i}\right\} \quad \ldots\ldots (256)$$

The radial distance c from point O to the axis of the disk is

found from the condition that the sum of all forces over the cross section must be zero, because there is no net external force acting in the plane of the disk. Since the bending stresses σ_1'' have no force resultant, only the stress σ_1' due to the radial displacements need be considered. Thus

$$\int_{c-r_o}^{c-r_i} \sigma_1' t dx = 0$$

or using Equation 248

$$\int_{c-r_o}^{c-r_i} \frac{x dx}{c-x} = 0$$

Integrating this and solving for c

$$c = \frac{r_o - r_i}{\log_e \frac{r_o}{r_i}} \qquad \text{.....(257)}$$

Substituting Equation 257 in Equation 256,

$$M_1 = \frac{E\phi d\theta}{1-\mu^2} \left\{ \left[\frac{r_o^2 - r_i^2}{2} - \frac{2(r_o - r_i)^2}{\log_e \frac{r_o}{r_i}} + \frac{(r_o - r_i)^2}{\log_e \frac{r_o}{r_i}} \right] \times \right.$$

$$\left. (\beta - \phi)\left(\beta - \frac{\phi}{2}\right) t + \frac{t^3}{12} \log_e \frac{r_o}{r_i} \right\} \qquad \text{.....(258)}$$

This moment must be equal to the external moment on the sector $d\theta$ (*Fig.* 124*a*) which is

$$M_1 = \frac{P(r_o - r_i) d\theta}{2\pi}$$

Solving for P,

$$P = \frac{2\pi M_1}{(r_o - r_i) d\theta} \qquad \text{.....(259)}$$

Taking

$$\beta \approx \frac{h}{r_o - r_i} \; ; \; \phi = \frac{\delta}{r_o - r_i} \; ; \text{ and } \frac{r_o}{r_i} = \alpha$$

δ being the total deflection of the spring and using Equation 258 in Equation 259,

$$P=\frac{E\delta}{(1-\mu^2)r_o^2}\left[C_2(h-\delta)\left(h-\frac{\delta}{2}\right)t+C_2''t^3\right] \quad \text{.....(260)}$$

where

$$C_2=\left(\frac{\alpha+1}{\alpha-1}-\frac{2}{\log_e\alpha}\right)\pi\left(\frac{\alpha}{\alpha-1}\right)^2 \quad \text{.....(261)}$$

$$C_2''=\frac{\pi}{6}\log_e\alpha\left(\frac{\alpha}{\alpha-1}\right)^2 \quad \text{.....(262)}$$

A calculation shows that $C_2=C_2''$ for practical purposes. Hence the load becomes

$$P=\frac{E\delta C_2}{(1-\mu^2)r_o^2}\left[(h-\delta)\left(h-\frac{\delta}{2}\right)t+t^3\right] \quad \text{.....(263)}$$

Values of C_2 are plotted as functions of the ratio $\alpha=r_o/r_i$ in *Fig.* 125. From Equation 263 it may be seen that the load P is nonlinear function of the deflection δ. By using this equation, load-deflection characteristics may be determined for various values of h and t, *Fig.* 122. The application of Equation 263

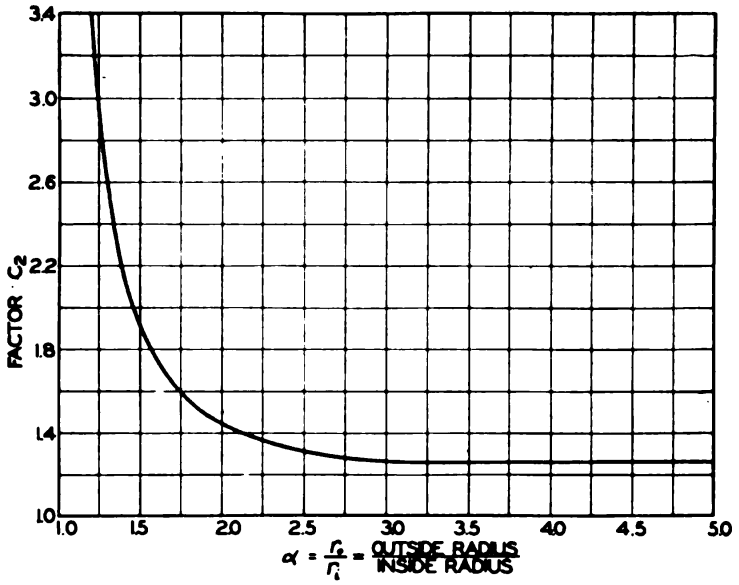

Fig. 125—Curve for determining factor C_2

in practical calculations is facilitated by the method described on Page 249.

The resultant tangential stress at a point at a distance x from O will be the sum of the stresses σ_1' and σ_1''. Hence, using Equations 248 and 254

$$\sigma=\sigma_1'+\sigma_1''=\frac{E\phi}{(1-\mu^2)(c-x)}\left[x\left(\beta-\frac{\phi}{2}\right)+y\right] \quad \ldots\ldots\ldots\ldots\ldots\ldots (264)$$

The maximum stress σ_1 at the upper surface of the spring will occur when $x=c-r_i$ and $y=t/2$. Taking these values together with $\beta=h/(r_o-r_i)$, $\phi=\delta/(r_o-r_i)$ and substituting the value of c given by Equation 257 in Equation 264 this maximum stress σ_1 becomes

$$\sigma_1=-\frac{E\delta C_2}{(1-\mu^2)r_o^2}\left[C_1'\left(h-\frac{\delta}{2}\right)+C_2't\right] \quad \ldots\ldots\ldots\ldots\ldots\ldots\ldots\ldots (265)$$

where

$$C_1'=\left(\frac{\alpha-1}{\log_e\alpha}-1\right)\frac{6}{\pi\log_e\alpha} \quad \ldots\ldots\ldots\ldots\ldots\ldots\ldots\ldots\ldots\ldots (266)$$

$$C_2'=\frac{3(\alpha-1)}{\pi\log_e\alpha} \quad \ldots\ldots\ldots\ldots\ldots\ldots\ldots\ldots\ldots\ldots\ldots\ldots\ldots (267)$$

The stress σ_2 at the lower inner edge of the spring is obtained by taking $y=-t/2$ in Equation 264. This yields

$$\sigma_2=-\frac{E\delta C_2}{(1-\mu^2)r_o^2}\left[C_1'\left(h-\frac{\delta}{2}\right)-C_2't\right] \quad \ldots\ldots\ldots\ldots\ldots\ldots\ldots\ldots (268)$$

In these equations a negative value signifies compression, a positive value tension.

PRACTICAL DESIGN

To simplify the application of Equations 263 and 264 in the practical design of initially coned disk springs the following procedure may be used. For determining the load-deflection characteristic of the spring, Equation 263 may be written:

$$P = C_1 C_2 \frac{Et^4}{r_o^2} \quad \text{.....(269)}$$

where

$$C_1 = \frac{\delta}{(1-\mu^2)t}\left[\left(\frac{h}{t}-\frac{\delta}{t}\right)\left(\frac{h}{t}-\frac{\delta}{2t}\right)+1\right] \quad \text{.....(270)}$$

The factor C_1 thus depends on the ratios h/t and δ/t while the term C_2 depends on $\alpha = r_o/r_i$ only and may be taken from the curve of *Fig.* 125 or from Equation 261.

To facilitate practical computations, values of C_1 have been plotted as functions of δ/t for various values of h/t in *Figs.* 122

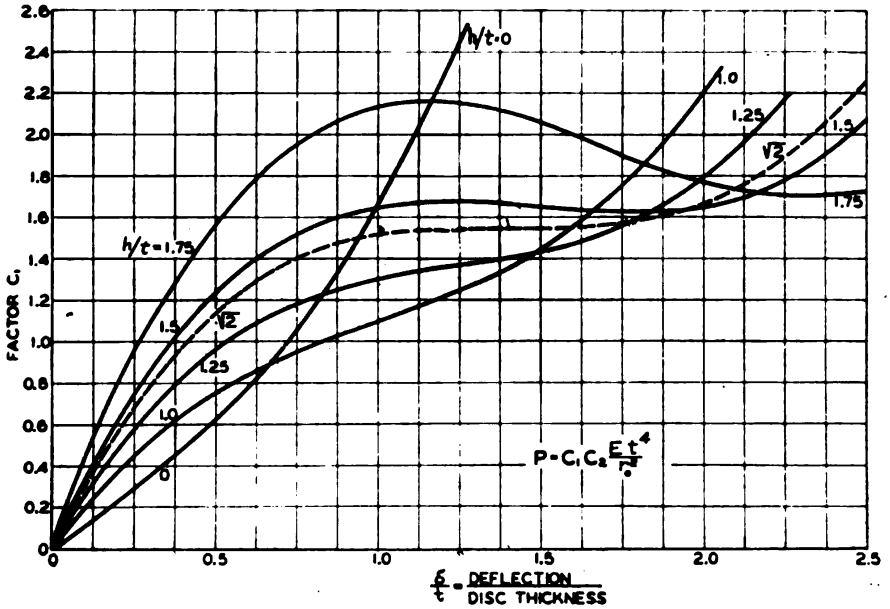

Fig. 126—Curves for deflection factor C_1 for Belleville springs
h/t = ratio initial cone height: thickness

and 126. The curve of *Fig.* 126 may be used to obtain greater accuracy for the smaller values of h/t.

It should be noted that the curves of *Figs.* 122 and 126 also represent load-deflection characteristics for springs having various ratios h/t between initial cone height and thickness. This is true since the load is directly proportional to the constant C_1. Since these curves are independent of the ratio r_o/r_i (and hence

of C_2) it follows that the shape of the load-deflection characteristic can be changed materially only by altering the ratio h/t between initial cone height and disk thickness. At $h/t=1.414$, shown dotted in *Fig.* 126, the curve has a horizontal tangent

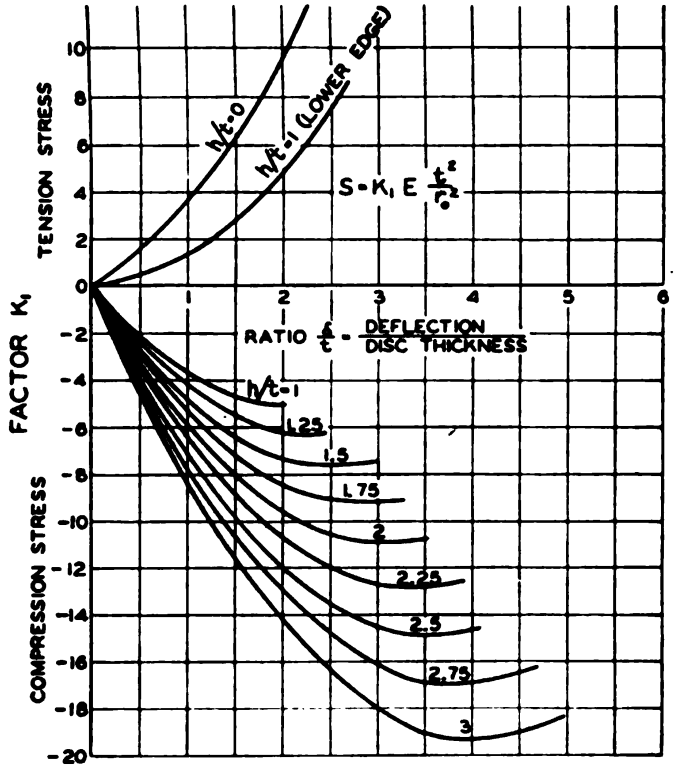

Fig. 127—Curves for determining stress factor K_1 for Belleville springs, $\alpha = r_o/r_i = 1.5$

and for a considerable range the spring rate is very low. For $h/t=1.5$ there is an even greater range of low spring rate but in this case the load drops slightly after reaching a maximum. When h/t reaches a value of about 2.8 the load drops below zero at the larger deflections, so that permanent buckling of the spring may occur. Interpolation for intermediate values of h/t may be used with sufficient accuracy for most practical purposes.

To facilitate the calculation of stress σ, Equations 265 and 268 may be written as follows

$$\sigma = K_1 \frac{Et^2}{r_o^2} \qquad (271)$$

where K_1 has the following value:

$$K_1 = \frac{-C_2\delta}{(1-\mu^2)t}\left[C_1'\left(\frac{h}{t} - \frac{\delta}{2t}\right) \pm C_2'\right] \quad \ldots\ldots\ldots\ldots\ldots\ldots\ldots\ldots (272)$$

If the positive sign is used before the constant C_2' the stress in the upper inner edge of the spring is obtained, while using the negative sign yields the stress at the lower inner edge. It is thus seen that the stress is a function of r_o/r_i, δ/t and h/t.

As an aid in practical computations, values of K_1 have been plotted as functions of the ratio δ/t for various values of h/t in *Figs.* 127 and 128. For ratios $\alpha = r_o/r_i$ equal to 1.5, the curves of *Fig.* 127 apply, a positive value of K_1 representing tension

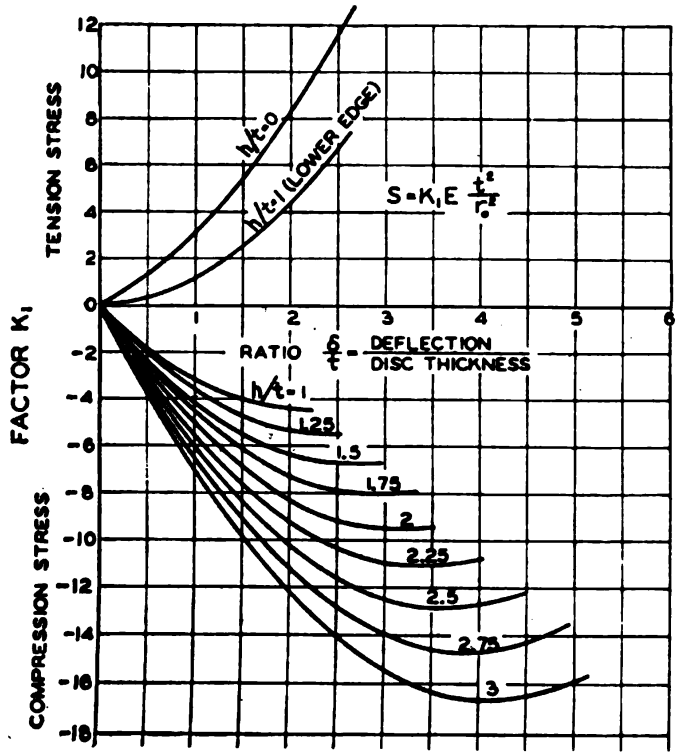

Fig. 128—Curves for determining stress factor K_1 for Belleville springs, $\alpha = r_o/r_i = 2$ to 2.5

stress, a negative value representing compression. It was found that within the range shown by the curves, for values of h/t between 1 and 3 the maximum stress will be compression at the

upper inner edge where $\delta<2h$. For deflection δ equal to $2h$, the tension in the lower inner edge equals the compression in the upper and for $\delta>2h$, the tension in the lower edge becomes the maximum stress. This is shown by the upper curve for $h/t=1$, i.e., when $\delta/t=2$ or $h=2t$ then the compression and tension stresses at the two edges become equal, and for $\delta/t>2$ the upper curve yields higher values. For most practical cases where h/t is between 1 and 3 the maximum stresses will be obtained by using the lower groups of curves. Interpolation may be used for intermediate values of h/t. In doubtful cases where $\delta>2h$, the stress should be checked by using Equation 271. A further discussion of the evaluation of stress in these springs is given on Page 259. *Fig.* 129 shows distribution of stress in a typical case.

Illustrative Examples—EXAMPLE 1: To illustrate the use of the curves of *Figs.* 126 to 128 in practical design a spring is to be designed for the following conditions: The spring is to be used in a gasket application where the load is to be held approximately constant at 6000 pounds so that the type of load-deflection curve desired is that for $h/t=1.5$, *Fig.* 121. The space available will permit using an 8½-inch outside diameter spring. The deflection of the spring may vary between ⅛ and ¼-inch at the design load and the maximum compression stress calculated by Equation 271 is to be limited to 200,000 pounds per square inch. This value has been found by experience to be safe provided the load is static or repeated but a few times[7].

Taking $r_o=4¼$ inches, $r_i=2⅛$ inches, $\alpha=r_o/r_i=2$, from Equation 271, $\sigma=K_1Et^2/r_o^2$ where $K_1=-6.7$ from *Fig.* 128 for $h/t=1.5$, this being the maximum value. Solving this for t and taking $\sigma=200{,}000$ pounds per square inch compression,

$$t=r_o\sqrt{\frac{\sigma}{K_1E}}=4.25\sqrt{\frac{200000}{6.7\times30\times10^6}}=.134\text{-in.}$$

From *Fig.* 126 for $h/t=1.5$, $C_1=1.68$ on the flat part of the curve and from *Fig.* 125 for $\alpha=2$, $C_2=1.45$. From Equation 269 the load per disk will be

$$P=C_1C_2\frac{Et^4}{r_o^2}=1300 \text{ lb.}$$

[7]For a further discussion of working stress see Page 259.

Since 6000 pounds is desired, it will be necessary to use 5 springs in parallel which will give approximately the right load. From *Fig.* 126 it is seen that for $h/t=1.5$, C_1 is approximately constant from $\delta/t=.75$ to $\delta/t=2.1$. Since $t=.134$ this means the load will be approximately constant from $\delta=.75(.134)=.1$-inch to $\delta=.28$-inch which is about what is required. If the maximum deflection is ¼-inch, the maximum value of δ/t will be .25/.134 or about 2. From *Fig.* 128 for $\delta/t=2$ the factor K_1 will be about —6.4 instead of —6.7 which means that the calculated maximum stress will be slightly less than 200,000 pounds per square inch. To reduce the calculated load from 6500 to 6000 pounds the thickness of the disk may be reduced about 2 per cent.

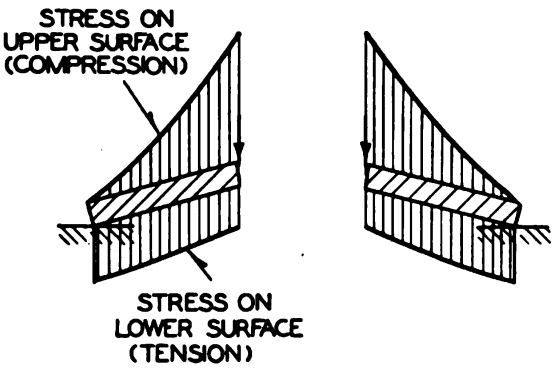

Fig. 129 — Approximate distribution of stress along radius for constant-load type of disk spring

EXAMPLE 2: A curve such as that shown in *Fig.* 122 for $h/t=2.5$ is desired for a snap action device to operate in such a way that, when the load reaches a certain point represented by the peak on the curve, the system becomes unstable and a large deflection occurs with resulting snap-action. Also, a maximum load of about 520 pounds is desired, space is available for an 8-inch diameter disk, and a stop is provided so that the spring may deflect ¼-inch before coming against the stop. It is desired at ¼-inch deflection when the spring is against the stop it will be represented by the point on the curve of *Fig.* 126 for $h/t=2.5$ corresponding to $\delta/t=3$. Since at maximum deflection $\delta=$¼-inch this means that $t=.25/3=.0833$-inch and $h=2.5\times.0833=.208$-inch. Assuming $\alpha=2$, from *Fig.* 128, $K_1=-12.5$ for $\delta/t=3$, $h/t=2.5$. From Equation 271 on Page 250, solving for r_o obtains the following relation:

$$r_o = t\sqrt{\frac{K_1 E}{\sigma}}$$

Taking $\sigma = -180{,}000$ pounds per square inch (compression), $t = .0833$-inch and solving, $r_o = 3.8$-inch say 3¾ inches. From *Fig.* 125 for $\alpha = 2$, $C_2 = 1.45$ and from *Fig.* 122 the maximum value of C_1 (corresponding to maximum load) for $h/t = 2.5$ is 4.6. From Equation 269 the peak load is

$$P_{max} = C_1 C_2 \frac{Et^4}{r_o^2} = 675 \text{ lb.}$$

This load is too high since 520 pounds were desired. To get a lower peak load, since the latter from Equation 269 increases as t^4 (other things being equal) the thickness may be reduced in the ratio $(520/675)^{1/4} = .935$. Thus $t = .0833 \times .935 = .078$-inch. For the same shape of curve h/t must be kept the same (or 2.5) so that $h = 2.5 \times .078 = .195$-inch. At ¼-inch deflection δ/t will be $.25/.078 = 3.2$ which will be somewhat beyond the point on the curve for $\delta/t = 3$, which in this case is permissible. Also the maximum stress will not be changed appreciably since from *Fig.* 128 for $h/t = 2.5$ and $\delta/t = 3.2$, the factor K_1 is practically the same as for $\delta/t = 3$. From *Fig.* 122 for $\delta/t = 3.2$, $h/t = 2.5$, $C_1 = 1.3$. Since $C_1 = 4.6$ at the peak load, the load when the spring is against the stop will be reduced to $1.3/4.6 \times 520 = 147$ pounds.

SIMPLIFIED DESIGN FOR CONSTANT-LOAD

Where the ratio $h/t = 1.5$, a load-deflection characteristic of the "constant-load" type is obtained as indicated by Curve *B* of *Fig.* 121 and the curve for $h/t = 1.5$ of *Fig.* 126 such that the load is constant within ±5 per cent from a deflection $\delta = .8t$ to $\delta = 2.25t$. Such springs, which are of particular value in many practical applications, may be designed in a simple manner[5] provided the maximum allowable stress is given. Letting D be the outside diameter of the spring, then the constant load P and the required thickness t to obtain this load are given by

$$P = CD^2 \quad \text{.....(273)}$$

[5]This method was suggested by R. C. Bergvall of the Westinghouse Company.

and, for the thickness,

$$t=\frac{D}{K} \qquad (274)$$

where the constants C and K depend on the maximum allowable stress and on the ratio D/d or (r_o/r_i) between outer and inner diameters. Values of these constants may be taken from the

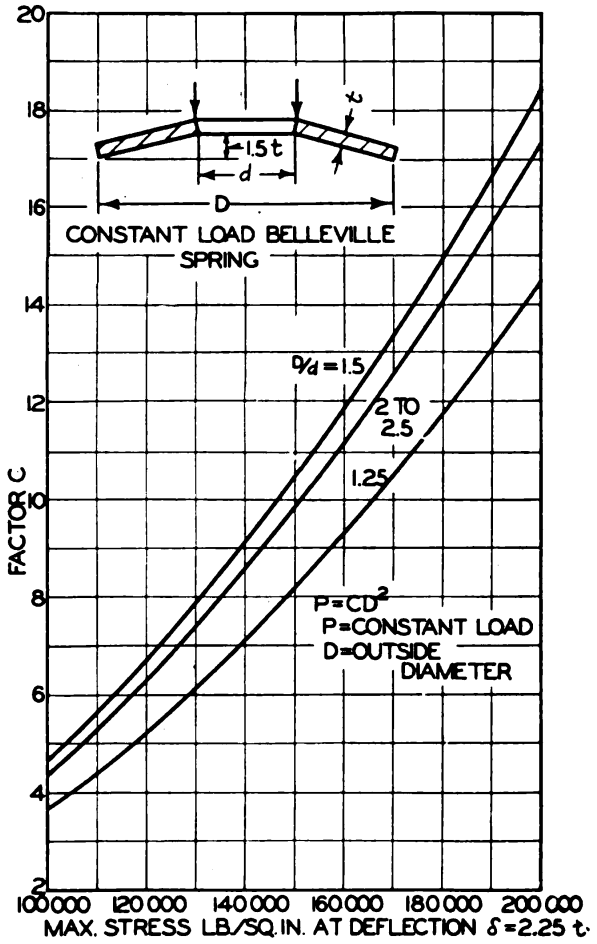

Fig. 130 — Curves for finding load P in constant-load Belleville springs. These curves apply only if the thickness t is chosen in accordance with *Fig.* 131 and if E is 30×10^6 pounds per square inch

curves of *Figs.* 130 and 131. It should be noted that the thickness t must always be held to the value given by Equation 274 to obtain the constant-load characteristic. In all cases the maximum deflection was assumed as 2.25 times the thickness.

In TABLE XXVI values of constant load P, thickness t, and maximum deflection $2.25t$ are tabulated for maximum stresses of 200,000, 150,000, and 100,000 pounds per square inch, and for ratios $\alpha = D/d$ varying from 1.25 to 2.5. It is assumed that

TABLE XXVI

Design Data—Constant Load Belleville Springs*

Maximum Stress (σ_{max}) (lb./sq. in.)	α (D/d)	Spring Thickness (t)	Maximum Deflection ($\delta = 2.25\,t$)	Constant Load (P)
200,000	1.25	D/80	D/35.5	14.5 D^2
	1.5	D/67.4	D/29.9	18.5 D^2
	2.0 to 2.5	D/63.8	D/28.3	17.4 D^2
150,000	1.25	D/92.5	D/41	8.15 D^2
	1.5	D/77.8	D/34.6	10.4 D^2
	2.0 to 2.5	D/73.7	D/32.7	9.8 D^2
100,000	1.25	D/113	D/50.2	3.62 D^2
	1.5	D/95.4	D/42.3	4.62 D^2
	2.0 to 2.5	D/90.2	D/40	4.35 D^2

* Modulus of elasticity taken as 30×10^6 lb./sq. in.

the springs are steel for which the modulus of elasticity E may be taken as 30×10^6 pounds per square inch.

The constants C and K of Equations 273 and 274 as well as the constants of TABLE XXVI may be calculated as follows: From Equation 271 it is possible to solve for the thickness t taking $r_o = D/2$:

$$t = \frac{D}{2}\sqrt{\frac{\sigma}{K_1 E}} = \frac{D}{K} \qquad \text{.....(275)}$$

where

$$K = 2\sqrt{\frac{K_1 E}{\sigma}} \qquad \text{.....(276)}$$

Taking K_1 from the curves of *Figs.* 127 and 128 or from Equation 272 for the given value of α, $E = 30 \times 10^6$ pounds per square inch and, assuming a given value of stress, the factor K may be computed.

Likewise from Equation 269, the load P is

$$P = C_1 C_2 \frac{E t^4}{r_o^2} = \frac{4 C_1 C_2 E t^4}{D^2}$$

Using $t=D/K$ from Equation 274 in this,

$$P=\frac{4C_1C_2ED^2}{K^4}=CD^2$$

where

$$C=\frac{4C_1C_2E}{K^4} \qquad \text{(277)}$$

This is the same as Equation 273.

For a given value of α and a given stress, the factor C_2 may be obtained from *Fig.* 125 while K will be found from Equation

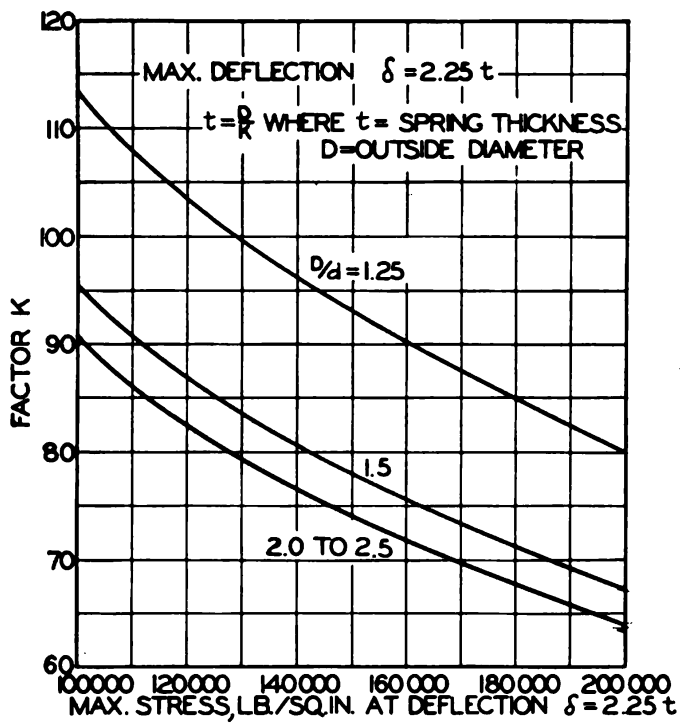

Fig. 131—Curves for determining thickness for constant-load Belleville steel springs

276. The value C_1 will be approximately that given by the flat part of the curve for $h/t=1.5$, *Fig.* 126. Using these values the constants C and K of *Figs.* 130 and 131 and the constants in TABLE XXVI were computed.

TESTS COMPARED WITH THEORY

A large number of tests have been carried out by Almen and Laszlo[4] on initially coned disk springs. These tests, made on springs of various proportions, show curves similar to those of *Fig.* 121 and indicate that the method of calculation developed is sufficiently accurate for most practical purposes. However, the final equations are not exact and, in practice, deviations in deflections as much as 10 to 15 per cent may be expected between test and calculated values. For highest accuracy in individual cases, tests should therefore be carried out.

Deflection—In *Fig.* 132, a load-deflection characteristic obtained on a stack of four disks in parallel is shown. These disks have a ratio h/t of about 1.45 and show clearly the constant-load characteristic. The initial large deflection was due to

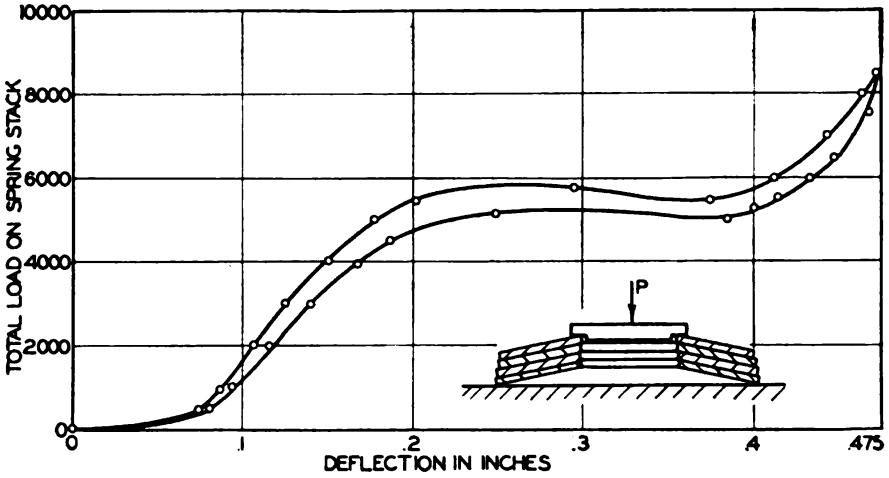

Fig. 132—Deflection test of stack of four steel Belleville springs, $r_o = 4\frac{1}{4}$. $r_i = 1\frac{3}{4}$, $h = .212$, $t = .148$

flattening out of irregularities between the disks. In spite of the fact that the surfaces of the individual springs were slightly oily, a considerable hysteresis loop between the loading and unloading curve was obtained, indicating considerable friction between the disks. By using a group of springs in parallel the load is increased approximately in proportion to the number of springs.

Stress—Although the approximate method of calculation

used appears to yield good results as far as deflections are concerned, it may be expected that deviations between test and theory will be greater for stress than for deflection. Comparison of the results as calculated by the theory were made by Laszlo[9] with the results of some tests carried out by Lehr and

TABLE XXVII

Comparison of Test and Calculated Stresses

Distance from Inner Edge (*mm*)	Measured Stress (*lb./sq. in.*)	Calculated Stress (Eq. 271) (*lb./sq. in.*)
0	70,500	69,200
1	63,900	66,700
3	56,000	62,200
7	45,900	54,500
10	41,400	49,000
20	29,200	35,300
30	22,100	25,200
40	16,450	17,450
50	11,750	11,350
60	8,450	6,400
70	5,630	2,520

Granacher[10] on relatively thick Belleville springs. The results of these strain measurements, obtained with a special extensometer on a 2 millimeter gage length, are compared with the results of the theory in TABLE XXVII.

In the case of the spring tested by these writers the deflection was not large. Such good agreement as TABLE XXVII indicates should not be expected for large deflections relative to the thickness. It may be expected, however, that even in such cases, approximate results may be obtained.

WORKING STRESSES

Static Loading—Where initially coned disk springs are subject to static loading, or to a load repeated a relatively few times during the spring life, experience shows that stresses of 200,000 to 220,000 pounds per square inch as calculated by Equation 271 may be used even though the yield point of the steel from which the spring is made is only 120,000 pounds per square inch in tension[11]. Although this stress seems extremely

[9]Discussion, *Machine Design*, May, 1939, Page 47.
[10]*Forschung*, V.D.I., 1936, Page 66.
[11]See article by Almen and Laszlo, loc. cit., Page 242.

high, it should be remembered that it is localized near the upper inner edge of the spring, *Fig.* 129. Consequently, any yielding which may occur will redistribute the stress and allow the remaining parts of the spring to take a greater share of the load. Then, too, the peak stress is compression in the usual application which also makes for a more favorable condition. Also due to presetting operations in the manufacture of the spring, residual stresses of opposite sign are induced and these reduce the maximum stress below that calculated.

Another way of evaluating working loads for static loading in the case of the constant-load type of spring is to figure the stress in the following way: Assuming that the spring is flattened out, the moment about a diameter of the vertical reaction acting on an outer half-circumference of the spring will be $(P/2)2r_o/\pi$ (since the center of gravity of a semicircle of radius r_o is at a distance $2r_o/\pi$ from the diameter). The moment of the vertical load acting on an inner half-circumference about a diameter will likewise be $(P/2)2r_i/\pi$. The net moment M acting on a diametral section of the spring will be the difference between these values. Hence

$$M=\frac{P}{\pi}(r_o-r_i) \qquad (278)$$

This moment will set up bending stresses across the diametral section. If these are figured from the ordinary beam formula, thus neglecting the stress-concentration effects of the hole in the spring, the expression for maximum stress σ becomes (taking the value of M given by Equation 278)

$$\sigma=\frac{6M}{2(r_o-r_i)t^2}=\frac{3}{\pi}\frac{P}{t^2} \qquad (279)$$

This follows since the section modulus of a diametral section is $2(r_o-r_i)t^2/6$.

EXAMPLE: As an example of the use of Equation 279: A constant-load spring has a calculated stress of 200,000 pounds per square inch figured from Equation 271 and has an outside diameter D of 2 inches. From TABLE XXVI the constant load will be 18.5 $D^2=74$ pounds for $D/d=1.5$. The thickness will be $D/67.4=2/67.4=.0297$-inches. Using $P=74$ pounds and

t=.0297-inch in Equation 279 the calculated stress (neglecting stress concentration) becomes

$$\sigma = \frac{3 \times 74}{\pi (.0297)^2} = 80{,}000 \text{ lb./sq. in.}$$

Thus it is seen that when figured in this way (i.e., stress concentration being neglected) the stress is only about 80,000 instead of the 200,000 pounds per square inch figure obtained by the more exact theory. This explains why springs designed on this basis stand up satisfactorily under static loads since the 80,000 pounds per square inch figure is well below the tension yield point for spring steels. In the case of the constant-load type of spring statically loaded, it may well be that the stress as figured from Equation 279 will yield a better picture of the ability of the spring to carry load. However, the more exact theory which takes stress concentration into account should be used where fatigue or repeated loading is involved.

Fatigue Loading—Where fatigue loading of initially-coned disk springs is involved, considerably lower stresses than those permissible for static loading may have to be used. So far, there appears to be little fatigue test data available by means of which the fatigue strength of such springs may be evaluated. A rough estimate of the fatigue strength of this type of spring may be made, however, as follows:

Assuming that the spring operates within a given range of deflection, the range of stress in the upper and lower surfaces of the spring may be found by using Equation 271. Assuming no residual stresses present in the usual case the range in the upper inner edge will be from an intermediate value to a maximum in compression, while that in the lower inner edge will be from some compression to a tension, or from an intermediate value to a maximum in tension. Residual stresses present in actual springs will modify these conditions.

In general, a range involving tension stress will be more dangerous than one involving compression stress only. However, in the usual case the calculated compression stress will be beyond the compression yield point of the material. Hence, yielding of the material will actually occur either on first loading or in the presetting operation, with the result that tension stresses will

be set up at one end of the range. In practice, therefore, it appears reasonable to use as a basis for design the maximum range of stress in the spring (which will usually be a range in compression) as figured from Equation 271. The actual stress range in the spring would then be compared with the endurance range of the material.

Since most initially coned disk springs are heat treated after forming, some decarburization of the surface material will no doubt be present. Hence the endurance range to be used for comparison should be that obtained on specimens with unmachined surfaces. As indicated in Chapter XXIII this latter value may probably be half or less of the value obtained on machined and ground specimens.

This method of evaluating the fatigue strength of Belleville springs should be considered as very rough and the final answer can only be obtained by actual fatigue tests.

CHAPTER XV

INITIALLY-FLAT DISK SPRINGS

As in the case of initially coned or Belleville springs, initially flat springs are of advantage where space is limited in the direction of load application while at the same time high loads are required. In contrast to the Belleville spring (which may be designed with a wide variety of load-deflection characteristics) the initially flat spring will have a load-deflection diagram which is linear for small deflections and concave upward for large ones. In the latter case the spring becomes stiffer as the load increases. Such springs may be made with a cross section of constant thickness as shown in *Fig.* 133 or with a radially-tapered cross-section as shown in *Fig.* 134[1]. As will be shown later the use of the latter section (where the thickness is proportional to the radius) results in a more uniform stress distribution and hence a more efficient utilization of the spring material. Such springs, either of the constant-thickness type or of the radially-tapered type may be stacked as shown in *Fig.* 135. By this means the spring flexibility may be increased without reducing the load-carrying ability. At the same time, the spring assembly is enabled to take lateral as well as vertical loads.

RADIALLY-TAPERED SPRINGS

An important application of the radially-tapered disk spring is shown in *Fig.* 136, which represents a sectional view of a commutator as used in large railway motors. The function of the disk spring in this case is to supply a constant pressure for holding the commutator bars together, while at the same time allowing sufficient flexibility so that expansions due to temperature changes may take place without producing excessive stress in the v-rings or commutator bars. For this purpose, the disk spring is well suited.

Approximate Theory—For an approximate calculation of the

[1] See paper by W. A. Brecht and the author, "The Radially Tapered Disk Spring", *Transactions* A.S.M.E., 1930 A.P.M. 52-4.

stress in radially-tapered[2] disk springs, as in the case of the approximate solutions previously discussed, it will be assumed that radial cross sections of the spring rotate during deflection

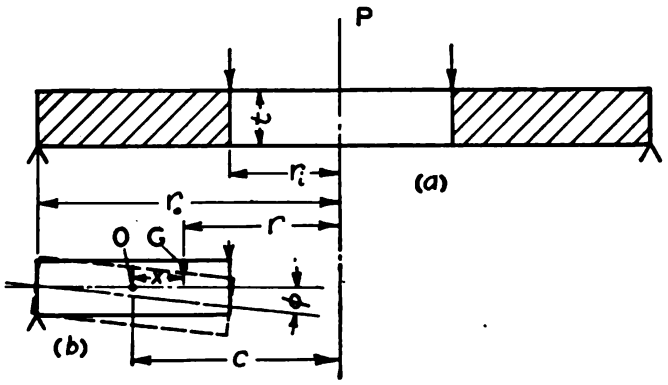

Fig. 133—Constant thickness, initially-flat disk spring

without distortion. Comparison with a more exact solution as given below indicates that this approximation is satisfactory for calculating deflections provided the ratio r_o/r_i between outer and inner radii is not over 3. For stress, the agreement between

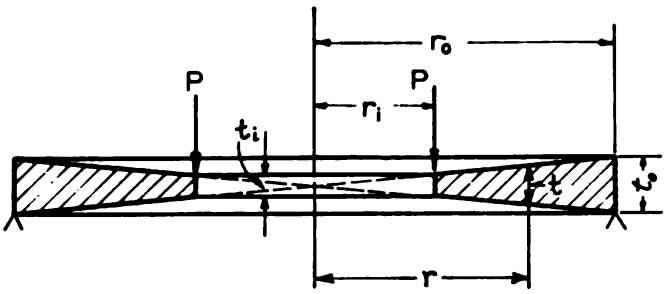

Fig. 134—Radially-tapered disk spring

exact and approximate theory is not so good where the ratio r_o/r_i exceeds 1.4. By using the approximate method, however, it is possible to calculate the nonlinear load-deflection characteristic for large deflections; this is far more complicated if the exact method is used.

To apply the approximate method, an element of a radially-

[2] In this discussion, by radially-tapered spring is meant a spring having a thickness proportional to the radius at any point.

tapered spring is assumed cut out by two neighboring radial planes subtending a small angle $d\theta$ as shown in *Fig.* 137, the complete spring being shown in *Fig.* 134. Under the load P the spring will deflect through an angle ϕ as shown by the dashed

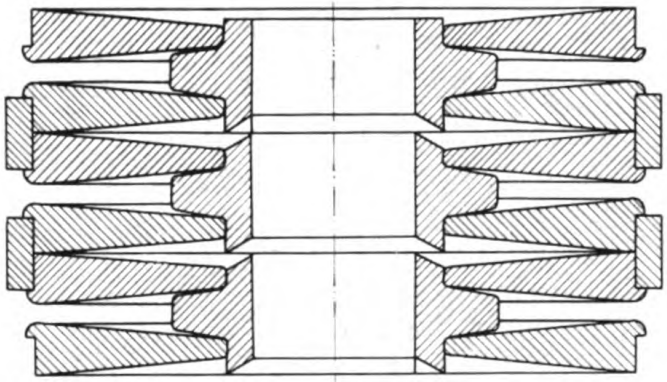

Fig. 135—Method of stacking radially-tapered disk springs

outline, *Fig.* 137*b;* the rotation is assumed to take place about some point O at a distance c from the spring axis.

Considering an element G initially at a distance x from O and at a distance y from the neutral surface (or middle plane) of the spring, the initial length of this element is

$$l_1 = (c-x)d\theta$$

After deflection through an angle ϕ the final length becomes

$$l_2 = (c - x\ cos\ \phi - y\ sin\ \phi)d\theta$$

The change in length of this element due to deflection of the spring is the difference between these expressions. Thus

$$l_1 - l_2 = d\theta[y\ sin\ \phi - x(1-cos\ \phi)]$$

Assuming that ϕ is small, sin $\phi = \phi$ and 1—cos $\phi = \phi^2/2$, approximately. Thus

$$l_1 - l_2 = d\theta\left(y\phi - \frac{x\phi^2}{2}\right)$$

The unit elongation ϵ will be this difference divided by the

initial length l_1 or

$$\epsilon=\frac{l_1-l_2}{l_1}=\frac{y\phi-\frac{x\phi^2}{2}}{c-x}$$

The stress σ will be equal to the unit elongation multiplied by the modulus of elasticity E (effects due to lateral contraction being neglected). Thus using this equation, the stress becomes

$$\sigma=\epsilon E=\frac{E\left(y\phi-\frac{x\phi^2}{2}\right)}{r} \quad \ldots\ldots (280)$$

where $r=c-x$. For a radially-tapered spring, the disk thickness is taken as $t=2kr$ where k is the thickness factor. If the

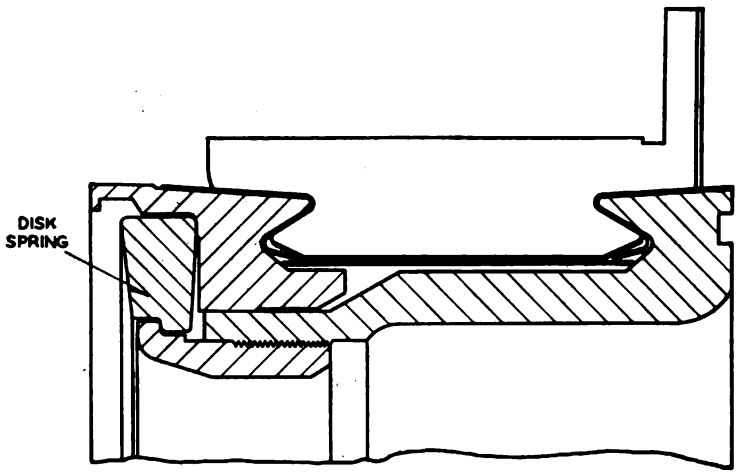

Fig. 136—Disk spring used in railway motor commutator

angle ϕ is small, i.e., if the spring deflection is small, the term $x\phi^2/2$ may be neglected and the stress will be given by $E\phi y/r$. The maximum stress σ_m will then occur when $y=t/2=kr$. Thus

$$\sigma_m=\frac{E\phi(kr)}{r}=E\phi k \quad \ldots\ldots (281)$$

Under the assumptions made, it is seen that for small deflections the maximum stress is constant along a radius for this type of spring.

The moment of the forces acting on the element G, *Fig.* 137, about an axis through O perpendicular to the paper will be

$$dM'' = \sigma y dx dy d\theta \quad \ldots\ldots (282)$$

This expression is obtained by taking the radial component of the tangential forces and multiplying by the lever arm y.

The total moment acting on the slice cut out of the disk will be the integral of these elementary forces over the cross-section, x being taken between the limits $c-r_o$ and $c-r_i$ and y being taken between the limits $-k(c-x)$ and $+k(c-x)$.

Substituting the expression for σ given by Equation 280 in Equation 282 the total moment becomes

$$M'' = d\theta \int_{c-r_o}^{c-r_i} \int_{-k(c-x)}^{k(c-x)} \frac{Ey\left(y\phi - \frac{x\phi^2}{2}\right) dy dx}{c-x} \quad \ldots\ldots (283)$$

This moment M'' must be equal to the moment due to the external load P which is

$$M'' = d\theta \frac{P(r_o - r_i)}{2\pi} \quad \ldots\ldots (284)$$

This equation simply states that the moment acting on the element subtended by two planes at an angle $d\theta$ will be $d\theta/2\pi$

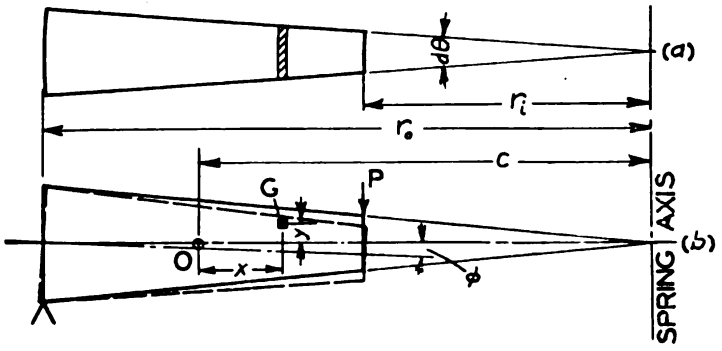

Fig. 137—Deflection of section, radially-tapered disk spring

times the total moment due to the load P which is $P(r_o - r_i)$.

Substituting the value of M'' given by Equation 283 in

Equation 284, integrating and solving for P,

$$P=\frac{4}{3}\pi E\phi k\left[\frac{\phi^2}{8}(r_o-r_i)^2+\frac{k^2}{3}(r_o^2+r_or_i+r_i^2)\right] \quad (285)$$

The maximum deflection δ is given by

$$\delta=\phi(r_o-r_i) \quad (286)$$

It will be seen that these two equations determine P as a function of δ. Solving Equation 286 for ϕ and substituting in Equation 285,

$$P=\frac{4.19Ek\delta}{(r_o-r_i)}\left[\frac{\delta^2}{8}+\frac{k^2}{3}(r_o^2+r_or_i+r_i^2)\right] \quad (287)$$

For *small deflections*, Equations 281 and 287 may be reduced to the following simple forms

$$\sigma_m=\frac{K'P}{t_b^2} \quad (288)$$

$$\delta=C'\frac{Pr_o^2}{Et_b^3} \quad (289)$$

where

$$K'=\frac{2.86}{\alpha^2+\alpha+1} \quad (290)$$

$$C'=\frac{5.73}{\alpha^2}\left(\frac{\alpha-1}{\alpha^2+\alpha+1}\right) \quad (291)$$

and $\alpha=r_o/r_i$.

For *large deflections*, Equation 287 may be written

$$P=\frac{Et_b^3\delta}{C'r_o^2}\left[1+\frac{1.5\delta^2}{t_b^2(\alpha^2+\alpha+1)}\right] \quad (292)$$

or

$$\delta=C'\frac{Pr_o^2}{Et_b^3}\left[\frac{1}{1+\frac{1.5\delta^2}{t_b^2(\alpha^2+\alpha+1)}}\right] \quad (293)$$

Since the term in the brackets is usually not greatly different from unity, a first approximation for δ will be obtained by using Equation 289. Using this value in Equation 293, a corrected value of deflection δ will be obtained. This corrected value may again be used in Equation 293 for a second approximation, if desired. This process will be found to converge rapidly. Another method of procedure is to assume a value of δ and calculate the corresponding value of P from Equation 292. By assuming several values of δ the load-deflection curve may be plotted readily.

Exact Theory—To check the accuracy of the results obtained by the approximate method developed previously, it is desirable to apply the more exact flat-plate theory to this problem. The differential equations[3] which must be satisfied at any radius r of a flat circular plate which is loaded by a load P uniformly distributed along its edges, are

$$m_1+\frac{dm_1}{dr}r-m_2+\frac{P}{2\pi}=0 \quad \ldots\ldots (294)$$

$$m_1=D\left(\frac{d\phi}{dr}+\mu\frac{\phi}{r}\right) \quad \ldots\ldots (295)$$

$$m_2=D\left(\frac{\phi}{r}+\mu\frac{d\phi}{dr}\right) \quad \ldots\ldots (296)$$

In these equations:

m_1 = Bending moment in a radial direction at radius r, inch-pounds per inch length
m_2 = Bending moment in tangential direction at radius r, inch-pounds per inch
μ = Poisson's ratio
w = Deflection of plate at radius r
ϕ = $-dw/dr$ = Slope in radial direction at radius r
D = Plate rigidity at radius r
D = k_1r^3 where $k_1=2Ek^3/3(1-\mu^2)$ for a radially-tapered disk where $t=2kr$.

Differentiating Equation 295 with respect to r gives

$$\frac{dm_1}{dr}=k_1r^3\left(\frac{d^2\phi}{dr^2}+\frac{\mu}{r}\frac{d\phi}{dr}-\frac{\mu\phi}{r^2}\right)+3k_1r^2\left(\frac{d\phi}{dr}+\mu\frac{\phi}{r}\right) \quad \ldots\ldots (297)$$

[3] A derivation of these differential equations is given by Timoshenko—*Strength of Materials*, 2nd Edition, Vol. 2, Page 135, Van Nostrand; also by A. Nadai—*Elastische Platten*, Berlin, J. Springer, Page 52.

Substituting expressions for m_1, m_2 and dm_1/dr given by Equations 295, 296, 297 in Equation 294 yields the following expression:

$$\frac{d^2\phi}{dr^2} + \frac{4}{r}\frac{d\phi}{dr} + (3\mu-1)\frac{\phi}{r^2} = -\frac{P}{2\pi k_1 r^4}$$

The complete solution to this equation[4] is

$$\phi = C_1 r^{(-3/2+s)} + C_2 r^{(-3/2-s)} - \frac{P}{6\pi k_1(\mu-1)r^2} \quad \ldots\ldots\ldots\ldots\ldots\ldots (298)$$

where

$$s = \sqrt{\frac{13}{4} - 3\mu}$$

The boundary conditions are: For $r=r_o$, $m_1=0$ since no radial moments act along the edge; hence from Equation 295,

$$\left(\frac{d\phi}{dr} + \mu\frac{\phi}{r}\right)_{r=r_o} = 0$$

For $r=r_i$, $m_1=0$ and

$$\left(\frac{d\phi}{dr} + \mu\frac{\phi}{r}\right)_{r=r_i} = 0$$

These two equations enable the determination of the two constants C_1 and C_2 of Equation 298. These values are

$$C_1 = \frac{P(2-\mu)}{6\pi k_1(1-\mu)\left(-\frac{3}{2}+s+\mu\right)}\left[\frac{r_o^{-1/2}r_i^{-s} - r_i^{-1/2}r_o^{-s}}{\alpha^s - \alpha^{-s}}\right] \quad \ldots\ldots\ldots (299)$$

$$C_2 = \frac{P(2-\mu)}{6\pi k_1(1-\mu)\left(-\frac{3}{2}-s+\mu\right)}\left[\frac{r_o^{s}r_i^{-1/2} - r_i^{s}r_o^{-1/2}}{\alpha^s - \alpha^{-s}}\right] \quad \ldots\ldots\ldots (300)$$

where

$$\alpha = \frac{r_o}{r_i}$$

[4] The author is indebted to Dr. A. Nadai of the Westinghouse Research Laboratories for suggestions regarding the method of integration of this equation.

The maximum stress in the plate will occur at the inner edge where $r=r_i$. This will be

$$\sigma_m=\frac{6(m_2)_{r=r_i}}{t_b^2} \quad \ldots\ldots (301)$$

where t_b=thickness at inner edge ($t_b=2kr_i$).

Using Equations 296, 298, 299, and 300, and the derivative of Equation 298 in Equation 301, and taking $r=r_i$ the maximum stress becomes

$$\sigma_m=K\frac{P}{t_b^2} \quad \ldots\ldots (302)$$

where

$$K=\frac{(2-\mu)(A-B)}{\pi(1-\mu)(\alpha^2-\alpha^{-2})}+\frac{1-2\mu}{\pi(1-\mu)} \quad \ldots\ldots (303)$$

and

$$A=\left(1-\frac{3\mu}{2}+s\mu\right)\left(\alpha^{-1/2}-\alpha^{-2}\right)\div\left(s+\mu-\frac{3}{2}\right)$$

$$B=\left(1-\frac{3\mu}{2}-s\mu\right)\left(\alpha^{-2}-\alpha^{-1/2}\right)\div\left(\mu-s-\frac{3}{2}\right)$$

Thus it is seen that the factor K depends primarily on the ratio $\alpha=r_o/r_i$ between outer and inner radius and on Poisson's ratio μ. In *Fig.* 138 values of K are plotted as functions of the ratio α for Poisson's ratio equal to .3, which is approximately true for steel. However, a considerable change in Poisson's ratio would affect the values of K but slightly.

Deflection is calculated from the equation

$$\phi=-\frac{dw}{dr} \quad \ldots\ldots (304)$$

or, integrating

$$w=-\int\phi dr+C_3$$

Using the value of ϕ given by Equation 298 and integrating the deflection w becomes

$$w = -\frac{C_1 r^{(-1/2+s)}}{-\frac{1}{2}+s} - \frac{C_2 r^{(-1/2-s)}}{-\frac{1}{2}-s} - \frac{P}{6\pi k_1(\mu-1)r} + C_3 \quad \ldots\ldots (305)$$

The integration constant C_3 is determined from the condition that the deflection w is zero at the outer edge of the plate where $r=r_o$. Using Equation 305 this condition gives

$$C_3 = \frac{C_1 r_o^{(-1/2+s)}}{-\frac{1}{2}+s} + \frac{C_2 r_o^{(-1/2-s)}}{-\frac{1}{2}-s} + \frac{P}{6\pi k_1(\mu-1)r_o} \quad \ldots\ldots (306)$$

Using this value of C_3 in Equation 305 and taking $r=r_i$ the maximum deflection δ becomes

$$\delta = C\frac{Pr_o^2}{Et_b^3} \quad \ldots\ldots (307)$$

where

$$C = \frac{.637(1+\mu)}{\alpha^2}\left\{\frac{(\mu-2)}{\alpha^s-\alpha^{-s}}\left[\frac{-\alpha^{(1-s)}-\alpha^s+2\sqrt{\alpha}}{\left(-\frac{3}{2}+s+\mu\right)\left(-\frac{1}{2}+s\right)}+\right.\right.$$

$$\left.\left.\frac{\alpha^{(s+1)}+\alpha^{-s}-2\sqrt{\alpha}}{\left(-\frac{3}{2}-s+\mu\right)\left(-\frac{1}{2}-s\right)}\right]+\alpha-1\right\} \quad \ldots\ldots (308)$$

In *Fig.* 139 values of the deflection constant C have been plotted as functions of $\alpha=r_o/r_i$ for Poisson's ratio $\mu=.3$.

Values of the constants C, C', K, K' figured by the exact and approximate methods, Equations 308, 291, 303, and 290, are listed in TABLE XXVIII.

An examination of this table shows that for values of the ratio α between inner and outer diameters less than 3 there is agreement between C and C' within about 10 per cent. This means that *for small deflections* (say, less than about half the thickness) there will be agreement within this percentage between deflections as figured by the exact and by the approximate methods. Since 10 per cent accuracy is usually sufficient for practical calculations, the approximate method may be used in

most cases for diameter ratios α less than 3. However, the agreement for stress is not so good, since the difference between K and K' will be over 10 per cent for values of α greater than about 1.4, the values given by the exact theory being somewhat higher than those given by the approximate theory.

It should be noted that Equations 302 and 307 were derived on the assumption of small deflections. However, when the de-

TABLE XXVIII

Constants C, C', and K and K' for Various Values of α

α	K	K'	C	C'
1	.985	.954	.0	.0
1.25	.819	.75	.243	.242
1.5	.696	.602	.271	.268
2	.536	.408	.213	.205
3	.382	.22	.110	.098
4	.315	.136	.062	.0506
5	.280	.092	.039	.0296

flections become large the exact flat-plate theory becomes extremely complicated[5]. An improvement in accuracy for calculating deflections may be obtained by multiplying Equation 307 for deflection, derived from the more exact plate theory by the term in brackets in Equation 293. This gives

$$\delta = C\frac{Pr_o^2}{Et_b^3}\left[\frac{1}{1+\dfrac{1.5\delta^2}{t_b^2(\alpha^2+\alpha+1)}}\right] \qquad (309)$$

or

$$P = \frac{Et_b^3\delta}{Cr_o^2}\left[1+\frac{1.5\delta^2}{t_b^2(\alpha^2+\alpha+1)}\right] \qquad (310)$$

For small deflections relative to thickness Equation 309 reduces to Equation 307 since the term in the brackets becomes unity. For large deflections, the equation corrects for the effect of dish in the same proportion as is done in the approximate Equation 293.

An investigation[6] based on the approximate theory shows that for a given load, outside diameter and stress the deflection

[5] *Elastische Platten*, by A. Nadai, Page 284 presents a further discussion of this.
[6] Reference of Footnote 1 gives additional details.

of the disk spring becomes a maximum for values of diameter ratios α around 2. Such proportions also result in better conditions for heat treating and forging than disks of larger ratios. For these reasons it is better in practice to use values of α around 2 unless design conditions dictate otherwise.

Application of Formulas—In the practical use of radially-tapered springs the load is applied a small distance inside the edge as indicated in *Fig.* 140. In such cases it is advisable to

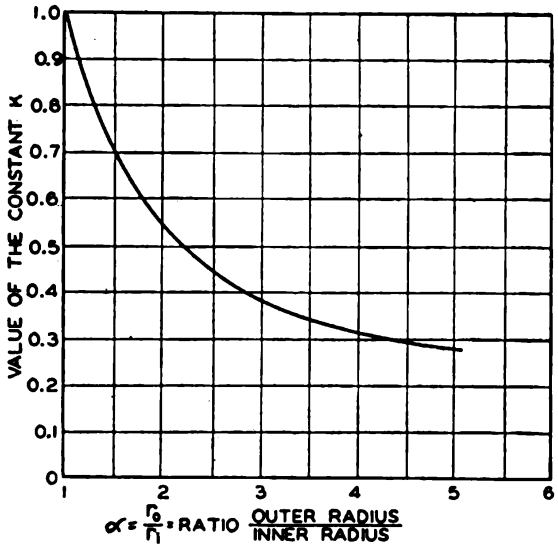

Fig. 138—Values for stress constant K for radially-tapered disk springs

figure the spring as though the load were applied exactly at the edge. The resulting stress is then multiplied by the ratio $d/(r_o—r_i)$, where d=radial distance between points of contact, to take into account the reduction of stress caused by this effect. This yields an approximation since the moment per inch of circumferential length (which is proportional to stress) has been reduced by this amount. The deflection of the inner edge of the spring with respect to the outer will also be reduced in the ratio $d(r_o—r_i)$ but the deflection of the points of load application will be reduced somewhat more than this or approximately in the ratio $d^2/(r_o—r_i)^2$. The use of these corrections will improve the accuracy of the calculation.

As an example of the application in practical calculation of

the equations given in this chapter: It is desired to determine maximum stress and deflection for a radially-tapered disk spring for the railway motor commutator application in *Fig.* 136. The dimensions are as follows: $r_o = 9$ inches, $r_i = 6$ inches, $\alpha = 1.5$

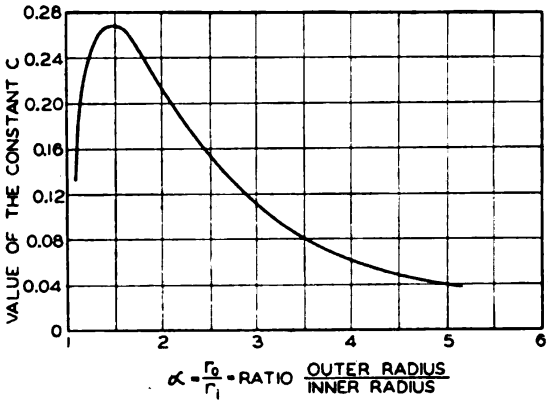

Fig. 139—Deflection constant C for radial-tapered disk springs

inches, $t_b = \frac{3}{4}$ inch. The maximum load P is 90,000 pounds.

From *Figs.* 138 and 139 or TABLE XXVIII $C = .271$ and $K = .696$ for $\alpha = 1.5$. Then from Equations 302 and 307,

$$\sigma_m = \frac{KP}{t_b^2} = 111{,}000 \text{ lb./sq. in.}$$

$$\delta = C\frac{Pr_o^2}{Et_b^3} = .157\text{- inch}$$

These values should be corrected because in the actual design the point of load application is ⅛-inch inside the edge as in-

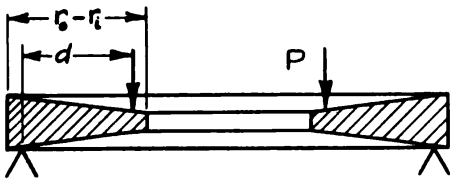

Fig. 140—Load is displaced inward from edge in disk spring

dicated in *Fig.* 140. Thus the distance $d = 2\frac{3}{4}$ inches and $r_o - r_i = 3$ inches. The corrected value of stress will be $110{,}000 \times 2.75/3 = 101{,}000$ pounds per square inch and the deflection at the points of application of the load will be $.157(2.75/3)^2 = .132$-inch.

Since these deflections are much smaller than half the thickness it may be expected that the load-deflection characteristic of this spring will be approximately linear, being modified only by friction along the edges. By supporting the spring at the neutral axis by means of a stepped edge (*Fig.* 136) this friction may be greatly reduced.

COMPARISONS WITH THEORY

As a check on the theory given in this chapter, some tests were made using the test arrangement shown schematically in *Fig.* 141. In this arrangement, the load was applied in a testing machine through steel cylinders to a heavy ring which applied the load uniformly around the outer circumference of the disk spring. The disk spring was supported by a cylinder rest-

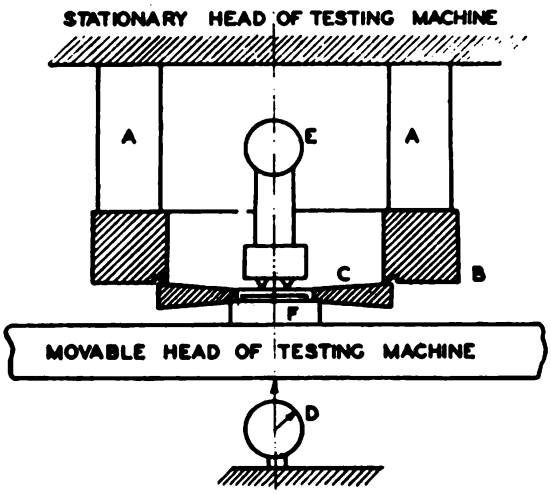

Fig. 141 — Arrangement for testing disk springs. A = steel cylinder, B = ring, C = disk spring, F = cylinder, E = extensometer, D = dial gage

ing on the lower head of the testing machine. Sufficient clearance was allowed between the edges of the disk spring, the cylinder and the ring, respectively, to make certain there would be no binding during application of the load. In most of the tests the supporting edge of the ring was beveled as shown, greatly exaggerated, so that the point of load application was definite. Huggenberger extensometers, placed along the inner edge of the spring made possible the measurement of maximum stress. At the same time it was possible to read the extensometers while the

spring was loaded. In all cases strain measurements were made on diametrically opposite sides of the spring to determine whether or not the load was central. For measuring deflections a dial gage was used.

Tests were carried out on a total of seven radially tapered disk springs having outer diameters varying from 3.8 to 4¼ inches,

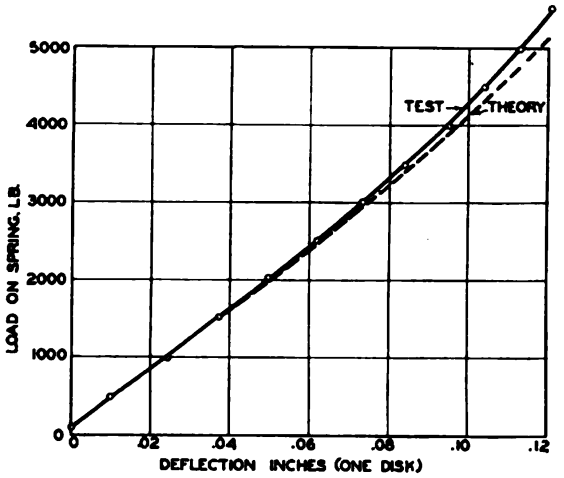

Fig. 142—Deflection test on disk spring *C*

inner diameters varying from 1½ to 2½ inches, and minimum thickness t_h from ⅛ to ⅜ inches.

Typical load-deflection and load-stress diagrams as obtained on these springs are shown by the full lines of the curves of *Figs.* 142 and 143 while the theoretically determined curves using Equations 302 and 309 (correction being made for the inward displacement of the point of load application) are shown by the dotted curves. The stresses were determined from the strains at the inside edge of the spring where the maximum stress occurs. (This is also the point where failure starts as shown by actual fatigue tests). A modulus of elasticity $E = 30 \times 10^6$ pounds per square inch was used in converting the strain readings to stress.

In all cases, good agreement was found between test and calculated values for stress. At the lower loads for deflection in all cases the agreement was found to be quite good, but at the higher loads in some cases there was a small deviation between test and theory, due probably to the fact that the point of appli-

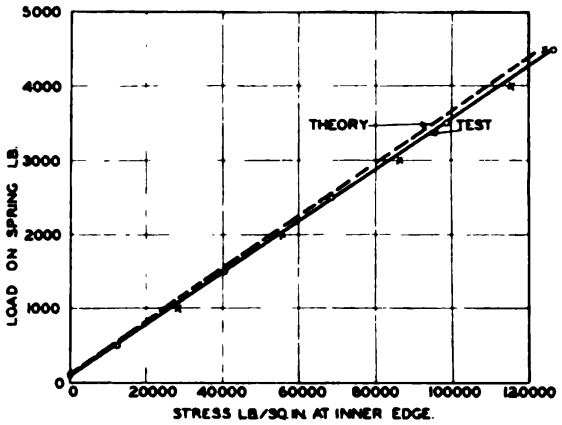

Fig. 143—Stress test on disk spring *A'*

cation of the load tended to move inward so that the distance *d* (*Fig.* 140) became less, thus making the spring slightly stiffer at these loads. However, the agreement in all cases between test and theory was sufficiently good for most practical purposes.

SPRINGS OF CONSTANT THICKNESS

The initially-flat disk spring of constant thickness, *Fig.* 133*a*, may be analyzed in a similar manner as was done in the case of the radially-tapered disk spring.

Approximate Theory—For an approximate theory[7] the assumption is again made that radial cross-sections rotate without distortion through an angle ϕ as indicated by the dotted outline in *Fig.* 133*b*. As in the case of the radially-tapered spring for small deflections the stress in an element *G* at a radius *r* from the axis and at a distance *y* from the middle surface of the disk will be

$$\sigma = \frac{E\phi y}{r} \qquad \ldots\ldots(311)$$

for small deflections (Equation 280). The moment of the forces acting on the element *G* about an axis through *O* will be as before $\sigma y dx dy d\theta$ assuming that the element *G* is cut out by two slices at an angle $d\theta$, *Fig.* 137*a*. The total moment *M''* will be the integral

[7] Timoshenko—*Strength of Materials*, Part II, Second Edition, Page 179, Van Nostrand, 1941.

of these elementary moments taken over the area of the section. Thus

$$M'' = d\theta \int_{c-r_o}^{c-r_i} \int_{-t/2}^{t/2} \frac{E\phi y^2}{c-x} dy\, dx$$

Integrating and substituting limits

$$M'' = \frac{d\theta E \phi t^3 \log_e \alpha}{12} \quad \text{(312)}$$

Since the total load acting on the spring is equal to P, the external moment acting on the element will be the same as that given by Equation 284 for the radially-tapered spring. Equating the value of M'' given by Equation 312 to that given by Equation 284 and solving for ϕ,

$$\phi = \frac{6P(r_o - r_i)}{\pi E t^3 \log_e \alpha} \quad \text{(312a)}$$

The maximum deflection is then

$$\delta = \phi(r_o - r_i) = \frac{6Pr_o^2\left(1 - \frac{1}{\alpha}\right)^2}{\pi E t^3 \log_e \alpha} \quad \text{(313)}$$

This may be written

$$\delta = C' \frac{Pr_o^2}{Et^3} \quad \text{(314)}$$

where

$$C' = \frac{6\left(1 - \frac{1}{\alpha}\right)^2}{\pi \log_e \alpha} \quad \text{(315)}$$

From Equation 311 it is clear that the stress will be a maximum when $y = t/2$ and $r = r_i$. Using these values and the value of ϕ given by Equation 312*a* in Equation 311 and simplifying, the maximum stress becomes

$$\sigma_m = K' \frac{P}{t^2} \quad \text{(316)}$$

where

$$K' = \frac{3}{\pi} \frac{\alpha - 1}{\log_e \alpha} \quad \text{.....(317)}$$

Exact Theory—The exact theory for calculating initially-flat disk springs of constant thickness is based on the known plate theory[3]. Letting ϕ be the slope at any radius r of a circular plate symmetrically loaded, then from plate theory the following differential equation must be satisfied:

$$\frac{d^2\phi}{dr^2} + \frac{1}{r}\frac{d\phi}{dr} - \frac{\phi}{r^2} = -\frac{Q}{D} \quad \text{.....(318)}$$

where

D = Plate rigidity $= Et^3/12(1-\mu^2)$
μ = Poisson's ratio
Q = Shearing force per unit circumferential length at any radius r.

For the case shown in *Fig.* 133 where the load P is distributed uniformly along the edges

$$Q = \frac{P}{2\pi r}$$

Using this value in Equation 318 and integrating

$$\phi = -\frac{Pr}{8\pi D}\left(2\log_e r - 1\right) + \frac{C_1 r}{2} + \frac{C_2}{r} \quad \text{.....(319)}$$

where C_1 and C_2 are integration constants to be determined later. If w is the deflection at any radius r, the slope $\phi = -dw/dr$. Integrating Equation 319 with respect to r,

$$w = \frac{Pr^2}{8\pi D}\left(\log_e r - 1\right) - \frac{C_1 r^2}{4} - C_2 \log_e r + C_3 \quad \text{.....(320)}$$

The integration constants C_1, C_2, C_3 are found from the following conditions: At the outer and inner edges where $r = r_o$ and $r = r_i$, the radial bending moments m_1 must be zero. From Equation 295 this means that

$$\left(\frac{d\phi}{dr} + \mu\frac{\phi}{r}\right)_{r=r_o} = 0$$

$$\left(\frac{d\phi}{dr}+\mu\frac{\phi}{r}\right)_{r=r_i}=0$$

Also when $r=r_o$, $w=0$

These three equations enable the determination of the three constants C_1, C_2, C_3 in Equation 320.

From Equation 296 the tangential bending moment m_2 per unit length is

$$m_2=D\left(\frac{\phi}{r}+\mu\frac{d\phi}{dr}\right)$$

It may be shown that this moment is a maximum when $r=r_i$; the maximum stress is then

$$\sigma_m=\frac{6(m_2)_{r=r_i}}{t^2}=\frac{6D}{t^2}\left(\frac{\phi}{r}+\mu\frac{d\phi}{dr}\right)_{r=r_i} \quad \ldots\ldots (321)$$

Differentiating Equation 319 and taking $r=r_i$ in the resulting expressions for ϕ and $d\phi/dr$, substituting in Equation 321 the maximum stress becomes (for $\mu=.3$):

$$\sigma_m=K\frac{P}{t^2} \quad \ldots\ldots (322)$$

where

$$K=.3343+\frac{1.242\,\alpha^2 \log_e\alpha}{\alpha^2-1} \quad \ldots\ldots (323)$$

The maximum deflection δ is obtained from Equation 320 by taking $r=r_i$. This then becomes (for $\mu=.3$)

$$\delta=C\frac{Pr_o^2}{Et^3} \quad \ldots\ldots (324)$$

where

$$C=.6514\left(\frac{\alpha^2-1}{\alpha^2}\right)+\frac{1.614(\log_e\alpha)^2}{\alpha^2-1} \quad \ldots\ldots (325)$$

It will be noted that these expressions for stress and deflections are of the same form as those obtained by the approximate method (Equations 314 and 316). Comparisons of the numer-

TABLE XXIX

Stress and Deflection Constants for Disk Springs

	Values of α						
	1	1.25	1.5	2	3	4	5
K	.955	1.10	1.26	1.48	1.88	2.17	2.34
K'	.955	1.07	1.18	1.38	1.74	2.07	2.37
C	0	.341	.519	.672	.734	.724	.704
C'	0	.343	.524	.689	.773	.775	.760

ical values of C, C', K, K' obtained by the exact and approximate methods is given in TABLE XXIX.

Comparison of these values shows that up to a ratio for α of

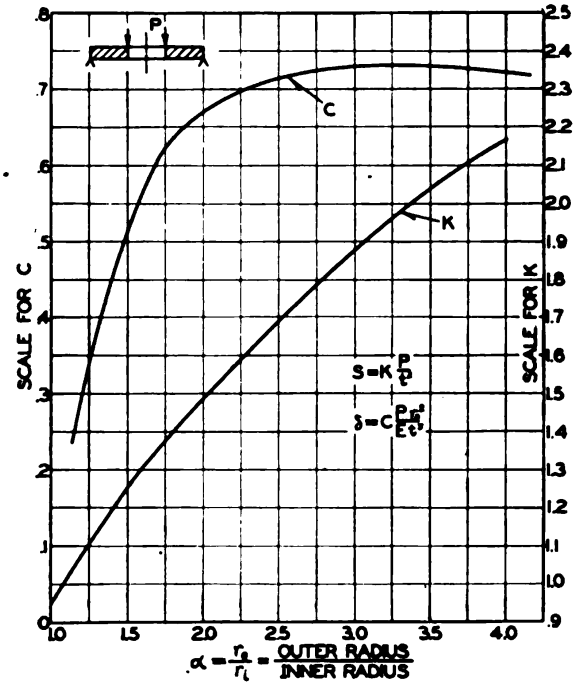

Fig. 144—Curve for determining constants C and K for flat disk springs of constant thickness

5, there is good agreement between the exact and approximate values of the constants[8].

For convenience in calculation, values of C and K are plotted against the diameter ratio α in *Fig.* 144.

[8] Paper on "Stresses and Deflections in Flat Circular Plates with Central Holes" by G. Lobo, Jr. and the writer, *Transactions* ASME, 1930, A.P.M. 52-3 gives a further discussion of flat circular plates with various loading and edge conditions.

LARGE DEFLECTIONS

The exact theory previously discussed for calculating initially-flat disk springs is based on the assumption that deflections are small, say, not over half the spring thickness, for reasonably accurate results. Where deflections are large, the exact theory is too complicated for practical use; however, the approximate method for initially-coned disk springs Chapter XIV may be used with sufficient accuracy for most purposes. It is only necessary to take $h=0$ (for an initially-flat spring) in Equations 269 and 270. This gives the following expression for the load P:

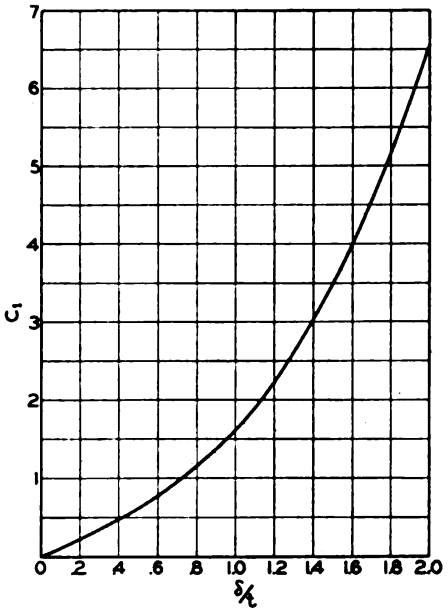

Fig. 145 — Deflection constant C_1 for initially-flat disk spring

$$P = C_1 C_2 \frac{Et^4}{r_o^2} \quad \ldots\ldots (326)$$

where

$$C_1 = \frac{\delta}{(1-\mu^2)t}\left(\frac{\delta^2}{2t^2}+1\right) \quad \ldots\ldots (327)$$

and C_2 is given by Equation 261 or *Fig.* 125.

Values of C_1 are given as a function of the ratio δ/t between

deflection and thickness in the curve of *Fig.* 145. This curve shows how the deflection curve deviates from a straight line after the deflection becomes greater than about half the thickness.

The maximum stress may be obtained from Equations 271 and 272 taking $h=0$. This gives:

$$\sigma_m = K_1 \frac{Et^2}{r_o^2} \qquad (328)$$

where

$$K_1 = \frac{C_2\delta}{(1-\mu^2)t}\left(C_1' \frac{\delta}{2t} + C_2' \right) \qquad (329)$$

where C_1' and C_2' are given as functions of $\alpha = r_o/r_i$ in Equations 266 and 267. Values of K_1 are also given by the curves for $h/t=0$ in *Figs.* 127 and 128 for different ratios of r_o/r_i.

SIMPLIFIED CALCULATION

If it be assumed that a load-deflection characteristic of the shape shown in *Fig.* 146 is desired, the calculation of required spring thickness and diameters becomes simple[9]. By proceeding in a similar way as was done for the case of initially-coned disk

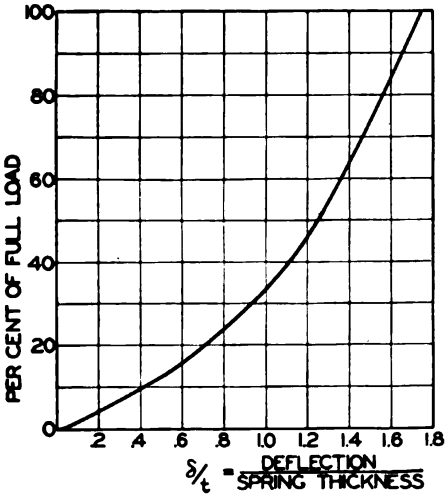

Fig. 146—Load-deflection diagram for initially-flat disk spring with maximum $\delta/t=1.75$

springs (Page 254) values may be calculated for steel springs

[9]This method was suggested by R. C. Bergvall of the Westinghouse Company.

(modulus of elasticity $E=30\times10^6$ lb./sq. in.) as in TABLE XXX.

The deflection at any other load less than the maximum load (at $\delta=1.75t$) may be found by using the curve of *Fig.* 146.

By using TABLE XXX a relatively simple method of design for initially-flat disk springs with a given load-deflection characteristic is obtained. This approximate method involves the assumption that radial cross-sections rotate without distortion, but available data indicate that the results are sufficiently accurate for most purposes.

TABLE XXX

Proportions of Initially-Flat Steel Disk Springs*

Maximum Stress, σ_m (lb./sq. in.)	Diameter Ratio ($\alpha = D/d$)	Spring Thickness (t)	Maximum Deflection ($\delta = 1.75t$)	Load P ($\delta = 1.75t$)
200,000	1.25	$D/80$	$D/45.7$	$42D^2$
	1.5	$D/67.4$	$D/38.5$	$53.8D^2$
	2 to 2.5	$D/63.8$	$D/36.4$	$50.5D^2$
150,000	1.25	$D/92.5$	$D/52.8$	$23.7D^2$
	1.5	$D/77.8$	$D/44.4$	$30.1D^2$
	2 to 2.5	$D/73.7$	$D/42.2$	$28.4D^2$
100,000	1.25	$D/113$	$D/64.5$	$10.5D^2$
	1.5	$D/95.4$	$D/54.5$	$13.4D^2$
	2 to 2.5	$D/90.2$	$D/51.5$	$12.6D^2$

*For load-deflection curve of *Fig.* 146 when maximum deflection $\delta = 1.75t$.

CHAPTER XVI

FLAT AND LEAF SPRINGS

Broadly speaking, the term "flat springs" is a generic term referring to springs of flat strip or bar stock made in a wide variety of forms. Because of the shapes which are possible for this type of spring, a complete discussion is beyond the scope of this book. In this chapter only the fundamental principles underlying the calculation of the simpler forms of flat springs such as the flat cantilever spring (*Figs.* 147 and 148) and their application in practical design will be considered. In addition the effects of large deflections, stress concentration, and combined axial and lateral loading will also be treated. More complicated shapes may, however, be analyzed by similar methods.

An advantage of the flat cantilever spring over the helical spring is that the end of the spring may be guided along a definite path as it deflects. Thus the spring may function as a structural member as well as an energy absorbing device. By making the spring in a particular shape it may be possible to combine several functions, thus simplifying design. For example, an automobile leaf spring may be designed not only to absorb road shocks, but also to carry lateral loads and, in some cases to take the brake torque as well.

CANTILEVER SPRINGS

A simple cantilever spring is a flat strip or plate of rectangular profile and constant cross section as shown in *Fig.* 147. Assuming the spring built in at one end and loaded at the other, the maximum deflection is given by the well-known cantilever formula:

$$\delta = \frac{Pl^3}{3EI} \qquad (330)$$

where l=length of spring, E=modulus of elasticity of the material and I=moment of inertia of spring cross-section. ($I = b_o h^3/12$ where b_o=width of spring, h=thickness.)

Fig. 147—Simple cantilever spring of rectangular profile

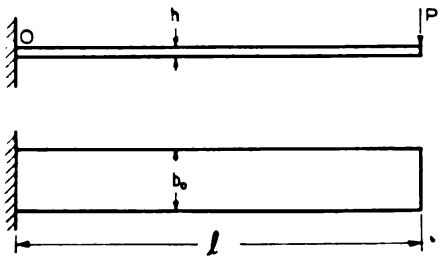

More exact considerations of the deflection show that if b_o is large compared to h (as for springs of clock-spring steel) the deflection will be given by:

$$\delta = \frac{Pl^3}{3EI}(1-\mu^2) \quad \ldots\ldots (331)$$

where μ=Poissons' ratio. Since for most materials μ is around .3, the deflection given by this equation is about 10 per cent less than that given by Equation 330. The reason for this difference lies in the fact that for a spring of relatively great width compared to thickness, lateral expansion or contraction of elements near the surface of the spring is prevented, which results in a slightly stiffer spring than figured from beam theory. This stiffening is taken into account by the term $(1-\mu^2)$ in Equation 331. In many practical flat spring applications the deflection will probably be

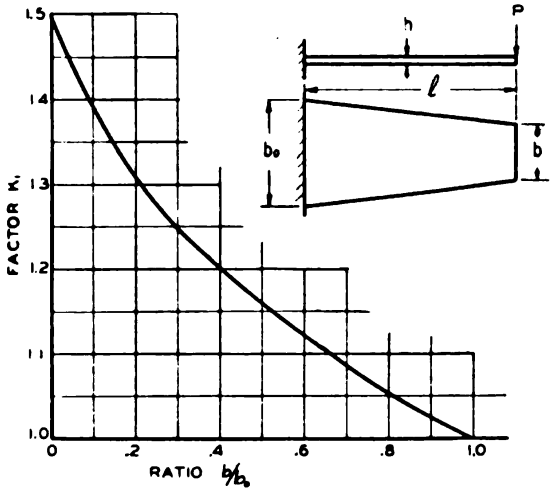

Fig. 148—Curves for calculating deflections of cantilever springs of trapezoidal profile

closer to the value calculated by Equation 331 than to that calculated by Equation 330[1].

The nominal stress at the built-in edge *O*, *Fig.* 147, is given by[2]

$$\sigma = \frac{6Pl}{b_o h^2} \qquad (332)$$

It should be noted that these formulas are based on usual beam theory which assumes small deflections. The case where deflections are large will be considered later. Where variable stresses (fatigue loading) are involved, the stresses must be multiplied by *stress concentration factors* which depend on the conditions near the built-in edge. A discussion of this will also be given later.

Trapezoidal Profile Springs—In many cases, leaf springs of the usual shape as shown in *Fig.* 149 may, for practical purposes of analysis, be considered as cantilever springs of trapezoidal profile as shown in *Fig.* 148. Such a profile makes a more efficient use of the material than does the rectangular profile of *Fig.* 147. For a given load P the maximum stress is again given by Equation 332, where in this case b_o is the width at the built-in end. Analysis based on ordinary beam theory, however, shows that the deflections are increased over those obtained in the simple cantilever spring of rectangular profile by an amount depending on the ratio b/b_o between width at the free and built-in ends, respectively. The analysis shows that in this case the maximum deflection is given by

$$\delta = K_1 \frac{Pl^3}{3EI_o} \qquad (333)$$

where

$$K_1 = \frac{3}{\left(1 - \frac{b}{b_o}\right)^3}\left[\frac{1}{2} - 2\frac{b}{b_o} + \left(\frac{b}{b_o}\right)^2\left(\frac{3}{2} - \log_e \frac{b}{b_o}\right)\right]$$

and I_o=moment of inertia at built-in ends. The factor K_1 depends on b/b_o and may be taken from the curve of *Fig.* 148. It

[1] Page 243 of Chapter XIV gives a further discussion of this correction.

[2] The *nominal* stress is obtained by dividing the bending moment by the section modulus of the minimum or net section.

is thus seen that the deflection of a trapezoidal profile spring is equal to that of a rectangular profile spring $Pl^3/3EI_o$ multiplied by a factor K_1 varying from 1 for $b/b_o=1$ (rectangular profile) to 1.5 for $b/b_o=0$ (triangular profile). Theoretically the most efficient spring is obtained where $b/b_o=0$ since other things being equal this gives the maximum deflection for a given value of load. Practical considerations however, usually dictate a value of b/b_o greater than zero. For cases where b_o is large compared to the thickness h it is necessary to multiply the deflection given by Equation 333 by a factor $(1-\mu^2)$ as explained previously.

Large Deflections—As mentioned previously, the beam theory on which Equations 331 to 333 are based assumes small

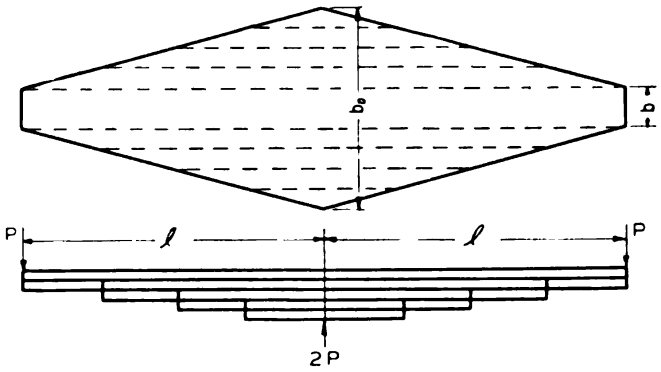

Fig. 149—Leaf spring is equivalent to a cantilever spring of trapezoidal profile

deflections relative to the spring length. In some practical cases, however, the actual deflections cannot be considered small. This is illustrated by *Fig.* 150. When the spring is deflected by an amount δ_1 the ordinary theory will hold. However, when the deflection is increased to, say, δ_2 it may be seen that the moment arm of the load x_o is considerably less than the length l of the spring. This results in a decrease in both stress and deflection from the values calculated from Equations 332 and 333.

To analyze the case where the deflection is large compared to the thickness, the more accurate mathematical expression for curvature of the center line of the beam is used. If x is the distance from the built-in end O of the beam (*Fig.* 150) and δ the deflection at this distance, then by equating the curvature of the beam to the external bending moment divided by EI_x,

the following equation results:

$$\frac{\frac{d^2y}{dx^2}}{\left[1+\left(\frac{dy}{dx}\right)^2\right]^{3/2}} = \frac{P(x_o-x)}{EI_x} \qquad \text{.....(334)}$$

where I_x = moment of inertia at distance x.

Since for a trapezoid the width is a linear function of the length, for constant thickness the moment of inertia at a distance x from the end is given approximately by

$$I_x = I_o\left[1-\frac{x}{x_o}\left(1-\frac{b}{b_o}\right)\right]$$

Substituting this expression in Equation 334, the following expression results:

$$\frac{\frac{d^2y}{dx^2}}{\left[1+\left(\frac{dy}{dx}\right)^2\right]^{3/2}} = \frac{P(x_o-x)}{EI_o\left[1-\frac{x}{x_o}\left(1-\frac{b}{b_o}\right)\right]} \qquad \text{.....(335)}$$

By integrating this equation[3] utilizing the boundary conditions which require that at $x=0$, $y=0$, and $dy/dx=0$, the reduc-

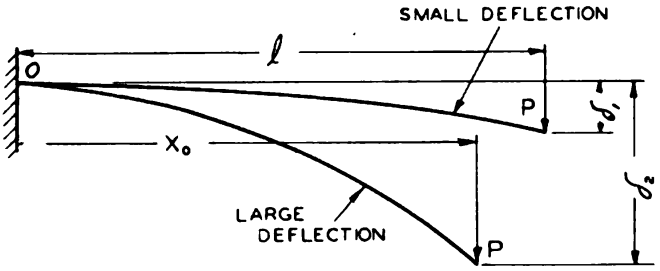

Fig. 150—Cantilever spring with deflections

tion in stress and deflection below those calculated from Equations 332 and 333 may be expressed as functions of the dimensionless quantity $c=Pl^2/EI_o$ and the ratio b/b_o between width at end of spring and width at built-in edge. In *Fig.* 151 are given some curves based on Equation 335 for estimating the percentage

[3] See *Die Federn*, by Gross and Lehr, published by V.D.I., Berlin, 1938, Page 133, for details of method of integration.

stress reduction in cantilever springs of trapezoidal profile for various ratios b/b_o and values of $c=Pl^2/EI_o$ as compared with the calculated stress value using Equation 332. Where $b/b_o=0$ triangular profile is obtained and, in this case, the stress reduc-

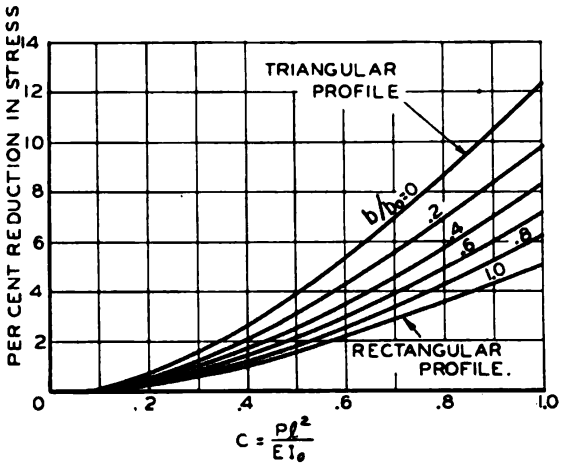

Fig. 151—Curves for estimating stress reduction due to large deflections of cantilever springs

tion varies from about 0 to 12 per cent for values of c between 0 and 1. This means that, for example, if $c=1$ and the stress is computed from Equation 332, the actual stress will be 12 per cent less than this. For springs of rectangular profile the variation is from 0 to 5 per cent within a range $c=0$ to $c=1$. In *Fig.* 152, curves are also given to estimate the percentage reduction in deflection from the value calculated by using Equation 333. For a range $c=0$ to $c=1$, this correction varies from 0 to 8 per cent for the rectangular profile ($b/b_o=1$) and from 0 to 18 per cent for the triangular profile ($b/b_o=0$). It is clear that the corrections become larger as b/b_o becomes smaller. Although in most practical applications, these corrections may be neglected, for highest accuracy particularly where b/b_o is small, they should be considered.

Example—As an example, to illustrate the practical utilization of *Figs.* 151 and 152, a cantilever spring of trapezoidal profile is assumed to have the following dimensions (*Fig.* 148): $l=$ 30 in., $h=$¼-in., $b/b_o=.2$, $b_o=6$ in., $P=200$ lb. The material is steel with $E=30\times10^6$ pounds per square inch. For this value of P the quantity c becomes

$$c = \frac{Pl^2}{EI_o} = \frac{200 \times (30)^2 \times 12}{30 \times 10^6 \times 6 \times (1/4)^3} = .77$$

From Equation 332 the nominal stress is

$$\sigma = \frac{6Pl}{b_o h^2} = 96000 \text{ lb./sq. in.}$$

However, from Fig. 151, for $c = .77$, $b/b_o = .2$, there is a 6½ per cent reduction in stress as a consequence of the large deflec-

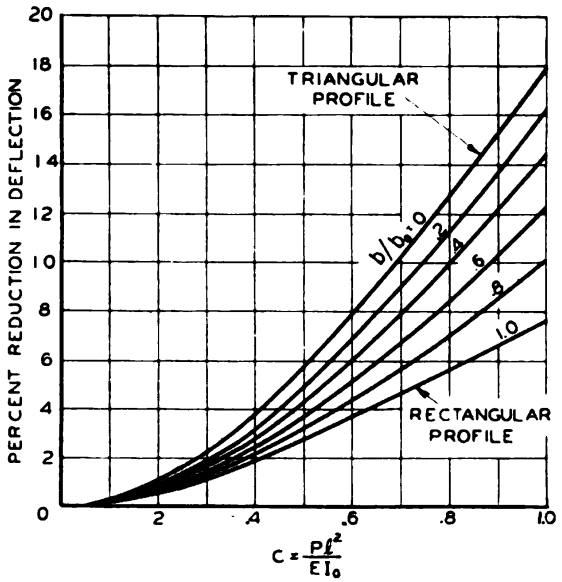

Fig. 152—Curves for the calculation of large deflections of cantilever springs

tion. Thus the actual stress is $96000(1-.065) = 89{,}700$ pounds per square inch. From *Fig.* 148 for $b/b_o = .2$, $K_1 = 1.31$ and the deflection becomes from Equation 333,

$$\delta = K_1 \frac{Pl^3}{3EI_o} = 10.1 \text{ inches}$$

This deflection should be corrected by the percentage given on the curve of *Fig.* 152 for $c = .77$ and $b/b_o = .2$ which indicates that the deflection is over-estimated 10½ per cent if Equation 333 is used. Hence the deflection is corrected by a factor (1—

.105) giving a value 10.1(1—.105)=9.05 inches. In addition since in this case the width b_o is large compared with the thickness ($b_o/t=24$), a further reduction by multiplying by $(1-\mu^2)=.91$ should be made (as was discussed previously). This gives a final deflection value of 9.05(.91)=8.25 inches is considerably less than the value of 10.1 figured by the simple formula of Equation 333.

SIMPLE LEAF SPRING

In *Fig.* 149 is shown a sketch of a simple leaf spring loaded by forces P at each end and supported by a force $2P$ at the bottom. Neglecting interleaf friction as a first approximation, this spring may be calculated as a simple trapezoidal spring. If there are n_1 leaves of length $2l$ and width b_1 and if there are a total

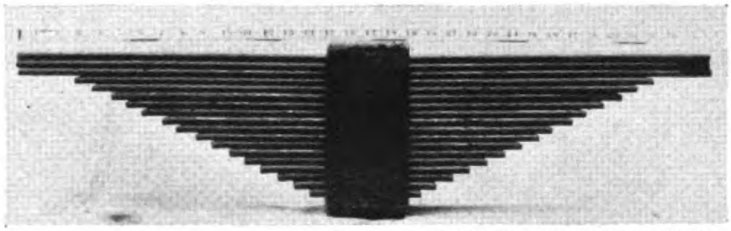

—Courtesy, Baldwin Locomotive Works

Fig. 153—Large leaf spring for locomotive

of n leaves, then from *Fig.* 149, $b=n_1b_1$ and $b_o=nb_1$. The ratio b/b_o will be n_1/n and the curves of *Figs.* 148, 151, and 152 may still be used[4]. A photo of a large leaf spring as used in locomotive design is shown in *Fig.* 153.

CANTILEVER SPRING UNDER COMBINED LOADING

A type of spring loading which frequently occurs in practice is the cantilever spring with one end rigidly built in and the other end free to move laterally but restrained from rotation; the deflection being of the type shown schematically in *Fig.* 154. The spring may support a weight in the vertical direction, this weight being represented by the axial force P. Such cases occur

[4] For more complicated cases of elliptic leaf springs and those supported by links or shackles, the reader is referred to the book by Gross and Lehr, loc. cit.

where a vibrating table is supported by springs of this type, the vibration being actuated by a crank arrangement. An example of this type of spring is shown in *Fig.* 155 which shows an application to a Fourdrinier paper machine. The vertical strips visible in the photo are flat strips of Micarta (known as *shake springs*) which support the weight of the table. These springs are subject to essentially the loading conditions shown schematically in *Fig.* 154. If the axial load P is very small compared to the buckling load, the deflection and stress may easily be figured from ordinary beam theory. The resulting equations are

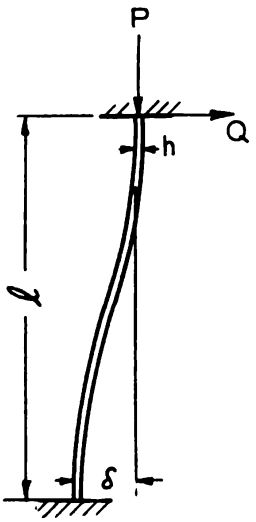

Fig. 154 — Cantilever under combined axial and transverse loading

$$\delta = \frac{Ql^3}{12EI} \qquad (336)$$

$$\sigma = \frac{3\delta Eh}{l^2} \qquad (337)$$

where l=length of beam (*Fig.* 154), Q=lateral load, $I=bh^3/12$=moment of inertia of section, b=width, h=thickness, δ=total deflection, σ=nominal stress at built-in edge (stress concentration neglected). When springs are subject to fatigue loading as mentioned previously the nominal stress σ should be multiplied by a fatigue strength reduction factor to take into account the stress concentration at the clamped edge. Actual test data relative to the values of such factors are meagre.

Where the axial load P, *Fig.* 154 is not small compared to the buckling load, Equations 336 and 337 no longer apply accurately. In such cases a more accurate analysis shows that the stress and deflection may be found by multiplying the results calculated from these equations by factors C_1 and K_2 which depend on the ratio $P/P_{cr}=Pl^2/EI\pi^2$. In this $P_{cr}=EI\pi^2/l^2$ is the Euler critical or buckling load for hinged ends. These factors are:

$$C_1 = \frac{1}{1-\frac{P}{P_{cr}}} \qquad (338)$$

$$K_2 = 1 - .178\frac{P}{P_{cr}} \quad \ldots\ldots (339)$$

The stress and deflection thus become:

$$\sigma = K_2\frac{3\delta Eh}{l^2} \quad \ldots\ldots (340)$$

$$\delta = C_1\frac{Ql^3}{12EI} \quad \ldots\ldots (341)$$

In *Figs.* 156 and 157 values of C_1 and K_2 are plotted against the ratio P/P_{cr}. An approximate method of calculating[5] the fac-

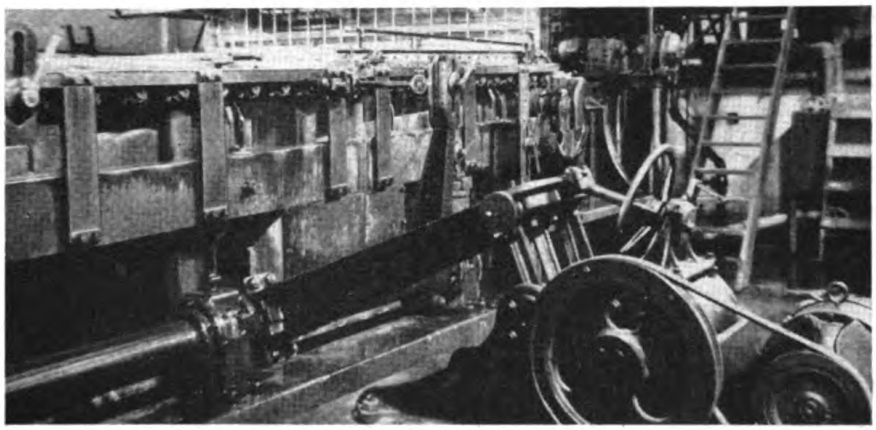

Fig. 155—Micarta shake springs of cantilever type on Fourdrinier paper machine are subject to combined lateral and axial loading

tor C_1 is as follows: Under the action of the loads P and Q the spring deflects into a cosine curve of the form

$$y = \frac{\delta}{2}\left(1 - \cos\frac{\pi x}{l}\right)$$

The potential energy stored in the beam is (using this equation)

$$V = \frac{EI}{2}\int_0^l \left(\frac{d^2y}{dx^2}\right)^2 dx = \frac{EI\pi^4}{16l^3}\delta^2 \quad \ldots\ldots (342)$$

[5] A more exact method is applied to the case of a simply supported beam in *Theory of Elastic Stability* by Timoshenko, McGraw-Hill, 1936, Page 28.

Assuming now that the deflection δ increases by a small amount $\Delta\delta$, from Equation 342 the potential energy V changes by an amount $EI\pi^4(2\delta)\Delta\delta/16l^3$, neglecting small quantities of higher order. The lateral force Q does the work $Q\Delta\delta$ and it may be shown that the vertical movement of the axial force P is approximately $\pi^2\delta\Delta\delta/8l$ which means that the work done is

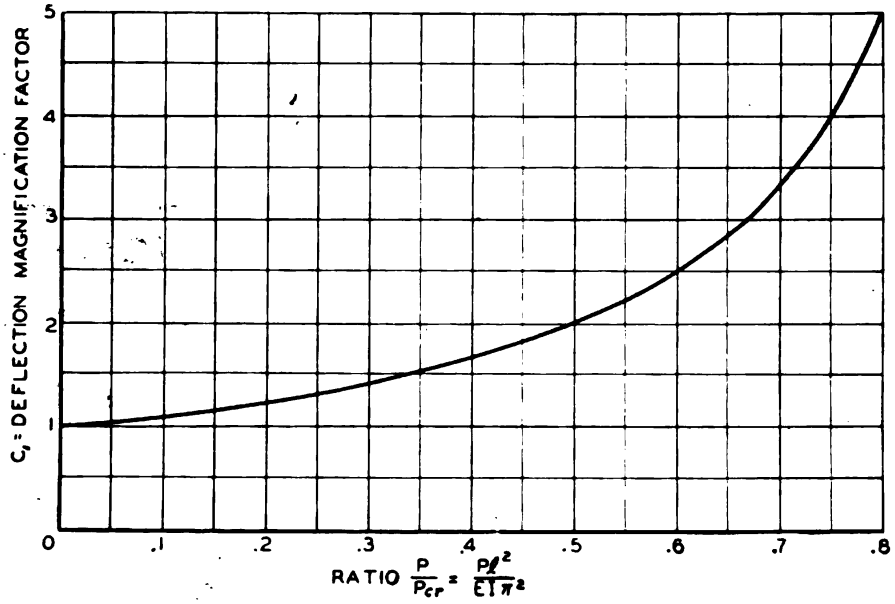

Fig. 156—Curve for calculating the deflection of a cantilever spring under combined lateral and axial type of load

$P\pi^2\delta\Delta\delta/8l$. Equating the change in potential energy to the work done by the forces P and Q, the following equation results:

$$\delta = \frac{Ql^3}{12.2EI}\left(\frac{1}{1-\frac{P}{P_{cr}}}\right) = C_1\frac{Ql^3}{12.2EI}$$

which is practically the same as Equation 341. Maximum stress is

$$\sigma = \frac{Ql}{2Z} + \frac{P\delta}{2Z}$$

where Z is the section modulus ($Z = b\,h^2/6$).

Substituting the expression for Q obtained from Equation

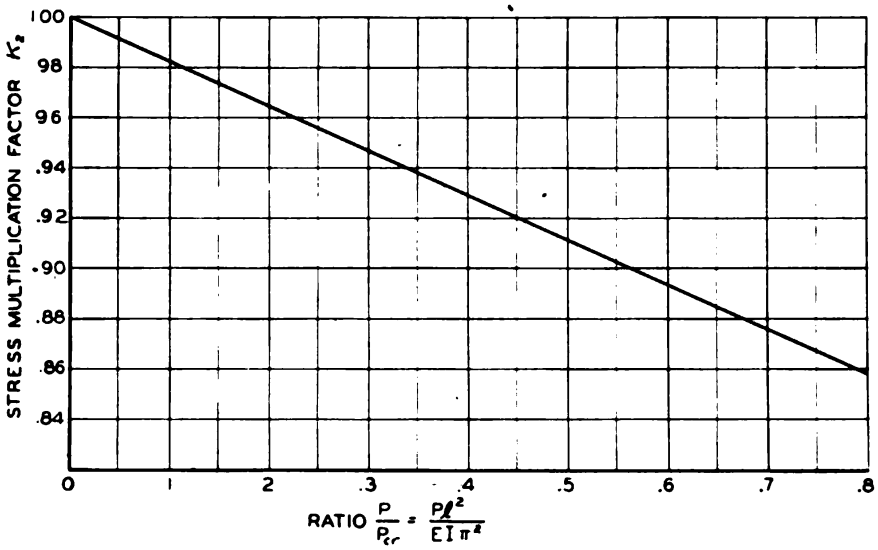

Fig. 157—Stress correction factor for cantilever springs under combined lateral and axial loads plotted against load ratios

341 in this expression, Equation 340 is obtained.

The curve of *Fig.* 156 shows that where the axial load is half the critical buckling load, the factor $C_1 = 2$, i.e., twice as much deflection may be expected than if Equation 336 based on ordinary beam theory were used. On the other hand for ratios P/P_{cr} equal to .5 or less, the curve of *Fig.* 157 indicates that the stress formula of Equation 337 is less than 10 per cent in error. In addition, where δ is given (as in the case where a crank arrangement is used to actuate the spring) the stresses figured from Equation 337 are always somewhat higher than the actual stresses.

It should also be noted that when the spring width is large compared to its thickness (as it usually is) the calculated deflection as given by Equation 341 should be multiplied by $1-\mu^2$ as before and the calculated stress as given by Equation 340 divided by $1-\mu^2$ where μ = Poisson's ratio. For most materials this will mean about a 10 per cent increase in stress.

PLATE SPRING

An interesting application of the use of large flat springs in machine design is shown schematically in *Fig.* 158 which represents a stack of plate springs supporting the frame of a 60,000

kilovolt-ampere single-phase alternating-current turbo-generator. The purpose of this arrangement is to absorb the periodic torque pulsations inherent in a single-phase generator of this type without the transmission of objectionable vibration to the foundation.

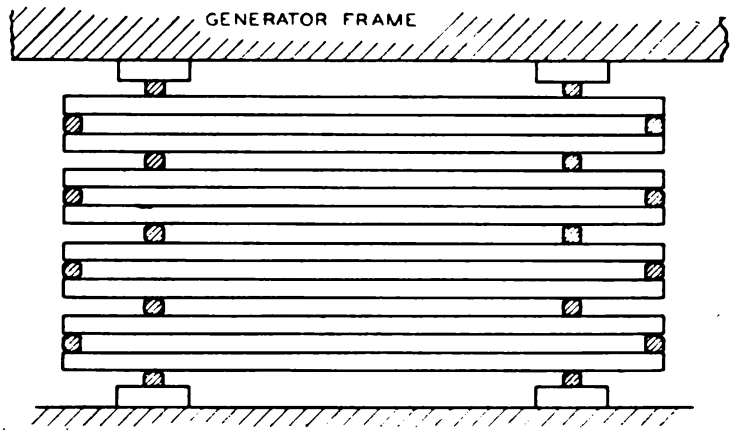

Fig. 158—Schematic arrangement of plate spring assembly for a spring-mounted alternating-current generator

The mode of deflection of this type of spring is shown by the dashed line of *Fig.* 159. From the beam theory, the deflection per spring may be calculated as

$$\delta = \frac{Pl_2^2 l_1}{2EI}\left(1 + \frac{2}{3}\,\frac{l_2}{l_1}\right) \quad \text{(343)}$$

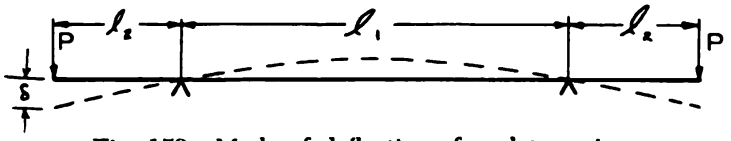

Fig. 159—Mode of deflection of a plate spring

where l_2 and l_1 are the dimensions shown on *Fig.* 159 and P is the load at each end. For very wide springs in relation to the thickness this deflection should be multiplied by $1-\mu^2$ as explained previously. The maximum stress is given by

$$\sigma = \frac{6Pl_2}{bh^2} \quad \text{(344)}$$

Springs of this type are normally subject to relatively low stresses. It is only under severe short circuit conditions (which occur infrequently) that the design stresses are reached.

STRESS CONCENTRATION EFFECTS

In the preceding sections, methods for calculating nominal stresses and deflections in various flat and leaf spring applications were described. In most cases, however, the effect of these nominal stresses is augmented by *stress concentration*, which may be due to holes, notches, clamped edges, sharp bends, sudden changes in section, etc. If the spring is under a purely static loading or if the loads are repeated a relatively few times, such stress concentration effects may usually be neglected, in practical design, for spring materials of good quality. However,

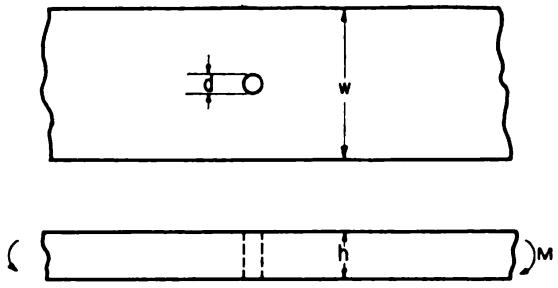

Fig. 160—Strip with hole under bending, hole where diameter d is small compared to strip thickness h. In this case upper curve of Fig. 161 for tension may be used to find theoretical stress concentration factor

where fatigue or repeated loading occurs, careful consideration should be given to such "stress raisers" by the designer, since otherwise cracks may start at localized points of stress concentration and precipitate complete failure of the spring.

To take stress concentration into account, it is necessary to know the range of nominal stress to which the spring is subjected. In accordance with the discussion of Chapter I the stress is then divided into a mean stress σ_o and a variable stress σ_v. If σ_{max} and σ_{min} are the maximum and minimum nominal stresses, then $\sigma_o = \frac{1}{2}(\sigma_{max} + \sigma_{min})$ and $\sigma_v = \frac{1}{2}(\sigma_{max} - \sigma_{min})$.

In figuring the variable stress σ_v a fatigue strength reduction factor K_f should be used. To be on the safe side, in the absence of actual test data the value of K_f may be taken equal to the theoretical stress concentration factor K_t (see Page 125). In some cases the actual fatigue factor K_f may be appreciably below K_t, but in other cases the two factors may be nearly equal. Fatigue tests indicate that this is particularly true of the fine-grained, high-strength materials used for springs. For this reason the theoretical stress concentration factors given in the following sections probably will be satisfactory for use until more test data are available.

Holes—Frequently it is desirable or necessary to provide a hole in a flat spring for holding the spring in place or for manu-

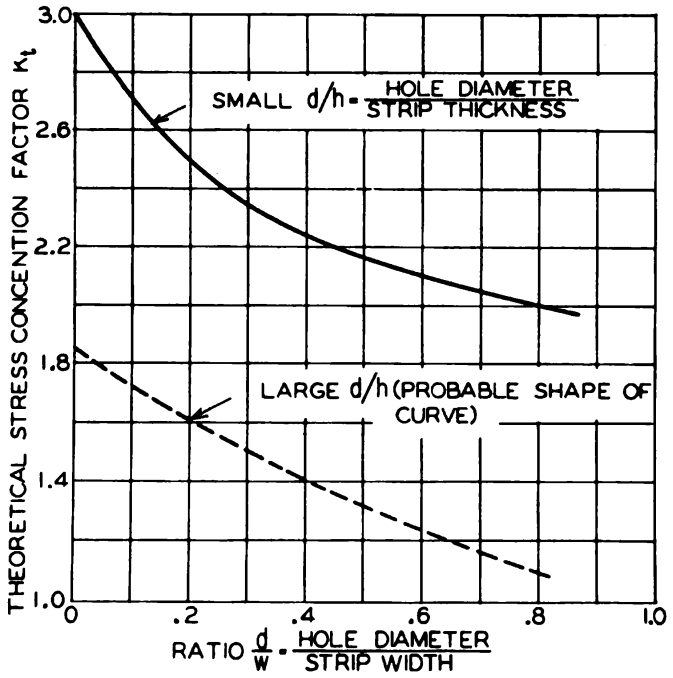

Fig. 161—Theoretical stress concentration factors for strips with holes in bending. Note that the lower curve may also be used for semicircular notches

facturing reasons. A common example is the semielliptic automobile leaf spring which usually is provided with a hole in the center. A bolt through this hole holds the leaves together and

prevents relative motion between the leaves.

For flat springs having holes small in diameter relative to the spring thicknesses as shown in *Fig.* 160 (this may occur in large and heavy plate springs), it appears reasonable to apply the results of photoelastic tests on tension bars with holes[6]. The

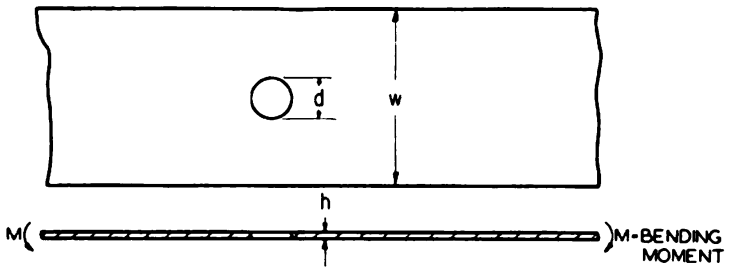

Fig. 162—Flat spring with hole large in diameter compared to thickness. In this case where d/h is large considerably lower stress concentration factors may be expected. For small ratio d/w and d/h, factor is 3 compared to 1.85 for small d/w and large d/h ratios

upper curve of *Fig.* 161 shows values of theoretical stress concentration factor K_t determined photoelastically as a function of ratio d/w between hole diameter and plate width. Thus where this ratio is small the factor K_t approaches 3, a well known result for a plate in tension. However, for small holes it is possible that the actual fatigue strength reduction factor K_f will be considerably less than 3 since the "size effect" may be pronounced.

On the other hand, for thin springs (for example, those made of clock spring material) where the hole diameter d is large compared to the strip thickness h as shown in *Fig.* 162, both tests and theory indicate considerably lower values of K_t will exist than is the case where d/h is small. A mathematical analysis by Goodier[7] shows that for a small hole in a wide strip under pure bending in one direction where d/h is large this factor $K_t = 1.85$. This value is considerably smaller than the value of 3 found for a thicker plate where d/h is small. Since when the hole diameter approaches the strip width a factor of 1 may be expected,

[6] *Transactions* ASME, Aug., 1934, Page 617, and *Mechanical Engineering*, Aug., 1936, Page 485 discuss descriptions of such tests, together with theoretical stress concentration factors.

[7] *Philosophical Magazine*, V. 22, 1936, Page 69. This work has also been checked experimentally by C. Dumont using strain-measurements on a large aluminum plate. See N.A.C.A. *Technical Note* No. 740. Values of $K_t = 1.59$ were found for $d/w = .145$ and large d/h.

the probable shape of this curve is that shown dashed in *Fig.* 161 for large d/h.

The practical use of these stress concentration factors is illustrated by the curve of *Fig.* 163 which shows an estimated endurance diagram for a very high quality spring-steel strip in a ground and polished condition (thickness .006-inch). The endurance limit of this material was found by tests (carried out by T. F. Hengstenberg of the Westinghouse Research Laboratories) to be $\pm 130{,}000$ pounds per square inch in reversed bending while the ultimate strength was 275,000. It may be expected that the material when subject to a stress range between σ_{min} and σ_{max} will have a characteristic approximately as shown by the full lines of *Fig.* 163. Thus the stress range for complete reversal is between points A and B or between $+130{,}000$ and $-130{,}000$ pounds per square inch. For a range from 0 to maximum the limiting points are G and H from 0 to 180,000. Now, if a small hole is put into the strip, assuming that d/w is small and d/h large (*Fig.* 162) the factor $K_t = 1.85$. Since this material will probably be fairly sensitive to stress concentration, it may not be so far off to assume that the fatigue strength reduction factor K_f is approximately equal to this value. On this basis a strip with a hole would show a diagram as indicated by the dashed lines of *Fig.* 163, the point C and D representing nominal stresses of $130{,}000/1.85 = \pm 70{,}000$. The ordinates between the mean stress line σ_o and either the upper or lower full line are also divided by 1.85. Thus a zero to maximum stress range for the strip with the hole is represented by the line EF or 0 to 112,000 pounds per square inch. In this case, therefore, the strength for this type of stress application has been reduced by the presence of the hole from 180,000 to 112,000 pounds per square inch or by a factor of $180{,}000/112{,}000 = 1.6$. This is considerably less than the fatigue strength reduction factor assumed for completely reversed stress which was 1.85. This difference is a consequence of the assumption that stress concentration effects may be neglected as far as the static component of the applied stress is concerned.

It should be noted that actual tests would probably show a somewhat higher endurance limit for the strip with a hole than the figures determined in this way, due to "size effect" for such thin material; in any case, however, the method of calculation

should be on the safe side for design. Also the assumption that stress concentration effects may be neglected in calculating the static component of stress may not be entirely correct (See Page 131), and this may introduce a further deviation between the theoretical and test results.

The curve of *Fig.* 163 represents the values to be expected

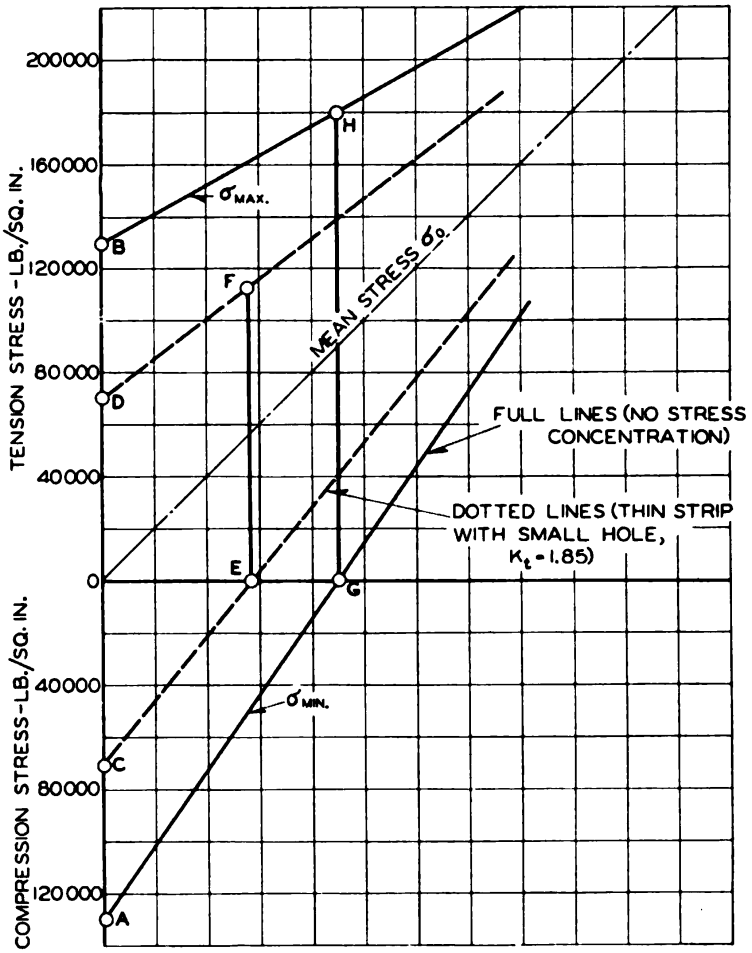

Fig. 163—Endurance curves for a high-grade spring-steel strip, thickness .006-inch, surface ground and polished

for an exceptionally high-grade strip material in a very thin size (.006-in.) and with the surface in good condition, i.e., ground and polished. For the thicker sections, such as are used in leaf and plate springs, with the surface in the condition left by rolling

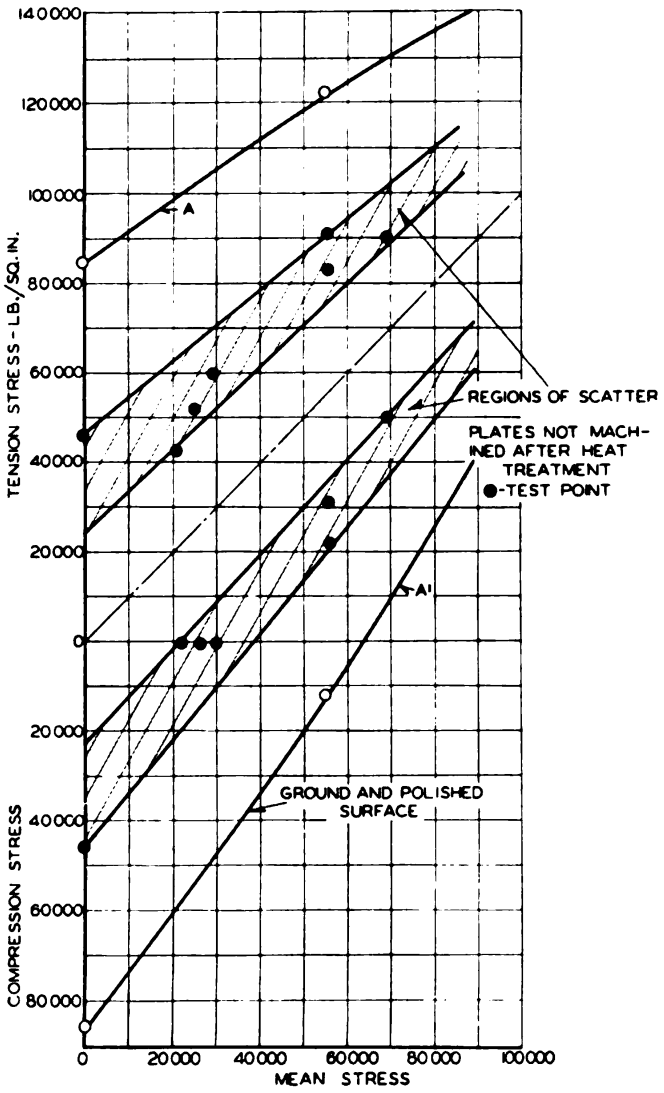

Fig. 164—Typical endurance curves on leaf spring material

and not ground after heat treatment on the basis of available test data very much lower values of endurance limit may be expected than those shown in *Fig.* 163. The results of endurance tests on typical steels as used in leaf springs are indicated in *Fig.* 164. The upper and lower curves *A* and *A'* represent the results of tests on typical steel plates as used in leaf springs with surfaces ground to remove the decarburized layer left by heat treatment. The points in the shaded area represent test results

reported by Hankins[8], Batson and Bradley[9], and Houdremont and Bennek[10] on springs with the surfaces untouched after heat-treatment. It may be expected that, for leaf springs the results of endurance tests will fall somewhere within the shaded area shown; in any case a lowering of the endurance range to from ¼ to ½ that found for machined or ground specimens is to be expected as a consequence of the decarburized surface layer

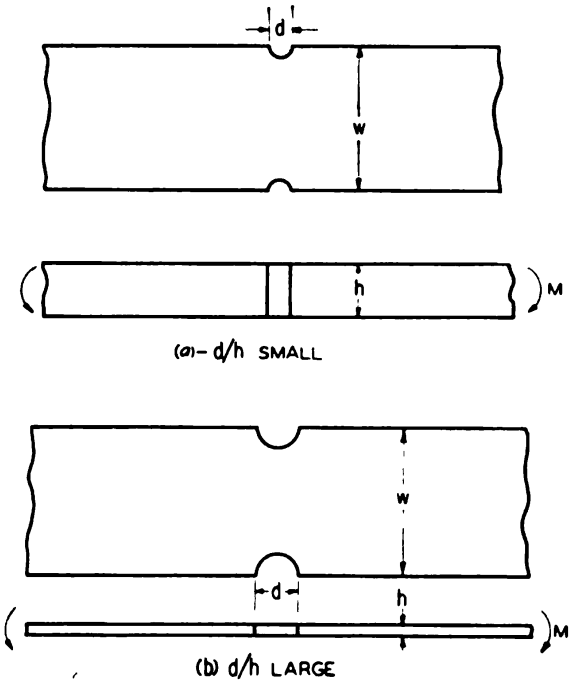

Fig. 165—Strips with notches in bending. Where *d/h* is small as in *a*, use curve of *Fig.* 166. Where *d/h* is large as in *b*, use lower curve of *Fig.* 161

left by heat treatment. However, for high quality materials and carefully controlled heat treatments it is possible that improved results may be obtained over the values indicated on *Fig.* 164.

It should be noted that if stress concentration effects (holes, notches, etc.) are present, the values of limiting stress range as shown in *Fig.* 164 are reduced still lower.

[8] Department of Scientific and Industrial Research, (British) Spec. Report No. 5.
[9] *Proceedings*, Institution of Mechanical Engineers, 1931, Page 301.
[10] "*Federstaehle*", published in Stahl und Eisen, July 7, 1932, Page 660.

Notches—Sometimes it is necessary for various practical reasons to cut small notches in the sides of flat springs. When these notches are of semicircular form, the stress concentration effect may be estimated as follows: If the strip is relatively thick so that the ratio d/h between notch diameter and spring thickness is small as indicated in *Fig.* 165*a*, it appears reasonable to apply the results of photoelastic tests on notched bars in tension[11]. In *Fig.* 166, values of the theoretical stress concentration

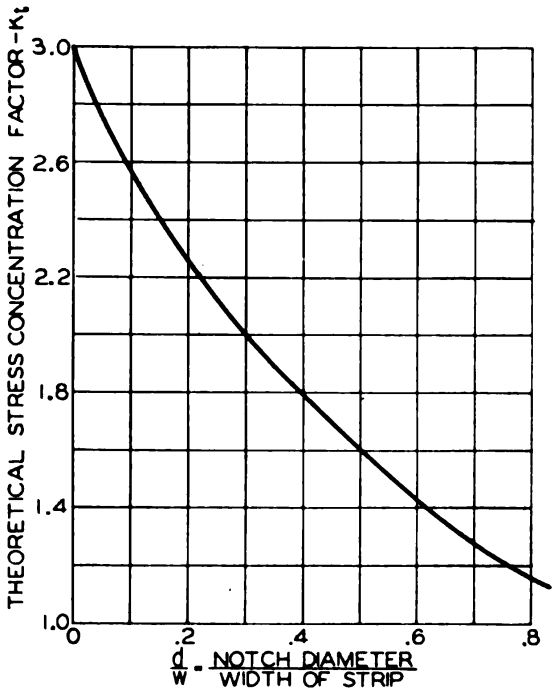

Fig. 166—Theoretical stress concentration factors for semicircular notches in thick strips, small d/h

factor K_t as found in this way are plotted as a function of the ratio d/w between notch diameter and plate width.

For semicircular notches in thin strip materials as shown in *Fig.* 165*b* where the ratio d/h is large, it is reasonable to expect that the factor K_t would be practically the same as that for a strip with a hole of the same diameter d and the same width w. It is, therefore, suggested that the lower curve of *Fig.* 161 may also be used as an approximation for this case. The dashed curve

[11] References in Footnote 6 discuss results of such photoelastic tests.

of *Fig.* 163, may, therefore, represent the endurance diagram for the case of a wide strip with semicircular notches under bending (where d/h is large, d/w small).

Sharp Bends—In forming flat springs, sharp bends are frequently used. An example of this is the bend at *A* in the spring

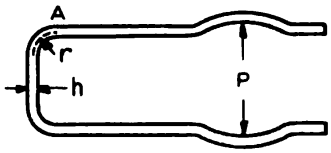

Fig. 167—Spring clip showing stress concentration effect due to sharp curvature of bend at *A*

clip shown in *Fig.* 167. Because of their sharp curvature, these bends introduce a further stress concentration effect which may be taken into account for repeated loading by using a stress concentration factor K_t derived from curved bar theory[12]. Values of K_t thus found for various values of the ratio r/h between mean radius of bend and thickness of material are given in *Fig.* 168. It may be seen that this factor K_t increases rapidly as r/h approaches unity. The importance of avoiding very sharp bends in such springs, particularly when subject to repeated loading is obvious.

Clamped Ends—Mention was made previously of the effect of clamping the ends of plate springs in certain applications. Such clamping is frequently necessary but because of the clamping pressures, a certain amount of stress concentration is set up as at *A*, *Fig.* 169. Under fatigue loading this will result in a reduction of fatigue strength below that obtained when the spring is tested in the form shown by the dashed line *b* in *Fig.* 169 which practically eliminates stress concentration. In addition, under repeated loading there is also a certain amount of rubbing at the clamped edges, point *A*, which results in this so-called rubbing corrosion or brown rust. This latter results in a further lowering of the fatigue strength which may be particularly great for the higher strength materials.

Although there appears to be little data available on the subject, particularly as applied to spring steels, some results of fatigue tests were published by Hankins[8]. These tests were made

[12] This theory is discussed more fully in Chapter XVII.

on flat specimens of leaf spring steel (⅜-inch thick) with the surface left untouched after heat treatment, the loading conditions being essentially those of *Fig.* 169. When the specimens were clamped and of uniform width the endurance limit in completely reversed bending stress for a .48 per cent carbon steel

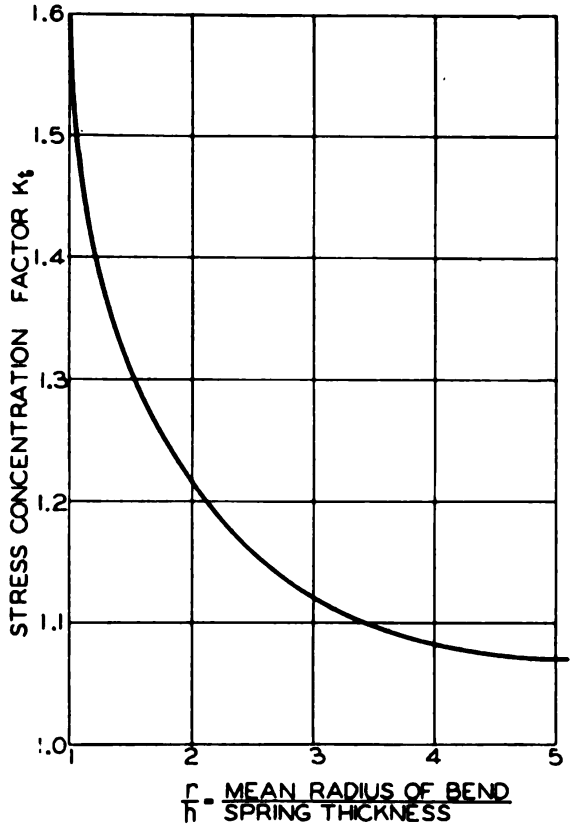

Fig. 168—Stress concentration factors K_t for sharp bends in flat springs

was ±33,600 while tests on the specimens without stress concentration showed an average value of ±47,000. The fatigue strength reduction factor K_f therefore, was 47,000/33,600=1.4. Similar tests on a .6 per cent carbon spring steel showed a reduction in endurance limit from 60,500 to 45,000 and a fatigue factor K_f of 1.35. No data were given as to the actual clamping pressures in these tests. It should be noted that for higher strength materials (where the surface has been ground after heat treat-

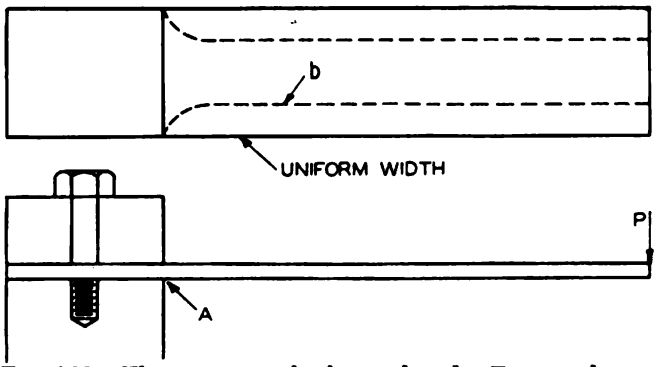

Fig. 169—Flat spring with clamped end. Due to clamping pressure, stress concentration occurs at *A*

ment) much larger values of K_f than these are possible. For example, in press fits as used in roller and ball bearings where a similar condition exists, values of K_f as high as 3 to 4 have been found when alloy steels shafts are used. For a medium-carbon-steel collar pressed on a 2-inch diameter carbon-steel shaft values of K_f ranging from 1.4 to 2, depending on fit pressure, may be expected[13].

APPLICATIONS OF FLAT SPRINGS

A sketch showing a rather unusual application where the use of flat springs worked out advantageously is the lateral extensometer[14] shown in *Fig.* 170. The purpose of this instrument (used in photoelastic work) is to measure minute lateral contractions which occur in a model of Bakelite when stressed. These are of the order of .001-inch total; to obtain say one per cent accuracy it is necessary to measure these movements to .00001-inch. It is well known that these lateral contractions are directly proportional to the sum of the *principal stresses*[15] at any point in a flat specimen under load. By thus determining the sum of these stresses at any point, and determining their difference by well known photoelastic methods the complete stress

[13] Article by Peterson and Wahl, "Fatigue of Shafts at Fitted Members", *Journal Applied Mechanics*, 1935, Page A-1 gives further details.

[14] *Machine Design*, Nov., 1939, presents a more complete description of these extensometers.

[15] If a square element is imagined as cut out of a flat specimen under load and if this element is imagined to be rotated until no shearing stresses act on its sides, the two stresses acting on perpendicular planes are called *principal stresses*.

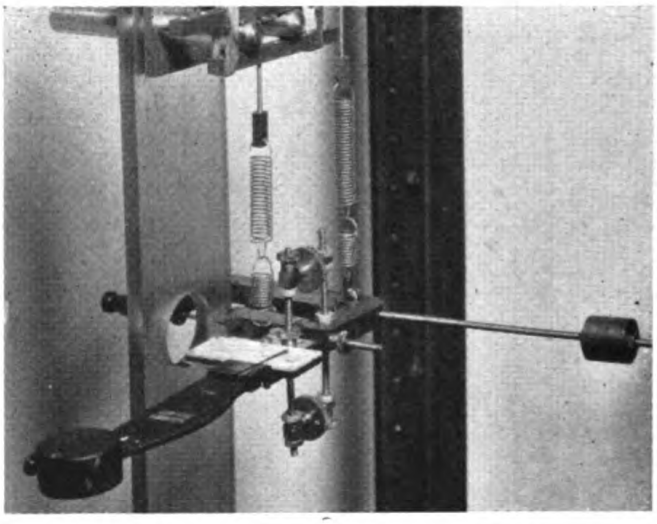

Fig. 170—Lateral extensometer utilizes flat springs

distribution in the test specimen may be found.

A sketch of this lateral extensometer is shown in *Fig.* 171. The two rounded points *P* and *P'* are pressed lightly against the Bakelite test specimen, the pressure exerted by the flat springs *C* and *C'* being sufficient to hold the points at a definite location on the test specimen. The whole assembly is supported by the helical springs shown in *Fig.* 170, a static balance of the instrument being effected by means of the weights shown. Because of the considerable flexibility of the supporting helical springs, slight movements of distortions of the test specimen may occur without

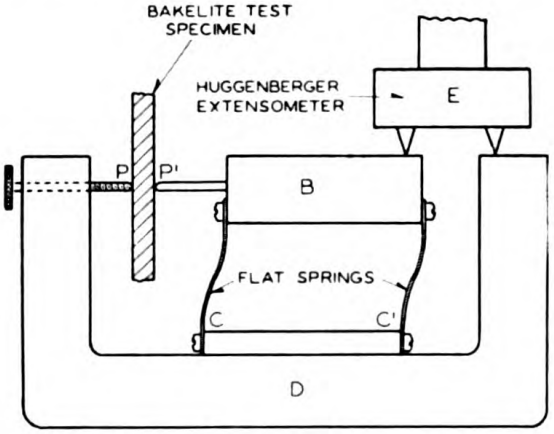

Fig. 171—Sketch of lateral extensometer

causing lateral slippage of the points P and P' (*Fig.* 171) resting on the specimen.

From *Fig.* 171 it may be seen that any lateral contraction of the test specimen will cause a relative motion of points P and P' which in turn results in a motion of the bar B with respect to the frame D. This motion is recorded on the Huggenberger extensometer E whose points are held against the instrument by a clamp not shown.

Another application where flat springs have been used to form elastic hinges[16] is the short gage-length extensometer shown sche-

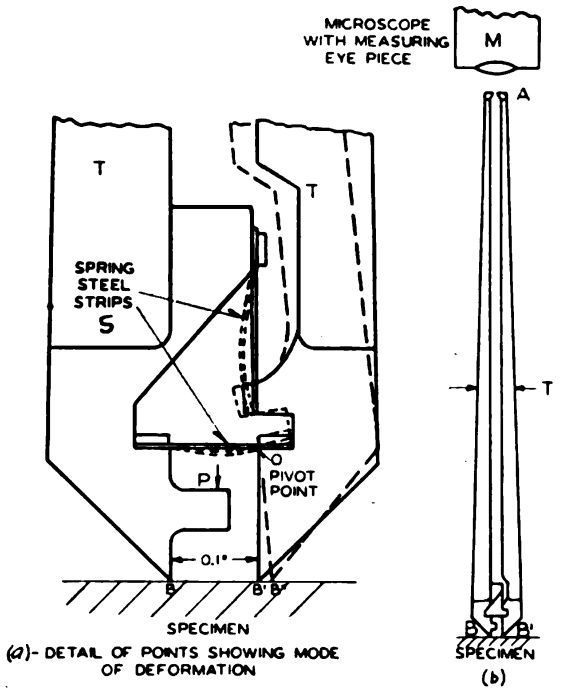

Fig. 172—Schematic sketch for arrangement of short gage length extensometer

matically in *Fig.* 172. This instrument is used in the determination of stress concentration where a short gage-length is necessary. Essentially the instrument consists of two light, hollow tubes attached to two knife edges B and B'. These knife edges are held together by the spring steel strips S (*Fig.* 172*a*) which are

[16] Paper by W. E. Young, "An Investigation of the Cross-Spring Pivot", presented at 1943 Annual A.S.M.E. meeting gives design formulas for elastic hinges. These may be used for deflection angles as high as 45 degrees.

essentially flat springs. The extensometer points are pressed against the specimen by means of a special clamping arrangement shown in *Fig.* 173. Referring to *Fig.* 172*a* when deformation of the specimen occurs point B' moves to say B''. This causes rotation of the movable lever arm T as indicated by the dashed lines, with resulting deformation of the spring steel strips. The result is that the whole assembly pivots about the point O, and because of the length of the lever arms a considerable magnification takes place (about 35 in this case). Thus any relative motion of points B and B' is thus communicated to the targets A after being magnified by the lever ratio. The relative motion of the targets A is determined by means of a microscope with a measuring eyepiece. By this method a high magnification is obtained.

In designing the flat strips S (*Fig.* 172*a*) it was necessary to make them stiff enough so that buckling due to the clamping load will not occur, while at the same time sufficient flexibility must be present so that no appreciable restraint to the deformation of the specimen is imposed. By using flat springs in this way, the use of knife edges with their disadvantages was avoided.

Further application of flat springs is shown in the special clamp (*Fig.* 173) used for holding the extensometer points against the test specimen. The clamping pressure is supplied by the U-shaped magnet shown. The flat springs D and D' allow a horizontal motion of the clamp when the screw E is turned.

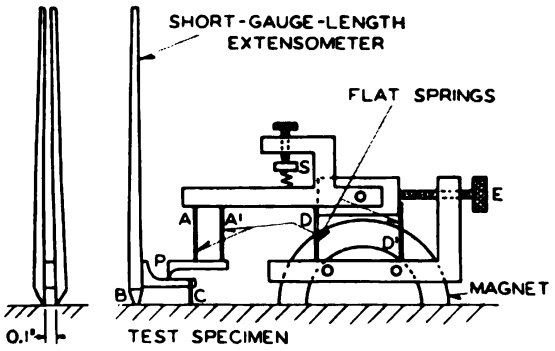

Fig. 173—Sketch of special clamp for extensometer

By this means the point P may be located accurately. A definite load is applied to the extensometer by compressing the helical spring S a given amount. It is important to maintain a definite clamping load sufficiently high to prevent slippage of the points and yet not so high as to cause buckling of the flat springs. A

lateral adjustment of the clamping point P (not shown) is also provided. The strip A' is essentially a flat spring while A is a thin round bar. The purpose of this arrangement is to allow slight movements of the extensometer relative to the clamp,

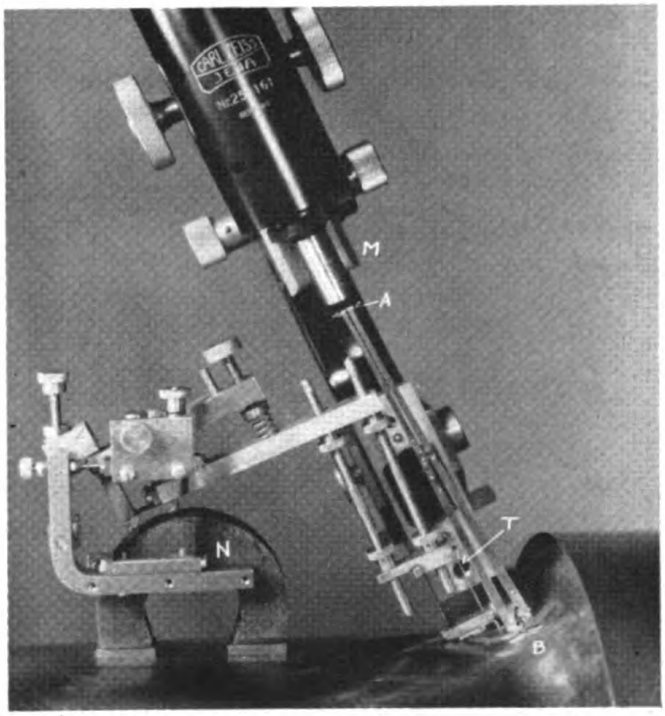

Fig. 174—View of extensometer and magnet clamping arrangement shown in position on shaft fillet

caused by distortion of the test specimen, both laterally and longitudinally without resulting in lateral forces which may cause distortion in the instrument or slippage of the gage points. Either of these latter effects would produce errors in the results. The flexible strip C makes possible a three-point support for the clamping load P, while at the same time slight distortions of the specimen between points B and C may be taken up by deflection of the strip without imposing appreciable lateral load on the points. In designing these flat springs it was again necessary to guard against buckling under the action of the clamping force.

A view of the extensometer clamped on to a large shaft fillet is shown in *Fig.* 174. The microscope M, the target A, the flexible strips T, the points B, and the magnet N are indicated.

CHAPTER XVII

HELICAL TORSION SPRINGS

Helical torsion springs have essentially the same shape as helical compression or tension springs except that the ends are formed in such a way that the spring may be subject to torque about the coil axis. Because of the mode of stressing such springs the primary stress is *flexural,* in contrast to the helical compression or tension spring where the primary stress is *torsional.* Some typical shapes of ends for torsion springs are shown in *Figs.* 175 and 176. The design of spring end is made primarily from the point of view of transmitting external torque to the spring. Tor-

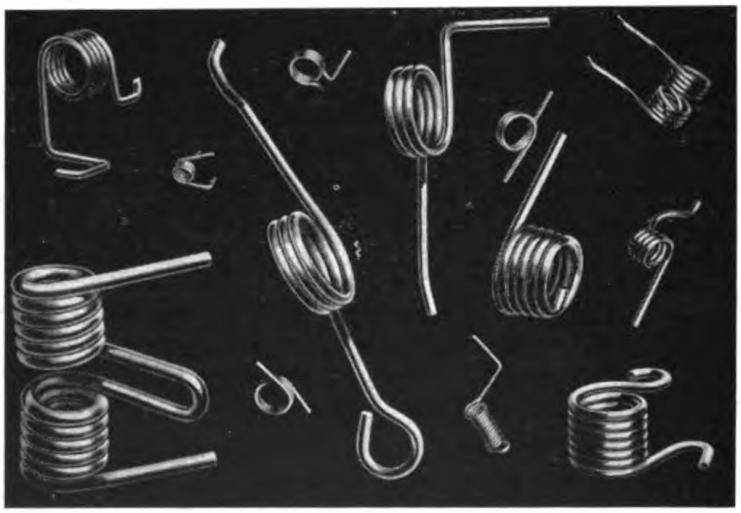

—Courtesy, Wallace-Barnes Co.

Fig. 175—Typical group of torsion springs

sion springs are used in a wide variety of applications among which may be mentioned door hinge springs, springs for starters in automobiles and springs for brushholders in electric motors.

Loading—A typical method of loading a torsion spring is indicated in *Fig.* 177. Here the spring is supposed to be wound around a rod, one end of it being fastened to the rod while the other has a straight portion projecting outward. If this arm is

loaded by a force P at a radius R from the axis in such a manner as to wind the spring, then the moment tending to twist the spring will be PR as indicated in the figure. Because of friction between the spring and guide, the actual moment may decrease along the spring so that an exact calculation becomes involved.

Since most torsion springs are wound cold, it is advisable to load them in such a way that the spring tends to wind up as the

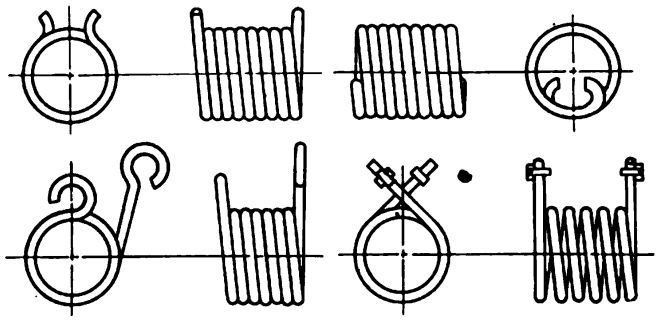

Fig. 176—Various styles of ends used in torsion springs

load is applied. The reason for this is that the residual stresses set up as a consequence of the cold winding are in such a direction as to subtract from the peak stress due to the loading, provided that the load is in the same direction as that in which the

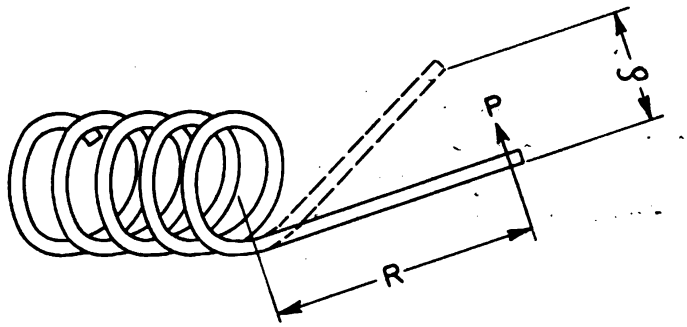

Fig. 177—Torsion spring subject to force P at radius R

spring was wound. If the direction of loading is such as to unwind the spring, it is advisable to heat treat by means of a bluing treatment to remove such residual stresses.

There is another reason for loading the spring in this man-

ner. Referring to *Fig.* 177 for a load tending to wind up the spring, the reaction will be against the arbor and the peak bending moment in the spring will be PR. However, if the load is in the opposite direction to that shown, the peak moment will be $P(R+r)$ where r is the mean coil radius. This means a considerable increase in stress, particularly if r is about as large as R.

End Conditions—For many cases where the ends of the spring are clamped, or if special ends are used, some stress concentration may be expected near the ends. These stress concentrations should be carefully considered particularly if the spring is subject to fatigue loading, or if it is to be subject to a large number of load repetitions during its life. On the other hand, if the number of load applications is small during the spring life, such stress concentrations may probably be neglected.

Binding—Because a torsion spring (for usual applications) tends to wind up with load, its diameter decreases. In design it is important that sufficient clearance be allowed between the arbor or rod, about which the spring is wound, and the inner diameter of the spring. If this is not done, the spring may bind or wrap around the arbor and high stresses may be set up. The clearance necessary may be estimated from the calculated deflection of the ends of the spring as given by Equation 367. Thus, if the spring end deflects 90 degrees or ¼-turn and the spring has 8 turns, the diameter will change in the ratio of ¼ to 8 or about 3 per cent. This can be allowed for in design.

If the spring fits inside a tube and is loaded so as to unwind, sufficient clearance must be allowed between the outside diameter of the spring and the inside diameter of the tube. This clearance may be estimated in the same manner as before.

Buckling—Sometimes quite long torsion springs are used. Where this is done, there is always the possibility of torsional buckling. This may be avoided by providing such springs with guides such as rods or tubes. By properly clamping the ends or by applying an initial tension load, it is possible to avoid buckling in some cases without the use of guides.

Wire Section—Usually for manufacturing reasons, torsion springs are made of round wire. However, where maximum energy storage is required in a given space, the use of square or rectangular wire may be advisable. The reason for this is that

in bending, the square or rectangular section has a larger proportion of material subjected to stresses near the peak value than is the case for circular wire. Consequently, for the same peak stress, greater energy storage may be obtained for a given volume of material for square or rectangular wire than for circular wire. Also, for a given spring index, more material may be compressed within a given outside diameter in the case of rectangular wire; this further increases the amount of energy which may be stored in a given space. Chapter XXII discusses this further.

THEORY

If the ends are properly designed, most torsion springs may be considered as subject to a pure bending moment about the axis of the coil. For the usual small pitch angles, the spring may

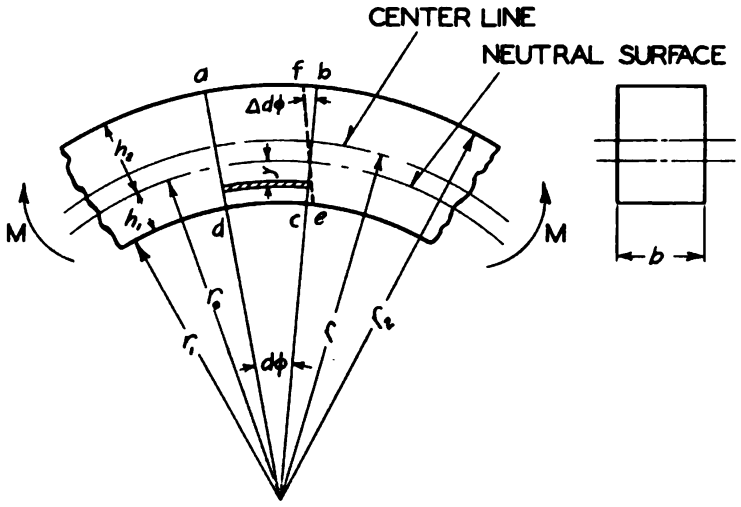

Fig. 178—Torsion spring element acted on by bending moment M

also be assumed as a curved bar subject to a bending moment M, and the results of curved bar theory may be applied[1].

Considering an element *abcd, Fig.* 178, cut from the spring by two neighboring planes passing through the center of curvature (or the spring axis) and including a small angle $d\phi$, the radius of the center line of the bar, ½ the mean coil diameter, is

[1] Timoshenko—*Strength of Materials*, Part II, Second Edition, page 65 gives a further discussion of this theory.

designated by r. At a certain radius r_o there will be no stress in the spring; the surface corresponding to this radius is known as the *neutral surface.*

When a bending moment M acts on this element, if it is assumed that plane cross sections normal to the center line remain so after bending, the section bc deflects through a small angle $\Delta d\phi$ and takes up the position ef.

Length of the longitudinal element shown shaded at a distance y from the neutral surface is $(r_o - y)d\phi$ before bending occurs. After bending, the length increases by an amount $y(\Delta d\phi)$. The unit elongation will thus be

$$\frac{y(\Delta d\phi)}{(r_o - y)d\phi}$$

and the stress σ_x acting will be this elongation times the modulus of elasticity of the spring material. Thus,

$$\sigma_x = \frac{Ey(\Delta d\phi)}{(r_o - y)d\phi} \qquad (345)$$

This equation shows that the stress distribution across the section is hyperbolic in form as indicated in the diagram of *Fig.* 179.

To determine the unknown radius r_o of the neutral surface, and the unknown angular deflection $\Delta d\phi$, two equations are needed. These are obtained from two conditions:

1. The sum of the normal forces acting over a radial cross section must be zero since no net external force (but only an external moment) acts
2. The sum of the moments of the elementary forces about the neutral axis must be equal to the external moment M.

If dA is the element of area over which the stress σ_x acts $dA = bdy$ for a rectangular cross section where b is the width of the cross section. Then, from the first condition mentioned, using Equation 345,

$$\int \sigma_x dA = \frac{E(\Delta d\phi)}{d\phi} \int \frac{y dA}{r_o - y} = 0 \qquad (346)$$

From the second condition,

$$\int \sigma_x y dA = \frac{E(\Delta d\phi)}{d\phi} \int \frac{y^2 dA}{r_o - y} = M$$

This latter equation may be written as

$$\frac{E(\Delta d\phi)}{d\phi}\int\frac{y^2dA}{r_o-y}=\frac{-E(\Delta d\phi)}{d\phi}\int\left(y-\frac{r_oy}{r_o-y}\right)dA=M$$

Since

$$\int\frac{r_oy}{r_o-y}dA=0$$

from Equation 346, this gives

$$\frac{E\Delta d\phi}{d\phi}\int ydA=M \qquad \text{.....(347).}$$

Letting e be the distance of the centroid of the section from the neutral axis, then,

$$\int ydA=Ae$$

Substituting this in Equation 347,

$$\frac{E(\Delta d\phi)}{d\phi}=\frac{M}{Ae}$$

Using this in Equation 345, the expression for stress σ_x becomes

$$\sigma_x=\frac{My}{Ae(r_o-y)} \qquad \text{.....(348)}$$

For springs of circular and rectangular cross sections the maximum stress will occur at the inside surface of the spring where $y=h_1$ and $r_o-y=r_1$, the inside radius of the bar, *Fig.* 178. Hence, substituting these values in Equation 348, expression for maximum stress σ_{max} at the inside of the coil, *Fig.* 179, becomes

$$\sigma_{max}=\frac{Mh_1}{Aer_1}$$

The stress σ_{min} on the outside of the coil is obtained by taking $y=-h_2$ and $r_o-y=r_2$ in Equation 348. Thus,

$$\sigma_{min}=\frac{-Mh_2}{Aer_2}$$

In this the negative sign signifies compression for the direction of the moment M indicated in *Fig.* 178.

RECTANGULAR BAR TORSION SPRINGS

For a rectangular cross section of width b, *Fig.* 178, $dA=bdy$ and, by substitution in Equation 346,

$$\int \frac{ydA}{r_o-y}=\int_{-h_2}^{h_1}\frac{ybdy}{r_o-y}=0 \qquad (349)$$

By integrating this equation, the value of r_o may be determined. However, the calculation is facilitated by the following method suggested by Timoshenko[2]. Letting $y_1=y+e$ where y_1 is the distance of a point on the cross section from the centroid, then, since $r_o-y=r-y_1$ and $e=r-r_o$, from Equation 349

$$\int \frac{ydA}{r_o-y}=\int\frac{(y_1-e)dA}{r-y_1}=\int\frac{y_1dA}{r-y_1}-e\int\frac{dA}{r-y_1}=0 \qquad (350)$$

Letting

$$\int\frac{y_1dA}{r-y_1}=mA \qquad (351)$$

Also, using Equation 351,

$$\int\frac{dA}{r-y_1}=\frac{1}{r}\int\left[1+\frac{y_1}{r-y_1}\right]dA=\frac{A}{r}(1+m) \qquad (352)$$

By substituting Equations 351 and 352 in Equation 350,

$$mA-\frac{e(1+m)A}{r}=0$$

or

$$e=r\left(\frac{m}{1+m}\right) \qquad (353)$$

To calculate the value of m for a rectangular cross section, the

[2] Loc. cit. Page 72.

term $1/(r—y_1)$ in Equation 351 may be expressed in series form

$$\frac{1}{r-y_1}=\frac{1}{r}\left(1+\frac{y_1}{r}+\frac{y_1^2}{r^2}+\frac{y_1^3}{r^3}+\ldots+\left(\frac{y_1}{r}\right)^{n-1}+\ldots\right)$$

Substituting this in Equation 351, taking $dA=bdy_1$, and solving for m,

$$m=\frac{1}{h}\int_{-h/2}^{h/2}\frac{y_1dy_1}{r-y_1}=\frac{1}{h}\int_{-h/2}^{h/2}\left(\frac{y_1}{r}+\frac{y_1^2}{r^2}+\frac{y_1^3}{r^3}+---\right)dy_1$$

Integrating and putting $c=2r/h$, the value of m becomes

$$m=\frac{1}{3c^2}+\frac{1}{5c^4}+\frac{1}{7c^6}+\cdots+\frac{1}{(2n+1)c^{2n}}+\ldots\ldots\ldots\ldots\ldots\ldots\ldots\ldots\ldots\ldots(354)$$

Since $h_1=(h/2)—e$ for rectangular section, by substitution of the value of e given by Equation 353,

$$h_1=\frac{h}{2}-\frac{rm}{1+m}\ldots\ldots\ldots\ldots\ldots\ldots\ldots\ldots\ldots\ldots\ldots\ldots\ldots\ldots\ldots\ldots\ldots\ldots\ldots\ldots(355)$$

Maximum Stress—Substituting Equations 353 and 355 in Equation 348, and taking $r_1=r—h/2$ and $A=bh$, the maximum stress for a rectangular section becomes

$$\sigma_{max}=\frac{M\left(\frac{h}{2}-\frac{rm}{1+m}\right)}{bh\left(\frac{rm}{1+m}\right)\left(r-\frac{h}{2}\right)}$$

Putting in this equation, the spring index $c=2r/h$ for a rectangular section,

$$\sigma_{max}=\frac{M}{bhr}\left(\frac{1+\frac{1}{m}-c}{c-1}\right)\ldots\ldots\ldots\ldots\ldots\ldots\ldots\ldots\ldots\ldots\ldots\ldots\ldots\ldots\ldots\ldots\ldots\ldots\ldots\ldots(356)$$

For practical springs where c is over three, the series of Equation 354 for m converges very rapidly and sufficient accuracy for practical purposes may be obtained by taking two terms. This gives

$$m=\frac{1}{3c^2}+\frac{1}{5c^4}=\frac{1}{3c^2}\left(1+\frac{.6}{c^2}\right)$$

Since the term $.6/c^2$ in this equation is very small compared to unity for most practical springs, this may be written:

$$m=\frac{1}{3c^2}\left(\frac{1}{1-\frac{.6}{c^2}}\right)=\frac{1}{3c^2-1.8}$$

Substituting this value for m in Equation 356, the maximum stress becomes

$$\sigma_{max}=K_2\frac{6M}{bh^2} \quad \text{.....(357)}$$

where

$$K_2=\frac{3c^2-c-.8}{3c(c-1)}$$

It is seen that this formula is simply the ordinary formula for stress in a rectangular bar subject to a bending moment M (i.e., $6M/bh^2$) multiplied by a factor K_2 greater than unity which depends on the spring index c and which may be considered as a stress concentration factor. Values of K_2 are plotted as functions of c in *Fig.* 180. It is seen that, as would be expected, the value K_2 drops with increase in index, since the spring bar then approaches the condition of a straight bar under a bending moment. For a spring with an index of 3, the correction factor $K_2=1.30$, which means that the peak stress is about 30 per cent greater in this case than that figured by the usual formula in which the effect of curvature is neglected.

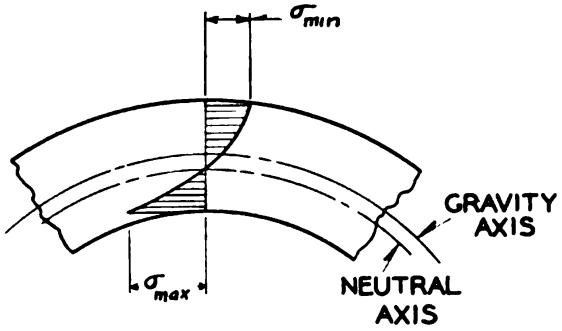

Fig. 179 — Hyperbolic distribution of stress in helical torsion spring

Deflection—To calculate the *deflection* of a torsion spring of rectangular or square-section wire, the usual beam equation

may be used[2]. Neglecting effects of friction and assuming that the spring is subject to a constant moment M as before, the angular deflection of an element of the spring of length ds will be

$$d\phi = \frac{Mds}{EI} = \frac{12Mds}{Ebh^3}$$

where I is the moment of inertia of the wire section. The total deflection of the spring (in radians) will be the integral of this, or

$$\phi = \int \frac{12Mds}{Ebh^3} = \frac{12Ml}{Ebh^3}$$

where $l = 2\pi nr$ is the active length of the spring wire and n the

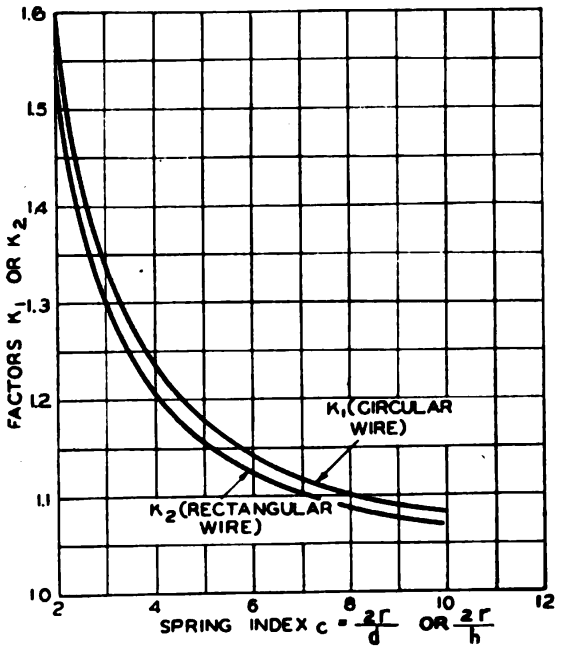

Fig. 180—Torsion stress concentration factors K_1 and K_2 for circular and rectangular wire

number of active coils. Using this value of l, the angular deflection ϕ becomes

[2] Comparison of the usual beam equation with more exact results calculated from curved-bar theory shows that the difference is negligible for practical purposes. This is analogous to helical compression springs, where the usual equation for deflection is accurate enough for most practical purposes, although derived in an elementary way.

$$\phi = \frac{24\pi Mrn}{Ebh^3} \text{ radians} \quad \ldots\ldots (358)$$

The angular twist of the spring in degrees will be 57.3 times this value.

Assuming that the spring is subject to a force P at the end of an arm of length R as indicated in *Fig.* 177, the moment $M = PR$ and the circumferential deflection δ at the end of this arm will be ϕR. Using Equation 358 the deflection at radius R is

$$\delta = \frac{24\pi PR^2rn}{Ebh^3} \quad \ldots\ldots (359)$$

CIRCULAR WIRE TORSION SPRINGS

Maximum Stress—Although the rectangular-wire torsion spring makes a more efficient use of material, springs of circular wire are more frequently used for reasons of economy. The stress in such springs may be figured in a similar way as before. If d is the wire diameter, by using Equation 348 the maximum stress σ_{max} may be expressed as follows:

$$\sigma_{max} = \frac{M\left(\frac{d}{2} - e\right)}{Ae\left(r - \frac{d}{2}\right)} \quad \ldots\ldots (360)$$

To calculate e, a similar procedure may be used as in the case of the rectangular bar spring. From Equation 360, taking $e = rm/(1+m)$,

$$\sigma_{max} = \frac{M\left(\frac{d}{2} - \frac{rm}{1+m}\right)}{Ar\left(\frac{m}{1+m}\right)\left(r - \frac{d}{2}\right)}$$

Taking the spring index $c = 2r/d$ and $A = \pi d^2/4$ for circular wire, this equation may be written

$$\sigma_{max} = \frac{8M}{\pi d^3}\left(\frac{1 + \frac{1}{m}}{\frac{c}{c-1}} - 1\right) \quad \ldots\ldots (361)$$

To find the value of m, Equation 352 is used. Taking

$$dA = 2\sqrt{\frac{d^2}{4} - y_1^2}\, dy_1$$

from *Fig.* 181, this gives

$$\frac{A}{r}(1+m) = \int \frac{dA}{r-y_1} = 2\int_{-d/2}^{d/2} \frac{\sqrt{d^2/4 - y_1^2}\, dy_1}{r-y_1} = 2\pi\left(r - \sqrt{r^2 - \frac{d^2}{4}}\right) \quad (362)$$

Putting $c = 2r/d$, the expression under the radical may be written in series form as follows:

$$\sqrt{r^2 - \frac{d^2}{4}} = r\left(1 - \frac{1}{2c^2} - \frac{1}{8c^4} - \frac{1}{16c^6} - \text{- - - - -}\right)$$

Substituting this in Equation 362, taking $A = (\pi/4)d^2$ and solving for m,

$$m = \frac{1}{4c^2} + \frac{1}{8c^4} + \frac{1}{16c^6} + \text{- - - -}$$

(It should be noted that for a rectangular cross-section, the index $c = 2r/h$; for a circular section $c = 2r/d$)

For practical springs where the index $c > 3$, this series converges rapidly and two terms are sufficient for practical use. Thus

$$m = \frac{1}{4c^2} + \frac{1}{8c^4} = \frac{1}{4c^2}\left(1 + \frac{1}{2c^2}\right) \quad \text{.....(363)}$$

Since the last term in the brackets of this expression is small this equation may be written with sufficient accuracy as

$$m = \frac{1}{4c^2}\left(\frac{1}{1 - \frac{1}{2c^2}}\right) = \frac{1}{4c^2 - 2}$$

Putting this value of m in Equation 361, and simplifying, the expression for maximum stress becomes

$$\sigma_{max} = K_1 \frac{32M}{\pi d^3} \quad \text{.....(364)}$$

where K_1 replaces the following expression

$$K_1=\frac{4c^2-c-1}{4c(c-1)} \quad \ldots\ldots (365)$$

The term $32M/\pi d^3$ in Equation 364 represents the stress figured from the usual formula for a straight circular bar, i.e., stress equals bending moment over section modulus. The factor K_1 represents the stress increase due to the hyperbolic stress distribution, *Fig.* 179. Values of K_1 are plotted as functions of the spring index c in *Fig.* 180. It is seen that for an index of 3 the stress multiplication factor K_1 is about 1.33. It may also be noted from *Fig.* 180 that the values of K_1 do not differ much from those of K_2 for rectangular wire, for the same index.

Deflection—To calculate the deflection of a torsion spring of circular wire the same expression may be used as that used for rectangular wire except that the moment of inertia I is taken as $\pi d^4/64$ in this case. This gives for the angular deflection

$$\phi=\int\frac{Mds}{EI}=\frac{64Ml}{\pi d^4E}$$

Since the effective length $l=2\pi rn$, this expression may be written

$$\phi=\frac{128Mrn}{Ed^4}\ \text{radians} \quad \ldots\ldots (366)$$

If ϕ is given in number of turns, since one turn $=2\pi$ radians, this equation becomes

$$\phi=\frac{64Mrn}{\pi Ed^4}\ \text{turns} \quad \ldots\ldots (367)$$

If the spring is subject to a moment set up by a force P at the end of a lever arm of radius R, *Fig.* 177, then $M=PR$ and the circumferential deflection at this radius will be equal to $R\phi$, where ϕ is given in radians. Hence, using Equation 366, the deflection at the load becomes

$$\delta=\frac{128PR^2rn}{Ed^4} \quad \ldots\ldots (368)$$

Example Calculation—As an example, the design of a brush-holder spring loaded as indicated in *Fig.* 177 will be considered. (This type of spring is used to apply pressure on the carbon

brushes of small motors). Assuming the following dimensions: load arm R=⅞-inch; mean coil-radius r=3/16-inch; wire diameter d=.04-inch; spring index $c=2r/d=9.4$, the load P at the

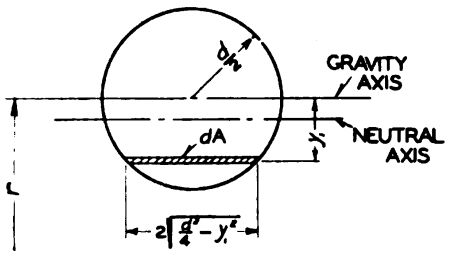

Fig. 181—Curved bar with circular section

end of the lever arm is 1¼ pounds. From *Fig.* 180 the factor K_1 for c=9.4 is 1.08. Using Equation 364 the maximum stress is, taking $M=PR$,

$$\sigma_{max}=K_1\frac{32M}{\pi d^3}=\frac{1.08\times32\times1.25\times.875}{\pi\times(.04)^3}=188000 \text{ lb./sq. in.}$$

If there are 10 active turns, from Equation 367 the deflection in turns is, for $E=30\times10^6$ pounds per square inch,

$$\phi=\frac{64Mrn}{\pi Ed^4}=\frac{64\times1.25\times.875\times.187\times10}{\pi\times30\times10^6\times(.04)^4}=.54 \text{ turns}$$

This corresponds to a deflection of slightly more than 180 degrees.

TABLE XXXI

Suggested Working Stresses for Torsion Springs

(lb./sq. in.)

Spring Material	Wire Size Less than ⅛-inch		Wire Sizes ⅛ to ¼-inch	
	Maximum Working Stress	Maximum Total Stress	Maximum Working Stress	Maximum Total Stress
Music wire	200,000	240,000	180,000	215,000
Oil-tempered wire	180,000	215,000	140,000	180,000
Hard-drawn wire	155,000	180,000	120,000	155,000
Stainless-steel 18-8	155,000	180,000	115,000	145,000
Phosphor bronze	60,000	85,000	48,000	70,000
Brass	45,000	70,000	35,000	60,000

Working Stresses—Working stresses for torsion springs of circular wire up to ¼-inch diameter are suggested by Wallace

[4] *The Mainspring*, June 1941.

Barnes Company[4] as a good guide in designing springs of reasonable proportions for general use. These are shown in TABLE XXXI.

The American Steel & Wire Company (*Manual of Spring Engineering*, Page 36) gives values of maximum design stress varying with the wire size as indicated in TABLE XXXII. These recommended values are for average service conditions, defined as noncorrosive atmosphere, temperatures not exceeding 150 degrees Fahr. and relatively slowly varying or static loads. The

TABLE XXXII

Recommended Maximum Design Stresses

(for average service conditions)

		Kind of Wire		
Material	**Wire Diameter *d***	**Hard Drawn**	**Tempered**	**Music**
Plain carbon steels	.004-.009	.....	.....	280,000
	.010-.020	.....	.....	270,000
	.021-.040	160,000	.....	240,000
	.041-.060	160,000	180,000	220,000
	.061-.080	160,000	180,000	210,000
	.081-.100	140,000	180,000	200,000
	.101-.150	130,000	165,000	185.000
	.151-.225	110,000	145,000	165,000
	.226-.400	.....	135,000	.....
	.401-.625	.....	125,000	.....
Stainless steel 18-8		.....	140,000	.....
Monel metal		.....	60,000	.....
Brass		.....	30,000	.....

working stresses are reduced in general for the larger sizes of wire, as indicated. Values are also given for stainless steel, monel metal and brass.

These stresses will probably be satisfactory when computed using Equations 357 or 364 which take into account the stress augment due to curvature and provided the spring is subject to relatively few cycles of stress during its life.

Where the spring is subject to repeated or fatigue stresses through a considerable range, in general it will be necessary to use lower working stresses than those suggested in TABLES XXXI and XXXII. This is also true if the spring is subject to elevated temperatures so that creep of the material may occur.

CHAPTER XVIII

SPIRAL SPRINGS

Flat spiral springs, consisting essentially of flat strip wound to form a spiral, have many advantages from the standpoint of energy storage within a limited space, particularly if the spring is required to deliver torque. In addition, such springs are relatively simple to manufacture. Because of these advantages, spiral springs are widely used in clocks, watches, electrical instruments and similar devices. Other applications include brush-holder springs, *Fig.* 182, phonograph motors, etc. An un-

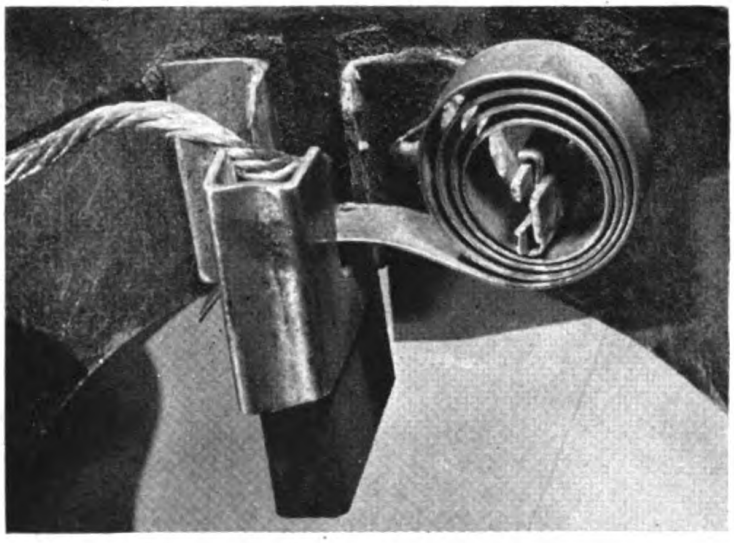

Fig. 182—Spiral brusholder spring for motor

usual use of this type of spring as an energy storing device is shown in the experimental circuit-breaker mechanism of *Fig.* 183.

If the spiral spring is so wound that individual turns do not come in contact, the analysis for the spring may be carried out with considerable accuracy. Such an example is provided by the hairspring of a watch. On the other hand, if the turns of the spring are wound tightly together, as is true of a phonograph motor spring, a different sort of analysis must be made because

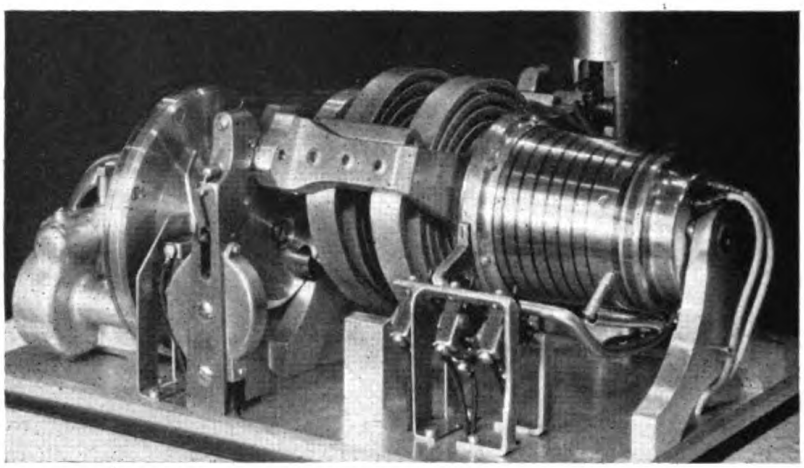

Fig. 183—Experimental mechanism utilizes spiral springs

of friction between turns. These cases will therefore be treated separately, the primary purpose of this chapter being a discussion of the fundamentals of spiral spring calculations.

SPRINGS WITH MANY TURNS WITHOUT CONTACT

Clamped outer end—In the first analysis it will be assumed that the outer end of the spring is clamped by a moment M_1 as indicated in *Fig.* 184. It also will be assumed that the spring has a large number of turns which are, however, separated sufficiently so that adjacent turns do not come in contact during deflection[1]. The inner end of the spring is fastened to an arbor which pivots about point O and is acted on by a torque M_o.

For a built-in condition, at the outer end A of the spring a tangential force P, a radial force R (passing through O) and a moment M_1, will act. The external torque M_o is

$$M_o = Pr + M_1 \quad \ldots\ldots (369)$$

If M is the bending moment at any point of the spiral having the coordinates x and y, then from the statical conditions of equilibrium,

$$M = P(r+y) + M_1 - Rx \quad \ldots\ldots (370)$$

[1]R. V. Southwell—*Theory of Elasticity*, Oxford, Clarendon Press, 1936, Page 66.

Solving for Pr in Equation 369 and substituting in Equation 370,

$$M=M_o\left(1+\frac{y}{r}\right)-M_1\frac{y}{r}-Rx \quad \ldots\ldots\ldots\ldots\ldots\ldots\ldots\ldots\ldots\ldots\ldots\ldots (371)$$

The energy stored in a short length ds of the spring acted on by a moment M is, from ordinary beam theory[2]

$$dU=\frac{M^2ds}{2EI}$$

where E is the modulus of elasticity and I the moment of inertia of the cross section. Where strip material is used as indicated in Chapter XVI, more accurate results will be obtained by replacing E by $E/(1-\mu^2)$ where μ=Poisson's ratio.

Total energy U stored in the spring is

$$U=\int_0^l dU=\int_0^l \frac{M^2ds}{2EI} \quad \ldots\ldots\ldots\ldots\ldots\ldots\ldots\ldots\ldots\ldots\ldots\ldots (372$$

In this the integral is taken over the total length of the spiral.

The Castigliano theorem[2] states that the partial derivative of the stored energy U with respect to a statically indeterminate

[2]Timoshenko, S.—*Strength of Materials*, Part I, Second Edition, Van Nostrand Pages 296 and 308.

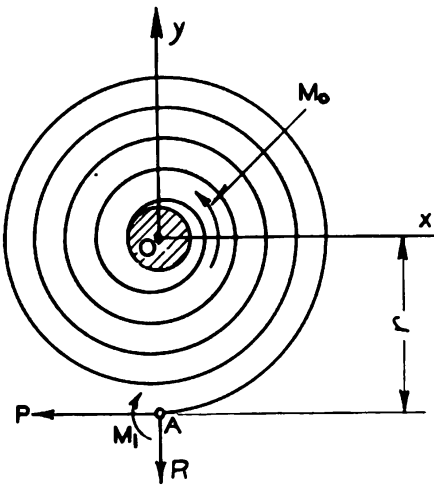

Fig. 184—Spiral spring with large number of turns, clamped outer end

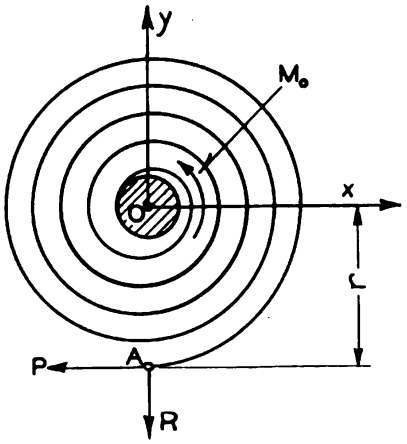

Fig. 185—Pinned outer end of a spiral spring, large number of turns

force or moment which does no work, must be zero. Since neither the force R nor the moment M_1 do work as the spring deflects, this means that

$$\frac{\partial U}{\partial R}=0; \quad \frac{\partial U}{\partial M_1}=0$$

Using Equation 372 and differentiating under the integral sign, these conditions give

$$\int_0^l \frac{M}{EI}\frac{\partial M}{\partial R}ds=0 \qquad (373)$$

$$\int_0^l \frac{M}{EI}\frac{\partial M}{\partial M_1}ds=0 \qquad (374)$$

In these l is the total length of the spiral.

Since EI is assumed constant, from these equations the following conditions hold:

$$\int_0^l M\frac{\partial M}{\partial R}ds=0 \qquad (375)$$

$$\int_0^l M\frac{\partial M}{\partial M_1}ds=0 \qquad (376)$$

From Equation 371,

$$\frac{\partial M}{\partial M_1}=-\frac{y}{r}; \quad \frac{\partial M}{\partial R}=-x$$

Using these equations together with Equation 371 in Equation 376,

$$\int_0^l \left[M_o\left(1+\frac{y}{r}\right)-M_1\frac{y}{r}-Rx\right]\frac{yds}{r}=0 \qquad (377)$$

Similarly, using Equations 371 and 375,

$$\int_0^l \left[M_o\left(1+\frac{y}{r}\right)-M_1\frac{y}{r}-Rx\right]xds=0 \qquad (378)$$

The Castigliano theorem[2] also states that the partial derivative of the stored energy U with respect to an external moment gives

the angular deflection due to this moment. Thus the angular deflection ϕ due to the external moment M_o becomes (using Equation 372)

$$\phi=\frac{\partial U}{\partial M_o}=\int_0^l \frac{M}{EI}\frac{\partial M}{\partial M_o}ds \quad (379)$$

Differentiating Equation 371 with respect to M_o,

$$\frac{\partial M}{\partial M_o}=1+\frac{y}{r} \quad (380)$$

Using Equations 371 and 380 in 379 angular deflection ϕ becomes

$$\phi=\frac{1}{EI}\int_0^l\left[M_o\left(1+\frac{y}{r}\right)-M_1\frac{y}{r}-Rx\right]\left(1+\frac{y}{r}\right)ds \quad (381)$$

Equation 378 may be written

$$\int_0^l M_o x ds+\int_0^l M_o\frac{xy}{r}ds-\int_0^l M_1\frac{xy}{r}ds-\int_0^l Rx^2ds=0 \quad (382)$$

For a spiral spring with a large number of turns, the following equations also hold with sufficient exactitude for practical purposes:

$$\int_0^l x ds=0\ ;\ \int_0^l y ds=0\ ;\ \int_0^l xy ds=0$$

This means that the first three integrals of Equation 382 are zero. Hence

$$\int_0^l Rx^2ds=0$$

Since $\int x^2ds$ cannot be zero it follows from this equation that $R=0$. In other words, at the outer end A of such a spring, *Fig.* 184, the radial load R will be zero. For a small number of turns, this will not be true, however.

From Equation 377,

$$\int_0^l M_o\frac{y}{r}ds+\int_0^l M_o\frac{y^2}{r^2}ds-\int_0^l M_1\frac{y^2}{r^2}ds-\int_0^l R\frac{xy}{r}ds=0$$

Since $R=0$, $\int y/r\ ds=0$ and $\int (xy/r)ds=0$ for a large number of turns, this equation reduces to

$$\int_0^l (M_o-M_1)\frac{y^2}{r^2}ds=0 \quad \ldots\ldots (383)$$

Since $\int (y^2/r^2)ds$ cannot be zero, Equation 383 shows that $M_o-M_1=0$ or $M_o=M_1$. Using this condition in Equation 369, $P=0$ which means that the tangential force at the end A, *Fig.* 184, also vanishes for the condition assumed. Since R is also zero, and $M_1=M_o$, Equation 371 shows that $M=M_o$ which means that the moment is constant along the length of the spring.

Taking $M_1=M_o$ and $R=0$, Equation 381 reduces to

$$\phi=\frac{1}{EI}\left[\int_0^l M_o ds+\int_0^l M_o\frac{y}{r}ds\right] \quad \ldots\ldots (384)$$

Again for a large number of turns $\int (y/r)ds=0$ and $\int ds=l$ Hence the angular deflection ϕ becomes

$$\phi=\frac{M_o l}{EI} \quad \ldots\ldots (385)$$

In this ϕ is given in radians (or degrees divided by 57.3). This equation thus states that the angular deflection of a spiral spring with a large number of turns and a length l with built-in outer end is the same as that of a straight beam of length l built in at one end and loaded by a moment at the other.

Since the moment is constant along the length of the spiral the nominal stress σ (neglecting curvature effects) for the case of *Fig.* 184 will be given by

$$\sigma=\frac{6M_o}{bh^2} \quad \ldots\ldots (386)$$

where b=width of spring cross section and h=thickness of strip.

Usually there is some stress concentration at the clamped ends of the spring. If fatigue or repeated loading is present (as in the hairspring of a watch), in accordance with the discussion in Chapter XVI this should be taken into account by multiplying the stress calculated from Equation 386 by a stress concentration factor. For most applications where the number of repetitions

of load during the life of the spring is small, stress concentration effects are neglected, however.

Where a small number of turns is involved, Equations 385 and 386 should be modified as discussed later.

Pinned Outer End—Frequently in practice, for manufacturing reasons the outer end of a spiral spring may be held with a pin instead of being clamped. Neglecting friction no moment will act at the pinned end A and the loading conditions will be those shown in *Fig.* 185. In this case the external moment M_o will be

$$M_o = Pr \qquad (387)$$

Assuming that the coils do not touch each other, the moment at any point of the spiral having the coordinates x and y becomes

$$M = P(r+y) - Rx \qquad (388)$$

Using Equation 387, this expression may be written

$$M = M_o\left(1 + \frac{y}{r}\right) - Rx \qquad (389)$$

From the Castigliano theorem, as before,

$$\frac{\partial U}{\partial R} = 0$$

This follows as a consequence of the fact that the radial force R does no work during deflection of the spring. Therefore Equation 373 also applies.

Differentiating Equation 388 with respect to R and substituting in Equation 373, the following expression is obtained:

$$\int_0^l \left[Pr\left(1 + \frac{y}{r}\right) - Rx\right] x\,ds = 0$$

or

$$P\int_0^l rx\,ds + P\int_0^l xy\,ds - R\int_0^l x^2\,ds = 0$$

As before, for a large number of turns, the first two integrals

may be taken as zero. Hence this equation gives

$$\int_0^l Rx^2 ds = 0 \quad \ldots\ldots (390)$$

Since $\int x^2 ds$ is different from zero this means that the radial force R is also equal to zero for the pin-ended case, *Fig.* 185.

As before the angular rotation ϕ is given by Equation 379, using the value of M given by Equation 389. Differentiating the latter partially with respect to M_o and substituting the result together with Equation 389 in Equation 379,

$$\phi = \frac{1}{EI}\int_0^l \left[M_o\left(1+\frac{y}{r}\right) - Rx\right]\left(1+\frac{y}{r}\right) ds$$

Since R was found to be zero this simplifies to

$$\phi = \frac{M_o}{EI}\int_0^l \left(1+\frac{2y}{r}+\frac{y^2}{r^2}\right) ds$$

From the condition that $\int y ds = 0$ for a large number of turns, this equation becomes

$$\phi = \frac{M_o}{EI}\int_0^l \left(1+\frac{y^2}{r^2}\right) ds \quad \ldots\ldots (391)$$

Also for a large number of turns

$$\int_0^l \frac{y^2}{r^2} ds = \frac{l}{4}$$

This value is approximate. Using it in Equation 391, the expression for ϕ simplifies to

$$\phi = 1.25\frac{M_o l}{EI} \quad \ldots\ldots (392)$$

Comparing this with Equation 385 it is seen that, for the same external moment M_o, a spiral spring with a hinged outer end will have about 25 per cent more angular deflection than the corresponding one with clamped outer end, provided adjacent turns do not come in contact.

The maximum moment in the spring will occur when $y = r$ (approximately). Taking $y = r$ in Equation 389, since $R = 0$, this

gives a maximum value $M=2M_o$. The maximum stress is then

$$\sigma=\frac{6(2M_o)}{bh^2}=\frac{12M_o}{bh^2} \quad \text{.....(393)}$$

For a given external moment M_o this stress is twice that for a spring with a clamped outer edge (Equation 386). However, it should be noted that it occurs at a point opposite to the pinned end where there is no stress concentration. If the arbor diameter is small compared to r, the moment at the inner clamped end will be M_o which is the same as that for a spring with clamped outer end. This means that the stress at this end will also be the same and, since there is always some stress concentration at this point, it may still happen that in some cases this is the limiting stress. Also touching of the coils, as may easily occur in practice, will tend to reduce the stress given by Equation 393. For a more extensive discussion of spiral springs with large numbers of turns the reader is referred to the article by Van den Broek[3].

EXAMPLE: A steel torsion spring having a pinned end *A Fig.* 185 is subject to an external torque M_o equal to 25 inch-pounds. The outer diameter is 2 inches, the bar section is ½ by .06-inch, and the total length 15 inches. Required the stress and the deflection. Assuming a modulus $E=30\times10^6$ pounds per square inch,

$$I=\frac{bh^3}{12}=\frac{.5(.06)^3}{12}=9\times10^{-6}$$

From Equation 392 for a pinned end

$$\phi=1.25\frac{M_o l}{EI}=\frac{1.25\times25\times15}{30\times10^6\times9\times10^{-6}}=1.73 \text{ radians}$$

This corresponds to an angular rotation of $1.73(57.3)=99$ degrees.

From Equation 393 the maximum stress is

$$\sigma=\frac{12M_o}{bh^2}=\frac{12\times25}{.5(.06)^2}=167000 \text{ lb./sq. in.}$$

The stress at the clamped end O where stress concentration

[3] J. A. Van den Broek—"Spiral Springs" *Transactions*, A.S.M.E., 1931, 53-18. Also *Elastic Energy Theory*, Wiley, 1942.

occurs will be about half this or 84,000 pounds per square inch assuming an arbor diameter small compared to r. However, as indicated previously this latter stress will be augmented by stress concentration effects due to clamping of the end.

SPRINGS WITH FEW TURNS

In some practical cases where large torques are involved it is necessary to use a relatively heavy cross section for the spiral spring as well as an arbor of larger diameter. This means that the number of turns in the spring may be relatively small so that the previously discussed theory (based on a large number of turns) no longer applies. However, an analysis of this case may be made by using similar methods to those described previously[4]. This analysis will be briefly outlined.

Considering a spring with a small number of turns as shown in *Fig.* 186, it is assumed that the spring is clamped or built in at point B at a radius r_1 while the outer end A may move in an arc about point O. The angular deflection of the end A (in radians) is equal to the movement of A along the arc divided by the outer radius r_2.

The moment M at any point on the spiral having the coordinates x and y will be given by Equation 370, using r_2 for r,

$$M=P(r_2+y)+M_1-Rx \qquad (394)$$

The three unknown quantities M_1, P and R in this equation may be determined from three equations obtained by using the Castigliano theorem. Since the point A is assumed constrained to move along a circular arc about O, the work done by the force R must be zero. This means $\partial U/\partial R=0$ and Equation 375 holds.

By differentiating Equation 394 partially with respect to R,

$$\frac{\partial M}{\partial R}=-x$$

Using this and Equation 394 in Equation 375, the following expression is obtained:

$$\int_0^l [P(r_2+y)x+M_1x-Rx^2]ds=0 \qquad (395)$$

[4]Kroon and Davenport—"Spiral Springs with Small Number of Turns", *Journal*, Franklin Institute, Vol. 225, 1938, Page 171.

During deflection of the end of the spring through an angle ϕ, the moment M_1 will also move through the same angle. From the Castigliano theorem this condition gives

$$\phi = \frac{\partial U}{\partial M_1} = \frac{1}{EI}\int_0^l M \frac{\partial M}{\partial M_1} ds \quad \text{.....(396)}$$

From Equation 394, $\partial M/\partial M_1 = 1$. Using this in Equation 396, together with Equation 394,

$$\phi = \frac{1}{EI}\int_0^l M ds = \frac{1}{EI}\int_0^l \Big[P(r_2+y) + M_1 - Rx\Big] ds \quad \text{.....(397)}$$

Another equation is also obtained from the Castigliano theorem which states that the total deflection in the direction of the force P must be equal to $\partial U/\partial P$. Since P is always assumed to be directed along the arc of motion of the end A, *Fig.* 186, this deflection will be $r_2\phi$. Hence

$$r_2\phi = \frac{\partial U}{\partial P} = \frac{1}{EI}\int_0^l M \frac{\partial M}{\partial P} ds \quad \text{.....(398)}$$

But from Equation 394, $\partial M/\partial P = r_2 + y$. Using this together with Equation 394 in Equation 398,

$$r_2\phi = \frac{1}{EI}\int_0^l \Big[P(r_2+y) + M_1 - Rx\Big](r_2+y) ds \quad \text{.....(399)}$$

If the center line of the spring is taken in the form of a spiral, Equations 395, 397 and 399 may be integrated over the total length l. This gives three simultaneous equations in P, M_1 and R from which these latter quantities may be found. Knowing these, the bending moment M at any point may be found from Equation 394. By differentiation the location of the maximum value of the moment along the spiral may be obtained and from this the actual value of the maximum moment M_m. If M_o

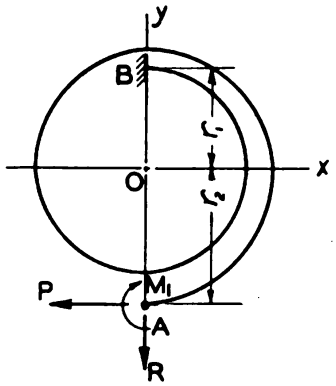

Fig. 186—Spiral spring with small number of turns

is the external moment (this is also the maximum moment for a spring with clamped ends and a large number of turns) the ratio M_m/M_o between maximum moment and external moment may be considered as a stress concentration factor. Values of this ratio

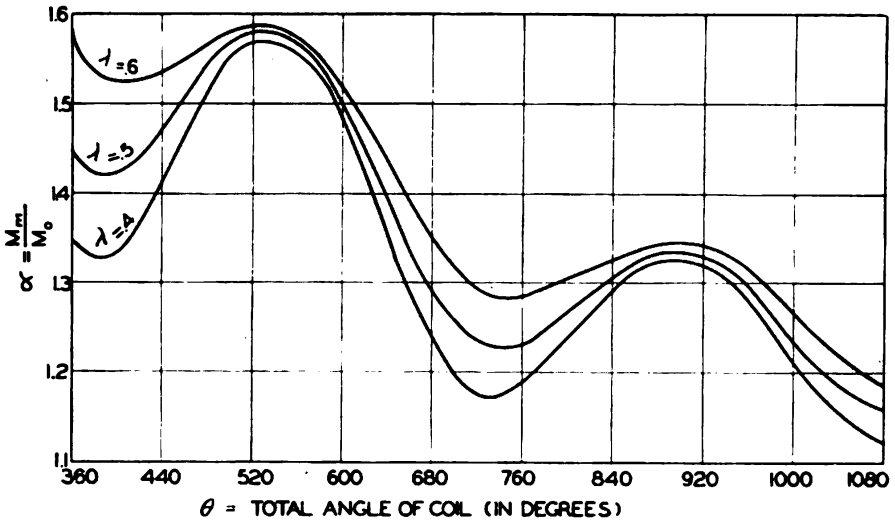

Fig. 187—Stress concentration factor α for spring with few turns

M_m/M_o plotted in *Fig.* 187 as functions of the total spiral angle θ for various values of the function $\lambda=(r_2-r_1)/r_2$ have been obtained by Kroon and Davenport[4]. The value of θ is taken as the angle swept out by the radius vector in traveling from one end of the spiral to the other.

From *Fig.* 187 it is seen that the stress concentration effect due to a small number of turns is somewhat greater for the larger values of λ. In addition the stress concentration values are smaller when the total coil angle θ is near 360, 720 or 1080 degrees, i.e. for 1, 2, or 3 full turns. This is shown by the dips in the curves and suggests that it is of advantage when designing spiral springs of this type to use a whole rather than a fractional, number of turns if possible. From *Fig.* 187 it is also seen that as the total coil angle θ increases, the maximum values of the ratio M_m/M_o also decrease, i.e., the stress concentration effect decreases. However, even for $\theta=1080$ degrees (3 turns) and $\lambda=.6$, the ratio M_m/M_o is still equal to almost 1.2 which means that maximum stress will still be almost 20 per cent higher than that given by Equation 386, derived on the assumption of a large

angle θ. These values for stress concentration effect may be modified slightly by the effects of imperfect clamping at the ends of the spring.

In addition it will be found that because of the small number of turns the spring is somewhat stiffer than would be expected on the basis of the simple formula (Equation 385) derived for a large number of turns. The more accurate analysis[4] shows that the angular deflection at a moment M_o is given by

$$\phi = \frac{1}{\beta}\frac{M_o l}{EI} \qquad (400)$$

In this the factor β (which is greater than unity) depends on the total angle θ of the spiral and on the ratio λ. Values of this factor are given in *Fig.* 188. However, for ratios λ between .4

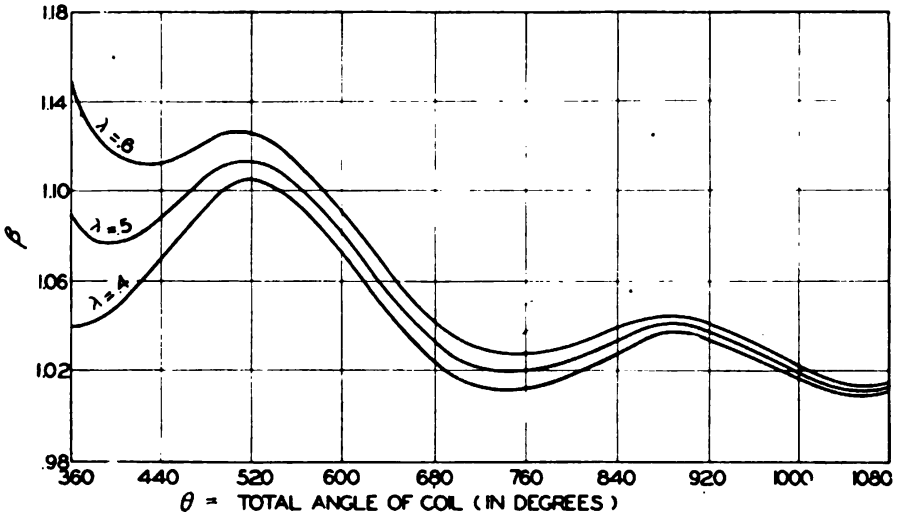

Fig. 188—Stiffness factor β for spiral spring with small number of turns

and .6 and for more than two turns of the spiral this factor differs from unity by less than 4 per cent and may usually be neglected for practical purposes, i.e., the usual formula (Equation 385) may be applied. However, from *Fig.* 188 it may be seen that a 15 per cent error is involved in the usual formula where $\lambda = .6$ for a spring with only one turn.

Values of the radial deflection at various points along the spiral are of interest since in general the designer should try to

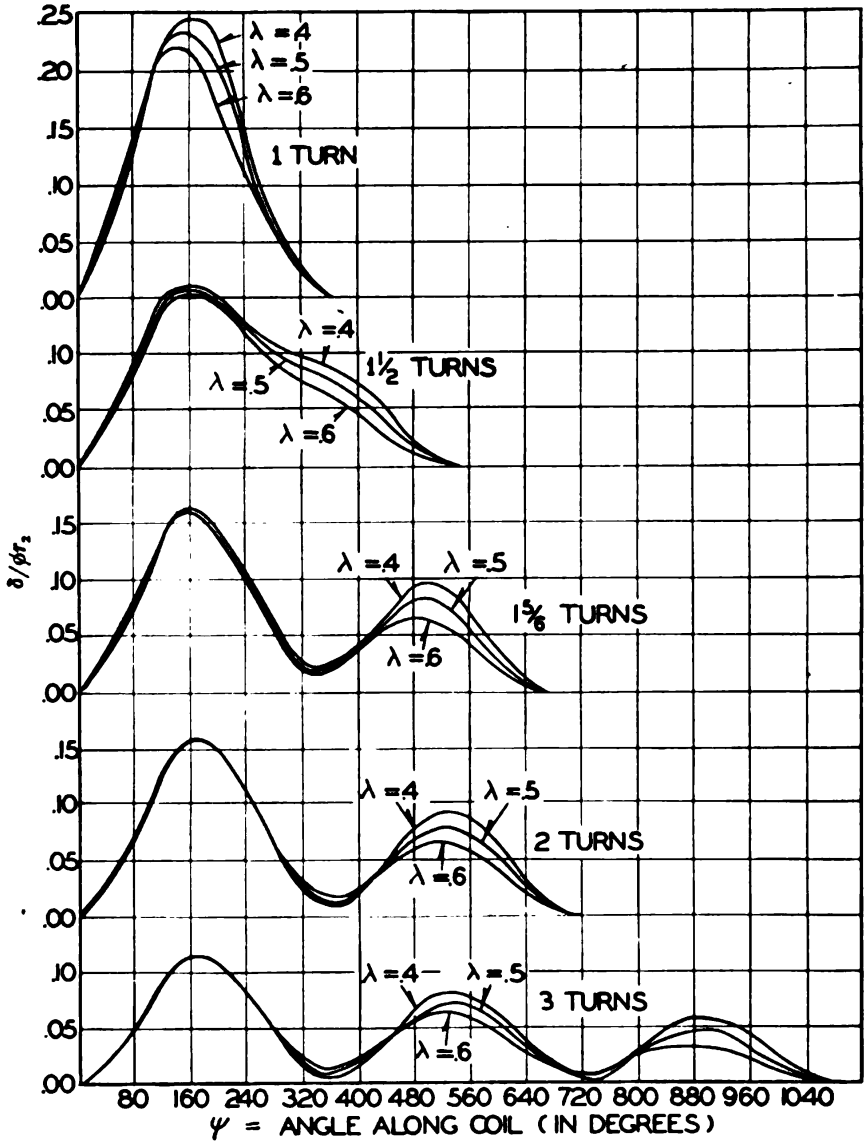

Fig. 189—Curves for finding the radial deflection of coils of spiral spring. Angle ψ measured from outer end

avoid having the coils touch during deflection. These quantities have been worked out[4] as functions of the angle along the spiral for various numbers of turns and for various values of the ratio λ; the results are plotted in *Fig.* 189. The ordinates represent radial deflection δ divided by ϕr_2. In this ϕ is the angular deflection of the spring due to the external moment while ψ is the angle meas-

ured along the spiral from the outer end. By using these curves the necessary spacing between coils may be worked out for springs with various numbers of turns. For further details the reader is referred to the paper by Kroon and Davenport[4].

In the design of spiral springs where the thickness is fairly large, a further stress concentration enters due to the fact that the spring is, in effect, a curved bar. This stress concentration is usually small but may be determined for a given thickness and radius of curvature by using curves given for torsion springs in *Fig.* 180, Chapter XVII.

The curves of *Figs.* 187 and 188 apply only to spiral springs with clamped outer ends. Where the outer end is pin connected and few turns are involved, an analysis may be carried out using similar methods, and more exact expressions for deflection and stress obtained. These expressions are rather cumbersome and for further details the reader is referred to the publication by Gross and Lehr[5].

WORKING STRESSES

Calculated working stresses in spiral springs may run as high as 175,000 to 250,000 pounds per square inch or more where fatigue conditions are not a factor. For example, an ordinary clock spring during its life may be subject to less than 5000 cycles and hence may be stressed much higher than would be the case where millions of cycles are involved. Where fatigue conditions are present (as for example in the spiral spring for the balance wheel of a watch) the stress range should be kept well below the endurance range of the material, stress concentration conditions at the clamped edges being considered. Some data on endurance ranges in bending for spring materials are given in Chapter XXIII.

LARGE DEFLECTION—COILS IN CONTACT

The foregoing discussion has been based on the assumption that individual coils do not touch each other. This condition, however does not apply in many cases, as for example in the mainspring of a watch or power spring of a phonograph where the

[5] Gross and Lehr—*Die Federn*, Page 73, 1938, V.D.I., Berlin.

spring is usually placed inside a hollow case as indicated in *Fig.* 190. Here the spring is shown wound up on the arbor. When the spring is unwound it rests against the inside of the case as indicated in *Fig.* 191.

The number of turns delivered by such a spring may be estimated approximately as follows[6]: If l is total length of spring strip and h is the thickness, the total sectional area of the wound spring will be lh. But from *Fig.* 190 this is also equal to $(\pi/4)(d_2^2-d_1^2)$ assuming that the coils are wound tightly so that adjacent turns touch, and neglecting the turns connecting the wound part with the case. Thus,

$$lh=\frac{\pi}{4}(d_2^2-d_1^2)$$

Solving this for d_2,

$$d_2=\sqrt{\frac{4}{\pi}lh+d_1^2} \qquad (401)$$

Also assuming that adjacent coils touch, the number of turns n becomes

$$n=\frac{d_2-d_1}{2h} \qquad (402)$$

Substituting the value of d_2 given by Equation 401, the expression for n becomes

$$n=\frac{\sqrt{\frac{4}{\pi}lh+d_1^2}-d_1}{2h} \qquad (403)$$

It should be noted that if the spring is oiled, adjacent turns will be separated by the thickness of the oil film and this will introduce some error in the equation.

Considering the condition when the spring is unwound as indicated in *Fig.* 191, if n' be the number of turns of the unwound spring, and again neglecting the turns connecting the inside of the wound portion with the arbor,

[6] "Number of Turns Delivered by Flat Coiled Springs", *The Mainspring*, Spring 7, Coil 2, August, 1937, published by Wallace Barnes Co.

$$n' = \frac{D_2 - D_1}{2h} \quad \ldots\ldots (404)$$

Also, as before, since the area of the wound portion must be equal to hl

$$hl = \frac{\pi}{4}(D_2^2 - D_1^2) \quad \ldots\ldots (405)$$

From this

$$D_1 = \sqrt{D_2^2 - \frac{4}{\pi}hl} \quad \ldots\ldots (406)$$

Substituting Equation 406 in 404,

$$n' = \frac{D_2 - \sqrt{D_2^2 - \frac{4}{\pi}hl}}{2h} \quad \ldots\ldots (407)$$

The total number of turns N delivered by the spring in unwinding from the wound position of *Fig.* 190 to the unwound

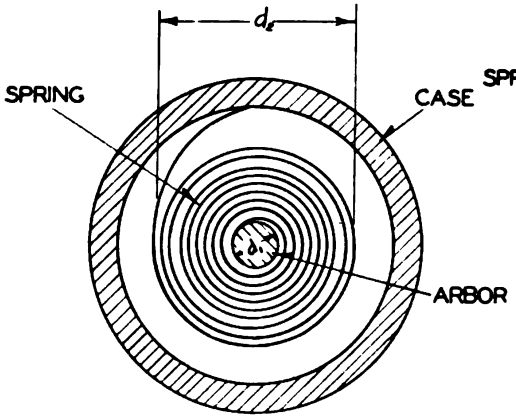

Fig. 190—Spiral spring wound on the arbor

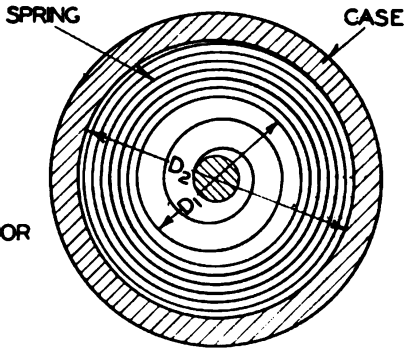

Fig. 191—Unwound spring against case

position of *Fig.* 191 will be the difference between n and n'. Hence the number of turns delivered becomes:

$$N = n - n' = \frac{\sqrt{\frac{4}{\pi}lh + d_1^2} + \sqrt{D_2^2 - \frac{4}{\pi}lh} - (D_2 + d_1)}{2h} \quad \ldots\ldots (408)$$

Since the turns connecting the wound part of the spring with the arbor or case are neglected in this derivation the results given by Equation 408 are somewhat high. To obtain more accurate results, the value of N should be multiplied with a correction factor k less than unity. Values of this correction factor are dependent on the ratio m of drum area minus arbor area divided by spring area, where

$$m=\frac{\frac{\pi}{4}(D_2^2-d_1^2)}{lh} \qquad (409)$$

Values of k for various values of m as suggested by Wallace Barnes Co.[6] are given in TABLE XXXIII.

It is seen that for values of m between 5 and 1.5 a reduction in number of turns below that calculated from Equation 408 of from 15 to 33 per cent may be expected.

To avoid excessive stress concentration due to curvature effects, the arbor diameter is usually made around 15 to 25 times the strip thickness.

EXAMPLE: A spiral spring is wound from a strip ¾-inch wide, .015-inch thick and 100 inches long. The arbor diameter

TABLE XXXIII

Values of k for Various Values of m

m	5	4	3	2	1.5
k	.672	.702	.739	.796	.85

is ¾-inch and the inner diameter of the case 2¼ inches. The problem is to find the number of turns delivered from the solid to the free condition. Thus $h=.015$, $l=100$, $D_2=2.25$, $d_1=.375$.

From Equation 409,

$$m=\frac{\frac{\pi}{4}[(2.25)^2-(.375)^2]}{.015\times 100}=2.58$$

From TABLE XXXIII, by interpolation for $m=2.58$, $k=.76$.

Using the given values of h, l, D_2 and d_1 in Equation 408 the calculated value of N becomes 19.6 turns. This must be multiplied by the correction factor $k=.76$ which yields a value

$19.6 \times .76 = 14.9$ turns for the number of turns delivered.

Where a spiral spring has a large number of turns the equations for calculating stress and deflection become simple provided the coils do not come in contact during deflection. Where the number of turns is small and the outer end is clamped the peak moment and deflection may be calculated by means of the curves given.

Where the spring is wound tightly, as in the case of the mainspring of a watch, the relatively simple expressions given facilitate calculation of the turns delivered. Because of friction and other uncertainties, in this case a determination of torque delivered as a function of the angle or number of turns is rather uncertain and will not be discussed here.

CHAPTER XIX

RING SPRINGS

Where space is limited and a relatively large amount of energy must be absorbed, a type of spring known as the "ring spring" may well merit consideration by the designer[1]. This is particularly true if the application is one where a large amount of damping is also desirable, such as for example, draft gear springs for railway use[2].

As its name implies the ring spring consists essentially of a series of rings having conical surfaces and assembled as indicated in *Figs.* 192 and 193. When an axial load is applied, sliding oc-

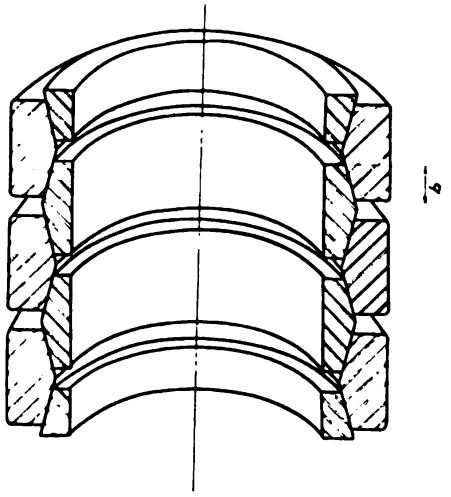

Fig. 192—Diametral section through ring spring

curs along the conical surfaces with the result that the inner rings are compressed and the outer rings extended. In this manner an approximately uniform distribution of circumferential stress is obtained in both inner and outer rings. Because of this approximate uniformity of stress distribution, the ring spring is

[1] O. R. Wikander—"The Ring Spring", *Mechanical Engineering*, Feb., 1926, Page 139 and "Characteristics of the Ring Spring", *American Machinist*, Feb. 14, 1924.

[2] L. E. Endsley—"Draft Gear Springs—Past and Present", *Railway Mechanical Engineer*, July 1933.

commonly assumed to act essentially as a bar in simple tension and to have a correspondingly high efficiency (considered on the basis of allowable energy storage per pound of metal). Actually, because of compression stresses at the conical surfaces of the outside rings, there will be a slight nonuniformity in *equiva-*

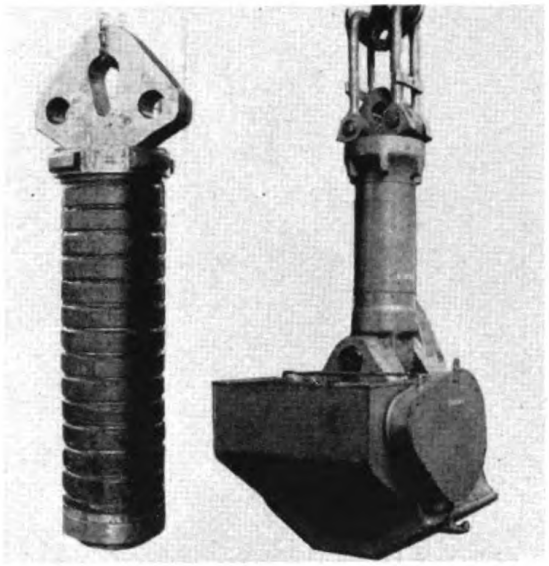

—Courtesy, United Engineering and Foundry Co.

Fig. 193—Ring spring and rotating block for forging press in which the spring is utilized

lent stress distribution. Where a tension and compression stress act at right angles as in this case, the *equivalent stress*—on the basis of the maximum shear theory of strength—will be the sum of the numerical magnitudes of these tension and compression stresses.

In addition, where the radial thickness of the rings is appreciable, there is some nonuniformity in circumferential stress since the ring behaves like a thick cylinder under internal or external pressure. For most springs, however, this nonuniformity in equivalent stress distribution will not be large and hence this type of spring will have a relatively high efficiency. On the other hand, it should be noted that the damping in this spring is obtained at the expense of a certain amount of wear on the sliding surfaces even if lubricated according to usual practice.

STRESS CALCULATIONS

A typical load-deflection hysteresis loop for the ring spring is shown in *Fig.* 194. From this it may be seen that on the compression stroke a much higher spring constant (in terms of pounds per inch deflection) is obtained than for the return stroke. This is due to the friction forces on the conical faces of the rings which, for an increasing load, are added to the elastic forces caused by distortion of the rings but for a decreasing load are subtracted

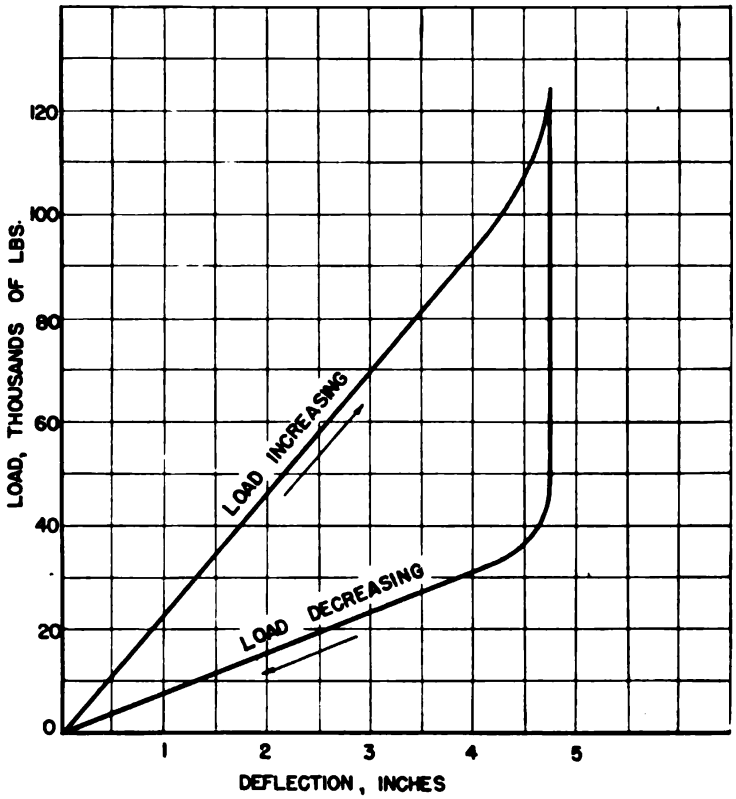

Fig. 194—Typical load-deflection diagram of ring spring showing typical hysteresis loop during loading and unloading

from the elastic forces. Thus a large hysteresis loop is obtained with correspondingly high energy absorption per cycle.

Referring to *Fig.* 195, for practical purposes of analysis each conical surface of the ring spring may be considered as subject to a total normal force N distributed uniformly around the cir-

cumference and a friction force $F=\mu N$ (when μ is the coefficient of friction). This latter force acts in the direction shown when the spring is being compressed, and in an opposite direction when the spring is being extended. These forces N and F produce

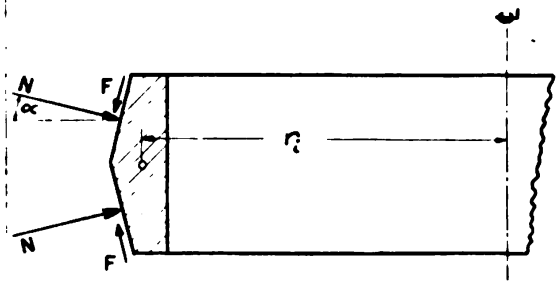

Fig. 195—Forces acting on element of ring spring

primarily a compression of the ring, although there is at the same time a tendency of the ring to bend like a bar on elastic foundation[3]. This latter effect, however, may be neglected for practical design purposes. It will also be assumed that the ring thickness is small compared to the mean diameter so that the nonuniform circumferential distribution due to the thick cylinder effect may be neglected[4].

Inner Ring—Considering the inner ring of Fig. 195 and assuming the spring is being compressed so that the friction force acts in the direction shown, the total radial force acting will be equal to $2(N \cos \alpha - F \sin \alpha)$ where α is the angle of taper of the conical surfaces. The radial load p per inch of the circumferential center line of the ring will be the total radial force divided by $2\pi r_i$, where r_i is the mean radius of the ring. Hence this load may be expressed as

$$p=\frac{2(N\cos\alpha-F\sin\alpha)}{2\pi r_i}$$

Taking $F=\mu N$ this equation becomes

$$p=\frac{N(\cos\alpha-\mu\sin\alpha)}{\pi r_i} \qquad (410)$$

[3] S. Timoshenko—*Strength of Materials*, Van Nostrand, Second Edition, Part 2, Page 164.

[4] S. Timoshenko, loc. cit., Page 236.

For a thin ring, the compressive stress will be

$$\sigma_c = \frac{pr_i}{A_i} \quad (411)$$

where A_i = sectional area of the inner ring. Substituting Equation 410 in 411,

$$\sigma_c = \frac{N(\cos\alpha - \mu \sin\alpha)}{\pi A_i} \quad (412)$$

The axial load P acting on the spring during the compression stroke is found by taking the components of N and F along the axis, *Fig.* 195. Hence

$$P = N\sin\alpha + F\cos\alpha = N(\sin\alpha + \mu\cos\alpha)$$

Solving this for N and substituting in Equation 412, the circumferential compressive stress σ_c in the inner rings becomes

$$\sigma_c = \frac{P}{\pi A_i}\,\frac{\cos\alpha - \mu\sin\alpha}{\sin\alpha + \mu\cos\alpha} \quad (413)$$

This equation may be reduced to the simpler form:

$$\sigma_c = \frac{P\tan\alpha}{\pi A_i K} \quad (414)$$

where

$$K = \frac{\tan\alpha(\mu + \tan\alpha)}{1 - \mu\tan\alpha} \quad (415)$$

To facilitate practical use of Equation 414, values of K are plotted against the angle α for various friction coefficients μ in the upper group of curves of *Fig.* 196. Where maximum accuracy is desired, computation should be made by using Equation 415.

A similar procedure for calculating the circumferential tension stress σ_t in the outer rings is used. This gives

$$\sigma_t = \frac{P\tan\alpha}{\pi A_o K} \quad (416)$$

where in this case A_o = sectional area of outer ring and K is given by *Fig.* 196. It should be noted that Equations 414 and 416 give the stresses in the spring as a function of load for *increasing* load P only.

Outer Ring—As indicated previously, to obtain the *equivalent stress* in the outer rings, the compressive stresses due to the normal forces N, *Fig.* 195 should be added to the circumferential tension stress σ_t calculated from Equation 416. These compressive stresses may be computed as follows: For the outer ring the radial load p per inch of mean circumference is obtained from Equation 410 using r_o instead of r_i. Thus

$$p=\frac{N(\cos\alpha-\mu\sin\alpha)}{\pi r_o}$$

Solving for N, this gives

$$N=\frac{p\pi r_o}{\cos\alpha-\mu\sin\alpha} \qquad (417)$$

If σ_t is the circumferential tension stress, from the ring formula:

$$p=\frac{\sigma_t A_o}{r_o}$$

Substituting in Equation 417.

$$N=\frac{\sigma_t A_o\pi}{\cos\alpha-\mu\sin\alpha} \qquad (418)$$

Letting b equal the projected axial length of contact area at the load P and stress σ_t, *Fig.* 192 (which length may be obtained from the calculated deflection of the spring and its geometrical proportions), then the average compression stress σ_c' in the contact region is

$$\sigma_c'=\frac{N\cos\alpha}{2\pi r_m b} \qquad (419)$$

where $r_m=(r_o+r_i)/2$ = mean radius of inner and outer rings. This holds since the total area over which the force N acts is $2\pi r_m b/\cos\alpha$. Substituting in this the value of N given by Equation 418 the contact stress becomes

$$\sigma_c' = \frac{\sigma_t A_o}{2r_m b(1-\mu \tan \alpha)} \quad \ldots\ldots (420)$$

DEFLECTION

To calculate the total deflection of the spring, the radial deflections of the rings must first be found. For the inner ring the radial deflection will be approximately equal to $\sigma_c r_m/E$ where E is the modulus of elasticity. The axial deflection of the spring due to each inner ring will be two times the radial value $\sigma_c r_m/E$ divided by $\tan \alpha$. (The factor two is used since there are two conical surfaces per ring). Hence if n_i is the total number of inner rings in the spring (a ring of half the full section being considered as half a ring), the deflection δ_i due to these rings is

$$\delta_i = \frac{2\sigma_c n_i r_m}{E \tan \alpha} \quad \ldots\ldots (421)$$

Similarly the total axial deflection δ_o due to outer rings is

$$\delta_o = \frac{2\sigma_t n_o r_m}{E \tan \alpha} \quad \ldots\ldots (422)$$

where n_o is the number of outer rings. This will also equal n_i.

Letting $n = n_o + n_i$ = total number of "elements" in the spring, each element consisting of a half inner and a half outer ring, and adding Equations 421 and 422,

$$\delta = \delta_o + \delta_i = \frac{r_m n}{E \tan \alpha}(\sigma_t + \sigma_c) \quad \ldots\ldots (423)$$

Using values of σ_c and σ_t given by Equations 414 and 416 in this, the deflection during the compression stroke may be expressed in terms of the load P.

$$\delta = \frac{P r_m n}{\pi E A_i K}\left(1 + \frac{A_i}{A_o}\right) \quad \ldots\ldots (424)$$

In this K is given by Equation 415 or *Fig.* 196.

The deflection and loads occuring during the unloading or return stroke may be analyzed in a similar manner by considering that in this case the direction of the friction forces F, *Fig.*

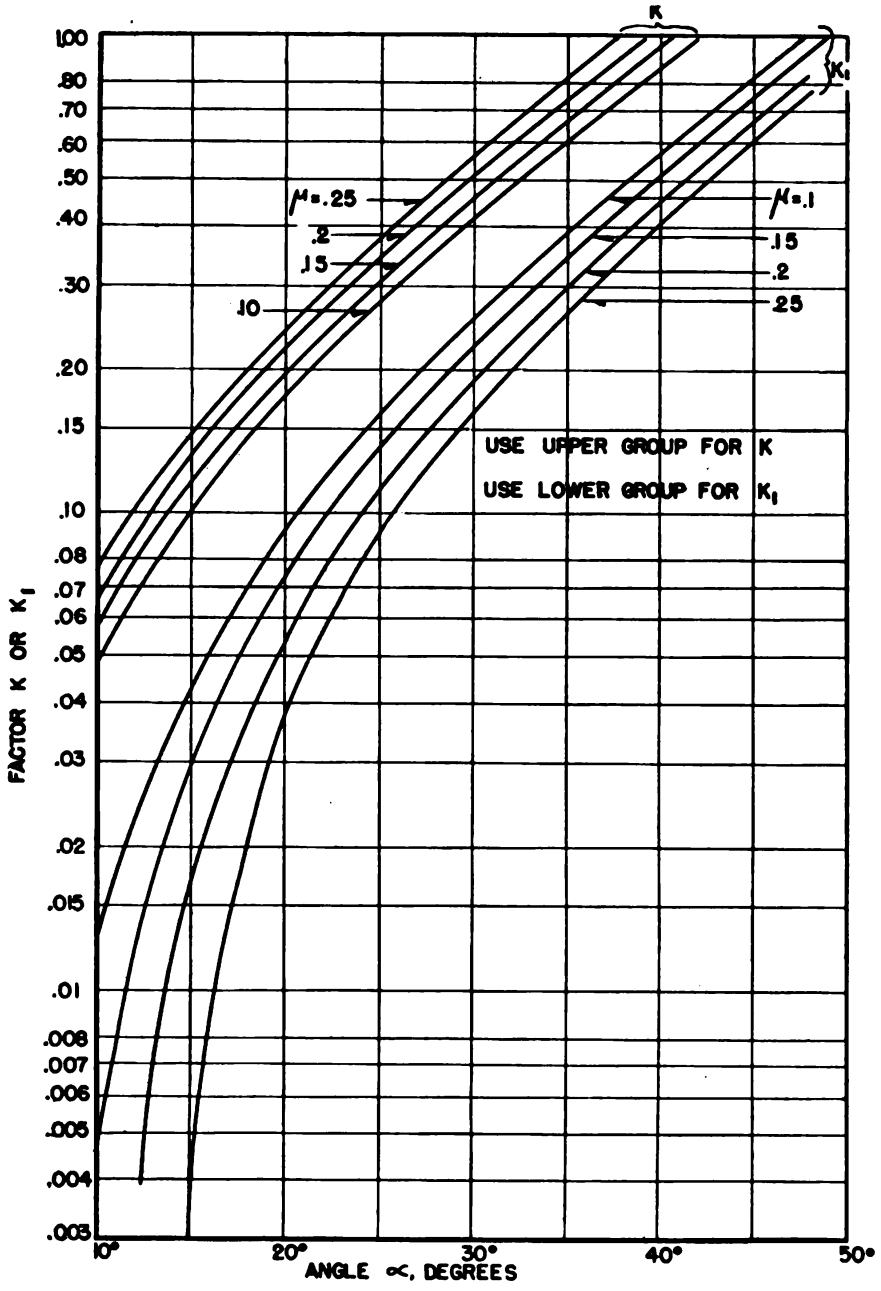

Fig. 196—Curves for finding factors K and K_1 for use in the formulas

195 will be reversed. If P_1 is the load and δ_1 the corresponding deflection during the return stroke,

$$\delta_1 = \frac{P_1 r_m n}{\pi E A_i K_1}\left(1 + \frac{A_i}{A_o}\right) \quad \ldots\ldots (425)$$

where

$$K_1 = \frac{\tan\alpha(\tan\alpha - \mu)}{1 + \mu\tan\alpha} \quad \ldots\ldots (426)$$

Values of K_1 are plotted for convenience in the lower group of curves of *Fig.* 196.

The ratio between the load P_1 (return stroke) and the load P (compression stroke) at any given deflection is obtained by equating δ and δ_1, Equations 424 and 425. This gives

$$\frac{P_1}{P} = \frac{K_1}{K} \quad \ldots\ldots (427)$$

Hence to find the ratio of the spring constants for the return and compression strokes respectively it is only necessary to take the ratio K_1/K for the given values of μ and α. This is true since the spring constants are proportional to the respective loads at any given deflection.

DESIGN CALCULATION

As an example of the application of these formulas in practical design, a ring spring of the following dimensions as tested by Wikander[1] may be considered: $A_o = A_i = .584$ in.^{2}, $r_i = 4.42$ in., $r_o = 4.74$ in., $r_m = 4.58$ in. $\tan\alpha = .25$, $\alpha = 14°$ (approx.), $E = 29 \times 10^6$, $n_o = n_i = 9$, n = 18. Tests on this ring spring indicated a coefficient of friction $\mu = .12$. From *Fig.* 196, for $\alpha = 14°$ and $\mu = .12$, by interpolation $K = .095$ and $K_1 = .031$.

Assuming a peak load $P_1 = 100{,}000$ pounds, from Equation 424 for an increasing load the deflection δ is

$$\delta = \frac{100000 \times 4.58 \times 18 \times 2}{\pi \times 29 \times 10^6 \times .584 \times .095} = 3.26 \text{ in.}$$

The load P_1 on the return stroke for this same deflection will be equal to P multiplied by the ratio K_1/K. This gives

$$P_1 = 100000 \times \frac{.031}{.095} = 32{,}700 \text{ lb}$$

The spring constant for the compression stroke is

$$\frac{P}{\delta} = \frac{100000}{3.26} = 30{,}700 \text{ lb/in.}$$

That for the return stroke is:

$$30700 \times \frac{K_1}{K} = 30700 \times \frac{.031}{.095} = 10{,}000 \text{ lb/in.}$$

The tension stress σ_t in the outer ring at $P_1 = 100{,}000$ pounds is obtained from Equation 416,

$$\sigma_t = \frac{100000 \times .25}{\pi \times .584 \times .095} = 143{,}000 \text{ lb/sq n.}$$

Since $A_o = A_i$ in this case, from Equation 414, the foregoing will also be equal to the compression stress in the inner ring. Usually in practice, however, the inner ring area A_i is made smaller than A_o since it has been found from experience that higher working stresses may be used in compression than in tension. For example, draft gear springs have been designed for a circumferential tension stress of 125,000 pounds per square inch in the outer rings as compared with a compression stress of 210,000 pounds per square inch in inner rings when spring is solid[2].

Assuming that the design proportions of the spring are so chosen that the projected contact length b, *Fig.* 192, is .79-inch at a load of 100,000 pounds, then from Equation 420 the compressive stress σ_c' in the contact area is

$$\sigma_c' = \frac{143000 \times .584}{2 \times 4.58 \times .79 \times .97} = 11{,}900 \text{ lb/sq in.}$$

Adding this to the tension stress $\sigma_t = 143{,}000$ pounds per square inch, the equivalent stress in the outer ring becomes $143{,}000 + 11{,}900 = 144{,}900$ pounds per square inch. This is a slightly higher value than would be obtained if the contact compressive stresses were neglected.

As an approximate indication of loads and deflections possible for this type of spring. TABLE XXXIV, is useful[5].

[5] Data from Edgewater Steel Co.

TABLE XXXIV

Load and Deflection Ratings*

Inches				Pounds		
O.D.	I.D.	B_1	δ/n	W	P	P_1
3.750	3.020	.750	·250	.778	1135	382
3.093	2.240	.540	·152	.480	1420	450
1.521	1.275	.1750	·0265	.0286	3000	1630
2.124	1.856	.230	·041	.0378	3250	1465
.980	.724	.1785	.0164	.0179	3500	1430
1.813	1.498	.204	.0366	.0522	5000	1880
1.906	1.530	.2000	.0323	.0602	5000	2720
4.305	3.982	.420	.085	.1436	5760	2600
1.917	1.530	.2000	.0348	.0625	6000	2970
2.242	1.785	.2250	.0378	.0961	6800	3700
1.875	1.327	.200	.0344	.0806	7000	4390
2.048	1.660	.2635	.0376	.0889	7900	3910
2.587	2.040	.2500	.0434	.1469	9000	4900
1.470	.880	.212	.0248	.0668	9420	3540
3.152	2.550	.3000	.0537	.2409	12000	6500
3.441	3.024	.360	.0719	.2367	12150	4550
1.875	1.203	.290	.0316	.1365	13875	9000
3.549	2.800	.325	.0595	.357	16000	8700
3.441	2.419	.275	.0560	.375	22500	9150
3.441	2.353	.375	.0575	.540	27750	18000
4.375	2.976	.312	.0830	.732	32000	11400
3.663	2.302	.500	.059	.916	50500	25000
4.938	3.134	.375	.0830	1.235	52000	20400
5.625	3.758	.645	.0800	2.312	97000	44600
8.188	6.496	.786	.1680	4.57	100000	35800
7.500	5.189	.692	.1215	4.61	110000	43000
6.500	3.881	.593	.110	3.64	128000	45000
8.188	4.599	.692	.1281	7.08	186000	73000

*Ring Spring to be guided, either on the outside in a cylinder of 2% greater diameter than the O. D. or on the inside by a mandrel of 2% smaller than the I. D. of the spring.

O.D. = Outside diameter of spring.
I.D. = Inside diameter of spring.
B_1 = Solid height of one spring element (one-half the width of one outer ring).
δ/n = Travel of one spring element.
$B_1 + \delta/n$ = Free height of one spring element.
W = Weight of one spring element.
P = Compression force of spring.
P_1 = Recoil force of spring.

Ring springs must be provided with lubrication since a dry spring will gall and stick under comparatively light service. A graphite grease may be used for this purpose. Such a lubricant not only decreases the friction coefficient, thereby reducing the heat generated, but also acts as a coolant.

In general, ring springs must also be provided with guides, either internal or external, to prevent sidewise buckling. Such guides are usually provided with a clearance of about two per cent of the diameter.

Besides the applications previously mentioned, ring springs have been used in a variety of types of service including elastic supports for bedplates in presses, shock absorbers for guns, flexible draw-bars for trailers and buffers for cranes.

CHAPTER XX

VOLUTE SPRINGS

The volute spring consists essentially of a relatively wide and relatively thin bar or blade, which has been wound to form the shape shown in cross section in *Fig.* 197. Before winding, the blade has the shape shown in *Fig.* 199. After winding but before cold-setting, such a spring will have either a constant or a variable helix angle and a variable coil radius as shown in *Fig.* 197*b*. The cold-setting operation usually employed will, in general, result in a change in the helix angle distribution and a more favorable stress condition. When loaded axially each element of the spring behaves essentially as a curved bar under torsion, the principal stresses being torsional.

Because of certain inherent advantages, the volute spring has found increasing application in recent years, particularly in the military field. Among these advantages are the following: Compactness, ease of manufacture, damping produced by friction between turns, and a spring rate which increases at high deflection, thus tending to protect the spring against overload. These advantages are partially offset by a rather unfavorable stress distribution within the spring which tends to lower the endurance or fatigue strength.

The curved load-deflection characteristic of the volute springs is due primarily to the "bottoming" of the coils above a

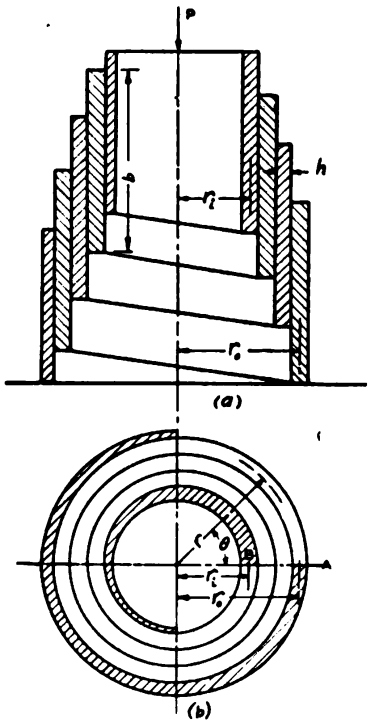

Fig. 197—Volute spring

certain load. This means that beyond a certain load some of the outer coils contact the supporting plate, increasing the stiffness.

To obtain a more favorable stress distribution the thickness of the bar is frequently tapered near the inner end of the coil[1].

CONSTANT HELIX ANGLE

Method of Analysis—To calculate stresses and deflections in volute springs, each element of the coil may, for practical purposes, be considered essentially as a portion of an axially loaded helical spring of the same coil radius and having a rectangular cross-section. This method thus neglects friction between ad-

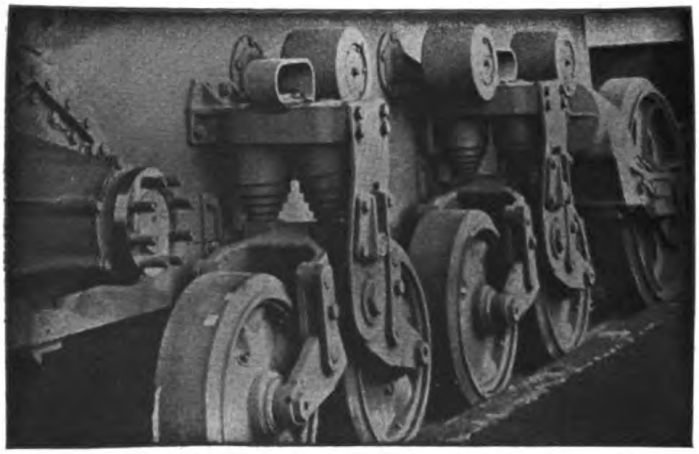

Fig. 198—Volute spring suspension for M-5 tank

jacent turns, as well as certain secondary stresses which are difficult to compute. Some of these stresses arise from the fact that the resultant load *P*, *Fig.* 197*a* in general will not be axial as assumed in the calculations but will be displaced from the axis of the spring, thus giving rise to additional stresses caused by this eccentricity[2]. In addition, certain stresses known as *cone* and *arch* stresses are present which may modify the results[1]. To simplify

[1] For a comprehensive discussion of volute spring calculations including the effect of tapering the inner end thickness see article by B. Sterne, "Characteristics of the Volute Spring," *Journal* S.A.E., June 1942, Page 221. See also paper by H. O. Fuchs, "Notes on Secondary Stresses in Volute Springs," *Transactions* ASME, July 1943, Page 543; and "A Design Method for Volute Springs", *Journal* S.A.E., Sept. 1943, Page 317. Results of fatigue tests are given in article by B. Sterne, *Transactions A.S.M.E.*, July 1943, Page 523.

[2] Paper by Dohrenwend, *Proceedings Society for Experimental Stress Analysis*, Vol. 1, Page 94, gives results of strain measurements and eccentricity determinations on volute springs.

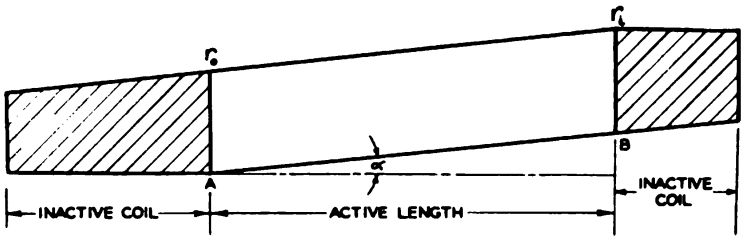

Fig. 199—Developed volute spring

the problem, a constant, free helix angle will first be assumed. Later, effects of variable helix angle will be treated.

Bottoming Loads—Referring to *Fig.* 200 which represents the developed center line of the blade of a volute spring, the spring at zero load is indicated by the line *AB*, α being the free helix angle (assumed constant). In this the ordinate represents the height of the blade center line, and the abscissa the distance from outer end *A*. At moderate loads before the outer end starts to bottom, the developed length will be represented by the dashed line *AE*, while at heavy loads when a portion *AC* of the outer coil is bottomed the developed length is represented by *ACD*.

Up to a certain load P_1 (which will be called the initial bottoming load) at which the outer coil just starts to bottom, the load-deflection characteristic will be a straight line as indicated in *Fig.* 201. Above this load, as the coils bottom, the spring becomes stiffer as indicated and the load-deflection characteristic curves upward.

In calculating the initial bottoming load it will be assumed

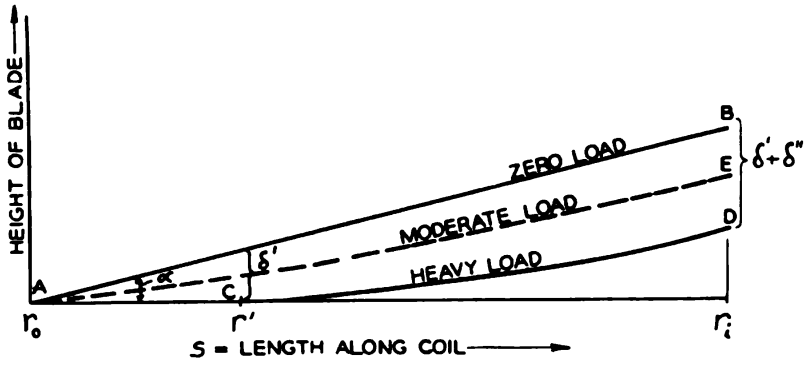

Fig. 200—Development of center line of volute spring for constant free helix angle. At heavy loads spring bottoms between r_o and r'

that the coil radius r at any angle θ from the built-in outer end A (*Fig.* 197*b*) may be represented approximately by a spiral. This will be sufficiently accurate for most practical purposes. Thus

$$r=r_o\left(1-\frac{\beta\theta}{2\pi n}\right) \quad \text{.....(428)}$$

where

$$\beta=\frac{r_o-r_i}{r_o} \quad \text{.....(429)}$$

r_o, r_i are the radii at the beginning and end, respectively, of the active portion of the spring (*Fig.* 197) and n is the number of active coils.

The deflection per turn of a helical spring of narrow rectangular cross section, where the long side of the section is parallel to the spring axis and where the width b (*Fig.* 197*a*) is greater than $2.7h$, as is usually the case in volute springs, is given with sufficient accuracy by the following equation[3]:

$$\delta_t=\frac{6\pi Pr^3}{Gbh^3\left(1-.63\frac{h}{b}\right)} \quad \text{.....(430)}$$

where P=load on spring, h=thickness of blade, b=blade width, G=modulus of rigidity, r=coil radius.

In a small angle $d\theta$, the increment of the deflection $d\delta$ will be equal to δ_t multiplied by $d\theta/2\pi$. Hence, using Equation 430

$$d\delta=\delta_t\frac{d\theta}{2\pi}=\frac{3Pr^3d\theta}{Gbh^3\left(1-.63\frac{h}{b}\right)} \quad \text{.....(431)}$$

In this r=mean coil radius at angle θ (*Fig.* 197*b*).

From *Fig.* 200, bottoming of the outer coil may be expected to start for constant, free helix angle when the slope $d\delta/ds$ at the outer mean radius r_o (*Fig.* 197) is equal to the tangent of the helix angle α, or when

$$\left(\frac{d\delta}{ds}\right)_{r=r_o}=\tan\alpha$$

Since α is usually small in practical volute springs the tangent of

[3] Chapter XII, Page 216.

the angle may with sufficient accuracy be taken equal to the angle in radians. Taking $ds = rd\theta$ and $\tan \alpha = \alpha$, this condition becomes

$$\left(\frac{d\delta}{rd\theta}\right)_{r=r_o} = \alpha \qquad (432).$$

Putting $r = r_o$ in Equation 431, and substituting in Equation 432, the initial bottoming load P_1 for constant free helix angle becomes

$$P_1 = \frac{Gbh^3\alpha\left(1 - .63\frac{h}{b}\right)}{3r_o^2} \qquad (433)$$

In this the helix angle α is expressed in radians (degrees divided by 57.3).

Deflection—Calculation of deflection will be discussed for two conditions, namely, where the loads are less than initial bottoming loads and where they are greater.

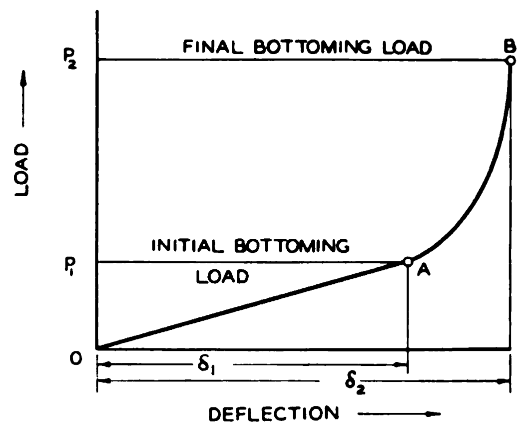

Fig. 201 — Load-deflection characteristic of volute spring

WHEN $P < P_1$: To calculate the deflection δ for loads P that are less than the initial bottoming load P_1, Equation 428 and 431 may be used. Substituting the value of r given by Equation 428 in 431, the increment of deflection in small angle $d\theta$ becomes

$$d\delta = \frac{3Pr_o^3\left(1 - \frac{\beta\theta}{2\pi n}\right)^3 d\theta}{Gbh^3\left(1 - .63\frac{h}{b}\right)} \qquad (434)$$

Integrating this between the limits $\theta=0$ and $\theta=2\pi n$ where n is the number of active coils, the total deflection (for loads under the initial bottoming load) may be expressed as

$$\delta=\frac{P}{P_1}(2\pi nr_o\alpha K_1), \text{ when } P<P_1 \quad \ldots\ldots\ldots\ldots\ldots\ldots\ldots\ldots\ldots\ldots (435)$$

where P_1 is given by Equation 433, and

$$K_1=1-\frac{3}{2}\beta+\beta^2-\frac{\beta^3}{4} \quad \ldots\ldots\ldots\ldots\ldots\ldots\ldots\ldots\ldots\ldots (436)$$

Values of K_1 are plotted as functions of $\beta=(r_o-r_i)/r_o$ in *Fig.* 202. The values r_o and r_i in this expression depend on the design of the end coils (*Fig.* 197). Where these latter are tapered as indicated in *Fig.* 197, three-fourths turn at each end is fre-

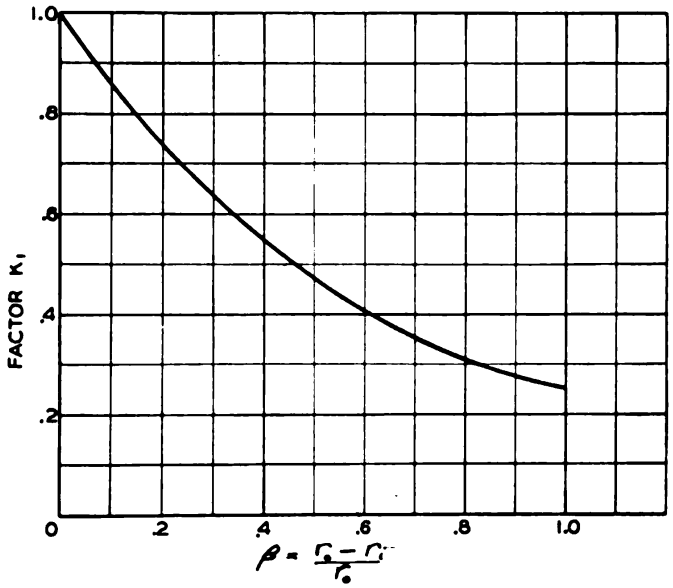

Fig. 202—Curve for finding factor K_1 as function of β

quently considered inactive, but this figure may be changed as further test data become available.

Thus to calculate deflection at any load P less than P_1 the simple formula of Equation 435 may be used, the value K_1 being read from the curve of *Fig.* 202. It should be noted that Equation

435 will also apply for the case of a variable free helix angle provided no bottoming of the coils occurs.

WHEN $P>P_1$: Where the load P is above the bottoming load P_1, the deflection δ for a constant free helix angle may be considered as composed of two parts, e.g., a part δ' (*Fig.* 200) due to the compression of the bottomed portion AC of the spring and a part δ'' due to the deflection of the free portion CD. Assuming that the coils have bottomed to a radius r' and angle θ' as indicated in *Fig.* 200, then from the condition $d\delta/ds=\alpha$ at the radius $r=r'$ and by proceeding as before the following is obtained:

$$c'=2\sqrt{\frac{\alpha Gbh\left(1-.63\frac{h}{b}\right)}{3P}} \qquad (437)$$

In this, $c'=2r'/h=$spring index at $r=r'$.

Also by taking $r=r'$ and $\theta=\theta'$ in Equation 428, the angle θ' may be expressed as follows:

$$\theta'=\frac{2\pi n}{\beta}\left(1-\frac{c'}{c_o}\right) \qquad (438)$$

where $c_o=2r_o/h=$spring index at $r=r_o$.

Assuming as before that $\tan\alpha=\alpha$, the deflection δ' is given by

$$\delta'=\int_0^{\theta'}\alpha r d\theta \qquad (439)$$

Using Equation 428 in this and integrating,

$$\delta'=\alpha r_o\theta'\left(1-\frac{\beta\theta'}{4\pi n}\right) \qquad (440)$$

By using Equations 433, 437 and 438 this equation may be expressed in terms of the ratio P/P_1 as follows:

$$\delta'=\frac{\pi\alpha r_o n}{\beta}\left(1-\frac{P_1}{P}\right) \qquad (441)$$

The deflection δ'' will be obtained by summing up the elementary deflection $d\delta$ between the limits $\theta=\theta'$ and $\theta=2\pi n$. Thus, using Equation 434,

$$\delta'' = \int_{\theta'}^{2\pi n} \frac{3Pr_o^3(1-\beta\vartheta/2\pi n)^2 d\theta}{Gbh^3(1-.63h/b)} \quad \ldots\ldots (442)$$

Integrating this, simplifying and adding to the value of δ' given by Equation 441, the total deflection δ becomes for $P > P_1$:

$$\delta = \delta' + \delta'' = 2\pi n r_o \alpha \left(\frac{P}{P_1} K_1 - \frac{K_2}{\beta} \right) \quad \ldots\ldots (443)$$

where K_2 is a function of the ratio P/P_1.

$$K_2 = \frac{1}{2}\left(\frac{P_1}{2P} + \frac{P}{2P_1} - 1 \right) \quad \ldots\ldots (444)$$

Values of K_2 are given as functions of P/P_1, in *Fig.* 203. By using this curve and that of *Fig.* 202, the deflection at any load P may easily be calculated. In this manner the complete load-deflection characteristic of the spring for a constant initial helix angle may be obtained.

To find the load P_2 at which all coils bottom the procedure is as follows. From Equation 437, by using the expression for P_1 given by Equation 433,

$$\frac{c'}{c_o} = \frac{r'}{r_o} = \sqrt{\frac{P_1}{P}} \quad \ldots\ldots (445)$$

Bottoming of all active coils will occur when $r' = r_i$ and $P = P_2$. Using Equation 445 and taking $\beta = (r_o - r_i)/r_o$ the final bottoming load P_2 becomes

$$P_2 = \frac{P_1}{(1-\beta)^2} = P_1 \left(\frac{r_o}{r_i} \right)^2 \quad \ldots\ldots (446)$$

The deflection δ_2 at the load P_2 is obtained by taking $\theta' = 2\pi n$ in Equation 439 and integrating, using the value of r given by Equation 428. This also gives the difference between free and solid height:

$$\delta_2 = \int_0^{2\pi n} \alpha r_o \left(1 - \frac{\beta\theta}{2\pi n} \right) d\theta = 2\pi n r_o \alpha \left(1 - \frac{\beta}{2} \right) \quad \ldots\ldots (447)$$

Solving this for α the helix angle in terms of δ_2 is

$$\alpha = \frac{\delta_2}{2\pi n r_o \left(1 - \frac{\beta}{2}\right)} \quad \ldots\ldots (448)$$

Since the free and solid heights of the spring are known, the helix angle α (in radians) may be calculated from this equation. The deflection δ_1 at which initial bottoming occurs is obtained from Equation 435 taking $P = P_1$. This gives

$$\delta_1 = 2\pi n r_o \alpha K_1 \quad \ldots\ldots (449)$$

To construct an approximate load-deflection curve for any

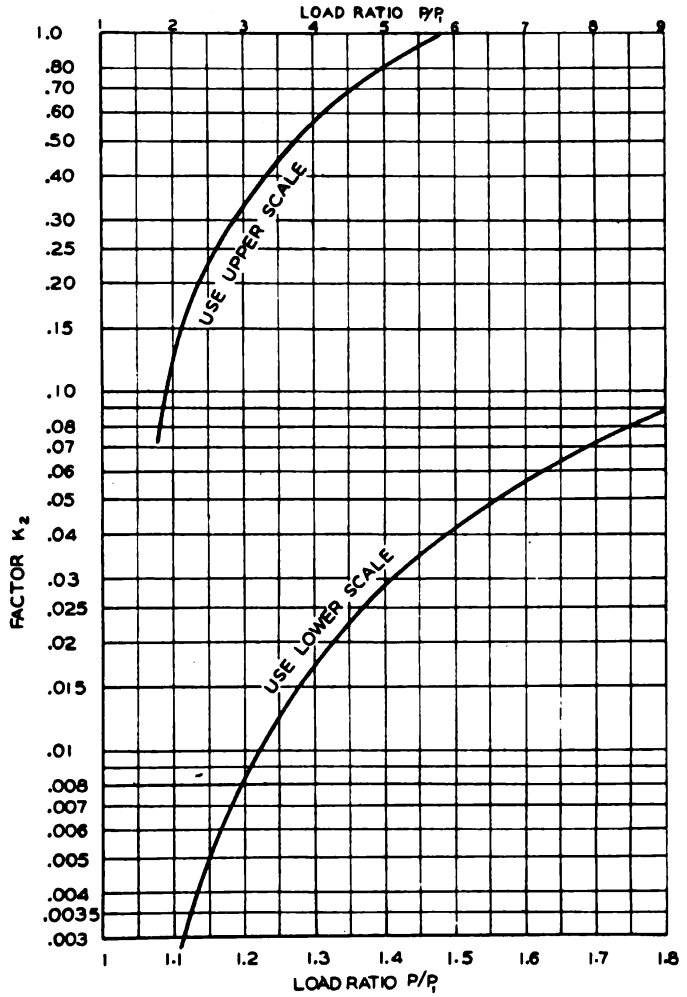

Fig. 203—Curves for finding factor K_2 from load ratio P/P_1

spring having a constant initial helix angle it is only necessary to calculate P_1, P_2, δ_1 and δ_2 from Equations 433, 446, 447 and 449. A straight line is then drawn between the origin and point A representing P_1 and δ_1 (*Fig.* 201). Point B (representing P_2 and δ_2) is connected to A by a smooth curve concave upward. For greater accuracy, if desired, additional points on this curve may be calculated from Equation 443. Thus the load-deflection diagram may be determined simply.

Stress Calculations—To calculate the stress, the formulas for rectangular bar helical springs will be used, modified to apply to the volute spring. As mentioned previously, these stresses should be considered only as first approximations because additional secondary stress usually will be present.

WHEN $P<P_1$: Where the load P is less than the initial bottoming load P_1, the peak stress will occur at the maximum radius $r=r_0$. Using the approximate equation for a rectangular bar spring with $b>3h$ and with the long side of the rectangle parallel to the spring axis as discussed previously[4], the maximum shear stress τ (where $P \leqq P_1$) becomes

$$\tau = \frac{3P(c_o+1)}{2hb\left(1 - .63\frac{h}{b}\right)} \text{ when } P \leqq P_1 \quad \ldots\ldots (450)$$

In this $c_0=2r_0/h=$spring index at $r=r_0$. Where h/b is small, i.e., where the blade is wide compared to the thickness, the term $1-.63h/b$ may be taken as unity. This gives, approximately,

$$\tau = \frac{3P(c_o+1)}{2hb} \quad \ldots\ldots (451)$$

WHEN $P>P_1$: Where the load is greater than the initial bottoming load, the maximum shear stress τ will occur at $r=r'$ where r' is the radius at which bottoming occurs. Thus Equation 450 may be used, putting $c_o=c'$ where $c'=2r'/h=$spring index at $r=r'$. This gives

$$\tau = \frac{3P(c'+1)}{2hb\left(1 - .63\frac{h}{b}\right)}, \text{ when } P>P_1 \quad \ldots\ldots (452)$$

[4] Chapter XII, Page 213.

Since from Equation 445, $c'=c_o\sqrt{P_1/P}$, by substitution of this in Equation 452, the stress at any load P (for $P>P_1$) becomes

$$\tau=\frac{3P\left(c_o\sqrt{\frac{P_1}{P}}+1\right)}{2hb\left(1-.63\frac{h}{b}\right)} \qquad (453)$$

When final bottoming occurs, the load $P=P_2$. Using the value of P_1/P_2 given by Equation 446 in Equation 453 the peak stress τ_2 at the final bottoming load P_2 may be expressed by

$$\tau_2=\frac{3P_2(c_i+1)}{2hb\left(1-.63\frac{h}{b}\right)} \qquad (454)$$

where $c_i=2r_i/h$=spring index at $r=r_i$.

Substituting in this the value of P_2 given by Equation 446

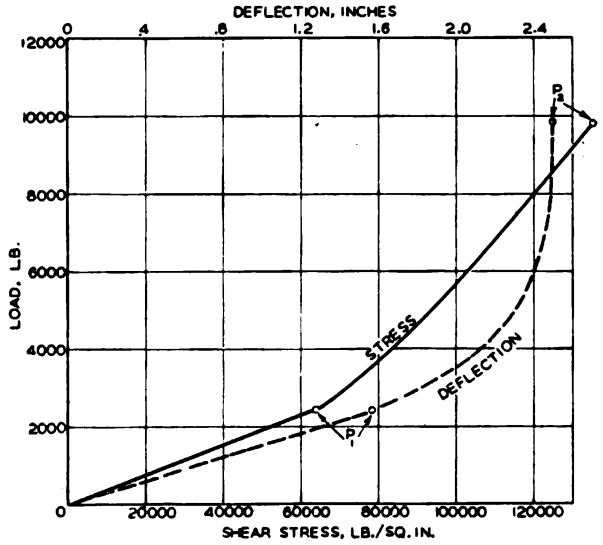

Fig. 204—Load-deflection and load-stress curves, P_1, P_2 initial and final bottoming loads

and the value of P_1 given by Equation 433, the stress τ_2 for final bottoming reduces to the simple expression

$$\tau_2=\frac{2G\alpha(c_i+1)}{c_i^2} \qquad (455)$$

These formulas include the effect of bar curvature. If it is desired to neglect this effect where static loading is present, the calculation may be made using the same equations (450 to 455), but reducing the expression in the parenthesis of the numerator by unity. (Thus in Equation 450, to do this c_o is taken instead of c_o+1 in the numerator). For most volute springs this will not make a great deal of difference, however.

Application to Practical Design—As an example of the use of these equations in practical design a volute spring with a constant initial helix angle and with the following dimensions may be considered: $r_o=2\frac{1}{2}$-inch, $r_i=1\frac{1}{4}$-inch, $h=\frac{1}{4}$-inch, $b=5$-inch=solid height, free height=$7\frac{1}{2}$-inch, $c_o=2r_o/h=20$, $c_i=2r_i/h=10$, $n=4$=number of active coils, $\beta=(r_o-r_i)/r_o=.5$.

The solid deflection δ_2 will be the difference between the free and solid heights; thus $\delta_2=2\frac{1}{2}$-inch. From Equation 448 the helix angle α is

$$\alpha=\frac{\delta_2}{2\pi n r_o\left(1-\frac{\beta}{2}\right)}=\frac{2.5}{2\pi\times4\times2.5\times.75}=.0531 \text{ radians}$$

Taking $G=11.5\times10^6$ for steel, the peak shear stress with the spring solid becomes, from Equation 455,

$$\tau_2=\frac{2\times11.5\times(10)^6\times.0531\times11}{(10)^2}=135000 \text{ lb/sq in.}$$

The initial bottoming load P_1 is, from Equation 433,

$$P_1=\frac{11.5\times(10)^6\times5\times(.25)^3\times.0531\times.969}{3(2.5)^2}=2460 \text{ lb}$$

Shear stress at the initial bottoming load P_1 from Equation 450 is

$$\tau_1=\frac{3\times2460\times21}{2\times.25\times5\times.969}=64000 \text{ lb/sq in.}$$

From Equation 446 the final load P_2 is found:

$$P_2=\frac{2460}{(.5)^2}=9840 \text{ lb}$$

The deflection δ_1 at the initial bottoming load P_1 is given by

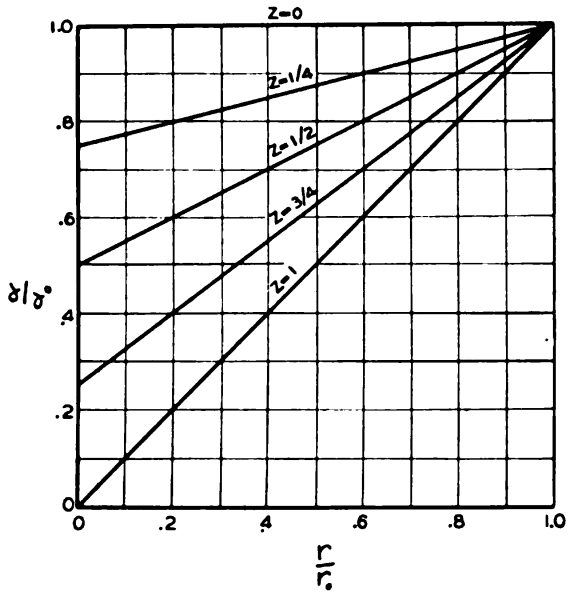

Fig. 205—Assumed distribution of helix angle as function of radius for various z values

Equation 449, using the value of $K_1 = .47$ given by *Fig.* 202 for $\beta = .5$. This gives

$$\delta_1 = 2\pi n r_o \alpha K_1 = 2\pi \times 4 \times 2.5 \times .0531 \times .47 = 1.57 \text{ in.}$$

The value δ_2 for the final bottoming load P_2 will be the difference between the free and solid height, i.e., $\delta_2 = 7.5 - 5 = 2.5$-inch. Knowing δ_1, δ_2, P_1, and P_2 a load deflection curve similar to *Fig.* 201 may be plotted for this particular spring. A similar load-stress curve may be plotted, since the stress will vary linearly with load up to initial bottoming load P_1. The stress at any load between P_1 and P_2 may be calculated from Equation 453. In this manner the complete load-stress and load-deflection diagrams as given in *Fig.* 204 are obtained for this case. From these diagrams, if desired, a stress-deflection curve may also be plotted.

VARIABLE HELIX ANGLE

As mentioned previously, the process of manufacture in general results in a helix angle which increases from inside to outside of the spring. The amount of this variation in helix

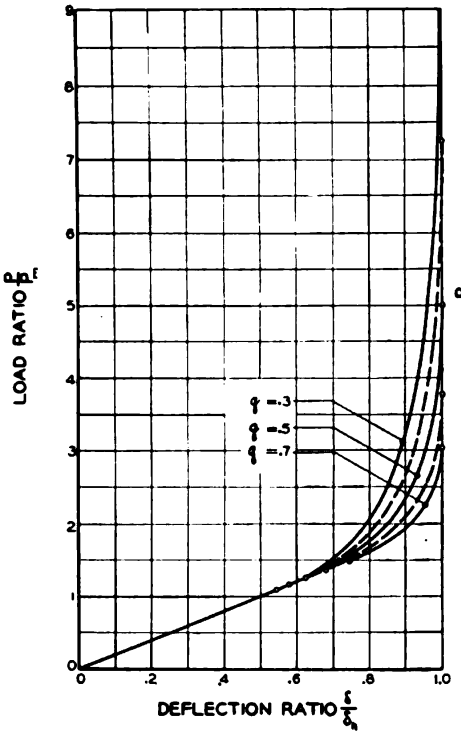

Fig. 206—Type curve for $z=0$, constant helix angle, $q=r_i/r_o$

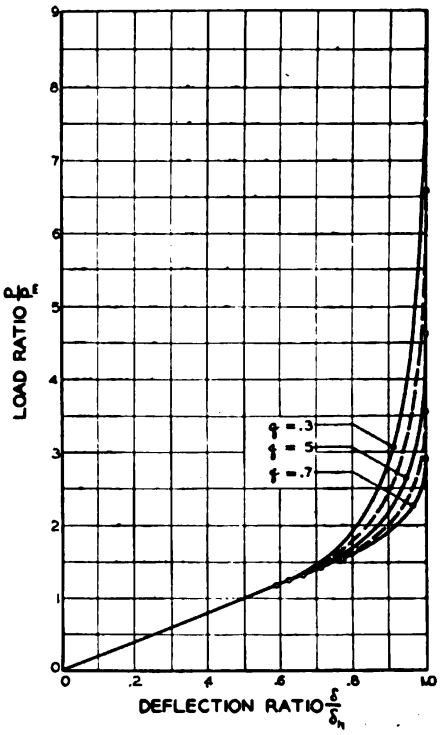

Fig. 207—Type curves for $z=\frac{1}{4}$, volute spring, $q=r_i/r_o$

angle depends on the conditions obtaining during the cold-setting process and on the method of winding. An analysis based on the assumption that the variation of free helix angle is linear from the inner to the outer radius has been carried out by Fuchs[5]. This assumption may be expressed by

$$\frac{\alpha_o-\alpha}{\alpha_o-\alpha_i}=\frac{r_o-r}{r_o-r_i} \qquad (456)$$

In this α_o, α_i and α are the helix angles at radii r_o, r_i and r respectively (*Fig.* 197). The relative variation of the helix angle may be expressed by a number z where

$$z=\frac{1-\frac{\alpha_i}{\alpha_o}}{1-\frac{r_i}{r_o}} \qquad (457)$$

[5] S.A.E. *Journal*, Sept. 1943, Page 317. This also discusses design of presetting bowls for volute springs.

For $z=0$ the case of constant free helix angle is obtained while for $z=1$ approximately constant bottoming stress will exist (neglecting corrections for curvature). Ratios of α/α_o are plotted against r'/r_o in *Fig.* 205, for the various values of z. This gives an idea of the relative variation in free helix angle with radius, for different values of z.

Load-Deflection—Assuming elastic conditions, similar load-deflection diagrams will be obtained for all springs with given values of z and q. Thus the actual load-deflection diagram may be found by multiplying a given "type curve" by certain scale ratios. Approximate type curves for values of $z=0$, ¼, ½, ¾ and 1 have been computed by Fuchs[5] and are given in *Figs.* 206, 207, 208, 209, and 210. On each figure curves are drawn for r_i/r_o equal to .3, .4, .5, .6, and .7 corresponding to springs with small, medium or large ratios of inside to outside diameters. Initial and final bottoming loads are indicated by the circles on each curve. The abscissas

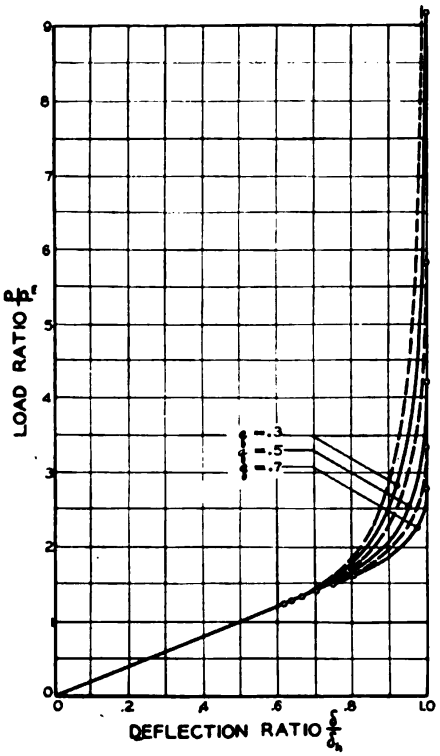

Fig. 208—Type curves for $z=½$, volute spring, $q=r_i/r_o$

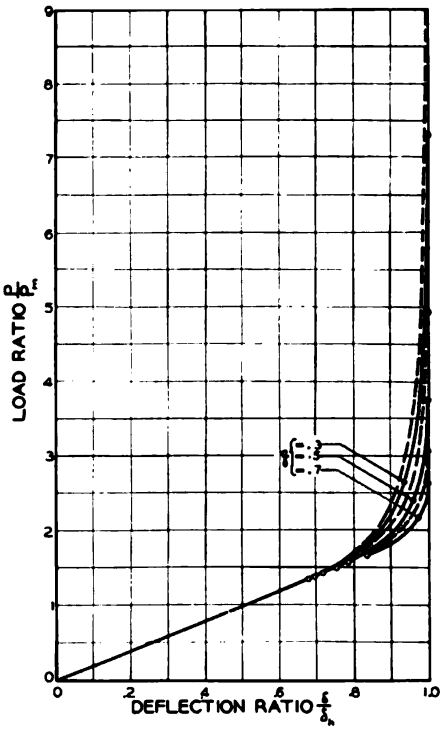

Fig. 209—Type curves for $z=¾$, volute spring, $q=r_i/r_o$

of these figures are plotted in terms of the maximum possible deflection δ_h, the ordinates in terms of a load P_m, where

$$\delta_h = nr_o\alpha_i K_3 \quad \text{.....(458)}$$

$$K_3 = \frac{2\pi}{1-q-(1-q)^2 z}\left[\frac{z(1-q^3)}{3}+\frac{(1-z)(1-q^2)}{2}\right] \quad \text{.....(459)}$$

In this $q = r_i/r_o$ and z is given by Equation 457. Values of K_3 may be taken from the curve of *Fig.* 211 for various values of z.

$$P_m = \frac{bh^3\alpha_i K_3 K_4 G}{r_o^2} \quad \text{.....(460)}$$

where

$$K_4 = \frac{1}{\pi^2}\left(\frac{1-q}{1-q^4}\right) \quad \text{.....(461)}$$

Values of K_4 are plotted in *Fig.* 212 against $q = r_i/r_o$. For further details the reader is referred to the article by Fuchs[5].

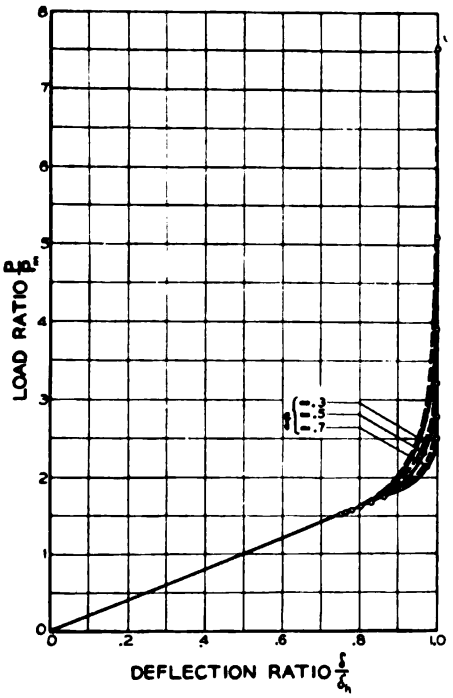

Fig. 210—Type curves for $z = 1$, uniform bottoming stress, $q = r_i/r_o$

Thus to get the actual load-deflection curve for any spring with a given value of z and q the ordinates of the corresponding type curve must be multiplied by P_m and the abscissas by δ_h. Interpolation can be used if necessary.

It should be noted that the initial bottoming load P_1 may be

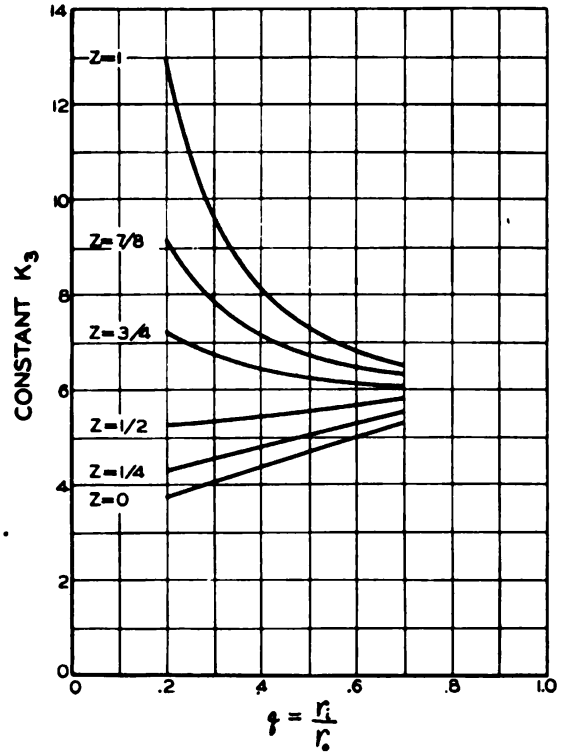

Fig. 211—Constant K_3 plotted as a function of r_i/r_o for various z values

obtained from Equation 433 using $\alpha=\alpha_o$. For the usual spring where h/b is small the shear stress τ_o at which bottoming starts is found by using Equation 450 taking $P=P_1$. This gives

$$\tau_o=\frac{3}{2}\frac{P_1(c_o+1)}{hb} \qquad (462)$$

In this c_o=index $2r_o/h$ at $r=r_o$. If the value of P_1 given by Equation 433 is substituted in this the initial bottoming stress becomes:

$$\tau_o=\frac{Gh^2\alpha_o(c_o+1)}{2r_o^2} \qquad (463)$$

If curvature effects are neglected the term unity in the parentheses of this expression is dropped, obtaining the simple formula

$$\tau_o = \frac{Gh\alpha_o}{r_o} \quad \text{.....(464)}$$

In a similar manner the final bottoming load is given by Equation 433 taking $\alpha = \alpha_i$ and using r_i instead of r_o. This gives

$$P_2 = \frac{Gbh^3\alpha_i}{3r_i^2}\left(1 - .63\frac{h}{b}\right) \quad \text{.....(465)}$$

Shear stress at the inner end ($r = r_i$) at final bottoming load is given by Equation 455 using α_i in this case instead of α:

$$\tau_i = \frac{Gh\alpha_i}{r_i}\left(\frac{c_i+1}{c_i}\right) \quad \text{.....(466)}$$

where $c_i = 2r_i/h$ = index at $r = r_i$.

If curvature effects are neglected this reduces to the simple expression:

$$\tau_i = \frac{Gh\alpha_i}{r_i} \quad \text{.....(467)}$$

Design Calculation—As an example of the use of these formulas in design assuming $r_o = 3.75$, $r_i = 1.93$, $b = 7.50$, $h = .40$ inches, $n = 4$, $G = 11 \times 10^6$ lb./sq. in., $\alpha_o = .076$, $\alpha_i = .060$, $q = .515$, $z = .434$ from Equation 457. From *Fig.* 211, for $q = .515$, $z = .434$, $K_3 = 5.5$, and from *Fig.* 212, $K_4 = .053$. Using Equations 460 and 458

$$P_m = \frac{11 \times 10^6 \times 7.5 \times (.4)^3 \times .060 \times .053 \times 5.5}{(3.75)^2} = 6550 \text{ lb}$$

$$\delta_h = 4 \times 3.75 \times .060 \times 5.5 = 4.95$$

The difference in deflection obtained by using the curves for $z = \frac{1}{4}$ and $z = \frac{1}{2}$, (*Figs.* 207 and 208) for $q = .5$ does not amount to more than .1-inch at any load, which is very small compared to the peak deflection. Hence either curve may be used for constructing an approximate load-deflection diagram.

To find the initial bottoming stress τ_o, neglecting curvature, Equation 464 is used. This gives

$$\tau_o = \frac{11 \times 10^6 \times .4 \times .076}{3.75} = 89{,}000 \text{ lb/sq in.}$$

To include the effect of curvature this stress is multiplied

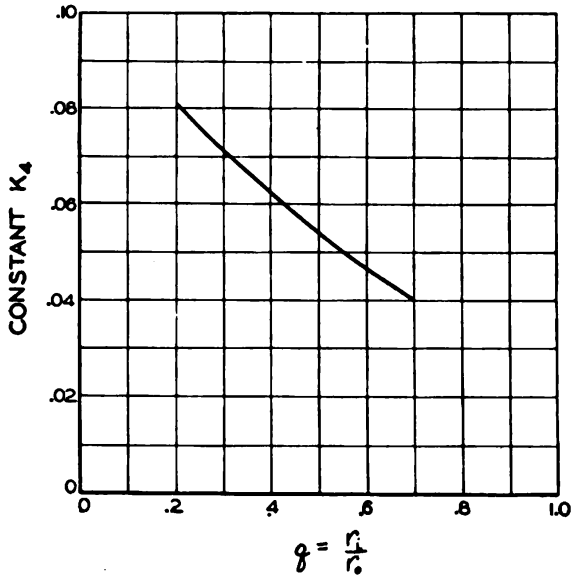

Fig. 212—Constant K_4 as a function of r_i/r_o

by the ratio $(c_o+1)/c_o$ where $c_o = 2r_o/h = 18.7$. This gives $r_o = 89{,}000 \times 19.7/18.7 = 94{,}000$ pounds per square inch.

To find the peak bottoming stress τ_i, neglecting curvature, Equation 467 is used. This gives

$$\tau_i = \frac{11 \times 10^6 \times .4 \times .06}{1.93} = 137{,}000 \text{ lb/sq in.}$$

To include effects of curvature the stress thus found is multiplied by $(c_i+1)/c_i$ where c_i = index $2r_i/h = 9.7$. The stress then becomes $r_i = 137{,}000(10.7/9.7) = 151{,}000$ pounds per square inch.

CHAPTER XXI

RUBBER SPRINGS AND MOUNTINGS

Inherent advantages of rubber springs include high energy storage per unit volume and the possibility of forming in complicated shapes. For these reasons such springs have found increasing application as vibration isolators for machinery, flexible mountings for automobile and aircraft engines, mount-

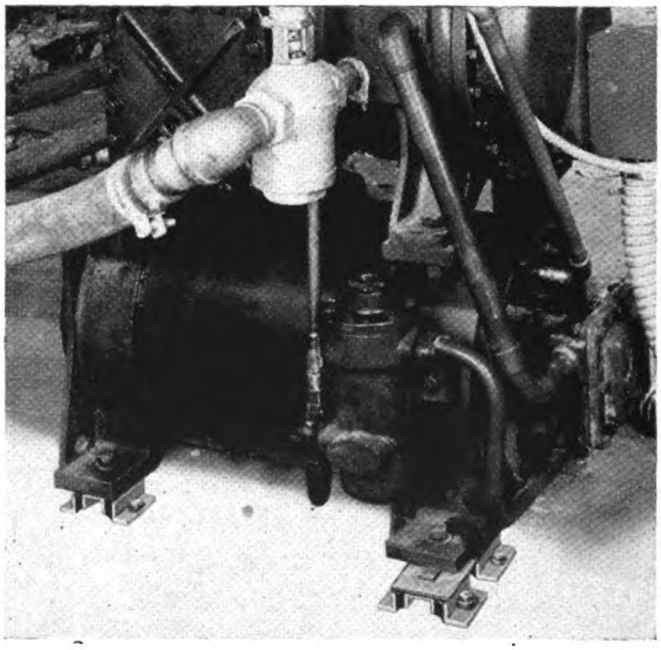

—Courtesy, B. F. Goodrich Co.

Fig. 213—Rubber springs applied to compressor mounting

ings for instruments, flexible elements in couplings, and many others. An example of the application of rubber springs to a refrigerant compressor mounting is shown in *Fig.* 213.

Although the subject is so large that an extensive treatment of rubber springs and mountings is beyond the scope of this book, completeness requires that at least the fundamental principles of design be touched upon. It should be emphasized that the ex-

tent of our knowledge of the behavior of rubber under stress is not comparable to that of the more usual spring materials such as the various steels, phosphor bronze and the like. Consequently, the calculation of rubber springs by available methods is at best only approximate. Among the reasons for variations between the predicted and actual behavior of such springs are the following:

1. Variations in elastic or shear moduli may occur among different rubber compounds even though of the same hardness reading.
2. In the case of compression springs of rubber, friction between compressed surfaces may vary through wide limits thus affecting the behavior of the spring. Where rubber pads are bonded to steel plates, such variations will not occur, however.
3. The static and dynamic moduli of elasticity will differ.
4. In general, rubber springs are deflected by relatively large amounts, and such deflections are more difficult to calculate accurately

Methods of calculating stress and deflection of various types of rubber mountings will first be treated after which the fundamental principles involved in the choice of flexibilities for such mountings will be discussed.

COMPRESSION SPRINGS

One of the most commonly used types of rubber springs is the simple compression block shown in *Fig.* 214 which represents a rectangular slab of rubber compressed between two steel plates.

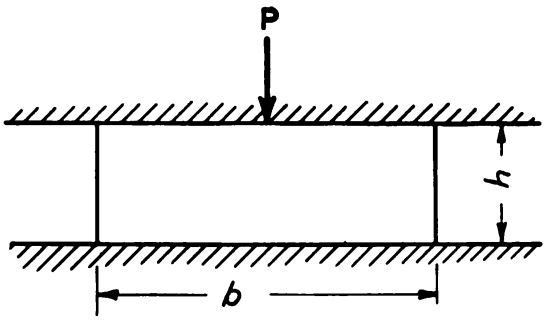

Fig. 214—Compression block of rubber, loaded

Because of tangential forces developed at the surfaces of the block during compression, the stiffness of such a spring is far larger when h is small (compared to the other two dimensions) than

when h is large. If the rubber is not bonded on, the stiffness may vary considerably for different amounts of friction between the surfaces of contact. Thus if the plates are lubricated with vaseline (or heavy grease) much larger deflections may be expected for short slabs than would be the case if dry surfaces

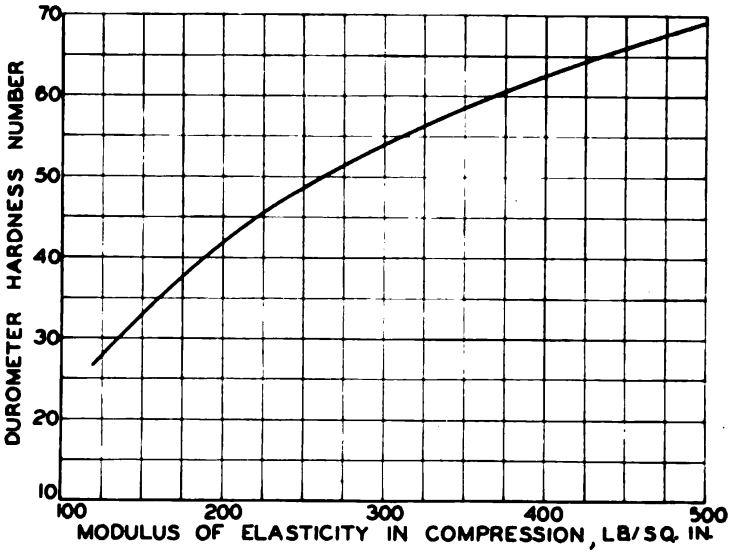

—J. F. D. Smith, *Journal of Applied Mechanics*, 1938.

Fig. 215—Modulus of elasticity of rubber in compression as function of durometer hardness number

were used. Because of the uncertain amount of friction present, when no bonding is used calculations of deflection in such cases must be considered roughly approximate only.

The following empirical method was developed by Smith[1], taking as a basis an average of a considerable number of tests. For this discussion, n = percentage deflection of slab of rubber at a given unit pressure, A = sectional area of slab, β = ratio of length of slab to width, h = thickness, E = modulus of elasticity of the rubber used. An average curve of the variation of modulus

[1] For further details see "Rubber Mountings"—J. F. Downie Smith, *Journal of Applied Mechanics*, March, 1938, Page A13; and "Rubber Springs—Shear Loading" by the same author, *Journal of Applied Mech.*, Dec., 1939, Page A159. Other articles of interest on rubber are: "Rubber Springs"—W. O. Keys, *Mechanical Engineering*, May, 1937, Page 345; "Elastic Behavior of Vulcanized Rubber"—H. Hencky, *Transactions* ASME, 1933, Page 45; "Rubber Cushioning Devices"—Hirschfield and Piron, *Transactions* ASME, Aug. 1937, Page 471; "The Mechanical Characteristics of Rubber"—F. L. Haushalter, *Transactions* ASME, Feb., 1939, Page 149. "Use of Rubber in Vibration Isolation"—E. H. Hull, *Journal of Applied Mechanics*, Sept. 1937, Page 109.

of elasticity in compression with durometer hardness is given in *Fig*. 215. E_o=modulus of elasticity of rubber having 55 durometer hardness, n_o=percentage deflection of a 1-inch cube of 55 durometer hardness rubber; n_o may be taken from the average curve of *Fig*. 216 if the loading is known. Then an empirical expression for percentage compression of rubber slabs is

$$n=\frac{n_o E_o}{E}\,\frac{(h\beta)^{2/3}}{\sqrt{A}} \qquad (468)$$

EXAMPLE. As an example of the use of this equation, assuming a rubber slab of 65 durometer hardness, a sectional area $A=8\times4=32$ in.², thickness=1 inch, and load=10,000 pounds,

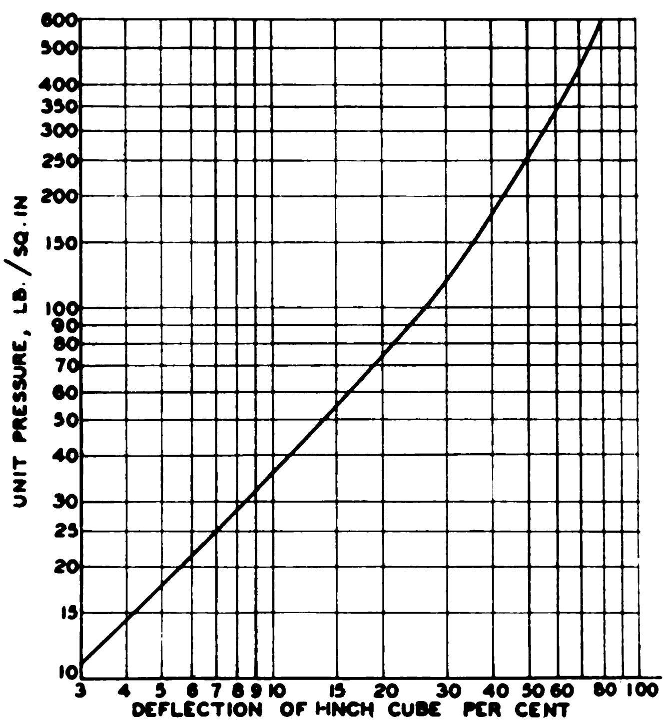

—from J. F. D. Smith

Fig. 216—Mean load-deflection curve for 55 duro rubber

the ratio β will be $8/4=2$. From *Fig*. 215 the modulus of elasticity for 55 durometer rubber is $E=310$ pounds per square inch. For 65 durometer rubber $E=430$ pounds per square inch. The unit pressure will be $10000/32=312$ pounds per square inch.

From *Fig.* 216 the deflection n_o of a 1-inch cube of 55 durometer rubber at this pressure will be 57 per cent. Using these values in Equation 468, the percentage compression at 10,000 pounds load becomes:

$$n=\frac{57\times310}{430}\,\frac{(1\times2)^{2/3}}{\sqrt{32}}=11.6\%$$

By finding values of n at other loads, a load-deflection diagram may be constructed.

SIMPLE SHEAR SPRING

Since rubber in pure shear involves no volume change, frictional effects at surfaces of contact such as may occur in compression slabs are not present and better accuracy in calculation may be expected. Rubber shear springs which have essentially the form shown in *Fig.* 217 consisting of two rubber pads bonded to steel plates are widely used for vibration isolation and machine mounting. Such an application is shown in *Fig.* 213.

This type of spring may be calculated as follows: Assuming that the shear angle γ in radians is proportional to shear stress

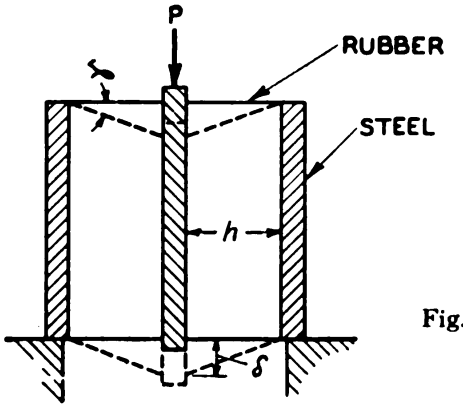

Fig. 217—Simple rubber shear spring

and inversely proportional to the modulus of rigidity G (according to Smith[1] this assumption gives the better agreement between theory and practice), then the shear stress $\tau=P/2A$ and

$$\gamma=\frac{P}{2AG}\text{ radians} \qquad (469)$$

where A is the sectional area of each pad. The factor 2 is used

since in this case there are two pads subjected to the load P. (To obtain the angle in degrees the value given by Equation 469 must be multiplied by 57.3). The modulus of rigidity G depends

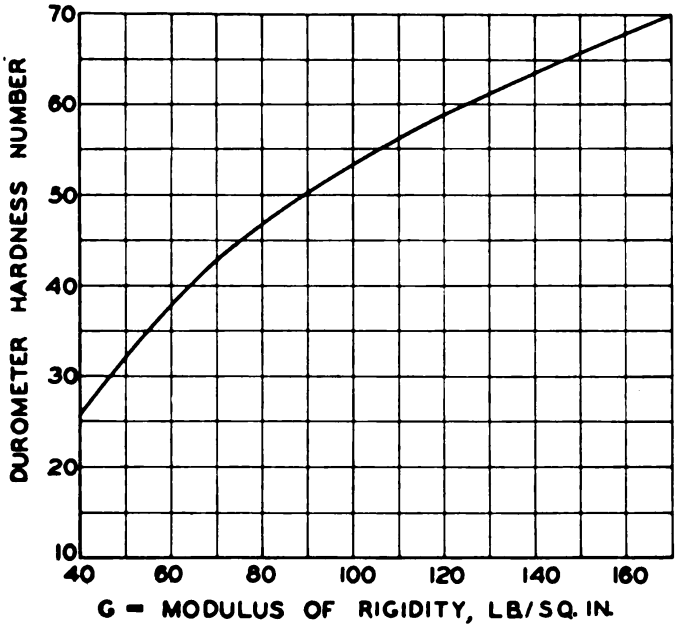

—from J. F. D. Smith

Fig. 218—Modulus of rigidity as function of hardness

on the durometer hardness of the rubber and may be estimated from the curve of *Fig.* 218.

To calculate the deflection δ of the spring of *Fig.* 217, if the shear angle γ is known,

$$\delta = h \tan \gamma \quad \ldots\ldots (470)$$

In this h= thickness of the pad and γ=the angle figured from Equation 469.

If the angle γ is not too large (say below 20 degrees), for practical purposes, the tangent may be taken equal to the angle. Using Equations 469 and 470 the deflection δ then becomes

$$\delta = \frac{Ph}{2AG} \quad \ldots\ldots (471)$$

Usually in practice rubber springs are made initially oblique

as indicated by the full lines of *Fig.* 219, the position of the rubber after final deflection being indicated by the dashed lines. By forming the pads in this manner, it is possible to introduce additional compression stresses during deflection. These stresses

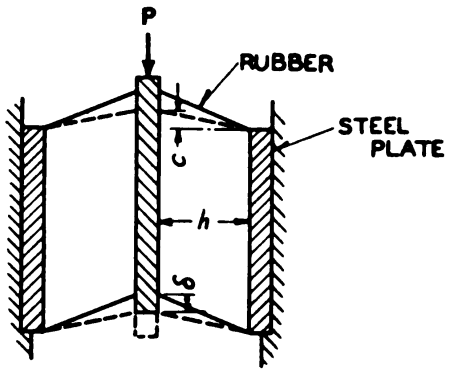

Fig. 219—Simple rubber spring with initially oblique pads. With this design, lateral compression is produced under load

are beneficial from the standpoint of the adhesion of the bond between the rubber and the steel. If the final deflection leaves the rubber approximately flat so that c/h is not large, as is usually the case, and if δ/h is not too great, it may be shown that Equation 471 can be used with enough accuracy for practical purposes[2].

CYLINDRICAL SHEAR SPRING

Constant Height—This type of shear spring consists essentially of a circular pad bonded to a steel ring on the outside and to a shaft or ring on the inside as indicated in *Fig.* 220*a*. A load P is applied along the axis as shown. The shear stress τ at any radius r will be

$$\tau = \frac{P}{2\pi r h} \qquad (472)$$

If y is the deflection at the same radius (*Fig.* 220*b*) the slope dy/dr will be equal to the negative value of the shear angle. The negative sign is taken since y decreases with increase in r. Since the shear angle γ is equal to τ/G (approximately) and the derivative is equal to the tangent of the shear angle, using Equation 472,

[2] J. F. D. Smith, *Journal of Applied Mechanics*, December, 1939, Page A-159.

$$\frac{dy}{dr} = -\tan\ \gamma = -\tan\left(\frac{P}{2\pi rhG}\right) \quad \text{.....(473)}$$

Letting $b = P/2\pi hG$, then using the known series expression for the tangent of an angle,

$$-\frac{dy}{dr} = \frac{b}{r} + \frac{b^3}{3r^3} + \frac{2b^5}{15r^5} + \frac{17b^7}{315r^7} + - - - + \text{.....(474)}$$

Integrating this between $r = r_i$ and $r = r_o$, the total deflection δ becomes

$$\delta = b \log_e \frac{r_o}{r_i} - \frac{b^3}{6}\left(\frac{1}{r_o^2} - \frac{1}{r_i^2}\right) - \frac{b^5}{30}\left(\frac{1}{r_o^4} - \frac{1}{r_i^4}\right) -$$

$$\frac{17b^7}{1890}\left(\frac{1}{r_o^6} - \frac{1}{r_i^6}\right) + - - - + \text{.....(475)}$$

For most practical cases (where $b/r_o < .4$) the terms of this series beyond the first may be neglected without serious error. This gives for a first approximation the following formula:

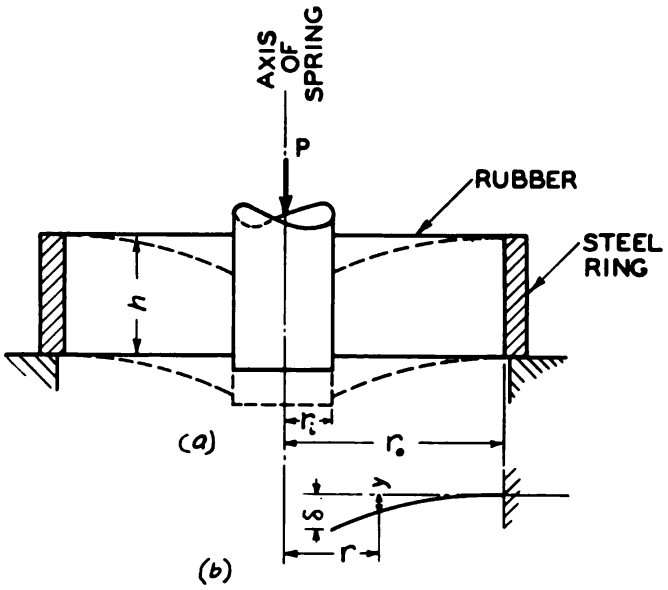

Fig. 220—Cylindrical rubber spring of constant height h subject to shear loading along axis

$$\delta \approx \frac{P}{2\pi hG} \log_e \frac{r_o}{r_i} \quad \text{.....(476)}$$

Constant Stress—If the thickness h of a cylindrical rubber spring is inversely proportional to the radius r, as indicated in *Fig.* 221 the shear stress τ will be constant and better utilization

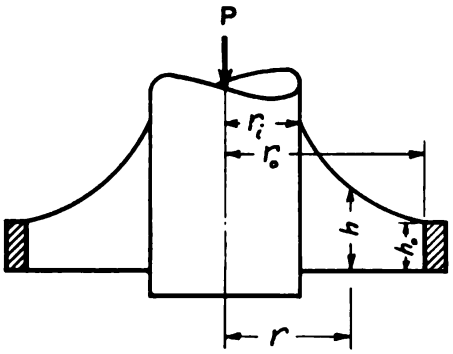

Fig. 221—Cylindrical rubber spring with constant shear stress, load is axial and h is inversely proportional to r

of the material will be obtained. This follows from the equation for stress:

$$\tau = \frac{P}{2\pi rh}$$

If $r = K_o/h$, by substitution in this formula,

$$\tau = \frac{P}{2\pi\left(\frac{K_o}{h}\right)h} = \frac{P}{2\pi K_o} = \frac{P}{2\pi r_o h_o} = \text{Const.} \quad \text{.....(477)}$$

In this h_o = thickness at outer radius r_o, *Fig.* 221. Since the stress τ is constant in this case, the shear angle $\gamma = \tau/G$ will also be constant. The deflection will be

$$\delta = (r_o - r_i)\tan\frac{\tau}{G}$$

or using Equation 477 for τ

$$\delta = (r_o - r_i)\tan\left(\frac{P}{2\pi r_o h_o G}\right) \quad \text{.....(478)}$$

For small angles γ (say less than 20 degrees) where the

tangent may be taken approximately equal to the angle, the deflection δ may be written

$$\delta = \frac{P(r_o - r_i)}{2\pi r_o h_o G} \quad \ldots\ldots (479)$$

This equation is sufficiently accurate for most practical uses.

CYLINDRICAL TORSION SPRING

Constant Thickness—In this case the thickness h of the spring is taken constant, *Fig.* 222 while a moment M is assumed to act about the spring axis as indicated. The shear stress τ at radius r due to the moment M is

$$\tau = \frac{M}{2\pi r^2 h} \quad \ldots\ldots (480)$$

In this case the maximum shear stress will occur when $r = r_i$ and is

$$\tau_m = \frac{M}{2\pi r_i^2 h} \quad \ldots\ldots (481)$$

Letting $d\theta$ = relative angular deflection about the spring axis

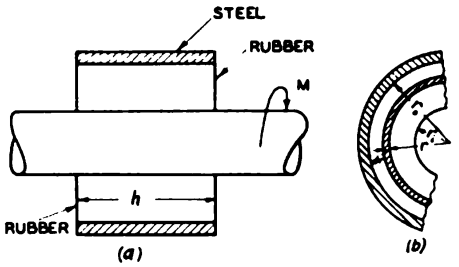

Fig. 222—Cylindrical torsion spring, constant thickness h

contributed by the shear stress acting on the elemental ring shown shaded in *Fig.* 222*b*, then

$$d\theta = \frac{dr \tan \gamma}{r} \quad \ldots\ldots (482)$$

This follows since the tangential deformation of the outer circumference of the element with respect to the inner is $dr \tan \gamma$

where γ is the shear angle τ/G. Dividing this by r yields the elemental angular deflection $d\theta$. Since $\gamma=\tau/G$, by using Equation 480,

$$d\theta=\frac{dr}{r}\tan\left(\frac{M}{2\pi r^2hG}\right)$$

Putting c equal to $M/2\pi hG$, this expression becomes

$$d\theta=\frac{1}{r}\left(\tan\frac{c}{r^2}\right)dr \quad \ldots\ldots(483)$$

Using the known tangent series as before, the angular deflection becomes

$$\theta=\int_{r_i}^{r_o}\left(\frac{c}{r^3}+\frac{1}{3}\frac{c^3}{r^7}+\frac{2}{15}\frac{c^5}{r^{11}}+---+---\right)dr$$

By integrating and substituting limits this equation reduces to

$$\theta=\frac{M}{4\pi hG}\left[\left(\frac{1}{r_i^2}-\frac{1}{r_o^2}\right)+\frac{1}{9}\left(\frac{1}{r_i^6}-\frac{1}{r_o^6}\right)\frac{M^2}{4\pi^2h^2G^2}+---\right] \quad \ldots(484)$$

In practice it will be found that this series converges rapidly so that the first term usually will be sufficient. This gives

$$\theta=\frac{M}{4\pi hG}\left(\frac{1}{r_i^2}-\frac{1}{r_o^2}\right) \quad \ldots\ldots(485)$$

Constant Stress—If the cylindrical rubber spring is made so that the thickness h, *Fig.* 223 varies inversely as the square of the radius r, as shown by Equation 480 the shear stress will be constant. Thus, in this case, the depth is taken equal to

$$h=h_i\frac{r_i^2}{r^2} \quad \ldots\ldots(486)$$

where h_i=thickness of rubber at the inside radius $r=r_i$, *Fig.* 223. By substitution in Equation 480 the stress becomes

$$\tau=\frac{M}{2\pi r_i^2h_i}=\text{Const.} \quad \ldots\ldots(487)$$

Letting $\gamma=\tau/G$ as before, then the angular deflection due to

the elemental ring shown shaded in *Fig.* 223*b* will be, as before,

$$d\theta = \frac{dr \tan \gamma}{r}$$

or

$$d\theta = \frac{dr}{r} \tan\left(\frac{M}{2\pi r_i^2 h_i G}\right)$$

Integrating between $r = r_i$ and $r = r_o$, the total angular deflection θ (in radians) becomes

$$\theta = \left[\tan\left(\frac{M}{2\pi r_i^2 h_i G}\right) \right] \log_e \frac{r_o}{r_i} \quad \text{.....(488)}$$

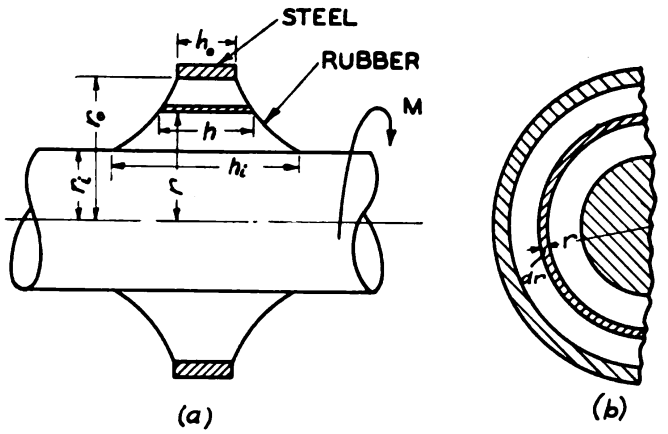

Fig. 223—Cylindrical torsion spring with constant stress

Assuming the tangent of the angle equal to the angle (which is accurate enough if the deflection is not too large),

$$\theta = \frac{M \log_e \frac{r_o}{r_i}}{2\pi r_i^2 h_i G} \quad \text{.....(489)}$$

EXAMPLE—Assuming a cylindrical rubber spring (60 durometer) of constant depth h loaded as in *Fig.* 222 under a torque of 10,000 in-lb, with dimensions as follows: $r_o = 3$ inches, $r_i = 2$ inches, $h = 5$ inches, from Equation 481 the maximum stress at the inner radius, in pounds per square inch, is

$$\tau_m = \frac{M}{2\pi r_i^2 h} = \frac{10000}{2\pi \times 4 \times 5} = 80 \text{ lb/sq in.}$$

For 60 durometer rubber, from *Fig.* 218 the modulus of rigidity is 125 pounds per square inch. Using the first term of the series of Equation 484 the angular deflection becomes:

$$\theta = \frac{10000}{4\pi(5)(125)}\left(\frac{1}{4} - \frac{1}{9}\right) = .177 \text{ radians or } 10.2 \text{ degrees}$$

If the second term of Equation 484 is used, this result will change by about 7 per cent.

If the spring were of the constant stress type (*Fig.* 223) with $h_i = 5$ inches, $h_o = 2.22$ inches from Equation 487 the stress is the same as that found previously. From Equation 489 assuming small deflections, the angular deflection at 10,000 inch-pounds moment is

$$\theta = \frac{10000 \times .405}{2\pi \times 4 \times 5 \times 125} = .258 \text{ radians} = 14.8 \text{ degrees}$$

where $\log_e (r_o/r_i) = \log_e 1.5 = .405$.

The use of Equation 488 would give a result equal to 17.2 degrees or about 16 per cent greater than that found from Equation 489 .

It should be recognized that as mentioned previously the equations given here should be considered approximate only particularly if deflections and stresses are large.

ALLOWABLE STRESSES

There is not a great deal of data in the literature on allowable working stress for rubber springs. Hirschfield and Piron[3] suggest that the working stresses in rubber shear springs (and also on rubber to metal bonds) be limited to 25 to 30 pounds per square inch in shear except in cases which have been thoroughly tested. They also state that under favorable conditions these bonds may withstand considerably higher unit loads, values of to 50 to 60 pounds per square inch having been used.

[3] *Transactions* ASME, Aug., 1937, Page 489.

These values agree roughly with those of Keys[4] who states that stresses of 25 to 50 pounds per square inch are used on metal to rubber bonds. Also it is suggested that the thickness of a shear sandwich be not greater than one-fourth of the smaller of the other two dimensions.

Haushalter[5] reports the results of long-time creep tests on rubber of about 45 durometer hardness. When tested in the form of a flat shear spring, *Fig.* 217, at 50 pounds per square inch shear the rubber showed a total creep of about .017-inch for 5/16-inch thickness (corresponding to a shear angle of .055-radian) after 20 days at normal temperature. At 140 degrees Fahr., at the same shear stress, the creep was .15-inch in 5/16-inch or .48-radian shear angle in 100 days. Other tests on 1-inch thick rubber sandwiches of a different compound (38 durometer) at 40 pounds per square inch shear stress and at normal temperature showed .055-inch deflection (or a shear angle of .055-radian) after 500 days. In all cases the creep-time relation was approximately logarithmic. This work showed that the creep may be greatly increased by a rise in temperature and that wide variations may occur if different compounds are used. The necessity for keeping down working stresses if excessive creep is to be avoided was clearly brought out by these tests.

Regarding allowable strains on rubber compression springs, *Fig.* 214, Hirschfield and Piron[3] suggest a maximum compression equal to 10 to 20 per cent of the free thickness, and an upper limit of compressive stress equal to 700 pounds per square inch for conservative design. Haushalter[5] also suggests that the deflection of compression springs be limited to 15 to 20 per cent to avoid excessive creep. Where fatigue loading is involved (as in the case of rubber springs for couplings in electric motor applications where continuous starting and stopping is involved) probably even lower percentage compressions should be allowed.

In designing rubber sandwiches for use in shear or compression springs it is usually desirable to keep the maximum thickness below 2 inches and if possible below 1 inch. This is done in order to provide for better curing during vulcanization. If more deflection is required, a stack of rubber sandwiches in series

[4] *Mechanical Engineering*, May, 1937, Page 347.
[5] *Transactions* ASME, Feb., 1939, Page 157.

may be used. In doing this, care must be taken to avoid instability or buckling effects. This can happen not only in compression springs but also in shear springs.

VIBRATION AND SHOCK ISOLATION

The previous discussion has been concerned primarily with the problem of calculating stresses and deflections of rubber mountings of various types. However, the designer is also faced with the necessity for deciding what flexibility, or deflection, is actually required for a given mounting. In doing this he must be guided by known principles for vibration and shock isolation. Some of the more important of these principles particularly as regards the design of mountings for machinery, and military equipment will now be briefly considered[6]. For purposes of discussion the problem is divided into two parts:

1. Steady-state vibration.
2. Transient oscillation or shock.

The former can be considered as a vibration which lasts continuously, while the latter is considered as a motion which dies out after a relatively short time.

Steady-State Vibration—This kind of vibration is encountered for example in rotating electrical machinery as a consequence of unbalance of the rotating parts. It may also be set up by magnetic forces due to alternating currents. A further example is the vibration present in aircraft structures due to engine unbalance and pulsating explosion forces[7]. In machinery mountings, the vibration due to unbalanced reciprocating masses is usually of most importance.

In the design of a resilient mounting for steady-state vibration, it is necessary to consider the various possible modes of vibration. However, in many cases the system can be simplified into a system, known as a *single degree-of-freedom* system, consisting essentially of a single spring-mounted mass on a vibrating support, (as shown on *Fig.* 117 of Chapter XIII). This is the

[6] A more complete discussion of the general vibration problem is given in *Mechanical Vibrations*—J. P. Den Hartog, McGraw-Hill, Second Edition 1940, and *Vibration Problems in Engineering*—S. Timoshenko, Van Nostrand. Second Edition 1937.

[7] Article by P. C. Roche, *Mechanical Engineering*, August 1943, Page 581 presents a more comprehensive discussion of rubber mountings for aircraft and military equipment.

case for example, in certain instrument mountings in aircraft. Such a system will have a natural frequency given by[6]

$$f_n = \frac{1}{2\pi}\sqrt{\frac{g}{\delta_s}} = \frac{3.14}{\sqrt{\delta_s}} \quad \ldots\ldots (490)$$

where δ_s = static deflection of the mass under gravity, inches, f_n = natural frequency of system in cycles per second. In practical design the spring constant of the rubber mounting should usually be chosen such that f_n will be considerably lower than the lowest frequency of vibration of the support. For machinery mountings values of f_n equal to 1/3 to 1/10 the normal operating speed in revolutions per second are used in practice[8].

To determine the reduction in vibration realized by a rubber mounting, it is assumed that the support (*Fig.* 117, Chapter XIII) is subject to a vibration amplitude given by $a_o \sin \omega t$ where t = time, $\omega = 2\pi f$ and f is the frequency of the external vibration in cycles per second. Neglecting damping the differential equation for the relative motion y between the mass and the support may be shown to be[9]

$$m\frac{d^2y}{dt^2} + ky = ma_o\omega^2 \sin \omega t \quad \ldots\ldots (491)$$

In this m = mass and k = spring constant of spring. For a steady-state vibration the solution to this equation is

$$y = \left(\frac{a_o\dfrac{\omega^2}{\omega_n^2}}{1-\dfrac{\omega^2}{\omega_n^2}}\right)\sin \omega t \quad \ldots\ldots (492)$$

where $\omega_n^2 = k/m$

The absolute motion x of the spring supported mass will be $y + a_o \sin \omega t$ or using Equation 492 for y and taking $\omega/\omega_n = f/f_n$

$$x = \frac{a_o \sin \omega t}{\dfrac{f^2}{f_n^2} - 1} \quad \ldots\ldots (493)$$

[6] "Shear-Stressed Rubber Compounds in Isolating Machinery Vibration"—B. C. Madden, *Transactions* ASME, August 1943, Page 619.

[9] Den Hartog, loc. cit. Page 41.

Near resonance, where f/f_n approaches unity, this equation does not apply since in such cases the effect of damping (which was neglected in the derivation) is very important. However, Equation 493 will yield an approximation for frequencies considerably removed from resonance, and in such cases, it may be seen that the amplitude of motion of the mass has been reduced by a factor (f^2/f_n^2)—1 as compared with the amplitude experienced if it were not spring mounted. The accelerations to which the mass is subjected will also be reduced in the same ratio. Thus

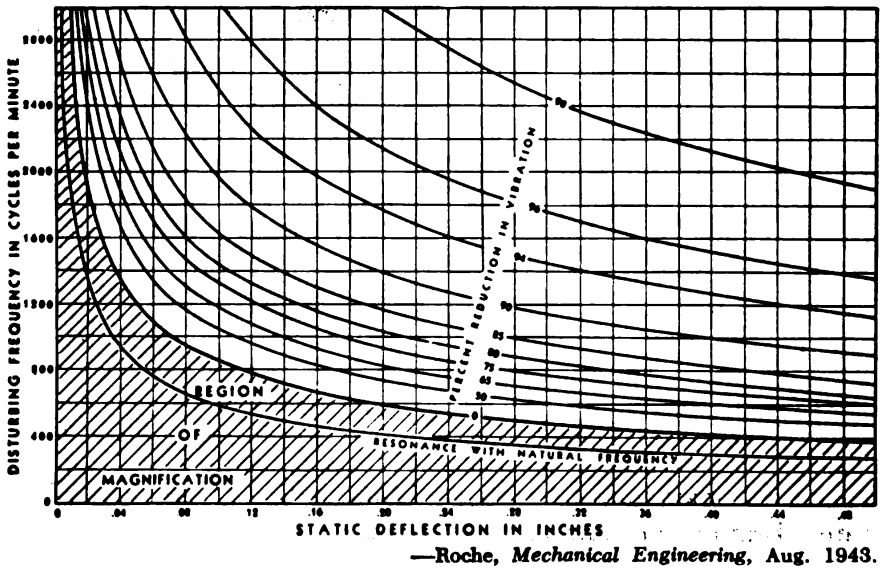

—Roche, *Mechanical Engineering*, Aug. 1943.

Fig. 224—Mounting efficiency in terms of frequency and static deflection

for example, for a vibration frequency, $f=30$ cycles per second, if the rubber mountings are so chosen that the natural frequency f_n is 10 cycles per second, $f/f_n=3$ and from Equation 493, the peak amplitude x of the mass will be $a_0/(3^2-1)=a_0/8$. This means that a reduction in vibration amplitude and acceleration in the ratio of 8:1 has been obtained with a flexible mounting.

The chart of *Fig.* 224, based on Equations 490 and 493, and plotted by Roche[7] may be used to estimate the percentage reduction in vibration achieved by the use of rubber mountings having a given static deflection δ_s. The ordinates of this diagram represent the disturbing frequency in cycles per minute, while the abscissas represent the static deflection of the mounting.

Each curve corresponds to a definite amount of reduction in vibration amplitude, while the shaded area represents a region of increase in vibration amplitude. Thus, for example, if the disturbing frequency is, say, 800 cycles per minute and the static deflection .3-inch under the weight of the mounted apparatus, a reduction in amplitude of 80 per cent normally would be expected.

Damping— It should be emphasized that Equation 493 and the chart of *Fig.* 224 are based on the assumption that damping may be neglected. For most practical purposes this will probably yield results sufficiently close to actual conditions. However, for best accuracy, damping must be taken into account. The usual method of treating this problem is to assume that the damping force is equal to a constant c times the velocity. This is equivalent to adding a term cdy/dt to the left side of Equation 491. The equation can then be solved for steady-state conditions in the usual way[6]. Actual tests, however, show that the internal damping constant c is a function of frequency and in many cases may be taken approximately as inversely proportional to the frequency for rubber compounds[10]. In addition, it has also been found that the modulus of elasticity of the material and hence the spring constant k as used in Equation 491 may in some cases vary with amplitude. This results, for some rubber compounds, in a considerable deviation between calculated and theoretical resonance curves based on constant values of c and k. In other cases, however, close agreement between theoretical curves, based on constant c and k values, and test curves have been obtained for a limited range of frequencies[8].

In some practical applications an alternating load $P=P_o \sin \omega t$ acts on a spring-mounted mass, the support or foundation being rigid in contrast to the previous case considered where the support was assumed to vibrate. An example of such an application is an electric motor mounted on rubber bushings, the force due to unbalance being the alternating load in question. In this case a similar analysis shows that if damping is neglected the load transmitted to the foundation is given by

[10] Discussion by H. O. Fuchs, *Transactions* ASME, August 1943, Page 623; paper on "Rubber in Vibration" by S. D. Gehman, *Journal Applied Physics*, June 1942, Page 402; and "Some Dynamical Properties of Rubber" by C. O. Harris, *Journal Applied Mechanics*, 1942, Page A-132 give additional data.

$$P_1 = \frac{P_o}{\frac{f^2}{f_n^2} - 1} \quad \text{.....(494)}$$

This equation shows that the reduction in vibration for the no-damping case is given by the same expression (f^2/f_n^2)—1 as that obtained for the case of a vibrating support in Equation 493. If a damping force proportional to velocity is assumed, an analysis by Den Hartog[11] shows that the ratio of the force P_1 (transmitted to the foundation) to impressed force P_o is given by

$$\frac{P_1}{P_o} = \sqrt{\frac{1+(2cf/c_c f_n)^2}{\left[1-\left(\frac{f}{f_n}\right)^2\right]^2 + \left(\frac{2c}{c_c}\,\frac{f}{f_n}\right)^2}} \quad \text{.....(495)}$$

In this formula, c=damping factor, $c_c = 2\sqrt{mk}$ defined as the "critical damping". In some cases values of c/c_c around .02 to .08 have been observed but this may vary considerably for different types of mountings[8]. A curve showing the effect of damping on the transmissibility (i.e., ratio P_1/P_o) is given in *Fig.* 225[7].

The full curve represents effect with no damping present, while the dashed curve is calculated on the assumption of a constant damping ratio c/c_c. This curve also indicates that, for constant c/c_c, damping increases the transmissibility above $f/f_n = 1.41$ and decreases it below this value. Because of variation in c this statement does not hold true in all cases particularly where a wide range in frequency is involved[12]. Thus for an effective mounting the spring flexibility should be chosen so as to obtain a ratio f/f_n considerably above 1.4. If the mounting is made too flexible, however, the structure may not function satisfactorily. Hence, a compromise must usually be reached. Values of ratios f/f_n equal to 1.6 and higher have been used in tank and aircraft design[7]. It should also be noted that a structure such as an airplane may have several different frequencies of vibration (due to harmonics in the engine torque, for example) while these may vary over a considerable range at various speeds. Consideration

[11] *Mechanical Vibrations*, loc. cit., Page 87.
[12] See discussion by Fuchs, Footnote 10.

of these various frequencies is necessary if resonance and excessive vibration are to be avoided.

Shock Isolation—This problem is particularly important in the design of flexible mountings for protecting equipment in naval vessels or tanks from the sudden motions resulting from firing of guns, dropping of depth charges, or enemy action. Thus, for example an instrument in a ship may be flexibly mounted so as to function in spite of the transient motions caused

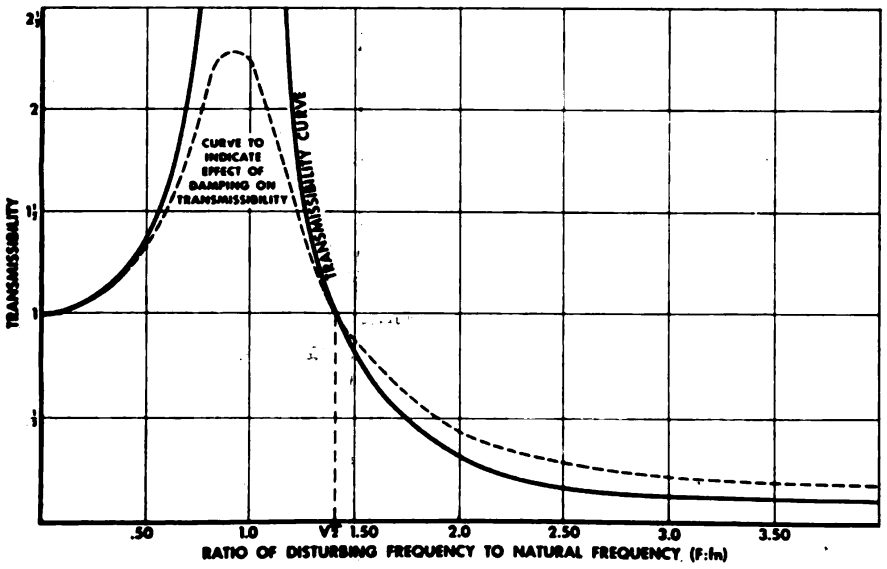

—Roche, *Mechanical Engineering*, Aug. 1943.

Fig. 225—Effect of damping on transmissibility at various ratios f/f_n between disturbing frequency and natural frequency

by a shell impact close by. In general the impacts or explosions result in low frequency oscillations combined with high frequency oscillations of much lower amplitudes, the frequencies involved being determined by the structural characteristics of the ship or tank. The high frequency motions may result in very high accelerations in equipment rigidly attached to the structure. By the use of flexible mountings the damaging effect of these high frequencies can be entirely eliminated. However, it is necessary to consider also the low frequency large amplitudes and to design the mountings so that the motion across the mountings will not build up during the time of the transient to

a point where the allowable motion across the mounting is exceeded. This means that each case must be considered with respect to the type of motion that is expected and the design carried out accordingly.

Where resonance is possible, for instance at low speeds, two methods of attack may be employed. The first is to introduce damping by friction or other means, while the second is to use a mounting with a curved load-deflection characteristic so that the mounting becomes stiffer with increased deflection. Such mountings with snubbing action can be obtained by using stops or other methods.

This means that, if the oscillations occur at a given frequency which is in resonance with the natural frequency for low amplitudes, the amplitude will tend to build up. As it builds up, however, because of the curved load-deflection characteristic, the effective stiffness also increases and with it the natural frequency. This will tend to throw the system out of resonance and result in snubbing action. The mounting must, of course, be designed so as to obtain the required characteristics at the given load.

In designing flexible mountings for a given machine it is desirable, in general, to locate them in one plane coinciding with the center of gravity. In this manner the tendency of different modes of vibration to become coupled is reduced while at the same time, greater stability is obtained.

After the required flexibility has been determined for a given system, the rubber mountings may be designed by using the equations given. The size of the mounting must be so chosen that excessive stresses in the rubber are avoided under the anticipated maximum amplitude of motion, while at the same time, the required flexibility is maintained.

CHAPTER XXII

ENERGY-STORAGE CAPACITY OF VARIOUS SPRINGS

Although a great many factors must be taken into account in the choice of spring type for a given application, to the practical spring designer the amount of energy which can be stored in a given spring is usually of primary importance. This is true since in most cases, load and deflection are given, which means that the spring must store a given amount of energy. This is the case, for example, in the design of landing gear springs for airplane application, where the springs must be able to absorb the kinetic energy of the mass of the plane falling through a certain height. The purpose of the present chapter is to compare various types of springs, such as helical, leaf, cantilever, etc., from the standpoint of energy-storage capacity per unit volume of material, assuming a given maximum stress. This will give the designer an idea of the *minimum* volume of space needed for a given application. (The actual volume may be much greater depending on the spring compactness). It may be noted that this approach to the problem is somewhat different from that of Chapter X, where a *single type* of spring (i.e., the helical) was discussed from the standpoint of total space occupied.

SIMPLE TENSION-BAR SPRINGS

This case may be considered as an ideal spring, consisting simply of a straight bar of uniform section subject to an axial load P at its end[1]. Since the bar is loaded axially, the stress distribution across the section is uniform and for this reason this case represents the optimum condition from the viewpoint of maximum energy storage per unit volume of material. If l is the length and A the cross-section area, the stress σ will be P/A. The unit elongation will be σ/E, where E is the modulus of elasticity of the material, and the total elongation δ will be $\sigma l/E$. The energy stored will be equal to the area under the load-deflec-

[1] This will be called a "tension-bar" spring to distinguish it from the helical tension spring which is also known as a tension spring.

tion curve. Hence, the energy $U=\frac{1}{2}P\delta$. This condition gives:

$$U=\frac{\sigma^2 Al}{2E}=\frac{\sigma^2 V}{2E}$$

In this $V=Al=$total volume of material.

Static Loads—For static loads, the tension yield point σ_y will be considered the limiting stress. The criterion of energy storage for static loads will therefore be the value of U when $\sigma=\sigma_y$. This value is

$$U_s=\frac{\sigma_y^2 V}{2E} \quad \text{.....(496)}$$

Fatigue Loads—On the other hand, if the spring is subject to fatigue or repeated loading, the stress at the endurance limit should be used in determining energy-storage capacity. Because of stress concentration which is usually present near the ends of the spring where it is clamped, it is also necessary to introduce a fatigue strength reduction factor[2]. If this fatigue factor is K_f, a similar analysis shows that for variable loads the energy stored at the endurance limit will be

$$U_s=\frac{\sigma_e^2 V}{2EK_f^2} \quad \text{.....(497)}$$

This equation shows that because of the presence of stress concentration, the energy storage capacity for repeated loading will be considerably below the ideal value (which would exist if no stress concentration were present).

CANTILEVER SPRINGS

Rectangular Profile — This spring consists essentially of a simple cantilever of rectangular profile and constant thickness (*Fig.* 147, Chapter XVI). For small deflections, the deflection from beam theory is, using the notation of Chapter XVI,

$$\delta=\frac{4Pl^3}{Ebh^3} \quad \text{.....(498)}$$

The nominal stress is given by the following equation:

[2] The applications of such factors have been discussed in Chapter VI.

$$\sigma = \frac{6Pl}{bh^2} \text{ or } P = \frac{\sigma bh^2}{6l} \quad \text{.....(499)}$$

Using Equation 498, the energy stored may be expressed as

$$U = \frac{1}{2} P\delta = \frac{2P^2l^3}{Ebh^3} \quad \text{.....(500)}$$

Using Equation 499 in this, and taking the volume V of the material equal to $V = bhl$, the energy U becomes

$$U = \frac{\sigma^2 V}{18E} \quad \text{.....(501)}$$

Static Loads—For static loads, the maximum energy stored when the stress is just equal to the yield stress σ_y will be, from Equation 501,

$$U_s = \frac{\sigma_y^2 V}{18E} \quad \text{.....(502)}$$

Comparing this with Equation 496, it is seen that this value is only 1/9 the value of energy which may be stored in the ideal (tension-bar) spring of the same volume at the yield point. However, it should be noted that, when the extreme fiber is stressed to the yield point, the cantilever spring will still have a considerable margin before general yielding over the cross section occurs. This will increase the stored energy by a factor of about two to one as shown later. Since the tension-bar spring does not have this margin, the ratio of 1/9 mentioned previously is pessimistic as far as the energy storage capacity of the simple cantilever spring is concerned. For this reason, probably a better basis of comparison *for static loads* is the energy stored at a load producing complete yielding over the section at the built-in end of the cantilever. The analysis may be made as follows:

It is assumed that a rectangular distribution of stress exists over the cross section for complete yielding. This means that, on the tension side, the stress is a constant tension equal to the yield stress σ_y, while on the compression side, the stress[3] is equal to $-\sigma_y$. For a rectangular section, the external bending moment

[3] Actually, for most spring steels the stress will tend to rise after the yield point is reached (stress-strain diagram of Fig. 61). However, the assumption of a constant stress is satisfactory for the present purpose.

will be expressed by the following relation:

$$Pl = 2\int_0^{h/2} \sigma_y b x dx = \frac{\sigma_y h^2 b}{4} \quad \text{.....(503)}$$

This corresponds to a value of load 50 per cent above the value by Equation 499 which is based on a linear stress distribution over the cross section. The load-deflection curve up to this load will not be exactly linear because of yielding effects. However, on *unloading*, the curve will be approximately linear and for further load applications in one direction, the energy stored will correspond to that figured from Equation 500, using the higher value of P. Hence, it seems reasonable to use the latter equation, which is based on a linear condition, as a basis for comparison. Thus using a load P as calculated from Equation 503 and substituting in Equation 500 the expression for energy stored becomes

$$U_s = \left(\frac{3}{2}\right)^2 \frac{\sigma_y^2 V}{18E} = \frac{\sigma_y^2 V}{8E} \quad \text{.....(504)}$$

This is one-fourth the value for the ideal case. (Equation 496).

Fatigue Loads—Where the load is variable, the stress given by Equation 499 must be multiplied by a fatigue strength reduction factor K_f to take into account the stress concentration at the built-in end of the cantilever. The stored energy at the endurance limit σ_e will then be

$$U_v = \frac{\sigma_e^2 V}{18 K_f^2 E} \quad \text{.....(505)}$$

If the same fatigue-strength reduction is assumed for the cantilever spring as for that in a simple tension-bar spring, the energy-storage capacity in the former for fatigue conditions will be only 1/9 that of the latter[4]. The reason for this may be found in the fact that in a cantilever spring of rectangular profile only a very small portion of the total volume of material (i.e., that near the fixed end) is subject to anything approaching the maximum stress. Nevertheless, in spite of its relative inefficiency in this respect, the cantilever spring still finds a field of use particularly in cases where the spring must function as a guide in addi-

[4] Actually the fatigue-strength reduction factor may be considerably less in the cantilever spring, the actual value depending on the design.

tion to its energy-absorption function.

Triangular Profile and Leaf Spring—The efficiency of utilization of the material in a cantilever spring may be increased by making the profile of triangular or trapezoidal form so that the nominal stress along the length of the spring will be approximately constant. This is the condition in the usual type of leaf spring also. For a spring of triangular profile, the deflection at the end due to a load P is, using the notation of Chapter XVI,

$$\delta = \frac{6Pl^3}{Eb_o h^3} \qquad (506)$$

The maximum stress is the same as that given by Equation 499. Using Equation 506, the stored energy may be expressed as

$$U = \frac{1}{2} P\delta = \frac{3P^2 l^3}{Eb_o h^3} \qquad (507)$$

Using Equation 506 in Equation 507 and taking the volume $V = \frac{1}{2} b_o hl$, the energy becomes

$$U = \frac{\sigma^2 V}{6E} \qquad (508)$$

Static Loads—For static loads, the energy stored when the stress just reaches the yield point σ_y is

$$U_s = \frac{\sigma_y^2 V}{6E} \qquad (509)$$

This value of stored energy is about one-third that for the ideal spring at the yield point, Equation 496. For complete yielding over the section of the spring, the load will be about 50 per cent above the value given by Equation 509 and for this condition (as for the cantilever spring of rectangular profile) the energy-storage capacity may be assumed to increase roughly in the ratio $(1.5)^2$ to 1. This gives

$$U_s = \frac{\sigma_y^2 V}{2.67E} \qquad (510)$$

This value of energy-storage capacity is about 25 per cent below that obtainable for the ideal case.

Fatigue Loads—For fatigue loading the energy stored in the

cantilever spring of triangular profile is

$$U_v=\frac{\sigma_c^2 V}{6K_f^2 E} \quad \text{.....(511)}$$

In this, K_f is the fatigue strength reduction factor at the clamped end. Assuming equal values of K_f, this value is approximately 1/3 that obtainable in the ideal case.

HELICAL TORSION SPRINGS

Rectangular Wire—Assuming a helical torsion spring of rectangular wire, subject to a constant moment M (*Fig.* 178), the bending stress is, from Equation 357,

$$\sigma=K_2\frac{6M}{bh^2}$$

or, solving for M,

$$M=\frac{\sigma bh^2}{6K_2} \quad \text{.....(512)}$$

where K_2 (*Fig.* 180) depends on the spring index to take into account the stress increase due to curvature of the bar. From Equation 358 the angular deflection of the end of the spring is

$$\phi=\frac{24\pi Mrn}{Ebh^3} \text{ radians}$$

The energy U stored in this case will be half the product of the moment and the angle. Using this equation the energy becomes

$$U=\frac{1}{2}M\phi=\frac{12\pi M^2 rn}{Ebh^3}$$

Using the value of M given by Equation 512 in this and taking the volume of material equal to $2\pi rnbh$,

$$U=\frac{\sigma^2 V}{6EK_2^2} \quad \text{.....(513)}$$

Static Loads—For static loads, the curvature correction factor K_2 may be considered as a stress-concentration factor and

hence may be neglected. The energy stored at the yield point σ_y will then be

$$U_s = \frac{\sigma_y^2 V}{6E} \quad \ldots\ldots (514)$$

This is the same as Equation 509 for a cantilever spring of triangular profile. For complete yielding, conditions will be the same as for a triangular cantilever spring; hence Equation 510 may also be used for this case.

Fatigue Loads—For variable loading the energy stored will be

$$U_s = \frac{\sigma_e^2 V}{6EK_2^2} \quad \ldots\ldots (515)$$

Usually, because of clamping at the ends in a torsion spring, there will be a stress concentration effect which may be represented by a fatigue strength reduction factor K_f. If this factor is higher than the curvature factor K_2, *Fig.* 180, the former should be used in Equation 515 instead of the latter.

Circular Wire—For a torsion spring of circular wire the stress (given by Equation 364) is

$$\sigma = K_1 \frac{32M}{\pi d^3}$$

where K_1 is the curvature correction factor.
From this

$$M = \frac{\pi d^3 \sigma}{32K_1} \quad \ldots\ldots (516)$$

The angular deflection in radians is, from Equation 366,

$$\phi = \frac{128Mrn}{Ed^4}$$

The energy stored is (as before)

$$U = \frac{1}{2} M\phi = \frac{64M^2rn}{Ed^4} \quad \ldots\ldots (517)$$

Taking the volume $V = \pi^2 rnd^2/2$ and using Equation 516 in equation 517, the stored energy becomes

$$U=\frac{\sigma^2 V}{8K_1^2 E} \quad \text{.....(518)}$$

Static Loads—For a static load, the energy stored when the stress reaches the yield point σ_y is, neglecting the curvature factor K_1 as before,

$$U_s=\frac{\sigma_y^2 V}{8E} \quad \text{.....(519)}$$

This appears to be about ¼ the energy stored in the ideal (tension-bar) spring at the yield point. However, an increase in moment approximately in the ratio of 1:1.7 is necessary to cause complete yielding over the cross section for a round-wire torsion spring. This may be shown as before by assuming yielding at constant stress and integrating over the circular cross section. This would correspond to an increase in energy to about 2.89 times that given in Equation 519. Thus, for complete yielding,

$$U=\frac{\sigma_y^2 V}{2.77E} \quad \text{.....(520)}$$

This value is about 28 per cent below that corresponding to the ideal spring.

Variable Loads—For variable loads, the energy stored will be, using σ_e in Equation 518,

$$U_v=\frac{\sigma_e^2 V}{8K_1^2 E} \quad \text{.....(521)}$$

If the fatigue strength reduction factor K_f at the clamped end is higher than K_1, the former should be used in this expression. Assuming the same value of K_f for both cases, Equation 521 thus indicates that for variable loading the round-wire torsion spring is about ¼ as efficient as the ideal (tension-bar) spring.

SPIRAL SPRINGS

A spiral spring of flat strip or rectangular bar material with a large number of turns will have the same energy-storage capacity per unit volume of material as the torsion spring of rectangular wire, provided that the ends are clamped and that there

is sufficient space between the turns so that they do not come in contact (see Chapter XVIII). In such a case as shown previously the moment is approximately constant along the length of the spring, as it is in the case of a helical torsion spring under a constant moment. For fatigue loading, however, the stress concentration factors may be different, depending on the method of fastening or clamping the ends.

ROUND BAR UNDER TORSION

For a straight round bar subject to a torsion moment M_t about its axis, the torsion stress τ is given by Equation 4, taking $Pr = M_t$

$$\tau = \frac{16M_t}{\pi d^3}$$

solving for M_t,

$$M_t = \frac{\pi d^3}{16}\tau \qquad (522)$$

The angular deflection ϕ, in radians, of a round bar of length l under a torque M_t is

$$\phi = \frac{32M_t l}{\pi d^4 G}$$

where G is the torsional modulus of elasticity.

The energy stored will be one-half the product of the moment and the angle in radians. Hence

$$U = \frac{1}{2}M_t\phi = \frac{16M_t^2 l}{\pi G d^4}$$

Substituting in this the value of M_t given by Equation 522 and taking the volume of material $V = \pi d^2 l/4$,

$$U = \frac{\tau^2 V}{4G} \qquad (523)$$

Static Loads—For static loads, when the shear stress τ just reaches the yield point in torsion τ_y, the energy stored becomes

$$U_s=\frac{\tau_y^2 V}{4G} \quad \ldots\ldots (524)$$

The torsional modulus is

$$G=\frac{E}{2(1+\mu)}$$

where μ = Poisson's ratio[5]. For most materials μ may be taken as about .3. This gives $G=E/2.6$. Also from the shear-energy theory (Chapter II) the shearing yield point τ_y may be taken as $1/\sqrt{3}$ times the tension yield point σ_y. Thus

$$\tau_y=\frac{\sigma_y}{\sqrt{3}} \quad \ldots\ldots (525)$$

Using these values in Equation 524, for static loading the energy stored when the stress just reaches the yield point is

$$U_s=\frac{\sigma_y^2 V}{4.62E} \quad \ldots\ldots (526)$$

This is considerably more than that stored in either the round or the rectangular-wire helical torsion springs (Equations 514 and 519). However, it should be noted that these latter springs have a considerable margin between the load at which yielding starts and that for complete yielding over the section. This margin is not as great in the case of the torsionally loaded round-bar spring (since a greater part of the section is stressed to values near the maximum) and hence for static loading comparison on the basis of Equations 519 and 526 is probably too favorable for the round bar in torsion. A fairer comparison may be made by assuming complete yielding over the section as follows:

For a rectangular distribution of stress over the cross section of the round bar (as would occur after complete yielding at constant stress τ_y has taken place), the moment M_t is given by

$$M_t=2\pi\int_0^{d/2}\tau_y r^2 dr=\frac{4}{3}\left(\frac{\pi d^3\tau_y}{16}\right) \quad \ldots\ldots (527)$$

Comparing this with Equation 522 this means that, for complete yielding, the moment is equal to 4/3 times the value when

[5] Timoshenko, *Strength of Materials*, Part I, Page 57, Second Edition.

the stress in the outer fiber just reaches the yield point in torsion. Assuming a linear moment-angle curve (which will be realized approximately after the first load application) the energy stored may be taken proportional to the square of the moment. Thus, the value given by Equation 526 will be increased in the ratio $(4/3)^2$. This gives

$$U_s = \frac{\sigma_y^2 V}{2.6E} \quad \text{.....(528)}$$

This value is only about 23 per cent lower than the stored energy in the ideal case and shows that the helical compression or tension spring of large index (which approximates a condition of pure torsion) is relatively efficient as far as energy storage per unit volume of material is concerned.

Fatigue Loading—For a straight bar in torsion under fatigue or repeated loading, Equation 522 may be used. However, in practice there will usually be some stress concentration (at clamped ends, for instance), and hence the value of M_t given by this equation must be divided by a fatigue strength reduction factor K_f to take this into account. Taking τ_e as the endurance limit in torsion, from Equation 523 the energy stored thus becomes

$$U_s = \frac{\tau_e^2 V}{4GK_f^2} \quad \text{.....(529)}$$

Again it may be assumed roughly that the endurance limit[6] in torsion τ_e is equal to that in tension σ_e divided by $\sqrt{3}$. Using Equation 529 and taking $G = E/2.6$ as before, the following expression is obtained:

$$U_s = \frac{\sigma_e^2 V}{4.62EK_f^2} \quad \text{.....(530)}$$

Thus, for variable loading, and assuming equal fatigue-strength reduction factors, the energy-storage capacity of a straight bar in torsion would be somewhat less than half that of a simple tension-bar spring. However, as previously indicated this comparison may be invalidated by differences in the actual fatigue factors which depend both on design and material.

[6] This is based on the shear-energy theory.

HELICAL COMPRESSION OR TENSION SPRINGS

The deflection of a helical spring, axially loaded (from Equation 7) is

$$\delta = \frac{64Pr^3n}{Gd^4}$$

Using this, the energy stored becomes

$$U = \frac{1}{2}P\delta = \frac{32P^2r^3n}{Gd^4} \quad \text{.....(531)}$$

Static Loads—For static loads, the stress is calculated from Equation 89

$$\tau_s = K_s\frac{16Pr}{\pi d^3}$$

or

$$P = \frac{\pi d^3\tau_s}{16rK_s}$$

In this case, K_s is the shear stress multiplication factor, *Fig.* 63.

Substituting this in Equation 531, taking the volume of material in the spring as $V = \pi^2d^2rn/2$, and the stress equal to the yield point in shear τ_y, this gives

$$U_s = \frac{\tau_y^2V}{4GK_s^2} \quad \text{.....(532)}$$

This is the same as the factor for a straight bar in torsion, with the exception of the factor K_s. Again taking τ_s equal to the tension yield point divided by $\sqrt{3}$ and taking $E = G/2.6$ this equation becomes

$$U_s = \frac{\sigma_y^2V}{4.62K_s^2E} \quad \text{.....(533)}$$

To get the energy storage for complete yielding over the section, this value must be multiplied by $(4/3)^2$ as in the case of a straight bar under torsion[7]. This gives

[7] Chapters V and VI give a more complete discussion of helical springs under static and variable loading.

$$U_s = \frac{\sigma_y^2 V}{2.6\, K_s^2 E} \quad \ldots\ldots (534)$$

Fatigue Loads—For fatigue or repeated loading, for a rough comparison the same method may be applied except that instead of using the factor K_s a factor K (*Fig.* 30, Chapter II) which takes into account both effects due to curvature and to direct shear should be used[7]. This gives (from Equation 533), taking the endurance limit σ_e instead of σ_y

$$U_s = \frac{\sigma_e^2 V}{4.62 K^2 E} \quad \ldots\ldots (535)$$

From Equations 533 and 535 it is seen that the larger the spring index, the larger the energy storage per unit volume of material, since K_s and K decrease with increase in the index. However, if the comparison is made on the basis of total volume of space occupied, it will be found that the use of moderate index springs will give the maximum efficiency (Chapter X).

COMPARATIVE STORAGE CAPACITIES

On the basis of the equations for spring capacity as previously derived, the figures listed in TABLE XXXV have been computed. These represent energy-storage capacity as fractions of that of an ideal (simple tension-bar) spring. Thus for static loading, in terms of the energy storage when first yielding occurs the simple cantilever spring will absorb an amount of energy equal to .11 times that of the ideal spring. If comparison is made on the basis of energy storage at first yielding, it appears that the simple tension-bar spring is far more efficient than other types. On the other hand, if comparison is made on the more logical basis of energy storage for complete yielding over the section, it appears that the ideal spring is not a great deal more efficient than other types. Thus, for example on this basis (from the second row of the table), the triangular cantilever spring, the torsion spring of rectangular section, and the round bar in torsion all have about 75 per cent of the capacity of the ideal spring assuming static loading. For a helical spring of index 5, $K_s = 1.1$ and from the last column of TABLE XXXV, the energy-

storage capacity per unit of volume on this basis will be $.77/(1.1)^2 = .64$ times that of the ideal spring. However, when comparison is made on the basis of energy-storage capacity for variable loading, if the same fatigue strength reduction factors are assumed, the ideal spring is far more efficient than the other types. However, in practice these fatigue factors may vary con-

TABLE XXXV

Comparison of Energy-Storage Capacity for Different Types of Springs

(Expressed in fractions of that in the ideal case of a simple tension-bar spring*)

	Simple Tension-Bar Spring	Simple Cantilever Spring	Triangular Cantilever Spring	Torsion Spring (Rectangular bar) Spiral Spring	Torsion Spring (Round Bar)	Straight Round Bar in Torsion	Helical Compression or Tension Spring
Energy stored at first yielding—static loads	1	.11	.33	.33	.25	.43	$.43/K_s^2$
Energy stored at complete yielding— static loads	1	.25	.75	.75	.72	.77	$.77/K_s^2$
Energy stored at endurance limit — variable loads†	$1/K_f^2$	$.11/K_f^2$	$.33/K_f^2$	$33/K_f^2$	$.25/K_f^2$	$.43/K_f^2$	$.43/K^2$

*Energy stored at first or complete yielding (static loads) for ideal case $\sigma^2 V/2E$. Energy stored at endurance limit (variable loads) for ideal case $\sigma_e^2 V/2E$.

†Values of fatigue strength reduction factors K_f in this row will vary among the different types of springs. Endurance limit in torsion taken as $\sigma_e/\sqrt{3}$.

siderably and for this reason the figures given should be considered only as a rough indication of the capacities of the various types.

It should be emphasized that in the choice of spring type by the designer a great many factors are involved besides energy storage per unit volume. Thus ability to fit into a machine or mechanism is often of paramount importance. However, the comparison of spring types as given in TABLE XXXV may be helpful in enabling the designer to form some judgement as to the best type of spring for use under given conditions.

CHAPTER XXIII

SPRING MATERIALS

The present chapter will be concerned primarily with a discussion of the more important spring materials, their properties, composition and uses. Particular reference will be made to possible substitutions which may be required as a consequence of wartime restrictions. The emphasis will, however, be placed on the properties of the material itself rather than on those of the complete spring[1].

In the choice of spring materials, it should be borne in mind that, in view of present restrictions, wherever possible plain carbon steels (such as music wire, oil-tempered wire, hot-rolled high-carbon steels) should be used instead of alloy steels, stainless steel, and nonferrous materials, all of which utilize severely restricted materials. In many practical applications such alternatives may be used without loss of essential properties.

PHYSICAL PROPERTIES OF MATERIALS

A summary of the more important properties of the different spring materials is given in TABLES XXXVI, XXXVII and XXXVIII. TABLE XXXVI gives a tabulation of the composition of various spring steels according to specifications of the American Society for Testing Materials. TABLES XXXVII and XXXVIII give typical values of physical properties, including ultimate strength, elastic limit in tension, modulus of rigidity, modulus of elasticity, and elongation for ferrous and nonferrous spring materials[2]. It should be emphasized that in individual cases, spring properties may deviate somewhat from the values shown.

Endurance limits—A summary of available data on endurance limits of spring materials as found in the literature is given in TABLES XXXIX and XL, the former applying to torsion and

[1] Static and endurance properties of helical springs were discussed in Chapter IV.
[2] Article by C. T. Eakin, *Iron Age*, August 16, 1934, Page 18, "Mechanical Springs", published by Wallace Barnes Co., 1944, and "Manual on Design and Application of Helical and Spiral Springs for Ordnance", published by S.A.E. War Engineering Board, 1943, give additional data on spring materials.

the latter to bending. Pertinent information, including kind of material, heat treatment, surface condition (i.e., whether ground and polished, or untouched), ultimate and yield strengths in tension, modulus of rupture and yield strength in torsion, and literature reference are given, together with the limiting endurance range values. Thus an endurance range from 0-110,000 pounds

TABLE XXXVI

Composition of Various Spring Materials

(ASTM Standard Specifications)

Material	ASTM Specification	Carbon	Manganese	Phosphorus (max.	Sulphur (max.	Silicon	Chromium	Vanadium
		(%)	(%)	%)	%)	(%)	(%)	(%)
Music wire	A228-41	.70 to 1	.20 to .60	.03	.03	.12 to .30		
Oil-tempered wire over $\frac{1}{32}$ dia. (comp. A)	A229-41	.55 to .75	.80 to 1.20	.045	.050	.10 to .30		
Oil-tempered wire under $\frac{1}{32}$ dia. (comp. B)	A229-41	.55 to .75	.60 to .90	.045	.050	.10 to .30		
Hard-drawn spring wire	A227-41	.45 to .75	.60 to 1.20	.045	.050	.10 to .30		
Hot-wound carbon steel helical springs*	A 68-39	.90 to 1.05	.25 to .50	.05	.05	.15		
Chrome-vanadium valve spring wire†	A232-41	.45 to .55	.60 to .90	.03	.03	.12 to .30	.80 to 1.10	.15 to .25

*Heat treated after forming.

†For ordinary chrome-vanadium wire, somewhat higher amounts of phosphorus (.04%) and sulphur (.05%) are allowed.

per square inch means that the bar will withstand indefinitely a stress range between these limits. Completely reversed stress is indicated by the $\pm$ sign.

In general, a study of TABLES XXXIX and XL shows that, where the test specimen is ground and polished, a considerably higher endurance limit is obtained than is the case where the surface is in the "as received" condition. This difference in endurance limits probably may be attributed largely to surface decarburization due to the manufacturing process, although other factors such as surface flaws or defects may also be present.

A summary of endurance ranges and physical properties, together with other pertinent data for leaf and flat spring materials as obtained from the literature are given in TABLE XLI. The highest endurance limits were obtained on thin polished specimens (.006 inch thick) of Swedish spring steel strip. On

the basis of these data, the endurance diagram of *Fig.* 226 has been drawn up. This represents what may be expected for good quality leaf or flat-spring material in thicknesses around ¼ to ½-inch. Again, it may be seen that for ground and polished specimens considerably higher endurance limits may be expected than for the others. Higher values may also be expected for high-quality, thin-strip materials.

It should be noted that because of stress concentration effects due to holes, notches, clamped edges, etc., the actual endurance limits obtained in leaf or flat springs in general are considerably lower[3] than those shown in *Fig.* 226. This is shown by the tests on actual elliptic leaf springs reported by Batson and Bradley and summarized in TABLE XLII. For these tests, as shown on this Table, the limiting range of stress in the master leaf of the spring was only about 30,000 to 40,000 pounds per square inch. For

TABLE XXXVII

Tensile Properties of Typical Spring Steels

Material	Ultimate tensile strength (lb./sq. in.)	Elastic limit in tension (lb./sq. in.)	Modulus of elasticity (lb./sq. in.)	Elongation in 2 inches (%)	Modulus of Rigidity* (lb./sq. in.)
Hard-drawn spring wire	160,000 to 310,000†	60% of *T.S.*‡	30×10^6	5	11.4×10^6
Oil-tempered spring wire	170 000 to 310,000†	70 to 85% of *T.S.*	30×10^6	8	11.4×10^6
Music wire	255,000 to 440,000†	60 to 75% of *T.S.*	30×10^6	8	11.5×10^6
Annealed, high-carbon wire	250,000 to 300,000	200,000 to 275,000	30×10^6	7	11.5×10^6
Hot-rolled, high-carbon steel	175,000 to 195,000	75 to 85% of *T.S.*	29×10^6	6	10.5×10^6§
Chrome-vanadium steel	210,000 to 300,000	80 to 90% of *T.S.*	30×10^6	10	11.5×10^6

†Depending on size.
‡*T.S.* = Tensile strength.
*See Chapter IV for further data on modulus of rigidity.
§Low value probably due to surface decarburization.

good quality leaf spring steel of this thickness, tested without stress concentration but with surface untouched, as seen from *Fig.* 226, this range should be around 80,000 pounds per square inch. While the springs tested by these investigators may not have been of very good quality, at least part of this difference is

[3] Methods of taking such effects into account were discussed in Chapter XVI.

no doubt due to stress concentration effects present in the actual spring. Thus as discussed in Chapter XVI a small hole in a flat strip may reduce the endurance range about 50 per cent.

DESCRIPTION OF SPRING WIRES AND MATERIALS

In the following, the properties and uses of the more important kinds of spring wire and spring materials will be briefly discussed, with particular reference to the data given in TABLES XXXVI, XXXVII, and XXXVIII. Pertinent data of importance in

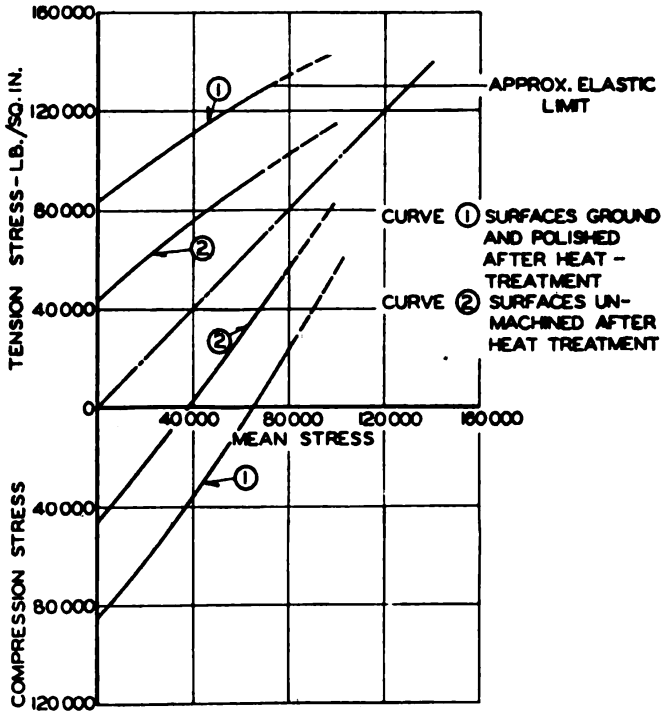

Fig. 226—Approximate endurance diagrams for good quality leaf and plate spring materials

connection with the application and use of the various materials will be briefly summarized.

Music wire—A high-quality carbon steel, this wire is widely used for small-sized helical springs, particularly those subject to severe stress conditions. The high strength of the material is obtained by using a steel of about .70 to 1.00 per cent carbon, patenting and cold drawing to size. The composition as specified

by ASTM A228-41 is given in TABLE XXXVI and typical physical properties in TABLE XXXVII. This specification also calls for minimum and maximum tensile strength values as shown by the upper and lower curves of *Fig.* 227. As will be seen from these

TABLE XXXVIII

Typical Physical Properties of Stainless Steel and Non-Ferrous Metals

(as used in Springs)

Kind of Material	Ultimate tensile strength (psi)	Elastic limit in tension (psi)	Modulus of elasticity (psi)	Elongation in 2 inches (%)	Endurance limit in bending (psi)	Modulus of rigidity (psi)
Stainless steel (18-8)	160,000 to 320,000†	70,000 to 230,000	26 to 28 x 10^6	....	.....	10 to 11.2 x 10^6
Phosphor bronze (4-6% tin)	100,000 to 150,000	50,000 to 110,000	15 x 10^6	2–3	.....	6 x 10^6
K-Monel (spring temper, heat-treated)	160,000 to 200,000	110,000 to 140,000	26 x 10^6	3–8	50,000	9.5 x 10^6
Z-nickel (spring temper, heat-treated)	180,000 to 230,000	130,000 to 170,000	30 x 10^6	5–10	.....	11 x 10^6
Beryllium copper	160,000 to 200,000	100,000 to 150,000	16 to 19 x 10^{6*}	1–2	40,000	6 to 7.5 x 10^{6*}
Spring brass	90,000 to 130,000	30,000 to 60,000	15 x 10^6	5	20,000 to 25,000	5.5 x 10^6

† Depending on size. * Depending on heat treatment.

curves the tensile strength of music wire may vary from 255,000 pounds per square inch for the larger wire sizes to 440,000 pounds per square inch for the smaller. The carbon content of this material usually will vary with the wire size, the smaller sizes having the lower amounts. Some specifications call for a limited range within .1 per cent in carbon content for a given wire size. Usually music wire is not used for springs larger than about ⅛-inch wire diameter, but it can be supplied in larger sizes on special order.

In forming helical springs of music wire, the winding is done cold over a mandrel. After winding, it is advisable to give the springs a low-temperature heat treatment to relieve coiling stresses. This bluing treatment may call for heating the springs to a temperature of around 500 degrees Fahr. for one hour for the larger sizes and for 15 to 30 minutes for the smaller sizes.

Formerly music wire was made largely from Swedish steels because of their uniformity and high quality. At present, Ameri-

TABLE XXXIX

Endurance Limits and Physical Properties of Spring Materials in Torsion

Material	Specimen or Wire Dia. inches	Heat Treatment	Condition of Surface	Hardness	Ult. Strength (Tension) lb./sq. in.	Yield Point (Tension) lb./sq. in.	Mod. of Rupture (Torsion) lb./sq. in.	Yield Point (Torsion)** lb./sq. in.	Limiting Endurance Range in Torsion§ lb./sq. in.	Investigator
Tempered Swedish Steel Wire	.125		As received	45 Rock. C	226,000	203,000	166,000	139,000	0 to 110,000*	Weibel[1]
.60% C	.187		"	43 Rock. C	211,000	190,000	162,000	125,000	0 to 107,000*	"
.35% Mn (approx.)	.225		"	42 Rock. C	204,000	181,000	166,000	120,000	± 56,000 0 to 100,000*	"
.6% C Spring Steel	.13†	O.Q. 950°C T. 500°C	Ground and polished	365 Brinell	177,000	161,000	150,000		± 52600 4500 to 103,000 55000 to 125,000	Hankins[2]
Cr Va Spring Steel	.13†	O.Q. 850°C T. 600°C	Ground and polished	385 Brinell	177,000	168,000	148,000		± 56000 10000 to 111,000 57000 to 131,000	Hankins[2]
Cold Drawn Steel Wire	.160		As received	350 Brinell	202,000		155,000		± 36400††	Lea and Dick[3]
High Carbon O.H. Steel .91% C .38% Mn	.25	O.Q. 1575°F D. 940°F	Ground and polished	438-450 Brinell	225,000	179,000	173,000	118,000	± 52000 0 to 102,000	Johnson[4]
Cr Va Electric .52% C .88% Cr .21% Va	.25	O.Q. 1600°F D. 810°F	Ground and polished	477-488 Brinell	237,000	229,000	183,000	141,000	± 75000 0 to 128,000	Johnson[4]
High Carbon Electric Steel	.25	O.Q. 1550°F D. 800°F	Ground and polished	430-470 Brinell	237,000	194,000	194,000	126,000	0 to 123,000	Johnson[4]
Beryllium Bronze	.25			303 Brinell	166,000	132,000	110,000	95,000	± 16000 0 to 30,000	Johnson[4]

* These figures probably represent ideal conditions when no flaws are present.
** Based on .2% plastic strain.
† Specimen turned down to this diameter.
†† Low value attributed by investigators to defects set up by drawing operation.
§ Where more than one figure is listed for a given material, this means that tests were made at different stress ranges, i.e., ± or completely reversed stress, 0 to maximum, or intermediate to maximum stress as indicated

1 *Trans. A.S.M.E.*, Nov. 1935, p. 501.
2 *Eng. Research Special Report* No. 9, Dept. of Scientific & Industrial Research (British).
3 *Proc. Inst. Mech. Engrs.* 1931, p. 661.
4 *Iron Age*, March 15, 1934, p. 12.

can steels are being used to make this material with satisfactory results in most cases.

Music wire may also be obtained with cadmium-plated surfaces for applications where corrosion is a factor (in the application of the coating, care must be taken to guard against hydrogen embrittlement). For such applications, cadmium-plated springs may offer a satisfactory substitute for 18-8 stainless steel wire.

Oil-tempered spring wire—This is a good-quality, high-carbon steel wire, made by the open hearth or electric furnace

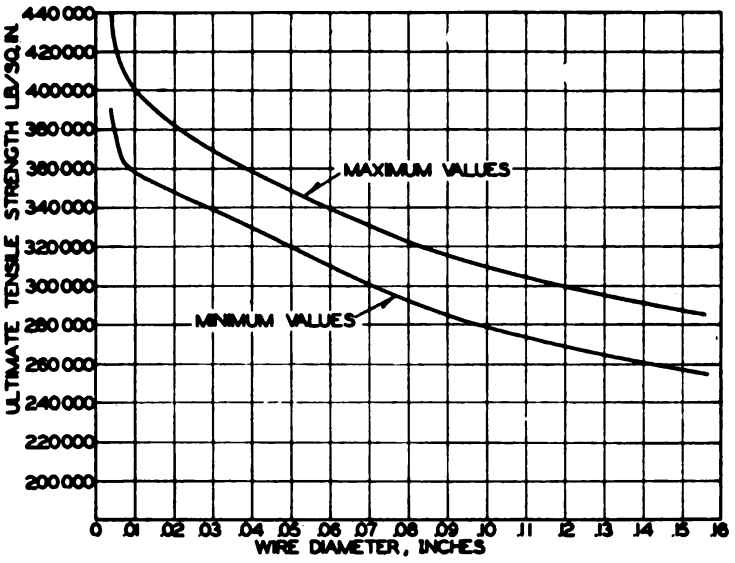

Fig. 227—Maximum and minimum tensile strength characteristics of music wire for various sizes, from ASTM A228-41

process, which is used for cold-wound springs. ASTM A229-41 calls for the compositions listed in TABLE XXXVI, Composition A being preferred for sizes over 7/32-inch.

In manufacturing, the wire is cold drawn to size and then heat treated. Upper and lower limits for tensile ultimate strengths for oil-tempered wire as given by the foregoing specifications are plotted against wire size in *Fig.* 228. Further limitations on the tensile strength call for a variation in tensile strength of not more than 30,000 pounds per square inch in a single lot in sizes below .120-inch, and not more than 25,000 pounds per square inch in sizes above .120-inch. It will be noted that the tensile strengths of this wire are somewhat below the values for

TABLE XL

Endurance Limits and Physical Properties of Spring Materials in Bending

(Round Specimens)

Material	Dia. of Specimen or Wire inches	Heat Treatment*	Condition of Surface	Hardness	Ult. Strength (Tension) lb./sq. in.	Yield Point (Tension) lb./sq. in.	Elongation Per Cent	Endurance Limit in Reversed Bending lb./sq. in.	Investigator
.6% C. Steel		O.Q. 950 C T. 500°C	Ground and Polished	365 Br.	177000	161000	7**	±85000	Hankins[1]
Cr. Va. Spring Steel		O.Q. 850°C T. 600°C	Ground and Polished	385 Br.	177000	168000	7**	±95000	Hankins[1]
.65% C. Steel	.162		As recd.		221000			±76000	Shelton, Swanger[2]
.65% C. Steel	.130		Ground and Polished		221000			±126000	" "
.65% C. Steel	.148		As recd.		217000			±65000	" "
Tempered Swedish Valve Spring Wire	.225		As recd.	42 Rock. C	204000	181000	10.5§	±67000	Weibel[3]
Tempered Swedish Valve Spring Wire	.225		Rough ground 60 grit wheel 1 pass	42 Rock. C	204000	181000	10.5§	±81000	"
Tempered Swedish Valve Spring Wire	.225		Shot blasted	42 Rock. C	204000	181000	10.5§	±85000	
High Carbon O.H. Steel .91% C .38% Mn	.273	O.Q. 1575°F D. 940°F	Ground and Polished	438-450 Br.	225000	179000	7§	±80000	Johnson[4]
Cr. Va. Steel .52% C.88% Cr .21% Va		O.Q. 1600°F D. 810°F	Ground and Polished	477-488 Br.	237000	229000	11§	±104000	"
High Carbon Electric Steel 1.04% C. .36% Mn.		O.Q. 1550°F D. 800°F	Ground and Polished	430-470 Br.	237000	194000	5§	±98000	"

* O.Q. = oil quenched. T = tempered. D = drawn.

** In 8 inches.

§ In 2 inches.

1 Dept. of Sci. and Ind. Research, Eng. Res. Spec. Rep. No. 9.
2 Bureau of Stds. *J. of Research*, V. 14, 1935, RP 754, p. 17-32.
3 *Trans.* A.S.M.E., Nov. 1935, p. 501.
4 *Iron Age*, March 15, 1934, p. 12.

corresponding sizes of music wire, *Fig.* 227. Other physical properties are listed in TABLE XXXVII.

As in the case of music wire, springs made from oil-tempered wire are usually wound cold and then given a thermal treatment to relieve coiling stresses. This may be done by heating at 500-535 degrees Fahr. for ½-hour.

Hard-drawn spring wire—Of lower quality than music or oil-tempered wire, this material is utilized in cases where the stresses are low or where a high degree of uniformity is not essential. The chemical composition as specified by ASTM A227-

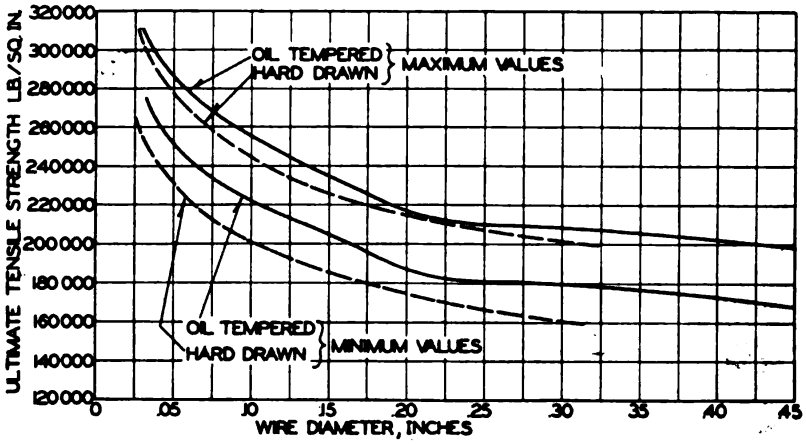

Fig. 228—Maximum and minimum values of ultimate tensile strength for hard-drawn and oil-tempered wire, ASTM A221-41 and 229-41

41 is given in TABLE XXXVI. This specification further requires that the carbon in any one lot of material shall not vary by more than .20 per cent and the manganese by not more than .30 per cent. Usually the higher carbon contents are used for the larger wire sizes to obtain higher values of tensile strength in these sizes.

Minimum and maximum values of ultimate tensile strengths for hard-drawn wire as given in ASTM A227-41 are shown by the dashed lines of *Fig.* 228 as a function of wire diameter. A further requirement of this specification is that the ultimate strength in a single lot shall not vary more than 40,000 pounds per square inch for sizes below .072-inch, nor by more than 30,000 pounds per square inch for sizes above .072-inch. Winding is done cold followed by a thermal treatment.

Annealed high-carbon wire—With high ductility in the annealed state, this material is utilized in cases where severe forming operations are necessary in the manufacture of the spring such as, for example, in torsion springs with certain shapes of end

TABLE XLI

Endurance Ranges and Physical Properties of Leaf and Flat Spring Materials in Bending

Material	Thickness of Specimen Inches	Heat Treatment	Condition of Surface	Brinell Hardness	Ult. Strength (Tension) lb./sq. in.	End Limit or Limiting Stress Range in Bending* lb./sq. in.	Investigator
.6% Commercial Carbon Spring Steel	⅛	Hardened and Tempered	As Recd.	350-370		0 to 42000	Batson and Bradley[1]
.6% Commercial Carbon Spring Steel	⅛	Hardened and Tempered	.062 inch machined from surface after heat treatment	350-370		0 to 128000	"
Silico-Manganese Steel	⅛	O.Q. 900°C T. 540°C	As Recd.	390-400		0 to 63000	"
Silico-Manganese Steel	⅛	O.Q. 900°C T. 540°C	.062 inch machined from surface	390-400		0 to 110000	"
.6% C. Spring Steel	⅛	Quenched and Tempered	As rolled			± 49000	Hankins[2]
Swedish Spring Steel	.006		Polished		275000	± 130000	Hengstenberg[3]
Carbon Spring Steel 1%C	1¼	Quenched and Tempered	As rolled	Approx. 400		0 to 86000	Beauwhes[3]
Carbon Spring Steel .5%C .56% Mn			As rolled		156000	34000 to 79000 51000 to 91000	Lehr[4]
Chrome Va. Spring Steel			As rolled		164000	21000 to 92000	"
Chrome Va. Spring Steel			Polished		171000	—12000 to 126000	"
Manganese Spring Steel			As rolled		188000	30000 to 84000	"

[1] *Proc. Inst. Mech. Engrs.*, 1931, V. 120, p. 301.
[2] Dept. of Sci. & Ind. Research, Special Rep. No. 5.
[3] Tests made at Westinghouse Research Laboratories.
[4] *Stahl und Eisen*, July 7, 1932, p. 653.
* Where two values are given for the same material, these correspond to actual ranges used in tests.

turns. The springs are first formed from the annealed wire and then heat treated after winding in order to obtain the required physical properties. A typical specification for this material calls for the following composition:

Carbon	.80-.95%
Manganese, max.	.50%
Phosphorus, max.	.03%
Sulphur, max.	.03%

Approximate physical properties as obtained after heat treatment are listed in TABLE XXXVII.

Hot-wound helical springs, heat treated after forming—For the larger sizes of helical springs (over about ⅜ to ½-inch wire diameter) it is not practical to wind the springs cold. In such cases, the springs may be wound hot from either carbon or alloy-steel bars and then heat-treated. For carbon steel bars, the composition required by ASTM A68-39 is given in TABLE XXXVI.

For winding of these springs, ASTM A125-39 calls for heating to a temperature of 1700 degrees Fahr. and coiling on a preheated mandrel. The springs are then allowed to cool uniformly

TABLE XLII

Endurance Limits of Elliptic Leaf Springs*

Spring Material	Thickness (in.)	Brinell Hardness	Limiting Stress Range§ (lb/sq in.)
Cr-Va spring steel	¼	445	3,000 to 32,000†
6% carbon spring steel	¼	349	2,500 to 46,000
Silico-manganese steel	¼	342	4,100 to 43,000

*Found by Batson and Bradley, Dept. of Sci. & Ind. Research (British) *Special Report* No. 13.

§ In master leaf.

† Stress concentration effects act to reduce strength. These are due to clamps used and to holes in the springs.

to a black heat, after which they are heat-treated to a temperature around 1475-1500 degrees Fahr. and quenched in oil. After quenching, the springs are tempered by heating to 800 degrees Fahr. in a salt bath. This will give a hardness around 375 to 425 Brinell. Typical physical properties of this material are shown on TABLE XXXVII.

Chrome-vanadium steel wire—In the past this alloy-steel wire has been frequently specified where a high-quality material is needed and where temperatures are somewhat higher than normal, such as is the case for automotive valve springs. Because of present restrictions on alloy steels, however, its use should be avoided where possible. In this connection it should be noted that relaxation tests by Zimmerli[4] did not show a marked superiority of chrome-vanadium steel compared to carbon steels as far as resistance to creep and relaxation at elevated temperature was concerned.

The composition of chrome-vanadium valve spring quality

[4] "Effect of Temperature on Coiled Steel Springs Under Various Loadings", *Transactions* ASME, May 1941, Page 363.

wire as given by ASTM A232-41 is listed in TABLE XXXVI. For ordinary chrome-vanadium steel spring wire (as distinguished from the "quality" wire), somewhat higher amounts of phosphorus (.04%) and sulphur (.05%) are allowed.

This type of wire may be obtained either in the annealed or in the heat-treated condition. When wound from annealed wire, the springs must be heat-treated after coiling. After winding from oil-tempered chrome-vanadium wire, a low temperature heat treatment at around 500-700 degrees Fahr. should be given, the higher bluing temperatures being preferred for applications involving elevated temperatures. Other tensile properties of this material are listed in TABLE XXXVII.

Stainless steel (18-8) spring wire—Stainless steels having a composition of about 18 per cent chromium and 8 per cent nickel are widely used for springs subject to corrosion conditions. They are also of value for elevated-temperature conditions. A typical specification for this material calls for the following composition:

Carbon, max.	.15%
Chromium	16.00-20.00%
Nickel	8.00-12.00%
Nickel plus Chromium, min.	26%

The tensile strength of this wire is developed by cold drawing and may vary from 160,000 to 320,000 pounds per square inch depending on wire size as shown in TABLE XLIII.

Other important physical properties of this type of steel are listed in TABLE XXXVIII.

Springs of 18-8 stainless steel wire are wound cold and may be given a stress-relieving heat treatment at a temperature of 750 degrees Fahr. for 15 minutes to an hour, the shorter time being used for the smaller wire sizes.

Phosphor bronze—Finding its greatest use in cases where a spring with good electrical conductivity is desired, phosphor bronze is also used for applications where corrosion resistance is important. However, at present because of high tin content (5 to 8 per cent) its use is severely restricted. A possible substitute where high conductivity is desired is beryllium copper. Typical physical properties are given in TABLE XXXVIII.

Beryllium copper—This is an alloy consisting essentially of about 2 per cent beryllium and the rest copper together with small amounts of other alloys[5]. It has the advantage of having a high electrical conductivity while not requiring any tin in its

TABLE XLIII

18-8 Stainless Steel Spring Wire

Wire Size (in.)	Ultimate Tensile Strength (lb/sq in.)
.0104	320,000
.0135	313,000
.0173	306,000
.0258	288,000
.0410	269,000
.0625	251,000
.0915	234,000
.1480	207,000
.207	185,000
.263	171,000
.307	162,000

manufacture. In general, wire made from this material is quenched from 1475 degrees Fahr. and then cold drawn to increase the hardness. After coiling, it is heat treated to increase the physical properties. This heat treatment may also be varied to change the modulus of elasticity or the amount of drift or creep. Further data on the properties of this material are given in TABLE XXXVIII.

Spring brass—This is an alloy composed of about 70 per cent copper and 30 per cent zinc which is cold rolled to give it high strength. Typical properties are listed in TABLE XXXVIII. Because of its low strength, stresses must be kept moderate if this material is used. However, it has the advantage of not requiring any tin in its manufacture, while at the same time possessing good electrical conductivity and corrosion resistance.

K-Monel—This is a copper-nickel alloy to which 2 to 4 per cent of aluminum has been added. A typical composition is: Copper 29 per cent; nickel 66 per cent; aluminum 2.75 per cent. Wire of this material is given a solution heat treatment and then cold drawn. After winding, springs are given a final heat treatment to increase the hardness and strength. By this means, ulti-

[5] Articles by R. W. Carson, "Springs of Beryllium Copper," *Aero Digest*, July 1942, and "New Alloys for Springs," *Product Engineering*, June 1938, give additional data on this alloy.

mate strengths around 160,000 to 200,000 pounds per square inch can be obtained. Further data on physical properties are given in TABLE XXXVIII. Springs of this alloy are used for corrosion conditions and for resistance to elevated temperatures[6].

Z-nickel—A corrosion-resistant alloy containing about 98 per cent nickel, this material also has good mechanical properties. It is used for springs subject to elevated temperatures. Because it has fair ductility after heat treatment, springs of this material may often be wound from heat treated wire. Further data are given in TABLE XXXVIII.

Other possible substitutions for critical spring materials—One which may be considered for use as a substitute material where both corrosion conditions and static loading are involved is copper-clad steel. For spring use, this material consists essentially of a high-strength steel having a thin coating of copper for protection against corrosion. Tensile properties in the heat treated condition may be obtained which approach those of hot-rolled spring steel heat treated. Where fatigue loading is involved, however, it may not be advisable to use this material because of danger of fatigue failure of the relatively weak surface material. This danger is not present for static loading.

Helical springs coiled from glass rods and tempered have also been used for springs under corrosion conditions[7]. The tempering consists in inducing surface compression stresses by suitable heat treatment, thereby greatly increasing the tensile strength. Because of the low tensile strength of glass relative to that of spring steel (even after tempering), much lower working stresses are used in practical design. Since the energy-storage capacity of a spring increases as the square of the stress, other things being equal, this means that the glass spring will usually have to be much larger than a corresponding one made of spring steel. This is true even though the modulus of elasticity of glass is only 1/3 that of steel. However, where space is available for the spring so that stresses may be kept to low values, this material offers some promise for use particularly where corrosion conditions are severe.

---

[6] Article by Betty, et al., *Transactions* ASME, July 1942, Page 465 gives data on relaxation resistance of this and other nickel alloys at elevated temperatures.

[7] Article by Colin Carmichael, *Machine Design*, August 1942, Page 85, gives further details on the use of glass, as well as article by T. J. Thompson, *Product Engineering*, May 1940, Page 196.

INDEX

A

B

C

D

E

F

G

H

I

K

L

M

N

O

P

R

S

T

U

V

W

Y

Z